CHEM 235: ANALYTICAL CHEMISTRY



Kathryn Davis
Manchester University

LibreTexts™

CHEM 235: Analytical Chemistry

Kathryn Davis

Manchester University

This text is disseminated via the Open Education Resource (OER) LibreTexts Project (https://LibreTexts.org) and like the thousands of other texts available within this powerful platform, it is freely available for reading, printing, and "consuming."

The LibreTexts mission is to bring together students, faculty, and scholars in a collaborative effort to provide an accessible, and comprehensive platform that empowers our community to develop, curate, adapt, and adopt openly licensed resources and technologies; through these efforts we can reduce the financial burden born from traditional educational resource costs, ensuring education is more accessible for students and communities worldwide.

Most, but not all, pages in the library have licenses that may allow individuals to make changes, save, and print this book. Carefully consult the applicable license(s) before pursuing such effects. Instructors can adopt existing LibreTexts texts or Remix them to quickly build course-specific resources to meet the needs of their students. Unlike traditional textbooks, LibreTexts' web based origins allow powerful integration of advanced features and new technologies to support learning.



LibreTexts is the adaptable, user-friendly non-profit open education resource platform that educators trust for creating, customizing, and sharing accessible, interactive textbooks, adaptive homework, and ancillary materials. We collaborate with individuals and organizations to champion open education initiatives, support institutional publishing programs, drive curriculum development projects, and more.

The LibreTexts libraries are Powered by NICE CXone Expert and was supported by the Department of Education Open Textbook Pilot Project, the California Education Learning Lab, the UC Davis Office of the Provost, the UC Davis Library, the California State University Affordable Learning Solutions Program, and Merlot. This material is based upon work supported by the National Science Foundation under Grant No. 1246120, 1525057, and 1413739.

Any opinions, findings, and conclusions or recommendations expressed in this material are those of the author(s) and do not necessarily reflect the views of the National Science Foundation nor the US Department of Education.

Have questions or comments? For information about adoptions or adaptions contact info@LibreTexts.org or visit our main website at https://LibreTexts.org.

This text was compiled on 01/28/2026

TABLE OF CONTENTS

Licensing

1: All Measurements Are Uncertain

- 1.1: Classifying Analytical Techniques
- 1.2: Measurements in Analytical Chemistry
- 1.3: Characterizing Measurements and Results
- 1.4: Characterizing Experimental Errors
- 1.5: Propagation of Uncertainty
- 1.6: The Distribution of Measurements and Results
- 1.7: Statistical Analysis of Data
- 1.8: Statistical Methods for Normal Distributions

2: The Return of Stoichiometry

- 2.1: Concentration
- 2.2: Stoichiometric Calculations
- 2.3: Preparing Solutions

3: Acid-Base Equilibria Affect Solution Conditions

- 3.1: Acid–Base Titrations
- 3.2: Ladder Diagrams for Acid-Base Equilibria
- 3.3: Solving Acid-Base Equilibrium Problems
- 3.4: Buffer Solutions

4: There Are Other Titration Methods!

- 4.1: Complexation Titrations
- 4.2: EDTA Ladder Diagrams
- 4.3: Redox Titrations
- 4.4: Ladder Diagrams for Redox Titrations

5: Electrochemical Instrumental Analysis

- 5.1: Overview of Electrochemistry
- 5.2: Potentiometric Methods
- 5.3: Coulometric Methods
- 5.4: Voltammetric and Amperometric Methods

6: Beyond Beer's Law- Quantitative Spectroscopic Analysis

- 6.1: Overview of Spectroscopy
- 6.2: Spectroscopy Based on Absorption
- 6.3: UV/Vis and IR Spectroscopy
- 6.4: Atomic Absorption Spectroscopy
- 6.5: Photoluminescent Spectroscopy
- 6.6: Atomic Emission Spectroscopy

7: Mass Spectrometry

- 7.1: Mass Spectrometers
- 7.2: Inductively Coupled Plasma Mass Spectrometer
- 7.3: Molecular Mass Spectra
- 7.4: Mass Spectrometers
- 7.5: Ion Sources
- 7.6: Applications of Molecular Mass Spectrometry

8: Analysis and Separation of Mixtures

- 8.1: UV/Vis Analysis of Two-Component Mixtures
- 8.2: Classifying Separation Techniques
- 8.3: Liquid-Liquid Extractions
- 8.4: Overview of Analytical Separations
- 8.5: General Theory of Column Chromatography
- 8.6: Optimizing Chromatographic Separations
- 8.7: Gas Chromatography
- 8.8: High-Performance Liquid Chromatography
- 8.9: Other Forms of Chromatography
- 8.10: Electrophoresis

9: Solubility Equilibria

- 9.1: Ladder Diagrams
- 9.2: Solving Equilibrium Problems
- 9.3: Activity Effects
- 9.4: Precipitation Gravimetry

Index

Glossary

Detailed Licensing

Licensing

*A detailed breakdown of this resource's licensing can be found in **Back Matter/Detailed Licensing**.*

CHAPTER OVERVIEW

1: All Measurements Are Uncertain

1.1: Classifying Analytical Techniques
1.2: Measurements in Analytical Chemistry
1.3: Characterizing Measurements and Results
1.4: Characterizing Experimental Errors
1.5: Propagation of Uncertainty
1.6: The Distribution of Measurements and Results
1.7: Statistical Analysis of Data
1.8: Statistical Methods for Normal Distributions

This page titled 1: All Measurements Are Uncertain is shared under a not declared license and was authored, remixed, and/or curated by Kathryn Davis.

1.1: Classifying Analytical Techniques

The analysis of a sample generates a chemical or physical signal that is proportional to the amount of analyte in the sample. This signal may be anything we can measure, such as volume or absorbance. It is convenient to divide analytical techniques into two general classes based on whether the signal is proportional to the mass or moles of analyte, or is proportional to the analyte's concentration

Consider the two graduated cylinders in Figure 3.3.1 , each of which contains a solution of 0.010 M $Cu(NO_3)_2$. Cylinder 1 contains 10 mL, or $\mathbf{1.0 \times 10^{-4}}$ moles of Cu^{2+}, and cylinder 2 contains 20 mL, or $\mathbf{2.0 \times 10^{-4}}$ moles of Cu^{2+}. If a technique responds to the absolute amount of analyte in the sample, then the signal due to the analyte S_A

$$S_A = k_A n_A \tag{1.1.1}$$

where n_A is the moles or grams of analyte in the sample, and k_A is a proportionality constant. Because cylinder 2 contains twice as many moles of Cu^{2+} as cylinder 1, analyzing the contents of cylinder 2 gives a signal twice as large as that for cylinder 1.



Figure 3.3.1 : Two graduated cylinders, each containing 0.10 M $Cu(NO_3)_2$. Although the cylinders contain the same concentration of Cu^{2+}, the cylinder on the left contains $\mathbf{1.0 \times 10^{-4}}$ mol Cu^{2+} and the cylinder on the right contains $\mathbf{2.0 \times 10^{-4}}$ mol Cu^{2+}.

A second class of analytical techniques are those that respond to the analyte's concentration, C_A

$$S_A = k_A C_A \tag{1.1.2}$$

Since the solutions in both cylinders have the same concentration of Cu^{2+}, their analysis yields identical signals.

A technique that responds to the absolute amount of analyte is a ***total analysis*** technique. Mass and volume are the most common signals for a total analysis technique, and the corresponding techniques are gravimetry (Chapter 8) and titrimetry (Chapter 9). With a few exceptions, the signal for a total analysis technique is the result of one or more chemical reactions, the stoichiometry of which determines the value of k_A in Equation 1.1.1.

> Historically, most early analytical methods used a total analysis technique. For this reason, total analysis techniques are often called "classical" techniques.

Spectroscopy (Chapter 10) and electrochemistry (Chapter 11), in which an optical or an electrical signal is proportional to the relative amount of analyte in a sample, are examples of concentration techniques. The relationship between the signal and the analyte's concentration is a theoretical function that depends on experimental conditions and the instrumentation used to measure the signal. For this reason the value of k_A in Equation 1.1.2 is determined experimentally.

> Since most concentration techniques rely on measuring an optical or electrical signal, they also are known as "instrumental" techniques.

This page titled 1.1: Classifying Analytical Techniques is shared under a CC BY-NC-SA 4.0 license and was authored, remixed, and/or curated by Kathryn Davis.

- **3.3: Classifying Analytical Techniques** by David Harvey is licensed CC BY-NC-SA 4.0.

1.2: Measurements in Analytical Chemistry

Analytical chemistry is a quantitative science. Whether determining the concentration of a species, evaluating an equilibrium constant, measuring a reaction rate, or drawing a correlation between a compound's structure and its reactivity, analytical chemists engage in "measuring important chemical things" [Murray, R. W. *Anal. Chem.* **2007**, *79*, 1765]. In this section we review briefly the basic units of measurement and the proper use of significant figures.

Units of Measurement

A measurement usually consists of a unit and a number that expresses the quantity of that unit. We can express the same physical measurement with different units, which creates confusion if we are not careful to specify the unit. For example, the mass of a sample that weighs 1.5 g is equivalent to 0.0033 lb or to 0.053 oz. To ensure consistency, and to avoid problems, scientists use the common set of fundamental base units listed in Table 2.1.1 . These units are called SI units after the Système International d'Unités.

> It is important for scientists to agree upon a common set of units. In 1999, for example, NASA lost a Mars Orbiter spacecraft because one engineering team used English units in their calculations and another engineering team used metric units. As a result, the spacecraft came too close to the planet's surface, causing its propulsion system to overheat and fail.
>
> Some measurements, such as absorbance, do not have units. Because the meaning of a unitless number often is unclear, some authors include an artificial unit. It is not unusual to see the abbreviation AU—short for absorbance unit—following an absorbance value, which helps clarify that the measurement is an absorbance value.

Table 2.1.1 : Fundamental Base SI Units

Measurement	Unit	Symbol	Definition (1 unit is...)
mass	kilogram	kg	...the mass of the international prototype, a Pt-Ir object housed at the Bureau International de Poids and Measures at Sèvres, France. (Note: The mass of the international prototype changes at a rate of approximately 1 μg per year due to reversible surface contamination. The reference mass, therefore, is determined immediately after its cleaning using a specified procedure. Current plans call for retiring the international prototype and defining the kilogram in terms of Planck's constant; see this link for more details.)
distance	meter	m	...the distance light travels in $(299\ 792\ 458)^{-1}$ seconds.
temperature	kelvin	K	...equal to $(273.16)^{-1}$, where 273.16 K is the triple point of water (where its solid, liquid, and gaseous forms are in equilibrium. and where 0 is the lowest possible temperature).
time	second	s	...the time it takes for 9 192 631 770 periods of radiation corresponding to a specific transition of the ^{133}Cs atom.
current	ampere	A	...the current producing a force of 2×10^{-7} N/m between two straight parallel conductors of infinite length separated by one meter (in a vacuum).
amount of substance	mole	mol	...the amount of a substance containing as many particles as there are atoms in exactly 0.012 kilogram of ^{12}C.
light	candela	cd	...the luminous intensity of a source with a monochromatic frequency of 540×10^{12} hertz and a radiant power of $(683)^{-1}$ watts per steradian.

There is some disagreement on the use of "amount of substance" to describe the measurement for which the mole is the base SI unit; see "What's in a Name? Amount of Substance, Chemical Amount, and Stoichiometric Amount," the full reference for

which is Giunta, C. J. *J. Chem. Educ.* **2016**, *93*, 583–586.

We define other measurements using these fundamental SI units. For example, we measure the quantity of heat produced during a chemical reaction in joules, (J), where 1 J is equivalent to 1 m kg/s . Table 2.1.2 provides a list of some important derived SI units, as well as a few common non-SI units.

Table 2.1.2 : Derived SI Units and Non-SI Units of Importance to Analytical Chemistry

Measurement	Unit	Symbol	Equivalent SI Units
length	angstrom (non-SI)	Å	$1\ Å = 1 \times 10^{-10}$ m
volume	liter (non-SI)	L	$1\ L = 10^{-3}\ m^3$
force	newton (SI)	N	$1\ N = 1\ m{\cdot}kg/s^2$
pressure	pascal (SI) atmosphere (non-SI)	Pa atm	$1\ Pa = 1\ N/m^3 = 1\ kg/(m{\cdot}s^2)$ 1 atm = 101 325 Pa
energy, work, heat	joule (SI) calorie (non-SI) electron volt (non-SI)	J cal eV	$1\ J = 1\ N{\cdot}m = 1\ m^2{\cdot}kg/s^2$ 1 cal = 4.184 J $1\ eV = 1.602\ 177\ 33 \times 10^{-19}$ J
power	watt (SI)	W	$1\ W = 1\ J/s = 1\ m^2{\cdot}kg/s^3$
charge	coulomb (SI)	C	$1\ C = 1\ A{\cdot}s$
potential	volt (SI)	V	$1\ V = 1\ W/A = 1\ m^2{\cdot}kg/(s^3{\cdot}A)$
frequency	hertz (SI)	Hz	$1\ Hz = s^{-1}$
temperature	Celcius (non-SI)	°C	°C = K – 273.15

Chemists frequently work with measurements that are very large or very small. A mole contains 602 213 670 000 000 000 000 000 particles and some analytical techniques can detect as little as 0.000 000 000 000 001 g of a compound. For simplicity, we express these measurements using scientific notation; thus, a mole contains $6.022\ 136\ 7 \times 10^{23}$ particles, and the detected mass is 1×10^{-15} g. Sometimes we wish to express a measurement without the exponential term, replacing it with a prefix (Table 2.1.3). A mass of $\mathbf{1 \times 10^{-15}}$ g, for example, is the same as 1 fg, or femtogram.

Writing a lengthy number with spaces instead of commas may strike you as unusual. For a number with more than four digits on either side of the decimal point, however, the recommendation from the International Union of Pure and Applied Chemistry is to use a thin space instead of a comma.

Table 2.1.3 : Common Prefixes for Exponential Notation

Prefix	Symbol	Factor	Prefix	Symbol	Factor	Prefix	Symbol	Factor
yotta	Y	10^{24}	kilo	k	10^{3}	micro	μ	10^{-6}
zetta	Z	10^{21}	hecto	h	10^{2}	nano	n	10^{-9}
eta	E	10^{18}	deka	da	10^{1}	pico	p	10^{-12}
peta	P	10^{15}	—	—	10^{0}	femto	f	10^{-15}
tera	T	10^{12}	deci	d	10^{-1}	atto	a	10^{-18}
giga	G	10^{9}	centi	c	10^{-2}	zepto	z	10^{-21}
mega	M	10^{6}	milli	m	10^{-3}	yocto	y	10^{-24}

Uncertainty in Measurements

A measurement provides information about both its magnitude and its uncertainty. Consider, for example, the three photos in Figure 2.1.1 , taken at intervals of approximately 1 sec after placing a sample on the balance. Assuming the balance is properly calibrated, we are certain that the sample's mass is more than 0.5729 g and less than 0.5731 g. We are uncertain, however, about the sample's mass in the last decimal place since the final two decimal places fluctuate between 29, 30, and 31. The best we can do is to report the sample's mass as 0.5730 g ± 0.0001 g, indicating both its magnitude and its absolute uncertainty.



Figure 2.1.1 : When weighing a sample on a balance, the measurement fluctuates in the final decimal place. We record this sample's mass as 0.5730 g ± 0.0001 g.

Significant Figures

A measurement's significant figures convey information about a measurement's magnitude and uncertainty. The number of significant figures in a measurement is the number of digits known exactly plus one digit whose value is uncertain. The mass shown in Figure 2.1.1 , for example, has four significant figures, three which we know exactly and one, the last, which is uncertain.

Suppose we weigh a second sample, using the same balance, and obtain a mass of 0.0990 g. Does this measurement have 3, 4, or 5 significant figures? The zero in the last decimal place is the one uncertain digit and is significant. The other two zeros, however, simply indicates the decimal point's location. Writing the measurement in scientific notation, $\mathbf{9.90 \times 10^{-2}}$, clarifies that there are three significant figures in 0.0990.

> In the measurement **0.0990** g, the zero in **green** is a significant digit and the zeros in **red** are not significant digits.

Example 2.1.1

How many significant figures are in each of the following measurements? Convert each measurement to its equivalent scientific notation or decimal form.

a. 0.0120 mol HCl
b. 605.3 mg $CaCO_3$
c. $\mathbf{1.043 \times 10^{-4}}$ mol Ag^+
d. $\mathbf{9.3 \times 10^{4}}$ mg NaOH

Solution

(a) Three significant figures; $\mathbf{1.20 \times 10^{-2}}$ mol HCl.

(b) Four significant figures; $\mathbf{6.053 \times 10^{2}}$ mg $CaCO_3$.

(c) Four significant figures; 0.000 104 3 mol Ag^+.

(d) Two significant figures; 93 000 mg NaOH.

There are two special cases when determining the number of significant figures in a measurement. For a measurement given as a logarithm, such as pH, the number of significant figures is equal to the number of digits to the right of the decimal point. Digits to

the left of the decimal point are not significant figures since they indicate only the power of 10. A pH of 2.45, therefore, contains two significant figures.

> The log of 2.8×10^2 is 2.45. The log of 2.8 is 0.45 and the log of 10^2 is 2. The 2 in 2.45, therefore, only indicates the power of 10 and is not a significant digit.

An exact number, such as a stoichiometric coefficient, has an infinite number of significant figures. A mole of $CaCl_2$, for example, contains exactly two moles of chloride ions and one mole of calcium ions. Another example of an exact number is the relationship between some units. There are, for example, exactly 1000 mL in 1 L. Both the 1 and the 1000 have an infinite number of significant figures.

Using the correct number of significant figures is important because it tells other scientists about the uncertainty of your measurements. Suppose you weigh a sample on a balance that measures mass to the nearest ±0.1 mg. Reporting the sample's mass as 1.762 g instead of 1.7623 g is incorrect because it does not convey properly the measurement's uncertainty. Reporting the sample's mass as 1.76231 g also is incorrect because it falsely suggests an uncertainty of ±0.01 mg.

Significant Figures in Calculations

Significant figures are also important because they guide us when reporting the result of an analysis. When we calculate a result, the answer cannot be more certain than the least certain measurement in the analysis. Rounding an answer to the correct number of significant figures is important.

For addition and subtraction, we round the answer to the last decimal place in common for each measurement in the calculation. The exact sum of 135.621, 97.33, and 21.2163 is 254.1673. Since the last decimal place common to all three numbers is the hundredth's place

$$\begin{array}{r} 135.621 \\ 97.33 \\ 21.2163 \\ \hline 254.1673 \end{array}$$

we round the result to 254.17.

> The last common decimal place shared by 135.621, 97.33, and 21.2163 is shown in **red**.

When working with scientific notation, first convert each measurement to a common exponent before determining the number of significant figures. For example, the sum of 6.17×10^7, 4.3×10^5, and 3.23×10^4 is 6.22×10^7.

$$\begin{array}{rl} 6.17 & \times 10^7 \\ 0.043 & \times 10^7 \\ \underline{0.00323} & \underline{\times 10^7} \\ 6.21623 & \times 10^7 \end{array}$$

> The last common decimal place shared by 6.17×10^7, 4.3×10^5 and 3.23×10^4 is shown in **red**.

For multiplication and division, we round the answer to the same number of significant figures as the measurement with the fewest number of significant figures. For example, when we divide the product of 22.91 and 0.152 by 16.302, we report the answer as 0.214 (three significant figures) because 0.152 has the fewest number of significant figures.

$$\frac{22.91 \times 0.152}{16.302} = 0.2136 = 0.214$$

There is no need to convert measurements in scientific notation to a common exponent when multiplying or dividing.

It is important to recognize that the rules presented here for working with significant figures are generalizations. What actually is conserved is uncertainty, not the number of significant figures. For example, the following calculation

$$101/99 = 1.02$$

is correct even though it violates the general rules outlined earlier. Since the relative uncertainty in each measurement is approximately 1% (101 ± 1 and 99 ± 1), the relative uncertainty in the final answer also is approximately 1%. Reporting the answer as 1.0 (two significant figures), as required by the general rules, implies a relative uncertainty of 10%, which is too large. The correct answer, with three significant figures, yields the expected relative uncertainty. Chapter 4 presents a more thorough treatment of uncertainty and its importance in reporting the result of an analysis.

Finally, to avoid "round-off" errors, it is a good idea to retain at least one extra significant figure throughout any calculation. Better yet, invest in a good scientific calculator that allows you to perform lengthy calculations without the need to record intermediate values. When your calculation is complete, round the answer to the correct number of significant figures using the following simple rules.

1. Retain the least significant figure if it and the digits that follow are less than halfway to the next higher digit. For example, rounding 12.442 to the nearest tenth gives 12.4 since 0.442 is less than half way between 0.400 and 0.500.
2. Increase the least significant figure by 1 if it and the digits that follow are more than halfway to the next higher digit. For example, rounding 12.476 to the nearest tenth gives 12.5 since 0.476 is more than halfway between 0.400 and 0.500.
3. If the least significant figure and the digits that follow are exactly halfway to the next higher digit, then round the least significant figure to the nearest even number. For example, rounding 12.450 to the nearest tenth gives 12.4, while rounding 12.550 to the nearest tenth gives 12.6. Rounding in this manner ensures that we round up as often as we round down.

? Exercise 2.1.1

For a problem that involves both addition and/or subtraction, and multiplication and/or division, be sure to account for significant figures at each step of the calculation. With this in mind, report the result of this calculation to the correct number of significant figures.

$$\frac{0.250 \times (9.93 \times 10^{-3}) - 0.100 \times (1.927 \times 10^{-2})}{9.93 \times 10^{-3} + 1.927 \times 10^{-2}} =$$

Answer

The correct answer to this exercise is 1.9×10^{-2}. To see why this is correct, let's work through the problem in a series of steps. Here is the original problem

$$\frac{0.250 \times (9.93 \times 10^{-3}) - 0.100 \times (1.927 \times 10^{-2})}{9.93 \times 10^{-3} + 1.927 \times 10^{-2}} =$$

Following the correct order of operations we first complete the two multiplications in the numerator. In each case the answer has three significant figures, although we retain an extra digit, highlight in **red**, to avoid round-off errors.

$$\frac{2.482 \times 10^{-3} - 1.927 \times 10^{-3}}{9.93 \times 10^{-3} + 1.927 \times 10^{-2}} =$$

Completing the subtraction in the numerator leaves us with two significant figures since the last significant digit for each value is in the hundredths place.

$$\frac{0.555 \times 10^{-3}}{9.93 \times 10^{-3} + 1.927 \times 10^{-2}} =$$

The two values in the denominator have different exponents. Because we are adding together these values, we first rewrite them using a common exponent.

$$\frac{0.555 \times 10^{-3}}{0.993 \times 10^{-2} + 1.927 \times 10^{-2}} =$$

The sum in the denominator has four significant figures since each of the addends has three decimal places.

$$\frac{0.555 \times 10^{-3}}{2.920 \times 10^{-2}} =$$

Finally, we complete the division, which leaves us with a result having two significant figures.

$$\frac{0.555 \times 10^{-3}}{2.920 \times 10^{-2}} = 1.9 \times 10^{-2}$$

This page titled 1.2: Measurements in Analytical Chemistry is shared under a CC BY-NC-SA 4.0 license and was authored, remixed, and/or curated by Kathryn Davis.

- **2.1: Measurements in Analytical Chemistry** by David Harvey is licensed CC BY-NC-SA 4.0.

1.3: Characterizing Measurements and Results

Let's begin by choosing a simple quantitative problem that requires a single measurement: What is the mass of a penny? You probably recognize that our statement of the problem is too broad. For example, are we interested in the mass of a United States penny or of a Canadian penny, or is the difference relevant? Because a penny's composition and size may differ from country to country, let's narrow our problem to pennies from the United States.

There are other concerns we might consider. For example, the United States Mint produces pennies at two locations (Figure 4.1.1). Because it seems unlikely that a penny's mass depends on where it is minted, we will ignore this concern. Another concern is whether the mass of a newly minted penny is different from the mass of a circulating penny. Because the answer this time is not obvious, let's further narrow our question and ask "What is the mass of a circulating United States Penny?"



Figure 4.1.1 : An uncirculated 2005 Lincoln head penny. The "D" below the date indicates that this penny was produced at the United States Mint at Denver, Colorado. Pennies produced at the Philadelphia Mint do not have a letter below the date. Source: United States Mint image.

A good way to begin our analysis is to gather some preliminary data. Table 4.1.1 shows masses for seven pennies collected from my change jar. In examining this data we see that our question does not have a simple answer. That is, we can not use the mass of a single penny to draw a specific conclusion about the mass of any other penny (although we might reasonably conclude that all pennies weigh at least 3 g). We can, however, characterize this data by reporting the spread of the individual measurements around a central value.

Table 4.1.1 : Masses of Seven Circulating U. S. Pennies

Penny	Mass (g)
1	3.080
2	3.094
3	3.107
4	3.056
5	3.112
6	3.174
7	3.198

Measures of Central Tendency

One way to characterize the data in Table 4.1.1 is to assume that the masses of individual pennies are scattered randomly around a central value that is the best estimate of a penny's expected, or "true" mass. There are two common ways to estimate central tendency: the mean and the median.

Mean

The ***mean***, $\overline{X}$, is the numerical average for a data set. We calculate the mean by dividing the sum of the individual values by the size of the data set

$$\overline{X} = \frac{\sum_{i=1}^{n} X_i}{n}$$

where X_i is the i^{th} measurement, and n is the size of the data set.

Example 4.1.1

What is the mean for the data in Table 4.1.1 ?

Solution

To calculate the mean we add together the results for all measurements

$$3.080 + 3.094 + 3.107 + 3.056 + 3.112 + 3.174 + 3.198 = 21.821 \text{ g}$$

and divide by the number of measurements

$$\overline{X} = \frac{21.821 \text{ g}}{7} = 3.117 \text{ g}$$

The mean is the most common estimate of central tendency. It is not a robust estimate, however, because a single extreme value—one much larger or much smaller than the remainder of the data—influences strongly the mean's value [Rousseeuw, P. J. *J. Chemom.* **1991**, *5*, 1–20]. For example, if we accidently record the third penny's mass as 31.07 g instead of 3.107 g, the mean changes from 3.117 g to 7.112 g!

> An estimate for a statistical parameter is robust if its value is not affected too much by an unusually large or an unusually small measurement.

Median

The ***median***, $\widetilde{X}$, is the middle value when we order our data from the smallest to the largest value. When the data has an odd number of values, the median is the middle value. For an even number of values, the median is the average of the $n/2$ and the $(n/2) + 1$ values, where n is the size of the data set.

> When $n = 5$, the median is the third value in the ordered data set; for $n = 6$, the median is the average of the third and fourth members of the ordered data set.

Example 4.1.2

What is the median for the data in Table 4.1.1 ?

Solution

To determine the median we order the measurements from the smallest to the largest value

$$3.056 \quad 3.080 \quad 3.094 \quad 3.107 \quad 3.112 \quad 3.174 \quad 3.198$$

Because there are seven measurements, the median is the fourth value in the ordered data; thus, the median is 3.107 g.

As shown by Example 4.1.1 and Example 4.1.2 , the mean and the median provide similar estimates of central tendency when all measurements are comparable in magnitude. The median, however, is a more robust estimate of central tendency because it is less sensitive to measurements with extreme values. For example, if we accidently record the third penny's mass as 31.07 g instead of 3.107 g, the median's value changes from 3.107 g to 3.112 g.

Measures of Spread

If the mean or the median provides an estimate of a penny's expected mass, then the spread of individual measurements about the mean or median provides an estimate of the difference in mass among pennies or of the uncertainty in measuring mass with a balance. Although we often define the spread relative to a specific measure of central tendency, its magnitude is independent of the central value. Although shifting all measurements in the same direction by adding or subtracting a constant value changes the mean or median, it does not change the spread. There are three common measures of spread: the range, the standard deviation, and the variance.

Problem 13 at the end of the chapter asks you to show that this is true.

Range

The ***range***, *w*, is the difference between a data set's largest and smallest values.

$$w = X_{\text{largest}} - X_{\text{smallest}}$$

The range provides information about the total variability in the data set, but does not provide information about the distribution of individual values. The range for the data in Table 4.1.1 is

$$w = 3.198\ \text{g} - 3.056\ \text{g} = 0.142\ \text{g}$$

Standard Deviation

The ***standard deviation***, *s*, describes the spread of individual values about their mean, and is given as

$$s = \sqrt{\frac{\sum_{i=1}^{n}(X_i - \overline{X})^2}{n-1}} \tag{1.3.1}$$

where X_i is one of the *n* individual values in the data set, and $\overline{X}$ is the data set's mean value. Frequently, we report the relative standard deviation, s_r, instead of the absolute standard deviation.

$$s_r = \frac{s}{\overline{X}}$$

The percent relative standard deviation, $\%s_r$, is $s_r \times 100$.

The relative standard deviation is important because it allows for a more meaningful comparison between data sets when the individual measurements differ significantly in magnitude. Consider again the data in Table 4.1.1 . If we multiply each value by 10, the absolute standard deviation will increase by 10 as well; the relative standard deviation, however, is the same.

Example 4.1.3

Report the standard deviation, the relative standard deviation, and the percent relative standard deviation for the data in Table 4.1.1 ?

Solution

To calculate the standard deviation we first calculate the difference between each measurement and the data set's mean value (3.117), square the resulting differences, and add them together to find the numerator of Equation 1.3.1

$$\begin{aligned}
(3.080 - 3.117)^2 &= (-0.037)^2 = 0.001369 \\
(3.094 - 3.117)^2 &= (-0.023)^2 = 0.000529 \\
(3.107 - 3.117)^2 &= (-0.010)^2 = 0.000100 \\
(3.056 - 3.117)^2 &= (-0.061)^2 = 0.003721 \\
(3.112 - 3.117)^2 &= (-0.005)^2 = 0.000025 \\
(3.174 - 3.117)^2 &= (+0.057)^2 = 0.003249 \\
(3.198 - 3.117)^2 &= (+0.081)^2 = \underline{0.006561} \\
&\qquad\qquad\qquad\quad 0.015554
\end{aligned}$$

For obvious reasons, the numerator of Equation 1.3.1 is called a sum of squares. Next, we divide this sum of squares by *n* – 1, where *n* is the number of measurements, and take the square root.

$$s = \sqrt{\frac{0.015554}{7-1}} = 0.051\ \text{g}$$

Finally, the relative standard deviation and percent relative standard deviation are

$$s_r = \frac{0.051\ \text{g}}{3.117\ \text{g}} = 0.016$$

$$\%s_r = (0.016) \times 100 = 1.6\%$$

It is much easier to determine the standard deviation using a scientific calculator with built in statistical functions.

Many scientific calculators include two keys for calculating the standard deviation. One key calculates the standard deviation for a data set of *n* samples drawn from a larger collection of possible samples, which corresponds to Equation 1.3.1. The other key calculates the standard deviation for all possible samples. The latter is known as the population's standard deviation, which we will cover later in this chapter. Your calculator's manual will help you determine the appropriate key for each.

Variance

Another common measure of spread is the ***variance***, which is the square of the standard deviation. We usually report a data set's standard deviation, rather than its variance, because the mean value and the standard deviation share the same unit. As we will see shortly, the variance is a useful measure of spread because its values are additive.

Example 4.1.4

What is the variance for the data in Table 4.1.1 ?

Solution

The variance is the square of the absolute standard deviation. Using the standard deviation from Example 4.1.3 gives the variance as

$$s^2 = (0.051)^2 = 0.0026$$

Exercise 4.1.1

The following data were collected as part of a quality control study for the analysis of sodium in serum; results are concentrations of Na^+ in mmol/L.

140 143 141 137 132 157 143 149 118 145

Report the mean, the median, the range, the standard deviation, and the variance for this data. This data is a portion of a larger data set from Andrew, D. F.; Herzberg, A. M. *Data: A Collection of Problems for the Student and Research Worker*, Springer-Verlag:New York, 1985, pp. 151–155.

Answer

Mean: To find the mean we add together the individual measurements and divide by the number of measurements. The sum of the 10 concentrations is 1405. Dividing the sum by 10, gives the mean as 140.5, or 1.40×10^2 mmol/L.

Median: To find the median we arrange the 10 measurements from the smallest concentration to the largest concentration; thus

118 132 137 140 141 143 143 145 149 157

The median for a data set with 10 members is the average of the fifth and sixth values; thus, the median is (141 + 143)/2, or 142 mmol/L.

Range: The range is the difference between the largest value and the smallest value; thus, the range is 157 – 118 = 39 mmol/L.

Standard Deviation: To calculate the standard deviation we first calculate the absolute difference between each measurement and the mean value (140.5), square the resulting differences, and add them together. The differences are

–0.5 2.5 0.5 –3.5 –8.5 16.5 2.5 8.5 –22.5 4.5

and the squared differences are

$$0.25 \quad 6.25 \quad 0.25 \quad 12.25 \quad 72.25 \quad 272.25 \quad 6.25 \quad 72.25 \quad 506.25 \quad 20.25$$

The total sum of squares, which is the numerator of Equation 1.3.1, is 968.50. The standard deviation is

$$s = \sqrt{\frac{968.50}{10-1}} = 10.37 \approx 10.4$$

Variance: The variance is the square of the standard deviation, or 108.

This page titled 1.3: Characterizing Measurements and Results is shared under a CC BY-NC-SA 4.0 license and was authored, remixed, and/or curated by Kathryn Davis.

- **4.1: Characterizing Measurements and Results** by David Harvey is licensed CC BY-NC-SA 4.0.

1.4: Characterizing Experimental Errors

Characterizing a penny's mass using the data in Table 4.1.1 suggests two questions. First, does our measure of central tendency agree with the penny's expected mass? Second, why is there so much variability in the individual results? The first of these questions addresses the accuracy of our measurements and the second addresses the precision of our measurements. In this section we consider the types of experimental errors that affect accuracy and precision.

Errors That Affect Accuracy

Accuracy is how close a measure of central tendency is to its expected value, μ. We express accuracy either as an absolute error, e

$$e = \overline{X} - \mu \tag{1.4.1}$$

or as a percent relative error, $\%e$

$$\%e = \frac{\overline{X} - \mu}{\mu} \times 100 \tag{1.4.2}$$

Although Equation 1.4.1 and Equation 1.4.2 use the mean as the measure of central tendency, we also can use the median.

> The convention for representing a statistical parameter is to use a Roman letter for a value calculated from experimental data, and a Greek letter for its corresponding expected value. For example, the experimentally determined mean is $\overline{X}$ and its underlying expected value is μ. Likewise, the experimental standard deviation is s and the underlying expected value is σ.

We identify as determinate an error that affects the accuracy of an analysis. Each source of a ***determinate error*** has a specific magnitude and sign. Some sources of determinate error are positive and others are negative, and some are larger in magnitude and others are smaller in magnitude. The cumulative effect of these determinate errors is a net positive or negative error in accuracy.

> It is possible, although unlikely, that the positive and negative determinate errors will offset each other, producing a result with no net error in accuracy.

We assign determinate errors into four categories—sampling errors, method errors, measurement errors, and personal errors—each of which we consider in this section.

Sampling Errors

A determinate sampling error occurs when our sampling strategy does not provide a us with a representative sample. For example, if we monitor the environmental quality of a lake by sampling from a single site near a point source of pollution, such as an outlet for industrial effluent, then our results will be misleading. To determine the mass of a U. S. penny, our strategy for selecting pennies must ensure that we do not include pennies from other countries.

> An awareness of potential sampling errors especially is important when we work with heterogeneous materials. Strategies for obtaining representative samples are covered in Chapter 5.

Method Errors

In any analysis the relationship between the signal, S_{total}, and the absolute amount of analyte, n_A, or the analyte's concentration, C_A, is

$$S_{total} = k_A n_A + S_{mb} \tag{1.4.3}$$

$$S_{total} = k_A C_A + S_{mb} \tag{1.4.4}$$

where k_A is the method's sensitivity for the analyte and S_{mb} is the signal from the method blank. A ***method error*** exists when our value for k_A or for S_{mb} is in error. For example, a method in which S_{total} is the mass of a precipitate assumes that k is defined by a

pure precipitate of known stoichiometry. If this assumption is not true, then the resulting determination of n_A or C_A is inaccurate. We can minimize a determinate error in k_A by calibrating the method. A method error due to an interferent in the reagents is minimized by using a proper method blank.

Measurement Errors

The manufacturers of analytical instruments and equipment, such as glassware and balances, usually provide a statement of the item's maximum ***measurement error***, or ***tolerance***. For example, a 10-mL volumetric pipet (Figure 4.2.1) has a tolerance of ±0.02 mL, which means the pipet delivers an actual volume within the range 9.98–10.02 mL at a temperature of 20 °C. Although we express this tolerance as a range, the error is determinate; that is, the pipet's expected volume, μ, is a fixed value within this stated range.



Figure 4.2.1 : Close-up of a 10-mL volumetric pipet showing that it has a tolerance of ±0.02 mL at 20 °C.

Volumetric glassware is categorized into classes based on its relative accuracy. Class A glassware is manufactured to comply with tolerances specified by an agency, such as the National Institute of Standards and Technology or the American Society for Testing and Materials. The tolerance level for Class A glassware is small enough that normally we can use it without calibration. The tolerance levels for Class B glassware usually are twice that for Class A glassware. Other types of volumetric glassware, such as beakers and graduated cylinders, are not used to measure volume accurately. Table 4.2.1 provides a summary of typical measurement errors for Class A volumetric glassware. Tolerances for digital pipets and for balances are provided in Table 4.2.2 and Table 4.2.3 .

Table 4.2.1 : Measurement Errors for Type A Volumetric Glassware

Transfer Pipets		Volumetric Flasks		Burets	
Capacity (mL)	Tolerance (mL)	Capacity (mL)	Tolerance (mL)	Capacity (mL)	Tolerance (mL)
1	±0.006	5	±0.02	10	±0.02
2	±0.006	10	±0.02	25	±0.03
5	±0.01	25	±0.03	50	±0.05
10	±0.02	50	±0.05		
20	±0.03	100	±0.08		
25	±0.03	250	±0.12		
50	±0.05	500	±0.20		
100	±0.08	1000	±0.30		
		2000			

Table 4.2.2 : Measurement Errors for Digital Pipets

Pipet Range	Volume (mL or μL)	Percent Measurement Error
10–100 μL	10	±3.0%
	50	±1.0%
	100	±0.8%
100–1000 μL	100	±3.0%
	500	±1.0%
	1000	±0.6%
1–10 mL	1	±3.0%
	5	±0.8%
	10	±0.6%

The tolerance values for the volumetric glassware in Table 4.2.1 are from the ASTM E288, E542, and E694 standards. The measurement errors for the digital pipets in Table 4.2.2 are from www.eppendorf.com.

Table 4.2.3 : Measurement Errors for Selected Balances

Balance	Capacity (g)	Measurement Error
Precisa 160M	160	±1 mg
A & D ER 120M	120	±0.1 mg
Metler H54	160	±0.01 mg

We can minimize a determinate measurement error by calibrating our equipment. Balances are calibrated using a reference weight whose mass we can trace back to the SI standard kilogram. Volumetric glassware and digital pipets are calibrated by determining the mass of water delivered or contained and using the density of water to calculate the actual volume. It is never safe to assume that a calibration does not change during an analysis or over time. One study, for example, found that repeatedly exposing volumetric glassware to higher temperatures during machine washing and oven drying, led to small, but significant changes in the glassware's calibration [Castanheira, I.; Batista, E.; Valente, A.; Dias, G.; Mora, M.; Pinto, L.; Costa, H. S. *Food Control* **2006**, *17*, 719–726]. Many instruments drift out of calibration over time and may require frequent recalibration during an analysis.

Personal Errors

Finally, analytical work is always subject to ***personal error***, examples of which include the ability to see a change in the color of an indicator that signals the endpoint of a titration, biases, such as consistently overestimating or underestimating the value on an instrument's readout scale, failing to calibrate instrumentation, and misinterpreting procedural directions. You can minimize personal errors by taking proper care.

Identifying Determinate Errors

Determinate errors often are difficult to detect. Without knowing the expected value for an analysis, the usual situation in any analysis that matters, we often have nothing to which we can compare our experimental result. Nevertheless, there are strategies we can use to detect determinate errors.

The magnitude of a constant ***determinate error*** is the same for all samples and is more significant when we analyze smaller samples. Analyzing samples of different sizes, therefore, allows us to detect a constant determinate error. For example, consider a quantitative analysis in which we separate the analyte from its matrix and determine its mass. Let's assume the sample is 50.0% w/w analyte. As we see in Table 4.2.4 , the expected amount of analyte in a 0.100 g sample is 0.050 g. If the analysis has a positive

constant determinate error of 0.010 g, then analyzing the sample gives 0.060 g of analyte, or an apparent concentration of 60.0% w/w. As we increase the size of the sample the experimental results become closer to the expected result. An upward or downward trend in a graph of the analyte's experimental concentration versus the sample's mass (Figure 4.2.2) is evidence of a constant determinate error.

Table 4.2.4 : Effect of a Constant Determinate Error on the Analysis of a Sample That is 50.0% w/w Analyte

Mass of Sample (g)	Expected Mass of Analyte (g)	Constant Error (g)	Experimental Mass of Analyte (g)	Experimental Concentration of Analyte (% w/w)
0.100	0.050	0.010	0.060	60.0
0.200	0.100	0.010	0.110	55.0
0.400	0.200	0.010	0.210	52.5
0.800	0.400	0.010	0.410	51.2
1.600	0.800	0.010	0.810	50.6

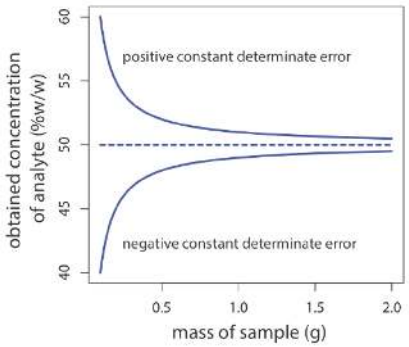


Figure 4.2.2 : Effect of a constant positive determinate error of +0.01 g and a constant negative determinate error of –0.01 g on the determination of an analyte in samples of varying size. The analyte's expected concentration of 50% w/w is shown by the dashed line.

A ***proportional determinate error***, in which the error's magnitude depends on the amount of sample, is more difficult to detect because the result of the analysis is independent of the amount of sample. Table 4.2.5 outlines an example that shows the effect of a positive proportional error of 1.0% on the analysis of a sample that is 50.0% w/w in analyte. Regardless of the sample's size, each analysis gives the same result of 50.5% w/w analyte.

Table 4.2.5 : Effect of a Proportional Determinate Error on the Analysis of a Sample That is 50.0% w/w Analyte

Mass of Sample (g)	Expected Mass of Analyte (g)	Proportional Error (%)	Experimental Mass of Analyte (g)	Experimental Concentration of Analyte (% w/w)
0.100	0.050	1.00	0.0505	50.5
0.200	0.100	1.00	0.101	50.5
0.400	0.200	1.00	0.202	50.5
0.800	0.400	1.00	0.404	50.5
1.600	0.800	1.00	0.808	50.5

One approach for detecting a proportional determinate error is to analyze a standard that contains a known amount of analyte in a matrix similar to our samples. Standards are available from a variety of sources, such as the National Institute of Standards and

Technology (where they are called Standard Reference Materials) or the American Society for Testing and Materials. Table 4.2.6 , for example, lists certified values for several analytes in a standard sample of *Gingko biloba* leaves. Another approach is to compare our analysis to an analysis carried out using an independent analytical method that is known to give accurate results. If the two methods give significantly different results, then a determinate error is the likely cause.

Table 4.2.6 : Certified Concentrations for SRM 3246: *Gingko bilbo* (Leaves)

Class of Analyte	Analyte	Mass Fraction (mg/g or ng/g)
Flavonoids/Ginkgolide B (mass fraction in mg/g)	Qurecetin	2.69 ± 0.31
	Kaempferol	3.02 ± 0.41
	Isorhamnetin	$0.517 \pm 0.0.99$
	Total Aglycones	6.22 ± 0.77
Selected Terpenes (mass fraction in mg/g)	Ginkgolide A	0.57 ± 0.28
	Ginkgolide B	0.470 ± 0.090
	Ginkgolide C	0.59 ± 0.22
	Ginkgolide J	0.18 ± 0.10
	Bilobalide	1.52 ± 0.40
	Total Terpene Lactones	3.3 ± 1.1
Selected Toxic Elements (mass fraction in ng/g)	Cadmium	20.8 ± 1.0
	Lead	995 ± 30
	Mercury	23.08 ± 0.17

> The primary purpose of this Standard Reference Material is to validate analytical methods for determining flavonoids, terpene lactones, and toxic elements in *Ginkgo biloba* or other materials with a similar matrix. Values are from the official Certificate of Analysis available at www.nist.gov.

Constant and proportional determinate errors have distinctly different sources, which we can define in terms of the relationship between the signal and the moles or concentration of analyte (Equation 1.4.3 and Equation 1.4.4). An invalid method blank, S_{mb}, is a constant determinate error as it adds or subtracts the same value to the signal. A poorly calibrated method, which yields an invalid sensitivity for the analyte, k_A, results in a proportional determinate error.

Errors that Affect Precision

As we saw in Section 4.1, precision is a measure of the spread of individual measurements or results about a central value, which we express as a range, a standard deviation, or a variance. Here we draw a distinction between two types of precision: repeatability and reproducibility. ***Repeatability*** is the precision when a single analyst completes an analysis in a single session using the same solutions, equipment, and instrumentation. ***Reproducibility***, on the other hand, is the precision under any other set of conditions, including between analysts or between laboratory sessions for a single analyst. Since reproducibility includes additional sources of variability, the reproducibility of an analysis cannot be better than its repeatability.

> The ratio of the standard deviation associated with reproducibility to the standard deviation associated with repeatability is called the Horowitz ratio. For a wide variety of analytes in foods, for example, the median Horowtiz ratio is 2.0 with larger

values for fatty acids and for trace elements; see Thompson, M.; Wood, R. “The ‘Horowitz Ratio’–A Study of the Ratio Between Reproducibility and Repeatability in the Analysis of Foodstuffs,” *Anal. Methods*, **2015**, *7*, 375–379.

Errors that affect precision are indeterminate and are characterized by random variations in their magnitude and their direction. Because they are random, positive and negative ***indeterminate errors*** tend to cancel, provided that we make a sufficient number of measurements. In such situations the mean and the median largely are unaffected by the precision of the analysis.

Sources of Indeterminate Error

We can assign indeterminate errors to several sources, including collecting samples, manipulating samples during the analysis, and making measurements. When we collect a sample, for instance, only a small portion of the available material is taken, which increases the chance that small-scale inhomogeneities in the sample will affect repeatability. Individual pennies, for example, may show variations in mass from several sources, including the manufacturing process and the loss of small amounts of metal or the addition of dirt during circulation. These variations are sources of indeterminate sampling errors.

During an analysis there are many opportunities to introduce indeterminate method errors. If our method for determining the mass of a penny includes directions for cleaning them of dirt, then we must be careful to treat each penny in the same way. Cleaning some pennies more vigorously than others might introduce an indeterminate method error.

Finally, all measuring devices are subject to indeterminate measurement errors due to limitations in our ability to read its scale. For example, a buret with scale divisions every 0.1 mL has an inherent indeterminate error of ±0.01–0.03 mL when we estimate the volume to the hundredth of a milliliter (Figure 4.2.3).

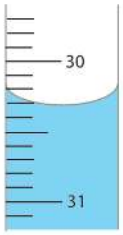


Figure 4.2.3 : Close-up of a buret showing the difficulty in estimating volume. With scale divisions every 0.1 mL it is difficult to read the actual volume to better than ±0.01–0.03 mL.

Evaluating Indeterminate Error

Indeterminate errors associated with our analytical equipment or instrumentation generally are easy to estimate if we measure the standard deviation for several replicate measurements, or if we monitor the signal’s fluctuations over time in the absence of analyte (Figure 4.2.4) and calculate the standard deviation. Other sources of indeterminate error, such as treating samples inconsistently, are more difficult to estimate.

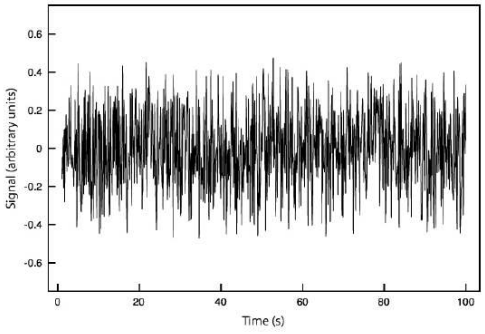


Figure 4.2.4 : Background noise in an instrument showing the random fluctuations in the signal.

To evaluate the effect of an indeterminate measurement error on our analysis of the mass of a circulating United States penny, we might make several determinations of the mass for a single penny (Table 4.2.7). The standard deviation for our original experiment (see Table 4.1.1) is 0.051 g, and it is 0.0024 g for the data in Table 4.2.7 . The significantly better precision when we determine the

mass of a single penny suggests that the precision of our analysis is not limited by the balance. A more likely source of indeterminate error is a variability in the masses of individual pennies.

Table 4.2.7 : Replicate Determinations of the Mass of a Single Circulating U. S. Penny

Replicate	Mass (g)	Replicate	Mass (g)
1	3.025	6	3.023
2	3.024	7	3.022
3	3.028	8	3.021
4	3.027	9	3.026
5	3.028	10	3.024

> In Section 4.5 we will discuss a statistical method—the *F*-test—that you can use to show that this difference is significant.

Error and Uncertainty

Analytical chemists make a distinction between error and uncertainty [Ellison, S.; Wegscheider, W.; Williams, A. *Anal. Chem.* **1997**, *69*, 607A–613A]. ***Error*** is the difference between a single measurement or result and its expected value. In other words, error is a measure of ***bias***. As discussed earlier, we divide errors into determinate and indeterminate sources. Although we can find and correct a source of determinate error, the indeterminate portion of the error remains.

Uncertainty expresses the range of possible values for a measurement or result. Note that this definition of uncertainty is not the same as our definition of precision. We calculate precision from our experimental data and use it to estimate the magnitude of indeterminate errors. Uncertainty accounts for all errors—both determinate and indeterminate—that reasonably might affect a measurement or a result. Although we always try to correct determinate errors before we begin an analysis, the correction itself is subject to uncertainty.

Here is an example to help illustrate the difference between precision and uncertainty. Suppose you purchase a 10-mL Class A pipet from a laboratory supply company and use it without any additional calibration. The pipet's tolerance of ±0.02 mL is its uncertainty because your best estimate of its expected volume is 10.00 mL ± 0.02 mL. This uncertainty primarily is determinate. If you use the pipet to dispense several replicate samples of a solution and determine the volume of each sample, the resulting standard deviation is the pipet's precision. Table 4.2.8 shows results for ten such trials, with a mean of 9.992 mL and a standard deviation of ±0.006 mL. This standard deviation is the precision with which we expect to deliver a solution using a Class A 10-mL pipet. In this case the pipet's published uncertainty of ±0.02 mL is worse than its experimentally determined precision of ±0.006 ml. Interestingly, the data in Table 4.2.8 allows us to calibrate this specific pipet's delivery volume as 9.992 mL. If we use this volume as a better estimate of the pipet's expected volume, then its uncertainty is ±0.006 mL. As expected, calibrating the pipet allows us to decrease its uncertainty [Kadis, R. *Talanta* **2004**, *64*, 167–173].

Table 4.2.8 : Experimental Results for Volume Dispensed by a 10–mL Class A Transfer Pipet

Replicate	Volume (ml)	Replicate	Volume (mL)
1	10.002	6	9.983
2	9.993	7	9.991
3	9.984	8	9.990
4	9.996	9	9.988
5	9.989	10	9.999

This page titled 1.4: Characterizing Experimental Errors is shared under a CC BY-NC-SA 4.0 license and was authored, remixed, and/or curated by Kathryn Davis.

- **4.2: Characterizing Experimental Errors** by David Harvey is licensed CC BY-NC-SA 4.0.

1.5: Propagation of Uncertainty

Suppose we dispense 20 mL of a reagent using the Class A 10-mL pipet whose calibration information is given in Table 4.2.8. If the volume and uncertainty for one use of the pipet is 9.992 ± 0.006 mL, what is the volume and uncertainty if we use the pipet twice?

As a first guess, we might simply add together the volume and the maximum uncertainty for each delivery; thus

$$(9.992\text{ mL} + 9.992\text{ mL}) \pm (0.006\text{ mL} + 0.006\text{ mL}) = 19.984 \pm 0.012\text{ mL}$$

It is easy to appreciate that combining uncertainties in this way overestimates the total uncertainty. Adding the uncertainty for the first delivery to that of the second delivery assumes that with each use the indeterminate error is in the same direction and is as large as possible. At the other extreme, we might assume that the uncertainty for one delivery is positive and the other is negative. If we subtract the maximum uncertainties for each delivery,

$$(9.992\text{ mL} + 9.992\text{ mL}) \pm (0.006\text{ mL} - 0.006\text{ mL}) = 19.984 \pm 0.000\text{ mL}$$

we clearly underestimate the total uncertainty.

So what is the total uncertainty? From the discussion above, we reasonably expect that the total uncertainty is greater than ±0.000 mL and that it is less than ±0.012 mL. To estimate the uncertainty we use a mathematical technique known as the propagation of uncertainty. Our treatment of the propagation of uncertainty is based on a few simple rules.

A Few Symbols

A ***propagation of uncertainty*** allows us to estimate the uncertainty in a result from the uncertainties in the measurements used to calculate that result. For the equations in this section we represent the result with the symbol R, and we represent the measurements with the symbols A, B, and C. The corresponding uncertainties are u_R, u_A, u_B, and u_C. We can define the uncertainties for A, B, and C using standard deviations, ranges, or tolerances (or any other measure of uncertainty), as long as we use the same form for all measurements.

> The requirement that we express each uncertainty in the same way is a critically important point. Suppose you have a range for one measurement, such as a pipet's tolerance, and standard deviations for the other measurements. All is not lost. There are ways to convert a range to an estimate of the standard deviation. See Appendix 2 for more details.

Uncertainty When Adding or Subtracting

When we add or subtract measurements we propagate their absolute uncertainties. For example, if the result is given by the equation

$$R = A + B - C$$

the the absolute uncertainty in R is

$$u_R = \sqrt{u_A^2 + u_B^2 + u_C^2} \tag{1.5.1}$$

Example 4.3.1

If we dispense 20 mL using a 10-mL Class A pipet, what is the total volume dispensed and what is the uncertainty in this volume? First, complete the calculation using the manufacturer's tolerance of 10.00 mL±0.02 mL, and then using the calibration data from Table 4.2.8.

Solution

To calculate the total volume we add the volumes for each use of the pipet. When using the manufacturer's values, the total volume is

$$V = 10.00\text{ mL} + 10.00\text{ mL} = 20.00\text{ mL}$$

and when using the calibration data, the total volume is

$$V = 9.992\ \text{mL} + 9.992\ \text{mL} = 19.984\ \text{mL}$$

Using the pipet's tolerance as an estimate of its uncertainty gives the uncertainty in the total volume as

$$u_R = \sqrt{(0.02)^2 + (0.02)^2} = 0.028\ \text{mL} = 0.028\ \text{mL}$$

and using the standard deviation for the data in Table 4.2.8 gives an uncertainty of

$$u_R = \sqrt{(0.006)^2 + (0.006)^2} = 0.0085\ \text{mL}$$

Rounding the volumes to four significant figures gives 20.00 mL ± 0.03 mL when we use the tolerance values, and 19.98 ± 0.01 mL when we use the calibration data.

Uncertainty When Multiplying or Dividing

When we multiple or divide measurements we propagate their relative uncertainties. For example, if the result is given by the equation

$$R = \frac{A \times B}{C}$$

then the relative uncertainty in R is

$$\frac{u_R}{R} = \sqrt{\left(\frac{u_A}{A}\right)^2 + \left(\frac{u_B}{B}\right)^2 + \left(\frac{u_C}{C}\right)^2} \tag{1.5.2}$$

Example 4.3.2

The quantity of charge, Q, in coulombs that passes through an electrical circuit is

$$Q = i \times t$$

where i is the current in amperes and t is the time in seconds. When a current of 0.15 A ± 0.01 A passes through the circuit for 120 s ± 1 s, what is the total charge and its uncertainty?

Solution

The total charge is

$$Q = (0.15\ \text{A}) \times (120\ \text{s}) = 18\ \text{C}$$

Since charge is the product of current and time, the relative uncertainty in the charge is

$$\frac{u_R}{R} = \sqrt{\left(\frac{0.01}{0.15}\right)^2 + \left(\frac{1}{120}\right)^2} = 0.0672$$

and the charge's absolute uncertainty is

$$u_R = R \times 0.0672 = (18\ \text{C}) \times (0.0672) = 1.2\ \text{C}$$

Thus, we report the total charge as 18 C ± 1 C.

Uncertainty for Mixed Operations

Many chemical calculations involve a combination of adding and subtracting, and of multiply and dividing. As shown in the following example, we can calculate the uncertainty by separately treating each operation using Equation 1.5.1 and Equation 1.5.2 as needed.

Example 4.3.3

For a concentration technique, the relationship between the signal and the an analyte's concentration is

$$S_{total} = k_A C_A + S_{mb}$$

What is the analyte's concentration, C_A, and its uncertainty if S_{total} is 24.37 ± 0.02, S_{mb} is 0.96 ± 0.02, and k_A is $0.186 \pm 0.003\ \text{ppm}^{-1}$?

Solution

Rearranging the equation and solving for C_A

$$C_A = \frac{S_{total} - S_{mb}}{k_A} = \frac{24.37 - 0.96}{0.186\ \text{ppm}^{-1}} = \frac{23.41}{0.186\ \text{ppm}^{-1}} = 125.9\ \text{ppm}$$

gives the analyte's concentration as 126 ppm. To estimate the uncertainty in C_A, we first use Equation 1.5.1 to determine the uncertainty for the numerator.

$$u_R = \sqrt{(0.02)^2 + (0.02)^2} = 0.028$$

The numerator, therefore, is 23.41 ± 0.028. To complete the calculation we use Equation 1.5.2 to estimate the relative uncertainty in C_A.

$$\frac{u_R}{R} = \sqrt{\left(\frac{0.028}{23.41}\right)^2 + \left(\frac{0.003}{0.186}\right)^2} = 0.0162$$

The absolute uncertainty in the analyte's concentration is

$$u_R = (125.9\ \text{ppm}) \times (0.0162) = 2.0\ \text{ppm}$$

Thus, we report the analyte's concentration as 126 ppm ± 2 ppm.

? Exercise 4.3.1

To prepare a standard solution of Cu^{2+} you obtain a piece of copper from a spool of wire. The spool's initial weight is 74.2991 g and its final weight is 73.3216 g. You place the sample of wire in a 500-mL volumetric flask, dissolve it in 10 mL of HNO_3, and dilute to volume. Next, you pipet a 1 mL portion to a 250-mL volumetric flask and dilute to volume. What is the final concentration of Cu^{2+} in mg/L, and its uncertainty? Assume that the uncertainty in the balance is ±0.1 mg and that you are using Class A glassware.

Answer

The first step is to determine the concentration of Cu^{2+} in the final solution. The mass of copper is

$$74.2991\ \text{g} - 73.3216\ \text{g} = 0.9775\ \text{g Cu}$$

The 10 mL of HNO_3 used to dissolve the copper does not factor into our calculation. The concentration of Cu^{2+} is

$$\frac{0.9775\ \text{g Cu}}{0.5000\ \text{L}} \times \frac{1.000\ \text{mL}}{250.0\ \text{mL}} \times \frac{1000\ \text{mg}}{\text{g}} = 7.820\ \text{mg Cu}^{2+}/\text{L}$$

Having found the concentration of Cu^{2+}, we continue with the propagation of uncertainty. The absolute uncertainty in the mass of Cu wire is

$$u_{\text{g Cu}} = \sqrt{(0.0001)^2 + (0.0001)^2} = 0.00014\ \text{g}$$

The relative uncertainty in the concentration of Cu^{2+} is

$$\frac{u_{\text{mg/L}}}{7.820\ \text{mg/L}} = \sqrt{\left(\frac{0.00014}{0.9775}\right)^2 + \left(\frac{0.20}{500.0}\right)^2 + \left(\frac{0.006}{1.000}\right)^2 + \left(\frac{0.12}{250.0}\right)^2} = 0.00603$$

Solving for $u_{\text{mg/L}}$ gives the uncertainty as 0.0472. The concentration and uncertainty for Cu^{2+} is 7.820 mg/L ± 0.047 mg/L.

Uncertainty for Other Mathematical Functions

Many other mathematical operations are common in analytical chemistry, including the use of powers, roots, and logarithms. Table 4.3.1 provides equations for propagating uncertainty for some of these function where A and B are independent measurements and where k is a constant whose value has no uncertainty.

Table 4.3.1 : Propagation of Uncertainty for Selected Mathematical Functions

Function	u_R	Function	u_R
$R = kA$	$u_R = ku_A$	$R = \ln(A)$	$u_R = \frac{u_A}{A}$
$R = A + B$	$u_R = \sqrt{u_A^2 + u_B^2}$	$R = \log(A)$	$u_R = 0.4343 \times \frac{u_A}{A}$
$R = A - B$	$u_R = \sqrt{u_A^2 + u_B^2}$	$R = e^A$	$\frac{u_R}{R} = u_A$
$R = A \times B$	$\frac{u_R}{R} = \sqrt{\left(\frac{u_A}{A}\right)^2 + \left(\frac{u_B}{B}\right)^2}$	$R = 10^A$	$\frac{u_R}{R} = 2.303 \times u_A$
$R = \frac{A}{B}$	$\frac{u_R}{R} = \sqrt{\left(\frac{u_A}{A}\right)^2 + \left(\frac{u_B}{B}\right)^2}$	$R = A^k$	$\frac{u_R}{R} = k \times \frac{u_A}{A}$

Example 4.3.4

If the pH of a solution is 3.72 with an absolute uncertainty of ±0.03, what is the $[H^+]$ and its uncertainty?

Solution

The concentration of H^+ is

$$[H^+] = 10^{-pH} = 10^{-3.72} = 1.91 \times 10^{-4}\ M$$

or 1.9×10^{-4} M to two significant figures. From Table 4.3.1 the relative uncertainty in $[H^+]$ is

$$\frac{u_R}{R} = 2.303 \times u_A = 2.303 \times 0.03 = 0.069$$

The uncertainty in the concentration, therefore, is

$$(1.91 \times 10^{-4}\ M) \times (0.069) = 1.3 \times 10^{-5}\ M$$

We report the $[H^+]$ as $1.9(\pm 0.1) \times 10^{-4}$ M, which is equivalent to $1.9 \times 10^{-4}\ M\ \pm 0.1 \times 10^{-4}\ M$.

Exercise 4.3.2

A solution of copper ions is blue because it absorbs yellow and orange light. Absorbance, A, is defined as

$$A = -\log T = -\log\left(\frac{P}{P_o}\right)$$

where, T is the transmittance, P_o is the power of radiation as emitted from the light source and P is its power after it passes through the solution. What is the absorbance if P_o is 3.80×10^2 and P is 1.50×10^2? If the uncertainty in measuring P_o and P is 15, what is the uncertainty in the absorbance?

Answer

The first step is to calculate the absorbance, which is

$$A = -\log T = -\log \frac{P}{P_o} = -\log \frac{1.50 \times 10^2}{3.80 \times 10^2} = 0.4037 \approx 0.404$$

Having found the absorbance, we continue with the propagation of uncertainty. First, we find the uncertainty for the ratio P/P_o, which is the transmittance, T.

$$\frac{u_T}{T} = \sqrt{\left(\frac{15}{3.80\times10^2}\right)^2 + \left(\frac{15}{1.50\times10^2}\right)^2} = 0.1075$$

Finally, from Table 4.3.1 the uncertainty in the absorbance is

$$u_A = 0.4343 \times \frac{u_T}{T} = (0.4343) \times (0.1075) = 4.669 \times 10^{-2}$$

The absorbance and uncertainty is 0.40 ± 0.05 absorbance units.

Is Calculating Uncertainty Actually Useful?

Given the effort it takes to calculate uncertainty, it is worth asking whether such calculations are useful. The short answer is, yes. Let's consider three examples of how we can use a propagation of uncertainty to help guide the development of an analytical method.

One reason to complete a propagation of uncertainty is that we can compare our estimate of the uncertainty to that obtained experimentally. For example, to determine the mass of a penny we measure its mass twice—once to tare the balance at 0.000 g and once to measure the penny's mass. If the uncertainty in each measurement of mass is ±0.001 g, then we estimate the total uncertainty in the penny's mass as

$$u_R = \sqrt{(0.001)^2 + (0.001)^2} = 0.0014 \text{ g}$$

If we measure a single penny's mass several times and obtain a standard deviation of ±0.050 g, then we have evidence that the measurement process is out of control. Knowing this, we can identify and correct the problem.

We also can use a propagation of uncertainty to help us decide how to improve an analytical method's uncertainty. In Example 4.3.3 , for instance, we calculated an analyte's concentration as 126 ppm ± 2 ppm, which is a percent uncertainty of 1.6%. Suppose we want to decrease the percent uncertainty to no more than 0.8%. How might we accomplish this? Looking back at the calculation, we see that the concentration's relative uncertainty is determined by the relative uncertainty in the measured signal (corrected for the reagent blank)

$$\frac{0.028}{23.41} = 0.0012 \text{ or } 0.12\%$$

and the relative uncertainty in the method's sensitivity, k_A,

$$\frac{0.003 \text{ ppm}^{-1}}{0.186 \text{ ppm}^{-1}} = 0.016 \text{ or } 1.6\%$$

Of these two terms, the uncertainty in the method's sensitivity dominates the overall uncertainty. Improving the signal's uncertainty will not improve the overall uncertainty of the analysis. To achieve an overall uncertainty of 0.8% we must improve the uncertainty in k_A to ±0.0015 ppm^{-1}.

? Exercise 4.3.3

Verify that an uncertainty of ±0.0015 ppm^{-1} for k_A is the correct result.

Answer

An uncertainty of 0.8% is a relative uncertainty in the concentration of 0.008; thus, letting u be the uncertainty in k_A

$$0.008 = \sqrt{\left(\frac{0.028}{23.41}\right)^2 + \left(\frac{u}{0.186}\right)^2}$$

Squaring both sides of the equation gives

$$6.4 \times 10^{-5} = \left(\frac{0.028}{23.41}\right)^2 + \left(\frac{u}{0.186}\right)^2$$

Solving for the uncertainty in k_A gives its value as $\mathbf{1.47 \times 10^{-3}}$ or ±0.0015 ppm^{-1}.

Finally, we can use a propagation of uncertainty to determine which of several procedures provides the smallest uncertainty. When we dilute a stock solution usually there are several combinations of volumetric glassware that will give the same final concentration. For instance, we can dilute a stock solution by a factor of 10 using a 10-mL pipet and a 100-mL volumetric flask, or using a 25-mL pipet and a 250-mL volumetric flask. We also can accomplish the same dilution in two steps using a 50-mL pipet and 100-mL volumetric flask for the first dilution, and a 10-mL pipet and a 50-mL volumetric flask for the second dilution. The overall uncertainty in the final concentration—and, therefore, the best option for the dilution—depends on the uncertainty of the volumetric pipets and volumetric flasks. As shown in the following example, we can use the tolerance values for volumetric glassware to determine the optimum dilution strategy [Lam, R. B.; Isenhour, T. L. *Anal. Chem.* **1980**, *52*, 1158–1161].

Example 4.3.5 :

Which of the following methods for preparing a 0.0010 M solution from a 1.0 M stock solution provides the smallest overall uncertainty?

(a) A one-step dilution that uses a 1-mL pipet and a 1000-mL volumetric flask.

(b) A two-step dilution that uses a 20-mL pipet and a 1000-mL volumetric flask for the first dilution, and a 25-mL pipet and a 500-mL volumetric flask for the second dilution.

Solution

The dilution calculations for case (a) and case (b) are

$$\text{case (a): } 1.0\ \text{M} \times \frac{1.000\ \text{mL}}{1000.0\ \text{mL}} = 0.0010\ \text{M}$$

$$\text{case (b): } 1.0\ \text{M} \times \frac{20.00\ \text{mL}}{1000.0\ \text{mL}} \times \frac{25.00\ \text{mL}}{500.0\text{mL}} = 0.0010\ \text{M}$$

Using tolerance values from Table 4.2.1, the relative uncertainty for case (a) is

$$u_R = \sqrt{\left(\frac{0.006}{1.000}\right)^2 + \left(\frac{0.3}{1000.0}\right)^2} = 0.006$$

and for case (b) the relative uncertainty is

$$u_R = \sqrt{\left(\frac{0.03}{20.00}\right)^2 + \left(\frac{0.3}{1000}\right)^2 + \left(\frac{0.03}{25.00}\right)^2 + \left(\frac{0.2}{500.0}\right)^2} = 0.002$$

Since the relative uncertainty for case (b) is less than that for case (a), the two-step dilution provides the smallest overall uncertainty. Of course we must balance the smaller uncertainty for case (b) against the increased opportunity for introducing a determinate error when making two dilutions instead of just one dilution, as in case (a).

This page titled 1.5: Propagation of Uncertainty is shared under a CC BY-NC-SA 4.0 license and was authored, remixed, and/or curated by Kathryn Davis.

- **4.3: Propagation of Uncertainty** by David Harvey is licensed CC BY-NC-SA 4.0.

1.6: The Distribution of Measurements and Results

Earlier we reported results for a determination of the mass of a circulating United States penny, obtaining a mean of 3.117 g and a standard deviation of 0.051 g. Table 1.6.1 shows results for a second, independent determination of a penny's mass, as well as the data from the first experiment. Although the means and standard deviations for the two experiments are similar, they are not identical. The difference between the two experiments raises some interesting questions. Are the results for one experiment better than the results for the other experiment? Do the two experiments provide equivalent estimates for the mean and the standard deviation? What is our best estimate of a penny's expected mass? To answer these questions we need to understand how we might predict the properties of all pennies using the results from an analysis of a small sample of pennies. We begin by making a distinction between populations and samples.

Table 1.6.1 : Results for Two Determinations of the Mass of a Circulating U. S. Penny

First Experiment		Second Experiment	
Penny	Mass (g)	Penny	Mass (g)
1	3.080	1	3.052
2	3.094	2	3.141
3	3.107	3	3.083
4	3.056	4	3.083
5	3.112	5	3.048
6	3.174		
7	3.198		
$\overline{X}$	3.117		3.081
s	0.051		0.037

Populations and Samples

A ***population*** is the set of all objects in the system we are investigating. For the data in Table 1.6.1 , the population is all United States pennies in circulation. This population is so large that we cannot analyze every member of the population. Instead, we select and analyze a limited subset, or ***sample*** of the population. The data in Table 1.6.1 , for example, shows the results for two such samples drawn from the larger population of all circulating United States pennies.

Probability Distributions for Populations

Table 1.6.1 provides the means and the standard deviations for two samples of circulating United States pennies. What do these samples tell us about the population of pennies? What is the largest possible mass for a penny? What is the smallest possible mass? Are all masses equally probable, or are some masses more common?

To answer these questions we need to know how the masses of individual pennies are distributed about the population's average mass. We represent the distribution of a population by plotting the probability or frequency of obtaining a specific result as a function of the possible results. Such plots are called ***probability distributions***.

There are many possible probability distributions; in fact, the probability distribution can take any shape depending on the nature of the population. Fortunately many chemical systems display one of several common probability distributions. Two of these distributions, the binomial distribution and the normal distribution, are discussed in this section.

The Binomial Distribution

The binomial distribution describes a population in which the result is the number of times a particular event occurs during a fixed number of trials. Think "heads/tails," "yes/no," "right answer/wrong answer," "patient recovered/patient did not recover," etc. There

are separate mathematical and statistical descriptions for binomial distributions. However, we'll skip over those in this course because they are not the typical outcomes of analytical methods.

The Normal Distribution

A population is continuous if its members may take on any value. The efficiency of extracting cholesterol from a sample, for example, can take on any value between 0% (no cholesterol is extracted) and 100% (all cholesterol is extracted).

The most common continuous distribution is the Gaussian, or ***normal distribution***, the equation for which is

$$f(X) = \frac{1}{\sqrt{2\pi\sigma^2}} e^{-\frac{(X-\mu)^2}{2\sigma^2}}$$

where μ is the expected mean for a population with n members

$$\mu = \frac{\sum_{i=1}^{n} X_i}{n}$$

and σ^2 is the population's variance.

$$\sigma^2 = \frac{\sum_{i=1}^{n} (X_i - \mu)^2}{n} \tag{1.6.1}$$

Examples of three normal distributions, each with an expected mean of 0 and with variances of 25, 100, or 400, respectively, are shown in Figure 1.6.2 . Two features of these normal distribution curves deserve attention. First, note that each normal distribution has a single maximum that corresponds to μ, and that the distribution is symmetrical about this value. Second, increasing the population's variance increases the distribution's spread and decreases its height; the area under the curve, however, is the same for all three distributions.

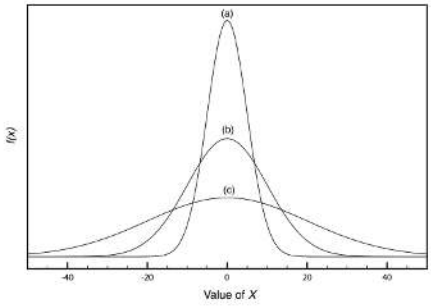


Figure 1.6.2 : Normal distribution curves for: (a) $\mu = 0$; $\sigma^2 = 25$ (b) $\mu = 0$; $\sigma^2 = 100$ (c) $\mu = 0$; $\sigma^2 = 400$.

The area under a normal distribution curve is an important and useful property as it is equal to the probability of finding a member of the population within a particular range of values. In Figure 1.6.2 , for example, 99.99% of the population shown in curve (a) have values of X between –20 and +20. For curve (c), 68.26% of the population's members have values of X between –20 and +20.

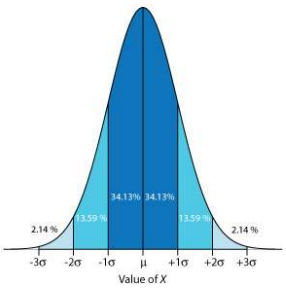


Figure 1.6.3 : Normal distribution curve showing the area under the curve for several different ranges of values of X.

Confidence Intervals for Populations

If we select at random a single member from a population, what is its most likely value? This is an important question, and, in one form or another, it is at the heart of any analysis in which we wish to extrapolate from a sample to the sample's parent population. One of the most important features of a population's probability distribution is that it provides a way to answer this question.

Figure 1.6.3 shows that for a normal distribution, 68.26% of the population's members have values within the range $\mu \pm 1\sigma$. Stating this another way, there is a 68.26% probability that the result for a single sample drawn from a normally distributed population is in the interval $\mu \pm 1\sigma$. In general, if we select a single sample we expect its value, X_i is in the range

$$X_i = \mu \pm z\sigma \tag{1.6.2}$$

where the value of z is how confident we are in assigning this range. Values reported in this fashion are called ***confidence intervals***. Equation 1.6.2, for example, is the confidence interval for a single member of a population. Table 1.6.2 gives the confidence intervals for several values of z. For reasons discussed later in the chapter, a 95% confidence level is a common choice in analytical chemistry.

> When z = 1, we call this the 68.26% confidence interval.

Table 1.6.2 : Confidence Intervals for a Normal Distribution

z	Confidence Interval
0.50	38.30
1.00	68.26
1.50	86.64
1.96	95.00
2.00	95.44
2.50	98.76
3.00	99.73
3.50	99.95

Example 1.6.3

What is the 95% confidence interval for the amount of aspirin in a single analgesic tablet drawn from a population for which μ is 250 mg and for which σ is 5?

Solution

Using Table 1.6.2 , we find that z is 1.96 for a 95% confidence interval. Substituting this into Equation 1.6.2 gives the confidence interval for a single tablet as

$$X_i = \mu \pm 1.96\sigma = 250 \text{ mg} \pm (1.96 \times 5) = 250 \text{ mg} \pm 10\text{mg}$$

A confidence interval of 250 mg ± 10 mg means that 95% of the tablets in the population contain between 240 and 260 mg of aspirin.

Typically, we collect n samples drawn from a population of known σ, and report the mean, X . The standard deviation of the mean, $\sigma_{\overline{X}}$, which also is known as the ***standard error of the mean***, is

$$\sigma_{\overline{X}} = \frac{\sigma}{\sqrt{n}}$$

The confidence interval for the population's mean, therefore, is

$$\mu = \overline{X} \pm \frac{z\sigma}{\sqrt{n}}$$

Example 1.6.5

What is the 95% confidence interval for a population of analgesic tablets if an analysis of five tablets yields a mean of 245 mg of aspirin?

Solution

In this case the confidence interval is

$$\mu = 245 \text{ mg} \pm \frac{1.96 \times 7}{\sqrt{5}} \text{ mg} = 245 \text{ mg} \pm 6 \text{ mg}$$

We estimate a 95% probability that the population's mean is between 239 mg and 251 mg of aspirin. As expected, the confidence interval when using the mean of five samples is smaller than that for a single sample.

? Exercise 1.6.2

An analysis of seven aspirin tablets from a population known to have a standard deviation of 5, gives the following results in mg aspirin per tablet:

$$246 \quad 249 \quad 255 \quad 251 \quad 251 \quad 247 \quad 250$$

What is the 95% confidence interval for the population's expected mean?

Answer

The mean is 249.9 mg aspirin/tablet for this sample of seven tablets. For a 95% confidence interval the value of z is 1.96, which makes the confidence interval

$$249.9 \pm \frac{1.96 \times 5}{\sqrt{7}} = 249.9 \pm 3.7 \approx 250 \text{ mg} \pm 4 \text{ mg}$$

Probability Distributions for Samples

In earlier examples, we assumed that the amount of aspirin in analgesic tablets is normally distributed. Without analyzing every member of the population, how can we justify this assumption? In a situation where we cannot study the whole population, or when we cannot predict the mathematical form of a population's probability distribution, we must deduce the distribution from a limited sampling of its members.

Sample Distributions and the Central Limit Theorem

Let's return to the problem of determining a penny's mass to explore further the relationship between a population's distribution and the distribution of a sample drawn from that population. It turns out that if you examine a larger sample of 100 pennies, you get a histogram of results like those in (Figure 1.6.5). To create the histogram, we divide the sample into intervals, by mass, and determine the percentage of pennies within each interval (Table 1.6.4). Note that the sample's mean is the midpoint of the histogram.

Table 1.6.4 : Frequency Distribution for the Data in Table 4.4.3

Mass Interval	Frequency (as % of Sample)	Mass Interval	Frequency (as % of Sample)
2.991 – 3.009	2	3.105 – 3.123	19
3.010 – 3.028	0	3.124 – 3.142	12
3.029 – 3.047	4	3.143 – 3.161	3
3.048 – 3.066	19	3.162 – 3.180	1
3.067 – 3.085	14	3.181 – 3.199	2
3.086 – 3.104	24	3.200 – 3.218	0

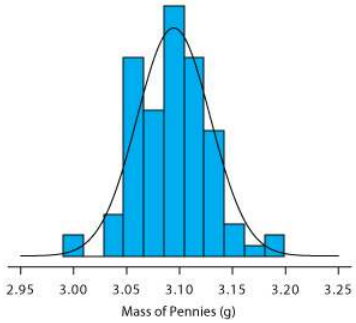


Figure 1.6.5 : The blue bars show a histogram for the data in Table 1.6.3 . The height of each bar corresponds to the percentage of pennies within one of the mass intervals in Table 1.6.4 . Superimposed on the histogram is a normal distribution curve based on the assumption that μ and σ^2 for the population are equivalent to $\overline{X}$ and σ^2 for the sample. The total area of the histogram's bars and the area under the normal distribution curve are equal.

Figure 1.6.5 also includes a normal distribution curve for the population of pennies, based on the assumption that the mean and the variance for the sample are appropriate estimates for the population's mean and variance. Although the histogram is not perfectly symmetric in shape, it provides a good approximation of the normal distribution curve, suggesting that the sample of 100 pennies is normally distributed and also that a still larger sample will even better match the normal distribution.

We will not offer a formal proof that the population of all circulating U. S. pennies are normally distributed; however, the evidence in Figure 1.6.5 strongly suggests this is true. Although we cannot claim that the results of all experiments are normally distributed, in most cases our data are normally distributed. According to the ***central limit theorem***, when a measurement is subject to a variety of indeterminate errors, the results for that measurement will approximate a normal distribution [Mark, H.; Workman, J. *Spectroscopy* **1988**, *3*, 44–48]. The central limit theorem holds true even if the individual sources of indeterminate error are not normally distributed. The chief limitation to the central limit theorem is that the sources of indeterminate error must be independent and of similar magnitude so that no one source of error dominates the final distribution.

Degrees of Freedom

Did you notice the differences between the equation for the variance of a population and the variance of a sample? If not, here are the two equations:

$$\sigma^2 = \frac{\sum_{i=1}^{n}(X_i - \mu)^2}{n}$$

$$s^2 = \frac{\sum_{i=1}^{n}(X_i - \overline{X})^2}{n-1}$$

Both equations measure the variance around the mean, using μ for a population and $\overline{X}$ for a sample. Although the equations use different measures for the mean, the intention is the same for both the sample and the population. A more interesting difference is between the denominators of the two equations. When we calculate the population's variance we divide the numerator by the population's size, *n*; for the sample's variance, however, we divide by *n* – 1, where *n* is the sample's size. Why do we divide by *n* – 1 when we calculate the sample's variance?

A variance is the average squared deviation of individual results relative to the mean. When we calculate an average we divide the sum by the number of independent measurements, or ***degrees of freedom***, in the calculation. For the population's variance, the degrees of freedom is equal to the population's size, *n*. When we measure every member of a population we have complete information about the population.

When we calculate the sample's variance, however, we replace μ with $\overline{X}$, which we also calculate using the same data. If there are *n* members in the sample, we can deduce the value of the n^{th} member from the remaining *n* – 1 members and the mean. For example, if \(*n* = 5\) and we know that the first four samples are 1, 2, 3 and 4, and that the mean is 3, then the fifth member of the sample must be

$$X_5 = (\overline{X} \times n) - X_1 - X_2 - X_3 - X_4 = (3 \times 5) - 1 - 2 - 3 - 4 = 5$$

Because we have just four independent measurements, we have lost one degree of freedom. Using $n - 1$ in place of n when we calculate the sample's variance ensures that s^2 is an unbiased estimator of σ^2.

> Here is another way to think about degrees of freedom. We analyze samples to make predictions about the underlying population. When our sample consists of n measurements we cannot make more than n independent predictions about the population. Each time we estimate a parameter, such as the population's mean, we lose a degree of freedom. If there are n degrees of freedom for calculating the sample's mean, then $n - 1$ degrees of freedom remain when we calculate the sample's variance.

Confidence Intervals for Samples

Earlier we introduced the confidence interval as a way to report the most probable value for a population's mean, μ

$$\mu = \overline{X} \pm \frac{z\sigma}{\sqrt{n}} \tag{1.6.3}$$

where $\overline{X}$ is the mean for a sample of size n, and σ is the population's standard deviation. For most analyses we do not know the population's standard deviation. We can still calculate a confidence interval, however, if we make two modifications to Equation 1.6.3.

The first modification is straightforward—we replace the population's standard deviation, σ, with the sample's standard deviation, s. The second modification is not as obvious. The values of z in Table 1.6.2 are for a normal distribution, which is a function of $sigma^2$, not s^2. Although the sample's variance, s^2, is an unbiased estimate of the population's variance, σ^2, the value of s^2 will only rarely equal σ^2. To account for this uncertainty in estimating σ^2, we replace the variable z in Equation 1.6.3 with the variable t, where t is defined such that $t \geq z$ at all confidence levels.

$$\mu = \overline{X} \pm \frac{ts}{\sqrt{n}} \tag{1.6.4}$$

Values for t at the 95% confidence level are shown in Table 1.6.5 . Note that t becomes smaller as the number of degrees of freedom increases, and that it approaches z as n approaches infinity. The larger the sample, the more closely its confidence interval for a sample (Equation 1.6.4) approaches the confidence interval for the population (Equation ???). Appendix 4 provides additional values of t for other confidence levels.

Table 1.6.5 : Values of t for a 95% Confidence Interval

Degrees of Freedom	t	Degrees of Freedom	t	Degrees of Freedom	t	Degrees of Freedom	t
1	12.706	6	2.447	12	2.179	30	2.042
2	4.303	7	2.365	14	2.145	40	2.021
3	3.181	8	2.306	16	2.120	60	2.000
4	2.776	9	2.262	18	2.101	100	1.984
5	2.571	10	2.228	20	2.086	\(\infty	1.960

Example 1.6.6

What are the 95% confidence intervals for the two samples of pennies in Table 1.6.1 ?

Solution

The mean and the standard deviation for first experiment are, respectively, 3.117 g and 0.051 g. Because the sample consists of seven measurements, there are six degrees of freedom. The value of t from Table 1.6.5 , is 2.447. Substituting into Equation 1.6.4 gives

$$\mu = 3.117 \text{ g} \pm \frac{2.447 \times 0.051 \text{ g}}{\sqrt{7}} = 3.117 \text{ g} \pm 0.047 \text{ g}$$

For the second experiment the mean and the standard deviation are 3.081 g and 0.073 g, respectively, with four degrees of freedom. The 95% confidence interval is

$$\mu = 3.081 \text{ g} \pm \frac{2.776 \times 0.037 \text{ g}}{\sqrt{5}} = 3.081 \text{ g} \pm 0.046 \text{ g}$$

Based on the first experiment, the 95% confidence interval for the population's mean is 3.070–3.164 g. For the second experiment, the 95% confidence interval is 3.035–3.127 g. Although the two confidence intervals are not identical—remember, each confidence interval provides a different estimate for μ—the mean for each experiment is contained within the other experiment's confidence interval. There also is an appreciable overlap of the two confidence intervals. Both of these observations are consistent with samples drawn from the same population.

Note that our comparison of these two confidence intervals at this point is somewhat vague and unsatisfying. We will return to this point in the next section, when we consider a statistical approach to comparing the results of experiments.

? Exercise 1.6.3

What is the 95% confidence interval for the sample of 100 pennies in Table 1.6.3 ? The mean and the standard deviation for this sample are 3.095 g and 0.0346 g, respectively. Compare your result to the confidence intervals for the samples of pennies in Table 1.6.1 .

Answer

With 100 pennies, we have 99 degrees of freedom for the mean. Although Table 1.6.3 does not include a value for $t(0.05, 99)$, we can approximate its value by using the values for $t(0.05, 60)$ and $t(0.05, 100)$ and by assuming a linear change in its value.

$$t(0.05, 99) = t(0.05, 60) - \frac{39}{40}\{t(0.05, 60) - t(0.05, 100\})$$

$$t(0.05, 99) = 2.000 - \frac{39}{40}\{2.000 - 1.984\} = 1.9844$$

The 95% confidence interval for the pennies is

$$3.095 \pm \frac{1.9844 \times 0.0346}{\sqrt{100}} = 3.095 \text{ g} \pm 0.007 \text{ g}$$

From Example 1.6.6 , the 95% confidence intervals for the two samples in Table 1.6.1 are 3.117 g ± 0.047 g and 3.081 g ± 0.046 g. As expected, the confidence interval for the sample of 100 pennies is much smaller than that for the two smaller samples of pennies. Note, as well, that the confidence interval for the larger sample fits within the confidence intervals for the two smaller samples.

A Cautionary Statement

There is a temptation when we analyze data simply to plug numbers into an equation, carry out the calculation, and report the result. This is never a good idea, and you should develop the habit of reviewing and evaluating your data. For example, if you analyze five samples and report an analyte's mean concentration as 0.67 ppm with a standard deviation of 0.64 ppm, then the 95% confidence interval is

$$\mu = 0.67 \text{ ppm} \pm \frac{2.776 \times 0.64 \text{ ppm}}{\sqrt{5}} = 0.67 \text{ ppm} \pm 0.79 \text{ ppm}$$

This confidence interval estimates that the analyte's true concentration is between –0.12 ppm and 1.46 ppm. Including a negative concentration within the confidence interval should lead you to reevaluate your data or your conclusions. A closer examination of

your data may convince you that the standard deviation is larger than expected, making the confidence interval too broad, or you may conclude that the analyte's concentration is too small to report with confidence.

> We will return to the topic of detection limits near the end of this chapter.

Here is a second example of why you should closely examine your data: results obtained on samples drawn at random from a normally distributed population must be random. If the results for a sequence of samples show a regular pattern or trend, then the underlying population either is not normally distributed or there is a time-dependent determinate error. For example, if we randomly select 20 pennies and find that the mass of each penny is greater than that for the preceding penny, then we might suspect that our balance is drifting out of calibration.

This page titled 1.6: The Distribution of Measurements and Results is shared under a CC BY-NC-SA 4.0 license and was authored, remixed, and/or curated by Kathryn Davis.

- **4.4: The Distribution of Measurements and Results** by David Harvey is licensed CC BY-NC-SA 4.0.

1.7: Statistical Analysis of Data

A confidence interval is a useful way to report the result of an analysis because it sets limits on the expected result. In the absence of determinate error, a confidence interval based on a sample's mean indicates the range of values in which we expect to find the population's mean. When we report a 95% confidence interval for the mass of a penny as 3.117 g ± 0.047 g, for example, we are stating that there is only a 5% probability that the penny's expected mass is less than 3.070 g or more than 3.164 g.

Because a confidence interval is a statement of probability, it allows us to consider comparative questions, such as these: "Are the results for a newly developed method to determine cholesterol in blood significantly different from those obtained using a standard method?" or "Is there a significant variation in the composition of rainwater collected at different sites downwind from a coal-burning utility plant?" In this section we introduce a general approach to the statistical analysis of data. Specific statistical tests are presented in Section 4.6.

> The reliability of significance testing recently has received much attention—see Nuzzo, R. "Scientific Method: Statistical Errors," *Nature*, **2014**, *506*, 150–152 for a general discussion of the issues—so it is appropriate to begin this section by noting the need to ensure that our data and our research question are compatible so that we do not read more into a statistical analysis than our data allows; see Leek, J. T.; Peng, R. D. "What is the Question? *Science*, **2015**, *347*, 1314-1315 for a use-ul discussion of six common research questions.
>
> In the context of analytical chemistry, significance testing often accompanies an exploratory data analysis (Is there a reason to suspect that there is a difference between these two analytical methods when applied to a common sample?) or an inferential data analysis (Is there a reason to suspect that there is a relationship between these two independent measurements?). A statistically significant result for these types of analytical research questions generally leads to the design of additional experiments better suited to making predictions or to explaining an underlying causal relationship. A significance test is the first step toward building a greater understanding of an analytical problem, not the final answer to that problem.

Significance Testing

Let's consider the following problem. To determine if a medication is effective in lowering blood glucose concentrations, we collect two sets of blood samples from a patient. We collect one set of samples immediately before we administer the medication, and collect the second set of samples several hours later. After analyzing the samples, we report their respective means and variances. How do we decide if the medication was successful in lowering the patient's concentration of blood glucose?

One way to answer this question is to construct a normal distribution curve for each sample, and to compare the two curves to each other. Three possible outcomes are shown in Figure 1.7.1 . In Figure 1.7.1 a, there is a complete separation of the two normal distribution curves, which suggests the two samples are significantly different from each other. In Figure 1.7.1 b, the normal distribution curves for the two samples almost completely overlap, which suggests that the difference between the samples is insignificant. Figure 1.7.1 c, however, presents us with a dilemma. Although the means for the two samples seem different, the overlap of their normal distribution curves suggests that a significant number of possible outcomes could belong to either distribution. In this case the best we can do is to make a statement about the probability that the samples are significantly different from each other.

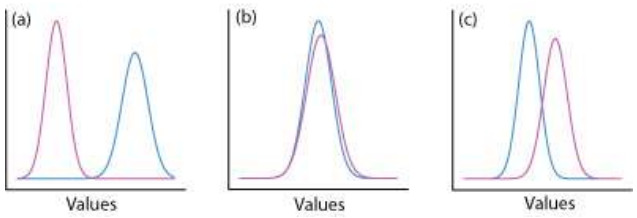


Figure 1.7.1 : Three examples of the possible relationships between the normal distribution curves for two samples. In (a) the curves do not overlap, which suggests that the samples are significantly different from each other. In (b) the two curves are almost identical, suggesting the samples are indistinguishable. The partial overlap of the curves in (c) means that the best we can do is evaluate the probability that there is a difference between the samples.

The process by which we determine the probability that there is a significant difference between two samples is called significance testing or hypothesis testing. Before we discuss specific examples we will first establish a general approach to conducting and interpreting a significance test.

Constructing a Significance Test

The purpose of a ***significance test*** is to determine whether the difference between two or more results is sufficiently large that it cannot be explained by indeterminate errors. The first step in constructing a significance test is to state the problem as a yes or no question, such as "Is this medication effective at lowering a patient's blood glucose levels?" A null hypothesis and an alternative hypothesis define the two possible answers to our yes or no question. The ***null hypothesis***, H_0, is that indeterminate errors are sufficient to explain any differences between our results. The ***alternative hypothesis***, H_A, is that the differences in our results are too great to be explained by random error and that they must be determinate in nature. We test the null hypothesis, which we either retain or reject. If we reject the null hypothesis, then we must accept the alternative hypothesis and conclude that the difference is significant.

Failing to reject a null hypothesis is not the same as accepting it. We retain a null hypothesis because we have insufficient evidence to prove it incorrect. It is impossible to prove that a null hypothesis is true. This is an important point and one that is easy to forget. To appreciate this point let's return to our sample of 100 pennies in Table 4.4.3. After looking at the data we might propose the following null and alternative hypotheses.

H_0: The mass of a circulating U.S. penny is between 2.900 g and 3.200 g

H_A: The mass of a circulating U.S. penny may be less than 2.900 g or more than 3.200 g

To test the null hypothesis we find a penny and determine its mass. If the penny's mass is 2.512 g then we can reject the null hypothesis and accept the alternative hypothesis. Suppose that the penny's mass is 3.162 g. Although this result increases our confidence in the null hypothesis, it does not prove that the null hypothesis is correct because the next penny we sample might weigh less than 2.900 g or more than 3.200 g.

After we state the null and the alternative hypotheses, the second step is to choose a confidence level for the analysis. The confidence level defines the probability that we will reject the null hypothesis when it is, in fact, true. We can express this as our confidence that we are correct in rejecting the null hypothesis (e.g. 95%), or as the probability that we are incorrect in rejecting the null hypothesis. For the latter, the confidence level is given as α, where

$$\alpha = 1 - \frac{\text{confidence interval (}}{100} \tag{1.7.1}$$

For a 95% confidence level, α is 0.05.

> In this textbook we use α to represent the probability that we incorrectly reject the null hypothesis. In other textbooks this probability is given as p (often read as "p- value"). Although the symbols differ, the meaning is the same.

The third step is to calculate an appropriate test statistic and to compare it to a critical value. The test statistic's critical value defines a breakpoint between values that lead us to reject or to retain the null hypothesis, which is the fourth, and final, step of a significance test. How we calculate the test statistic depends on what we are comparing, a topic we cover in Section 4.6. The last step is to either retain the null hypothesis, or to reject it and accept the alternative hypothesis.

> The four steps for a statistical analysis of data using a significance test:
>
> 1. Pose a question, and state the null hypothesis, H_0, and the alternative hypothesis, H_A.
> 2. Choose a confidence level for the statistical analysis.
> 3. Calculate an appropriate test statistic and compare it to a critical value.
> 4. Either retain the null hypothesis, or reject it and accept the alternative hypothesis.

One-Tailed and Two-tailed Significance Tests

Suppose we want to evaluate the accuracy of a new analytical method. We might use the method to analyze a Standard Reference Material that contains a known concentration of analyte, μ. We analyze the standard several times, obtaining a mean value, $\overline{X}$, for the analyte's concentration. Our null hypothesis is that there is no difference between $\overline{X}$ and μ

$$H_0: \overline{X} = \mu$$

If we conduct the significance test at $\alpha = 0.05$, then we retain the null hypothesis if a 95% confidence interval around $\overline{X}$ contains μ. If the alternative hypothesis is

$$H_A: \overline{X} \neq \mu$$

then we reject the null hypothesis and accept the alternative hypothesis if μ lies in the shaded areas at either end of the sample's probability distribution curve (Figure 1.7.2 a). Each of the shaded areas accounts for 2.5% of the area under the probability distribution curve, for a total of 5%. This is a ***two-tailed significance test*** because we reject the null hypothesis for values of μ at either extreme of the sample's probability distribution curve.

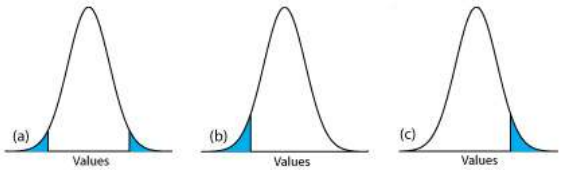


Figure 1.7.2 : Examples of (a) two-tailed, and (b, c) one-tailed, significance test of $\overline{X}$ and μ. The probability distribution curves, which are normal distributions, are based on the sample's mean and standard deviation. For α = 0.05, the blue areas account for 5% of the area under the curve. If the value of μ falls within the blue areas, then we reject the null hypothesis and accept the alternative hypothesis. We retain the null hypothesis if the value of μ falls within the unshaded area of the curve.

We also can write the alternative hypothesis in two additional ways

$$H_A: \overline{X} > \mu$$

$$H_A: \overline{X} < \mu$$

rejecting the null hypothesis if n falls within the shaded areas shown in Figure 1.7.2 b or Figure 1.7.2 c, respectively. In each case the shaded area represents 5% of the area under the probability distribution curve. These are examples of a ***one-tailed significance test***.

For a fixed confidence level, a two-tailed significance test is the more conservative test because rejecting the null hypothesis requires a larger difference between the parameters we are comparing. In most situations we have no particular reason to expect that one parameter must be larger (or must be smaller) than the other parameter. This is the case, for example, when we evaluate the accuracy of a new analytical method. A two-tailed significance test, therefore, usually is the appropriate choice.

We reserve a one-tailed significance test for a situation where we specifically are interested in whether one parameter is larger (or smaller) than the other parameter. For example, a one-tailed significance test is appropriate if we are evaluating a medication's ability to lower blood glucose levels. In this case we are interested only in whether the glucose levels after we administer the medication are less than the glucose levels before we initiated treatment. If a patient's blood glucose level is greater after we administer the medication, then we know the answer—the medication did not work—and do not need to conduct a statistical analysis.

Error in Significance Testing

Because a significance test relies on probability, its interpretation is subject to error. In a significance test, a defines the probability of rejecting a null hypothesis that is true. When we conduct a significance test at $\alpha = 0.05$, there is a 5% probability that we will incorrectly reject the null hypothesis. This is known as a ***type 1 error***, and its risk is always equivalent to α. A type 1 error in a two-tailed or a one-tailed significance tests corresponds to the shaded areas under the probability distribution curves in Figure 1.7.2 .

A second type of error occurs when we retain a null hypothesis even though it is false. This is as a ***type 2 error***, and the probability of its occurrence is β. Unfortunately, in most cases we cannot calculate or estimate the value for β. The probability of a type 2 error, however, is inversely proportional to the probability of a type 1 error.

Minimizing a type 1 error by decreasing α increases the likelihood of a type 2 error. When we choose a value for α we must compromise between these two types of error. Most of the examples in this text use a 95% confidence level ($\alpha = 0.05$) because this usually is a reasonable compromise between type 1 and type 2 errors for analytical work. It is not unusual, however, to use a more stringent (e.g. $\alpha = 0.01$) or a more lenient (e.g. $\alpha = 0.10$) confidence level when the situation calls for it.

This page titled 1.7: Statistical Analysis of Data is shared under a CC BY-NC-SA 4.0 license and was authored, remixed, and/or curated by Kathryn Davis.

- **4.5: Statistical Analysis of Data** by David Harvey is licensed CC BY-NC-SA 4.0.

1.8: Statistical Methods for Normal Distributions

The most common distribution for our results is a normal distribution. Because the area between any two limits of a normal distribution curve is well defined, constructing and evaluating significance tests is straightforward.

One-sample t-test compares $\overline{X}$ to μ

One way to validate a new analytical method is to analyze a sample that contains a known amount of analyte, μ. To judge the method's accuracy we analyze several portions of the sample, determine the average amount of analyte in the sample, $\overline{X}$, and use a significance test to compare $\overline{X}$ to μ. Our null hypothesis is that the difference between $\overline{X}$ and μ is explained by indeterminate errors that affect the determination of $\overline{X}$. The alternative hypothesis is that the difference between $\overline{X}$ and μ is too large to be explained by indeterminate error.

$$H_0: \overline{X} = \mu$$

$$H_A: \overline{X} \neq \mu$$

The test statistic is t_{exp}, which we substitute into the confidence interval for μ given by Equation 4.4.5

$$\mu = \overline{X} \pm \frac{t_{exp} s}{\sqrt{n}} \tag{1.8.1}$$

Rearranging this equation and solving for t_{exp}

$$t_{exp} = \frac{|\mu - \overline{X}|\sqrt{n}}{s} \tag{1.8.2}$$

gives the value for t_{exp} when μ is at either the right edge or the left edge of the sample's confidence interval (Figure 1.8.1 a)

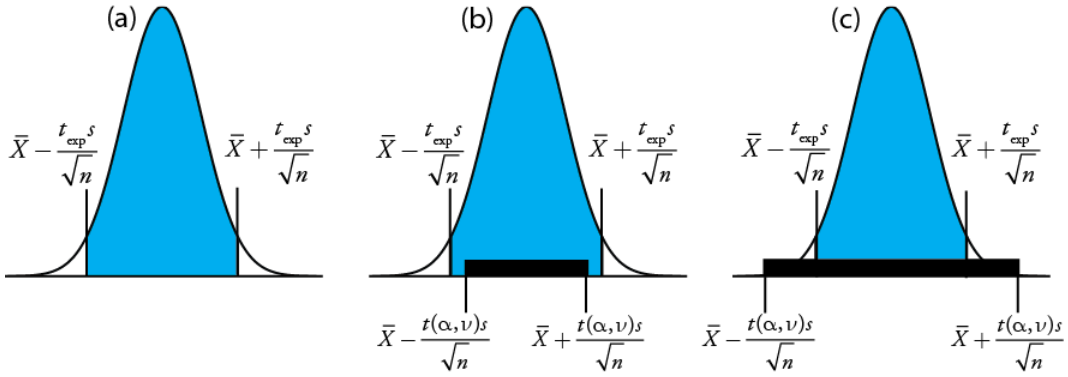


Figure 1.8.1 : Relationship between a confidence interval and the result of a significance test. (a) The shaded area under the normal distribution curve shows the sample's confidence interval for μ based on t_{exp}. The solid bars in (b) and (c) show the expected confidence intervals for μ explained by indeterminate error given the choice of α and the available degrees of freedom, ν. For (b) we reject the null hypothesis because portions of the sample's confidence interval fall outside the confidence interval explained by indeterminate error. In the case of (c) we retain the null hypothesis because the confidence interval explained by indeterminate error completely encompasses the sample's confidence interval.

To determine if we should retain or reject the null hypothesis, we compare the value of t_{exp} to a critical value, $t(\alpha, \nu)$, where α is the confidence level and ν is the degrees of freedom for the sample. The critical value $t(\alpha, \nu)$ defines the largest confidence interval explained by indeterminate error. If $t_{exp} > t(\alpha, \nu)$, then our sample's confidence interval is greater than that explained by indeterminate errors (Figure 1.8.1 b). In this case, we reject the null hypothesis and accept the alternative hypothesis. If $t_{exp} \leq t(\alpha, \nu)$, then our sample's confidence interval is smaller than that explained by indeterminate error, and we retain the null hypothesis (Figure 1.8.1 c). Example 1.8.1 provides a typical application of this significance test, which is known as a **t-test** of $\overline{X}$ to μ.

> You will find values for $t(\alpha, \nu)$ in Appendix 4.

Another name for the *t*-test is Student's *t*-test. Student was the pen name for William Gossett (1876-1927) who developed the *t*-test while working as a statistician for the Guiness Brewery in Dublin, Ireland. He published under the name Student because the brewery did not want its competitors to know they were using statistics to help improve the quality of their products.

Example 1.8.1

Before determining the amount of Na_2CO_3 in a sample, you decide to check your procedure by analyzing a standard sample that is 98.76% w/w Na_2CO_3. Five replicate determinations of the %w/w Na_2CO_3 in the standard gave the following results

$$98.71\% \quad 98.59\% \quad 98.62\% \quad 98.44\% \quad 98.58\%$$

Using $\alpha = 0.05$, is there any evidence that the analysis is giving inaccurate results?

Solution

The mean and standard deviation for the five trials are

$$\overline{X} = 98.59 \qquad s = 0.0973$$

Because there is no reason to believe that the results for the standard must be larger or smaller than μ, a two-tailed *t*-test is appropriate. The null hypothesis and alternative hypothesis are

$$H_0\text{: } \overline{X} = \mu \qquad H_A\text{: } \overline{X} \neq \mu$$

The test statistic, t_{exp}, is

$$t_{exp} = \frac{|\mu - \overline{X}|\sqrt{n}}{s} = \frac{|98.76 - 98.59|\sqrt{5}}{0.0973} = 3.91$$

The critical value for $t(0.05, 4)$ from Appendix 4 is 2.78. Since t_{exp} is greater than $t(0.05, 4)$, we reject the null hypothesis and accept the alternative hypothesis. At the 95% confidence level the difference between $\overline{X}$ and μ is too large to be explained by indeterminate sources of error, which suggests there is a determinate source of error that affects the analysis.

There is another way to interpret the result of this *t*-test. Knowing that t_{exp} is 3.91 and that there are 4 degrees of freedom, we use Appendix 4 to estimate the α value corresponding to a $t(\alpha, 4)$ of 3.91. From Appendix 4, $t(0.02, 4)$ is 3.75 and $t(0.01, 4)$ is 4.60. Although we can reject the null hypothesis at the 98% confidence level, we cannot reject it at the 99% confidence level. For a discussion of the advantages of this approach, see J. A. C. Sterne and G. D. Smith "Sifting the evidence—what's wrong with significance tests?" *BMJ* **2001**, *322*, 226–231.

Exercise 1.8.1

To evaluate the accuracy of a new analytical method, an analyst determines the purity of a standard for which μ is 100.0%, obtaining the following results.

$$99.28\% \quad 103.93\% \quad 99.43\% \quad 99.84\% \quad 97.60\% \quad 96.70\% \quad 98.02\%$$

Is there any evidence at $\alpha = 0.05$ that there is a determinate error affecting the results?

Answer

The null hypothesis is $H_0\text{: } \overline{X} = \mu$ and the alternative hypothesis is $H_A\text{: } \overline{X} \neq \mu$. The mean and the standard deviation for the data are 99.26% and 2.35%, respectively. The value for t_{exp} is

$$t_{exp} = \frac{|100.0 - 99.26|\sqrt{7}}{2.35} = 0.833$$

and the critical value for $t(0.05, 6)$ is 2.477. Because t_{exp} is less than $t(0.05, 6)$ we retain the null hypothesis and have no evidence for a significant difference between $\overline{X}$ and μ.

Earlier we made the point that we must exercise caution when we interpret the result of a statistical analysis. We will keep returning to this point because it is an important one. Having determined that a result is inaccurate, as we did in Example 1.8.1 , the next step is to identify and to correct the error. Before we expend time and money on this, however, we first should examine critically our data. For example, the smaller the value of s, the larger the value of t_{exp}. If the standard deviation for our analysis is unrealistically small, then the probability of a type 2 error increases. Including a few additional replicate analyses of the standard and reevaluating the t-test may strengthen our evidence for a determinate error, or it may show us that there is no evidence for a determinate error.

F-test compares s^2 to σ^2

If we analyze regularly a particular sample, we may be able to establish an expected variance, σ^2, for the analysis. This often is the case, for example, in a clinical lab that analyze hundreds of blood samples each day. A few replicate analyses of a single sample gives a sample variance, s^2, whose value may or may not differ significantly from σ^2.

We can use an F-test to evaluate whether a difference between s^2 and σ^2 is significant. The null hypothesis is H_0: $s^2 = \sigma^2$ and the alternative hypothesis is H_A: $s^2 \neq \sigma^2$. The test statistic for evaluating the null hypothesis is F_{exp}, which is given as either

$$F_{exp} = \frac{s^2}{\sigma^2} \text{ if } s^2 > \sigma^2 \text{ or } F_{exp} = \frac{\sigma^2}{s^2} \text{ if } \sigma^2 > s^2 \tag{1.8.3}$$

depending on whether s^2 is larger or smaller than σ^2. This way of defining F_{exp} ensures that its value is always greater than or equal to one.

If the null hypothesis is true, then F_{exp} should equal one; however, because of indeterminate errors F_{exp} usually is greater than one. A critical value, $F(\alpha, \nu_{num}, \nu_{den})$, is the largest value of F_{exp} that we can attribute to indeterminate error given the specified significance level, α, and the degrees of freedom for the variance in the numerator, ν_{num}, and the variance in the denominator, ν_{den}. The degrees of freedom for s^2 is $n - 1$, where n is the number of replicates used to determine the sample's variance, and the degrees of freedom for σ^2 is defined as infinity, ∞. Critical values of F for $\alpha = 0.05$ are listed in Appendix 5 for both one-tailed and two-tailed F-tests.

Example 1.8.2

A manufacturer's process for analyzing aspirin tablets has a known variance of 25. A sample of 10 aspirin tablets is selected and analyzed for the amount of aspirin, yielding the following results in mg aspirin/tablet.

$$254 \quad 249 \quad 252 \quad 252 \quad 249 \quad 249 \quad 250 \quad 247 \quad 251 \quad 252$$

Determine whether there is evidence of a significant difference between the sample's variance and the expected variance at $\alpha = 0.05$.

Solution

The variance for the sample of 10 tablets is 4.3. The null hypothesis and alternative hypotheses are

$$H_0: s^2 = \sigma^2 \qquad H_A: s^2 \neq \sigma^2$$

and the value for F_{exp} is

$$F_{exp} = \frac{\sigma^2}{s^2} = \frac{25}{4.3} = 5.8$$

The critical value for $F(0.05, \infty, 9)$ from Appendix 5 is 3.333. Since F_{exp} is greater than $F(0.05, \infty, 9)$, we reject the null hypothesis and accept the alternative hypothesis that there is a significant difference between the sample's variance and the expected variance. One explanation for the difference might be that the aspirin tablets were not selected randomly.

F-tests also compare variances for two samples

We can extend the F-test to compare the variances for two samples, A and B, by rewriting Equation 1.8.3 as

$$F_{exp} = \frac{s_A^2}{s_B^2}$$

defining A and B so that the value of Fexp is greater than or equal to 1.

Example 1.8.3

Table 4.4.1 shows results for two experiments to determine the mass of a circulating U.S. penny. Determine whether there is a difference in the variances of these analyses at $\alpha = 0.05$.

Solution

The standard deviations for the two experiments are 0.051 for the first experiment (A) and 0.037 for the second experiment (B). The null and alternative hypotheses are

$$H_0\text{: } s_A^2 = s_B^2 \qquad H_A\text{: } s_A^2 \neq s_B^2$$

and the value of F_{exp} is

$$F_{exp} = \frac{s_A^2}{s_B^2} = \frac{(0.051)^2}{(0.037)^2} = \frac{0.00260}{0.00137} = 1.90$$

From Appendix 5, the critical value for F(0.05, 6, 4) is 9.197. Because $F_{exp} < F$(0.05, 6, 4), we retain the null hypothesis. There is no evidence at $\alpha = 0.05$ to suggest that the difference in variances is significant.

Exercise 1.8.2

To compare two production lots of aspirin tablets, we collect an analyze samples from each, obtaining the following results (in mg aspirin/tablet).

Lot 1: **256 248 245 245 244 248 261**

Lot 2: **241 258 241 244 256 254**

Is there any evidence at $\alpha = 0.05$ that there is a significant difference in the variances for these two samples?

Answer

The standard deviations are 6.451 mg for Lot 1 and 7.849 mg for Lot 2. The null and alternative hypotheses are

$$H_0\text{: } s_{\text{Lot 1}}^2 = s_{\text{Lot 2}}^2 \qquad H_A\text{: } s_{\text{Lot 1}}^2 \neq s_{\text{Lot 2}}^2$$

and the value of F_{exp} is

$$F_{exp} = \frac{(7.849)^2}{(6.451)^2} = 1.480$$

The critical value for F(0.05, 5, 6) is 5.988. Because $F_{exp} < F$(0.05, 5, 6), we retain the null hypothesis. There is no evidence at $\alpha = 0.05$ to suggest that the difference in the variances is significant.

Two-sample t-tests compare means for two samples

Three factors influence the result of an analysis: the method, the sample, and the analyst. We can study the influence of these factors by conducting experiments in which we change one factor while holding constant the other factors. For example, to compare two analytical methods we can have the same analyst apply each method to the same sample and then examine the resulting means. In a similar fashion, we can design experiments to compare two analysts or to compare two samples.

It also is possible to design experiments in which we vary more than one of these factors. We will return to this point in Chapter 14.

Before we consider the significance tests for comparing the means of two samples, we need to make a distinction between ***unpaired data*** and ***paired data***. This is a critical distinction and learning to distinguish between these two types of data is important. Here are two simple examples that highlight the difference between unpaired data and paired data. In each example the goal is to compare two balances by weighing pennies.

- Example 1: We collect 10 pennies and weigh each penny on each balance. This is an example of paired data because we use the same 10 pennies to evaluate each balance.
- Example 2: We collect 10 pennies and divide them into two groups of five pennies each. We weigh the pennies in the first group on one balance and we weigh the second group of pennies on the other balance. Note that no penny is weighed on both balances. This is an example of unpaired data because we evaluate each balance using a different sample of pennies.

In both examples the samples of 10 pennies were drawn from the same population; the difference is how we sampled that population. We will learn why this distinction is important when we review the significance test for paired data; first, however, we present the significance test for unpaired data.

> One simple test for determining whether data are paired or unpaired is to look at the size of each sample. If the samples are of different size, then the data must be unpaired. The converse is not true. If two samples are of equal size, they may be paired or unpaired.

Unpaired t-tests are for same method, two different samples

Consider two analyses, *A* and *B* with means of $\overline{X}_A$ and $\overline{X}_B$, and standard deviations of s_A and s_B. The confidence intervals for μ_A and for μ_B are

$$\mu_A = \overline{X}_A \pm \frac{ts_A}{\sqrt{n_A}} \tag{1.8.4}$$

$$\mu_B = \overline{X}_B \pm \frac{ts_B}{\sqrt{n_B}} \tag{1.8.5}$$

where n_A and n_B are the sample sizes for *A* and for *B*. Our null hypothesis, H_0: $\mu_A = \mu_B$, is that and any difference between μ_A and μ_B is the result of indeterminate errors that affect the analyses. The alternative hypothesis, H_A: $\mu_A \neq \mu_B$, is that the difference between $\mu_A$and μ_B is too large to be explained by indeterminate error.

To derive an equation for t_{exp}, we assume that μ_A equals μ_B, and combine Equation 1.8.4 and Equation 1.8.5

$$\overline{X}_A \pm \frac{t_{exp}s_A}{\sqrt{n_A}} = \overline{X}_B \pm \frac{t_{exp}s_B}{\sqrt{n_B}}$$

Solving for $|\overline{X}_A - \overline{X}_B|$ and using a propagation of uncertainty, gives

$$|\overline{X}_A - \overline{X}_B| = t_{exp} \times \sqrt{\frac{s_A^2}{n_A} + \frac{s_B^2}{n_B}} \tag{1.8.6}$$

Finally, we solve for t_{exp}

$$t_{exp} = \frac{|\overline{X}_A - \overline{X}_B|}{\sqrt{\frac{s_A^2}{n_A} + \frac{s_B^2}{n_B}}} \tag{1.8.7}$$

and compare it to a critical value, $t(\alpha, \nu)$, where α is the probability of a type 1 error, and ν is the degrees of freedom.

> Problem 9 asks you to use a propagation of uncertainty to show that Equation 1.8.6 is correct.

Thus far our development of this *t*-test is similar to that for comparing $\overline{X}$ to μ, and yet we do not have enough information to evaluate the *t*-test. Do you see the problem? With two independent sets of data it is unclear how many degrees of freedom we have.

Suppose that the variances s_A^2 and s_B^2 provide estimates of the same σ^2. In this case we can replace s_A^2 and s_B^2 with a pooled variance, s_{pool}^2, that is a better estimate for the variance. Thus, Equation 1.8.7 becomes

$$t_{exp} = \frac{|\overline{X}_A - \overline{X}_B|}{s_{pool} \times \sqrt{\frac{1}{n_A} + \frac{1}{n_B}}} = \frac{|\overline{X}_A - \overline{X}_B|}{s_{pool}} \times \sqrt{\frac{n_A n_B}{n_A + n_B}} \tag{1.8.8}$$

where s_{pool}, the pooled standard deviation, is

$$s_{pool} = \sqrt{\frac{(n_A - 1)s_A^2 + (n_B - 1)s_B^2}{n_A + n_B - 2}} \tag{1.8.9}$$

The denominator of Equation 1.8.9 shows us that the degrees of freedom for a pooled standard deviation is $n_A + n_B - 2$, which also is the degrees of freedom for the *t*-test. Note that we lose two degrees of freedom because the calculations for s_A^2 and s_B^2 require the prior calculation of $\overline{X}_A$ amd $\overline{X}_B$.

So how do you determine if it is okay to pool the variances? Use an *F*-test.

If s_A^2 and s_B^2 are significantly different, then we calculate t_{exp} using Equation 1.8.7. In this case, we find the degrees of freedom using the following imposing equation.

$$\nu = \frac{\left(\frac{s_A^2}{n_A} + \frac{s_B^2}{n_B}\right)^2}{\frac{\left(\frac{s_A^2}{n_A}\right)^2}{n_A+1} + \frac{\left(\frac{s_B^2}{n_B}\right)^2}{n_B+1}} - 2 \tag{1.8.10}$$

Because the degrees of freedom must be an integer, we round to the nearest integer the value of ν obtained using Equation 1.8.10.

Equation 1.8.10, which is from Miller, J.C.; Miller, J.N. *Statistics for Analytical Chemistry*, 2nd Ed., Ellis-Horward: Chichester, UK, 1988. In the 6th Edition, the authors note that several different equations have been suggested for the number of degrees of freedom for *t* when s_A and s_B differ, reflecting the fact that the determination of degrees of freedom an approximation. An alternative equation—which is used by statistical software packages, such as R, Minitab, Excel—is

$$\nu = \frac{\left(\frac{s_A^2}{n_A} + \frac{s_B^2}{n_B}\right)^2}{\frac{\left(\frac{s_A^2}{n_A}\right)^2}{n_A-1} + \frac{\left(\frac{s_B^2}{n_B}\right)^2}{n_B-1}} = \frac{\left(\frac{s_A^2}{n_A} + \frac{s_B^2}{n_B}\right)^2}{\frac{s_A^4}{n_A^2(n_A-1)} + \frac{s_B^4}{n_B^2(n_B-1)}}$$

For typical problems in analytical chemistry, the calculated degrees of freedom is reasonably insensitive to the choice of equation.

Regardless of whether we calculate t_{exp} using Equation 1.8.7 or Equation 1.8.8, we reject the null hypothesis if t_{exp} is greater than $t(\alpha, \nu)$ and retain the null hypothesis if t_{exp} is less than or equal to $t(\alpha, \nu)$.

Example 1.8.4

Table 4.4.1 provides results for two experiments to determine the mass of a circulating U.S. penny. Determine whether there is a difference in the means of these analyses at $\alpha = 0.05$.

Solution

First we use an *F*-test to determine whether we can pool the variances. We completed this analysis in Example 1.8.3 , finding no evidence of a significant difference, which means we can pool the standard deviations, obtaining

$$s_{pool} = \sqrt{\frac{(7-1)(0.051)^2 + (5-1)(0.037)^2}{7+5-2}} = 0.0459$$

with 10 degrees of freedom. To compare the means we use the following null hypothesis and alternative hypotheses

$$H_0\text{: } \mu_A = \mu_B \qquad H_A\text{: } \mu_A \neq \mu_B$$

Because we are using the pooled standard deviation, we calculate t_{exp} using Equation 1.8.8.

$$t_{exp} = \frac{|3.117 - 3.081|}{0.0459} \times \sqrt{\frac{7 \times 5}{7 + 5}} = 1.34$$

The critical value for $t(0.05, 10)$, from Appendix 4, is 2.23. Because t_{exp} is less than $t(0.05, 10)$ we retain the null hypothesis. For $\alpha = 0.05$ we do not have evidence that the two sets of pennies are significantly different.

Example 1.8.5

One method for determining the %w/w Na_2CO_3 in soda ash is to use an acid–base titration. When two analysts analyze the same sample of soda ash they obtain the results shown here.

Analyst A: 86.82% 87.04% 86.93% 87.01% 86.20% 87.00%

Analyst B: 81.01% 86.15% 81.73% 83.19% 80.27% 83.93%

Determine whether the difference in the mean values is significant at $\alpha = 0.05$.

Solution

We begin by reporting the mean and standard deviation for each analyst.

$$\overline{X}_A = 86.83\% \qquad s_A = 0.32\%$$

$$\overline{X}_B = 82.71\% \qquad s_B = 2.16\%$$

To determine whether we can use a pooled standard deviation, we first complete an F-test using the following null and alternative hypotheses.

$$H_0\text{: } s_A^2 = s_B^2 \qquad H_A\text{: } s_A^2 \neq s_B^2$$

Calculating F_{exp}, we obtain a value of

$$F_{exp} = \frac{(2.16)^2}{(0.32)^2} = 45.6$$

Because F_{exp} is larger than the critical value of 7.15 for $F(0.05, 5, 5)$ from Appendix 5, we reject the null hypothesis and accept the alternative hypothesis that there is a significant difference between the variances; thus, we cannot calculate a pooled standard deviation.

To compare the means for the two analysts we use the following null and alternative hypotheses.

$$H_0\text{: } \overline{X}_A = \overline{X}_B \qquad H_A\text{: } \overline{X}_A \neq \overline{X}_B$$

Because we cannot pool the standard deviations, we calculate t_{exp} using Equation 1.8.7 instead of Equation 1.8.8

$$t_{exp} = \frac{|86.83 - 82.71|}{\sqrt{\frac{(0.32)^2}{6} + \frac{(2.16)^2}{6}}} = 4.62$$

and calculate the degrees of freedom using Equation 1.8.10.

$$\nu = \frac{\left(\frac{(0.32)^2}{6} + \frac{(2.16)^2}{6}\right)^2}{\frac{\left(\frac{(0.32)^2}{6}\right)^2}{6+1} + \frac{\left(\frac{(2.16)^2}{6}\right)^2}{6+1}} - 2 = 5.3 \approx 5$$

From Appendix 4, the critical value for $t(0.05, 5)$ is 2.57. Because t_{exp} is greater than $t(0.05, 5)$ we reject the null hypothesis and accept the alternative hypothesis that the means for the two analysts are significantly different at $\alpha = 0.05$.

Exercise 1.8.3

To compare two production lots of aspirin tablets, you collect samples from each and analyze them, obtaining the following results (in mg aspirin/tablet).

Lot 1: **256 248 245 245 244 248 261**

Lot 2: **241 258 241 244 256 254**

Is there any evidence at $\alpha = 0.05$ that there is a significant difference in the variance between the results for these two samples? This is the same data from Exercise 1.8.2 .

Answer

To compare the means for the two lots, we use an unpaired *t*-test of the null hypothesis H_0: $\overline{X}_{\text{Lot 1}} = \overline{X}_{\text{Lot 2}}$ and the alternative hypothesis H_A: $\overline{X}_{\text{Lot 1}} \neq \overline{X}_{\text{Lot 2}}$. Because there is no evidence to suggest a difference in the variances (see Exercise 1.8.2) we pool the standard deviations, obtaining an s_{pool} of

$$s_{\text{pool}} = \sqrt{\frac{(7-1)(6.451)^2 + (6-1)(7.849)^2}{7+6-2}} = 7.121$$

The means for the two samples are 249.57 mg for Lot 1 and 249.00 mg for Lot 2. The value for t_{exp} is

$$t_{\text{exp}} = \frac{|249.57 - 249.00|}{7.121} \times \sqrt{\frac{7 \times 6}{7+6}} = 0.1439$$

The critical value for $t(0.05, 11)$ is 2.204. Because t_{exp} is less than $t(0.05, 11)$, we retain the null hypothesis and find no evidence at $\alpha = 0.05$ that there is a significant difference between the means for the two lots of aspirin tablets.

Paired t-tests are for same samples using different methods

Suppose we are evaluating a new method for monitoring blood glucose concentrations in patients. An important part of evaluating a new method is to compare it to an established method. What is the best way to gather data for this study? Because the variation in the blood glucose levels amongst patients is large we may be unable to detect a small, but significant difference between the methods if we use different patients to gather data for each method. Using paired data, in which the we analyze each patient's blood using both methods, prevents a large variance within a population from adversely affecting a *t*-test of means.

> Typical blood glucose levels for most non-diabetic individuals ranges between 80–120 mg/dL (4.4–6.7 mM), rising to as high as 140 mg/dL (7.8 mM) shortly after eating. Higher levels are common for individuals who are pre-diabetic or diabetic.

When we use paired data we first calculate the difference, d_i, between the paired values for each sample. Using these difference values, we then calculate the average difference, $\overline{d}$, and the standard deviation of the differences, s_d. The null hypothesis, H_0: $d = 0$, is that there is no difference between the two samples, and the alternative hypothesis, H_A: $d \neq 0$, is that the difference between the two samples is significant.

The test statistic, t_{exp}, is derived from a confidence interval around $\overline{d}$

$$t_{\text{exp}} = \frac{|\overline{d}|\sqrt{n}}{s_d}$$

where n is the number of paired samples. As is true for other forms of the *t*-test, we compare t_{exp} to $t(\alpha, \nu)$, where the degrees of freedom, ν, is $n - 1$. If t_{exp} is greater than $t(\alpha, \nu)$, then we reject the null hypothesis and accept the alternative hypothesis. We retain the null hypothesis if t_{exp} is less than or equal to $t(a, o)$. This is known as a ***paired t-test.***

Example 1.8.6

Marecek et. al. developed a new electrochemical method for the rapid determination of the concentration of the antibiotic monensin in fermentation vats [Marecek, V.; Janchenova, H.; Brezina, M.; Betti, M. *Anal. Chim. Acta* **1991**, *244*, 15–19]. The standard method for the analysis is a test for microbiological activity, which is both difficult to complete and time-consuming. Samples were collected from the fermentation vats at various times during production and analyzed for the concentration of monensin using both methods. The results, in parts per thousand (ppt), are reported in the following table.

Sample	Microbiological	Electrochemical
1	129.5	132.3
2	89.6	91.0
3	76.6	73.6
4	52.2	58.2
5	110.8	104.2
6	50.4	49.9
7	72.4	82.1
8	141.4	154.1
9	75.0	73.4
10	34.1	38.1
11	60.3	60.1

Is there a significant difference between the methods at $\alpha = 0.05$?

Solution

Acquiring samples over an extended period of time introduces a substantial time-dependent change in the concentration of monensin. Because the variation in concentration between samples is so large, we use a paired *t*-test with the following null and alternative hypotheses.

$$H_0\colon \bar{d} = 0 \qquad H_A\colon \bar{d} \neq 0$$

Defining the difference between the methods as

$$d_i = (X_{\text{elect}})_i - (X_{\text{micro}})_i$$

we calculate the difference for each sample.

sample	1	2	3	4	5	6	7	8	9	10	11
d_i	2.8	1.4	–3.0	6.0	–6.6	–0.5	9.7	12.7	–1.6	4.0	–0.2

The mean and the standard deviation for the differences are, respectively, 2.25 ppt and 5.63 ppt. The value of t_{exp} is

$$t_{\text{exp}} = \frac{|2.25|\sqrt{11}}{5.63} = 1.33$$

which is smaller than the critical value of 2.23 for *t*(0.05, 10) from Appendix 4. We retain the null hypothesis and find no evidence for a significant difference in the methods at $\alpha = 0.05$.

? Exercise 1.8.4

Suppose you are studying the distribution of zinc in a lake and want to know if there is a significant difference between the concentration of Zn^{2+} at the sediment-water interface and its concentration at the air-water interface. You collect samples from six locations—near the lake's center, near its drainage outlet, etc.—obtaining the results (in mg/L) shown in the table. Using this data, determine if there is a significant difference between the concentration of Zn^{2+} at the two interfaces at $\alpha = 0.05$. Complete this analysis treating the data as (a) unpaired and as (b) paired. Briefly comment on your results.

Location	Air-Water Interface	Sediment-Water Interface
1	0.430	0.415
2	0.266	0.238
3	0.457	0.390
4	0.531	0.410
5	0.707	0.605
6	0.716	0.609

Complete this analysis treating the data as (a) unpaired and as (b) paired. Briefly comment on your results.

Answer

Treating as Unpaired Data: The mean and the standard deviation for the concentration of Zn^{2+} at the air-water interface are 0.5178 mg/L and 0.1732 mg/L, respectively, and the values for the sediment-water interface are 0.4445 mg/L and 0.1418 mg/L, respectively. An *F*-test of the variances gives an F_{exp} of 1.493 and an $F(0.05, 5, 5)$ of 7.146. Because F_{exp} is smaller than $F(0.05, 5, 5)$, we have no evidence at $\alpha = 0.05$ to suggest that the difference in variances is significant. Pooling the standard deviations gives an s_{pool} of 0.1582 mg/L. An unpaired *t*-test gives t_{exp} as 0.8025. Because t_{exp} is smaller than $t(0.05, 11)$, which is 2.204, we have no evidence that there is a difference in the concentration of Zn^{2+} between the two interfaces.

Treating as Paired Data: To treat as paired data we need to calculate the difference, d_i, between the concentration of Zn^{2+} at the air-water interface and at the sediment-water interface for each location, where

$$d_i = \left([Zn^{2+}]_{\text{air-water}}\right)_i - \left([Zn^{2+}]_{\text{sed-water}}\right)_i$$

The mean difference is 0.07333 mg/L with a standard deviation of 0.0441 mg/L. The null hypothesis and the alternative hypothesis are

$$H_0: \bar{d} = 0 \qquad H_A: \bar{d} \neq 0$$

and the value of t_{exp} is

$$t_{exp} = \frac{|0.07333|\sqrt{6}}{0.0441} = 4.073$$

Because t_{exp} is greater than $t(0.05, 5)$, which is 2.571, we reject the null hypothesis and accept the alternative hypothesis that there is a significant difference in the concentration of Zn^{2+} between the air-water interface and the sediment-water interface.

The difference in the concentration of Zn^{2+} between locations is much larger than the difference in the concentration of Zn^{2+} between the interfaces. Because out interest is in studying the difference between the interfaces, the larger standard deviation when treating the data as unpaired increases the probability of incorrectly retaining the null hypothesis, a type 2 error.

One important requirement for a paired *t*-test is that the determinate and the indeterminate errors that affect the analysis must be independent of the analyte's concentration. If this is not the case, then a sample with an unusually high concentration of analyte

will have an unusually large d_i. Including this sample in the calculation of $\bar{d}$ and s_d gives a biased estimate for the expected mean and standard deviation. This rarely is a problem for samples that span a limited range of analyte concentrations, such as those in Example 1.8.6 or Exercise 1.8.4 . When paired data span a wide range of concentrations, however, the magnitude of the determinate and indeterminate sources of error may not be independent of the analyte's concentration; when true, a paired *t*-test may give misleading results because the paired data with the largest absolute determinate and indeterminate errors will dominate $\bar{d}$. In this situation a regression analysis, which is the subject of the next chapter, is more appropriate method for comparing the data.

Statistical tests to identify sample outliers

Earlier in the chapter we examined several data sets consisting of the mass of a circulating United States penny. Table 1.8.1 provides one more data set. Do you notice anything unusual in this data? Of the 112 pennies included in Table 4.4.1 and Table 4.4.3, no penny weighed less than 3 g. In Table 4.6.1, however, the mass of one penny is less than 3 g. We might ask whether this penny's mass is so different from the other pennies that it is in error.

Table 1.8.1 : Mass (g) for Additional Sample of Circulating U. S. Pennies

3.067	2.514	3.094
3.049	3.048	3.109
3.039	3.079	3.102

A measurement that is not consistent with other measurements is called outlier. An ***outlier*** might exist for many reasons: the outlier might belong to a different population (Is this a Canadian penny?); the outlier might be a contaminated or otherwise altered sample (Is the penny damaged or unusually dirty?); or the outlier may result from an error in the analysis (Did we forget to tare the balance?). Regardless of its source, the presence of an outlier compromises any meaningful analysis of our data. There are many significance tests that we can use to identify a potential outlier, three of which we present here.

Dixon's *Q*-Test (for information - we won't use this very often)

The Dixon's *Q*-test is one way to test for outliers by comparing the gap between a possible outlier to the range of the data set, as in (Figure 1.8.2).

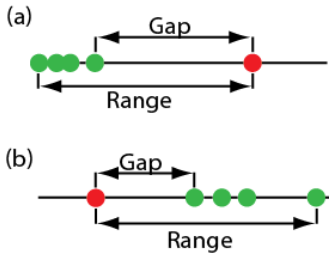


Figure 1.8.2 : Dotplots showing the distribution of two data sets containing a possible outlier. In (a) the possible outlier's value is larger than the remaining data, and in (b) the possible outlier's value is smaller than the remaining data.

The test statistic, Q_{exp}, is

$$Q_{\text{exp}} = \frac{\text{gap}}{\text{range}} = \frac{|\text{outlier's value} - \text{nearest value}|}{\text{largest value} - \text{smallest value}}$$

This equation is appropriate for evaluating a single outlier. Other forms of Dixon's *Q*-test allow its extension to detecting multiple outliers [Rorabacher, D. B. *Anal. Chem.* **1991**, *63*, 139–146].

Grubb's Test (this is the one we will use)

Although Dixon's *Q*-test is a common method for evaluating outliers, it is no longer favored by the International Standards Organization (ISO), which recommends the ***Grubb's test***. There are several versions of Grubb's test depending on the number of potential outliers. Here we will consider the case where there is a single suspected outlier.

For details on this recommendation, see International Standards ISO Guide 5752-2 “Accuracy (trueness and precision) of measurement methods and results–Part 2: basic methods for the determination of repeatability and reproducibility of a standard measurement method,” 1994.

The test statistic for Grubb’s test, G_{exp}, is the distance between the sample’s mean, $\overline{X}$, and the potential outlier, X_{out}, in terms of the sample’s standard deviation, s.

$$G_{exp} = \frac{|X_{out} - \overline{X}|}{s}$$

We compare the value of G_{exp} to a critical value $G(\alpha, n)$, where α is the probability that we will reject a valid data point and n is the number of data points in the sample. If G_{exp} is greater than $G(\alpha, n)$, then we may reject the data point as an outlier, otherwise we retain the data point as part of the sample. Table 1.8.3 provides values for $G(0.05, n)$ for a sample containing 3–10 values. A more extensive table is in Appendix 7. Values for $G(\alpha, n)$ assume an underlying normal distribution.

Table 1.8.3 : Grubb's Test

n	$G(0.05, n)$
3	1.115
4	1.481
5	1.715
6	1.887
7	2.020
8	2.126
9	2.215
10	2.290

Chauvenet's Criterion (don't worry about it)

Our final method for identifying an outlier is ***Chauvenet’s criterion***. Unlike Dixon’s Q-Test and Grubb’s test, you can apply this method to any distribution as long as you know how to calculate the probability for a particular outcome. Chauvenet’s criterion states that we can reject a data point if the probability of obtaining the data point’s value is less than $(2n)^{-1}$, where n is the size of the sample. For example, if n = 10, a result with a probability of less than $(2 \times 10)^{-1}$, or 0.05, is considered an outlier.

To calculate a potential outlier’s probability we first calculate its standardized deviation, z

$$z = \frac{|X_{out} - \overline{X}|}{s}$$

where X_{out} is the potential outlier, $\overline{X}$ is the sample’s mean and s is the sample’s standard deviation. Note that this equation is identical to the equation for G_{exp} in the Grubb’s test. For a normal distribution, we can find the probability of obtaining a value of z using the probability table in Appendix 3.

You also can adopt a more stringent requirement for rejecting data. When using the Grubb’s test, for example, the ISO 5752 guidelines suggests retaining a value if the probability for rejecting it is greater than $\alpha = 0.05$, and flagging a value as a “straggler” if the probability for rejecting it is between $\alpha = 0.05$ and $\alpha = 0.01$. A “straggler” is retained unless there is compelling reason for its rejection. The guidelines recommend using $\alpha = 0.01$ as the minimum criterion for rejecting a possible outlier.

Testing for outliers can provide useful information if we try to understand the source of the suspected outlier. For example, the outlier in Table 1.8.1 represents a significant change in the mass of a penny (an approximately 17% decrease in mass), which is the

result of a change in the composition of the U.S. penny. In 1982 the composition of a U.S. penny changed from a brass alloy that was 95% w/w Cu and 5% w/w Zn (with a nominal mass of 3.1 g), to a pure zinc core covered with copper (with a nominal mass of 2.5 g) [Richardson, T. H. *J. Chem. Educ.* **1991**, *68*, 310–311]. The pennies in Table 1.8.1 , therefore, were drawn from different populations.

This page titled 1.8: Statistical Methods for Normal Distributions is shared under a CC BY-NC-SA 4.0 license and was authored, remixed, and/or curated by Kathryn Davis.

- **4.6: Statistical Methods for Normal Distributions** by David Harvey is licensed CC BY-NC-SA 4.0.

CHAPTER OVERVIEW

2: The Return of Stoichiometry

2.1: Concentration

2.2: Stoichiometric Calculations

2.3: Preparing Solutions

This page titled 2: The Return of Stoichiometry is shared under a not declared license and was authored, remixed, and/or curated by Kathryn Davis.

2.1: Concentration

Concentration is a general measurement unit that reports the amount of solute present in a known amount of solution or solvent

$$\text{concentration} = \frac{\text{amount of solute}}{\text{amount of solution}} \tag{2.1.1}$$

Although we associate the terms "solute" and "solution" with liquid samples, we can extend their use to gas-phase and solid-phase samples as well. Table 2.1.1 lists the most common units of concentration.

Table 2.1.1 : Common Units for Reporting Concentration

Name	Units	Symbol
molarity	$\frac{\text{moles solute}}{\text{liters solution}}$	M
formality	$\frac{\text{moles solute}}{\text{liters solution}}$	F
normality	$\frac{\text{equivalents solute}}{\text{liters solution}}$	N
molality	$\frac{\text{moles solute}}{\text{kilograms solvent}}$	m
weight percent	$\frac{\text{grams solute}}{\text{100 grams solution}}$	% w/w
volume percent	$\frac{\text{mL solute}}{\text{100 mL solution}}$	% v/v
weight-to-volume percent	$\frac{\text{grams solute}}{\text{100 mL solution}}$	% w/v
parts per million	$\frac{\text{grams solute}}{10^6 \text{ grams solution}}$	ppm
parts per billion	$\frac{\text{grams solute}}{10^9 \text{ grams solution}}$	ppb

An alternative expression for weight percent is

$$\frac{\text{grams solute}}{\text{grams solution}} \times 100$$

You can use similar alternative expressions for volume percent and for weight-to-volume percent.

Molarity and Formality

Both molarity and formality express concentration as moles of solute per liter of solution; however, there is a subtle difference between them. ***Molarity*** is the concentration of a particular chemical species. ***Formality***, on the other hand, is a substance's total concentration without regard to its specific chemical form. There is no difference between a compound's molarity and formality if it dissolves without dissociating into ions. The formal concentration of a solution of glucose, for example, is the same as its molarity.

For a compound that ionizes in solution, such as $CaCl_2$, molarity and formality are different. When we dissolve 0.1 moles of $CaCl_2$ in 1 L of water, the solution contains 0.1 moles of Ca^{2+} and 0.2 moles of Cl^-. The molarity of $CaCl_2$, therefore, is zero since there is no undissociated $CaCl_2$ in solution; instead, the solution is 0.1 M in Ca^{2+} and 0.2 M in Cl^-. The formality of $CaCl_2$, however, is 0.1 F since it represents the total amount of $CaCl_2$ in solution. This more rigorous definition of molarity, for better or worse, largely is ignored in the current literature, as it is in this textbook. When we state that a solution is 0.1 M $CaCl_2$ we understand it to consist of Ca^{2+} and Cl^- ions. We will reserve the unit of formality to situations where it provides a clearer description of solution chemistry.

Molarity is used so frequently that we use a symbolic notation to simplify its expression in equations and in writing. Square brackets around a species indicate that we are referring to that species' molarity. Thus, $[Ca^{2+}]$ is read as "the molarity of calcium

ions."

> For a solute that dissolves without undergoing ionization, molarity and formality have the same value. A solution that is 0.0259 M in glucose, for example, is 0.0259 F in glucose as well.

Normality

Normality is a concentration unit that no longer is in common use; however, because you may encounter normality in older handbooks of analytical methods, it is helpful to understand its meaning. ***Normality*** defines concentration in terms of an equivalent, which is the amount of one chemical species that reacts stoichiometrically with another chemical species. Note that this definition makes an equivalent, and thus normality, a function of the chemical reaction in which the species participates. Although a solution of H_2SO_4 has a fixed molarity, its normality depends on how it reacts. You will find a more detailed treatment of normality in Appendix 1.

> One handbook that still uses normality is *Standard Methods for the Examination of Water and Wastewater*, a joint publication of the American Public Health Association, the American Water Works Association, and the Water Environment Federation. This handbook is one of the primary resources for the environmental analysis of water and wastewater.

Molality

Molality is used in thermodynamic calculations where a temperature independent unit of concentration is needed. Molarity is based on the volume of solution that contains the solute. Since density is a temperature dependent property, a solution's volume, and thus its molar concentration, changes with temperature. By using the solvent's mass in place of the solution's volume, the resulting concentration becomes independent of temperature.

Weight, Volume, and Weight-to-Volume Percent

Weight percent (% w/w), ***volume percent*** (% v/v) and ***weight-to-volume percent*** (% w/v) express concentration as the units of solute present in 100 units of solution. A solution that is 1.5% w/v NH_4NO_3, for example, contains 1.5 gram of NH_4NO_3 in 100 mL of solution.

Parts Per Million and Parts Per Billion

Parts per million (ppm) and ***parts per billion*** (ppb) are ratios that give the grams of solute in, respectively, one million or one billion grams of sample. For example, a sample of steel that is 450 ppm in Mn contains 450 μg of Mn for every gram of steel. If we approximate the density of an aqueous solution as 1.00 g/mL, then we can express solution concentrations in ppm or ppb using the following relationships.

$$\text{ppm} = \frac{\mu\text{g}}{\text{g}} = \frac{\text{mg}}{\text{L}} = \frac{\mu\text{g}}{\text{mL}} \qquad \text{ppb} = \frac{\text{ng}}{\text{g}} = \frac{\mu\text{g}}{\text{L}} = \frac{\text{ng}}{\text{mL}}$$

For gases a part per million usually is expressed as a volume ratio; for example, a helium concentration of 6.3 ppm means that one liter of air contains 6.3 μL of He.

> You should be careful when using parts per million and parts per billion to express the concentration of an aqueous solute. The difference between a solute's concentration in mg/L and ng/g, for example, is significant if the solution's density is not 1.00 g/mL. For this reason many organizations advise against using the abbreviation ppm and ppb (see section 7.10.3 at www.nist.gov). If in doubt, include the exact units, such as 0.53 μg Pb^{2+}/L for the concentration of lead in a sample of seawater.

Converting Between Concentration Units

The most common ways to express concentration in analytical chemistry are molarity, weight percent, volume percent, weight-to-volume percent, parts per million and parts per billion. The general definition of concentration in Equation 2.1.1 makes it is easy to convert between concentration units. From there, it's all about detailed attention to unit analysis.

Example 2.1.1

A concentrated solution of ammonia is 28.0% w/w NH_3 and has a density of 0.899 g/mL. What is the molar concentration of NH_3 in this solution?

Solution

$$\frac{28.0\text{ g NH}_3}{100\text{ g soln}} \times \frac{0.899\text{ g soln}}{\text{ml soln}} \times \frac{1\text{ mol NH}_3}{17.03\text{ g NH}_3} \times \frac{1000\text{mL}}{\text{L}} = 14.8\text{ M}$$

Example 2.1.2

The maximum permissible concentration of chloride ion in a municipal drinking water supply is 2.50×10^2 ppm Cl^-. When the supply of water exceeds this limit it often has a distinctive salty taste. What is the equivalent molar concentration of Cl^-?

Solution

$$\frac{2.50 \times 10^2\text{ mg Cl}^-}{\text{L}} \times \frac{1\text{ g}}{1000\text{ mg}} \times \frac{1\text{ mol Cl}^-}{35.453\text{ gCl}^-} = 7.05 \times 10^{-3}\text{ M}$$

Exercise 2.1.1

Which solution—0.50 M NaCl or 0.25 M $SrCl_2$—has the larger concentration when expressed in mg/mL?

Answer

The concentrations of the two solutions are

$$\frac{0.50\text{ mol NaCl}}{\text{L}} \times \frac{58.44\text{ g NaCl}}{\text{mol NaCl}} \times \frac{10^6\ \mu\text{g}}{\text{g}} \times \frac{1\text{L}}{1000\text{ mL}} = 2.9 \times 10^4\ \mu\text{g/mL NaCl}$$

$$\frac{0.25\text{ mol SrCl}_2}{\text{L}} \times \frac{158.5\text{ g SrCl}_2}{\text{mol SrCl}_2} \times \frac{10^6\ \mu\text{g}}{\text{g}} \times \frac{1\text{L}}{1000\text{ mL}} = 4.0 \times 10^4\ \mu\text{g/ml SrCl}_2$$

The solution of $SrCl_2$ has the larger concentration when it is expressed in µg/mL instead of in mol/L.

This page titled 2.1: Concentration is shared under a CC BY-NC-SA 4.0 license and was authored, remixed, and/or curated by Kathryn Davis.

- **2.2: Concentration** by David Harvey is licensed CC BY-NC-SA 4.0.

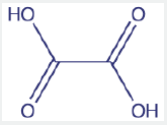
2.2: Stoichiometric Calculations

A balanced reaction, which defines the stoichiometric relationship between the moles of reactants and the moles of products, provides the basis for many analytical calculations. Consider, for example, an analysis for oxalic acid, $H_2C_2O_4$, in which Fe^{3+} oxidizes oxalic acid to CO_2

$$2Fe^{3+}(aq) + H_2C_2O_4(aq) + 2H_2O(l) \longrightarrow 2Fe^{2+}(aq) + 2CO_2(g) + 2H_3O^+(aq)$$

The balanced reaction shows us that one mole of oxalic acid reacts with two moles of Fe^{3+}. As shown in the following example, we can use this balanced reaction to determine the amount of $H_2C_2O_4$ in a sample of rhubarb if we know the moles of Fe^{3+} needed to react completely with oxalic acid.

In sufficient amounts, oxalic acid, the structure for which is shown to the right, is toxic. At lower physiological concentrations it leads to the formation of kidney stones. The leaves of the rhubarb plant contain relatively high concentrations of oxalic acid. The stalk, which many individuals enjoy eating, contains much smaller concentrations of oxalic acid.



In the examples that follow, note that we retain an extra significant figure throughout the calculation, rounding to the correct number of significant figures at the end. We will follow this convention in any calculation that involves more than one step. If we forget that we are retaining an extra significant figure, we might report the final answer with one too many significant figures. Here we mark the extra digit in **red** for emphasis. Be sure you pick a system for keeping track of significant figures.

Example 2.3.1

The amount of oxalic acid in a sample of rhubarb was determined by reacting with Fe^{3+}. After extracting a 10.62 g of rhubarb with a solvent, oxidation of the oxalic acid required 36.44 mL of 0.0130 M Fe^{3+}. What is the weight percent of oxalic acid in the sample of rhubarb?

Solution

We begin by calculating the moles of Fe^{3+} used in the reaction

$$\frac{0.0130 \text{ mol } Fe^{3+}}{\text{L}} \times 0.03644 \text{ M} = 4.737 \times 10^{-4} \text{ mol } Fe^{3+}$$

The moles of oxalic acid reacting with the Fe^{3+}, therefore, is

$$4.737 \times 10^{-4} \text{ mol } Fe^{3+} \times \frac{1 \text{ mol } H_2C_2O_4}{2 \text{ mol } Fe^{3+}} = 2.368 \times 10^{-4} \text{ mol } H_2C_2O_4$$

Converting the moles of oxalic acid to grams of oxalic acid

$$2.368 \times 10^{-4} \text{ mol } H_2C_2O_4 \times \frac{90.03 \text{ g } H_2C_2O_4}{\text{mol } H_2C_2O_4} = 2.132 \times 10^{-2} \text{ g } H_2C_2O_4$$

and calculating the weight percent gives the concentration of oxalic acid in the sample of rhubarb as

$$\frac{2.132 \times 10^{-2} \text{ g } H_2C_2O_4}{10.62 \text{ g rhubarb}} \times 100 = 0.201 H_2C_2O_4$$

Exercise 2.3.1

You can dissolve a precipitate of AgBr by reacting it with $Na_2S_2O_3$, as shown here.

$$AgBr(s) + 2Na_2S_2O_3(aq) \longrightarrow Ag(S_2O_3)_2^{3-}(aq) + Br^-(aq) + 4Na^+(aq)$$

How many mL of 0.0138 M $Na_2S_2O_3$ do you need to dissolve 0.250 g of AgBr?

Answer

First, we find the moles of AgBr

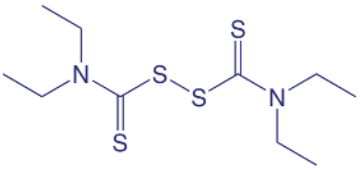
$$0.250 \text{ g AgBr} \times \frac{1 \text{ mol AgBr}}{187.8 \text{ g AgBr}} = 1.331 \times 10^{-3} \text{ mol AgBr}$$

and then the moles and volume of $Na_2S_2O_3$

$$1.331 \times 10^{-3} \text{ mol AgBr} \times \frac{2 \text{ mol } Na_2S_2O_3}{\text{mol AgBr}} = 2.662 \times 10^{-3} \text{ mol } Na_2S_2O_3$$

$$2.662 \times 10^{-3} \text{ mol } Na_2S_2O_3 \times \frac{1 \text{ L}}{0.0138 \text{ mol } Na_2S_2O_3} \times \frac{1000 \text{ mL}}{\text{L}} = 193 \text{ mL}$$

The analyte in Example 2.3.1 , oxalic acid, is in a chemically useful form because there is a reagent, Fe^{3+}, that reacts with it quantitatively. In many analytical methods, we first must convert the analyte into a more accessible form before we can complete the analysis. For example, one method for the quantitative analysis of disulfiram, $C_{10}H_{20}N_2S_4$—the active ingredient in the drug Antabuse, and whose structure is shown to the right —requires that we first convert the sulfur to SO_2 by combustion, and then oxidize the SO_2 to H_2SO_4 by bubbling it through a solution of H_2O_2. When the conversion is complete, the amount of H_2SO_4 is determined by titrating with NaOH.



To convert the moles of NaOH used in the titration to the moles of disulfiram in the sample, we need to know the stoichiometry of each reaction. Writing a balanced reaction for H_2SO_4 and NaOH is straightforward

$$H_2SO_4(aq) + 2NaOH(aq) \longrightarrow 2H_2O(l) + Na_2SO_4(aq)$$

but the balanced reactions for the oxidations of $C_{10}H_{20}N_2S_4$ to SO_2, and of SO_2 to H_2SO_4 are not as immediately obvious. Although we can balance these redox reactions, it is often easier to deduce the overall stoichiometry by using a little chemical logic.

Example 2.3.2

An analysis for disulfiram, $C_{10}H_{20}N_2S_4$, in Antabuse is carried out by oxidizing the sulfur to H_2SO_4 and titrating the H_2SO_4 with NaOH. If a 0.4613-g sample of Antabuse requires 34.85 mL of 0.02500 M NaOH to titrate the H_2SO_4, what is the %w/w disulfiram in the sample?

Solution

Calculating the moles of H_2SO_4 is easy—first, we calculate the moles of NaOH used in the titration

$$(0.02500 \text{ M}) \times (0.03485 \text{ L}) = 8.7125 \times 10^{-4} \text{ mol NaOH}$$

and then we use the titration reaction's stoichiometry to calculate the corresponding moles of H_2SO_4.

$$8.7125 \times 10^{-4} \text{ mol NaOH} \times \frac{1 \text{ mol } H_2SO_4}{2 \text{ mol NaOH}} = 4.3562 \times 10^{-4} \text{ mol } H_2SO_4$$

Here is where we use a little chemical logic. Instead of balancing the reactions for the combustion of $C_{10}H_{20}N_2S_4$ to SO_2 and for the subsequent oxidation of SO_2 to H_2SO_4, we recognize that a conservation of mass requires that all the sulfur in $C_{10}H_{20}N_2S_4$ ends up in the H_2SO_4; thus

$$4.3562 \times 10^{-4} \text{ mol } H_2SO_4 \times \frac{1 \text{ mol S}}{\text{mol } H_2SO_4} \times \frac{1 \text{ mol } C_{10}H_{20}N_2S_4}{4 \text{ mol S}} = 1.0890 \times 10^{-4} \text{ mol } C_{10}H_{20}N_2S_4$$

$$1.0890 \times 10^{-4} \text{ mol } C_{10}H_{20}N_2S_4 \times \frac{296.54 \text{ g } C_{10}H_{20}N_2S_4}{\text{mol } C_{10}H_{20}N_2S_4} = 0.032293 \text{ g } C_{10}H_{20}N_2S_4$$

$$\frac{0.032293 \text{ g } C_{10}H_{20}N_2S_4}{0.4613 \text{ g sample}} \times 100 = 7.000 C_{10}H_{20}N_2S_4$$

A conservation of mass is the essence of stoichiometry!

This page titled 2.2: Stoichiometric Calculations is shared under a CC BY-NC-SA 4.0 license and was authored, remixed, and/or curated by Kathryn Davis.

- **2.3: Stoichiometric Calculations** by David Harvey is licensed CC BY-NC-SA 4.0.

2.3: Preparing Solutions

Preparing a solution of known concentration is perhaps the most common activity in any analytical lab. The method for measuring out the solute and the solvent depend on the desired concentration and how exact the solution's concentration needs to be known. Pipets and volumetric flasks are used when we need to know a solution's exact concentration; graduated cylinders, beakers, and/or reagent bottles suffice when a concentrations need only be approximate. Two methods for preparing solutions are described in this section.

Preparing Stock Solutions

A ***stock solution*** is prepared by weighing out an appropriate portion of a pure solid or by measuring out an appropriate volume of a pure liquid, placing it in a suitable flask, and diluting to a known volume. Exactly how one measure's the reagent depends on the desired concentration unit. For example, to prepare a solution with a known molarity you weigh out an appropriate mass of the reagent, dissolve it in a portion of solvent, and bring it to the desired volume. To prepare a solution where the solute's concentration is a volume percent, you measure out an appropriate volume of solute and add sufficient solvent to obtain the desired total volume.

Example 2.5.1

Describe how to prepare the following three solutions: (a) 500 mL of approximately 0.20 M NaOH using solid NaOH; (b) 1 L of 150.0 ppm Cu^{2+} using Cu metal; and (c) 2 L of 4% v/v acetic acid using concentrated glacial acetic acid (99.8% w/w acetic acid).

Solution

(a) Because the desired concentration is known to two significant figures, we do not need to measure precisely the mass of NaOH or the volume of solution. The desired mass of NaOH is

$$\frac{0.20 \text{ mol NaOH}}{\text{L}} \times \frac{40.0 \text{ g NaOH}}{\text{mol NaOH}} \times 0.50 \text{ L} = 4.0 \text{ g NaOH}$$

To prepare the solution, place 4.0 grams of NaOH, weighed to the nearest tenth of a gram, in a bottle or beaker and add approximately 500 mL of water.

(b) Since the desired concentration of Cu^{2+} is given to four significant figures, we must measure precisely the mass of Cu metal and the final solution volume. The desired mass of Cu metal is

$$\frac{150.0 \text{ mg Cu}}{\text{L}} \times 1.000 \text{ M} \times \frac{1 \text{ g}}{1000 \text{ mg}} = 0.1500 \text{ g Cu}$$

To prepare the solution, measure out exactly 0.1500 g of Cu into a small beaker and dissolve it using a small portion of concentrated HNO_3. To ensure a complete transfer of Cu^{2+} from the beaker to the volumetric flask—what we call a ***quantitative transfer***—rinse the beaker several times with small portions of water, adding each rinse to the volumetric flask. Finally, add additional water to the volumetric flask's calibration mark.

(c) The concentration of this solution is only approximate so it is not necessary to measure exactly the volumes, nor is it necessary to account for the fact that glacial acetic acid is slightly less than 100% w/w acetic acid (it is approximately 99.8% w/w). The necessary volume of glacial acetic acid is

$$\frac{4 \text{ mL } CH_3COOH}{100 \text{ mL}} \times 2000 \text{ mL} = 80 \text{ mL } CH_3COOH$$

To prepare the solution, use a graduated cylinder to transfer 80 mL of glacial acetic acid to a container that holds approximately 2 L and add sufficient water to bring the solution to the desired volume.

Exercise 2.5.1

Provide instructions for preparing 500 mL of 0.1250 M $KBrO_3$.

Answer

Preparing 500 mL of 0.1250 M $KBrO_3$ requires

$$0.5000\ \text{L} \times \frac{0.1250\ \text{mol KBrO}_3}{\text{L}} \times \frac{167.00\ \text{g KBrO}_3}{\text{mol KBrO}_3} = 10.44\ \text{g KBrO}_3$$

Because the concentration has four significant figures, we must prepare the solution using volumetric glassware. Place a 10.44 g sample of $KBrO_3$ in a 500-mL volumetric flask and fill part way with water. Swirl to dissolve the $KBrO_3$ and then dilute with water to the flask's calibration mark.

Preparing Solutions by Dilution

Solutions are often prepared by diluting a more concentrated stock solution. A known volume of the stock solution is transferred to a new container and brought to a new volume. Since the total amount of solute is the same before and after dilution, we know that

$$C_o \times V_o = C_d \times V_d \tag{2.3.1}$$

where C_o is the stock solution's concentration, V_o is the volume of stock solution being diluted, C_d is the dilute solution's concentration, and V_d is the volume of the dilute solution. Again, the type of glassware used to measure V_o and V_d depends on how precisely we need to know the solution's concentration.

Note that Equation 2.3.1 applies only to those concentration units that are expressed in terms of the solution's volume, including molarity, formality, normality, volume percent, and weight-to-volume percent. It also applies to weight percent, parts per million, and parts per billion if the solution's density is 1.00 g/mL. We cannot use Equation 2.3.1 if we express concentration in terms of molality as this is based on the mass of solvent, not the volume of solution. See Rodríquez-López, M.; Carrasquillo, A. *J. Chem. Educ.* **2005**, *82*, 1327-1328 for further discussion.

Example 2.5.2

A laboratory procedure calls for 250 mL of an approximately 0.10 M solution of NH_3. Describe how you would prepare this solution using a stock solution of concentrated NH_3 (14.8 M).

Solution

Substituting known values into Equation 2.3.1

$$14.8\ \text{M} \times V_o = 0.10\ \text{M} \times 250\ \text{mL}$$

and solving for V_o gives 1.7 mL. Since we are making a solution that is approximately 0.10 M NH_3, we can use a graduated cylinder to measure the 1.7 mL of concentrated NH_3, transfer the NH_3 to a beaker, and add sufficient water to give a total volume of approximately 250 mL.

Although usually we express molarity as mol/L, we can express the volumes in mL if we do so both for both V_o and V_d.

Exercise 2.5.2

To prepare a standard solution of Zn^{2+} you dissolve a 1.004 g sample of Zn wire in a minimal amount of HCl and dilute to volume in a 500-mL volumetric flask. If you dilute 2.000 mL of this stock solution to 250.0 mL, what is the concentration of Zn^{2+}, in μg/mL, in your standard solution?

Answer

The first solution is a stock solution, which we then dilute to prepare the standard solution. The concentration of Zn^{2+} in the stock solution is

$$\frac{1.004\ \text{g Zn}^{2+}}{500.0\ \text{mL}} \times \frac{10^6\ \mu\text{g}}{\text{g}} = 2008\ \mu\text{g Zn}^{2+}/\text{mL}$$

To find the concentration of the standard solution we use Equation 2.3.1

$$\frac{2008\ \mu g\ Zn^{2+}}{mL} \times 2.000\ mL = C_d \times 250.0\ mL$$

where C_d is the standard solution's concentration. Solving gives a concentration of 16.06 μg Zn^{2+}/mL.

As shown in the following example, we can use Equation 2.3.1 to calculate a solution's original concentration using its known concentration after dilution.

Example 2.5.3

A sample of an ore was analyzed for Cu^{2+} as follows. A 1.25 gram sample of the ore was dissolved in acid and diluted to volume in a 250-mL volumetric flask. A 20 mL portion of the resulting solution was transferred by pipet to a 50-mL volumetric flask and diluted to volume. An analysis of this solution gives the concentration of Cu^{2+} as 4.62 μg/mL. What is the weight percent of Cu in the original ore?

Solution

Substituting known values (with significant figures appropriate for pipets and volumetric flasks) into Equation 2.3.1

$$(C_{Cu})_o \times 20.00\ mL = 4.62\ \mu g/mL\ Cu^{2+} \times 50.00\ mL$$

and solving for $(C_{Cu})_o$ gives the original concentration as 11.55 μg/mL Cu^{2+}. To calculate the grams of Cu^{2+} we multiply this concentration by the total volume

$$\frac{11.55 \mu g\ Cu^{2+}}{mL} \times 250.0\ mL \times \frac{1\ g}{10^6\ \mu g} = 2.888 \times 10^{-3}\ g\ Cu^{2+}$$

The weight percent Cu is

$$\frac{2.888 \times 10^{-3}\ g\ Cu^{2+}}{1.25\ g\ sample} \times 100 = 0.231 Cu^{2+}$$

This page titled 2.3: Preparing Solutions is shared under a CC BY-NC-SA 4.0 license and was authored, remixed, and/or curated by Kathryn Davis.

- **2.5: Preparing Solutions** by David Harvey is licensed CC BY-NC-SA 4.0.

CHAPTER OVERVIEW

3: Acid-Base Equilibria Affect Solution Conditions

3.1: Acid–Base Titrations

3.2: Ladder Diagrams for Acid-Base Equilibria

3.3: Solving Acid-Base Equilibrium Problems

3.4: Buffer Solutions

This page titled 3: Acid-Base Equilibria Affect Solution Conditions is shared under a not declared license and was authored, remixed, and/or curated by Kathryn Davis.

3.1: Acid–Base Titrations

Before 1800, most ***acid–base titrations*** used H_2SO_4, HCl, or HNO_3 as acidic titrants, and K_2CO_3 or Na_2CO_3 as basic titrants. A titration's end point was determined using litmus as an indicator, which is red in acidic solutions and blue in basic solutions, or by the cessation of CO_2 effervescence when neutralizing CO_3^{2-}. Early examples of acid–base titrimetry include determining the acidity or alkalinity of solutions, and determining the purity of carbonates and alkaline earth oxides.

> The determination of acidity and alkalinity continue to be important applications of acid–base titrimetry. We will take a closer look at these applications later in this section.

Three limitations slowed the development of acid–base titrimetry: the lack of a strong base titrant for the analysis of weak acids, the lack of suitable indicators, and the absence of a theory of acid–base reactivity. The introduction, in 1846, of NaOH as a strong base titrant extended acid–base titrimetry to the determination of weak acids. The synthesis of organic dyes provided many new indicators. Phenolphthalein, for example, was first synthesized by Bayer in 1871 and used as an indicator for acid–base titrations in 1877.

Despite the increased availability of indicators, the absence of a theory of acid–base reactivity made it difficult to select an indicator. The development of equilibrium theory in the late 19th century led to significant improvements in the theoretical understanding of acid–base chemistry, and, in turn, of acid–base titrimetry. Sørenson's establishment of the pH scale in 1909 provided a rigorous means to compare indicators. The determination of acid–base dissociation constants made it possible to calculate a theoretical titration curve, as outlined by Bjerrum in 1914. For the first time analytical chemists had a rational method for selecting an indicator, making acid–base titrimetry a useful alternative to gravimetry.

Acid–Base Titration Curves

In the overview to this chapter we noted that a titration's end point should coincide with its equivalence point. To understand the relationship between an acid–base titration's end point and its equivalence point we must know how the titrand's pH changes during a titration. In this section we will learn how to calculate a titration curve using the equilibrium calculations from Chapter 6. We also will learn how to sketch a good approximation of any acid–base titration curve using a limited number of simple calculations.

Titrating Strong Acids and Strong Bases

For our first titration curve, let's consider the titration of 50.0 mL of 0.100 M HCl using a titrant of 0.200 M NaOH. When a strong base and a strong acid react the only reaction of importance is

$$H_3O^+(aq) + OH^-(aq) \rightarrow 2H_2O(l) \tag{3.1.1}$$

> Although we have not written reaction 3.1.1 as an equilibrium reaction, it is at equilibrium; however, because its equilibrium constant is large—it is $(K_w)^{-1}$ or 1.00×10^{14}—we can treat reaction 3.1.1 as though it goes to completion.

The first task is to calculate the volume of NaOH needed to reach the equivalence point, V_{eq}. At the equivalence point we know from reaction 3.1.1 that

$$\text{moles HCl} = \text{moles NaOH}$$
$$M_a \times V_a = M_b \times V_b$$

where the subscript '*a*' indicates the acid, HCl, and the subscript '*b*' indicates the base, NaOH. The volume of NaOH needed to reach the equivalence point is

$$V_{eq} = V_b = \frac{M_a V_a}{M_b} = \frac{(0.100\ \text{M})(50.0\ \text{mL})}{(0.200\ \text{M})} = 25.0\ \text{mL}$$

Before the equivalence point, HCl is present in excess and the pH is determined by the concentration of unreacted HCl. At the start of the titration the solution is 0.100 M in HCl, which, because HCl is a strong acid, means the pH is

$$\text{pH} = -\log\left[\text{H}_3\text{O}^+\right] = -\log\left[\text{HCl}\right] = -\log(0.100) = 1.00$$

After adding 10.0 mL of NaOH the concentration of excess HCl is

$$[\text{HCl}] = \frac{(\text{mol HCl})_{\text{initial}} - (\text{mol NaOH})_{\text{added}}}{\text{total volume}} = \frac{M_a V_a - M_b V_b}{V_a + V_b}$$

$$[\text{HCl}] = \frac{(0.100\ \text{M})(50.0\ \text{mL}) - (0.200\ \text{M})(10.0\ \text{mL})}{50.0\ \text{mL} + 10.0\ \text{mL}} = 0.0500\ \text{M}$$

and the pH increases to 1.30.

At the equivalence point the moles of HCl and the moles of NaOH are equal. Since neither the acid nor the base is in excess, the pH is determined by the dissociation of water.

$$K_w = 1.00 \times 10^{-14} = \left[\text{H}_3\text{O}^+\right]\left[\text{OH}^-\right] = \left[\text{H}_3\text{O}^+\right]^2$$
$$\left[\text{H}_3\text{O}^+\right] = 1.00 \times 10^{-7}$$

Thus, the pH at the equivalence point is 7.00.

For volumes of NaOH greater than the equivalence point, the pH is determined by the concentration of excess OH^-. For example, after adding 30.0 mL of titrant the concentration of OH^- is

$$[\text{OH}^-] = \frac{(\text{mol NaOH})_{\text{added}} - (\text{mol HCl})_{\text{initial}}}{\text{total volume}} = \frac{M_b V_b - M_a V_a}{V_a + V_b}$$

$$[\text{OH}^-] = \frac{(0.200\ \text{M})(30.0\ \text{mL}) - (0.100\ \text{M})(50.0\ \text{mL})}{30.0\ \text{mL} + 50.0\ \text{mL}} = 0.0125\ \text{M}$$

To find the concentration of H_3O^+ we use the K_w expression

$$\left[\text{H}_3\text{O}^+\right] = \frac{K_\text{w}}{\left[\text{OH}^-\right]} = \frac{1.00 \times 10^{-14}}{0.0125} = 8.00 \times 10^{-13}\ \text{M}$$

to find that the pH is 12.10. Table 3.1.1 and Figure 3.1.1 show additional results for this titration curve. You can use this same approach to calculate the titration curve for the titration of a strong base with a strong acid, except the strong base is in excess before the equivalence point and the strong acid is in excess after the equivalence point.

Table 3.1.1 . Titration of 50.0 mL of 0.100 M HCl with 0.200 M NaOH

volume of NaOH (mL)	pH	volume of NaOH (mL)	pH
0.00	1.00	26.0	11.42
5.00	1.14	28.0	11.89
10.0	1.30	30.0	12.10
15.0	1.51	35.0	12.37
20.0	1.85	40.0	12.52
22.0	2.08	45.0	12.63
24.0	2.57	50.0	12.70
25.0	7.00		

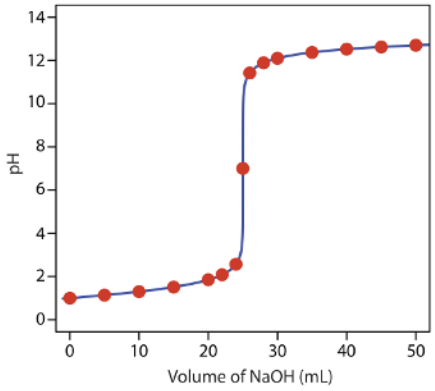


Figure 3.1.1 . Titration curve for the titration of 50.0 mL of 0.100 M HCl with 0.200 M NaOH. The red points correspond to the data in Table 3.1.1 . The blue line shows the complete titration curve.

Exercise 3.1.1

Construct a titration curve for the titration of 25.0 mL of 0.125 M NaOH with 0.0625 M HCl.

Answer

The volume of HCl needed to reach the equivalence point is

$$V_{eq} = V_a = \frac{M_b V_b}{M_a} = \frac{(0.125\ \text{M})(25.0\ \text{mL})}{(0.0625\ \text{M})} = 50.0\ \text{mL}$$

Before the equivalence point, NaOH is present in excess and the pH is determined by the concentration of unreacted OH^-. For example, after adding 10.0 mL of HCl

$$[OH^-] = \frac{(0.125\ \text{M})(25.0\ \text{mL}) - (0.0625\text{M})(10.0\ \text{mL})}{25.0\ \text{mL} + 10.0\ \text{mL}} = 0.0714\ \text{M}$$

$$[H_3O^+] = \frac{K_w}{[OH^-]} = \frac{1.00 \times 10^{-14}}{0.0714\ \text{M}} = 1.40 \times 10^{-13}\ \text{M}$$

the pH is 12.85.

For the titration of a strong base with a strong acid the pH at the equivalence point is 7.00.

For volumes of HCl greater than the equivalence point, the pH is determined by the concentration of excess HCl. For example, after adding 70.0 mL of titrant the concentration of HCl is

$$[HCl] = \frac{(0.0625\ \text{M})(70.0\ \text{mL}) - (0.125\ \text{M})(25.0\ \text{mL})}{70.0\ \text{mL} + 25.0\ \text{mL}} = 0.0132\ \text{M}$$

giving a pH of 1.88. Some additional results are shown here.

volume of HCl (mL)	pH	volume of HCl (mL)	pH
0	13.10	60	2.13
10	12.85	70	1.88
20	12.62	80	1.75
30	12.36	90	1.66
40	11.98	100	1.60
50	7.00		

Titrating a Weak Acid with a Strong Base

For this example, let's consider the titration of 50.0 mL of 0.100 M acetic acid, CH_3COOH, with 0.200 M NaOH. Again, we start by calculating the volume of NaOH needed to reach the equivalence point; thus

$$\text{mol } CH_3COOH = \text{mol NaOH}$$

$$M_a \times V_a = M_b \times V_b$$

$$V_{eq} = V_b = \frac{M_a V_a}{M_b} = \frac{(0.100\text{ M})(50.0\text{ mL})}{(0.200\text{ M})} = 25.0\text{ mL}$$

Before we begin the titration the pH is that for a solution of 0.100 M acetic acid. Because acetic acid is a weak acid, we calculate the pH using the method outlined in Chapter 6

$$CH_3COOH(aq) + H_2O(l) \rightleftharpoons H_3O^+(aq) + CH_3COO^-(aq)$$

$$K_a = \frac{[H_3O^+]\,[CH_3COO^-]}{[CH_3COOH]} = \frac{(x)(x)}{0.100 - x} = 1.75 \times 10^{-5}$$

finding that the pH is 2.88.

Adding NaOH converts a portion of the acetic acid to its conjugate base, CH_3COO^-.

$$CH_3COOH(aq) + OH^-(aq) \longrightarrow H_2O(l) + CH_3COO^-(aq) \tag{3.1.2}$$

> Because the equilibrium constant for reaction 3.1.2 is quite large
>
> $$K = K_a/K_w = 1.75 \times 10^9$$
>
> we can treat the reaction as if it goes to completion.

Any solution that contains comparable amounts of a weak acid, HA, and its conjugate weak base, A^-, is a buffer. As we learned in Chapter 6, we can calculate the pH of a buffer using the Henderson–Hasselbalch equation.

$$\text{pH} = \text{p}K_a + \log\frac{[A^-]}{[HA]}$$

Before the equivalence point the concentration of unreacted acetic acid is

$$[CH_3COOH] = \frac{(\text{mol } CH_3COOH)_{\text{initial}} - (\text{mol NaOH})_{\text{added}}}{\text{total volume}} = \frac{M_a V_a - M_b V_b}{V_a + V_b}$$

and the concentration of acetate is

$$[CH_3COO^-] = \frac{(\text{mol NaOH})_{\text{added}}}{\text{total volume}} = \frac{M_b V_b}{V_a + V_b}$$

For example, after adding 10.0 mL of NaOH the concentrations of CH_3COOH and CH_3COO^- are

$$[CH_3COOH] = \frac{(0.100\text{ M})(50.0\text{ mL}) - (0.200\text{ M})(10.0\text{ mL})}{50.0\text{ mL} + 10.0\text{ mL}} = 0.0500\text{ M}$$

$$[CH_3COO^-] = \frac{(0.200\text{ M})(10.0\text{ mL})}{50.0\text{ mL} + 10.0\text{ mL}} = 0.0333\text{ M}$$

which gives us a pH of

$$\text{pH} = 4.76 + \log\frac{0.0333\text{ M}}{0.0500\text{ M}} = 4.58$$

At the equivalence point the moles of acetic acid initially present and the moles of NaOH added are identical. Because their reaction effectively proceeds to completion, the predominate ion in solution is CH_3COO^-, which is a weak base. To calculate the pH we first determine the concentration of CH_3COO^-

$$[CH_3COO^-] = \frac{(\text{mol NaOH})_{\text{added}}}{\text{total volume}} = \frac{(0.200\ \text{M})(25.0\ \text{mL})}{50.0\ \text{mL} + 25.0\ \text{mL}} = 0.0667\ \text{M}$$

Alternatively, we can calculate acetate's concentration using the initial moles of acetic acid; thus

$$[CH_3COO^-] = \frac{(\text{mol } CH_3COOH)_{\text{initial}}}{\text{total volume}} = \frac{(0.100\ \text{M})(50.0\ \text{mL})}{50.0\ \text{mL} + 25.0\ \text{mL}} = 0.0667\ \text{M}$$

Next, we calculate the pH of the weak base as shown earlier in Chapter 6

$$CH_3COO^-(aq) + H_2O(l) \rightleftharpoons OH^-(aq) + CH_3COOH(aq)$$

$$K_b = \frac{[OH^-]\,[CH_3COOH]}{[CH_3COO^-]} = \frac{(x)(x)}{0.0667 - x} = 5.71 \times 10^{-10}$$

$$x = [OH^-] = 6.17 \times 10^{-6}\ \text{M}$$

$$[H_3O^+] = \frac{K_w}{[OH^-]} = \frac{1.00 \times 10^{-14}}{6.17 \times 10^{-6}} = 1.62 \times 10^{-9}\ \text{M}$$

finding that the pH at the equivalence point is 8.79.

After the equivalence point, the titrant is in excess and the titration mixture is a dilute solution of NaOH. We can calculate the pH using the same strategy as in the titration of a strong acid with a strong base. For example, after adding 30.0 mL of NaOH the concentration of OH^- is

$$[OH^-] = \frac{(0.200\ \text{M})(30.0\ \text{mL}) - (0.100\ \text{M})(50.0\ \text{mL})}{30.0\ \text{mL} + 50.0\ \text{mL}} = 0.0125\ \text{M}$$

$$[H_3O^+] = \frac{K_w}{[OH^-]} = \frac{1.00 \times 10^{-14}}{0.0125} = 8.00 \times 10^{-13}\ \text{M}$$

giving a pH of 12.10. Table 3.1.2 and Figure 3.1.2 show additional results for this titration. You can use this same approach to calculate the titration curve for the titration of a weak base with a strong acid, except the initial pH is determined by the weak base, the pH at the equivalence point by its conjugate weak acid, and the pH after the equivalence point by excess strong acid.

Table 3.1.2 . Titration of 50.0 mL of 0.100 M Acetic Acid with 0.200 M NaOH

volume of HCl (mL)	pH	volume of HCl (mL)	pH
0.00	2.88	26.0	11.43
5.00	4.16	28.0	11.89
10.0	4.58	30.0	12.10
15.0	4.94	35.0	12.37
20.0	5.36	40.0	12.52
22.0	5.63	45.0	12.63
24.0	6.14	50.0	12.70
25.0	8.79		

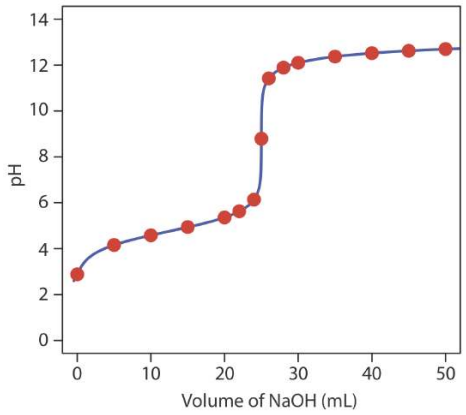


Figure 3.1.2 . Titration curve for the titration of 50.0 mL of 0.100 M CH_3COOH with 0.200 M NaOH. The red points correspond to the data in Table 3.1.2 . The blue line shows the complete titration curve.

Exercise 3.1.2

Construct a titration curve for the titration of 25.0 mL of 0.125 M NH_3 with 0.0625 M HCl.

Answer

The volume of HCl needed to reach the equivalence point is

$$V_{aq} = V_a = \frac{M_b V_b}{M_a} = \frac{(0.125\ \text{M})(25.0\ \text{mL})}{(0.0625\ \text{M})} = 50.0\ \text{mL}$$

Before adding HCl the pH is that for a solution of 0.100 M NH_3.

$$K_b = \frac{[OH^-]\,[NH_4^+]}{[NH_3]} = \frac{(x)(x)}{0.125 - x} = 1.75 \times 10^{-5}$$

$$x = [OH^-] = 1.48 \times 10^{-3}\ \text{M}$$

$$[H_3O^+] = \frac{K_w}{[OH^-]} = \frac{1.00 \times 10^{-14}}{1.48 \times 10^{-3}\ \text{M}} = 6.76 \times 10^{-12}\ \text{M}$$

The pH at the beginning of the titration, therefore, is 11.17.

Before the equivalence point the pH is determined by an NH_3/NH_4^+ buffer. For example, after adding 10.0 mL of HCl

$$[NH_3] = \frac{(0.125\ \text{M})(25.0\ \text{mL}) - (0.0625\ \text{M})(10.0\ \text{mL})}{25.0\ \text{mL} + 10.0\ \text{mL}} = 0.0714\ \text{M}$$

$$[NH_4^+] = \frac{(0.0625\ \text{M})(10.0\ \text{mL})}{25.0\ \text{mL} + 10.0\ \text{mL}} = 0.0179\ \text{M}$$

$$\text{pH} = 9.244 + \log \frac{0.0714\ \text{M}}{0.0179\ \text{M}} = 9.84$$

At the equivalence point the predominate ion in solution is NH_4^+. To calculate the pH we first determine the concentration of NH_4^+

$$[NH_4^+] = \frac{(0.125\ \text{M})(25.0\ \text{mL})}{25.0\ \text{mL} + 50.0\ \text{mL}} = 0.0417\ \text{M}$$

and then calculate the pH

$$K_a = \frac{[H_3O^+]\,[NH_3]}{[NH_4^+]} = \frac{(x)(x)}{0.0417 - x} = 5.70 \times 10^{-10}$$

obtaining a value of 5.31.

After the equivalence point, the pH is determined by the excess HCl. For example, after adding 70.0 mL of HCl

$$[\text{HCl}] = \frac{(0.0625\ \text{M})(70.0\ \text{mL}) - (0.125\ \text{M})(25.0\ \text{mL})}{70.0\ \text{mL} + 25.0\ \text{mL}} = 0.0132\ \text{M}$$

and the pH is 1.88. Some additional results are shown here.

volume of HCl (mL)	pH	volume of HCl (mL)	pH
0	11.17	60	2.13
10	9.84	70	1.88
20	9.42	80	1.75
30	9.07	90	1.66
40	8.64	100	1.60
50	5.31		

We can extend this approach for calculating a weak acid–strong base titration curve to reactions that involve multiprotic acids or bases, and mixtures of acids or bases. As the complexity of the titration increases, however, the necessary calculations become more time consuming. Not surprisingly, a variety of algebraic and spreadsheet approaches are available to aid in constructing titration curves.

The following papers provide information on algebraic approaches to calculating titration curves: (a) Willis, C. J. *J. Chem. Educ.* **1981**, *58*, 659–663; (b) Nakagawa, K. *J. Chem. Educ.* **1990**, *67*, 673–676; (c) Gordus, A. A. *J. Chem. Educ.* **1991**, *68*, 759–761; (d) de Levie, R. *J. Chem. Educ.* **1993**, *70*, 209–217; (e) Chaston, S. *J. Chem. Educ.* **1993**, *70*, 878–880; (f) de Levie, R. *Anal. Chem.* **1996**, *68*, 585–590.

The following papers provide information on the use of spreadsheets to generate titration curves: (a) Currie, J. O.; Whiteley, R. V. *J. Chem. Educ.* **1991**, *68*, 923–926; (b) Breneman, G. L.; Parker, O. J. *J. Chem. Educ.* **1992**, *69*, 46–47; (c) Carter, D. R.; Frye, M. S.; Mattson, W. A. *J. Chem. Educ.* **1993**, *70*, 67–71; (d) Freiser, H. *Concepts and Calculations in Analytical Chemistry*, CRC Press: Boca Raton, 1992.

Selecting and Evaluating the End Point

Earlier we made an important distinction between a titration's end point and its equivalence point. The difference between these two terms is important and deserves repeating. An **equivalence point,** which occurs when we react stoichiometrically equal amounts of the analyte and the titrant, is a theoretical not an experimental value. A titration's **end point** is an experimental result that represents our best estimate of the equivalence point. Any difference between a titration's equivalence point and its corresponding end point is a source of determinate error.

Where is the Equivalence Point?

Earlier we learned how to calculate the pH at the equivalence point for the titration of a strong acid with a strong base, and for the titration of a weak acid with a strong base. We also learned how to sketch a titration curve with only a minimum of calculations. Can we also locate the equivalence point without performing any calculations. The answer, as you might guess, often is yes!

For most acid–base titrations the inflection point—the point on a titration curve that has the greatest slope—very nearly coincides with the titration's equivalence point. The red arrows in Figure 3.1.4 , for example, identify the equivalence points for the titration curves in Example 3.1.1 . An inflection point actually precedes its corresponding equivalence point by a small amount, with the error approaching 0.1% for weak acids and weak bases with dissociation constants smaller than 10^{-9}, or for very dilute solutions [Meites, L.; Goldman, J. A. *Anal. Chim. Acta* **1963**, *29*, 472–479].

The principal limitation of an inflection point is that it must be present and easy to identify. For some titrations the inflection point is missing or difficult to find. Figure 3.1.5 , for example, demonstrates the affect of a weak acid's dissociation constant, K_a, on the shape of its titration curve. An inflection point is visible, even if barely so, for acid dissociation constants larger than 10^{-9}, but is missing when K_a is 10^{-11}.

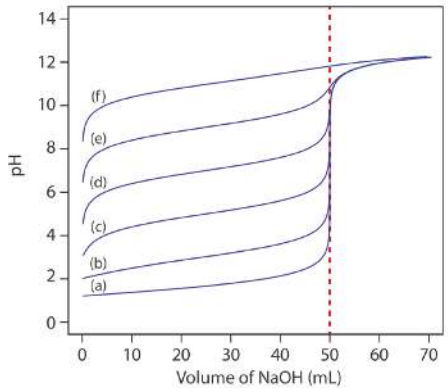


Figure 3.1.5 . Weak acid–strong base titration curves for the titration of 50.0 mL of 0.100 M HA with 0.100 M NaOH. The pK_a values for HA are (a) 1, (b) 3, (c) 5, (d) 7, (e) 9, and (f) 11. The dashed red line shows the equivalence point, which is 50.0 mL for all six analytes.

An inflection point also may be missing or difficult to see if the analyte is a multiprotic weak acid or weak base with successive dissociation constants that are similar in magnitude. To appreciate why this is true let's consider the titration of a diprotic weak acid, H_2A, with NaOH. During the titration the following two reactions occur.

$$\mathbf{H_2A}(aq) + \mathbf{OH^-}(aq) \longrightarrow \mathbf{H_2O}(l) + \mathbf{HA^-}(aq) \tag{3.1.3}$$

$$\mathbf{HA^-}(aq) + \mathbf{OH^-}(aq) \rightarrow \mathbf{H_2O}(l) + \mathbf{A^{2-}}(aq) \tag{3.1.4}$$

To see two distinct inflection points, reaction 3.1.3 must essentially be complete before reaction 3.1.4 begins.

Figure 3.1.6 shows titration curves for three diprotic weak acids. The titration curve for maleic acid, for which K_{a1} is approximately $\mathbf{20000\times}$ larger than K_{a2}, has two distinct inflection points. Malonic acid, on the other hand, has acid dissociation constants that differ by a factor of approximately 690. Although malonic acid's titration curve shows two inflection points, the first is not as distinct as the second. Finally, the titration curve for succinic acid, for which the two K_a values differ by a factor of only $\mathbf{27\times}$, has only a single inflection point that corresponds to the neutralization of $\mathbf{HC_2H_4O_4^-}$ to $\mathbf{C_2H_4O_4^{2-}}$. In general, we can detect separate inflection points when successive acid dissociation constants differ by a factor of at least 500 (a ΔK_a of at least 2.7).

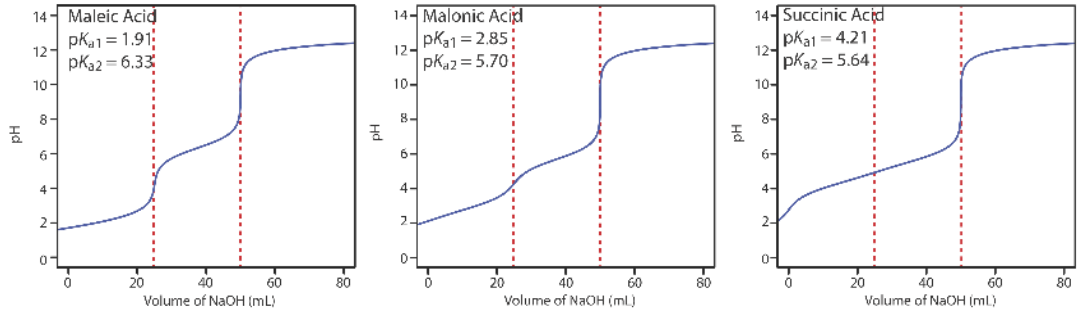


Figure 3.1.6 . Titration curves for the diprotic weak acids maleic acid, malonic acid, and succinic acid. Each titration curve is for 50.0 mL of 0.0500 M weak acid using 0.100 M NaOH as the titrant. Although each titration curve has equivalence points at 25.0 mL and 50.0 mL of NaOH (shown by the dashed red lines), the titration curve for succinic acid shows only one inflection point.

The same holds true for mixtures of weak acids or mixtures of weak bases. To detect separate inflection points when titrating a mixture of weak acids, their pK_a values must differ by at least a factor of 500.

Finding the End Point with an Indicator

One interesting group of weak acids and weak bases are organic dyes. Because an organic dye has at least one highly colored conjugate acid–base species, its titration results in a change in both its pH and its color. We can use this change in color to indicate the end point of a titration provided that it occurs at or near the titration's equivalence point.

As an example, let's consider an indicator for which the acid form, HIn, is yellow and the base form, In^-, is red. The color of the indicator's solution depends on the relative concentrations of HIn and In^-. To understand the relationship between pH and color we use the indicator's acid dissociation reaction

$$HIn(aq) + H_2O(l) \rightleftharpoons H_3O^+(aq) + In^-(aq)$$

and its equilibrium constant expression.

$$K_a = \frac{[H_3O^+]\,[In^-]}{[HIn]} \tag{3.1.5}$$

Taking the negative log of each side of Equation 3.1.5, and rearranging to solve for pH leaves us with a equation that relates the solution's pH to the relative concentrations of HIn and In^-.

$$pH = pK_a + \log \frac{[In^-]}{[HIn]} \tag{3.1.6}$$

If we can detect HIn and In^- with equal ease, then the transition from yellow-to-red (or from red-to-yellow) reaches its midpoint, which is orange, when the concentrations of HIn and In^- are equal, or when the pH is equal to the indicator's pK_a. If the indicator's pK_a and the pH at the equivalence point are identical, then titrating until the indicator turns orange is a suitable end point. Unfortunately, we rarely know the exact pH at the equivalence point. In addition, determining when the concentrations of HIn and In^- are equal is difficult if the indicator's change in color is subtle.

We can establish the range of pHs over which the average analyst observes a change in the indicator's color by making two assumptions: that the indicator's color is yellow if the concentration of HIn is $10\times$ greater than that of In^- and that its color is red if the concentration of HIn is $10\times$ smaller than that of In^-. Substituting these inequalities into Equation 3.1.6

$$pH = pK_a + \log \tfrac{1}{10} = pK_a - 1$$
$$pH = pK_a + \log \tfrac{10}{1} = pK_a + 1$$

shows that the indicator changes color over a pH range that extends ±1 unit on either side of its pK_a. As shown in Figure 3.1.7 , the indicator is yel-ow when the pH is less than pK_a – 1 and it is red when the pH is greater than pK_a + 1. For pH values between pK_a – 1 and pK_a + 1 the indicator's color passes through various shades of orange. The properties of several common acid–base indicators are listed in Table 3.1.3 .

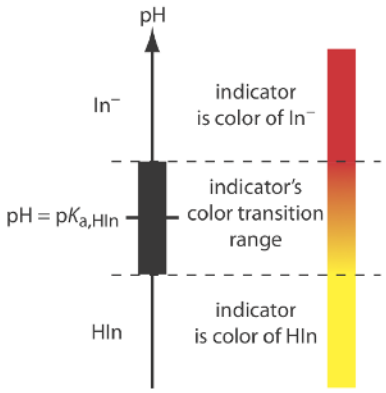


Figure 3.1.7 . Diagram showing the relationship between pH and an indicator's color. The ladder diagram defines pH values where HIn and In^- are the predominate species. The indicator changes color when the pH is between pK_a – 1 and pK_a+1.

Table 3.1.3 . Properties of Selected Acid–Base Indicators

https://chem.libretexts.org/@go/page/556120

indicator	acid color	base color	pH range	pK_a
cresol red	red	yellow	0.2–1.8	—
thymol blue	red	yellow	1.2–2.8	1.7
bromothymol blue	yellow	blue	3.0–4.6	4.1
methyl orange	red	yellow	3.4–4.4	3.7
Congo red	blue	red	3.0–5.0	—
bromocresol green	yellow	blue	3.8–5.4	4.7
methyl red	red	yellow	4.2–6.3	5.0
bromocresol purple	yellow	purple	5.2–6.8	6.1
litmus	red	blue	5.0–8.0	—
bromothymol blue	yellow	blue	6.0–7.6	7.1
phenol red	yellow	blue	6.8–8.4	7.8
cresol red	yellow	red	7.2–8.8	8.2
thymol blue	yellow	red	8.0–9.6	8.9
phenolphthalein	colorless	red	8.3–10.0	9.6
alizarin yellow R	yellow	orange-red	10.1–12.0	—

You may wonder why an indicator's pH range, such as that for phenolphthalein, is not equally distributed around its pK_a value. The explanation is simple. Figure 3.1.7 presents an idealized view in which our sensitivity to the indicator's two colors is equal. For some indicators only the weak acid or the weak base is colored. For other indicators both the weak acid and the weak base are colored, but one form is easier to see. In either case, the indicator's pH range is skewed in the direction of the indicator's less colored form. Thus, phenolphthalein's pH range is skewed in the direction of its colorless form, shifting the pH range to values lower than those suggested by Figure 3.1.7 .

The relatively broad range of pHs over which an indicator changes color places additional limitations on its ability to signal a titration's end point. To minimize a determinate titration error, the indicator's entire pH range must fall within the rapid change in pH near the equivalence point. For example, in Figure 3.1.8 we see that phenolphthalein is an appropriate indicator for the titration of 50.0 mL of 0.050 M acetic acid with 0.10 M NaOH. Bromothymol blue, on the other hand, is an inappropriate indicator because its change in color begins well before the initial sharp rise in pH, and, as a result, spans a relatively large range of volumes. The early change in color increases the probability of obtaining an inaccurate result, and the range of possible end point volumes increases the probability of obtaining imprecise results.

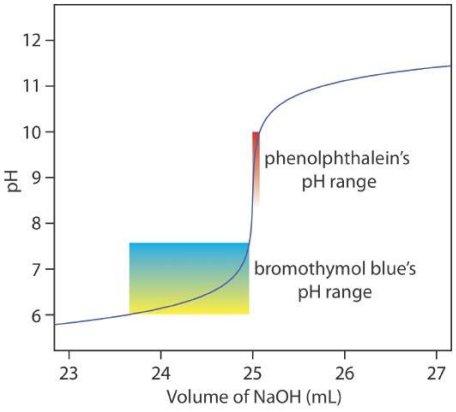


Figure 3.1.8 . Portion of the titration curve for 50.0 mL of 0.050 M CH_3COOH with 0.10 M NaOH, highlighting the region that contains the equivalence point. The end point transitions for the indicators phenolphthalein and bromothymol blue are superimposed on the titration curve.

? Exercise 3.1.5

Suggest a suitable indicator for the titration of 25.0 mL of 0.125 M NH_3 with 0.0625 M NaOH. You constructed a titration curve for this titration in Exercise 3.1.2 and Exercise 3.1.3 .

Answer

The pH at the equivalence point is 5.31 (see Exercise 3.1.2) and the sharp part of the titration curve extends from a pH of approximately 7 to a pH of approximately 4. Of the indicators in Table 3.1.3 , methyl red is the best choice because its pK_a value of 5.0 is closest to the equivalence point's pH and because the pH range of 4.2–6.3 for its change in color will not produce a significant titration error.

Finding the End Point by Monitoring pH

An alternative approach for locating a titration's end point is to monitor the titration's progress using a sensor whose signal is a function of the analyte's concentration. The result is a plot of the entire titration curve, which we can use to locate the end point with a minimal error. A pH electrode is the obvious sensor for monitoring an acid–base titration and the result is a ***potentiometric titration curve***. For example, Figure 3.1.9 a shows a small portion of the potentiometric titration curve for the titration of 50.0 mL of 0.050 M CH_3COOH with 0.10 M NaOH, which focuses on the region that contains the equivalence point.

There are four ways to use a potentiometric titration curve to locate the endpoint. The simplest method end point is to visually locate the titration curve's inflection point, which is shown by the arrow in Figure 3.1.9 a. This is also the least accurate method, particularly if the titration curve has a shallow slope at the equivalence point. Another method is to plot the first derivative of the titration curve, as in Figure 3.1.9 b, which gives its slope at each point along the *x*-axis. Similarly, the third way is to plot the second derivative of a titration curve as in Figure 3.1.9 c. This can be more useful than the first derivative because the equivalence point intersects the volume axis. Derivative methods in general are particularly useful when titrating a sample that contains more than one analyte.

However, derivative methods work well only if we record sufficient data during the rapid increase in pH near the equivalence point. This usually is not a problem if we use an automatic titrator. Because the pH changes so rapidly near the equivalence point—a change of several pH units over a span of several drops of titrant is not unusual—a manual titration does not provide enough data for a useful derivative titration curve. In these instances, we make a ***Gran plot*** as in Figure 3.1.9 d.

A manual titration does contain an abundance of data during the more gently rising portions of the titration curve before and after the equivalence point. This data also contains information about the titration curve's equivalence point.

Consider again the titration of acetic acid, CH_3COOH, with NaOH. At any point during the titration acetic acid is in equilibrium with H_3O^+ and CH_3COO^-

$$CH_3COOH(aq) + H_2O(l) \rightleftharpoons H_3O^+(aq) + CH_3COO^-(aq)$$

for which the equilibrium constant is

$$K_a = \frac{[H_3O^+]\,[CH_3COO^-]}{[CH_3COOH]}$$

Before the equivalence point the concentrations of CH_3COOH and CH_3COO^- are

$$[CH_3COOH] = \frac{(\text{mol } CH_3COOH)_{\text{initial}} - (\text{mol NaOH})_{\text{added}}}{\text{total volume}} = \frac{M_aV_a - M_bV_b}{V_a + V_b}$$

$$[CH_3COO^-] = \frac{(\text{mol NaOH})_{\text{added}}}{\text{total volume}} = \frac{M_bV_b}{V_a + V_b}$$

Substituting these equations into the K_a expression and rearranging leaves us with

$$K_a = \frac{[H_3O^+]\,(M_bV_b)\,/\,(V_a + V_b)}{\{M_aV_a - M_bV_b\}\,/\,(V_a + V_b)}$$

$$K_aM_aV_a - K_aM_bV_b = [H_3O^+]\,(M_bV_b)$$

$$\frac{K_aM_aV_a}{M_b} - K_aV_b = [H_3O^+]\,V_b$$

Finally, recognizing that the equivalence point volume is

$$V_{eq} = \frac{M_aV_a}{M_b}$$

leaves us with the following equation.

$$[H_3O^+] \times V_b = K_aV_{eq} - K_aV_b$$

For volumes of titrant before the equivalence point, a plot of $V_b \times [H_3O^+]$ versus V_b is a straight-line with an x-intercept of V_{eq} and a slope of $-K_a$. Figure 3.1.9 d shows a typical result. This method of data analysis, which converts a portion of a titration curve into a straight-line, is a ***Gran plot***.

> Values of K_a determined by this method may have a substantial error if the effect of activity is ignored. See Chapter 6.9 for a discussion of activity.

> See Chapter 11 for more details about pH electrodes.

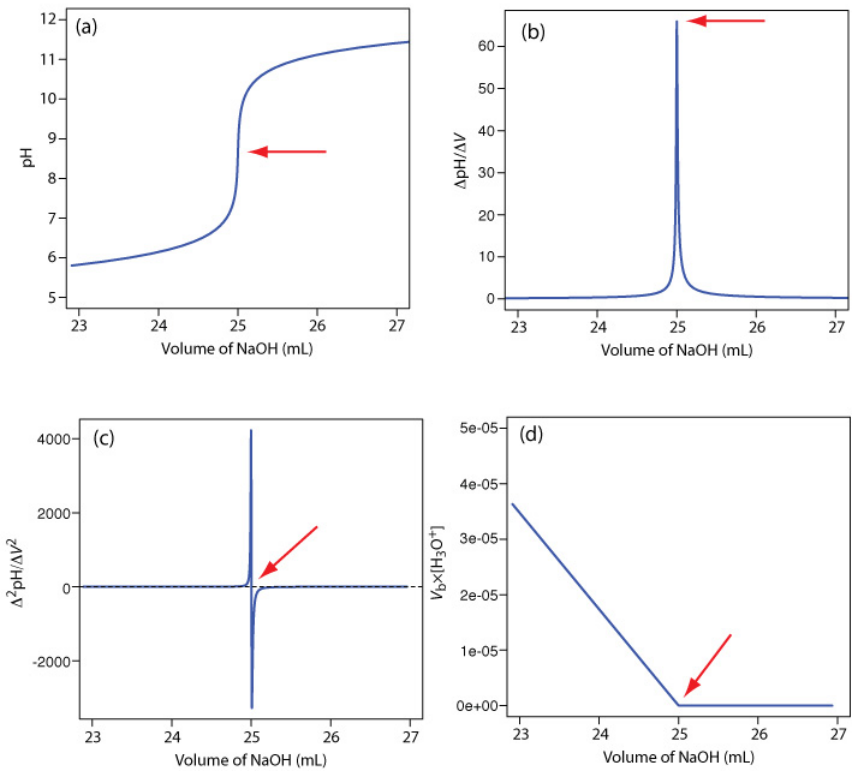


Figure 3.1.9 . Titration curves for the titration of 50.0 mL of 0.050 M CH_3COOH with 0.10 M NaOH: (a) normal titration curve; (b) first derivative titration curve; (c) second derivative titration curve; (d) Gran plot. The red arrows show the location of each titration's end point.

Quantitative Applications

Although many quantitative applications of acid–base titrimetry have been replaced by other analytical methods, a few important applications continue to find use. In this section we review the general application of acid–base titrimetry to the analysis of inorganic and organic compounds, with an emphasis on applications in environmental and clinical analysis. First, however, we discuss the selection and standardization of acidic and basic titrants.

Selecting and Standardizing a Titrant

The most common strong acid titrants are HCl, $HClO_4$, and H_2SO_4. Solutions of these titrants usually are prepared by diluting a commercially available concentrated stock solution. Because the concentration of a concentrated acid is known only approximately, the titrant's concentration is determined by standardizing against one of the primary standard weak bases listed in Table 3.1.4 .

The nominal concentrations of the concentrated stock solutions are 12.1 M HCl, 11.7 M $HClO_4$, and 18.0 M H_2SO_4. The actual concentrations of these acids are given as %w/v and vary slightly from lot-to-lot.

Table 3.1.4 . Selected Primary Standards for Standardizing Strong Acid and Strong Base Titrants

titrant type	primary standard	titration reaction	comment
strong acid	Na_2CO_3	$Na_2CO_3 + 2H_3O^+ \rightarrow H_2CO_3 + 2Na^+ + 2H_2O$	a
strong acid	$(HOCH_2)3CNH_2$	$(HOCH_2)_3\,CNH_2 + H_3O^+ \longrightarrow (HOCH_2)_3\,CNH_3^+ + H_2O$	b
strong acid	$Na2B_4O_7$	$Na_2B_4O_7 + 2H_3O^+ + 3H_2O \rightarrow 2Na^+ + 4H_3BO_3$	
strong base	$KHC_8H_4O_4$	$KHC_8H_4O_4 + OH^- \rightarrow K^+ + C_8H_4O_4^- + H_2O$	c
strong base	C_6H_5COOH	$C_6H_5COOH + OH^- \rightarrow C_6H_5COO^- + H_2O$	d
strong base	$KH(IO_3)_2$	$KH\,(IO_3)_2 + OH^- \rightarrow K^+ + 2IO_3^- + H_2O$	

(a) The end point for this titration is improved by titrating to the second equivalence point, boiling the solution to expel CO2, and retitrating to the second equivalence point. The reaction in this case is

$$Na_2CO_3 + 2H_3O^+ \rightarrow CO_2 + 2Na^+ + 3H_2O$$

(b) *Tris*-(hydroxymethyl)aminomethane often goes by the shorter name of TRIS or THAM.
(c) Potassium hydrogen phthalate often goes by the shorter name of KHP.
(d) Because it is not very soluble in water, dissolve benzoic acid in a small amount of ethanol before diluting with water.

The most common strong base titrant is NaOH, which is available both as an impure solid and as an approximately 50% w/v solution. Solutions of NaOH are standardized against any of the primary weak acid standards listed in Table **3.1.[4]**. Solid NaOH is always contaminated with carbonate due to its contact with the atmosphere, and we cannot use it to prepare a carbonate-free solution of NaOH. Solutions of carbonate-free NaOH are prepared from 50% w/v NaOH because Na_2CO_3 is insoluble in concentrated NaOH. When CO_2 is absorbed, Na_2CO_3 precipitates and settles to the bottom of the container, which allow access to the carbonate-free NaOH. When pre- paring a solution of NaOH, be sure to use water that is free from dissolved CO_2. Briefly boiling the water expels CO_2; after it cools, the water is used to prepare carbonate-free solutions of NaOH. A solution of carbonate-free NaOH is relatively stable if we limit its contact with the atmosphere. Standard solutions of sodium hydroxide are not stored in glass bottles as NaOH reacts with glass to form silicate; instead, store such solutions in polyethylene bottles.

Inorganic Analysis

Acid–base titrimetry is a standard method for the quantitative analysis of many inorganic acids and bases. A standard solution of NaOH is used to determine the concentration of inorganic acids, such as H_3PO_4 or H_3AsO_4, and inorganic bases, such as Na_2CO_3 are analyzed using a standard solution of HCl.

If an inorganic acid or base that is too weak to be analyzed by an aqueous acid–base titration, it may be possible to complete the analysis by adjusting the solvent or by an indirect analysis. For example, when analyzing boric acid, H_3BO_3, by titrating with NaOH, accuracy is limited by boric acid's small acid dissociation constant of 5.8×10^{-10}. Boric acid's K_a value increases to 1.5×10^{-4} in the presence of mannitol, because it forms a stable complex with the borate ion, which results is a sharper end point and a more accurate titration. Similarly, the analysis of ammonium salts is limited by the ammonium ion' small acid dissociation constant of 5.7×10^{-10}. We can determine NH_4^+ indirectly by using a strong base to convert it to NH_3, which is removed by distillation and titrated with HCl. Because NH_3 is a stronger weak base than NH_4^+ is a weak acid (its K_b is 1.58×10^{-5}), the titration has a sharper end point.

We can analyze a neutral inorganic analyte if we can first convert it into an acid or a base. For example, we can determine the concentration of NO_3^- by reducing it to NH_3 in a strongly alkaline solution using Devarda's alloy, a mixture of 50% w/w Cu, 45% w/w Al, and 5% w/w Zn.

$$3NO_3^-(aq) + 8Al(s) + 5OH^-(aq) + 2H_2O(l) \rightarrow 8AlO_2^-(aq) + 3NH_3(aq)$$

The NH_3 is removed by distillation and titrated with HCl. Alternatively, we can titrate NO_3^- as a weak base by placing it in an acidic nonaqueous solvent, such as anhydrous acetic acid, and using $HClO_4$ as a titrant.

Acid–base titrimetry continues to be listed as a standard method for the determination of alkalinity, acidity, and free CO_2 in waters and wastewaters. ***Alkalinity*** is a measure of a sample's capacity to neutralize acids. The most important sources of alkalinity are OH^-, HCO_3^-, and CO_3^{2-}, although other weak bases, such as phosphate, may contribute to the overall alkalinity. Total alkalinity is determined by titrating to a fixed end point pH of 4.5 (or to the bromocresol green end point) using a standard solution of HCl or H_2SO_4. Results are reported as mg $CaCO_3$/L.

> Although a variety of strong bases and weak bases may contribute to a sample's alkalinity, a single titration cannot distinguish between the possible sources. Reporting the total alkalinity as if $CaCO_3$ is the only source provides a means for comparing the acid-neutralizing capacities of different samples.

Acidity is a measure of a water sample's capacity to neutralize base and is divided into strong acid and weak acid acidity. Strong acid acidity from inorganic acids such as HCl, HNO_3, and H_2SO_4 is common in industrial effluents and in acid mine drainage. Weak acid acidity usually is dominated by the formation of H_2CO_3 from dissolved CO_2, but also includes contributions from hydrolyzable metal ions such as Fe^{3+}, Al^{3+}, and Mn^{2+}. In addition, weak acid acidity may include a contribution from organic acids.

Acidity is determined by titrating with a standard solution of NaOH to a fixed pH of 3.7 (or the bromothymol blue end point) and to a fixed pH of 8.3 (or the phenolphthalein end point). Titrating to a pH of 3.7 provides a measure of strong acid acidity, and titrating to a pH of 8.3 provides a measure of total acidity. Weak acid acidity is the difference between the total acidity and the strong acid acidity. Results are expressed as the amount of $CaCO_3$ that can be neutralized by the sample's acidity. An alternative approach for determining strong acid and weak acid acidity is to obtain a potentiometric titration curve and use a Gran plot to determine the two equivalence points. This approach has been used, for example, to determine the forms of acidity in atmospheric aerosols [Ferek, R. J.; Lazrus, A. L.; Haagenson, P. L.; Winchester, J. W. *Environ. Sci. Technol.* **1983**, *17*, 315–324].

> As is the case with alkalinity, acidity is reported as mg $CaCO_3$/L.

Water in contact with either the atmosphere or with carbonate-bearing sediments contains free CO_2 in equilibrium with $CO_2(g)$ and with aqueous H_2CO_3, HCO_3^- and CO_3^{2-}. The concentration of free CO_2 is determined by titrating with a standard solution of NaOH to the phenolphthalein end point, or to a pH of 8.3, with results reported as mg CO_2/L. This analysis essentially is the same as that for the determination of total acidity and is used only for water samples that do not contain strong acid acidity.

> Free CO_2 is the same thing as $CO_2(aq)$.

Organic Analysis

Acid–base titrimetry continues to have a small, but important role for the analysis of organic compounds in pharmaceutical, biochemical, agricultur- al, and environmental laboratories. Perhaps the most widely employed acid–base titration is the ***Kjeldahl analysis*** for organic nitrogen. Examples of analytes determined by a Kjeldahl analysis include caffeine and saccharin in pharmaceutical products, proteins in foods, and the analysis of nitrogen in fertilizers, sludges, and sediments. Any nitrogen present in a –3 oxidation state is oxidized quantitatively to NH_4^+. Because some aromatic heterocyclic compounds, such as pyridine, are difficult to oxidize, a catalyst is used to ensure a quantitative oxidation. Nitrogen in other oxidation states, such as nitro and azo nitrogens, are oxidized to N_2, which results in a negative determinate error. Including a reducing agent, such as salicylic acid, converts this nitrogen to a –3 oxidation state, eliminating this source of error. Table 3.1.6 provides additional examples in which an element is converted quantitatively into a titratable acid or base.

Table 3.1.6 . Selected Elemental Analyses Based on an Acid–Base Titration

element	convert to...	reaction producing titratable species	titration details
N	NH_3 (g)	NH3 (aq) + **HCl** (aq) → **NH_4^+** (aq) + Cl^- (aq)	add HCl in excess and back titrate with NaOH
S	SO_2(g)	SO_3 (g) + H_2O_2 (aq) → **H_2SO_4** (aq)	titrate H_2SO_4 with NaOH
C	CO_2 (g)	CO_2 (g) + **Ba(OH)$_2$** (aq) → $BaCO_3$ (s) + H_2O (l)	add excess $Ba(OH)_2$ and back titrate with HCl
Cl	**HCl** (g)	—	titrate HCl with NaOH
F	SiF_4 (g)	$3SiF_4$ (aq) + $2H_2O$ (l) → **$2H_3SiF_6$** (aq) + SiO2 (s)	titrate H_2SiF_6 with NaOH

the species that is titrated is shown in **bold**

Several organic functional groups are weak acids or weak bases. Carboxylic (–COOH), sulfonic ($–SO_3H$) and phenolic ($–C_6H_5OH$) functional groups are weak acids that are titrated successfully in either aqueous or non-aqueous solvents. Sodium hydroxide is the titrant of choice for aqueous solutions. Nonaqueous titrations often are carried out in a basic solvent, such as ethylenediamine, using tetrabutylammonium hydroxide, $(C_4H_9)_4NOH$, as the titrant. Aliphatic and aromatic amines are weak bases that are titrated using HCl in aqueous solutions, or $HClO_4$ in glacial acetic acid. Other functional groups are analyzed indirectly following a reaction that produces or consumes an acid or base. Typical examples are shown in Table 3.1.7 .

Table 3.1.7 . Selected Acid–Base Titrimetric Methods for Organic Functional Groups Based on the Production or Consumption of Acid or Base

functional group	reaction producing titratable species	titration details
ester	RCOOR' (aq) + **OH^-** (aq) → $RCOO^-$ (aq) + HOR' (aq)	titrate OH^- with HCl
carbonyl	R_2CO (aq) + NH4OH•HCl (aq) → R_2CNOH (aq) + **HCl** (aq) + H2O (l)	titrate HCl with NaOH
alcohol	[1]: $(CH_3CO)_2O$ + ROH → CH_3COOR + **CH_3COOH** [2]: $(CH_3CO)_2$) + H_2O → 2**CH_3COOH**	titrate CH_3COOH with NaOH; a blank titration of acetic anhydride, $(CH_3CO)_2O$, corrects for the contribution of reaction [2]

the species that is titrated is shown in **bold**
for alcohols, reaction [1] is carried out in pyridine to prevent the hydrolysis of acetic anhydride by water. After reaction [1] is complete, water is added to covert any unreacted acetic anhydride to acetic acid (reaction [2])

Many pharmaceutical compounds are weak acids or weak bases that are analyzed by an aqueous or a nonaqueous acid–base titration; examples include salicylic acid, phenobarbital, caffeine, and sulfanilamide. Amino acids and proteins are analyzed in glacial acetic acid using $HClO_4$ as the titrant. For example, a procedure for determining the amount of nutritionally available protein uses an acid–base titration of lysine residues [(a) Molnár-Perl, I.; Pintée-Szakács, M. *Anal. Chim. Acta* **1987**, *202*, 159–166; (b) Barbosa, J.; Bosch, E.; Cortina, J. L.; Rosés, M. *Anal. Chim. Acta* **1992**, *256*, 177–181].

Quantitative Calculations

The quantitative relationship between the titrand and the titrant is determined by the titration reaction's stoichiometry. If the titrand is polyprotic, then we must know to which equivalence point we are titrating. The following example illustrates how we can determine a titration reaction's stoichiometry.

✔ Example 3.1.2

A 50.00-mL sample of a citrus drink requires 17.62 mL of 0.04166 M NaOH to reach the phenolphthalein end point. Express the sample's acidity as grams of citric acid, $C_6H_8O_7$, per 100 mL.

Solution

Because citric acid is a triprotic weak acid, we first must determine if the phenolphthalein end point corresponds to the first, second, or third equivalence point. Citric acid's ladder diagram is shown in Figure 3.1.15 a. Based on this ladder diagram, the first equivalence point is between a pH of 3.13 and a pH of 4.76, the second equivalence point is between a pH of 4.76 and a pH of 6.40, and the third equivalence point is greater than a pH of 6.40. Because phenolphthalein's end point pH is 8.3–10.0 (see Table 3.1.3), the titration must proceed to the third equivalence point and the titration reaction is

$$C_6H_8O_7(aq) + 3OH^-(aq) \longrightarrow C_6H_5O_7^{3-}(aq) + 3H_2O(l)$$

To reach the equivalence point, each mole of citric acid consumes three moles of NaOH; thus

$$(0.04166\ \text{M NaOH})(0.01762\ \text{L NaOH}) = 7.3405 \times 10^{-4}\ \text{mol NaOH}$$

$$7.3405 \times 10^{-4}\ \text{mol NaOH} \times \frac{1\ \text{mol } C_6H_8O_7}{3\ \text{mol NaOH}} = 2.4468 \times 10^{-4}\ \text{mol } C_6H_8O_7$$

$$2.4468 \times 10^{-4}\ \text{mol } C_6H_8O_7 \times \frac{192.1\ \text{g } C_6H_8O_7}{\text{mol } C_6H_8O_7} = 0.04700\ \text{g } C_6H_8O_7$$

Because this is the amount of citric acid in a 50.00 mL sample, the concentration of citric acid in the citrus drink is 0.09400 g/100 mL. The complete titration curve is shown in Figure 3.1.15 b.

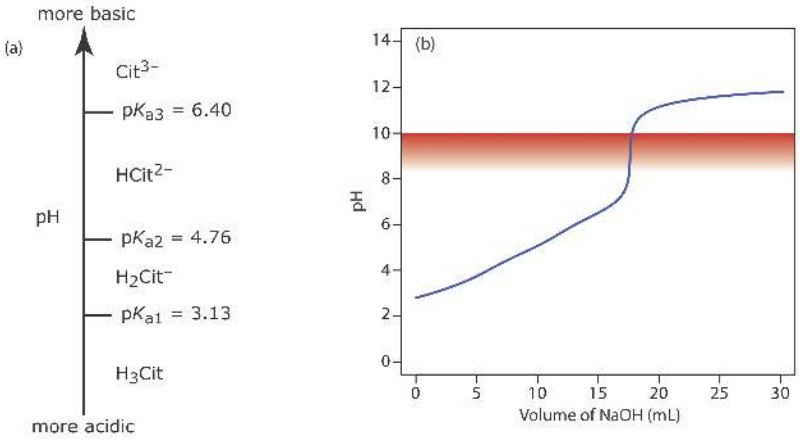


Figure 3.1.15 . (a) Ladder diagram for citric acid; (b) Titration curve for the sample in Example 3.1.2 showing phenolphthalein's pH transition region.In an indirect analysis the analyte participates in one or more preliminary reactions, one of which produces or consumes acid or base. Despite the additional complexity, the calculations are straightforward.

Example 3.1.3

The purity of a pharmaceutical preparation of sulfanilamide, $C_6H_4N_2O_2S$, is determined by oxidizing the sulfur to SO_2 and bubbling it through H_2O_2 to produce H_2SO_4. The acid is titrated to the bromothymol blue end point using a standard solution of NaOH. Calculate the purity of the preparation given that a 0.5136-g sample requires 48.13 mL of 0.1251 M NaOH.

Solution

The bromothymol blue end point has a pH range of 6.0–7.6. Sulfuric acid is a diprotic acid, with a pK_{a2} of 1.99 (the first K_a value is very large and the acid dissociation reaction goes to completion, which is why H_2SO4 is a strong acid). The titration, therefore, proceeds to the second equivalence point and the titration reaction is

$$H_2SO_4(aq) + 2OH^-(aq) \longrightarrow 2H_2O(l) + SO_4^{2-}(aq)$$

Using the titration results, there are

$$(0.1251\ \text{M NaOH})(0.04813\ \text{L NaOH}) = 6.021 \times 10^{-3}\ \text{mol NaOH}$$

$$6.012 \times 10^{-3}\ \text{mol NaOH} \times \frac{1\ \text{mol}\ H_2SO_4}{2\ \text{mol NaOH}} = 3.010 \times 10^{-3}\ \text{mol}\ H_2SO_4$$

$$3.010 \times 10^{-3}\ \text{mol}\ H_2SO_4 \times \frac{1\ \text{mol S}}{\text{mol}\ H_2SO_4} \times \frac{1\ \text{mol}\ C_6H_4N_2O_2S}{\text{mol S}} \times \frac{168.17\ \text{g}\ C_6H_4N_2O_2S}{\text{mol}\ C_6H_4N_2O_2S} = 0.5062\ \text{g}\ C_6H_4N_2O_2S$$

produced when the SO_2 is bubbled through H_2O_2. Because all the sulfur in H_2SO_4 comes from the sulfanilamide, we can use a conservation of mass to determine the amount of sulfanilamide in the sample.

$$\frac{0.5062\ \text{g}\ C_6H_4N_2O_2S}{0.5136\ \text{g sample}} \times 100 = 98.56\ \%\text{w/w}\ C_6H_4N_2O_2S$$

For a back titration we must consider two acid–base reactions. Again, the calculations are straightforward.

Example 3.1.4

The amount of protein in a sample of cheese is determined by a Kjeldahl analysis for nitrogen. After digesting a 0.9814-g sample of cheese, the nitrogen is oxidized to NH_4^+, converted to NH_3 with NaOH, and the NH_3 distilled into a collection flask that contains 50.00 mL of 0.1047 M HCl. The excess HCl is back titrated with 0.1183 M NaOH, requiring 22.84 mL to reach the bromothymol blue end point. Report the %w/w protein in the cheese assuming there are 6.38 grams of protein for every gram of nitrogen in most dairy products.

Solution

The HCl in the collection flask reacts with two bases

$$HCl(aq) + NH_3(aq) \rightarrow NH_4^+(aq) + Cl^-(aq)$$

$$HCl(aq) + OH^-(aq) \rightarrow H_2O(l) + Cl^-(aq)$$

The collection flask originally contains

$$(0.1047\ \text{M HCl})(0.05000\ \text{L HCl}) = 5.235 \times 10^{-3}\text{mol HCl}$$

of which

$$(0.1183\ \text{M NaOH})(0.02284\ \text{L NaOH}) \times \frac{1\ \text{mol HCl}}{\text{mol NaOH}} = 2.702 \times 10^{-3}\ \text{mol HCl}$$

react with NaOH. The difference between the total moles of HCl and the moles of HCl that react with NaOH is the moles of HCl that react with NH_3.

$$5.235 \times 10^{-3}\ \text{mol HCl} - 2.702 \times 10^{-3}\ \text{mol HCl} = 2.533 \times 10^{-3}\ \text{mol HCl}$$

Because all the nitrogen in NH_3 comes from the sample of cheese, we use a conservation of mass to determine the grams of nitrogen in the sample.

$$2.533 \times 10^{-3}\ \text{mol HCl} \times \frac{1\ \text{mol}\ NH_3}{\text{mol HCl}} \times \frac{14.01\ \text{g N}}{\text{mol}\ NH_3} = 0.03549\ \text{g N}$$

The mass of protein, therefore, is

$$0.03549\ \text{g N} \times \frac{6.38\ \text{g protein}}{\text{g N}} = 0.2264\ \text{g protein}$$

and the % w/w protein is

$$\frac{0.2264\ \text{g protein}}{0.9814\ \text{g sample}} \times 100 = 23.1\ \%\text{w/w protein}$$

Earlier we noted that we can use an acid–base titration to analyze a mixture of acids or bases by titrating to more than one equivalence point. The concentration of each analyte is determined by accounting for its contribution to each equivalence point.

Example 3.1.5

The alkalinity of natural waters usually is controlled by OH^-, HCO_3^-, and CO_3^{2-}, present singularly or in combination. Titrating a 100.0-mL sample to a pH of 8.3 requires 18.67 mL of 0.02812 M HCl. A second 100.0-mL aliquot requires 48.12 mL of the same titrant to reach a pH of 4.5. Identify the sources of alkalinity and their concentrations in milligrams per liter.

Solution

Because the volume of titrant to reach a pH of 4.5 is more than twice that needed to reach a pH of 8.3, we know from Table 3.1.5 , that the sample's alkalinity is controlled by CO_3^{2-} and HCO_3^-. Titrating to a pH of 8.3 neutralizes CO_3^{2-} to HCO_3^-

$$CO_3^{2-}(aq) + HCl(aq) \rightarrow HCO_3^-(aq) + Cl^-(aq)$$

but there is no reaction between the titrant and HCO_3^- (see Figure 3.1.14). The concentration of CO_3^{2-} in the sample, therefore, is

$$(0.02812 \text{ M HCl})(0.01867 \text{ L HCl}) \times \frac{1 \text{ mol } CO_3^{2-}}{\text{mol HCl}} = 5.250 \times 10^{-4} \text{ mol } CO_3^{2-}$$

$$\frac{5.250 \times 10^{-4} \text{ mol } CO_3^{2-}}{0.1000 \text{ L}} \times \frac{60.01 \text{ g } CO_3^{2-}}{\text{mol } CO_3^{2-}} \times \frac{1000 \text{ mg}}{\text{g}} = 315.1 \text{ mg/L}$$

Titrating to a pH of 4.5 neutralizes CO_3^{2-} to H_2CO_3 and neutralizes HCO_3^- to H_2CO_3 (see Figure 3.1.14).

$$CO_3^{2-}(aq) + 2HCl(aq) \rightarrow H_2CO_3(aq) + 2Cl^-(aq)$$
$$HCO_3^-(aq) + HCl(aq) \rightarrow H_2CO_3(aq) + Cl^-(aq)$$

Because we know how many moles of CO_3^{2-} are in the sample, we can calculate the volume of HCl it consumes.

$$5.250 \times 10^{-4} \text{ mol } CO_3^{2-} \times \frac{2 \text{ mol HCl}}{\text{mol } CO_3^{2-}} \times \frac{1 \text{ L HCl}}{0.02812 \text{ mol HCl}} \times \frac{1000 \text{ mL}}{\text{L}} = 37.34 \text{ mL HCl}$$

This leaves 48.12 mL–37.34 mL, or 10.78 mL of HCl to react with HCO_3^-. The amount of HCO_3^- in the sample is

$$(0.02812 \text{ M HCl})(0.01078 \text{ L HCl}) \times \frac{1 \text{ mol } HCO_3^-}{\text{mol HCl}} = 3.031 \times 10^{-4} \text{ mol } HCO_3^-$$

The sample contains 315.1 mg CO_3^{2-}/L and 185.0 mg HCO_3^-/L

Characterization Applications

In addition to a quantitative analysis and a qualitative analysis, we also can use an acid–base titration to characterize the chemical and physical properties of matter. Two useful characterization applications are the determination of a compound's equivalent weight and the determination of its acid dissociation constant or its base dissociation constant.

Equivalent Weights

Suppose we titrate a sample of an impure weak acid to a well-defined end point using a monoprotic strong base as the titrant. If we assume the titration involves the transfer of *n* protons, then the moles of titrant needed to reach the end point is

$$\text{moles titrant} = \frac{n \text{ moles titrant}}{\text{moles analyte}} \times \text{moles analyte}$$

If we know the analyte's identity, we can use this equation to determine the amount of analyte in the sample

$$\text{grams analyte} = \text{moles titrant} \times \frac{1 \text{ mole analyte}}{n \text{ moles analyte}} \times FW \text{ analyte}$$

where *FW* is the analyte's formula weight.

But what if we do not know the analyte's identify? If we titrate a pure sample of the analyte, we can obtain some useful information that may help us establish its identity. Because we do not know the number of protons that are titrated, we let n = 1 and replace the analyte's formula weight with its equivalent weight (EW)

$$\text{grams analyte} = \text{moles titrant} \times \frac{\text{1 equivalent analyte}}{\text{1 mole analyte}} = EW \text{ analyte}$$

where

$$FW = n \times EW$$

Example 3.1.6

A 0.2521-g sample of an unknown weak acid is titrated with 0.1005 M NaOH, requiring 42.68 mL to reach the phenolphthalein end point. Determine the compound's equivalent weight. Which of the following compounds is most likely to be the unknown weak acid?

acid	formula	formula weight (g/mol)	type
ascorbic acid	$C_8H_8O_6$	176.1	monoprotic
malonic acid	$C_3H_4O_4$	104.1	diprotic
succinic acid	C_4H_6O4	118.1	diprotic
citric acid	$C_6H_8O_7$	192.1	triprotic

Solution

The moles of NaOH needed to reach the end point is

$$(0.1005 \text{ M NaOH})(0.04268 \text{ L NaOH}) = 4.289 \times 10^{-3} \text{ mol NaOH}$$

The equivalents of weak acid are the same as the moles of NaOH used in the titration; thus, he analyte's equivalent weight is

$$EW = \frac{0.2521 \text{ g}}{4.289 \times 10^{-3} \text{ equivalents}} = 58.78 \text{ g/equivalent}$$

The possible formula weights for the weak acid are 58.78 g/mol (n = 1), 117.6 g/mol (n = 2), and 176.3 g/mol (n = 3). If the analyte is a monoprotic weak acid, then its formula weight is 58.78 g/mol, eliminating ascorbic acid as a possibility. If it is a diprotic weak acid, then the analyte's formula weight is either 58.78 g/mol or 117.6 g/mol, depending on whether the weak acid was titrated to its first or its second equivalence point. Succinic acid, with a formula weight of 118.1 g/mole is a possibility, but malonic acid is not. If the analyte is a triprotic weak acid, then its formula weight is 58.78 g/mol, 117.6 g/mol, or 176.3 g/mol. None of these values is close to the formula weight for citric acid, eliminating it as a possibility. Only succinic acid provides a possible match.

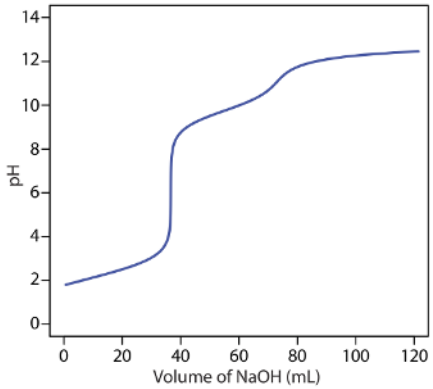


Figure 3.1.16 . Titration curve for Exercise 3.1.10 .

Exercise 3.1.10

Figure 3.1.16 shows the potentiometric titration curve for the titration of a 0.500-g sample an unknown weak acid. The titrant is 0.1032 M NaOH. What is the weak acid's equivalent weight?

Answer

The first of the two visible end points is approximately 37 mL of NaOH. The analyte's equivalent weight, therefore, is

$$(0.1032\ \text{M NaOH})(0.037\ \text{L}) \times \frac{1\ \text{equivalent}}{\text{mol NaOH}} = 3.8 \times 10^{-3}\ \text{equivalents}$$

$$EW = \frac{0.5000\ \text{g}}{3.8 \times 10^{-3}\ \text{equivalents}} = 1.3 \times 10^{2}\ \text{g/equivalent}$$

Equilibrium Constants

Another application of acid–base titrimetry is the determination of a weak acid's or a weak base's dissociation constant. Consider, for example, a solution of acetic acid, CH_3COOH, for which the dissociation constant is

$$K_a = \frac{[H_3O^+]\,[CH_3COO^-]}{[CH_3COOH]}$$

When the concentrations of CH_3COOH and CH_3COO^- are equal, the K_a expression reduces to $K_a = [H_3O^+]$, or pH = pK_a. If we titrate a solution of acetic acid with NaOH, the pH equals the pK_a when the volume of NaOH is approximately $\frac{1}{2}V_{eq}$. As shown in Figure 3.1.17 , a potentiometric titration curve provides a reasonable estimate of acetic acid's pK_a.

> Recall that pH = pK_a is a step on a ladder diagram, which divides the pH axis into two regions, one where the weak acid is the predominate species, and one where its conjugate weak base is the predominate species.

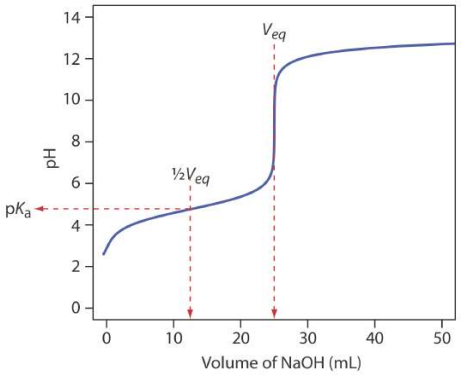


Figure 3.1.17 . Estimating acetic acid's pK_a using its potentiometric titration curve.

This method provides a reasonable estimate for a weak acid's pK_a if the acid is neither too strong nor too weak. These limitations are easy to appreciate if we consider two limiting cases. For the first limiting case, let's assume the weak acid, HA, is more than 50% dissociated before the titration begins (a relatively large K_a value); in this case the concentration of HA before the equivalence point is always less than the concentration of A^- and there is no point on the titration curve where [HA] = [A^-]. At the other extreme, if the acid is too weak, then less than 50% of the weak acid reacts with the titrant at the equivalence point. In this case the concentration of HA before the equivalence point is always greater than that of A^-. Determining the pK_a by the half-equivalence point method overestimates its value if the acid is too strong and underestimates its value if the acid is too weak.

Exercise 3.1.11

Use the potentiometric titration curve in Figure 3.1.16 to estimate the pK_a values for the weak acid in Exercise 3.1.10 .

Answer

At $1/2V_{eq}$, or approximately 18.5 mL, the pH is approximately 2.2; thus, we estimate that the analyte's pK_a is 2.2.

A second approach for determining a weak acid's pK_a is to use a Gran plot. For example, earlier in this chapter we derived the following equation for the titration of a weak acid with a strong base.

$$[H_3O^+] \times V_b = K_a V_{eq} - K_a V_b$$

A plot of $[H_3O^+] \times V_b$ versus V_b for volumes less than the equivalence point yields a straight line with a slope of $-K_a$. Other linearizations have been developed that use the entire titration curve or that require no assumptions [(a) Gonzalez, A. G.; Asuero, A. G. *Anal. Chim. Acta* **1992**, *256*, 29–33; (b) Papanastasiou, G.; Ziogas, I.; Kokkindis, G. *Anal. Chim. Acta* **1993**, *277*, 119–135]. This approach to determining an acidity constant has been used to study the acid–base properties of humic acids, which are naturally occurring, large molecular weight organic acids with multiple acidic sites. In one study a humic acid was found to have six titratable sites, three which were identified as carboxylic acids, two which were believed to be secondary or tertiary amines, and one which was identified as a phenolic group [Alexio, L. M.; Godinho, O. E. S.; da Costa, W. F. *Anal. Chim. Acta* **1992**, *257*, 35–39].

Values of K_a determined by this method may have a substantial error if the effect of activity is ignored. See Chapter 6.9 for a discussion of activity.

Evaluation of Acid–Base Titrimetry

Accuracy

When working with a macro–major or a macro–minor sample, an acid–base titration can achieve a relative error of 0.1–0.2%. The principal limitation to accuracy is the difference between the end point and the equivalence point.

Precision

An acid–base titration's relative precision depends primarily on the precision with which we can measure the end point volume and the precision in detecting the end point. Under optimum conditions, an acid–base titration has a relative precision of 0.1–0.2%. We can improve the relative precision by using the largest possible buret and by ensuring we use most of its capacity in reaching the end point. A smaller volume buret is a better choice when using costly reagents, when waste disposal is a concern, or when we must complete the titration quickly to avoid competing chemical reactions. An automatic titrator is particularly useful for titrations that require small volumes of titrant because it provides significantly better precision (typically about ±0.05% of the buret's volume).

The precision of detecting the end point depends on how it is measured and the slope of the titration curve at the end point. With an indicator the precision of the end point signal usually is ±0.03–0.10 mL. Potentiometric end points usually are more precise.

Sensitivity

For an acid–base titration we can write the following general analytical equation to express the titrant's volume in terms of the amount of titrand

$$\text{volume of titrant} = k \times \text{moles of titrand}$$

where k, the sensitivity, is determined by the stoichiometry between the titrand and the titrant. Consider, for example, the determination of sulfurous acid, H_2SO_3, by titrating with NaOH to the first equivalence point

$$H_2SO_3(aq) + OH^-(aq) \rightarrow H_2O(l) + HSO_3^-(aq)$$

At the equivalence point the relationship between the moles of NaOH and the moles of H_2SO_3 is

$$\text{mol NaOH} = \text{mol } H_2SO_3$$

Substituting the titrant's molarity and volume for the moles of NaOH and rearranging

$$M_{NaOH} \times V_{NNOH} = \text{mol } H_2SO_3$$

$$V_{NaOH} = \frac{1}{M_{NaOH}} \times \text{mol } H_2SO_3$$

we find that k is

$$k = \frac{1}{M_{NaOH}}$$

There are two ways in which we can improve a titration's sensitivity. The first, and most obvious, is to decrease the titrant's concentration because it is inversely proportional to the sensitivity, k. The second approach, which applies only if the titrand is multiprotic, is to titrate to a later equivalence point. If we titrate H_2SO_3 to its second equivalence point

$$H_2SO_3(aq) + 2OH^-(aq) \rightarrow 2H_2O(l) + SO_3^{2-}(aq)$$

then each mole of H_2SO_3 consumes two moles of NaOH

$$\text{mol NaOH} = 2 \times \text{mol } H_2SO_3$$

and the sensitivity becomes

$$k = \frac{2}{M_{NaOH}}$$

In practice, however, any improvement in sensitivity is offset by a decrease in the end point's precision if a larger volume of titrant requires us to refill the buret. For this reason, standard acid–base titrimetric procedures are written to ensure that a titration uses 60–100% of the buret's volume.

Selectivity

Acid–base titrants are not selective. A strong base titrant, for example, reacts with all acids in a sample, regardless of their individual strengths. If the titrand contains an analyte and an interferent, then selectivity depends on their relative acid strengths. Let's consider two limiting situations.

If the analyte is a stronger acid than the interferent, then the titrant will react with the analyte before it begins reacting with the interferent. The feasibility of the analysis depends on whether the titrant's reaction with the interferent affects the accurate location of the analyte's equivalence point. If the acid dissociation constants are substantially different, the end point for the analyte can be determined accurately. Conversely, if the acid dissociation constants for the analyte and interferent are similar, then there may not be an accurate end point for the analyte. In the latter case a quantitative analysis for the analyte is not possible.

In the second limiting situation the analyte is a weaker acid than the interferent. In this case the volume of titrant needed to reach the analyte's equivalence point is determined by the concentration of both the analyte and the interferent. To account for the interferent's contribution to the end point, an end point for the interferent must be available. Again, if the acid dissociation constants for the analyte and interferent are significantly different, then the analyte's determination is possible. If the acid dissociation constants are similar, however, there is only a single equivalence point and we cannot separate the analyte's and the interferent's contributions to the equivalence point volume.

Time, Cost, and Equipment

Acid–base titrations require less time than most gravimetric procedures, but more time than many instrumental methods of analysis, particularly when analyzing many samples. With an automatic titrator, however, concerns about analysis time are less significant. When performing a titration manually our equipment needs—a buret and, perhaps, a pH meter—are few in number, inexpensive, routinely available, and easy to maintain. Automatic titrators are available for between $3000 and $10 000.

Scale of Operation

In an acid–base titration, the volume of titrant needed to reach the equivalence point is proportional to the moles of titrand. Because the pH of the titrand or the titrant is a function of its concentration, the change in pH at the equivalence point—and thus the feasibility of an acid–base titration—depends on their respective concentrations. Figure 3.1.18 , for example, shows a series of titration curves for the titration of several concentrations of HCl with equimolar solutions NaOH. For titrand and titrant concentrations smaller than 10^{-3} M, the change in pH at the end point is too small to provide an accurate and a precise result.

Acid–base titrimetry is an example of a total analysis technique in which the signal is proportional to the absolute amount of analyte. See Chapter 3 for a discussion of the difference between total analysis techniques and concentration techniques.

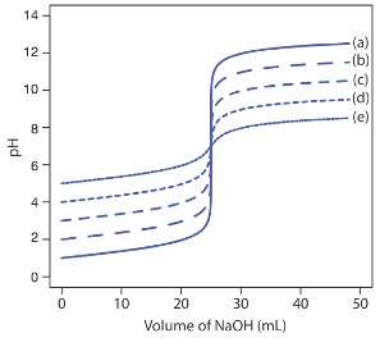


Figure 3.1.18 . Titration curves for 25.0 mL of (a) 10^{-1} M HCl, (b) 10^{-2} M HCl, (c) 10^{-3} M HCl, (d) 10^{-4} M HCl, and (e) 10^{-5} M HCl. In each case the titrant is an equimolar solution of NaOH.

A minimum concentration of 10^{-3} M places limits on the smallest amount of analyte we can analyze successfully. For example, suppose our analyte has a formula weight of 120 g/mol. To successfully monitor the titration's end point using an indicator or a pH probe, the titrand needs an initial volume of approximately 25 mL. If we assume the analyte's formula weight is 120 g/mol, then each sample must contain at least 3 mg of analyte. For this reason, acid–base titrations generally are limited to major and minor analytes. We can extend the analysis of gases to trace analytes by pulling a large volume of the gas through a suitable collection solution.

We need a volume of titrand sufficient to cover the tip of the pH probe or to allow for an easy observation of the indicator's color. A volume of 25 mL is not an unreasonable estimate of the minimum volume.

It is possible to perform titrations on smaller volume scales. In one experimental design (Figure 3.1.19), samples of 20–100 µL are held by capillary action between a flat-surface pH electrode and a stainless steel sample stage [Steele, A.; Hieftje, G. M. *Anal. Chem.* **1984**, *56*, 2884–2888]. The titrant is added using the oscillations of a piezoelectric ceramic device to move an angled glass rod in and out of a tube connected to a reservoir that contains the titrant. Each time the glass tube is withdrawn an approximately 2 nL microdroplet of titrant is released. The microdroplets are allowed to fall onto the sample, with mixing accomplished by spinning the sample stage at 120 rpm. A total of 450 microdroplets, with a combined volume of 0.81–0.84 µL, is dispensed between each pH measurement. This method has been used to titrate solutions of 0.1 M HCl and 0.1 M CH_3COOH with 0.1 M NaOH. Absolute errors ranged from a minimum of +0.1% to a maximum of –4.1%, with relative standard deviations from 0.15% to 4.7%. Samples as small as 20 µL were titrated successfully.

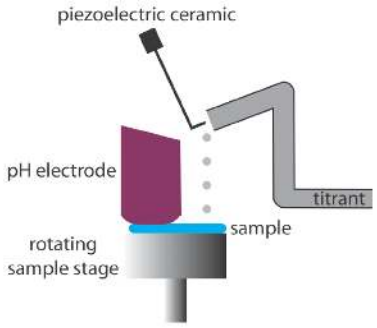


Figure 3.1.19 . Experimental design for a microdroplet titration apparatus.

Another approach carries out the acid–base titration in a single drop of solution [(a) Gratzl, M.; Yi, C. *Anal. Chem.* **1993**, *65*, 2085–2088; (b) Yi, C.; Gratzl, M. *Anal. Chem.* **1994**, *66*, 1976–1982; (c) Hui, K. Y.; Gratzl, M. *Anal. Chem.* **1997**, *69*, 695–698; (d) Yi, C.; Huang, D.; Gratzl, M. *Anal. Chem.* **1996**, *68*, 1580–1584; (e) Xie, H.; Gratzl, M. *Anal. Chem.* **1996**, *68*, 3665–3669]. The titrant is delivered using a microburet fashioned from a glass capillary micropipet (Figure 3.1.20). The microburet has a 1-2 µm tip filled

with an agar gel membrane. The tip of the microburet is placed within a drop of the sample solution, which is suspended in heptane, and the titrant is allowed to diffuse into the sample. The titration's progress is monitored using an acid–base indicator and the time needed to reach the end point is measured. The rate of the titrant's diffusion from the microburet is determined by a prior calibration. Once calibrated the end point time is converted to an end point volume. Samples usually consist of picoliter volumes (10^{-12} liters), with the smallest sample being 0.7 pL. The precision of the titrations is about 2%.

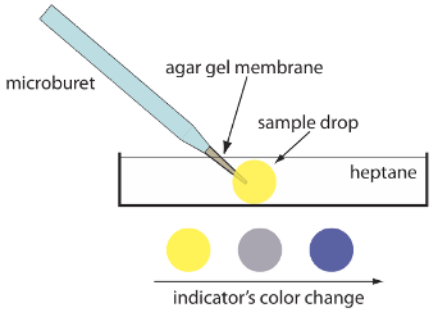


Figure 3.1.20 . Experimental set-up for a diffusional microtitration. The indicator is a mixture of bromothymol blue and bromocresol purple.

Titrations conducted with microliter or picoliter sample volumes require a smaller absolute amount of analyte. For example, diffusional titrations have been conducted on as little as 29 femtomoles (10^{-15} moles) of nitric acid. Nevertheless, the analyte must be present in the sample at a major or minor level for the titration to give accurate and precise results.

This page titled 3.1: Acid–Base Titrations is shared under a CC BY-NC-SA 4.0 license and was authored, remixed, and/or curated by Kathryn Davis.

- **9.2: Acid–Base Titrations** by David Harvey is licensed CC BY-NC-SA 4.0.

3.2: Ladder Diagrams for Acid-Base Equilibria

When we develop or evaluate an analytical method, we often need to understand how the chemistry that takes place affects our results. Suppose we wish to isolate Ag^+ by precipitating it as AgCl. If we also need to control pH, then we must use a reagent that does not adversely affect the solubility of AgCl. It is a mistake to use NH_3 to adjust the pH, for example, because it increases the solubility of AgCl (see reaction 6.5.4). One of the primary sources of determinate errors in many analytical methods is failing to account for potential chemical interferences.

In this section we introduce the ladder diagram as a simple graphical tool for visualizing equilibrium chemistry. We will use ladder diagrams to determine what reactions occur when we combine several reagents, to estimate the approximate composition of a system at equilibrium, and to evaluate how a change to solution conditions might affect an analytical method.

> Although not specifically on the topic of ladder diagrams as developed in this section, the following papers provide appropriate background information: (a) Runo, J. R.; Peters, D. G. *J. Chem. Educ.* **1993**, *70*, 708–713; (b) Vale, J.; Fernández-Pereira, C.; Alcalde, M. *J. Chem. Educ.* **1993**, *70*, 790–795; (c) Fernández-Pereira, C.; Vale, J. *Chem. Educator* **1996**, *6*, 1–18; (d) Fernández- Pereira, C.; Vale, J.; Alcalde, M. *Chem. Educator* **2003**, *8*, 15–21; (e) Fernández-Pereira, C.; Alcalde, M.; Villegas, R.; Vale, J. *J. Chem. Educ.* **2007**, *84*, 520–525. Ladder diagrams are a great tool for helping you to think intuitively about analytical chemistry. We will make frequent use of them in the chapters to follow.

Ladder Diagrams for Acid–Base Equilibria

Let's use acetic acid, CH_3COOH, to illustrate the process we will use to draw and to interpret an acid–base ladder diagram. Before we draw the diagram, however, let's consider the equilibrium reaction in more detail. Acetic acid's acid dissociation reaction and equilibrium constant expression are

$$CH_3COOH(aq) + H_2O(l) \rightleftharpoons H_3O^+(aq) + CH_3COO^-(aq)$$

$$K_a = \frac{[CH_3COO^-]\,[H_3O^+]}{[CH_3COOH]} = 1.75 \times 10^{-5}$$

First, let's take the logarithm of each term in this equation and multiply through by –1

$$-\log K_a = 4.76 = -\log [H_3O^+] - \log \frac{[CH_3COO^-]}{[CH_3COOH]}$$

Now, let's replace $-\log[H_3O^+]$ with pH and rearrange the equation to obtain the result shown here.

$$pH = 4.76 + \log \frac{[CH_3COO^-]}{[CH_3COOH]} \tag{3.2.1}$$

Equation 3.2.1 tells us a great deal about the relationship between pH and the relative amounts of acetic acid and acetate at equilibrium. If the concentrations of CH_3COOH and CH_3COO^- are equal, then Equation 3.2.1 reduces to

$$pH = 4.76 + \log(1) = 4.76 + 0 = 4.76$$

If the concentration of CH_3COO^- is greater than that of CH_3COOH, then the log term in Equation 3.2.1 is positive and the pH is greater than 4.76. This is a reasonable result because we expect the concentration of the conjugate base, CH_3COO^-, to increase as the pH increases. Similar reasoning will convince you that the pH is less than 4.76 when the concentration of CH_3COOH exceeds that of CH_3COO^-.

Now we are ready to construct acetic acid's ladder diagram (Figure 3.2.1). First, we draw a vertical arrow that represents the solution's pH, with smaller (more acidic) pH levels at the bottom and larger (more basic) pH levels at the top. Second, we draw a horizontal line at a pH equal to acetic acid's pK_a value. This line, or step on the ladder, divides the pH axis into regions where either CH_3COOH or CH_3COO^- is the predominate species. This completes the ladder diagram.

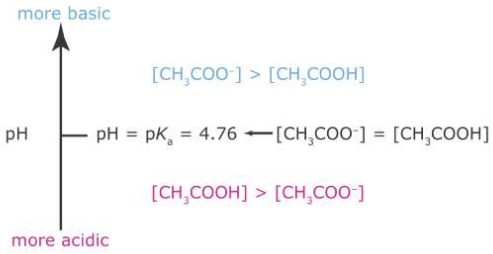


Figure 3.2.1 . Acid–base ladder diagram for acetic acid showing the relative concentrations of CH_3COOH and CH_3COO^-. A simpler version of this ladder diagram dispenses with the equalities and inequalities and shows only the predominate species in each region.

Using the ladder diagram, it is easy to identify the predominate form of acetic acid at any pH. At a pH of 3.5, for example, acetic acid exists primarily as CH_3COOH. If we add sufficient base to the solution such that the pH increases to 6.5, the predominate form of acetic acid is CH_3COO^-.

Example 3.2.1

Draw a ladder diagram for the weak base *p*-nitrophenolate and identify its predominate form at a pH of 6.00.

Solution

To draw a ladder diagram for a weak base, we simply draw the ladder diagram for its conjugate weak acid. From Appendix 11, the pK_a for *p*-nitrophenol is 7.15. The resulting ladder diagram is shown in Figure 3.2.2 . At a pH of 6.00, *p*-nitrophenolate is present primarily in its weak acid form.

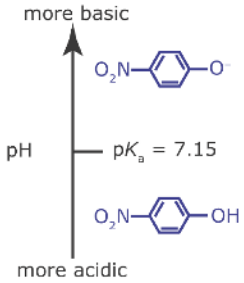


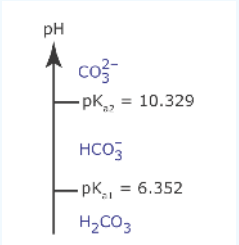
Figure 3.2.2 . Acid–base ladder diagram for *p*-nitrophenolate.

Exercise 3.2.1

Draw a ladder diagram for carbonic acid, H_2CO_3. Because H_2CO_3 is a diprotic weak acid, your ladder diagram will have two steps. What is the predominate form of carbonic acid when the pH is 7.00? Relevant equilibrium constants are in Appendix 11.

Answer

From Appendix 11, the pK_a values for H_2CO_3 are 6.352 and 10.329. The ladder diagram for H_2CO_3 is shown below. The predominate form at a pH of 7.00 is $\mathbf{HCO_3^-}$.



A ladder diagram is particularly useful for evaluating the reactivity between a weak acid and a weak base. Figure 3.2.3 , for example, shows a single ladder diagram for acetic acid/acetate and for *p*-nitrophenol/*p*-nitrophenolate. An acid and a base can not co-exist if their respective areas of predominance do not overlap. If we mix together solutions of acetic acid and sodium *p*-nitrophenolate, the reaction

$$\mathrm{C_6H_4NO_2^-}(aq) + \mathrm{CH_3COOH}(aq) \rightleftharpoons \mathrm{CH_3COO^-}(aq) + \mathrm{C_6H_4NO_2H}(aq) \tag{3.2.2}$$

occurs because the areas of predominance for acetic acid and *p*-nitrophenolate do not overlap. The solution's final composition depends on which species is the limiting reagent. The following example shows how we can use the ladder diagram in Figure 3.2.3 to evaluate the result of mixing together solutions of acetic acid and *p*-nitrophenolate.

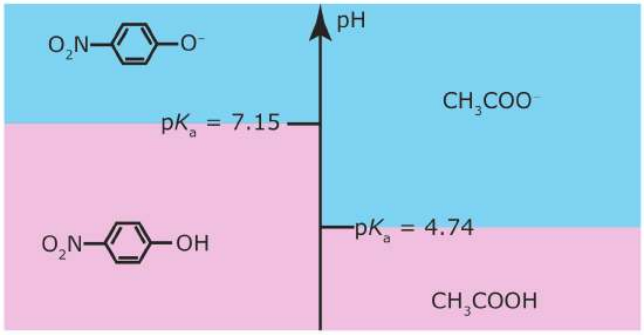


Figure 3.2.3 . Acid–base ladder diagram showing the areas of predominance for acetic acid/acetate and for *p*-nitrophenol/*p*-nitrophenolate. The areas shaded in blue shows the pH range where the weak bases are the predominate species; the weak acid forms are the predominate species in the areas shaded in pink.

Example 3.2.2

Predict the approximate pH and the final composition after mixing together 0.090 moles of acetic acid and 0.040 moles of *p*-nitrophenolate.

Solution

The ladder diagram in Figure 3.2.3 indicates that the reaction between acetic acid and *p*-nitrophenolate is favorable. Because acetic acid is in excess, we assume the reaction of *p*-nitrophenolate to *p*-nitrophenol is complete. At equilibrium essentially no *p*-nitrophenolate remains and there are 0.040 mol of *p*-nitrophenol. Converting *p*-nitrophenolate to *p*-nitrophenol consumes 0.040 moles of acetic acid; thus

$$\text{moles } \mathrm{CH_3COOH} = 0.090 - 0.040 = 0.050 \text{ mol}$$
$$\text{moles } \mathrm{CH_3COO^-} = 0.040 \text{ mol}$$

According to the ladder diagram, the pH is 4.74 when there are equal amounts of CH_3COOH and CH_3COO^-. Because we have slightly more CH_3COOH than CH_3COO^-, the pH is slightly less than 4.74.

Exercise 3.2.2

Using Figure 3.2.3 , predict the approximate pH and the composition of the solution formed by mixing together 0.090 moles of *p*-nitrophenolate and 0.040 moles of acetic acid.

Answer

The ladder diagram in Figure 3.2.3 indicates that the reaction between acetic acid and *p*-nitrophenolate is favorable. Because *p*-nitrophenolate is in excess, we assume the reaction of acetic acid to acetate is complete. At equilibrium essentially no acetic acid remains and there are 0.040 moles of acetate. Converting acetic acid to acetate consumes 0.040 moles of *p*-nitrophenolate; thus

$$\text{moles } p\text{-nitrophenolate } = 0.090 - 0.040 = 0.050 \text{ mol}$$

$$\text{moles } p\text{-nitrophenol } = 0.040 \text{ mol}$$

According to the ladder diagram for this system, the pH is 7.15 when there are equal concentrations of *p*-nitrophenol and *p*-nitrophenolate. Because we have slightly more *p*-nitrophenolate than we have *p*-nitrophenol, the pH is slightly greater than 7.15.

If the areas of predominance for an acid and a base overlap, then we do not expect that much of a reaction will occur. For example, if we mix together solutions of CH_3COO^- and *p*-nitrophenol, we do not expect a significant change in the moles of either reagent. Furthermore, the pH of the mixture must be between 4.76 and 7.15, with the exact pH depending upon the relative amounts of CH_3COO^- and *p*-nitrophenol.

We also can use an acid–base ladder diagram to evaluate the effect of pH on other equilibria. For example, the solubility of CaF_2

$$CaF_2(s) \rightleftharpoons Ca^{2+}(aq) + 2F^-(aq)$$

is affected by pH because F^- is a weak base. From Le Châtelier's principle, we know that converting F^- to HF will increase the solubility of CaF_2. To minimize the solubility of CaF_2 we need to maintain the solution's pH so that F^- is the predominate species. The ladder diagram for HF (Figure 3.2.4) shows us that maintaining a pH of more than 3.17 will minimize solubility losses.

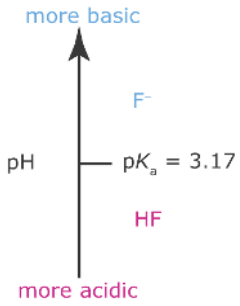


Figure 3.2.4 . Acid–base ladder diagram for HF. To minimize the solubility of CaF_2, we need to keep the pH above 3.17, with more basic pH levels leading to smaller solubility losses. See Chapter 8 for a more detailed discussion.

This page titled 3.2: Ladder Diagrams for Acid-Base Equilibria is shared under a CC BY-NC-SA 4.0 license and was authored, remixed, and/or curated by Kathryn Davis.

- **6.6: Ladder Diagrams** by David Harvey is licensed CC BY-NC-SA 4.0.

3.3: Solving Acid-Base Equilibrium Problems

Ladder diagrams are a useful tool for evaluating chemical reactivity and for providing a reasonable estimate of a chemical system's composition at equilibrium. If we need a more exact quantitative description of the equilibrium condition, then a ladder diagram is insufficient; instead, we need to find an algebraic solution. In this section we will learn how to set-up and solve equilibrium problems. We will start with a simple problem and work toward more complex problems.

A Systematic Approach to Solving Equilibrium Problems

Determining the equilibrium composition of a system with multiple equilibrium reactions is more complicated, but not irretrievably so. In this section we introduce a systematic approach to setting-up and solving equilibrium problems. As shown in Table 3.3.1 , this approach involves four steps.

Table 3.3.1 . Systematic Approach to Solving Equilibrium Problems

Step 1 Write all relevant equilibrium reactions and equilibrium constant expressions.
Step 2 Count the unique species that appear in the equilibrium constant expressions; these are your unknowns. You have enough information to solve the problem if the number of unknowns equals the number of equilibrium constant expressions. If not, add a mass balance equation and/or a charge balance equation. Continue adding equations until the number of equations equals the number of unknowns.
Step 3 Combine your equations and solve for one unknown. Whenever possible, simplify the algebra by making appropriate assumptions. If you make an assumption, set a limit for its error. This decision influences your evaluation of the assumption.
Step 4 Check your assumptions. If any assumption proves invalid, return to the previous step and continue solving. The problem is complete when you have an answer that does not violate any of your assumptions.

In addition to equilibrium constant expressions, two other equations are important to this systematic approach to solving an equilibrium problem. The first of these equations is a ***mass balance equation***, which simply is a statement that matter is conserved during a chemical reaction. In a solution of acetic acid, for example, the combined concentrations of the conjugate weak acid, CH_3COOH, and the conjugate weak base, CH_3COO^-, must equal acetic acid's initial concentration, C_{CH_3COOH}.

$$C_{CH_3COOH} = [CH_3COOH] + [CH_3COO^-]$$

> You may recall from Chapter 2 that this is the difference between a formal concentration and a molar concentration. The variable C represents a formal concentration.

The second equation is a ***charge balance equation***, which requires that the total positive charge from the cations equal the total negative charge from the anions. Mathematically, the charge balance equation is

$$\sum_{i=1}^{n} (z^+)_i \left[C^{z+}\right]_i = -\sum_{j=1}^{m} (z^-)_j \left[A^{z-}\right]_j$$

where $[C^{z+}]_i$ and $[A^{z-}]_j$ are, respectively, the concentrations of the i^{th} cation and the j^{th} anion, and $(z^+)_i$ and $(z^-)_j$ are the charges for the i^{th} cation and the j^{th} anion. Every ion in solution, even if it does not appear in an equilibrium reaction, must appear in the charge balance equation. For example, the charge balance equation for an aqueous solution of $Ca(NO_3)_2$ is

$$2 \times [Ca^{2+}] + [H_3O^+] = [OH^+] + [NO_3^-]$$

Note that we multiply the concentration of Ca^{2+} by two and that we include the concentrations of H_3O^+ and OH^-.

A charge balance is a conservation of a charge. The minus sign in front of the summation term on the right side of the charge balance equation ensures that both summations are positive. There are situations where it is impossible to write a charge balance equation because we do not have enough information about the solution's composition. For example, suppose we fix a solution's pH using a buffer. If the buffer's composition is not specified, then we cannot write a charge balance equation.

Example 3.3.2

Write mass balance equations and a charge balance equation for a 0.10 M solution of $NaHCO_3$.

Solution

It is easier to keep track of the species in solution if we write down the reactions that define the solution's composition. These reactions are the dissolution of a soluble salt

$$\mathrm{NaHCO_3}(s) \rightarrow \mathrm{Na^+}(aq) + \mathrm{HCO_3^-}(aq)$$

and the acid–base dissociation reactions of $\mathrm{HCO_3^-}$ and H_2O

$$\mathrm{HCO_3^-}(aq) + \mathrm{H_2O}(l) \rightleftharpoons \mathrm{H_3O^+}(aq) + \mathrm{CO_3^{2-}}(aq)$$

$$\mathrm{HCO_3^-}(aq) + \mathrm{H_2O}(l) \rightleftharpoons \mathrm{OH^-}(aq) + \mathrm{H_2CO_3}(aq)$$

$$2\mathrm{H_2O}(l) \rightleftharpoons \mathrm{H_3O^+}(aq) + \mathrm{OH^-}(aq)$$

The mass balance equations are

$$0.10\mathrm{M} = [\mathrm{H_2CO_3}] + [\mathrm{HCO_3^-}] + [\mathrm{CO_3^{2-}}]$$

$$0.10\ \mathrm{M} = [\mathrm{Na^+}]$$

and the charge balance equation is

$$[\mathrm{Na^+}] + [\mathrm{H_3O^+}] = [\mathrm{OH^-}] + [\mathrm{HCO_3^-}] + 2 \times [\mathrm{CO_3^{2-}}]$$

Exercise 3.3.3

Write appropriate mass balance and charge balance equations for a solution containing 0.10 M KH_2PO_4 and 0.050 M Na_2HPO_4.

Answer

To help us determine what ions are in solution, let's write down all the reaction needed to prepare the solutions and the equilibrium reactions that take place within these solutions. These reactions are the dissolution of two soluble salts

$$\mathrm{KH_2PO_4}(s) \longrightarrow \mathrm{K^+}(aq) + \mathrm{H_2PO_4^-}(aq)$$

$$\mathrm{NaHPO_4}(s) \longrightarrow \mathrm{Na^+}(aq) + \mathrm{HPO_4^{2-}}(aq)$$

and the acid–base dissociation reactions for $\mathrm{H_2PO_4^-}$, $\mathrm{HPO_4^{2-}}$. and H_2O.

$$\mathrm{H_2PO_4^-}(aq) + \mathrm{H_2O}(l) \rightleftharpoons \mathrm{H_3O^+}(aq) + \mathrm{HPO_4^{2-}}(aq)$$

$$\mathrm{H_2PO_4^-}(aq) + \mathrm{H_2O}(l) \rightleftharpoons \mathrm{OH^-}(aq) + \mathrm{H_3PO_4}(aq)$$

$$\mathrm{HPO_4^{2-}}(aq) + \mathrm{H_2O}(l) \rightleftharpoons \mathrm{H_3O^+}(aq) + \mathrm{PO_4^{3-}}(aq)$$

$$2\mathrm{H_2O}(l) \rightleftharpoons \mathrm{H_3O^+}(aq) + \mathrm{OH^-}(aq)$$

Note that we did not include the base dissociation reaction for $\mathrm{HPO_4^{2-}}$ because we already accounted for its product, $\mathrm{H_2PO_4^-}$, in another reaction. The mass balance equations for K^+ and Na^+ are straightforward

$$[\mathrm{K^+}] = 0.10\ \mathrm{M}\ \text{and}\ [\mathrm{Na^+}] = 0.10\ \mathrm{M}$$

but the mass balance equation for phosphate takes a bit more thought. Both $H_2PO_4^-$ and HPO_4^{2-} produce the same ions in solution. We can, therefore, imagine that the solution initially contains 0.15 M KH_2PO_4, which gives the following mass balance equation.

$$[H_3PO_4] + [H_2PO_4^-] + [HPO_4^{2-}] + [PO_4^{3-}] = 0.15\ M$$

The charge balance equation is

$$[H_3O^+] + [K^+] + [Na^+] = [H_2PO_4^-] + 2 \times [HPO_4^{2-}] + 3 \times [PO_4^{3-}] + [OH^-]$$

pH of a Monoprotic Weak Acid

To illustrate the systematic approach to solving equilibrium problems, let's calculate the pH of 1.0 M HF. Two equilibrium reactions affect the pH. The first, and most obvious, is the acid dissociation reaction for HF

$$HF(aq) + H_2O(l) \rightleftharpoons H_3O^+(aq) + F^-(aq)$$

for which the equilibrium constant expression is

$$K_a = \frac{[H_3O^+]\,[F^-]}{[HF]} = 6.8 \times 10^{-4} \tag{3.3.1}$$

The second equilibrium reaction is the dissociation of water, which is an obvious yet easily neglected reaction

$$2H_2O(l) \rightleftharpoons H_3O^+(aq) + OH^-(aq)$$

$$K_w = [H_3O^+]\,[OH^-] = 1.00 \times 10^{-14} \tag{3.3.2}$$

Counting unknowns, we find four: [HF], [F^-], [H_3O^+], and [OH^-]. To solve this problem we need two additional equations. These equations are a mass balance equation on hydrofluoric acid

$$C_{HF} = [HF] + [F^-] = 1.0M \tag{3.3.3}$$

and a charge balance equation

$$[H_3O^+] = [OH^-] + [F^-] \tag{3.3.4}$$

With four equations and four unknowns, we are ready to solve the problem. Before doing so, let's simplify the algebra by making two assumptions.

Assumption One. Because HF is a weak acid, we know that the solution is acidic. For an acidic solution it is reasonable to assume that

$$[H_3O^+] >> [OH^-]$$

which simplifies the charge balance equation to

$$[H_3O^+] = [F^-] \tag{3.3.5}$$

Assumption Two. Because HF is a weak acid, very little of it dissociates to form F^-. Most of the HF remains in its conjugate weak acid form and it is reasonable to assume that

$$[HF] >> [F^-]$$

which simplifies the mass balance equation to

$$C_{HF} = [HF] = 1.0\ M \tag{3.3.6}$$

For this exercise let's accept an assumption if it introduces an error of less than ±5%.

Substituting Equation 3.3.5 and Equation 3.3.6 into Equation 3.3.1, and solving for the concentration of H_3O^+ gives us

$$K_a = \frac{[H_3O^+]\,[F^-]}{[HF]} = \frac{[H_3O^+]\,[H_3O^+]}{C_{HF}} = \frac{[H_3O^+]^2}{C_{HF}} = 6.8 \times 10^{-4}$$

$$[H_3O^+] = \sqrt{K_a C_{HF}} = \sqrt{(6.8 \times 10^{-4})(1.0)} = 2.6 \times 10^{-2}$$

Before accepting this answer, we must verify our assumptions. The first assumption is that $[OH^-]$ is significantly smaller than $[H_3O^+]$. Using Equation 3.3.2, we find that

$$[OH^-] = \frac{K_w}{[H_3O^+]} = \frac{1.00 \times 10^{-14}}{2.6 \times 10^{-2}} = 3.8 \times 10^{-13}$$

Clearly this assumption is acceptable. The second assumption is that $[F^-]$ is significantly smaller than [HF]. From Equation 3.3.5 we have

$$[F^-] = 2.6 \times 10^{-2}\ M$$

Because $[F^-]$ is 2.60% of C_{HF}, this assumption also is acceptable. Given that $[H_3O^+]$ is 2.6×10^{-2} M, the pH of 1.0 M HF is 1.59.

How does the calculation change if we require that the error introduced in our assumptions be less than ±1%? In this case we no longer can assume that [HF] >> $[F^-]$ and we cannot simplify the mass balance equation. Solving the mass balance equation for [HF]

$$[HF] = C_{HF} - [F^-] = C_{HF} - [H_3O^+]$$

and substituting into the K_a expression along with Equation 3.3.5 gives

$$K_a = \frac{[H_3O^+]^2}{C_{HF} - [H_3O^+]}$$

Rearranging this equation leaves us with a quadratic equation

$$[H_3O^+]^2 + K_a[H_3O^+] - K_a C_{HF} = 0$$

which we solve using the quadratic formula

$$x = \frac{-b \pm \sqrt{b^2 - 4ac}}{2a}$$

where a, b, and c are the coefficients in the quadratic equation

$$ax^2 + bx + c = 0$$

Solving a quadratic equation gives two roots, only one of which has chemical significance. For our problem, the equation's roots are

$$x = \frac{-6.8 \times 10^{-4} \pm \sqrt{(6.8 \times 10^{-4})^2 - (4)(1)(-6.8 \times 10^{-4})}}{(2)(1)}$$

$$x = \frac{-6.8 \times 10^{-4} \pm 5.22 \times 10^{-2}}{2}$$

$$x = 2.57 \times 10^{-2} \text{ or } -2.64 \times 10^{-2}$$

Only the positive root is chemically significant because the negative root gives a negative concentration for H_3O^+. Thus, $[H_3O^+]$ is 2.57×10^{-2} M and the pH is 1.59.

You can extend this approach to calculating the pH of a monoprotic weak base by replacing K_a with K_b, replacing C_{HF} with the weak base's concentration, and solving for $[OH^-]$ in place of $[H_3O^+]$.

? Exercise 3.3.4

Calculate the pH of 0.050 M NH_3. State any assumptions you make in solving the problem, limiting the error for any assumption to ±5%. The K_b value for NH_3 is 1.75×10^{-5}.

Answer

To determine the pH of 0.050 M NH_3, we need to consider two equilibrium reactions: the base dissociation reaction for NH_3

$$NH_3(aq) + H_2O(l) \rightleftharpoons OH^-(aq) + NH_4^+(aq)$$

and water's dissociation reaction.

$$2H_2O(l) \rightleftharpoons H_3O^+(aq) + OH^-(aq)$$

These two reactions contain four species whose concentrations we need to consider: NH_3, NH_4^+, H_3O^+, and OH^-. We need four equations to solve the problem—these equations are the K_b equation for NH_3

$$K_b = \frac{[NH_4^+]\,[OH^-]}{[NH_3]} = 1.75 \times 10^{-5}$$

the K_w equation for H_2O

$$K_w = [H_3O^+]\,[OH^-]$$

a mass balance equation on ammonia

$$C_{NH_3} = 0.050\ M = [NH_3] + [NH_4^+]$$

and a charge balance equation

$$[H_3O^+] + [NH_4^+] = [OH^-]$$

To solve this problem, we will make two assumptions. Because NH_3 is a base, our first assumption is

$$[OH^-] >> [H_3O^+]$$

which simplifies the charge balance equation to

$$[NH_4^+] = [OH^-]$$

Because NH_3 is a weak base, our second assumption is

$$[NH_3] >> [NH_4^+]$$

which simplifies the mass balance equation to

$$C_{NH_3} = 0.050\ M = [NH_3]$$

Substituting the simplified charge balance equation and mass balance equation into the K_b equation leave us with

$$K_b = \frac{[NH_4^+]\,[OH^-]}{[NH_3]} = \frac{[OH^-]\,[OH^-]}{C_{NH_3}} = \frac{[OH^-]^2}{C_{NH_3}} = 1.75 \times 10^{-5}$$

$$[OH^-] = \sqrt{K_b C_{NH_3}} = \sqrt{(1.75 \times 10^{-5})\,(0.050)} = 9.35 \times 10^{-4}$$

Before we accept this answer, we must verify our two assumptions. The first assumption is that the concentration of OH^- is significantly greater than the concentration of H_3O^+. Using K_w, we find that

$$[H_3O^+] = \frac{K_w}{[OH^-]} = \frac{1.00 \times 10^{-14}}{9.35 \times 10^{-4}} = 1.07 \times 10^{-11}$$

Clearly this assumption is acceptable. Our second assumption is that the concentration of NH_3 is significantly greater than the concentration of NH_4^+. Using our simplified charge balance equation, we find that

$$[NH_4^+] = [OH^-] = 9.35 \times 10^{-4}$$

Because the concentration of NH_4^+ is 1.9% of C_{NH_3}, our second assumption also is reasonable. Given that $[H_3O^+]$ is 1.07×10^{-11}, the pH is 10.97.

pH of a Polyprotic Acid or Base

A more challenging problem is to find the pH of a solution that contains a polyprotic weak acid or one of its conjugate species. As an example, consider the amino acid alanine, whose structure is shown in Figure 3.3.1 . The ladder diagram in Figure 3.3.2 shows alanine's three acid–base forms and their respective areas of predominance. For simplicity, we identify these species as H_2L^+, HL, and L^-.

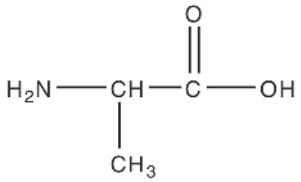


Figure 3.3.1 . Structure of the amino acid alanine, which has pK_a values of 2.348 (–COOH) and 9.867 (–NH_2).

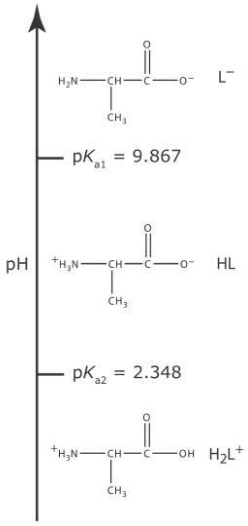


Figure 3.3.2 . Ladder diagram for alanine.

pH of 0.10 M Alanine Hydrochloride (H_2L^+)

Alanine hydrochloride is the salt of the diprotic weak acid H_2L^+ and Cl^-. Because H_2L^+ has two acid dissociation reactions, a complete systematic solution to this problem is more complicated than that for a monoprotic weak acid. The ladder diagram in Figure 3.3.2 helps us simplify the problem. Because the areas of predominance for H_2L^+ and L^- are so far apart, we can assume that a solution of H_2L^+ will not contain a significant amount of L^-. As a result, we can treat H_2L^+ as though it is a monoprotic weak acid. Calculating the pH of 0.10 M alanine hydrochloride, which is 1.72, is left to the reader as an exercise.

pH of 0.10 M Sodium Alaninate (L^-)

The alaninate ion is a diprotic weak base. Because L^- has two base dissociation reactions, a complete systematic solution to this problem is more complicated than that for a monoprotic weak base. Once again, the ladder diagram in Figure 3.3.2 helps us simplify the problem. Because the areas of predominance for H_2L^+ and L^- are so far apart, we can assume that a solution of L^- will not contain a significant amount of H_2L^+. As a result, we can treat L^- as though it is a monoprotic weak base. Calculating the pH of 0.10 M sodium alaninate, which is 11.42, is left to the reader as an exercise.

pH of 0.10 M Alanine (HL)

Finding the pH of a solution of alanine is more complicated than our previous two examples because we cannot ignore the presence of either H_2L^+ or L^-. To calculate the solution's pH we must consider alanine's acid dissociation reaction

$$\mathbf{HL}(aq) + \mathbf{H_2O}(l) \rightleftharpoons \mathbf{H_3O^+}(aq) + \mathbf{L^-}(aq)$$

and its base dissociation reaction

$$\mathbf{HL}(aq) + \mathbf{H_2O}(l) \rightleftharpoons \mathbf{OH^-}(aq) + \mathbf{H_2L^+}(aq)$$

and, as always, we must also consider the dissociation of water

$$\mathbf{2H_2O}(l) \rightleftharpoons \mathbf{H_3O^+}(aq) + \mathbf{OH^-}(aq)$$

This leaves us with five unknowns—[H_2L^+], [HL], [L^-], [H_3O^+], and [OH^-]—for which we need five equations. These equations are K_{a2} and K_{b2} for alanine

$$K_{a2} = \frac{[H_3O^+]\,[L^-]}{[HL]}$$

$$K_{b2} = \frac{K_w}{K_{a1}} = \frac{[OH^-]\,[H_2L^+]}{[HL]}$$

the K_w equation

$$K_w = [H_3O^+]\,[OH^-]$$

a mass balance equation for alanine

$$C_{HL} = [H_2L^+] + [HL] + [L^-]$$

and a charge balance equation

$$[H_2L^+] + [H_3O^+] = [OH^-] + [L^-]$$

Because HL is a weak acid and a weak base, it seems reasonable to assume that little of it will dissociate and that

$$[HL] >> [H_2L^+] + [L^-]$$

which allows us to simplify the mass balance equation to

$$C_{HL} = [HL]$$

Next we solve K_{b2} for [H_2L^+]

$$[H_2L^+] = \frac{K_w[HL]}{K_{a1}\,[OH^-]} = \frac{[H_3O^+]\,[HL]}{K_{a1}} = \frac{C_{HL}\,[H_3O^+]}{K_{a1}}$$

and solve K_{a2} for [L^-]

$$[L^-] = \frac{K_{a2}[HL]}{[H_3O^+]} = \frac{K_{a2}C_{HL}}{[H_3O^+]}$$

Substituting these equations for [H_2L^+] and [L^-], and the equation for K_w, into the charge balance equation give us

$$\frac{C_{HL}\,[H_3O^+]}{K_{a1}} + [H_3O^+] = \frac{K_w}{[H_3O^+]} + \frac{K_{a2}C_{HL}}{[H_3O^+]}$$

which we simplify to

$$[H_3O^+]\left(\frac{C_{HL}}{K_{a1}} + 1\right) = \frac{1}{[H_3O^+]}\left(K_w + K_{a2}C_{HL}\right)$$

$$[H_3O^+]^2 = \frac{(K_{a2}C_{HL} + K_w)}{\frac{C_{HL}}{K_{a1}} + 1} = \frac{K_{a1}\,(K_{a2}C_{HL} + K_w)}{C_{HL} + K_{a1}}$$

$$[H_3O^+] = \sqrt{\frac{(K_{a1}K_{a2}C_{HL} + K_{a1}K_w)}{C_{HL} + K_{a1}}}$$

We can further simplify this equation if $K_{a1}K_w << K_{a1}K_{a2}C_{HL}$, and if $K_{a1} << C_{HL}$, leaving us with

$$[H_3O^+] = \sqrt{K_{a1}K_{a2}}$$

For a solution of 0.10 M alanine the [H_3O^+] is

$$[H_3O^+] = \sqrt{\left(4.487 \times 10^{-3}\right)\left(1.358 \times 10^{-10}\right)} = 7.806 \times 10^{-7}\ \text{M}$$

or a pH of 6.11.

Exercise 3.3.5

Verify that each assumption in our solution for the pH of 0.10 M alanine is reasonable, using ±5% as the limit for the acceptable error.

Answer

In solving for the pH of 0.10 M alanine, we made the following three assumptions: (a) [HL] >> [H_2L^+] + [L^-]; (b) $K_{a1}K_w$ << $K_{a1}K_{a2}C_{HL}$; and (c) K_{a1} << C_{HL}. Assumptions (b) and (c) are easy to check. The value of K_{a1} ($\mathbf{4.487 \times 10^{-3}}$) is 4.5% of C_{HL} (0.10), and K_{a1}Kw ($\mathbf{4.487 \times 10^{-17}}$) is 0.074% of $K_{a1}K_{a2}C_{HL}$ ($\mathbf{6.093 \times 10^{-14}}$). Each of these assumptions introduces an error of less than ±5%.

To test assumption (a) we need to calculate the concentrations of H_2L^+ and L^-, which we accomplish using the equations for K_{a1} and K_{a2}.

$$[\mathbf{H_2L^+}] = \frac{[\mathbf{H_3O^+}]\,[\mathbf{HL}]}{K_{a1}} = \frac{(7.807 \times 10^{-7})\,(0.10)}{4.487 \times 10^{-3}} = 1.74 \times 10^{-5}$$

$$[\mathbf{L^-}] = \frac{K_{a2}[\mathbf{HL}]}{[\mathbf{H_3O^+}]} = \frac{(1.358 \times 10^{-10})\,(0.10)}{7.807 \times 10^{-7}} = 1.74 \times 10^{-5}$$

Because these concentrations are less than ±5% of *C*HL, the first assumption also is acceptable.

This page titled 3.3: Solving Acid-Base Equilibrium Problems is shared under a CC BY-NC-SA 4.0 license and was authored, remixed, and/or curated by Kathryn Davis.

- **6.7: Solving Equilibrium Problems** by David Harvey is licensed CC BY-NC-SA 4.0.

3.4: Buffer Solutions

Adding as little as 0.1 mL of concentrated HCl to a liter of H_2O shifts the pH from 7.0 to 3.0. Adding the same amount of HCl to a liter of a solution that 0.1 M in acetic acid and 0.1 M in sodium acetate, however, results in a negligible change in pH. Why do these two solutions respond so differently to the addition of HCl?

A mixture of acetic acid and sodium acetate is one example of an acid–base ***buffer***. To understand how this buffer works to limit the change in pH, we need to consider its acid dissociation reaction

$$\mathrm{CH_3COOH}(aq) + \mathrm{H_2O}(l) \rightleftharpoons \mathrm{H_3O^+}(aq) + \mathrm{CH_3COO^-}(aq)$$

and its corresponding acid dissociation constant

$$K_a = \frac{[\mathrm{CH_3COO^-}]\,[\mathrm{H_3O^+}]}{[\mathrm{CH_3COOH}]} = 1.75 \times 10^{-5} \tag{3.4.1}$$

Taking the negative log of the terms in Equation 3.4.1 and solving for pH leaves us with the result shown here.

$$\mathrm{pH} = \mathrm{p}K_\mathrm{a} + \log \frac{[\mathrm{CH_3COO^-}]}{[\mathrm{CH_3COOH}]}$$

$$\mathrm{pH} = 4.76 + \log \frac{[\mathrm{CH_3COO^-}]}{[\mathrm{CH_3COOH}]} \tag{3.4.2}$$

> You may recall that we developed these same equations in Chapter 6.6 when we introduced ladder diagrams.

Buffering occurs because of the logarithmic relationship between pH and the concentration ratio of acetate and acetic acid. Here is an example to illustrate this point. If the concentrations of acetic acid and acetate are equal, the buffer's pH is 4.76. If we convert 10% of the acetate to acetic acid, by adding a strong acid, the ratio $[CH_3COO^-]/[CH_3COOH]$ changes from 1.00 to 0.818, and the pH decreases from 4.76 to 4.67—a decrease of only 0.09 pH units.

> The ratio $[CH_3COO^-]/[CH_3COOH]$ becomes 0.9/1.1 = 0.818 and the pH becomes
>
> $$\mathrm{pH} = 4.76 + \log(0.818) = 4.67$$

Systematic Solution to Buffer Problems

Equation 3.4.2 is written in terms of the equilibrium concentrations of CH_3COOH and of CH_3COO^-. A more useful relationship relates a buffer's pH to the initial concentrations of the weak acid and the weak base. We can derive a general buffer equation by considering the following reactions for a weak acid, HA, and the soluble salt of its conjugate weak base, NaA.

$$\mathrm{NaA}(s) \rightarrow \mathrm{Na^+}(aq) + \mathrm{A^-}(aq)$$
$$\mathrm{HA}(aq) + \mathrm{H_2O}(l) \rightleftharpoons \mathrm{H_3O^+}(aq) + \mathrm{A^-}(aq)$$
$$2\mathrm{H_2O}(l) \rightleftharpoons \mathrm{H_3O^+}(aq) + \mathrm{OH^-}(aq)$$

Because the concentrations of Na^+, A^-, HA, H_3O^+, and OH^- are unknown, we need five equations to define the solution's composition. Two of these equations are the equilibrium constant expressions for HA and H_2O.

$$K_a = \frac{[\mathrm{H_3O^+}]\,[\mathrm{A^-}]}{[\mathrm{HA}]} \tag{3.4.3}$$

$$K_w = [\mathrm{H_3O^+}]\,[\mathrm{OH^-}]$$

The remaining three equations are mass balance equations for HA and Na^+

$$C_\mathrm{HA} + C_\mathrm{NaA} = [\mathrm{HA}] + [\mathrm{A^-}] \tag{3.4.4}$$

$$C_\mathrm{NaA} = [\mathrm{Na^+}] \tag{3.4.5}$$

and a charge balance equation

$$[H_3O^+] + [Na^+] = [OH^-] + [A^-] \tag{3.4.6}$$

Substituting Equation 3.4.5 into Equation 3.4.6 and solving for [A⁻] gives

$$[A^-] = C_{NaA} - [OH^-] + [H_3O^+] \tag{3.4.7}$$

Next, we substitute Equation 3.4.7 into Equation 3.4.4, which gives the concentration of HA as

$$[HA] = C_{HA} + [OH^-] - [H_3O^+] \tag{3.4.8}$$

Finally, we substitute Equation 3.4.7 and Equation 3.4.8 into Equation 3.4.3 and solve for pH to arrive at a general equation for a buffer's pH.

$$pH = pK_a + \log \frac{C_{NaA} - [OH^-] + [H_3O^+]}{C_{HA} + [OH^-] - [H_3O^+]}$$

If the initial concentrations of the weak acid, C_{HA}, and the weak base, C_{NaA}. are significantly greater than $[H_3O^+]$ and $[OH^-]$, then we can simplify the general equation to the ***Henderson–Hasselbalch equation***.

$$pH = pK_a + \log \frac{C_{NaA}}{C_{HA}} \tag{3.4.9}$$

As outlined below, the Henderson–Hasselbalch equation provides a simple way to calculate the pH of a buffer, and to determine the change in pH upon adding a strong acid or strong base.

Lawrence Henderson (1878-1942) first developed a relationship between $[H_3O^+]$, [HA], and $[A^-]$ while studying the buffering of blood. Kurt Hasselbalch (1874-1962) modified Henderson's equation by transforming it to the logarithmic form shown in Equation 3.4.9. The assumptions that lead to Equation 3.4.9 result in a minimal error in pH (<±5%) for larger concentrations of HA and A⁻, for concentrations of HA and A⁻ that are similar in magnitude, and for weak acid's with pK_a values closer to 7. For most problems in this textbook, Equation 3.4.9 provides acceptable results. Be sure, however, to test your assumptions. For a discussion of the Henderson–Hasselbalch equation, including the error inherent in Equation 3.4.9, see Po, H. N.; Senozan, N. M. "The Henderson–Hasselbalch Equation: Its History and Limitations," *J. Chem. Educ.* **2001**, *78*, 1499–1503.

Example 6.8.1

Calculate the pH of a buffer that is 0.020 M in NH_3 and 0.030 M in NH_4Cl. What is the pH after we add 1.0 mL of 0.10 M NaOH to 0.10 L of this buffer?

Solution

The acid dissociation constant for NH_4^+ is 5.70×10^{-10}, which is a pK_a of 9.24. Substituting the initial concentrations of NH_3 and NH_4Cl into Equation 3.4.9 and solving, we find that the buffer's pH is

$$pH = 9.24 + \log \frac{0.020}{0.030} = 9.06$$

With a pH of 9.06, the concentration of H_3O^+ is 8.71×10^{-10} and the concentration of OH^- is 1.15×10^{-5}. Because both of these concentrations are much smaller than either C_{NH_3} or C_{NH_4Cl}, the approximations used to derive Equation 3.4.9 are reasonable.

Adding NaOH converts a portion of the NH_4^+ to NH_3 following reaction

$$NH_4^+(aq) + OH^-(aq) \rightleftharpoons H_2O(l) + NH_3(aq)$$

Because this reaction's equilibrium constant is so large (it is equal to $(K_b)^{-1}$ or 5.7×10^4), we may treat the reaction as if it goes to completion. The new concentrations of NH_4^+ and NH_3 are

$$C_{NH_4^+} = \frac{\text{mol } NH_4^+ - \text{mol} OH^-}{V_{total}}$$

$$C_{NH_4^+} = \frac{(0.030\ \text{M})(0.10\ \text{L}) - (0.10\ \text{M})\left(1.0 \times 10^{-3}\ \text{L}\right)}{0.10\ \text{L} + 1.0 \times 10^{-3}\ \text{L}} = 0.029\ \text{M}$$

$$C_{NH_3} = \frac{\text{mol } NH_3 + \text{mol } OH^-}{V_{total}}$$

$$C_{NH_3} = \frac{(0.020\ \text{M})(0.10\ \text{L}) + (0.10\ \text{M})\left(1.0 \times 10^{-3}\ \text{L}\right)}{0.10\ \text{L} + 1.0 \times 10^{-3}\ \text{L}} = 0.021\ \text{M}$$

Substituting these concentrations into the equation 6.60 gives a pH of

$$\text{pH} = 9.24 + \log\frac{0.021}{0.029} = 9.10$$

Note that adding NaOH increases the pH from 9.06 to 9.10. As we expect, adding a base makes the pH more basic. Checking to see that the pH changes in the right direction is one way to catch a calculation error.

? Exercise 6.8.1

Calculate the pH of a buffer that is 0.10 M in KH_2PO_4 and 0.050 M in Na_2HPO_4. What is the pH after we add 5.0 mL of 0.20 M HCl to 0.10 L of this buffer. Use Appendix 11 to find the appropriate K_a value.

Answer

The acid dissociation constant for $H_2PO_4^-$ is 6.32×10^{-8}, or a pK_a of 7.199. Substituting the initial concentrations of $H_2PO_4^-$ and HPO_4^{2-} into Equation 3.4.9 and solving gives the buffer's pH as

$$\text{pH} = 7.199 + \log\frac{[HPO_4^{2-}]}{[H_2PO_4^-]} = 7.199 + \log\frac{0.050}{0.10} = 6.898 \approx 6.90$$

Adding HCl converts a portion of HPO_4^{2-} to $H_2PO_4^-$ as a result of the following reaction

$$HPO_4^{2-}(aq) + H_3O^+(aq) \rightleftharpoons H_2O(l) + H_2PO_4^-(aq)$$

Because this reaction's equilibrium constant is so large (it is 1.59×10^7), we may treat the reaction as if it goes to completion. The new concentrations of $H_2PO_4^-$ and HPO_4^{2-} are

$$C_{H_2PO_4^-} = \frac{\text{mol } H_2PO_4^- + \text{mol HCl}}{V_{total}}$$

$$C_{H_2PO_4^-} = \frac{(0.10\ \text{M})(0.10\ \text{L}) + (0.20\ \text{M})\left(5.0 \times 10^{-3}\ \text{L}\right)}{0.10\ \text{L} + 5.0 \times 10^{-3}\ \text{L}} = 0.105\ \text{M}$$

$$C_{HPO_4^{2-}} = \frac{\text{mol } HPO_4^{2-} - \text{mol HCl}}{V_{total}}$$

$$C_{HPO_4^{2-}} = \frac{(0.05\ \text{M})(0.10\ \text{L}) - (0.20\ \text{M})\left(5.0 \times 10^{-3}\ \text{L}\right)}{0.10\ \text{L} + 5.0 \times 10^{-3}\ \text{L}} = 0.0381\ \text{M}$$

Substituting these concentrations into Equation 3.4.9 gives a pH of

$$\text{pH} = 7.199 + \log\frac{[HPO_4^{2-}]}{[H_2PO_4^-]} = 7.199 + \log\frac{0.0381}{0.105} = 6.759 \approx 6.76$$

As we expect, adding HCl decreases the buffer's pH by a small amount, dropping from 6.90 to 6.76.

We can use a multiprotic weak acid to prepare buffers at as many different pH's as there are acidic protons, with the Henderson–Hasselbalch equation applying in each case. For example, for malonic acid (pK_{a1} = 2.85 and pK_{a2} = 5.70) we can prepare buffers with pH values of

$$\text{pH} = 2.85 + \log \frac{C_{\text{HM}^-}}{C_{\text{H}_2\text{M}}}$$

$$\text{pH} = 5.70 + \log \frac{C_{\text{M}^{2-}}}{C_{\text{HM}^-}}$$

where H_2M, HM^- and M^{2-} are malonic acid's different acid–base forms.

Although our treatment of buffers is based on acid–base chemistry, we can extend buffers to equilibria that involve complexation or redox reactions. For example, the Nernst equation for a solution that contains Fe^{2+} and Fe^{3+} is similar in form to the Henderson-Hasselbalch equation.

$$E = E^\circ_{\text{Fe}^{3+}/\text{Fe}^{2+}} - 0.05916 \log \frac{[\text{Fe}^{2+}]}{[\text{Fe}^{3+}]}$$

A solution that contains similar concentrations of Fe^{2+} and Fe^{3+} is buffered to a potential near the standard state reduction potential for Fe^{3+}. We call such solutions redox buffers. Adding a strong oxidizing agent or a strong reducing agent to a redox buffer results in a small change in potential.

Representing Buffer Solutions with Ladder Diagrams

A ladder diagram provides a simple way to visualize a solution's predominate species as a function of solution conditions. It also provides a convenient way to show the range of solution conditions over which a buffer is effective. For example, an acid–base buffer exists when the concentrations of the weak acid and its conjugate weak base are similar. For convenience, let's assume that an acid–base buffer exists when

$$\frac{1}{10} \leq \frac{[\text{CH}_3\text{COO}^-]}{[\text{CH}_3\text{COOH}]} \leq \frac{10}{1}$$

Substituting these ratios into the Henderson–Hasselbalch equation

$$\text{pH} = \text{p}K_\text{a} + \log \frac{1}{10} = \text{p}K_\text{a} - 1$$

$$\text{pH} = \text{p}K_\text{a} + \log \frac{10}{1} = \text{p}K_\text{a} + 1$$

shows that an acid–base buffer works over a pH range of $pK_a \pm 1$.

Using the same approach, it is easy to show that a metal-ligand complexation buffer for ML_n exists when

$$\text{pL} = \log K_n \pm 1 \text{ or } \text{pL} = \log \beta_n \pm \frac{1}{n}$$

where K_n or β_n is the relevant stepwise or overall formation constant. For an oxidizing agent and its conjugate reducing agent, a redox buffer exists when

$$E = E^\circ \pm \frac{1}{n} \times \frac{RT}{F} = E^\circ \pm \frac{0.05916}{n} \text{ (at 25°C)}$$

Figure 6.8.1 shows ladder diagrams with buffer regions for several equilibrium systems.

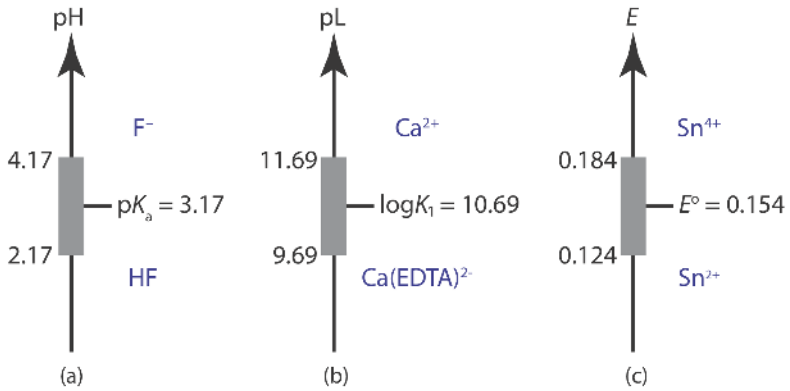


Figure 6.8.1 . Ladder diagrams showing buffer regions shaded in grey for (a) an acid–base buffer of HF and F^{-}; (b) a metal–ligand complexation buffer of Ca^{2+} and $Ca(EDTA)^{2-}$; and (c) an oxidation–reduction (redox) buffer of Sn^{4+} and Sn^{2+}.

Preparing a Buffer

Buffer capacity is the ability of a buffer to resist a change in pH when we add to it a strong acid or a strong base. A buffer's capacity to resist a change in pH is a function of the concentrations of the weak acid and the weak base, as well as their relative proportions. The importance of the weak acid's concentration and the weak base's concentration is obvious. The more moles of weak acid and weak base a buffer has, the more strong base or strong acid it can neutralize without a significant change in its pH.

> Although a higher concentration of buffering agents provides greater buffer capacity, there are reasons for using smaller concentrations, including the formation of unwanted precipitates and the tolerance of biological systems for high concentrations of dissolved salts.

The relative proportions of a weak acid and a weak base also affects how much the pH changes when we add a strong acid or a strong base. A buffer that is equimolar in weak acid and weak base requires a greater amount of strong acid or strong base to bring about a one unit change in pH. Consequently, a buffer is most effective against the addition of strong acids or strong bases when its pH is near the weak acid's pK_a value.

Buffer solutions are often prepared using standard "recipes" found in the chemical literature [see, for example, (a) Bower, V. E.; Bates, R. G. *J. Res. Natl. Bur. Stand. (U. S.)* **1955**, *55*, 197– 200; (b) Bates, R. G. *Ann. N. Y. Acad. Sci.* **1961**, *92*, 341–356; (c) Bates, R. G. *Determination of pH*, 2nd ed.; Wiley-Interscience: New York, 1973]. In addition, there are computer programs and on-line calculators to aid in preparing buffers [(a) Lambert, W. J. J. Chem. Educ. 1990, 67, 150–153; (b) http://www.bioinformatics.org/JaMBW/5/4/index.html.]. Perhaps the simplest way to make a buffer, however, is to prepare a solution that contains an appropriate conjugate weak acid and weak base, measure its pH, and then adjust the pH to the desired value by adding small portions of either a strong acid or a strong base.

> A good "rule of thumb" when choosing a buffer is to select one whose reagents have a pK_a value close to your desired pH.

This page titled 3.4: Buffer Solutions is shared under a CC BY-NC-SA 4.0 license and was authored, remixed, and/or curated by Kathryn Davis.

- **6.8: Buffer Solutions** by David Harvey is licensed CC BY-NC-SA 4.0.

CHAPTER OVERVIEW

4: There Are Other Titration Methods!

4.1: Complexation Titrations

4.2: EDTA Ladder Diagrams

4.3: Redox Titrations

4.4: Ladder Diagrams for Redox Titrations

This page titled 4: There Are Other Titration Methods! is shared under a not declared license and was authored, remixed, and/or curated by Kathryn Davis.

4.1: Complexation Titrations

The earliest examples of metal–ligand ***complexation titrations*** are Liebig's determinations, in the 1850s, of cyanide and chloride using, respectively, Ag^+ and Hg^{2+} as the titrant. Practical analytical applications of complexation titrimetry were slow to develop because many metals and ligands form a series of metal–ligand complexes. Liebig's titration of CN^- with Ag^+ was successful because they form a single, stable complex of $\mathbf{Ag(CN)_2^-}$, which results in a single, easily identified end point. Other metal–ligand complexes, such as $\mathbf{CdI_4^{2-}}$, are not analytically useful because they form a series of metal–ligand complexes (CdI^+, $CdI_2(aq)$, $\mathbf{CdI_3^-}$ and $\mathbf{CdI_4^{2-}}$) that produce a sequence of poorly defined end points.

> Recall that an acid–base titration curve for a diprotic weak acid has a single end point if its two K_a values are not sufficiently different. See Figure 9.2.6 for an example.

In 1945, Schwarzenbach introduced aminocarboxylic acids as multidentate ligands. The most widely used of these new ligands—ethylenediaminetetraacetic acid, or EDTA—forms a strong 1:1 complex with many metal ions. The availability of a ligand that gives a single, easily identified end point made complexation titrimetry a practical analytical method.

Chemistry and Properties of EDTA

Ethylenediaminetetraacetic acid, or EDTA, is an aminocarboxylic acid. EDTA, the structure of which is shown in Figure 4.1.1 a in its fully deprotonated form, is a Lewis acid with six binding sites—the four negatively charged carboxylate groups and the two tertiary amino groups—that can donate up to six pairs of electrons to a metal ion. The resulting metal–ligand complex, in which EDTA forms a cage-like structure around the metal ion (Figure 4.1.1 b), is very stable. The actual number of coordination sites depends on the size of the metal ion, however, all metal–EDTA complexes have a 1:1 stoichiometry.

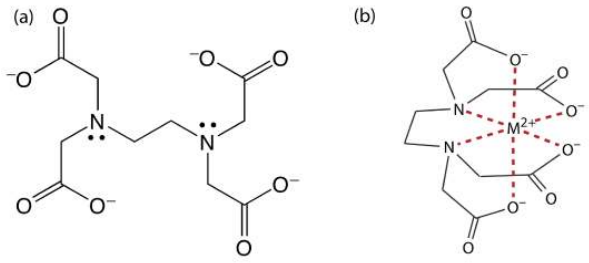


Figure 4.1.1 . Structures of (a) EDTA, in its fully deprotonated form, and (b) in a six-coordinate metal–EDTA complex with a divalent metal ion.

Metal–EDTA Formation Constants

To illustrate the formation of a metal–EDTA complex, let's consider the reaction between Cd^{2+} and EDTA

$$\mathbf{Cd^{2+}(aq) + Y^{4-}(aq) \rightleftharpoons CdY^{2-}(aq)} \tag{4.1.1}$$

where Y^{4-} is a shorthand notation for the fully deprotonated form of EDTA shown in Figure 4.1.1 a. Because the reaction's formation constant

$$K_f = \frac{[\mathbf{CdY^{2-}}]}{[\mathbf{Cd^{2+}}]\,[\mathbf{Y^{4-}}]} = \mathbf{2.9 \times 10^{16}} \tag{4.1.2}$$

is large, its equilibrium position lies far to the right. Formation constants for other metal–EDTA complexes are found in Appendix 12.

EDTA is a Weak Acid

In addition to its properties as a ligand, EDTA is also a weak acid. The fully protonated form of EDTA, H_6Y^{2+}, is a hexaprotic weak acid with successive pK_a values of

$$pK_{a1} = 0.0 \quad pK_{a2} = 1.5 \quad pK_{a3} = 2.0$$

$$pK_{a4} = 2.66 \quad pK_{a5} = 6.16 \quad pK_{a6} = 10.24$$

The first four values are for the carboxylic acid protons and the last two values are for the ammonium protons. Figure 4.1.2 shows a ladder diagram for EDTA. The specific form of EDTA in reaction 4.1.1 is the predominate species only when the pH is more basic than 10.24.

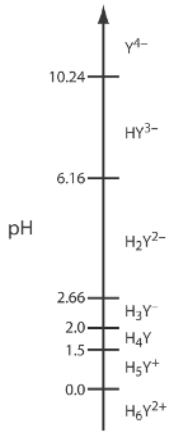


Figure 4.1.2 . Ladder diagram for EDTA.

Conditional Metal–Ligand Formation Constants

The formation constant for CdY^{2-} in Equation 4.1.2 assumes that EDTA is present as Y^{4-}. Because EDTA has many forms, when we prepare a solution of EDTA we know it total concentration, C_{EDTA}, not the concentration of a specific form, such as Y^{4-}. To use Equation 4.1.2, we need to rewrite it in terms of C_{EDTA}.

At any pH a mass balance on EDTA requires that its total concentration equal the combined concentrations of each of its forms.

$$C_{EDTA} = [H_6Y^{2+}] + [H_5Y^+] + [H_4Y] + [H_3Y^-] + [H_2Y^{2-}] + [HY^{3-}] + [Y^{4-}]$$

To correct the formation constant for EDTA's acid–base properties we need to calculate the fraction, $\alpha_{Y^{4-}}$, of EDTA that is present as Y^{4-}.

$$\alpha_{Y^{4-}} = \frac{[Y^{4-}]}{C_{EDTA}} \tag{4.1.3}$$

Table 4.1.1 provides values of $\alpha_{Y^{4-}}$ for selected pH levels. Solving Equation 4.1.3 for $[Y^{4-}]$ and substituting into Equation 4.1.2 for the CdY^{2-} formation constant

$$K_f = \frac{[CdY^{2-}]}{[Cd^{2+}]\,(\alpha_{Y^{4-}})C_{EDTA}}$$

and rearranging gives

$$K_f' = K_f \times \alpha_{Y^{4-}} = \frac{[CdY^{2-}]}{[Cd^{2+}]\,C_{EDTA}} \tag{4.1.4}$$

where K_f' is a pH-dependent ***conditional formation constant***. As shown in Table 4.1.2 , the conditional formation constant for CdY^{2-} becomes smaller and the complex becomes less stable at more acidic pHs.

Table 4.1.1 . Values of $\alpha_{Y^{4-}}$ for EDTA at Selected pH Levels

pH	$\alpha_{Y^{4-}}$	pH	$\alpha_{Y^{4-}}$
1	1.94×10^{-18}	8	5.68×10^{-3}
2	3.47×10^{-14}	9	5.47×10^{-2}
3	2.66×10^{-11}	10	0.367
4	3.80×10^{-9}	11	0.853
5	3.73×10^{-7}	12	0.983
6	2.37×10^{-5}	13	0.988
7	5.06×10^{-4}	14	1.00

Table 4.1.2 . Conditional Formation Constants for CdY^{2-}

pH	K'_f	pH	K'_f
1	5.6×10^{-2}	8	1.6×10^{14}
2	1.0×10^{3}	9	1.6×10^{15}
3	7.7×10^{5}	10	1.1×10^{16}
4	1.1×10^{8}	11	2.5×10^{16}
5	1.1×10^{10}	12	2.9×10^{16}
6	6.9×10^{11}	13	2.9×10^{16}
7	1.5×10^{13}	14	2.9×10^{16}

EDTA Competes With Other Ligands

To maintain a constant pH during a complexation titration we usually add a buffering agent. If one of the buffer's components is a ligand that binds with Cd^{2+}, then EDTA must compete with the ligand for Cd^{2+}. For example, an NH_4^+/NH_3 buffer includes NH_3, which forms several stable Cd^{2+}–NH_3 complexes. Because EDTA forms a stronger complex with Cd^{2+} than does NH_3, it displaces NH_3; however, the stability of the Cd^{2+}–EDTA complex decreases.

We can account for the effect of an ***auxiliary complexing agent***, such as NH_3, in the same way we accounted for the effect of pH. Before adding EDTA, the mass balance on Cd^{2+}, C_{Cd}, is

$$C_{Cd} = [Cd^{2+}] + [Cd(NH_3)^{2+}] + [Cd(NH_3)_2^{2+}] + [Cd(NH_3)_3^{2+}] + [Cd(NH_3)_4^{2+}]$$

and the fraction of uncomplexed Cd^{2+}, $\alpha_{Cd^{2+}}$, is

$$\alpha_{Cd^{2+}} = \frac{[Cd^{2+}]}{C_{Cd}} \tag{4.1.5}$$

> The value of $\alpha_{Cd^{2+}}$ depends on the concentration of NH_3. Contrast this with $\alpha_{Y^{4-}}$, which depends on pH.

Solving Equation 4.1.5 for $[Cd^{2+}]$ and substituting into Equation 4.1.4 gives

$$K'_f = K_f \times \alpha_{Y^{4-}} = \frac{[CdY^{2-}]}{\alpha_{Cd^{2+}} C_{Cd} C_{EDTA}}$$

Because the concentration of NH_3 in a buffer essentially is constant, we can rewrite this equation

$$K''_f = K_f \times \alpha_{Y^{4-}} \times \alpha_{Cd^{2+}} = \frac{[CdY^{2-}]}{C_{Cd} C_{EDTA}} \tag{4.1.6}$$

to give a conditional formation constant, K_f', that accounts for both pH and the auxiliary complexing agent's concentration. Table 4.1.3 provides values of $\alpha_{M^{2+}}$ for several metal ion when NH_3 is the complexing agent.

Table 4.1.3 . Values of $\alpha_{M^{2+}}$ for Selected Concentrations of Ammonia

$[NH_3]$ (M)	$\alpha_{Ca^{2+}}$	$\alpha_{Cd^{2+}}$	$\alpha_{Co^{2+}}$	$\alpha_{Cu^{2+}}$	$\alpha_{Mg^{2+}}$	$\alpha_{Ni^{2+}}$	$\alpha_{Zn^{2+}}$
1	5.50×10^{-1}	6.09×10^{-8}	1.00×10^{-6}	3.79×10^{-14}	1.76×10^{-1}	9.20×10^{-10}	3.95×10^{-10}
0.5	7.36×10^{-1}	1.05×10^{-6}	2.22×10^{-5}	6.86×10^{-13}	4.13×10^{-1}	3.44×10^{-8}	6.27×10^{-9}
0.1	9.39×10^{-1}	3.51×10^{-4}	6.64×10^{-3}	4.63×10^{-10}	8.48×10^{-1}	5.12×10^{-5}	3.68×10^{-6}
0.05	9.69×10^{-1}	2.72×10^{-3}	3.54×10^{-2}	7.17×10^{-9}	9.22×10^{-1}	6.37×10^{-4}	5.45×10^{-5}
0.01	9.94×10^{-1}	8.81×10^{-2}	3.55×10^{-1}	3.22×10^{-6}	9.84×10^{-1}	4.32×10^{-2}	1.82×10^{-2}
0.005	9.97×10^{-1}	2.27×10^{-1}	5.68×10^{-1}	3.62×10^{-5}	9.92×10^{-1}	1.36×10^{-1}	1.27×10^{-1}
0.001	9.99×10^{-1}	6.09×10^{-1}	8.84×10^{-1}	4.15×10^{-4}	9.98×10^{-1}	5.76×10^{-1}	7.48×10^{-1}

Complexometric EDTA Titration Curves

Now that we know something about EDTA's chemical properties, we are ready to evaluate its usefulness as a titrant. To do so we need to know the shape of a complexometric titration curve. In chapter 9.2 we learned that an acid–base titration curve shows how the titrand's pH changes as we add titrant. The analogous result for a complexation titration shows the change in pM, where M is the metal ion's concentration, as a function of the volume of EDTA. To look like titration curves that we already recognize, we graph volume of titrant (EDTA) on the *x*-axis and a *p* function on the *y*-axis. Since the metal ion is the analyte, we graph *pM* as

$$pM = -\log[M^{2+}]$$

The actual calculations are beyond what we're interested in here, but you can see a sample EDTA titration curve below for the titration of 50.0 mL of 0.00500 M Cd^{2+} with 0.0100 M EDTA at a pH of 10 and in the presence of 0.0100 M NH_3. Note that since Cd^{2+} reacts with EDTA in 1:1 stoichiometry, we see that at the equivalence point, moles of Cd^{2+} = moles EDTA.

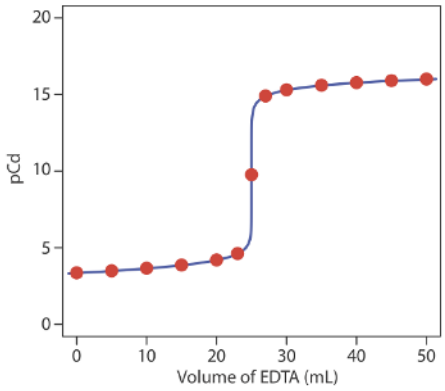


Figure 4.1.3 . Titration curve for the titration of 50.0 mL of 5.00×10^{-3} M Cd^{2+} with 0.0100 M EDTA at a pH of 10 and in the presence of 0.0100 M NH_3. The red points correspond to the data in Table 4.1.4 . The blue line shows the complete titration curve.

Selecting and Evaluating the Endpoint

The equivalence point of a complexation titration occurs when we react stoichiometrically equivalent amounts of the titrand and titrant. As is the case for an acid–base titration, we estimate the equivalence point for a complexation titration using an experimental end point. A variety of methods are available for locating the end point, including indicators and sensors that respond to a change in the solution conditions.

Finding the End Point with an Indicator

Most indicators for complexation titrations are organic dyes—known as ***metallochromic indicators***—that form stable complexes with metal ions. The indicator, In^{m-}, is added to the titrand's solution where it forms a stable complex with the metal ion, MIn^{n-}. As we add EDTA it reacts first with free metal ions, and then displaces the indicator from MIn^{n-}.

$$\mathbf{MIn^{n-}}(aq) + \mathbf{Y^{4-}}(aq) \rightarrow \mathbf{MY^{2-}}(aq) + \mathbf{In^{m-}}(aq)$$

If MIn^{n-} and In^{m-} have different colors, then the change in color signals the end point.

The accuracy of an indicator's end point depends on the strength of the metal–indicator complex relative to the strength of the metal–EDTA complex. If the metal–indicator complex is too strong, the change in color occurs after the equivalence point. If the metal–indicator complex is too weak, however, the end point occurs before we reach the equivalence point.

Most metallochromic indicators also are weak acids. One consequence of this is that the conditional formation constant for the metal–indicator complex depends on the titrand's pH. This provides some control over an indicator's titration error because we can adjust the strength of a metal–indicator complex by adjusted the pH at which we carry out the titration. Unfortunately, because the indicator is a weak acid, the color of the uncomplexed indicator also may change with pH. Figure 4.1.5 , for example, shows the color of the indicator calmagite as a function of pH and pMg, where H_2In^-, HIn^{2-}, and In^{3-} are different forms of the uncomplexed indicator, and $MgIn^-$ is the Mg^{2+}–calmagite complex. Because the color of calmagite's metal–indicator complex is red, its use as a metallochromic indicator has a practical pH range of approximately 8.5–11 where the uncomplexed indicator, HIn^{2-}, has a blue color.

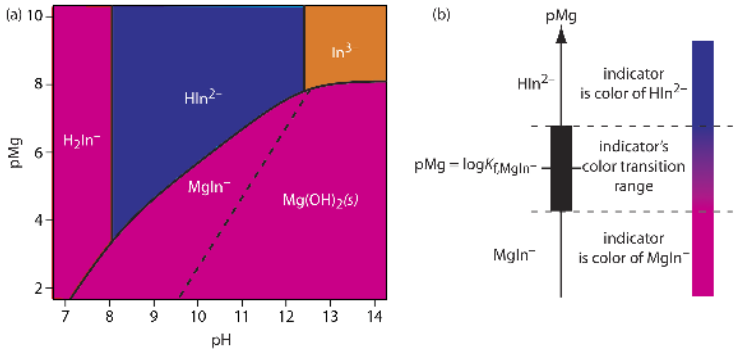


Figure 4.1.5 . (a) Predominance diagram for the metallochromic indicator calmagite showing the most important forms and colors of calmagite as a function of pH and pMg, where H_2In^-, HIn^{2-}, and In^{3-} are uncomplexed forms of calmagite, and $MgIn^-$ is its complex with Mg^{2+}. Conditions to the right of the dashed line, where Mg^{2+} precipitates as $Mg(OH)_2$, are not analytically useful for a complexation titration. A red to blue end point is possible if we maintain the titrand's pH in the range 8.5–11. (b) Diagram showing the relationship between the concentration of Mg^{2+} (as pMg) and the indicator's color. The ladder diagram defines pMg values where $MgIn^-$ and HIn^{2-} are predominate species. The indicator changes color when pMg is between $\log K_f - 1$ and $\log K_f + 1$. This figure is essentially a two-variable ladder diagram. The solid lines are equivalent to a step on a conventional ladder diagram, indicating conditions where two (or three) species are equal in concentration.

Table 4.1.5 provides examples of metallochromic indicators and the metal ions and pH conditions for which they are useful. Even if a suitable indicator does not exist, it often is possible to complete an EDTA titration by introducing a small amount of a secondary metal–EDTA complex if the secondary metal ion forms a stronger complex with the indicator and a weaker complex with EDTA than the analyte. For example, calmagite has a poor end point when titrating Ca^{2+} with EDTA. Adding a small amount of Mg^{2+}–EDTA to the titrand gives a sharper end point. Because Ca^{2+} forms a stronger complex with EDTA, it displaces Mg^{2+}, which then forms the red-colored Mg^{2+}–calmagite complex. At the titration's end point, EDTA displaces Mg^{2+} from the Mg^{2+}–calmagite complex, signaling the end point by the presence of the uncomplexed indicator's blue form.

Table 4.1.5 . Selected Metallochromic Indicators

indicator	pH range	metal ions	indicator	pH range	metal ions
calmagite	8.5–11	Ba, *Ca*, Mg, Zn	eriochrome Black T	7.5–10.5	Ba, *Ca*, Mg, Zn
eriochrome Blue Black R	8–12	*Ca*, Mg, Zn, Cu	PAN	2–11	Cd, Cu, Zn
murexide	6–13	Ca, Ni, Cu	salicylic acid	2–3	Fe
all metal ions carry a +2 charge expect for iron, which is +3 metal ions in *italic* font have poor end points					

Finding the End Point By Monitoring Absorbance

An important limitation when using a metallochromic indicator is that we must be able to see the indicator's change in color at the end point. This may be difficult if the solution is already colored. For example, when titrating Cu^{2+} with EDTA, ammonia is used to adjust the titrand's pH. The intensely colored $\mathbf{Cu(NH_3)_2^{4+}}$ complex obscures the indicator's color, making an accurate determination of the end point difficult. Other absorbing species present within the sample matrix may also interfere. This often is a problem when analyzing clinical samples, such as blood, or environmental samples, such as natural waters.

If at least one species in a complexation titration absorbs electromagnet- ic radiation, then we can identify the end point by monitoring the titrand's absorbance at a carefully selected wavelength. For example, we can identify the end point for a titration of Cu^{2+} with EDTA in the presence of NH_3 by monitoring the titrand's absorbance at a wavelength of 745 nm, where the $\mathbf{Cu(NH_3)_2^{4+}}$ complex absorbs strongly. At the beginning of the titration the absorbance is at a maximum. As we add EDTA, however, the reaction

$$\mathbf{Cu(NH_3)_4^{2+}}(aq) + \mathbf{Y^{4-}} \rightleftharpoons \mathbf{CuY^{2-}}(aq) + 4\mathbf{NH_3}(aq)$$

decreases the concentration of $\mathbf{Cu(NH_3)_2^{4+}}$ and decreases the absorbance until we reach the equivalence point. After the equivalence point the absorbance essentially remains unchanged. The resulting spectrophotometric titration curve is shown in Figure 4.1.6 a. Note that the titration curve's *y*-axis is not the measured absorbance, A_{meas}, but a corrected absorbance, A_{corr}

$$A_{corr} = A_{meas} \times \frac{V_{EDTA} + V_{Cu}}{V_{Cu}}$$

where V_{EDTA} and V_{Cu} are, respectively, the volumes of EDTA and Cu. Correcting the absorbance for the titrand's dilution ensures that the spectrophotometric titration curve consists of linear segments that we can extrapolate to find the end point. Other common spectrophotometric titration curves are shown in Figures 4.1.6 b-f.

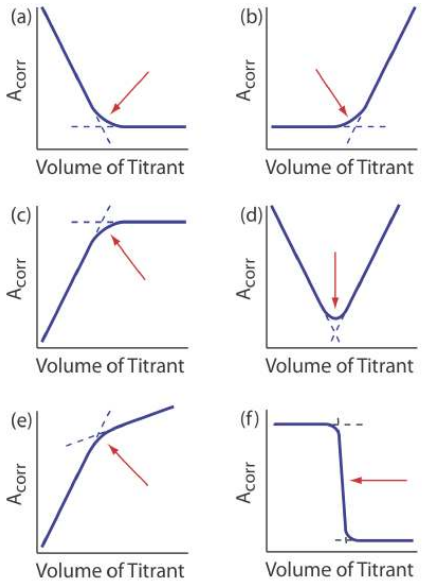


Figure 4.1.6 . Examples of spectrophotometric titration curves: (a) only the titrand absorbs; (b) only the titrant absorbs; (c) only the product of the titration reaction absorbs; (d) both the titrand and the titrant absorb; (e) both the titration reaction's product and the titrant absorb; (f) only the indicator absorbs. The red arrows indicate the end points for each titration curve.

Sample EDTA Method: Determination of Hardness of Water and Wastewater

The best way to appreciate the theoretical and the practical details discussed in this section is to carefully examine a typical complexation titrimetric method. Although each method is unique, the following description of the determination of the hardness of water provides an instructive example of a typical procedure. The description here is based on Method 2340C as published in *Standard Methods for the Examination of Water and Wastewater*, 20th Ed., American Public Health Association: Washington, D. C., 1998.

Description of the Method

The operational definition of water hardness is the total concentration of cations in a sample that can form an insoluble complex with soap. Although most divalent and trivalent metal ions contribute to hardness, the two most important metal ions are Ca^{2+} and Mg^{2+}. Hardness is determined by titrating with EDTA at a buffered pH of 10. Calmagite is used as an indicator. Hardness is reported as mg $CaCO_3$/L.

Procedure

Select a volume of sample that requires less than 15 mL of titrant to keep the analysis time under 5 minutes and, if necessary, dilute the sample to 50 mL with distilled water. Adjust the sample's pH by adding 1–2 mL of a pH 10 buffer that contains a small amount of Mg^{2+}–EDTA. Add 1–2 drops of indicator and titrate with a standard solution of EDTA until the red-to-blue end point is reached (Figure 4.1.7).

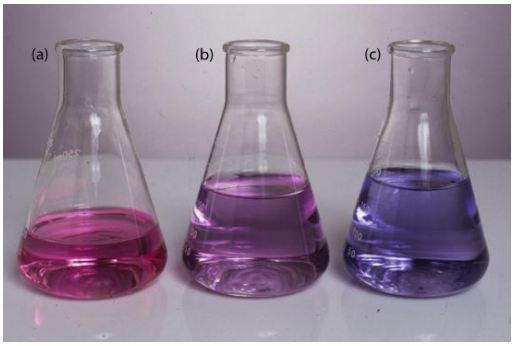


Figure 4.1.7 . End point for the titration of hardness with EDTA using calmagite as an indicator; the indicator is: (a) red prior to the end point due to the presence of the Mg^{2+}–indicator complex; (b) purple at the titration's end point; and (c) blue after the end point due to the presence of uncomplexed indicator.

Questions

1. Why is the sample buffered to a pH of 10? What problems might you expect at a higher pH or a lower pH?

Of the two primary cations that contribute to hardness, Mg^{2+} forms the weaker complex with EDTA and is the last cation to react with the titrant. Calmagite is a useful indicator because it gives a distinct end point when titrating Mg^{2+} (see Table 4.1.5). Because of calmagite's acid–base properties, the range of pMg values over which the indicator changes color depends on the titrand's pH (Figure 4.1.5). Figure 4.1.8 shows the titration curve for a 50-mL solution of 10^{-3} M Mg^{2+} with 10^{-2} M EDTA at pHs of 9, 10, and 11. Superimposed on each titration curve is the range of conditions for which the average analyst will observe the end point. At a pH of 9 an early end point is possible, which results in a negative determinate error. A late end point and a positive determinate error are possible if the pH is 11.

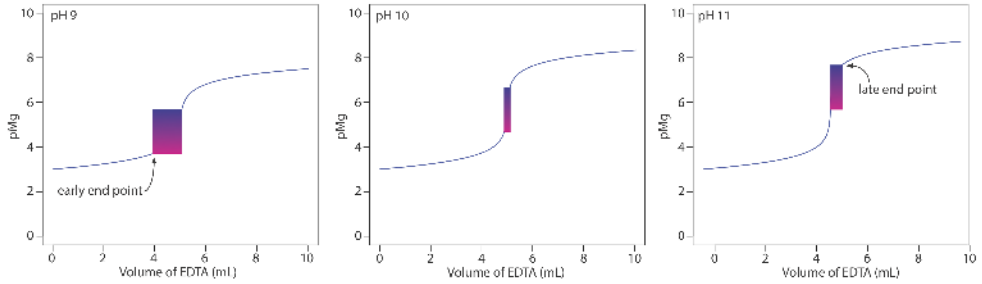


Figure 4.1.8 . Titration curves for 50 mL of 10^{-3} M Mg^{2+} with 10^{-3} M EDTA at pHs 9, 10, and 11 using calmagite as an indicator. The range of pMg and volume of EDTA over which the indicator changes color is shown for each titration curve.

2. Why is a small amount of the Mg^{2+}–EDTA complex added to the buffer?

The titration's end point is signaled by the indicator calmagite. The indicator's end point with Mg^{2+} is distinct, but its change in color when titrating Ca^{2+} does not provide a good end point (see Table 4.1.5). If the sample does not contain any Mg^{2+} as a source of hardness, then the titration's end point is poorly defined, which leads to an inaccurate and imprecise result. Adding a small amount of Mg^{2+}–EDTA to the buffer ensures that the titrand includes at least some Mg^{2+}. Because Ca^{2+} forms a stronger complex with EDTA, it displaces Mg^{2+} from the Mg^{2+}–EDTA complex, freeing the Mg^{2+} to bind with the indicator. This displacement is stoichiometric, so the total concentration of hardness cations remains unchanged. The displacement by EDTA of Mg^{2+} from the Mg^{2+}–indicator complex signals the titration's end point.

3. Why does the procedure specify that the titration take no longer than 5 minutes?

A time limitation suggests there is a kinetically-controlled interference, possibly arising from a competing chemical reaction. In this case the interference is the possible precipitation of $CaCO_3$ at a pH of 10.

Additional Considerations for Quantitative Applications of EDTA Titration

Although many quantitative applications of complexation titrimetry have been replaced by other analytical methods, a few important applications continue to find relevance. In the section we review the general application of complexation titrimetry with an emphasis on applications from the analysis of water and wastewater. First, however, we discuss the selection and standardization of complexation titrants.

Selection and Standardization of Titrants

EDTA is a versatile titrant that can be used to analyze virtually all metal ions. Although EDTA is the usual titrant when the titrand is a metal ion, it cannot be used to titrate anions, for which Ag^+ or Hg^{2+} are suitable titrants.

Solutions of EDTA are prepared from its soluble disodium salt, $Na_2H_2Y{\bullet}2H_2O$, and standardized by titrating against a solution made from the primary standard $CaCO_3$. Solutions of Ag^+ and Hg^{2+} are prepared using $AgNO_3$ and $Hg(NO_3)_2$, both of which are secondary standards. Standardization is accomplished by titrating against a solution prepared from primary standard grade NaCl.

Inorganic Analytes

Complexation titrimetry continues to be listed as a standard method for the determination of hardness, Ca^{2+}, CN^-, and Cl^- in waters and wastewaters. The evaluation of hardness was described earlier in Representative Method 9.3.1. The determination of Ca^{2+} is

complicated by the presence of Mg^{2+}, which also reacts with EDTA. To prevent an interference the pH is adjusted to 12–13, which precipitates Mg^{2+} as $Mg(OH)_2$. Titrating with EDTA using murexide or Eriochrome Blue Black R as the indicator gives the concentration of Ca^{2+}.

Cyanide is determined at concentrations greater than 1 mg/L by making the sample alkaline with NaOH and titrating with a standard solution of $AgNO_3$ to form the soluble $\mathbf{Ag(CN)_2^-}$ complex. The end point is determined using *p*-dimethylaminobenzalrhodamine as an indicator, with the solution turning from a yellow to a salmon color in the presence of excess Ag^+.

Chloride is determined by titrating with $Hg(NO_3)_2$, forming $HgCl_2(aq)$. The sample is acidified to a pH of 2.3–3.8 and diphenylcarbazone, which forms a colored complex with excess Hg^{2+}, serves as the indicator. The pH indicator xylene cyanol FF is added to ensure that the pH is within the desired range. The initial solution is a greenish blue, and the titration is carried out to a purple end point.

Quantitative Calculations

The quantitative relationship between the titrand and the titrant is determined by the titration reaction's stoichiometry. For a titration using EDTA, the stoichiometry is always 1:1.

Direct Titration Example 4.1.3

A 100.0-mL sample is analyzed for hardness using the procedure outlined in Representative Method 9.3.1, requiring 23.63 mL of 0.0109 M EDTA. Report the sample's hardness as mg $CaCO_3$/L.

Answer

In an analysis for hardness we treat the sample as if Ca^{2+} is the only metal ion that reacts with EDTA. The grams of Ca^{2+} in the sample, therefore, are

$$(0.0109\text{ M EDTA})(0.02363\text{ L}) \times \frac{1\text{ mol Ca}^{2+}}{\text{mol EDTA}} = 2.58 \times 10^{-4}\text{ mol Ca}^{2+}$$

$$2.58 \times 10^{-4}\text{ mol Ca}^{2+} \times \frac{1\text{ mol CaCO}_3}{\text{mol Ca}^{2+}} \times \frac{100.09\text{ g CaCO}_3}{\text{mol CaCO}_3} = 0.0258\text{ g CaCO}_3$$

and the sample's hardness is

$$\frac{0.0258\text{ g CaCO}_3}{0.1000\text{ L}} \times \frac{1000\text{ mg}}{\text{g}} = 258\text{ g CaCO}_3\text{/L}$$

Complex titrations involving multiple analytes or back titrations are also possible.

Back Titration Example 4.1.3

An alloy of chromel that contains Ni, Fe, and Cr is analyzed by a complexation titration using EDTA as the titrant. A 0.7176-g sample of the alloy is dissolved in HNO_3 and diluted to 250 mL in a volumetric flask. A 50.00-mL aliquot of the sample, treated with pyrophosphate to mask the Fe and Cr, requires 26.14 mL of 0.05831 M EDTA to reach the murexide end point. A second 50.00-mL aliquot is treated with hexamethylenetetramine to mask the Cr. Titrating with 0.05831 M EDTA requires 35.43 mL to reach the murexide end point. Finally, a third 50.00-mL aliquot is treated with 50.00 mL of 0.05831 M EDTA, and back titrated to the murexide end point with 6.21 mL of 0.06316 M Cu^{2+}. Report the weight percents of Ni, Fe, and Cr in the alloy.

Solution

The stoichiometry between EDTA and each metal ion is 1:1. For each of the three titrations, therefore, we can write an equation that relates the moles of EDTA to the moles of metal ions that are titrated.

titration 1: mol Ni = mol EDTA
titration 2: mol Ni +mol Fe = mol EDTA
titration 3: mol Ni + mol Fe + mol Cr + mol Cu = mol EDTA

We use the first titration to determine the moles of Ni in our 50.00-mL portion of the dissolved alloy. The titration uses

$$\frac{0.05831 \text{ mol EDTA}}{\text{L}} \times 0.02614 \text{ L} = 1.524 \times 10^{-3} \text{ mol EDTA}$$

which means the sample contains 1.524×10^{-3} mol Ni.

Having determined the moles of EDTA that react with Ni, we use the second titration to determine the amount of Fe in the sample. The second titration uses

$$\frac{0.05831 \text{ mol EDTA}}{\text{L}} \times 0.03543 \text{ L} = 2.066 \times 10^{-3} \text{ mol EDTA}$$

of which 1.524×10^{-3} mol are used to titrate Ni. This leaves 5.42×10^{-4} mol of EDTA to react with Fe; thus, the sample contains 5.42×10^{-4} mol of Fe.

Finally, we can use the third titration to determine the amount of Cr in the alloy. The third titration uses

$$\frac{0.05831 \text{ mol EDTA}}{\text{L}} \times 0.0500 \text{ L} = 3.926 \times 10^{-3} \text{ mol EDTA}$$

of which 1.524×10^{-3} mol are used to titrate Ni and 5.42×10^{-4} mol are used to titrate Fe. This leaves 8.50×10^{-4} mol of EDTA to react with Cu and Cr. The amount of EDTA that reacts with Cu is

$$\frac{0.06316 \text{ mol } Cu^{2+}}{\text{L}} \times 0.006211 \text{ L} \times \frac{1 \text{ mol EDTA}}{\text{mol } Cu^{2+}} = 3.92 \times 10^{-4} \text{ mol EDTA}$$

leaving 4.58×10^{-4} mol of EDTA to react with Cr. The sample, therefore, contains 4.58×10^{-4} mol of Cr.

Having determined the moles of Ni, Fe, and Cr in a 50.00-mL portion of the dissolved alloy, we can calculate the %w/w of each analyte in the alloy.

$$\frac{1.524 \times 10^{-3} \text{ mol Ni}}{50.00 \text{ mL}} \times \frac{58.69 \text{ g Ni}}{\text{mol Ni}} = 0.4472 \text{ g Ni}$$

$$\frac{0.4472 \text{ g Ni}}{0.7176 \text{ g sample}} \times 100 = 62.32$$

$$\frac{5.42 \times 10^{-4} \text{ mol Fe}}{50.00 \text{ mL}} \times \frac{55.845 \text{ g Fe}}{\text{mol Fe}} = 0.151 \text{ g Fe}$$

$$\frac{0.151 \text{ g Fe}}{0.7176 \text{ g sample}} \times 100 = 21.0$$

$$\frac{4.58 \times 10^{-4} \text{ mol Cr}}{50.00 \text{ mL}} \times \frac{51.996 \text{ g Cr}}{\text{mol Cr}} = 0.119 \text{ g Cr}$$

$$\frac{0.119 \text{ g Cr}}{0.7176 \text{ g sample}} \times 100 = 16.6$$

? Indirect Titration Example 4.1.5

An indirect complexation titration with EDTA can be used to determine the concentration of sulfate, SO_4^{2-}, in a sample. A 0.1557-g sample is dissolved in water and any sulfate present is precipitated as $BaSO_4$ by adding $Ba(NO_3)_2$. After filtering and rinsing the precipitate, it is dissolved in 25.00 mL of 0.02011 M EDTA. The excess EDTA is titrated with 0.01113 M Mg^{2+}, requiring 4.23 mL to reach the end point. Calculate the %w/w Na_2SO_4 in the sample.

Answer

The total moles of EDTA used in this analysis is

$$(0.02011\ \text{M EDTA})(0.02500\ \text{L}) = 5.028 \times 10^{-4}\ \text{mol EDTA}$$

Of this,

$$(0.01113\ \text{M Mg}^{2+})(0.00423\ \text{L}) \times \frac{1\ \text{mol EDTA}}{\text{mol Mg}^{2+}} = 4.708 \times 10^{-5}\ \text{mol EDTA}$$

are consumed in the back titration with Mg^{2+}, which means that

$$5.028 \times 10^{-4}\ \text{mol EDTA} - 4.708 \times 10^{-5}\ \text{mol EDTA} = 4.557 \times 10^{-4}\ \text{mol EDTA}$$

react with the $BaSO_4$. Each mole of $BaSO_4$ reacts with one mole of EDTA; thus

$$4.557 \times 10^{-4}\ \text{mol EDTA} \times \frac{1\ \text{mol BaSO}_4}{\text{mol EDTA}} \times \frac{1\ \text{mol Na}_2\text{SO}_4}{\text{mol BaSO}_4} \times \frac{142.04\ \text{g Na}_2\text{SO}_4}{\text{mol Na}_2\text{SO}_4} = 0.06473\ \text{g Na}_2\text{SO}_4$$

$$\frac{0.06473\ \text{g Na}_2\text{SO}_4}{0.1557\ \text{g sample}} \times 100 = 41.57_2\text{SO}_4$$

Evaluation of Complexation Titrimetry

The scale of operations, accuracy, precision, sensitivity, time, and cost of a complexation titration are similar to those described earlier for acid–base titrations. Complexation titrations, however, are more selective. Although EDTA forms strong complexes with most metal ion, by carefully controlling the titrand's pH we can analyze samples that contain two or more analytes. The reason we can use pH to provide selectivity is shown in Figure 4.1.9 a. A titration of Ca^{2+} at a pH of 9 has a distinct break in the titration curve because the conditional formation constant for CaY^{2-} of $\mathbf{2.6 \times 10^9}$ is large enough to ensure that the reaction of Ca^{2+} and EDTA goes to completion. At a pH of 3, however, the conditional formation constant of 1.23 is so small that very little Ca^{2+} reacts with the EDTA. Suppose we need to analyze a mixture of Ni^{2+} and Ca^{2+}. Both analytes react with EDTA, but their conditional formation constants differ significantly. If we adjust the pH to 3 we can titrate Ni^{2+} with EDTA without titrating Ca^{2+} (Figure 4.1.9 b). When the titration is complete, we adjust the titrand's pH to 9 and titrate the Ca^{2+} with EDTA.

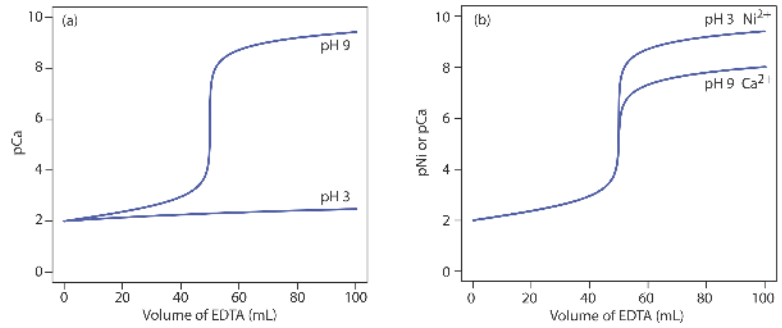


Figure 4.1.9 . Titration curves illustrating how we can use the titrand's pH to control EDTA's selectivity. (a) Titration of 50.0 mL of 0.010 M Ca^{2+} at a pH of 3 and a pH of 9 using 0.010 M EDTA. At a pH of 3 the CaY^{2-} complex is too weak to titrate successfully. (b) Titration of a 50.0 mL mixture of 0.010 M Ca^{2+} and 0.010 M Ni^{2+} at a pH of 3 and at a pH of 9 using 0.010 M EDTA. At a pH of 3 EDTA reacts only with Ni^{2+}. When the titration is complete, raising the pH to 9 allows for the titration of Ca^{2+}.

A spectrophotometric titration is a particularly useful approach for analyzing a mixture of analytes. For example, as shown in Figure 4.1.10 , we can determine the concentration of a two metal ions if there is a difference between the absorbance of the two metal-ligand complexes.

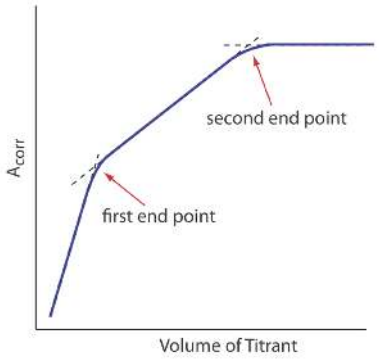


Figure 4.1.10 . Spectrophotometric titration curve for the complexation titration of a mixture of two analytes. The red arrows indicate the end points for each analyte.

This page titled 4.1: Complexation Titrations is shared under a CC BY-NC-SA 4.0 license and was authored, remixed, and/or curated by Kathryn Davis.

- **9.3: Complexation Titrations** by David Harvey is licensed CC BY-NC-SA 4.0.

4.2: EDTA Ladder Diagrams

When we develop or evaluate an analytical method, we often need to understand how the chemistry that takes place affects our results. Suppose we wish to isolate Ag^+ by precipitating it as AgCl. If we also need to control pH, then we must use a reagent that does not adversely affect the solubility of AgCl. It is a mistake to use NH_3 to adjust the pH, for example, because it increases the solubility of AgCl (see reaction 6.5.4). One of the primary sources of determinate errors in many analytical methods is failing to account for potential chemical interferences.

In this section we introduce the ladder diagram as a simple graphical tool for visualizing equilibrium chemistry. We will use ladder diagrams to determine what reactions occur when we combine several reagents, to estimate the approximate composition of a system at equilibrium, and to evaluate how a change to solution conditions might affect an analytical method.

> Although not specifically on the topic of ladder diagrams as developed in this section, the following papers provide appropriate background information: (a) Runo, J. R.; Peters, D. G. *J. Chem. Educ.* **1993**, *70*, 708–713; (b) Vale, J.; Fernández-Pereira, C.; Alcalde, M. *J. Chem. Educ.* **1993**, *70*, 790–795; (c) Fernández-Pereira, C.; Vale, J. *Chem. Educator* **1996**, *6*, 1–18; (d) Fernández- Pereira, C.; Vale, J.; Alcalde, M. *Chem. Educator* **2003**, *8*, 15–21; (e) Fernández-Pereira, C.; Alcalde, M.; Villegas, R.; Vale, J. *J. Chem. Educ.* **2007**, *84*, 520–525. Ladder diagrams are a great tool for helping you to think intuitively about analytical chemistry. We will make frequent use of them in the chapters to follow.

Ladder Diagrams for Complexation Equilibria

We can apply the same principles for constructing and interpreting an acid–base ladder diagram to equilibria that involve metal–ligand complexes. For a complexation reaction we define the ladder diagram's scale using the concentration of uncomplexed, or free ligand, pL. Using the formation of $Cd(NH_3)^{2+}$ as an example

$$Cd^{2+}(aq) + NH_3(aq) \rightleftharpoons Cd(NH_3)^{2+}(aq)$$

we can show that log K_1 is the dividing line between the areas of predominance for Cd^{2+} and for $Cd(NH_3)^{2+}$.

$$K_1 = 3.55 \times 10^2 = \frac{[Cd(NH_3)^{2+}]}{[Cd^{2+}]\,[NH_3]}$$

$$\log K_1 = \log\left(3.55 \times 10^2\right) = \log \frac{[Cd(NH_3)^{2+}]}{[Cd^{2+}]} - \log [NH_3]$$

$$\log K_1 = 2.55 = \log \frac{[Cd(NH_3)^{2+}]}{[Cd^{2+}]} + pNH_3$$

$$pNH_3 = \log K_1 + \log \frac{[Cd^{2+}]}{[Cd(NH_3)^{2+}]} = 2.55 + \log \frac{[Cd^{2+}]}{[Cd(NH_3)^{2+}]}$$

Thus, Cd^{2+} is the predominate species when pNH_3 is greater than 2.55 (a concentration of NH_3 smaller than 2.82×10^{-3} M) and for a pNH_3 value less than 2.55, $Cd(NH_3)^{2+}$ is the predominate species. Figure 4.2.5 shows a complete metal–ligand ladder diagram for Cd^{2+} and NH_3 that includes additional Cd–NH_3 complexes.

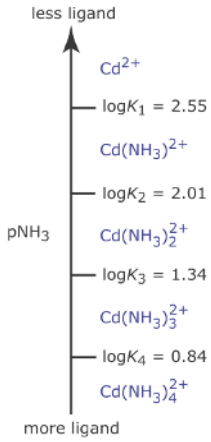


Figure 4.2.5 . Metal–ligand ladder diagram for Cd^{2+}–NH_3 complexation reactions. Note that higher-order complexes form when pNH_3 is smaller (which corresponds to larger concentrations of NH_3).

Example 4.2.3

Draw a single ladder diagram for the $Ca(EDTA)^{2-}$ and the $Mg(EDTA)^{2-}$ metal–ligand complexes. Use your ladder diagram to predict the result of adding 0.080 moles of Ca^{2+} to 0.060 moles of $Mg(EDTA)^{2-}$. EDTA is an abbreviation for the ligand ethylenediaminetetraacetic acid.

Solution

Figure 4.2.6 shows the ladder diagram for this system of metal–ligand complexes. Because the predominance regions for Ca^{2+} and $Mg(EDTA)^{2-}$ do not overlap, the reaction

$$\mathbf{Ca^{2+}}(aq) + \mathbf{Mg(EDTA)^{2-}}(aq) \rightleftharpoons \mathbf{Ca(EDTA)^{2-}}(aq) + \mathbf{Mg^{2+}}(aq)$$

proceeds essentially to completion. Because Ca^{2+} is the excess reagent, the composition of the final solution is approximately

$$\text{moles } \mathbf{Ca^{2+}} = 0.080 - 0.060 = 0.020 \text{ mol}$$

$$\text{moles } \mathbf{Ca(EDTA)^{2-}} = 0.060 \text{ mol}$$

$$\text{moles } \mathbf{Mg^{2+}} = 0.060 \text{ mol}$$

$$\text{moles } \mathbf{Mg(EDTA)^{2-}} = 0 \text{ mol}$$

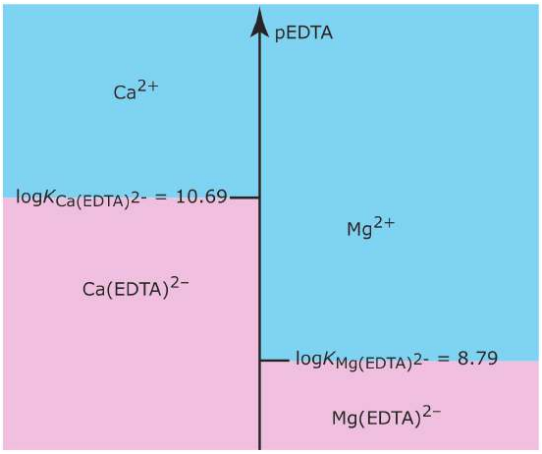


Figure 4.2.6 . Metal–ligand ladder diagram for $Ca(EDTA)^{2-}$ and for $Mg(EDTA)^{2-}$. The areas shaded in blue show the pEDTA range where the free metal ions are the predominate species; the metal–ligand complexes are the predominate species in the areas shaded in pink.

The metal–ligand ladder diagram in Figure 4.2.5 uses stepwise formation constants. We also can construct a ladder diagram using cumulative formation constants. For example, the first three stepwise formation constants for the reaction of Zn^{2+} with NH_3

$$Zn^{2+}(aq) + NH_3(aq) \rightleftharpoons Zn(NH_3)^{2+}(aq) \quad K_1 = 1.6 \times 10^2$$

$$Zn(NH_3)^{2+}(aq) + NH_3(aq) \rightleftharpoons Zn(NH_3)_2^{2+}(aq) \quad K_2 = 1.95 \times 10^2$$

$$Zn(NH_3)_2^{2+}(aq) + NH_3(aq) = Zn(NH_3)_3^{2+}(aq) \quad K_3 = 2.3 \times 10^2$$

suggests that the formation of $Zn(NH_3)_3^{2+}$ is more favorable than the formation of $Zn(NH_3)^{2+}$ or $Zn(NH_3)_2^{2+}$. For this reason, the equilibrium is best represented by the cumulative formation reaction shown here.

$$Zn^{2+}(aq) + 3NH_3(aq) \rightleftharpoons Zn(NH_3)_3^{2+}(aq) \quad \beta_3 = 7.2 \times 10^6$$

> Because K_3 is greater than K_2, which is greater than K_1, the formation of the metal-ligand complex $Zn(NH_3)_3^{2+}$ is more favorable than the formation of the other metal ligand complexes. For this reason, at lower values of pNH_3 the concentration of $Zn(NH_3)_3^{2+}$ is larger than the concentrations of $Zn(NH_3)^{2+}$ or $Zn(NH_3)_2^{2+}$. The value of β_3 is
>
> $$\beta_3 = K_1 \times K_2 \times K_3$$

To see how we incorporate this cumulative formation constant into a ladder diagram, we begin with the reaction's equilibrium constant expression.

$$\beta_3 = \frac{[Zn(NH_3)_3^{2+}]}{[Zn^{2+}][NH_3]^3}$$

Taking the log of each side

$$\log \beta_3 = \log \frac{[Zn(NH_3)_3^{2+}]}{[Zn^{2+}]} - 3 \log [NH_3]$$

and rearranging gives

$$pNH_3 = \frac{1}{3} \log \beta_3 + \frac{1}{3} \log \frac{[Zn^{2+}]}{[Zn(NH_3)_3^{2+}]}$$

When the concentrations of Zn and $Zn(NH_3)_3^{2+}$ are equal, then

$$pNH_3 = \frac{1}{3} \log \beta_3 = 2.29$$

In general, for the metal–ligand complex ML_n, the step for a cumulative formation constant is

$$pL = \frac{1}{n} \log \beta_n$$

Figure 4.2.7 shows the complete ladder diagram for the Zn^{2+}–NH_3 system.

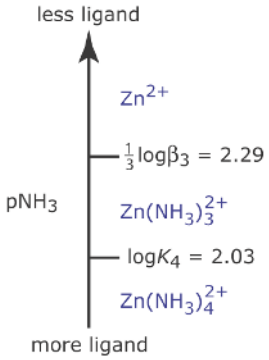


Figure 4.2.7 . Ladder diagram for Zn^{2+}–NH_3 metal–ligand complexation reactions showing both a step based on a cumulative formation constant and a step based on a stepwise formation constant.

This page titled 4.2: EDTA Ladder Diagrams is shared under a CC BY-NC-SA 4.0 license and was authored, remixed, and/or curated by Kathryn Davis.

- **6.6: Ladder Diagrams** by David Harvey is licensed CC BY-NC-SA 4.0.

4.3: Redox Titrations

Analytical titrations using oxidation–reduction reactions were introduced shortly after the development of acid–base titrimetry. The earliest ***redox titration*** took advantage of chlorine's oxidizing power. In 1787, Claude Berthollet introduced a method for the quantitative analysis of chlorine water (a mixture of Cl_2, HCl, and HOCl) based on its ability to oxidize indigo, a dye that is colorless in its oxidized state. In 1814, Joseph Gay-Lussac developed a similar method to determine chlorine in bleaching powder. In both methods the end point is a change in color. Before the equivalence point the solution is colorless due to the oxidation of indigo. After the equivalence point, however, unreacted indigo imparts a permanent color to the solution.

The number of redox titrimetric methods increased in the mid-1800s with the introduction of $\mathbf{MnO_4^-}$, $\mathbf{Cr_2O_7^{2-}}$, and I_2 as oxidizing titrants, and of Fe^{2+} and $\mathbf{S_2O_3^{2-}}$ as reducing titrants. Even with the availability of these new titrants, redox titrimetry was slow to develop due to the lack of suitable indicators. A titrant can serve as its own indicator if its oxidized and its reduced forms differ significantly in color. For example, the intensely purple $\mathbf{MnO_4^-}$ ion serves as its own indicator since its reduced form, Mn^{2+}, is almost colorless. Other titrants require a separate indicator. The first such indicator, diphenylamine, was introduced in the 1920s. Other redox indicators soon followed, increasing the applicability of redox titrimetry.

Redox Titration Curves

To evaluate a redox titration we need to know the shape of its titration curve. In an acid–base titration or a complexation titration, the titration curve shows how the concentration of H_3O^+ (as pH) or M^{n+} (as pM) changes as we add titrant. For a redox titration it is convenient to monitor the titration reaction's potential instead of the concentration of one species.

You may recall from Chapter 6 that the Nernst equation relates a solution's potential to the concentrations of reactants and products that participate in the redox reaction. Consider, for example, a titration in which a titrand in a reduced state, A_{red}, reacts with a titrant in an oxidized state, B_{ox}.

$$A_{red} + B_{ox} \rightleftharpoons B_{red} + A_{ox}$$

where A_{ox} is the titrand's oxidized form, B_{red} is the titrant's reduced form, and the stoichiometry between the two is 1:1. The reaction's potential, E_{rxn}, is the difference between the reduction potentials for each half-reaction.

$$E_{rxn} = E_{B_{ox}/B_{red}} - E_{A_{ox}/A_{red}}$$

After each addition of titrant the reaction between the titrand and the titrant reaches a state of equilibrium. Because the potential at equilibrium is zero, the titrand's and the titrant's reduction potentials are identical. This is an important observation as it allows us to use either half-reaction to monitor the titration's progress.

Before the equivalence point, the titration mixture consists of appreciable quantities of the titrand's oxidized and reduced forms. The concentration of unreacted titrant, however, is very small. The potential, therefore, is easier to calculate if we use the Nernst equation for the **titrand's** half-reaction

$$E = E_{A_{ox}/A_{red}} = E^\circ_{A_{ox}/A_{red}} - \frac{RT}{nF}\ln\frac{[A_{red}]}{[A_{ox}]}$$

After the equivalence point it is easier to calculate the potential using the Nernst equation for the **titrant's** half-reaction.

$$E = E_{B_{ox}/B_{red}} = E^\circ_{B_{ox}/B_{red}} - \frac{RT}{nF}\ln\frac{[B_{red}]}{[B_{ox}]}$$

> Although the Nernst equation is written in terms of the half-reaction's standard state potential, a matrix-dependent ***formal potential*** often is used in its place. See Appendix 13 for the standard state potentials and formal potentials for selected half-reactions.

Calculating the Titration Curve

Let's calculate the titration curve for the titration of 50.0 mL of 0.100 M Fe^{2+} with 0.100 M Ce^{4+} in a matrix of 1 M $HClO_4$. The reaction in this case is

$$Fe^{2+}(aq) + Ce^{4+}(aq) \rightleftharpoons Ce^{3+}(aq) + Fe^{3+}(aq) \tag{4.3.1}$$

Because the equilibrium constant for reaction 4.3.1 is very large—it is approximately 6×10^{15}—we may assume that the analyte and titrant react completely.

> In 1 M $HClO_4$, the formal potential for the reduction of Fe^{3+} to Fe^{2+} is +0.767 V, and the formal potential for the reduction of Ce^{4+} to Ce^{3+} is +1.70 V.

The first task is to calculate the volume of Ce needed to reach the titration's equivalence point. From the reaction's stoichiometry we know that

$$\text{mol } Fe^{2+} = M_{Fe}V_{Fe} = M_{Ce}V_{Ce} = \text{mol } Ce^{4+}$$

Solving for the volume of Ce^{4+} gives the equivalence point volume as

$$V_{eq} = V_{Ce} = \frac{M_{Fe}V_{Fe}}{M_{Ce}} = \frac{(0.100\text{ M})(50.0\text{ mL})}{(0.100\text{ M})} = 50.0\text{ mL}$$

Before the equivalence point, the concentration of unreacted Fe^{2+} and the concentration of Fe^{3+} are easy to calculate. For this reason we find the potential using the Nernst equation for the Fe^{3+}/Fe^{2+} half-reaction.

$$E = +0.767\text{ V} - 0.05916 \log \frac{[Fe^{2+}]}{[Fe^{3+}]} \tag{4.3.2}$$

For example, the concentrations of Fe^{2+} and Fe^{3+} after adding 10.0 mL of titrant are

$$[Fe^{2+}] = \frac{(\text{mol } Fe^{2+})_{\text{initial}} - (\text{mol } Ce^{4+})_{\text{added}}}{\text{total volume}} = \frac{M_{Fe}V_{Fe} - M_{Ce}V_{Ce}}{V_{Fe} + V_{Ce}}$$

$$[Fe^{2+}] = \frac{(0.100\text{ M})(50.0\text{ mL}) - (0.100\text{ M})(10.0\text{ mL})}{50.0\text{ mL} + 10.0\text{ mL}} = 6.67 \times 10^{-2}\text{ M}$$

$$[Fe^{3+}] = \frac{(\text{mol } Ce^{4+})_{\text{added}}}{\text{total volume}} = \frac{M_{Ce}V_{Ce}}{V_{Fe} + V_{Ce}}$$

$$[Fe^{3+}] = \frac{(0.100\text{ M})(10.0\text{ mL})}{50.0\text{ mL} + 10.0\text{ mL}} = 1.67 \times 10^{-2}\text{ M}$$

Substituting these concentrations into Equation 4.3.2 gives the potential as

$$E = +0.767\text{ V} - 0.05916 \log \frac{6.67 \times 10^{-2}}{1.67 \times 10^{-2}} = +0.731\text{ V}$$

After the equivalence point, the concentration of Ce^{3+} and the concentration of excess Ce^{4+} are easy to calculate. For this reason we find the potential using the Nernst equation for the Ce^{4+}/Ce^{3+} half-reaction in a manner similar to that used above to calculate potentials before the equivalence point.

$$E = +1.70\text{ V} - 0.05916 \log \frac{[Ce^{3+}]}{[Ce^{4+}]} \tag{4.3.3}$$

For example, after adding 60.0 mL of titrant, the concentrations of Ce^{3+} and Ce^{4+} are

$$[Ce^{3+}] = \frac{(\text{mol } Fe^{2+})_{\text{initial}}}{\text{total volume}} = \frac{M_{Fe}V_{Fe}}{V_{Fe} + V_{Ce}}$$

$$[Ce^{3+}] = \frac{(0.100\text{ M})(50.0\text{ mL})}{50.0\text{ mL} + 60.0\text{ mL}} = 4.55 \times 10^{-2}\text{ M}$$

$$[Ce^{4+}] = \frac{(\text{mol } Ce^{4+})_{\text{added}} - (\text{mol } Fe^{2+})_{\text{initial}}}{\text{total volume}} = \frac{M_{Ce}V_{Ce} - M_{Fe}V_{Fe}}{V_{Fe} + V_{Ce}}$$

$$[Ce^{4+}] = \frac{(0.100\ M)(60.0\ mL) - (0.100\ M)(50.0\ mL)}{50.0\ mL + 60.0\ mL} = 9.09 \times 10^{-3}\ M$$

Substituting these concentrations into Equation 4.3.3 gives a potential of

$$E = +1.70\ V - 0.05916 \log \frac{4.55 \times 10^{-2}\ M}{9.09 \times 10^{-3}\ M} = +1.66\ V$$

At the titration's equivalence point, the potential, E_{eq}, in Equation 4.3.2 and Equation 4.3.3 are identical. Adding the equations together to gives

$$2E_{eq} = E^{\circ}_{Fe^{3+}/Fe^{2+}} + E^{\circ}_{Ce^{4+}/Ce^{3+}} - 0.05916 \log \frac{[Fe^{2+}][Ce^{3+}]}{[Fe^{3+}][Ce^{4+}]}$$

Because $[Fe^{2+}] = [Ce^{4+}]$ and $[Ce^{3+}] = [Fe^{3+}]$ at the equivalence point, the log term has a value of zero and the equivalence point's potential is

$$E_{eq} = \frac{E^{\circ}_{Fe^{3+}/Fe^{2+}} + E^{\circ}_{Ce^{4+}/Ce^{3+}}}{2} = \frac{0.767\ V + 1.70\ V}{2} = +1.23\ V$$

Additional results for this titration curve are shown in Table 4.3.1 and Figure 4.3.1 .

Table 4.3.1 . Data for the Titration of 50.0 mL of 0.100 M Fe^{2+} with 0.100 M Ce^{4+}

volume of Ce^{4+} (mL)	E (V)	volume of Ce^{4+} (mL)	E (V)
10.0	0.731	60.0	1.66
20.0	0.757	70.0	1.68
30.0	0.777	80.0	1.69
40.0	0.803	90.0	1.69
50.0	1.23	100.0	1.70

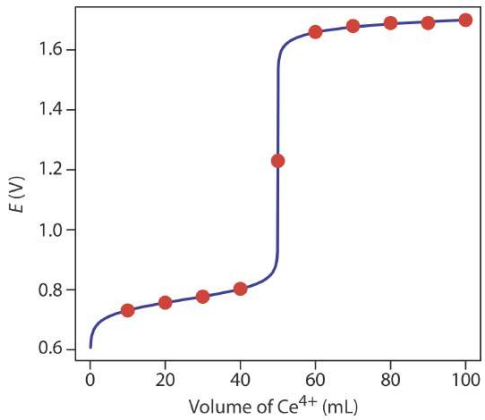


Figure 4.3.1 . Titration curve for the titration of 50.0 mL of 0.100 M Fe^{2+} with 0.100 M Ce^{4+}. The red points correspond to the data in Table 4.3.1 . The blue line shows the complete titration curve.

Quickly Sketching a Redox Titration Curve

To evaluate the relationship between a titration's equivalence point and its end point we need to construct only a reasonable approximation of the exact titration curve. In this section we demonstrate a simple method for sketching a redox titration curve. Our goal is to sketch the titration curve quickly, using as few calculations as possible. Let's use the titration of 50.0 mL of 0.100 M Fe^{2+} with 0.100 M Ce^{4+} in a matrix of 1 M $HClO_4$.

We begin by calculating the titration's equivalence point volume, which, as we determined earlier, is 50.0 mL. Next, we draw our axes, placing the potential, E, on the y-axis and the titrant's volume on the x-axis. To indicate the equivalence point's volume, we

draw a vertical line that intersects the *x*-axis at 50.0 mL of Ce^{4+}. Figure 4.3.2 a shows the result of the first step in our sketch.

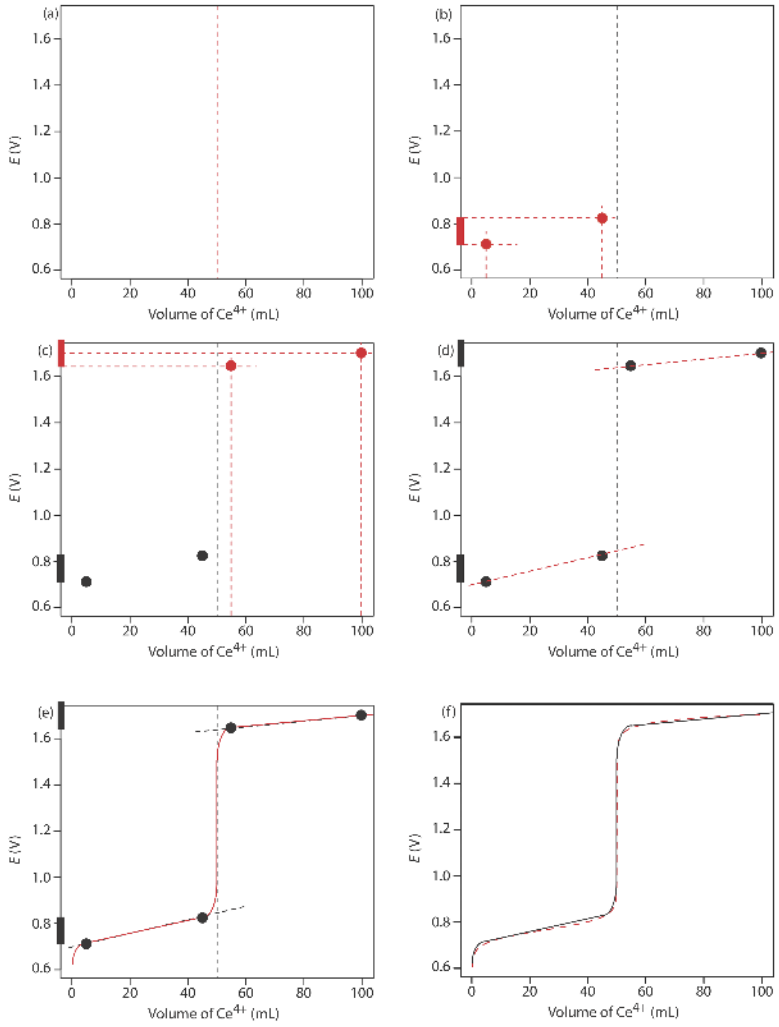


Figure 4.3.2 . Illustrations showing the steps in sketching an approximate titration curve for the titration of 50.0 mL of 0.100 M Fe^{2+} with 0.100 M Ce^{4+} in 1 M $HClO_4$: (a) locating the equivalence point volume; (b) plotting two points before the equivalence point; (c) plotting two points after the equivalence point; (d) preliminary approximation of titration curve using straight-lines; (e) final approximation of titration curve using a smooth curve; (f) comparison of approximate titration curve (solid black line) and exact titration curve (dashed red line). See the text for additional details.

Before the equivalence point, the potential is determined by a redox buffer of Fe^{2+} and Fe^{3+}. Although we can calculate the potential using the Nernst equation, we can avoid this calculation if we make a simple assumption. You may recall from Chapter 6 that a redox buffer operates over a range of potentials that extends approximately ±(0.05916/*n*) unit on either side of $E^\circ_{Fe^{3+}/Fe^{2+}}$. The potential at the buffer's lower limit is

$$E = E^\circ_{Fe^{3+}/Fe^{2+}} - 0.05916$$

when the concentration of Fe^{2+} is $10\times$ greater than that of Fe^{3+}. The buffer reaches its upper potential of

$$E = E^\circ_{Fe^{3+}/Fe^{2+}} + 0.05916$$

when the concentration of Fe^{2+} is $10\times$ smaller than that of Fe^{3+}. The redox buffer spans a range of volumes from approximately 10% of the equivalence point volume to approximately 90% of the equivalence point volume. Figure 4.3.2 b shows the second step in our sketch. First, we superimpose a ladder diagram for Fe on the *y*-axis, using its $E^\circ_{Fe^{3+}/Fe^{2+}}$ value of 0.767 V and including the buffer's range of potentials. Next, we add points for the potential at 10% of V_{eq} (a potential of 0.708 V at 5.0 mL) and for the potential at 90% of V_{eq} (a potential of 0.826 V at 45.0 mL).

We used a similar approach when sketching the acid–base titration curve for the titration of acetic acid with NaOH; see Chapter 9.2 for details.

The third step in sketching our titration curve is to add two points after the equivalence point. Here the potential is controlled by a redox buffer of Ce^{3+} and Ce^{4+}. The redox buffer is at its lower limit of

$$E = E^{\circ}_{Ce^{4+}/Ce^{3+}} - 0.05916$$

when the titrant reaches 110% of the equivalence point volume and the potential is $E^{\circ}_{Ce^{4+}/Ce^{3+}}$ when the volume of Ce is $2 \times V_{eq}$.

We used a similar approach when sketching the complexation titration curve for the titration of Mg^{2+} with EDTA; see Chapter 9.3 for details.

Figure 4.3.2 c shows the third step in our sketch. First, we superimpose a ladder diagram for Ce on the *y*-axis, using its $E^{\circ}_{Ce^{4+}/Ce^{3+}}$ value of 1.70 V and including the buffer's range. Next, we add points representing the potential at 110% of V_{eq} (a value of 1.66 V at 55.0 mL) and at 200% of V_{eq} (a value of 1.70 V at 100.0 mL).

Next, we draw a straight line through each pair of points, extending the line through the vertical line that indicates the equivalence point's volume (Figure 4.3.2 d). Finally, we complete our sketch by drawing a smooth curve that connects the three straight-line segments (Figure 4.3.2 e). A comparison of our sketch to the exact titration curve (Figure 4.3.2 f) shows that they are in close agreement.

Selecting and Evaluating the End Point

A redox titration's equivalence point occurs when we react stoichiometrically equivalent amounts of titrand and titrant. As is the case for acid–base titrations and complexation titrations, we estimate the equivalence point of a redox titration using an experimental end point. A variety of methods are available for locating a redox titration's end point, including indicators and sensors that respond to a change in the solution conditions.

Where is the Equivalence Point

For an acid–base titration or a complexometric titration the equivalence point is almost identical to the inflection point on the steeply rising part of the titration curve. If you look back at Figure 9.2.2 and Figure 9.3.3, you will see that the inflection point is in the middle of this steep rise in the titration curve, which makes it relatively easy to find the equivalence point when you sketch these titration curves. We call this a ***symmetric equivalence point***. If the stoichiometry of a redox titration is 1:1—that is, one mole of titrant reacts with each mole of titrand—then the equivalence point is symmetric. If the titration reaction's stoichiometry is not 1:1, then the equivalence point is closer to the top or to the bottom of the titration curve's sharp rise. In this case we have an ***asymmetric equivalence point***.

Example 4.3.1

Derive a general equation for the equivalence point's potential when titrating Fe^{2+} with MnO_4^-.

$$5Fe^{2+}(aq) + MnO_4^-(aq) + 8H^+(aq) \rightarrow 5Fe^{3+}(aq) + Mn^{2+}(aq) + 4H_2O(l)$$

Solution

The half-reactions for the oxidation of Fe^{2+} and the reduction of MnO_4^- are

$$Fe^{2+}(aq) \rightarrow Fe^{3+}(aq) + e^-$$

$$MnO_4^-(aq) + 8H^+(aq) + 5e^- \rightarrow Mn^{2+}(aq) + 4H_2O(l)$$

for which the Nernst equations are

$$E = E^{\circ}_{Fe^{3+}/Fe^{2+}} - 0.5916 \log \frac{[Fe^{2+}]}{[Fe^{3+}]}$$

$$E = E^\circ_{MnO_4^-/Mn^{2+}} - \frac{0.5916}{5}\log\frac{[Mn^{2+}]}{[MnO_4^-][H^+]^8}$$

Before we add together these two equations we must multiply the second equation by 5 so that we can combine the log terms; thus

$$6E_{eq} = E^\circ_{Fe^{3+}/Fe^{2+}} + 5E^\circ_{MnO_4^-/Mn^{2+}} - 0.05916\log\frac{[Fe^{2+}][Mn^{2+}]}{[Fe^{3+}][MnO_4^-][H^+]^8}$$

At the equivalance point we know that

$$[Fe^{2+}] = 5 \times [MnO_4^-] \text{ and } [Fe^{3+}] = 5 \times [Mn^{2+}]$$

Substituting these equalities into the previous equation and rearranging gives us a general equation for the potential at the equivalence point.

$$6E_{eq} = E^\circ_{Fe^{3+}/Fe^{2+}} + 5E^\circ_{MnO_4^-/Mn^{2+}} - 0.05916\log\frac{5[MnO_4^-][Mn^{2+}]}{5[Mn^{2+}][MnO_4^-][H^+]^8}$$

$$E_{eq} = \frac{E^\circ_{Fe^{3+}/Fe^{2+}} + 5E^\circ_{MnO_4^-/Mn^{2+}}}{6} - \frac{0.05916}{6}\log\frac{1}{[H^+]^8}$$

$$E_{eq} = \frac{E^\circ_{Fe^{3+}/Fe^{2+}} + 5E^\circ_{MnO_4^-/Mn^{2+}}}{6} + \frac{0.05916 \times 8}{6}\log[H^+]$$

$$E_{eq} = \frac{E^\circ_{Fe^{3+}/Fe^{2+}} + 5E^\circ_{MnO_4^-/Mn^{2+}}}{6} - 0.07888pH$$

Our equation for the equivalence point has two terms. The first term is a weighted average of the titrand's and the titrant's standard state potentials, in which the weighting factors are the number of electrons in their respective half-reactions. The second term shows that E_{eq} for this titration is pH-dependent. At a pH of 1 (in H_2SO_4), for example, the equivalence point has a potential of

$$E_{eq} = \frac{0.768 + 5 \times 1.51}{6} - 0.07888 \times 1 = 1.31 \text{ V}$$

Figure 4.3.3 shows a typical titration curve for titration of Fe^{2+} with MnO_4^-. Note that the titration's equivalence point is asymmetrical.

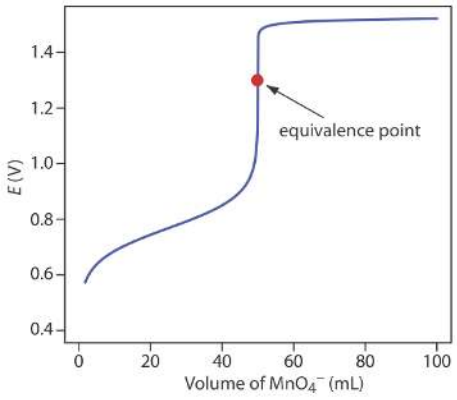


Figure 4.3.3 . Titration curve for the titration of 50.0 mL of 0.100 M Fe^{2+} with 0.0200 M MnO_4^- at a fixed pH of 1 (using H_2SO_4). The equivalence point is shown by the red dot.

? Exercise 4.3.3

Derive a general equation for the equivalence point's potential for the titration of U^{4+} with Ce^{4+}. The unbalanced reaction is

$$Ce^{4+}(aq) + U^{4+}(aq) \rightarrow UO_2^{2+}(aq) + Ce^{3+}(aq)$$

What is the equivalence point's potential if the pH is 1?

Answer

The two half reactions are

$$Ce^{4+}(aq) + e^- \rightarrow Ce^{3+}(aq)$$

$$U^{4+}(aq) + 2H_2O(l) \rightarrow UO_2^{2+}(aq)) + 4H^+(aq) + 2e^-$$

for which the Nernst equations are

$$E = E^\circ_{Ce^{4+}/Ce^{3+}} - 0.05916 \log \frac{[Ce^{3+}]}{[Ce^{4+}]}$$

$$E = E^\circ_{UO_2^{2+}/U^{4+}} - \frac{0.05916}{2} \log \frac{[U^{4+}]}{[UO_2^{2+}][H^+]^4}$$

Before adding these two equations together we must multiply the second equation by 2 so that we can combine the log terms; thus

$$3E = E^\circ_{Ce^{4+}/Ce^{3+}} + 2E^\circ_{UO_2^{2+}/U^{4+}} - 0.05916 \log \frac{[Ce^{3+}][U^{4+}]}{[Ce^{4+}][UO_2^{2+}][H^+]^4}$$

At the equivalence point we know that

$$[Ce^{3+}] = 2 \times [UO_2^{2+}] \text{ and } [Ce^{4+}] = 2 \times [U^{4+}]$$

Substituting these equalities into the previous equation and rearranging gives us a general equation for the potential at the equivalence point.

$$3E = E^\circ_{Ce^{4+}/Ce^{3+}} + 2E^\circ_{UO_2^{2+}/U^{4+}} - 0.05916 \log \frac{2[UO_2^{2+}][U^{4+}]}{2[U^{4+}][UO_2^{2+}][H^+]^4}$$

$$E = \frac{E^\circ_{Ce^{4+}/Ce^{3+}} + 2E^\circ_{UO_2^{2+}/U^{4+}}}{3} - \frac{0.05916}{3} \log \frac{1}{[H^+]^4}$$

$$E = \frac{E^\circ_{Ce^{4+}/Ce^{3+}} + 2E^\circ_{UO_2^{2+}/U^{4+}}}{3} + \frac{0.05916 \times 4}{3} \log [H^+]^4$$

$$E = \frac{E^\circ_{Ce^{4+}/Ce^{3+}} + 2E^\circ_{UO_2^{2+}/U^{4+}}}{3} - 0.07888 pH$$

At a pH of 1 the equivalence point has a potential of

$$E = \frac{1.72 + 2 \times 0.327}{3} - 0.07888 \times 1 = +0.712 \text{ V}$$

Finding the End Point With an Indicator

Three types of indicators are used to signal a redox titration's end point. The oxidized and reduced forms of some titrants, such as MnO_4^-, have different colors. A solution of MnO_4^- is intensely purple. In an acidic solution, however, permanganate's reduced form, Mn^{2+}, is nearly colorless. When using MnO_4^- as a titrant, the titrand's solution remains colorless until the equivalence point. The first drop of excess MnO_4^- produces a permanent tinge of purple, signaling the end point.

Some indicators form a colored compound with a specific oxidized or reduced form of the titrant or the titrand. Starch, for example, forms a dark purple complex with I_3^-. We can use this distinct color to signal the presence of excess I_3^- as a titrant—a change in color from colorless to purple—or the completion of a reaction that consumes I_3^- as the titrand— a change in color from purple to colorless. Another example of a specific indicator is thiocyanate, SCN^-, which forms the soluble red-colored complex of $Fe(SCN)^{2+}$ in the presence of Fe^{3+}.

The most important class of indicators are substances that do not participate in the redox titration, but whose oxidized and reduced forms differ in color. When we add a ***redox indicator*** to the titrand, the indicator imparts a color that depends on the solution's potential. As the solution's potential changes with the addition of titrant, the indicator eventually changes oxidation state and changes color, signaling the end point.

To understand the relationship between potential and an indicator's color, consider its reduction half-reaction

$$\mathrm{In_{ox}} + ne^- \rightleftharpoons \mathrm{In_{red}}$$

where $\mathrm{In_{ox}}$ and $\mathrm{In_{red}}$ are, respectively, the indicator's oxidized and reduced forms.

> For simplicity, $\mathrm{In_{ox}}$ and $\mathrm{In_{red}}$ are shown without specific charges. Because there is a change in oxidation state, $\mathrm{In_{ox}}$ and $\mathrm{In_{red}}$ cannot both be neutral.

The Nernst equation for this half-reaction is

$$E = E^\circ_{\mathrm{In_{ox}/In_{red}}} - \frac{0.05916}{n} \log \frac{[\mathrm{In_{red}}]}{[\mathrm{In_{ox}}]}$$

As shown in Figure 4.3.4 , if we assume the indicator's color changes from that of $\mathrm{In_{ox}}$ to that of $\mathrm{In_{red}}$ when the ratio $[\mathrm{In_{red}}]/[\mathrm{In_{ox}}]$ changes from 0.1 to 10, then the end point occurs when the solution's potential is within the range

$$E = E^\circ_{\mathrm{In_{ox}/In_{red}}} \pm \frac{0.05916}{n}$$

> This is the same approach we took in considering acid–base indicators and complexation indicators.

A partial list of redox indicators is shown in Table 4.3.2 . Examples of an appropriate and an inappropriate indicator for the titration of Fe^{2+} with Ce^{4+} are shown in Figure 4.3.5 .

Table 4.3.2 . Selected Examples of Redox Indicators

indicator	color $\mathrm{In_{ox}}$	color of $\mathrm{In_{red}}$	E^o (V)
indigo tetrasulfate	blue	colorless	0.36
methylene blue	blue	colorless	0.53
diphenylamine	violet	colorless	0.75
diphenylamine sulfonic acid	red-violet	colorless	0.85
tris(2,2'-bipyradine)iron	pale blue	red	1.120
ferroin	pale blue	red	1.147
tris(5-nitro-1,10-phenanthroline)iron	pale blue	red-violet	1.25

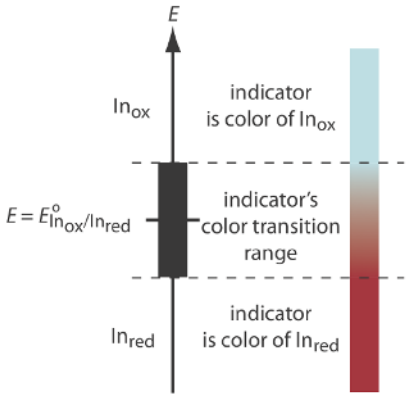


Figure 4.3.4 . Diagram showing the relationship between E and an indicator's color. The ladder diagram defines potentials where In_{red} and In_{ox} are the predominate species.

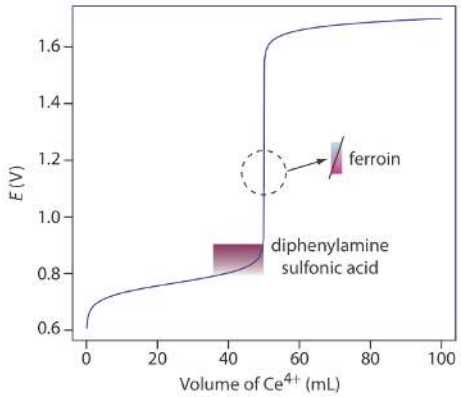


Figure 4.3.5 . Titration curve for titration of 50.0 mL of 0.100 M Fe^{2+} with 0.100 M Ce^{4+}. The end point transitions for the indicators diphenylamine sulfonic acid and ferroin are superimposed on the titration curve. Because the transition for ferroin is too small to see on the scale of the x-axis—it requires only 1–2 drops of titrant—the color change is expanded to the right.

Other Methods for Finding the End Point

Another method for locating a redox titration's end point is a potentiometric titration in which we monitor the change in potential while we add the titrant to the titrand. The end point is found by examining visually the titration curve. The simplest experimental design for a potentiometric titration consists of a Pt indicator electrode whose potential is governed by the titrand's or the titrant's redox half-reaction, and a reference electrode that has a fixed potential. Other methods for locating the titration's end point include thermometric titrations and spectrophotometric titrations.

> You will a further discussion of potentiometry in Chapter 11.

Example Use of Redox Titration: Determination of Total Chlorine Residual

The best way to appreciate the theoretical and the practical details discussed in this section is to carefully examine a typical redox titrimetric method. Although each method is unique, the following description of the determination of the total chlorine residual in water provides an instructive example of a typical procedure. The description here is based on Method 4500-Cl B as published in *Standard Methods for the Examination of Water and Wastewater*, 20th Ed., American Public Health Association: Washington, D. C., 1998.

Description of the Method

The chlorination of a public water supply produces several chlorine-containing species, the combined concentration of which is called the total chlorine residual. Chlorine is present in a variety of chemical states, including the free residual chlorine, which consists of Cl_2, HOCl and OCl^-, and the combined chlorine residual, which consists of NH_2Cl, $NHCl_2$, and NCl_3. The total chlorine residual is determined by using the oxidizing power of chlorine to convert I^- to I_3^-. The amount of I_3^- formed is then

https://chem.libretexts.org/@go/page/556126

determined by titrating with $Na_2S_2O_3$ using starch as an indicator. Regardless of its form, the total chlorine residual is reported as if Cl_2 is the only source of chlorine, and is reported as mg Cl/L.

Procedure

Select a volume of sample that requires less than 20 mL of $Na_2S_2O_3$ to reach the end point. Using glacial acetic acid, acidify the sample to a pH between 3 and 4, and add about 1 gram of KI. Titrate with $Na_2S_2O_3$ until the yellow color of I_3^- begins to disappear. Add 1 mL of a starch indicator solution and continue titrating until the blue color of the starch–I_3^- complex disappears (Figure 4.3.6). Use a blank titration to correct the volume of titrant needed to reach the end point for reagent impurities.

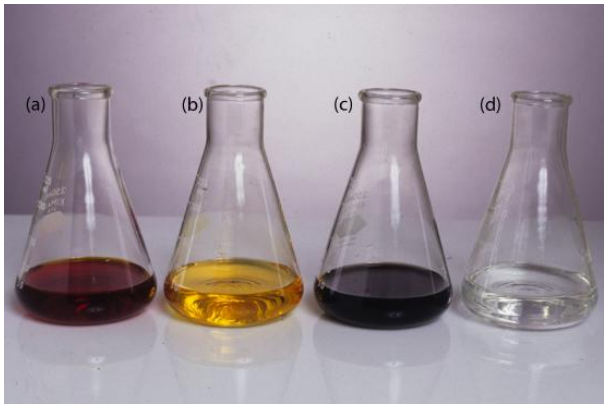


Figure 4.3.6 . Endpoint for the determination of the total chlorine residual. (a) Acidifying the sample and adding KI forms a brown solution of I_3^-. (b) Titrating with $Na_2S_2O_3$ converts I_3^- to I^- with the solution fading to a pale yellow color as we approach the end point. (c) Adding starch forms the deep purple starch–I_3^- complex. (d) As the titration continues, the end point is a sharp transition from a purple to a colorless solution. The change in color from (c) to (d) typically takes 1–2 drops of titrant.

Questions

1. Is this an example of a direct or an indirect analysis?

> This is an indirect analysis because the chlorine-containing species do not react with the titrant. Instead, the total chlorine residual oxidizes I^- to I_3^-, and the amount of I_3^- is determined by titrating with $Na_2S_2O_3$.

2. Why does the procedure rely on an indirect analysis instead of directly titrating the chlorine-containing species using KI as a titrant?

> Because the total chlorine residual consists of six different species, a titration with I^- does not have a single, well-defined equivalence point. By converting the chlorine residual to an equivalent amount of I_3^-, the indirect titration with $Na_2S_2O_3$ has a single, useful equivalence point. Even if the total chlorine residual is from a single species, such as HOCl, a direct titration with KI is impractical. Because the product of the titration, I_3^-, imparts a yellow color, the titrand's color would change with each addition of titrant, making it difficult to find a suitable indicator.

3. Both oxidizing and reducing agents can interfere with this analysis. Explain the effect of each type of interferent on the total chlorine residual.

> An interferent that is an oxidizing agent converts additional I^- to I_3^-. Because this extra I_3^- requires an additional volume of $Na_2S_2O_3$ to reach the end point, we overestimate the total chlorine residual. If the interferent is a reducing agent, it reduces back to I^- some of the I_3^- produced by the reaction between the total chlorine residual and iodide; as a result, we underestimate the total chlorine residual.

Quantitative Applications

Although many quantitative applications of redox titrimetry have been re- placed by other analytical methods, a few important applications continue to find relevance. In this section we review the general application of redox titrimetry with an emphasis on environmental, pharmaceutical, and industrial applications. We begin, however, with a brief discussion of selecting and characterizing redox titrants, and methods for controlling the titrand's oxidation state.

Adjusting the Titrand's Oxidation State

If a redox titration is to be used in a quantitative analysis, the titrand initially must be present in a single oxidation state. For example, iron is determined by a redox titration in which Ce^{4+} oxidizes Fe^{2+} to Fe^{3+}. Depending on the sample and the method of sample preparation, iron initially may be present in both the +2 and +3 oxidation states. Before titrating, we must reduce any Fe^{3+} to Fe^{2+} if we want to determine the total concentration of iron in the sample. This type of pretreatment is accomplished using an auxiliary reducing agent or oxidizing agent.

A metal that is easy to oxidize—such as Zn, Al, and Ag—can serve as an ***auxiliary reducing agent***. The metal, as a coiled wire or powder, is added to the sample where it reduces the titrand. Because any unreacted auxiliary reducing agent will react with the titrant, it is removed before we begin the titration by removing the coiled wire or by filtering.

An alternative method for using an auxiliary reducing agent is to immobilize it in a column. To prepare a reduction column an aqueous slurry of the finally divided metal is packed in a glass tube equipped with a porous plug at the bottom. The sample is placed at the top of the column and moves through the column under the influence of gravity or vacuum suction. The length of the reduction column and the flow rate are selected to ensure the analyte's complete reduction. Two common reduction columns are the ***Jones reductor***, in which the the column is filled with amalgamated zinc, Zn(Hg); and the ***Walden reductor*** the column is filled with granular Ag metal.

Several reagents are used as ***auxiliary oxidizing agents***, including ammonium peroxydisulfate, $(NH_4)_2S_2O_8$, and hydrogen peroxide, H_2O_2. Peroxydisulfate is a powerful oxidizing agent

$$S_2O_8^{2-}(aq) + 2e^- \rightarrow 2SO_4^{2-}(aq)$$

that is capable of oxidizing Mn^{2+} to MnO_4^-, Cr^{3+} to $Cr_2O_7^{2-}$, and Ce^{3+} to Ce^{4+}. Excess peroxydisulfate is destroyed by briefly boiling the solution. The reduction of hydrogen peroxide in an acidic solution

$$H_2O_2(aq) + 2H^+(aq) + 2e^- \rightarrow 2H_2O(l)$$

provides another method for oxidizing a titrand. Excess H_2O_2 is destroyed by briefly boiling the solution.

Selecting and Standardizing a Titrant

If it is to be used quantitatively, the titrant's concentration must remain stable during the analysis. Because a titrant in a reduced state is susceptible to air oxidation, most redox titrations use an oxidizing agent as the titrant. The two strongest oxidizing titrants are MnO_4^- and Ce^{4+}, for which the reduction half-reactions are

$$MnO_4^-(aq) + 8H^+(aq) + 5e^- \rightleftharpoons Mn^{2+}(aq) + 4H_2O(l)$$

$$Ce^{4+}(aq) + e^- \rightleftharpoons Ce^{3+}(aq)$$

Despite its availability as a primary standard and its ease of preparation, Ce^{4+} is not used as frequently as MnO_4^- because it is more expensive.

Potassium dichromate is a relatively strong oxidizing agent whose principal advantages are its availability as a primary standard and its long term stability when in solution. It is not, however, as strong an oxidizing agent as MnO_4^- or Ce^{4+}, which makes it less useful when the titrand is a weak reducing agent. Its reduction half-reaction is

$$Cr_2O_7^{2-}(aq) + 14H^+(aq) + 6e^- \rightleftharpoons 2Cr^{3+}(aq) + 7H_2O(l)$$

Although a solution of $Cr_2O_7^{2-}$ is orange and a solution of Cr^{3+} is green, neither color is intense enough to serve as a useful indicator. Diphenylamine sulfonic acid, whose oxidized form is red-violet and reduced form is colorless, gives a very distinct end point signal with $Cr_2O_7^{2-}$.

Iodine is another important oxidizing titrant. Because it is a weaker oxidizing agent than MnO_4^-, Ce^{4+}, and $Cr_2O_7^{2-}$, it is useful only when the titrand is a stronger reducing agent. This apparent limitation, however, makes I_2 a more selective titrant for the analysis of a strong reducing agent in the presence of a weaker reducing agent. The reduction half-reaction for I_2 is

$$I_2(aq) + 2e^- \rightleftharpoons 2I^-(aq)$$

Because iodine is not very soluble in water, solutions are prepared by adding an excess of I^-. The complexation reaction

$$I_2(aq) + I^-(aq) \rightleftharpoons I_3^-(aq)$$

increases the solubility of I_2 by forming the more soluble triiodide ion, I_3^-. Even though iodine is present as I_3^- instead of I_2, the number of electrons in the reduction half-reaction is unaffected.

$$I_3^-(aq) + 2e^-(aq) \rightleftharpoons 3I^-(aq)$$

Solutions of I_3^- normally are standardized against $Na_2S_2O_3$ using starch as a specific indicator for I_3^-.

An oxidizing titrant such as MnO_4^-, Ce^{4+}, $Cr_2O_7^{2-}$, and I_3^-, is used when the titrand is in a reduced state. If the titrand is in an oxidized state, we can first reduce it with an auxiliary reducing agent and then complete the titration using an oxidizing titrant. Alternatively, we can titrate it using a reducing titrant. Iodide is a relatively strong reducing agent that could serve as a reducing titrant except that its solutions are susceptible to the air-oxidation of I^- to I_3^-.

$$3I^-(aq) \rightleftharpoons I_3^-(aq) + 2e^-$$

> A freshly prepared solution of KI is clear, but after a few days it may show a faint yellow coloring due to the presence of I_3^-.

Instead, adding an excess of KI reduces the titrand and releases a stoichiometric amount of I_3^-. The amount of I_3^- produced is then determined by a back titration using thiosulfate, $S_2O_3^{2-}$, as a reducing titrant.

$$2S_2O_3^{2-}(aq) \rightleftharpoons S_4O_6^{2-}(aq) + 2e^-$$

Solutions of $S_2O_3^{2-}$ are prepared using $Na_2S_2O_3 \cdot 5H_2O$ and are standardized before use. Standardization is accomplished by dissolving a carefully weighed portion of the primary standard KIO_3 in an acidic solution that contains an excess of KI. The reaction between IO_3^- and I^-

$$IO_3^-(aq) + 8I^-(aq) + 6H^+(aq) \rightarrow 3I_3^-(aq) + 3H_2O(l)$$

liberates a stoichiometric amount of I-3 . By titrating this I_3^- with thiosulfate, using starch as a visual indicator, we can determine the concentration of $S_2O_3^{2-}$ in the titrant.

Although thiosulfate is one of the few reducing titrants that is not readily oxidized by contact with air, it is subject to a slow decomposition to bisulfite and elemental sulfur. If used over a period of several weeks, a solution of thiosulfate is restandardized periodically. Several forms of bacteria are able to metabolize thiosulfate, which leads to a change in its concentration. This problem is minimized by adding a preservative such as HgI_2 to the solution.

Another useful reducing titrant is ferrous ammonium sulfate, $Fe(NH_4)_2(SO_4)_2 \cdot 6H_2O$, in which iron is present in the +2 oxidation state. A solution of Fe^{2+} is susceptible to air-oxidation, but when prepared in 0.5 M H_2SO_4 it remains stable for as long as a month. Periodic restandardization with $K_2Cr_2O_7$ is advisable. Ferrous ammonium sulfate is used as the titrant in a direct analysis of the titrand, or, it is added to the titrand in excess and the amount of Fe^{3+} produced determined by back titrating with a standard solution of Ce^{4+} or $Cr_2O_7^{2-}$.

Inorganic Analysis

One of the most important applications of redox titrimetry is evaluating the chlorination of public water supplies as described earlier in this section.

Another important example of redox titrimetry, which finds applications in both public health and environmental analysis, is the determination of dissolved oxygen. In natural waters, such as lakes and rivers, the level of dissolved O_2 is important for two reasons: it is the most readily available oxidant for the biological oxidation of inorganic and organic pollutants; and it is necessary for the support of aquatic life. In a wastewater treatment plant dissolved O_2 is essential for the aerobic oxidation of waste materials. If the concentration of dissolved O_2 falls below a critical value, aerobic bacteria are replaced by anaerobic bacteria, and the oxidation of organic waste produces undesirable gases, such as CH_4 and H_2S.

One more important example of redox titrimetry is the determination of water in nonaqueous solvents. The titrant for this analysis is known as the Karl Fischer reagent and consists of a mixture of iodine, sulfur dioxide, pyridine, and methanol. Because the

concentration of pyridine is sufficiently large, I_2 and SO_2 react with pyridine (py) to form the complexes py•I_2 and py•SO_2. When added to a sample that contains water, I_2 is reduced to I^- and SO_2 is oxidized to SO_3.

$$\mathrm{py \cdot I_2 + py \cdot SO_2 + H_2O + 2py \rightarrow 2py \cdot HI + py \cdot SO_3}$$

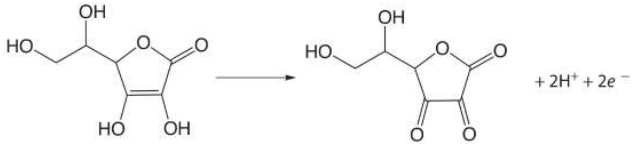
Methanol is included to prevent the further reaction of py•SO_3 with water. The titration's end point is signaled when the solution changes from the product's yellow color to the brown color of the Karl Fischer reagent.

Organic Analysis

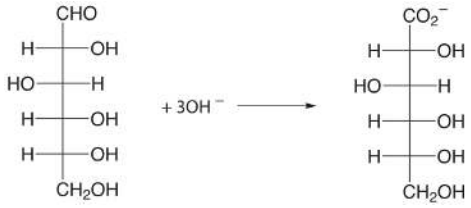
Redox titrimetry also is used for the analysis of organic analytes. One important example is the determination of the chemical oxygen demand (COD) of natural waters and wastewaters. The COD is a measure of the quantity of oxygen necessary to oxidize completely all the organic matter in a sample to CO_2 and H_2O. Because no attempt is made to correct for organic matter that is decomposed biologically, or for slow decomposition kinetics, the COD always overestimates a sample's true oxygen demand. The determination of COD is particularly important in the management of industrial wastewater treatment facilities where it is used to monitor the release of organic-rich wastes into municipal sewer systems or into the environment.

A sample's COD is determined by refluxing it in the presence of excess $K_2Cr_2O_7$, which serves as the oxidizing agent. The solution is acidified with H_2SO_4, using Ag_2SO_4 to catalyze the oxidation of low molecular weight fatty acids. Mercuric sulfate, $HgSO_4$, is added to complex any chloride that is present, which prevents the precipitation of the Ag^+ catalyst as AgCl. Under these conditions, the efficiency for oxidizing organic matter is 95–100%. After refluxing for two hours, the solution is cooled to room temperature and the excess $\mathrm{Cr_2O_7^{2-}}$ determined by a back titration using ferrous ammonium sulfate as the titrant and ferroin as the indicator. Because it is difficult to remove completely all traces of organic matter from the reagents, a blank titration is performed. The difference in the amount of ferrous ammonium sulfate needed to titrate the sample and the blank is proportional to the COD.

Iodine has been used as an oxidizing titrant for a number of compounds of pharmaceutical interest. Earlier we noted that the reaction of $\mathrm{S_2O_3^{2-}}$ with $\mathrm{I_3^-}$ produces the tetrathionate ion, $\mathrm{S_4O_6^{2-}}$. The tetrathionate ion is actually a dimer that consists of two thiosulfate ions connected through a disulfide (–S–S–) linkage. In the same fashion, $\mathrm{I_3^-}$ is used to titrate mercaptans of the general formula RSH, forming the dimer RSSR as a product. The amino acid cysteine also can be titrated with $\mathrm{I_3^-}$. The product of this titration is cystine, which is a dimer of cysteine. Triiodide also is used for the analysis of ascorbic acid (vitamin C) by oxidizing the enediol functional group to an alpha diketone



and for the analysis of reducing sugars, such as glucose, by oxidizing the aldehyde functional group to a carboxylate ion in a basic solution.



An organic compound that contains a hydroxyl, a carbonyl, or an amine functional group adjacent to an hydoxyl or a carbonyl group can be oxidized using metaperiodate, $\mathrm{IO_4^-}$, as an oxidizing titrant.

$$\mathrm{IO_4^-}(aq) + \mathrm{H_2O}(l) + 2e^- \rightleftharpoons \mathrm{IO_3^-}(aq) + 2\mathrm{OH^-}(aq)$$

A two-electron oxidation cleaves the C–C bond between the two functional groups with hydroxyl groups oxidized to aldehydes or ketones, carbonyl groups oxidized to carboxylic acids, and amines oxidized to an aldehyde and an amine (ammonia if a primary amine). The analysis is conducted by adding a known excess of $\mathrm{IO_4^-}$ to the solution that contains the analyte and allowing the oxidation to take place for approximately one hour at room temperature. When the oxidation is complete, an excess of KI is added, which converts any unreacted $\mathrm{IO_4^-}$ to $\mathrm{IO_3^-}$ and $\mathrm{I_3^-}$.

$$IO_4^-(aq) + 3I^-(aq) + H_2O(l) \rightarrow IO_3^-(aq) + I_3^-(aq) + 2OH^-(aq)$$

The I_3^- is then determined by titrating with $S_2O_3^{2-}$ using starch as an indicator.

Quantitative Redox Titration Calculations

The quantitative relationship between the titrand and the titrant is determined by the stoichiometry of the titration reaction. If you are unsure of the balanced reaction, you can deduce its stoichiometry by remembering that the electrons in a redox reaction are conserved.

Direct Titration Example 4.3.2

The amount of Fe in a 0.4891-g sample of an ore is determined by titrating with $K_2Cr_2O_7$. After dissolving the sample in HCl, the iron is brought into a +2 oxidation state using a Jones reductor. Titration to the diphenylamine sulfonic acid end point requires 36.92 mL of 0.02153 M $K_2Cr_2O_7$. Report the ore's iron content as %w/w Fe_2O_3.

Solution

Because we are not provided with the titration reaction, we will use a conservation of electrons to deduce the stoichiometry. During the titration the analyte is oxidized from Fe^{2+} to Fe^{3+}, and the titrant is reduced from $Cr_2O_7^{2-}$ to Cr^{3+}. Oxidizing Fe^{2+} to Fe^{3+} requires a single electron. Reducing $Cr_2O_7^{2-}$, in which each chromium is in the +6 oxidation state, to Cr^{3+} requires three electrons per chromium, for a total of six electrons. A conservation of electrons for the titration, therefore, requires that each mole of $K_2Cr_2O_7$ reacts with six moles of Fe^{2+}.

The moles of $K_2Cr_2O_7$ used to reach the end point is

$$(0.02153\ \text{M})(0.03692\ \text{L}) = 7.949 \times 10^{-4}\ \text{mol}\ K_2Cr_2O_7$$

which means the sample contains

$$7.949 \times 10^{-4}\ \text{mol}\ K_2Cr_2O_7 \times \frac{6\ \text{mol}\ Fe^{2+}}{\text{mol}\ K_2Cr_2O_7} = 4.769 \times 10^{-3}\ \text{mol}\ Fe^{2+}$$

Thus, the %w/w Fe_2O_3 in the sample of ore is

$$4.769 \times 10^{-3}\ \text{mol}\ Fe^{2+} \times \frac{1\ \text{mol}\ Fe_2O_3}{2\ \text{mol}\ Fe^{2+}} \times \frac{159.69\text{g}\ Fe_2O_3}{\text{mol}\ Fe_2O_3} = 0.3808\ \text{g}\ Fe_2O_3$$

$$\frac{0.3808\ \text{g}\ Fe_2O_3}{0.4891\ \text{g sample}} \times 100 = 77.86_2O_3$$

As shown in the following two examples, we can easily extend this approach to an analysis that requires an indirect analysis or a back titration.

Indirect Titration Example 4.3.3

A 25.00-mL sample of a liquid bleach is diluted to 1000 mL in a volumetric flask. A 25-mL portion of the diluted sample is transferred by pipet into an Erlenmeyer flask that contains an excess of KI, reducing the OCl^- to Cl^- and producing I_3^-. The liberated I_3^- is determined by titrating with 0.09892 M $Na_2S_2O_3$, requiring 8.96 mL to reach the starch indicator end point. Report the %w/v NaOCl in the sample of bleach.

Solution

To determine the stoichiometry between the analyte, NaOCl, and the titrant, $Na_2S_2O_3$, we need to consider both the reaction between OCl^- and I^-, and the titration of I_3^- with $Na_2S_2O_3$.

First, in reducing OCl^- to Cl^- the oxidation state of chlorine changes from +1 to –1, requiring two electrons. The oxidation of three I^- to form I_3^- releases two electrons as the oxidation state of each iodine changes from –1 in I^- to –1⁄3 in I_3^-. A conservation of electrons, therefore, requires that each mole of OCl^- produces one mole of I_3^-.

Second, in the titration reaction, I_3^- is reduced to I^- and $S_2O_3^{2-}$ is oxidized to $S_4O_6^{2-}$. Reducing I_3^- to $3I^-$ requires two elections as each iodine changes from an oxidation state of –1⁄3 to –1. In oxidizing $S_2O_3^{2-}$ to $S_4O_6^{2-}$, each sulfur changes its oxidation state from +2 to +2.5, releasing one electron for each $S_2O_3^{2-}$. A conservation of electrons, therefore, requires that each mole of I_3^- reacts with two moles of $S_2O_3^{2-}$.

Finally, because each mole of OCl^- produces one mole of I_3^-, and each mole of I_3^- reacts with two moles of $S_2O_3^{2-}$, we know that every mole of NaOCl in the sample ultimately results in the consumption of two moles of $Na_2S_2O_3$.

The moles of $Na_2S_2O_3$ used to reach the titration's end point is

$$(0.09892\ \text{M})(0.00896\ \text{L}) = 8.86 \times 10^{-4}\ \text{mol}\ Na_2S_2O_3$$

which means the sample contains

$$8.86 \times 10^{-4}\ \text{mol}\ Na_2S_2O_3 \times \frac{1\ \text{mol NaOCl}}{\text{mol}\ Na_2S_2O_3} \times \frac{74.44\ \text{g NaOCl}}{\text{mol NaOCl}} = 0.03299\ \text{g NaOCl}$$

Thus, the %w/v NaOCl in the diluted sample is

$$\frac{0.03299\ \text{g NaOCl}}{25.00\ \text{mL}} \times 100 = 0.132$$

Because the bleach was diluted by a factor of **40×** (25 mL to 1000 mL), the concentration of NaOCl in the bleach is 5.28% w/v.

Back Titration Example 4.3.4

The amount of ascorbic acid, $C_6H_8O_6$, in orange juice is determined by oxidizing ascorbic acid to dehydroascorbic acid, $C_6H_6O_6$, with a known amount of I_3^-, and back titrating the excess I_3^- with $Na_2S_2O_3$. A 5.00-mL sample of filtered orange juice is treated with 50.00 mL of 0.01023 M I_3^-. After the oxidation is complete, 13.82 mL of 0.07203 M $Na_2S_2O_3$ is needed to reach the starch indicator end point. Report the concentration ascorbic acid in mg/100 mL.

Solution

For a back titration we need to determine the stoichiometry between I_3^- and the analyte, $C_6H_8O_6$, and between I_3^- and the titrant, $Na_2S_2O_3$. The later is easy because we know from Example 4.3.3 that each mole of I_3^- reacts with two moles of $Na_2S_2O_3$.

In oxidizing ascorbic acid to dehydroascorbic acid, the oxidation state of carbon changes from +2⁄3 in $C_6H_8O_6$ to +1 in $C_6H_6O_6$. Each carbon releases 1⁄3 of an electron, or a total of two electrons per ascorbic acid. As we learned in Example 4.3.3 , reducing I_3^- requires two electrons; thus, a conservation of electrons requires that each mole of ascorbic acid consumes one mole of I_3^-.

The total moles of I_3^- that react with $C_6H_8O_6$ and with $Na_2S_2O_3$ is

$$(0.01023\ \text{M})(0.05000\ \text{L}) = 5.115 \times 10^{-4}\ \text{mol}\ I_3^-$$

The back titration consumes

$$0.01382\ \text{L}\ Na_2S_2O_3 \times \frac{0.07203\ \text{mol}\ Na_2S_2O_3}{\text{L}\ Na_2S_2O_3} \times \frac{1\ \text{mol}\ I_3^-}{2\ \text{mol}\ Na_2S_2O_3} = 4.977 \times 10^{-4}\ \text{mol}\ I_3^-$$

Subtracting the moles of I_3^- that react with $Na_2S_2O_3$ from the total moles of I_3^- gives the moles reacting with ascorbic acid.

$$5.115 \times 10^{-4}\ \text{mol}\ I_3^- - 4.977 \times 10^{-4}\ \text{mol}\ I_3^- = 1.38 \times 10^{-5}\ \text{mol}\ I_3^-$$

The grams of ascorbic acid in the 5.00-mL sample of orange juice is

$$1.38 \times 10^{-5}\ \text{mol}\ I_3^- \times \frac{1\ \text{mol}\ C_6H_8O_6}{\text{mol}\ I_3^-} \times \frac{176.12\ \text{g}\ C_6H_8O_6}{\text{mol}\ C_6H_8O_6} = 2.43 \times 10^{-3}\ \text{g}\ C_6H_8O_6$$

There are 2.43 mg of ascorbic acid in the 5.00-mL sample, or 48.6 mg per 100 mL of orange juice.

Evaluation of Redox Titrimetry

The scale of operations, accuracy, precision, sensitivity, time, and cost of a redox titration are similar to those described earlier in this chapter for an acid–base or a complexation titration. As with an acid–base titration, we can extend a redox titration to the analysis of a mixture of analytes if there is a significant difference in their oxidation or reduction potentials. Figure 4.3.7 shows an example of the titration curve for a mixture of Fe^{2+} and Sn^{2+} using Ce^{4+} as the titrant. A titration of a mixture of analytes is possible if their standard state potentials or formal potentials differ by at least 200 mV.

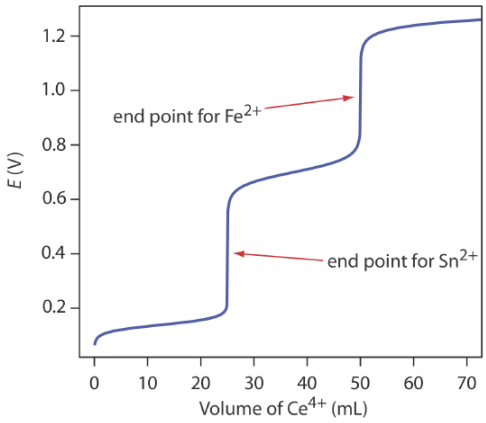


Figure 4.3.7 . Titration curve for the titration of 50.0 mL of 0.0125 M Sn^{2+} and 0.0250 M Fe^{2+} with 0.050 M Ce^{4+}. Both the titrand and the titrant are 1M in HCl.

This page titled 4.3: Redox Titrations is shared under a CC BY-NC-SA 4.0 license and was authored, remixed, and/or curated by Kathryn Davis.

- **9.4: Redox Titrations** by David Harvey is licensed CC BY-NC-SA 4.0.

4.4: Ladder Diagrams for Redox Titrations

When we develop or evaluate an analytical method, we often need to understand how the chemistry that takes place affects our results. Suppose we wish to isolate Ag^+ by precipitating it as AgCl. If we also need to control pH, then we must use a reagent that does not adversely affect the solubility of AgCl. It is a mistake to use NH_3 to adjust the pH, for example, because it increases the solubility of AgCl (see reaction 6.5.4). One of the primary sources of determinate errors in many analytical methods is failing to account for potential chemical interferences.

In this section we introduce the ladder diagram as a simple graphical tool for visualizing equilibrium chemistry. We will use ladder diagrams to determine what reactions occur when we combine several reagents, to estimate the approximate composition of a system at equilibrium, and to evaluate how a change to solution conditions might affect an analytical method.

Although not specifically on the topic of ladder diagrams as developed in this section, the following papers provide appropriate background information: (a) Runo, J. R.; Peters, D. G. *J. Chem. Educ.* **1993**, *70*, 708–713; (b) Vale, J.; Fernández-Pereira, C.; Alcalde, M. *J. Chem. Educ.* **1993**, *70*, 790–795; (c) Fernández-Pereira, C.; Vale, J. *Chem. Educator* **1996**, *6*, 1–18; (d) Fernández- Pereira, C.; Vale, J.; Alcalde, M. *Chem. Educator* **2003**, *8*, 15–21; (e) Fernández-Pereira, C.; Alcalde, M.; Villegas, R.; Vale, J. *J. Chem. Educ.* **2007**, *84*, 520–525. Ladder diagrams are a great tool for helping you to think intuitively about analytical chemistry. We will make frequent use of them in the chapters to follow.

Ladder Diagrams for Oxidation/Reduction Equilibria

We also can construct ladder diagrams to help us evaluate redox equilibria. Figure 4.4.8 shows a typical ladder diagram for two half-reactions in which the scale is the potential, *E*.

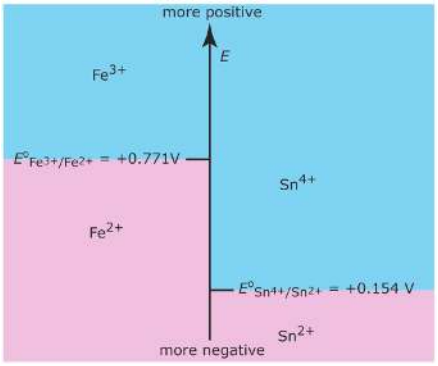


Figure 4.4.8 . Redox ladder diagram for Fe^{3+}/Fe^{2+} and for Sn^{4+}/Sn^{2+}. The areas shaded in blue show the potential range where the oxidized forms are the predominate species; the reduced forms are the predominate species in the areas shaded in pink. Note that a more positive potential favors the oxidized form.

The Nernst equation defines the areas of predominance. Using the Fe^{3+}/Fe^{2+} half-reaction as an example, we write

$$E = E^\circ - \frac{RT}{nF}\ln\frac{[Fe^{2+}]}{[Fe^{3+}]} = 0.771 - 0.05916\log\frac{[Fe^{2+}]}{[Fe^{3+}]}$$

At a potential more positive than the standard state potential, the predominate species is Fe^{3+}, whereas Fe^{2+} predominates at potentials more negative than E^o. When coupled with the step for the Sn^{4+}/Sn^{2+} half-reaction we see that Sn^{2+} is a useful reducing agent for Fe^{3+}. If Sn^{2+} is in excess, the potential of the resulting solution is near +0.154 V.

Because the steps on a redox ladder diagram are standard state potentials, a complication arises if solutes other than the oxidizing agent and reducing agent are present at non-standard state concentrations. For example, the potential for the half-reaction

$$UO_2^{2+}(aq) + 4H_3O^+(aq) + 2e^- \rightleftharpoons U^{4+}(aq) + 6H_2O(l)$$

depends on the solution's pH. To define areas of predominance in this case we begin with the Nernst equation

$$E = +0.327 - \frac{0.05916}{2} \log \frac{[U^{4+}]}{[UO_2^{2+}]\,[H_3O^+]^4}$$

and factor out the concentration of H_3O^+.

$$E = +0.327 + \frac{0.05916}{2} \log [H_3O^+]^4 - \frac{0.05916}{2} \log \frac{[U^{4+}]}{[UO_2^{2+}]}$$

From this equation we see that the area of predominance for UO_2^{2+} and U^{4+} is defined by a step at a potential where $[U^{4+}] = [UO_2^{2+}]$.

$$E = +0.327 + \frac{0.05916}{2} \log [H_3O^+]^4 = +0.327 - 0.1183pH$$

Figure 4.4.9 shows how pH affects the step for the UO_2^{2+} /U^{4+} half-reaction.

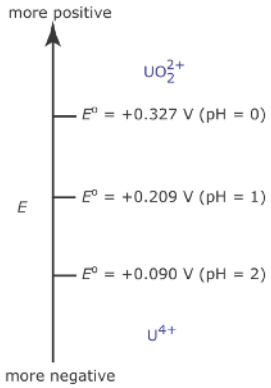


Figure 4.4.9 . Redox ladder diagram for the UO_2^{2+}/U^{4+} half-reaction showing the effect of pH on the step defined by the standard state's potential.

This page titled 4.4: Ladder Diagrams for Redox Titrations is shared under a CC BY-NC-SA 4.0 license and was authored, remixed, and/or curated by Kathryn Davis.

- **6.6: Ladder Diagrams** by David Harvey is licensed CC BY-NC-SA 4.0.

CHAPTER OVERVIEW

5: Electrochemical Instrumental Analysis

5.1: Overview of Electrochemistry

5.2: Potentiometric Methods

5.3: Coulometric Methods

5.4: Voltammetric and Amperometric Methods

This page titled 5: Electrochemical Instrumental Analysis is shared under a not declared license and was authored, remixed, and/or curated by Kathryn Davis.

5.1: Overview of Electrochemistry

The focus of this chapter is on analytical techniques that use a measurement of potential, current, or charge to determine an analyte's concentration or to characterize an analyte's chemical reactivity. Collectively we call this area of analytical chemistry ***electrochemistry*** because its originated from the study of the movement of electrons in an oxidation–reduction reaction.

Despite the difference in instrumentation, all electrochemical techniques share several common features. Before we consider individual examples in greater detail, let's take a moment to consider some of these similarities. As you work through the chapter, this overview will help you focus on similarities between different electrochemical methods of analysis. You will find it easier to understand a new analytical method when you can see its relationship to other similar methods.

Five Important Concepts

To understand electrochemistry we need to appreciate five important and interrelated concepts: (1) the electrode's potential determines the analyte's form at the electrode's surface; (2) the concentration of analyte at the electrode's surface may not be the same as its concentration in bulk solution; (3) in addition to an oxidation–reduction reaction, the analyte may participate in other chemical reactions; (4) current is a measure of the rate of the analyte's oxidation or reduction; and (5) we cannot control simultaneously current and potential.

> The material in this section—particularly the five important concepts—draws upon a vision for understanding electrochemistry outlined by Larry Faulkner in the article "Understanding Electrochemistry: Some Distinctive Concepts," *J. Chem. Educ.* **1983**, *60*, 262–264. See also, Kissinger, P. T.; Bott, A. W. "Electrochemistry for the Non-Electrochemist," *Current Separations*, **2002**, *20:2*, 51–53.

The Electrode's Potential Determines the Analyte's Form

In Chapter 6 we introduced the ladder diagram as a tool for predicting how a change in solution conditions affects the position of an equilibrium reaction. Figure 5.1.1 , for example, shows a ladder diagram for the Fe^{3+}/Fe^{2+} and the Sn^{4+}/Sn^{2+} equilibria. If we place an electrode in a solution of Fe^{3+} and Sn^{4+} and adjust its potential to +0.500 V, Fe^{3+} is reduced to Fe^{2+} but Sn^{4+} is not reduced to Sn^{2+}.

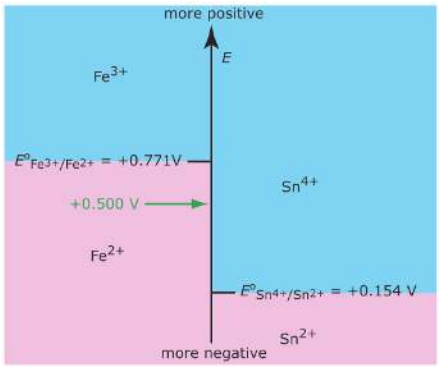


Figure 5.1.1 . Redox ladder diagram for Fe^{3+}/Fe^{2+} and for Sn^{4+}/Sn^{2+} redox couples. The areas in blue show the potential range where the oxidized forms are the predominate species; the reduced forms are the predominate species in the areas shown in pink. Note that a more positive potential favors the oxidized forms. At a potential of +0.500 V (green arrow) Fe^{3+} reduces to Fe^{2+}, but Sn^{4+} remains unchanged. You may wish to review the earlier treatment of oxidation–reduction reactions in Chapter 6.4 and the development of ladder diagrams for oxidation–reduction reactions in Chapter 6.6.

Interfacial Concentrations May Not Equal Bulk Concentrations

In Chapter 6 we introduced the Nernst equation, which provides a mathematical relationship between the electrode's potential and the concentrations of an analyte's oxidized and reduced forms in solution. For example, the Nernst equation for Fe^{3+} and Fe^{2+} is

$$E = E_{Fe^{3+}/Fe^{2+}} - \frac{RT}{nF}\ln\frac{[Fe^{2+}]}{[Fe^{3+}]} = \frac{0.05916}{1}\log\frac{[Fe^{2+}]}{[Fe^{3+}]} \quad (5.1.1)$$

where E is the electrode's potential and $E^{\circ}_{Fe^{3+}/Fe^{2+}}$ is the standard-state reduction potential for the reaction $Fe^{3+}(aq) \rightleftharpoons Fe^{2+}(aq) + e^{-}$. Because it is the potential of the electrode that determines the analyte's form at the electrode's surface, the concentration terms in Equation 5.1.1 are those of Fe^{2+} and Fe^{3+} at the electrode's surface, not their concentrations in bulk solution.

This distinction between a species' surface concentration and its bulk concentration is important. Suppose we place an electrode in a solution of Fe^{3+} and fix its potential at 1.00 V. From the ladder diagram in Figure 5.1.1 , we know that Fe^{3+} is stable at this potential and, as shown in Figure 5.1.2 a, the concentration of Fe^{3+} is the same at all distances from the electrode's surface. If we change the electrode's potential to +0.500 V, the concentration of Fe^{3+} at the electrode's surface decreases to approximately zero. As shown in Figure 5.1.2 b, the concentration of Fe^{3+} increases as we move away from the electrode's surface until it equals the concentration of Fe^{3+} in bulk solution. The resulting concentration gradient causes additional Fe^{3+} from the bulk solution to diffuse to the electrode's surface.

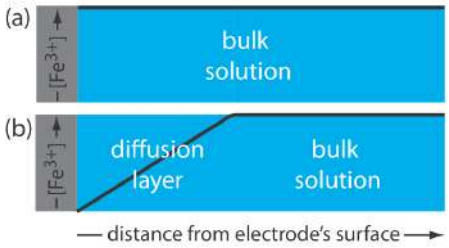


Figure 5.1.2 . Concentration of Fe^{3+} as a function of distance from the electrode's surface at (a) E = +1.00 V and (b) E = +0.500 V. The electrode is shown in gray and the solution in blue.

> We call the region of solution that contains this concentration gradient in Fe^{3+} the diffusion layer. We will have more to say about this in Chapter 11.4.

The Analyte May Participate in Other Reactions

Figure 5.1.1 and Figure 5.1.2 shows how the electrode's potential affects the concentration of Fe^{3+} and how the concentration of Fe^{3+} varies as a function of distance from the electrode's surface. The reduction of Fe^{3+} to Fe^{2+}, which is governed by Equation 5.1.1, may not be the only reaction that affects the concentration of Fe^{3+} in bulk solution or at the electrode's surface. The adsorption of Fe^{3+} at the electrode's surface or the formation of a metal–ligand complex in bulk solution, such as $Fe(OH)^{2+}$, also affects the concentration of Fe^{3+}.

Current is a Measure of Rate

The reduction of Fe^{3+} to Fe^{2+} consumes an electron, which is drawn from the electrode. The oxidation of another species, perhaps the solvent, at a second electrode is the source of this electron. Because the reduction of Fe^{3+} to Fe^{2+} consumes one electron, the flow of electrons between the electrodes—in other words, the current—is a measure of the rate at which Fe^{3+} is reduced. One important consequence of this observation is that the current is zero when the reaction $Fe^{3+}(aq) \rightleftharpoons Fe^{2+}(aq) + e^{-}$ is at equilibrium.

> The rate of the reaction $Fe^{3+}(aq) \rightleftharpoons Fe^{2+}(aq) + e^{-}$ is the change in the concentration of Fe^{3+} as a function of time.

We Cannot Control Simultaneously Both the Current and the Potential

If a solution of Fe^{3+} and Fe^{2+} is at equilibrium, the current is zero and the potential is given by Equation 5.1.1. If we change the potential away from its equilibrium position, current flows as the system moves toward its new equilibrium position. Although the initial current is quite large, it decreases over time, reaching zero when the reaction reaches equilibrium. The current, therefore, changes in response to the applied potential. Alternatively, we can pass a fixed current through the electrochemical cell, forcing the reduction of Fe^{3+} to Fe^{2+}. Because the concentrations of Fe^{3+} decreases and the concentration of Fe^{2+} increases, the potential, as given by Equation 5.1.1, also changes over time. In short, if we choose to control the potential, then we must accept the resulting current, and we must accept the resulting potential if we choose to control the current.

Controlling and Measuring Current and Potential

Electrochemical measurements are made in an electrochemical cell that consists of two or more electrodes and the electronic circuitry needed to control and measure the current and the potential. In this section we introduce the basic components of electrochemical instrumentation.

The simplest electrochemical cell uses two electrodes. The potential of one electrode is sensitive to the analyte's concentration, and is called the ***working electrode*** or the ***indicator electrode***. The second electrode, which we call the ***counter electrode***, completes the electrical circuit and provides a reference potential against which we measure the working electrode's potential. Ideally the counter electrode's potential remains constant so that we can assign to the working electrode any change in the overall cell potential. If the counter electrode's potential is not constant, then we replace it with two electrodes: a ***reference electrode*** whose potential remains constant and an ***auxiliary electrode*** that completes the electrical circuit.

Because we cannot control simultaneously the current and the potential, there are only three basic experimental designs: (1) we can measure the potential when the current is zero, (2) we can measure the potential while we control the current, and (3) we can measure the current while we control the potential. Each of these experimental designs relies on ***Ohm's law***, which states that the current, i, passing through an electrical circuit of resistance, R, generates a potential, E.

$$E = iR$$

Each of these experimental designs uses a different type of instrument. To help us understand how we can control and measure current and potential, *we will describe these instruments as if the analyst is operating them manually*. To do so the analyst observes a change in the current or the potential and manually adjusts the instrument's settings to maintain the desired experimental conditions. It is important to understand that modern electrochemical instruments provide an automated, electronic means for controlling and measuring current and potential, and that they do so by using very different electronic circuitry than that described here.

> This point bears repeating: It is important to understand that the experimental designs in Figure 5.1.3 , Figure 5.1.4 , and Figure 5.1.5 do not represent the electrochemical instruments you will find in today's analytical labs. For further information about modern electrochemical instrumentation, see this chapter's additional resources.

Potentiometers

To measure the potential of an electrochemical cell under a condition of zero current we use a ***potentiometer***. Figure 5.1.3 shows a schematic diagram for a manual potentiometer that consists of a power supply, an electrochemical cell with a working electrode and a counter electrode, an ammeter to measure the current that passes through the electrochemical cell, an adjustable, slide-wire resistor, and a tap key for closing the circuit through the electrochemical cell. Using Ohm's law, the current in the upper half of the circuit is

$$i_{\text{upper}} = \frac{E_{\text{PS}}}{R_{ab}}$$

where E_{PS} is the power supply's potential, and R_{ab} is the resistance between points a and b of the slide-wire resistor. In a similar manner, the current in the lower half of the circuit is

$$i_{\text{lower}} = \frac{E_{\text{cell}}}{R_{cb}}$$

where E_{cell} is the potential difference between the working electrode and the counter electrode, and R_{cb} is the resistance between the points c and b of the slide-wire resistor. When $i_{\text{upper}} = i_{\text{lower}} = 0$, no current flows through the ammeter and the potential of the electrochemical cell is

$$E_{\text{coll}} = \frac{R_{cb}}{R_{ab}} \times E_{\text{PS}} \tag{5.1.2}$$

To determine E_{cell} we briefly press the tap key and observe the current at the ammeter. If the current is not zero, then we adjust the slide wire resistor and remeasure the current, continuing this process until the current is zero. When the current is zero, we use

Equation 5.1.2 to calculate E_{cell}.

Using the tap key to briefly close the circuit through the electrochemical cell minimizes the current that passes through the cell and limits the change in the electrochemical cell's composition. For example, passing a current of 10^{-9} A through the electrochemical cell for 1 s changes the concentrations of species in the cell by approximately 10^{-14} moles. Modern potentiometers use operational amplifiers to create a high-impedance voltmeter that measures the potential while drawing a current of less than 10^{-9} A.

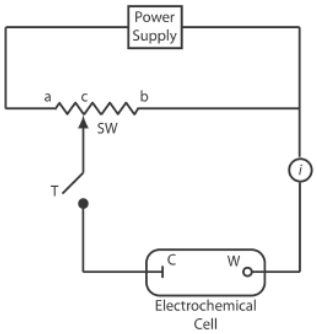


Figure 5.1.3 . Schematic diagram of a manual potentiometer: C is the counter electrode; W is the working electrode; SW is a slide-wire resistor; T is a tap key and *i* is an ammeter for measuring current.

Galvanostats

A ***galvanostat***, a schematic diagram of which is shown in Figure 5.1.4 , allows us to control the current that flows through an electrochemical cell. The current from the power supply through the working electrode is

$$i = \frac{E_{PS}}{R + R_{cell}}$$

where E_{PS} is the potential of the power supply, R is the resistance of the resistor, and R_{cell} is the resistance of the electrochemical cell. If $R >> R_{cell}$, then the current between the auxiliary and working electrodes

$$i = \frac{E_{PS}}{R} \approx \text{constant}$$

maintains a constant value. To monitor the working electrode's potential, which changes as the composition of the electrochemical cell changes, we can include an optional reference electrode and a high-impedance potentiometer.

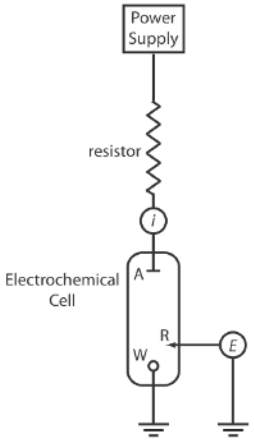


Figure 5.1.4 . Schematic diagram of a galvanostat: A is the auxiliary electrode; W is the working electrode; R is an optional reference electrode, *E* is a high-impedance potentiometer, and *i* is an ammeter. The working electrode and the optional reference electrode are connected to a ground.

Potentiostats

A ***potentiostat***, a schematic diagram of which is shown in Figure 5.1.5 , allows us to control the working electrode's potential. The potential of the working electrode is measured relative to a constant-potential reference electrode that is connected to the working

electrode through a high-impedance potentiometer. To set the working electrode's potential we adjust the slide wire resistor that is connected to the auxiliary electrode. If the working electrode's potential begins to drift, we adjust the slide wire resistor to return the potential to its initial value. The current flowing between the auxiliary electrode and the working electrode is measured with an ammeter. Modern potentiostats include waveform generators that allow us to apply a time-dependent potential profile, such as a series of potential pulses, to the working electrode.

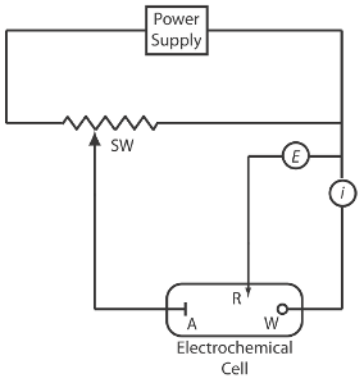


Figure 5.1.5 . Schematic diagram for a manual potentiostat: W is the working electrode; A is the auxiliary electrode; R is the reference electrode; SW is a slide-wire resistor, *E* is a high-impendance potentiometer; and *i* is an ammeter.

Interfacial Electrochemical Techniques

Because interfacial electrochemistry is such a broad field, let's use Figure 5.1.6 to organize techniques by the experimental conditions we choose to use (Do we control the potential or the current? How do we change the applied potential or applied current? Do we stir the solution?) and the analytical signal we decide to measure (Current? Potential?).

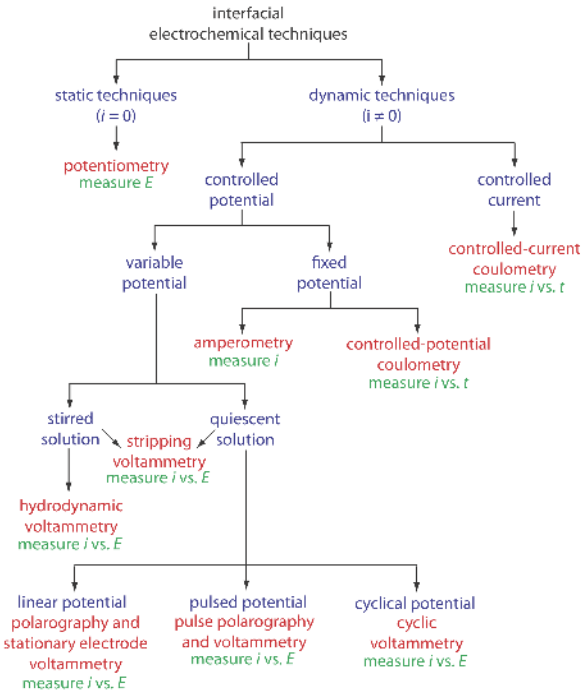


Figure 5.1.6 . Family tree that highlights the similarities and differences between a number of interfacial electrochemical techniques. The specific techniques are shown in red, the experimental conditions are shown in blue, and the analytical signals are shown in green.

At the first level, we divide interfacial electrochemical techniques into static techniques and dynamic techniques. In a static technique we do not allow current to pass through the electrochemical cell and, as a result, the concentrations of all species remain constant. Potentiometry, in which we measure the potential of an electrochemical cell under static conditions, is one of the most important quantitative electrochemical methods and is discussed in detail in Chapter 11.2.

Dynamic techniques, in which we allow current to flow and force a change in the concentration of species in the electrochemical cell, comprise the largest group of interfacial electrochemical techniques. Coulometry, in which we measure current as a function of time, is covered in Chapter 11.3. Amperometry and voltammetry, in which we measure current as a function of a fixed or variable potential, is the subject of Chapter 11.4.

This page titled 5.1: Overview of Electrochemistry is shared under a CC BY-NC-SA 4.0 license and was authored, remixed, and/or curated by Kathryn Davis.

- **11.1: Overview of Electrochemistry** by David Harvey is licensed CC BY-NC-SA 4.0.

5.2: Potentiometric Methods

In potentiometry we measure the potential of an electrochemical cell under static conditions. Because no current—or only a negligible current—flows through the electrochemical cell, its composition remains unchanged. For this reason, potentiometry is a useful quantitative method of analysis. The first quantitative potentiometric applications appeared soon after the formulation, in 1889, of the Nernst equation, which relates an electrochemical cell's potential to the concentration of electroactive species in the cell [Stork, J. T. *Anal. Chem.* **1993**, *65*, 344A–351A].

> For an on-line introduction to much of the material in this section, see Analytical Electrochemistry: Potentiometry by Erin Gross, Richard S. Kelly, and Donald M. Cannon, Jr., a resource that is part of the Analytical Sciences Digital Library.

Potentiometry initially was restricted to redox equilibria at metallic electrodes, which limited its application to a few ions. In 1906, Cremer discovered that the potential difference across a thin glass membrane is a function of pH when opposite sides of the membrane are in contact with solutions that have different concentrations of H_3O^+. This discovery led to the development of the glass pH electrode in 1909. Other types of membranes also yield useful potentials. For example, in 1937 Kolthoff and Sanders showed that a pellet of AgCl can be used to determine the concentration of Ag^+. Electrodes based on membrane potentials are called ion-selective electrodes, and their continued development extends potentiometry to a diverse array of analytes.

Potentiometric Measurements

As shown in Figure 11.1.3, we use a potentiometer to determine the difference between the potential of two electrodes. The potential of one electrode—the working or indicator electrode—responds to the analyte's activity and the other electrode—the counter or reference electrode—has a known, fixed potential. In this section we introduce the conventions for describing potentiometric electrochemical cells, and the relationship between the measured potential and the analyte's activity.

> In Chapter 6 we noted that a chemical reaction's equilibrium position is a function of the activities of the reactants and products, not their concentrations. To be correct, we should write the Nernst equation in terms of activities. So why didn't we use activities in Chapter 9 when we calculated redox titration curves? There are two reasons for that choice. First, concentrations are always easier to calculate than activities. Second, in a redox titration we determine the analyte's concentration from the titration's end point, not from the potential at the end point. The only reasons for calculating a titration curve is to evaluate its feasibility and to help us select a useful indicator. In most cases, the error we introduce by assuming that concentration and activity are identical is too small to be a significant concern.
>
> In potentiometry we cannot ignore the difference between activity and concentration. Later in this section we will consider how we can design a potentiometric method so that we can ignore the difference between activity and concentration. See Chapter 6.9 to review our earlier discussion of activity and concentration.

Potentiometric Electrochemical Cells

A schematic diagram of a typical potentiometric electrochemical cell is shown in Figure 5.2.1 . The electrochemical cell consists of two half-cells, each of which contains an electrode immersed in a solution of ions whose activities determine the electrode's potential. A ***salt bridge*** that contains an inert electrolyte, such as KCl, connects the two half-cells. The ends of the salt bridge are fixed with porous frits, which allow the electrolyte's ions to move freely between the half-cells and the salt bridge. This movement of ions in the salt bridge completes the electrical circuit.

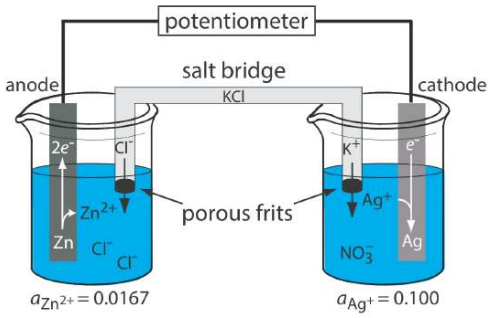


Figure 5.2.1 . Example of a potentiometric electrochemical cell. The activities of Zn^{2+} and Ag^{+} are shown below the two half-cells.

By convention, we identify the electrode on the left as the ***anode*** and assign to it the oxidation reaction; thus

$$\mathrm{Zn}(s) \rightleftharpoons \mathrm{Zn}^{2+}(aq) + 2e^{-}$$

The electrode on the right is the ***cathode***, where the reduction reaction occurs.

$$\mathrm{Ag}^{+}(aq) + e^{-} \rightleftharpoons \mathrm{Ag}(s)$$

The potential of the electrochemical cell in Figure 5.2.1 is for the reaction

$$\mathrm{Zn}(s) + 2\mathrm{Ag}^{+}(aq) \rightleftharpoons 2\mathrm{Ag}(s) + \mathrm{Zn}^{2+}(\mathrm{aq})$$

We also define potentiometric electrochemical cells such that the cathode is the indicator electrode and the anode is the reference electrode.

> The reason for separating the electrodes is to prevent the oxidation reaction and the reduction reaction from occurring at one of the electrodes. For example, if we place a strip of Zn metal in a solution of $AgNO_3$, the reduction of Ag^{+} to Ag occurs on the surface of the Zn at the same time as a potion of the Zn metal oxidizes to Zn^{2+}. Because the transfer of electrons from Zn to Ag^{+} occurs at the electrode's surface, we can not pass them through the potentiometer.

Shorthand Notation for Electrochemical Cells

Although Figure 5.2.1 provides a useful picture of an electrochemical cell, it is not a convenient way to represent it (Imagine having to draw a picture of each electrochemical cell you are using!). A more useful way to describe an electrochemical cell is a shorthand notation that uses symbols to identify different phases and that lists the composition of each phase. We use a vertical slash (|) to identify a boundary between two phases where a potential develops, and a comma (,) to separate species in the same phase or to identify a boundary between two phases where no potential develops. Shorthand cell notations begin with the anode and continue to the cathode. For example, we describe the electrochemical cell in Figure 5.2.1 using the following shorthand notation.

$$\mathrm{Zn}(s)\,|\mathrm{ZnCl_2}(aq, a_{\mathrm{Zn^{2+}}} = 0.0167)\,||\,\mathrm{AgNO_3}(aq, a_{\mathrm{Ag^{+}}} = 0.100)\,|\,\mathrm{Ag}(s)$$

The double vertical slash (||) represents the salt bridge, the contents of which we usually do not list. Note that a double vertical slash implies that there is a potential difference between the salt bridge and each half-cell.

✔ Example 5.2.1

What are the anodic, the cathodic, and the overall reactions responsible for the potential of the electrochemical cell in Figure 5.2.2 ? Write the shorthand notation for the electrochemical cell.

Solution

The oxidation of Ag to Ag^{+} occurs at the anode, which is the left half-cell. Because the solution contains a source of Cl^{-}, the anodic reaction is

$$\mathrm{Ag}(s) + \mathrm{Cl}^{-}(aq) \rightleftharpoons \mathrm{AgCl}(s) + e^{-}$$

The cathodic reaction, which is the right half-cell, is the reduction of Fe^{3+} to Fe^{2+}.

$$Fe^{3+}(aq) + e^- \rightleftharpoons Fe^{2+}(aq)$$

The overall cell reaction, therefore, is

$$Ag(s) + Fe^{3+}(aq) + Cl^-(aq) \rightleftharpoons AgCl(s) + Fe^{2+}(aq)$$

The electrochemical cell's shorthand notation is

$$Ag(s)\,|HCl(aq, a_{Cl^-} = 0.100), AgCl(sat'd)|$$
$$|FeCl_2(aq, a_{Fe^{2+}} = 0.0100),\ Fe^{3+}(aq, a_{Fe^{3+}} = 0.0500)|\,Pt(s)$$

Note that the Pt cathode is an inert electrode that carries electrons to the reduction half-reaction. The electrode itself does not undergo reduction.

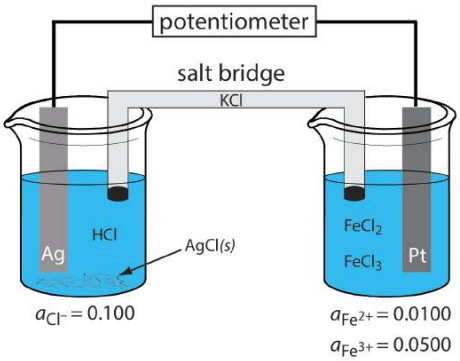


Figure 5.2.2 . Potentiometric electrochemical cell for Example 5.2.1 .

Potential and Activity—The Nernst Equation

The potential of a potentiometric electrochemical cell is

$$E_{cell} = E_{cathode} - E_{anode} \tag{5.2.1}$$

where $E_{cathode}$ and E_{anode} are reduction potentials for the redox reactions at the cathode and the anode, respectively. Each reduction potential is given by the Nernst equation

$$E = E^\circ - \frac{RT}{nF}\ln Q$$

where E^o is the standard-state reduction potential, R is the gas constant, T is the temperature in Kelvins, n is the number of electrons in the redox reaction, F is Faraday's constant, and Q is the reaction quotient. At a temperature of 298 K (25°C) the Nernst equation is

$$E = E^\circ - \frac{0.05916}{n}\log Q \tag{5.2.2}$$

where E is in volts.

Using Equation 5.2.2, the potential of the anode and cathode in Figure 5.2.1 are

$$E_{anode} = E^\circ_{Zn^{2+}/Zn} - \frac{0.05916}{2}\log\frac{1}{a_{Zn^{2+}}}$$

$$E_{anode} = E^\circ_{Ag^{+}/Ag} - \frac{0.05916}{1}\log\frac{1}{a_{Ag^{+}}}$$

Even though an oxidation reaction is taking place at the anode, we define the anode's potential in terms of the corresponding reduction reaction and the standard-state reduction potential. See Chapter 6.4 for a review of using the Nernst equation in calculations.

Substituting $E_{cathode}$ and E_{anode} into Equation 5.2.1, along with the activities of Zn^{2+} and Ag^{+} and the standard-state reduction potentials, gives E_{cell} as

$$E_{cell} = \left(E^{\circ}_{Ag^{+}/Ag} - \frac{0.05916}{1}\log\frac{1}{a_{Ag^{+}}}\right) - \left(E^{\circ}_{Zn^{2+}/Zn} - \frac{0.05916}{2}\log\frac{1}{a_{Zn^{2+}}}\right)$$

$$E_{cell} = \left(0.7996 - \frac{0.05916}{1}\log\frac{1}{0.100}\right) - \left(-0.7618 - \frac{0.05916}{2}\log\frac{1}{0.0167}\right) = 1.555 \text{ V}$$

You will find values for the standard-state reduction potentials in Appendix 13.

Example 5.2.2

What is the potential of the electrochemical cell shown in Example 5.2.1 ?

Solution

Substituting $E_{cathode}$ and E_{anode} into Equation 5.2.1, along with the concentrations of Fe^{3+}, Fe^{2+}, and Cl^{-} and the standard-state reduction potentials gives

$$E_{cell} = \left(E^{\circ}_{Fe^{3+}/Fe^{2+}} - \frac{0.05916}{1}\log\frac{a_{Fe^{2+}}}{a_{Fe^{3+}}}\right) - \left(E^{\circ}_{AgCl/Ag} - \frac{0.05916}{1}\log a_{Cl^{-}}\right)$$

$$E_{cell} = \left(0.771 - \frac{0.05916}{1}\log\frac{0.0100}{0.0500}\right) - \left(0.2223 - \frac{0.05916}{1}\log(0.100)\right) = 0.531 \text{ V}$$

In potentiometry, we assign the reference electrode to the anodic half-cell and assign the indicator electrode to the cathodic half-cell. Thus, if the potential of the cell in Figure 5.2.1 is +1.50 V and the activity of Zn^{2+} is 0.0167, then we can solve the following equation for $a_{Ag^{+}}$

$$1.50 \text{ V} = \left(0.7996 - \frac{0.05916}{1}\log\frac{1}{a_{Ag^{+}}}\right) - \left(-0.7618 - \frac{0.05916}{2}\log\frac{1}{0.0167}\right)$$

obtaining an activity of 0.0118. *(Note: activity is concentration adjusted for the presence of other species in solution. We'll get there.)*

Despite the apparent ease of determining an analyte's activity using the Nernst equation, there are several problems with this approach. One problem is that standard-state potentials are temperature-dependent and the values in reference tables usually are for a temperature of 25°C. We can overcome this problem by maintaining the electrochemical cell at 25°C or by measuring the standard-state potential at the desired temperature.

Another problem is that a standard-state reduction potential may have a significant matrix effect. For example, the standard-state reduction potential for the Fe^{3+}/Fe^{2+} redox couple is +0.735 V in 1 M $HClO_4$, +0.70 V in 1 M HCl, and +0.53 V in 10 M HCl. The difference in potential for equimolar solutions of HCl and $HClO_4$ is the result of a difference in the activity coefficients for Fe^{3+} and Fe^{2+} in these two media. The shift toward a more negative potential with an increase in the concentration of HCl is the result of chloride's ability to form a stronger complex with Fe^{3+} than with Fe^{2+}. We can minimize this problem by replacing the standard-state potential with a matrix-dependent formal potential. Most tables of standard-state potentials, including those in Appendix 13, include selected formal potentials.

Finally, a more serious problem is the presence of additional potentials in the electrochemical cell not included in Equation 5.2.1. In writing the shorthand notation for an electrochemical cell we use a double slash (||) to indicate the salt bridge, suggesting a potential exists at the interface between each end of the salt bridge and the solution in which it is immersed. The origin of this potential is discussed in the following section.

Junction Potentials

A ***junction potential*** develops at the interface between two ionic solution if there is a difference in the concentration and mobility of the ions. Consider, for example, a porous membrane that separations a solution of 0.1 M HCl from a solution of 0.01 M HCl (Figure 5.2.3 a). Because the concentration of HCl on the membrane's left side is greater than that on the right side of the membrane, H^+ and Cl^- will diffuse in the direction of the arrows. The mobility of H^+, however, is greater than that for Cl^-, as shown by the difference in the lengths of their respective arrows. Because of this difference in mobility, the solution on the right side of the membrane develops an excess concentration of H^+ and a positive charge (Figure 5.2.3 b). Simultaneously, the solution on the membrane's left side develops a negative charge because there is an excess concentration of Cl^-. We call this difference in potential across the membrane a junction potential and represent it as E_j.

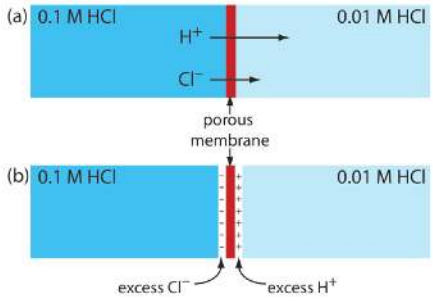


Figure 5.2.3 . Origin of the junction potential between a solution of 0.1 M HCl and a solution of 0.01 M HCl.

The magnitude of the junction potential depends upon the difference in the concentration of ions on the two sides of the interface, and may be as large as 30–40 mV. For example, a junction potential of 33.09 mV has been measured at the interface between solutions of 0.1 M HCl and 0.1 M NaCl [Sawyer, D. T.; Roberts, J. L., Jr. *Experimental Electrochemistry for Chemists*, Wiley-Interscience: New York, 1974, p. 22]. A salt bridge's junction potential is minimized by using a salt, such as KCl, for which the mobilities of the cation and anion are approximately equal. We also can minimize the junction potential by incorporating a high concentration of the salt in the salt bridge. For this reason salt bridges frequently are constructed using solutions that are saturated with KCl. Nevertheless, a small junction potential, generally of unknown magnitude, is always present.

When we measure the potential of an electrochemical cell, the junction potential also contributes to E_{cell}; thus, we rewrite Equation 5.2.1 as

$$E_{cell} = E_{cathode} - E_{anode} + E_j$$

to include its contribution. If we do not know the junction potential's actual value—which is the usual situation—then we cannot directly calculate the analyte's concentration using the Nernst equation. Quantitative analytical work is possible, however, if we use one of the standardization methods—external standards, the method of standard additions, or internal standards—discussed in Chapter 5.3.

Reference Electrodes

In a potentiometric electrochemical cell one of the two half-cells provides a fixed reference potential and the potential of the other half-cell responds the analyte's concentration. By convention, the reference electrode is the anode; thus, the short hand notation for a potentiometric electrochemical cell is

reference electrode || indicator electrode

and the cell potential is

$$E_{cell} = E_{ind} - E_{ref} + E_j$$

The ideal reference electrode provides a stable, known potential so that we can attribute any change in E_{cell} to the analyte's effect on the indicator electrode's potential. In addition, it should be easy to make and to use the reference electrode. Three common reference electrodes are discussed in this section.

Standard Hydrogen Electrode

Although we rarely use the ***standard hydrogen electrode*** (SHE) for routine analytical work, it is the reference electrode used to establish standard-state potentials for other half-reactions. The SHE consists of a Pt electrode immersed in a solution in which the activity of hydrogen ion is 1.00 and in which the fugacity of $H_2(g)$ is 1.00 (Figure 5.2.4). A conventional salt bridge connects the SHE to the indicator half-cell. The short hand notation for the standard hydrogen electrode is

$$\mathrm{Pt}(s),\ \mathrm{H_2}\,(g, f_{\mathrm{H_2}} = 1.00)\,|\,\mathrm{H^+}\,(aq, a_{\mathrm{H^+}} = 1.00)\,\|$$

and the standard-state potential for the reaction

$$\mathrm{H^+}(aq) + e^- = \frac{1}{2}\mathrm{H_2}(g)$$

is, by definition, 0.00 V at all temperatures. Despite its importance as the fundamental reference electrode against which we measure all other potentials, the SHE is rarely used because it is difficult to prepare and inconvenient to use.

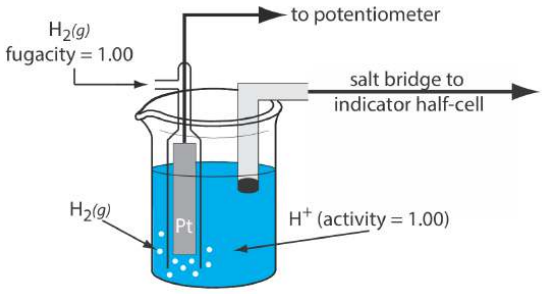


Figure 5.2.4 . Schematic diagram showing the standard hydrogen electrode.

Calomel Electrodes

A calomel reference electrode is based on the following redox couple between Hg_2Cl_2 and Hg (calomel is the common name for Hg_2Cl_2)

$$\mathrm{Hg_2Cl_2}(s) + 2e^- \rightleftharpoons 2\mathrm{Hg}(l) + 2\mathrm{Cl^-}(aq)$$

for which the potential is

$$E = E^\circ_{\mathrm{Hg_2Cl_2/Hg}} - \frac{0.05916}{2}\log\,(a_{\mathrm{Cl^-}})^2 = +0.2682\mathrm{V} - \frac{0.05916}{2}\log\,(a_{\mathrm{Cl^-}})^2$$

The potential of a calomel electrode, therefore, depends on the activity of Cl^- in equilibrium with Hg and Hg_2Cl_2.

As shown in Figure 5.2.5 , in a ***saturated calomel electrode*** (SCE) the concentration of Cl^- is determined by the solubility of KCl. The electrode consists of an inner tube packed with a paste of Hg, Hg_2Cl_2, and KCl, situated within a second tube that contains a saturated solution of KCl. A small hole connects the two tubes and a porous wick serves as a salt bridge to the solution in which the SCE is immersed. A stopper in the outer tube provides an opening for adding addition saturated KCl. The short hand notation for this cell is

$$\mathrm{Hg}(l)|\mathrm{Hg_2Cl_2}(s), \mathrm{KCl}(aq,\ \mathrm{sat'd}\ )\|$$

Because the concentration of Cl^- is fixed by the solubility of KCl, the potential of an SCE remains constant even if we lose some of the inner solution to evaporation. A significant disadvantage of the SCE is that the solubility of KCl is sensitive to a change in temperature. At higher temperatures the solubility of KCl increases and the electrode's potential decreases. For example, the potential of the SCE is +0.2444 V at 25°C and +0.2376 V at 35°C. The potential of a calomel electrode that contains an unsaturated solution of KCl is less dependent on the temperature, but its potential changes if the concentration, and thus the activity of Cl^-, increases due to evaporation.

> For example, the potential of a calomel electrode is +0.280 V when the concentration of KCl is 1.00 M and +0.336 V when the concentration of KCl is 0.100 M. If the activity of Cl^- is 1.00, the potential is +0.2682 V.

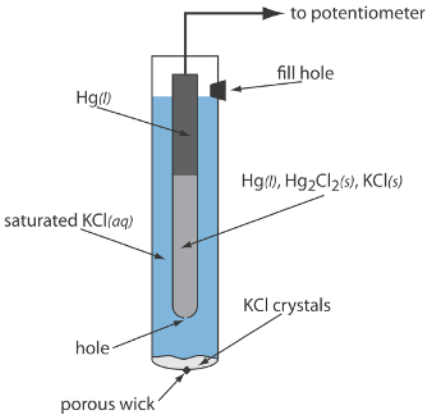


Figure 5.2.5 . Schematic diagram showing the saturated calomel electrode.

Silver/Silver Chloride Electrodes

Another common reference electrode is the ***silver/silver chloride electrode***, which is based on the reduction of AgCl to Ag.

$$\mathrm{AgCl}(s) + e^- \rightleftharpoons \mathrm{Ag}(s) + \mathrm{Cl}^-(aq)$$

As is the case for the calomel electrode, the activity of Cl^- determines the potential of the Ag/AgCl electrode; thus

$$E = E^\circ_{\mathrm{AgCl/Ag}} - 0.05916 \log a_{\mathrm{Cl}^-} = 0.2223\ \mathrm{V} - 0.05916 \log a_{\mathrm{Cl}^-}$$

When prepared using a saturated solution of KCl, the electrode's potential is +0.197 V at 25°C. Another common Ag/AgCl electrode uses a solution of 3.5 M KCl and has a potential of +0.205 V at 25°C. As you might expect, the potential of a Ag/AgCl electrode using a saturated solution of KCl is more sensitive to a change in temperature than an electrode that uses an unsaturated solution of KCl.

A typical Ag/AgCl electrode is shown in Figure 5.2.6 and consists of a silver wire, the end of which is coated with a thin film of AgCl, immersed in a solution that contains the desired concentration of KCl. A porous plug serves as the salt bridge. The electrode's short hand notation is

$$\mathrm{Ag}(s)|\,\mathrm{Ag\,Cl}(s), \mathrm{KCl}\,(aq, a_{\mathrm{Cl}^-} = x)\,\|$$

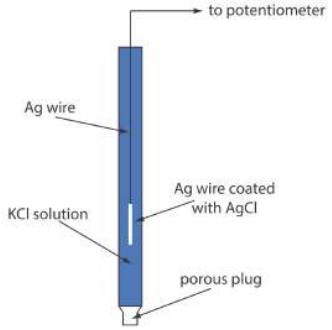


Figure 5.2.6 . Schematic diagram showing a Ag/AgCl electrode. Because the electrode does not contain solid KCl, this is an example of an unsaturated Ag/AgCl electrode.

Converting Potentials Between Reference Electrodes

The standard state reduction potentials in most tables are reported relative to the standard hydrogen electrode's potential of +0.00 V. Because we rarely use the SHE as a reference electrode, we need to convert an indicator electrode's potential to its equivalent value when using a different reference electrode. As shown in the following example, this is easy to do.

Example 5.2.4

The potential for an Fe^{3+}/Fe^{2+} half-cell is +0.750 V relative to the standard hydrogen electrode. What is its potential if we use a saturated calomel electrode or a saturated silver/silver chloride electrode?

Solution

When we use a standard hydrogen electrode the potential of the electrochemical cell is

$$E_{\text{cell}} = E_{\text{Fe}^{3+}/\text{Fe}^{2+}} - E_{\text{SHE}} = 0.750\ \text{V} - 0.000\ \text{V} = 0.750\ \text{V}$$

We can use the same equation to calculate the potential if we use a saturated calomel electrode

$$E_{\text{cell}} = E_{\text{Fe}^{3+}/\text{Fe}^{2+}} - E_{\text{SHE}} = 0.750\ \text{V} - 0.2444\ \text{V} = 0.506\ \text{V}$$

or a saturated silver/silver chloride electrode

$$E_{\text{cell}} = E_{\text{Fe}^{3+}/\text{Fe}^{2+}} - E_{\text{SHE}} = 0.750\ \text{V} - 0.197\ \text{V} = 0.553\ \text{V}$$

Figure 5.2.7 provides a pictorial representation of the relationship between these different potentials.

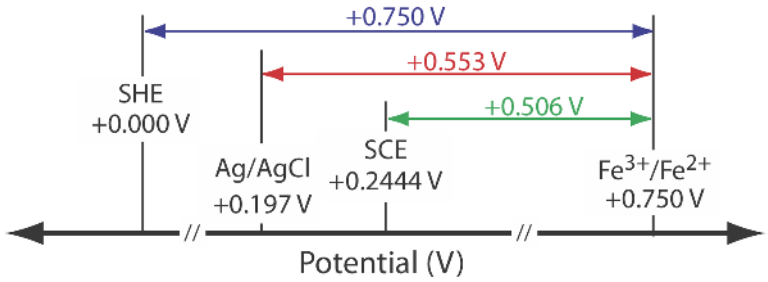


Figure 5.2.7 . Relationship between the potential of an Fe^{3+}/Fe^{2+} half-cell relative to the reference electrodes in Example 5.2.4 . The potential relative to a standard hydrogen electrode is shown in blue, the potential relative to a saturated silver/silver chloride electrode is shown in red, and the potential relative to a saturated calomel electrode is shown in green.

? Exercise 5.2.4

The potential of a UO_2^+/U^{4+} half-cell is –0.0190 V relative to a saturated calomel electrode. What is its potential when using a saturated silver/silver chloride electrode or a standard hydrogen electrode?

Answer

When using a saturated calomel electrode, the potential of the electro- chemical cell is

$$E_{\text{cell}} = E_{UO_2^+/U^{4+}} - E_{\text{SCE}}$$

Substituting in known values

$$-0.0190\ \text{V} = E_{UO_2^+/U^{4+}} - 0.2444\ \text{V}$$

and solving for $E_{UO_2^+/U^{4+}}$ gives its value as +0.2254 V. The potential relative to the Ag/AgCl electrode is

$$E_{\text{cell}} = E_{UO_2^+/U^{4+}} - E_{\text{Ag/AgCl}} = 0.2254\ \text{V} - 0.197\ \text{V} = 0.028\ \text{V}$$

and the potential relative to the standard hydrogen electrode is

$$E_{\text{cell}} = E_{UO_2^+/U^{4+}} - E_{\text{SHE}} = 0.2254\ \text{V} - 0.000\ \text{V} = 0.2254\ \text{V}$$

Metallic Indicator Electrodes

In potentiometry, the potential of the indicator electrode is proportional to the analyte's activity. Two classes of indicator electrodes are used to make potentiometric measurements: metallic electrodes, which are the subject of this section, and ion-selective electrodes, which are covered in the next section.

Electrodes of the First Kind

If we place a copper electrode in a solution that contains Cu^{2+}, the electrode's potential due to the reaction

$$Cu^{2+}(aq) + 2e^- \rightleftharpoons Cu(s)$$

is determined by the activity of Cu^{2+}.

$$E = E^\circ_{Cu^{2+}/Cu} - \frac{0.05916}{2}\log\frac{1}{a_{Cu^{2+}}} = +0.3419V - \frac{0.05916}{2}\log\frac{1}{a_{Cu^{2+}}}$$

If copper is the indicator electrode in a potentiometric electrochemical cell that also includes a saturated calomel reference electrode

$$SCE \| Cu^{2+}\,(aq, a_{Cu^{2+}} = x)\,|Cu(s)$$

then we can use the cell potential to determine an unknown activity of Cu^{2+} in the indicator electrode's half-cell

$$E_{cell} = E_{ind} - E_{SCE} + E_j = +0.3419V - \frac{0.05916}{2}\log\frac{1}{a_{Cu^{2+}}} - 0.2224V + E_j$$

An indicator electrode in which the metal is in contact with a solution containing its ion is called an ***electrode of the first kind***. In general, if a metal, M, is in a solution of M^{n+}, the cell potential is

$$E_{call} = K - \frac{0.05916}{n}\log\frac{1}{a_{M^{n+}}} = K + \frac{0.05916}{n}\log a_{M^{n+}}$$

where K is a constant that includes the standard-state potential for the M^{n+}/M redox couple, the potential of the reference electrode, and the junction potential.

> Note that including E_j in the constant K means we do not need to know the junction potential's actual value; however, the junction potential must remain constant if K is to maintain a constant value.

For a variety of reasons—including the slow kinetics of electron transfer at the metal–solution interface, the formation of metal oxides on the electrode's surface, and interfering reactions—electrodes of the first kind are limited to the following metals: Ag, Bi, Cd, Cu, Hg, Pb, Sn, Tl, and Zn.

> Many of these electrodes, such as Zn, cannot be used in acidic solutions because they are easily oxidized by H^+.
>
> $$Zn(s) + 2H^+(aq) \rightleftharpoons H_2(g) + Zn^{2+}(aq)$$

Electrodes of the Second Kind

The potential of an electrode of the first kind responds to the activity of M^{n+}. We also can use this electrode to determine the activity of another species if it is in equilibrium with M^{n+}. For example, the potential of a Ag electrode in a solution of Ag^+ is

$$E = 0.7996V + 0.05916\log a_{Ag^+} \tag{5.2.3}$$

If we saturate the indicator electrode's half-cell with AgI, the solubility reaction

$$AgI(s) \rightleftharpoons Ag^+(aq) + I^-(aq)$$

determines the concentration of Ag^+; thus

$$a_{Ag^+} = \frac{K_{sp,AgI}}{a_{I^-}} \tag{5.2.4}$$

where $K_{sp,AgI}$ is the solubility product for AgI. Substituting Equation 5.2.4 into Equation 5.2.3

$$E = 0.7996\ V + 0.05916\log\frac{K_{sp,\,AgI}}{a_{I^-}}$$

shows that the potential of the silver electrode is a function of the activity of I^-. If we incorporate this electrode into a potentiometric electrochemical cell with a saturated calomel electrode

$$\text{SCE}\|\text{AgI}(s),\ \text{I}^-\ (aq, a_{\text{I}^-} = x)\,|\text{Ag(s)}$$

then the cell potential is

$$E_{\text{cell}} = K - 0.05916 \log a_{\text{I}^-}$$

where K is a constant that includes the standard-state potential for the Ag^+/Ag redox couple, the solubility product for AgI, the reference electrode's potential, and the junction potential.

If an electrode of the first kind responds to the activity of an ion in equilibrium with M^{n+}, we call it an ***electrode of the second kind***. Two common electrodes of the second kind are the calomel and the silver/silver chloride reference electrodes.

> In an electrode of the second kind we link together a redox reaction and another reaction, such as a solubility reaction. You might wonder if we can link together more than two reactions. The short answer is yes. An electrode of the third kind, for example, links together a redox reaction and two other reactions. Such electrodes are less common and we will not consider them in this text.

Redox Electrodes

An electrode of the first kind or second kind develops a potential as the result of a redox reaction that involves the metallic electrode. An electrode also can serve as a source of electrons or as a sink for electrons in an unrelated redox reaction, in which case we call it a ***redox electrode.*** The Pt cathode in Figure 5.2.2 and Example 5.2.1 is a redox electrode because its potential is determined by the activity of Fe^{2+} and Fe^{3+} in the indicator half-cell. Note that a redox electrode's potential often responds to the activity of more than one ion, which limits its usefulness for direct potentiometry.

Membrane Electrodes

If metals were the only useful materials for constructing indicator electrodes, then there would be few useful applications of potentiometry. In 1906, Cremer discovered that the potential difference across a thin glass membrane is a function of pH when opposite sides of the membrane are in contact with solutions that have different concentrations of H_3O^+. The existence of this ***membrane potential*** led to the development of a whole new class of indicator electrodes, which we call ***ion-selective electrodes*** (ISEs). In addition to the glass pH electrode, ion-selective electrodes are available for a wide range of ions. It also is possible to construct a membrane electrode for a neutral analyte by using a chemical reaction to generate an ion that is monitored with an ion-selective electrode. The development of new membrane electrodes continues to be an active area of research.

Membrane Potentials

Figure 5.2.8 shows a typical potentiometric electrochemical cell equipped with an ion-selective electrode. The short hand notation for this cell is

$$\text{ref (sample)}\ \|[\text{A}]_{\text{samp}}\ (aq, a_{\text{A}} = x)\,|[\text{A}]_{\text{int}}\ (aq, a_{\text{A}} = y)\|\ \text{ref (internal)}$$

where the ion-selective membrane is represented by the vertical slash that separates the two solutions that contain analyte: the sample solution and the ion-selective electrode's internal solution. The potential of this electrochemical cell includes the potential of each reference electrode, a junction potential, and the membrane's potential

$$E_{\text{cell}} = E_{\text{ref(int)}} - E_{\text{ref(samp)}} + E_{\text{mem}} + E_j \tag{5.2.5}$$

where E_{mem} is the potential across the membrane and The notations ref(sample) and ref(internal) represent a reference electrode immersed in the sample and a reference electrode immersed in the ISE's internal solution. Because the junction potential and the potential of the two reference electrodes are constant, any change in E_{cell} reflects a change in the membrane's potential.

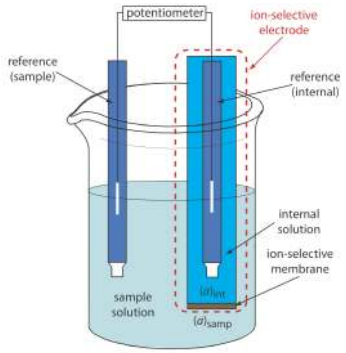


Figure 5.2.8 . Schematic diagram that shows a typical potentiometric cell with an ion-selective electrode. The ion-selective electrode's membrane separates the sample, which contains the analyte at an activity of $(a_A)_{samp}$, from an internal solution that contains the analyte with an activity of $(a_A)_{int}$.

The analyte's interaction with the membrane generates a membrane potential if there is a difference in its activity on the membrane's two sides. Current is carried through the membrane by the movement of either the analyte or an ion already present in the membrane's matrix. The membrane potential is given by the following Nernst-like equation

$$E_{mem} = E_{asym} - \frac{RT}{zF} \ln \frac{(a_A)_{int}}{(a_A)_{samp}} \tag{5.2.6}$$

where $(a_A)_{samp}$ is the analyte's activity in the sample, $(a_A)_{int}$ is the analyte's activity in the ion-selective electrode's internal solution, and z is the analyte's charge. Ideally, E_{mem} is zero when $(a_A)_{int} = (a_A)_{samp}$. The term E_{asym}, which is an ***asymmetry potential***, accounts for the fact that E_{mem} usually is not zero under these conditions.

> For now we simply note that a difference in the analyte's activity results in a membrane potential. As we consider different types of ion-selective electrodes, we will explore more specifically the source of the membrane potential.

Substituting Equation 5.2.6 into Equation 5.2.5, assuming a temperature of 25°C, and rearranging gives

$$E_{cell} = K + \frac{0.05916}{z} \log (a_A)_{samp} \tag{5.2.7}$$

where K is a constant that includes the potentials of the two reference electrodes, the junction potentials, the asymmetry potential, and the analyte's activity in the internal solution. Equation 5.2.7 is a general equation and applies to all types of ion-selective electrodes.

Selectivity of Membranes

A membrane potential results from a chemical interaction between the analyte and active sites on the membrane's surface. Because the signal depends on a chemical process, most membranes are not selective toward a single analyte. Instead, the membrane potential is proportional to the concentration of each ion that interacts with the membrane's active sites. We can rewrite Equation 5.2.7 to include the contribution to the potential of an interferent, I

$$E_{cell} = K + \frac{0.05916}{z_A} \log \left\{ a_A + K_{A,I} (a_I)^{z_A/z_I} \right\}$$

where z_A and z_I are the charges of the analyte and the interferent, and $K_{A,I}$ is a selectivity coefficient that accounts for the relative response of the interferent. The selectivity coefficient is defined as

$$K_{A,I} = \frac{(a_A)_e}{(a_I)_e^{z_A/z_I}} \tag{5.2.8}$$

where $(a_A)_e$ and $(a_I)_e$ are the activities of analyte and the interferent that yield identical cell potentials. When the selectivity coefficient is 1.00, the membrane responds equally to the analyte and the interferent. A membrane shows good selectivity for the analyte when $K_{A,I}$ is significantly less than 1.00.

Selectivity coefficients for most commercially available ion-selective electrodes are provided by the manufacturer. If the selectivity coefficient is not known, it is easy to determine its value experimentally by preparing a series of solutions, each of which contains the same activity of interferent, $(a_I)_{add}$, but a different activity of analyte. As shown in Figure 5.2.9 , a plot of cell potential versus the log of the analyte's activity has two distinct linear regions. When the analyte's activity is significantly larger than $K_{A,I} \times (a_I)_{add}$, the potential is a linear function of $\log(a_A)$, as given by Equation 5.2.7. If $K_{A,I} \times (a_I)_{add}$ is significantly larger than the analyte's activity, however, the cell's potential remains constant. The activity of analyte and interferent at the intersection of these two linear regions is used to calculate $K_{A,I}$.

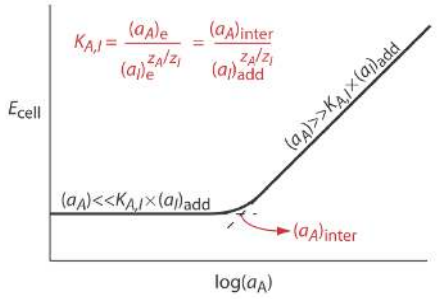


Figure 5.2.9 . Diagram showing the experimental determination of an ion-selective electrode's selectivity for an analyte. The activity of analyte that corresponds to the intersection of the two linear portions of the curve, $(a_A)_{inter}$, produces a cell potential identical to that of the interferent. The equation for the selectivity coefficient, $K_{A,I}$, is shown in red.

Example 5.2.5

Sokalski and co-workers described a method for preparing ion-selective electrodes with significantly improved selectivities [Sokalski, T.; Ceresa, A.; Zwicki, T.; Pretsch, E. *J. Am. Chem. Soc.* **1997**, *119*, 11347–11348]. For example, a conventional Pb^{2+} ISE has a $\log K_{Pb^{2+}/Mg^{2+}}$ of –3.6. If the potential for a solution in which the activity of Pb^{2+} is 4.1×10^{-12} is identical to that for a solution in which the activity of Mg^{2+} is 0.01025, what is the value of $\log K_{Pb^{2+}/Mg^{2+}}$ for their ISE?

Solution

Making appropriate substitutions into Equation 5.2.8, we find that

$$K_{Pb^{2+}/Mg^{2+}} = \frac{(a_{Pb^{2+}})_e}{(a_{Mg^{2+}})_e^{z_{Pb^{2+}}/z_{Mg^{2+}}}} = \frac{4.1 \times 10^{-12}}{(0.01025)^{+2/+2}} = 4.0 \times 10^{-10}$$

The value of $\log K_{Pb^{2+}/Mg^{2+}}$, therefore, is –9.40.

Exercise 5.2.5

A ion-selective electrode for NO_2^- has log$K_{A,I}$ values of –3.1 for F^-, –4.1 for SO_4^{2-}, –1.2 for I^-, and –3.3 for NO_3^-. Which ion is the most serious interferent and for what activity of this interferent is the potential equivalent to a solution in which the activity of NO_2^- is 2.75×10^{-4}?

Answer

The larger the value of $K_{A,I}$ the more serious the interference. Larger values for $K_{A,I}$ correspond to more positive (less negative) values for log$K_{A,I}$; thus, I^-, with a $K_{A,I}$ of 6.3×10^{-2}, is the most serious of these interferents. To find the activity of I^- that gives a potential equivalent to a NO_2^- activity of 2.75×10^{-4}, we note that

$$a_{NO_2^-} = K_{A,I} \times a_{I^-}$$

Making appropriate substitutions

$$2.75 \times 10^{-4} = (6.3 \times 10^{-2}) \times a_{I^-}$$

and solving for a_{I^-} gives its activity as 4.4×10^{-3}.

Glass Ion-Selective Electrodes

The first commercial ***glass electrodes*** were manufactured using Corning 015, a glass with a composition that is approximately 22% Na_2O, 6% CaO, and 72% SiO_2. When immersed in an aqueous solution for several hours, the outer approximately 10 nm of the membrane's surface becomes hydrated, resulting in the formation of negatively charged sites, —SiO^-. Sodium ions, Na^+, serve as counter ions. Because H^+ binds more strongly to —SiO^- than does Na^+, they displace the sodium ions

$$H^+ + -SiO^-Na^+ \rightleftharpoons -SiO^-H^+ + Na^+$$

explaining the membrane's selectivity for H^+. The transport of charge across the membrane is carried by the Na^+ ions. The potential of a glass electrode using Corning 015 obeys the equation

$$E_{cell} = K + 0.05916 \log a_{H^+} \tag{5.2.9}$$

over a pH range of approximately 0.5 to 9. At more basic pH values the glass membrane is more responsive to other cations, such as Na^+ and K^+.

Example 5.2.6

For a Corning 015 glass membrane, the selectivity coefficient K_{H^+/Na^+} is $\approx 10^{-11}$. What is the expected error if we measure the pH of a solution in which the activity of H^+ is 2×10^{-13} and the activity of Na^+ is 0.05?

Solution

A solution in which the actual activity of H^+, $(a_{H^+})_{act}$, is 2×10^{-13} has a pH of 12.7. Because the electrode responds to both H^+ and Na^+, the apparent activity of H^+, $(a_{H^+})_{app}$, is

$$(a_{H^+})_{app} = (a_{H^+})_{act} + (K_{H^+/Na^+} \times a_{Na^+}) = 2 \times 10^{-13} + (10^{-11} \times 0.05) = 7 \times 10^{-13}$$

The apparent activity of H^+ is equivalent to a pH of 12.2, an error of –0.5 pH units.

Replacing Na_2O and CaO with Li_2O and BaO extends the useful pH range of glass membrane electrodes to pH levels greater than 12.

Glass membrane pH electrodes often are available in a combination form that includes both the indicator electrode and the reference electrode. The use of a single electrode greatly simplifies the measurement of pH. An example of a typical combination electrode is shown in Figure 5.2.10 .

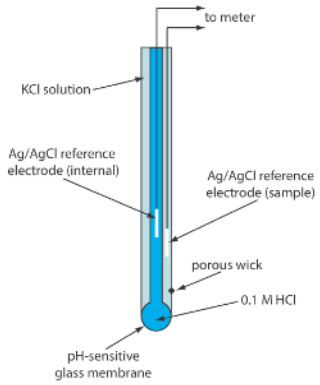


Figure 5.2.10 . Schematic diagram showing a combination glass electrode for measuring pH. The indicator electrode consists of a pH-sensitive glass membrane and an internal Ag/AgCl reference electrode in a solution of 0.1 M HCl. The sample's reference electrode is a Ag/AgCl electrode in a solution of KCl (which may be saturated with KCl or contain a fixed concentration of KCl). A porous wick serves as a salt bridge between the sample and its reference electrode.

The observation that the Corning 015 glass membrane responds to ions other than H^+ (see Example 5.2.6) led to the development of glass membranes with a greater selectivity for other cations. For example, a glass membrane with a composition of 11% Na_2O, 18% Al_2O_3, and 71% SiO_2 is used as an ion-selective electrode for Na^+. Other glass ion-selective electrodes have been developed for the analysis of Li^+, K^+, Rb^+, Cs^+, NH_4^+, Ag^+, and Tl^+. Table 5.2.1 provides several examples.

Table 5.2.1 . Representative Examples of Glass Membrane Ion-Selective Electrodes for Analytes Other Than H^+

analyte	membrane composition	selectivity coefficients
Na^+	11% Na_2O, 18% Al_2O_3, 71% SiO_2	$K_{Na^+/H^+} = 1000$ $K_{Na^+/K^+} = 0.001$ $K_{Na^+/Li^+} = 0.001$
Li^+	15% Li_2O, 25% Al_2O_3, 60% SiO_2	$K_{Li^+/Na^+} = 0.3$ $K_{Li^+/K^+} = 0.001$
K^+	27% Na_2O, 5% Al_2O_3, 68% SiO_2	$K_{K^+/Na^+} = 0.05$

Selectivity coefficients are approximate; values found experimentally may vary substantially from the listed values. See Cammann, K. *Working With Ion-Selective Electrodes*, Springer-Verlag: Berlin, 1977.

Because an ion-selective electrode's glass membrane is very thin—it is only about 50 μm thick—they must be handled with care to avoid cracks or breakage. Glass electrodes usually are stored in a storage buffer recommended by the manufacturer, which ensures that the membrane's outer surface remains hydrated. If a glass electrode dries out, it is reconditioned by soaking for several hours in a solution that contains the analyte. The composition of a glass membrane will change over time, which affects the electrode's performance. The average lifetime for a typical glass electrode is several years.

Solid-State Ion-Selective Electrodes

A s***olid-state ion-selective electrode*** has a membrane that consists of either a polycrystalline inorganic salt or a single crystal of an inorganic salt. We can fashion a polycrystalline solid-state ion-selective electrode by sealing a 1–2 mm thick pellet of AgS—or a mixture of AgS and a second silver salt or another metal sulfide—into the end of a nonconducting plastic cylinder, filling the cylinder with an internal solution that contains the analyte, and placing a reference electrode into the internal solution. Figure 5.2.11 shows a typical design.

> The NaCl in a salt shaker is an example of polycrystalline material because it consists of many small crystals of sodium chloride. The NaCl salt plates used in IR spectroscopy (see Chapter 10), on the other hand, are an example of a single crystal of sodium chloride.

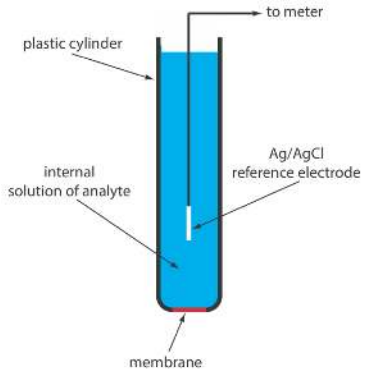


Figure 5.2.11 . Schematic diagram of a solid-state electrode. The internal solution contains a solution of analyte of fixed activity.

The membrane potential for a Ag_2S pellet develops as the result of a difference in the extent of the solubility reaction

$$Ag_2S(s) \rightleftharpoons 2Ag^+(aq) + S^{2-}(aq)$$

on the membrane's two sides, with charge carried across the membrane by Ag^+ ions. When we use the electrode to monitor the activity of Ag^+, the cell potential is

$$E_{cell} = K + 0.05916 \log a_{Ag^+}$$

The membrane also responds to the activity of S^{2-}, with a cell potential of

$$E_{cell} = K - \frac{0.05916}{2} \log a_{S^{2-}}$$

If we combine an insoluble silver salt, such as AgCl, with the Ag_2S, then the membrane potential also responds to the concentration of Cl^-, with a cell potential of

$$E_{cell} = K - 0.05916 \log a_{Cl^-}$$

By mixing Ag_2S with CdS, CuS, or PbS, we can make an ion-selective electrode that responds to the activity of Cd^{2+}, Cu^{2+}, or Pb^{2+}. In this case the cell potential is

$$E_{cell} = K + \frac{0.05916}{2} \ln a_{M^{2+}}$$

where $a_{M^{2+}}$ is the activity of the metal ion.

Table 5.2.2 provides examples of polycrystalline, Ag_2S-based solid-state ion-selective electrodes. The selectivity of these ion-selective electrodes depends on the relative solubility of the compounds. A Cl^- ISE using a Ag_2S/AgCl membrane is more selective for Br^- ($K_{Cl^-/Br^-} = 10^2$) and for I^- ($K_{Cl^-/I^-} = 10^6$) because AgBr and AgI are less soluble than AgCl. If the activity of Br^- is sufficiently high, AgCl at the membrane/solution interface is replaced by AgBr and the electrode's response to Cl^- decreases substantially. Most of the polycrystalline ion-selective electrodes listed in Table 5.2.2 operate over an extended range of pH levels. The equilibrium between S^{2-} and HS^- limits the analysis for S^{2-} to a pH range of 13–14.

5.2.2 . Representative Examples of Polycrystalline Solid-State Ion-Selective Electrodes

analyte	membrane composition	selectivity coefficients
Ag^+	Ag_2S	$K_{Ag^+/Cu^{2+}} = 10^{-6}$ $K_{Ag^+/Pb^{2+}} = 10^{-10}$ Hg^{2+} interferes
Cd^{2+}	CdS/Ag_2S	$K_{Cd^{2+}/Fe^{2+}} = 200$ $K_{Cd^{2+}/Pb^{2+}} = 6$ Ag^+, Hg^{2+}, and Cu^{2+} must be absent
Cu^{2+}	CuS/Ag_2S	$K_{Cu^{2+}/Fe^{3+}} = 10$ $K_{Cu^{2+}/Cu^+} = 10^{-6}$ Ag^+ and Hg^{2+} must be absent
Pb^{2+}	PbS/Ag_2S	$K_{Pb^{2+}/Fe^{3+}} = 1$ $K_{Pb^{2+}/Cd^{2+}} = 1$ Ag^+, Hg^{2+}, and Cu^{2+} must be absent
Br^-	$AgBr/Ag_2S$	$K_{Br^-/I^-} = 5000$ $K_{Br^-/Cl^-} = 0.005$ $K_{Br^-/OH^-} = 10^{-5}$ S^{2-} must be absent
Cl^-	$AgCl/Ag_2S$	$K_{Cl^-/I^-} = 10^6$ $K_{Cl^-/Br^-} = 100$ $K_{Cl^-/OH^-} = 0.01$ S^{2-} must be absent
I^-	AgI/Ag_2S	$K_{I^-/S^{2-}} = 30$ $K_{I^-/Br^-} = 10^{-4}$ $K_{I^-/Cl^-} = 10^{-6}$ $K_{I^-/OH^-} = 10^{-7}$
SCN^-	$AgSCN/Ag_2S$	$K_{SCN^-/I^-} = 10^3$ $K_{SCN^-/Br^-} = 100$ $K_{SCN^-/Cl^-} = 0.1 K_{SCN^-/OH^-} = 0.01$ S^{2-} must be absent
S^{2-}	Ag_2S	Hg^{2+} must be absent

Selectivity coefficients are approximate; values found experimentally may vary substantially from the listed values. See Cammann, K. *Working With Ion-Selective Electrodes*, Springer-Verlag: Berlin, 1977.

The membrane of a F^- ion-selective electrode is fashioned from a single crystal of LaF_3, which usually is doped with a small amount of EuF_2 to enhance the membrane's conductivity. Because EuF_2 provides only two F^- ions—compared to the three F^- ions in LaF_3—each EuF_2 produces a vacancy in the crystal's lattice. Fluoride ions pass through the membrane by moving into adjacent vacancies. As shown in Figure 5.2.11 , the LaF_3 membrane is sealed into the end of a non-conducting plastic cylinder, which contains a standard solution of F^-, typically 0.1 M NaF, and a Ag/AgCl reference electrode.

The membrane potential for a F^- ISE results from a difference in the solubility of LaF_3 on opposite sides of the membrane, with the potential given by

$$E_{cell} = K - 0.05916 \log a_{F^-}$$

One advantage of the F^- ion-selective electrode is its freedom from interference. The only significant exception is OH^- (K_{F^-/OH^-} = 0.1), which imposes a maximum pH limit for a successful analysis. Below a pH of 4 the predominate form of fluoride in solution is HF, which does not contribute to the membrane potential. For this reason, an analysis for fluoride is carried out at a pH greater than 4.

Example 5.2.7

What is the maximum pH that we can tolerate if we need to analyze a solution in which the activity of F^- is 1×10^{-5} with an error of less than 1%?

Solution

In the presence of OH^- the cell potential is

$$E_{cell} = K - 0.05916 \left\{ a_{F^-} + K_{F^-/OH^-} \times a_{OH^-} \right\}$$

To achieve an error of less than 1%, the term $K_{F^-/OH^-} \times a_{OH^-}$ must be less than 1% of a_{F^-}; thus

$$K_{F^-/OH^-} \times a_{OH^-} \leq 0.01 \times a_{F^-}$$

$$0.10 \times a_{OH^-} \leq 0.01 \times \left(1.0 \times 10^{-5}\right)$$

Solving for a_{OH^-} gives the maximum allowable activity for OH^- as 1×10^{-6}, which corresponds to a pH of less than 8.

Exercise 5.2.6

Suppose you wish to use the nitrite-selective electrode in Exercise 5.2.5 to measure the activity of NO_2^-. If the activity of NO_2^- is 2.2×10^{-4}, what is the maximum pH you can tolerate if the error due to OH^- must be less than 10%? The selectivity coefficient for OH^-, $K_{NO_2^-/OH^-}$, is 630. Do you expect the electrode to have a lower pH limit? Clearly explain your answer.

Answer

In the presence of OH^- the cell potential is

$$E_{cell} = K - 0.05916 \log \left\{ a_{NO_2^-} + K_{NO_2^-/OH^-} \times a_{OH^-} \right\}$$

To achieve an error of less than 10%, the term $K_{NO_2^-/OH^-} \times a_{OH^-}$ must be less than 1% of $a_{NO_2^-}$; thus

$$K_{NO_2^-/OH^-} \times a_{OH^-} \leq 0.10 \times a_{NO_2^-}$$

$$630 \times a_{OH^-} \leq 0.10 \times \left(2.2 \times 10^{-4}\right)$$

Solving for a_{OH^-} gives its maximum allowable activity as 3.5×10^{-8}, which corresponds to a pH of less than 6.54.

The electrode does have a lower pH limit. Nitrite is the conjugate weak base of HNO_2, a species to which the ISE does not respond. As shown by the ladder diagram below, at a pH of 4.15 approximately 10% of nitrite is present as HNO_2. A minimum pH of 4.5 is the usual recommendation when using a nitrite ISE. This corresponds to a NO_2^-/HNO_2 ratio of

$$pH = pK_a + \log \frac{[NO_2^-]}{[HNO_2]}$$

$$4.5 = 3.15 + \log \frac{[NO_2^-]}{[HNO_2]}$$

$$\frac{[NO_2^-]}{[HNO_2]} \approx 22$$

Thus, at a pH of 4.5 approximately 96% of nitrite is present as NO_2^-.

Unlike a glass membrane ion-selective electrode, a solid-state ISE does not need to be conditioned before it is used, and it may be stored dry. The surface of the electrode is subject to poisoning, as described above for a Cl^- ISE in contact with an excessive concentration of Br^-. If an electrode is poisoned, it can be returned to its original condition by sanding and polishing the crystalline membrane.

Poisoning simply means that the surface has been chemically modified, such as AgBr forming on the surface of a AgCl membrane.

Liquid-Based Ion-Selective Electrodes

Another class of ion-selective electrodes uses a hydrophobic membrane that contains a liquid organic complexing agent that reacts selectively with the analyte. Three types of organic complexing agents have been used: cation exchangers, anion exchangers, and neutral ionophores. A membrane potential exists if the analyte's activity is different on the two sides of the membrane. Current is carried through the membrane by the analyte.

An ***ionophore*** is a ligand whose exterior is hydrophobic and whose interior is hydrophilic. The crown ether shown here is one example of a neutral ionophore.



One example of a ***liquid-based ion-selective electrode*** is that for Ca^{2+}, which uses a porous plastic membrane saturated with the cation exchanger di-(*n*-decyl) phosphate. As shown in Figure 5.2.12 , the membrane is placed at the end of a non-conducting cylindrical tube and is in contact with two reservoirs. The outer reservoir contains di-(*n*-decyl) phosphate in di-*n*-octylphenylphosphonate, which soaks into the porous membrane. The inner reservoir contains a standard aqueous solution of Ca^{2+} and a Ag/AgCl reference electrode. Calcium ion-selective electrodes also are available in which the di-(*n*-decyl) phosphate is immobilized in a polyvinyl chloride (PVC) membrane that eliminates the need for the outer reservoir.

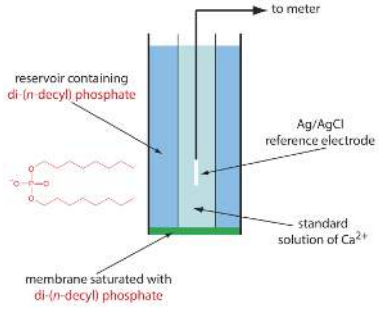


Figure 5.2.12 . Schematic diagram showing a liquid-based ion-selective electrode for Ca^{2+}. The structure of the cation exchanger, di-(*n*-decyl) phosphate, is shown in red.

The membrane potential for the Ca^{2+} ISE develops as the result of a difference in the extent of the complexation reaction

$$Ca^{2+}(aq) + 2\,(C_{10}H_{21}O)_2\,PO_2^-(mem) \rightleftharpoons Ca\,[(C_{10}H_{21}O)_2PO_2]_2\,(mem)$$

on the two sides of the membrane, where (*mem*) indicates a species that is present in the membrane. The cell potential for the Ca^{2+} ion-selective electrode is

$$E_{cell} = K + \frac{0.05916}{2}\log a_{Ca^{2+}}$$

The selectivity of this electrode for Ca^{2+} is very good, with only Zn^{2+} showing greater selectivity.

Table 5.2.3 lists the properties of several liquid-based ion-selective electrodes. An electrode using a liquid reservoir can be stored in a dilute solution of analyte and needs no additional conditioning before use. The lifetime of an electrode with a PVC membrane, however, is proportional to its exposure to aqueous solutions. For this reason these electrodes are best stored by covering the membrane with a cap along with a small amount of wetted gauze to maintain a humid environment. Before using the electrode it is conditioned in a solution of analyte for 30–60 minutes.

Table 5.2.3 . Representative Examples of Liquid-Based Ion-Selective Electrodes

analyte	membrane composition	selectivity coefficients
Ca^{2+}	di-(*n*-decyl) phosphate in PVC	$K_{Ca^{2+}/Zn^{2+}} = 1 - 5$ $K_{Ca^{2+}/Al^{3+}} = 0.90$ $K_{Ca^{2+}/Mn^{2+}} = 0.38$ $K_{Ca^{2+}/Cu^{2+}} = 0.070$ $K_{Ca^{2+}/Mg^{2+}} = 0.032$
K^+	valinomycin in PVC	$K_{K^+/Rb^+} = 1.9$ $K_{K^+/Cs^+} = 0.38$ $K_{K^+/Li^+} = 10^{-4}$
Li^+	ETH 149 in PVC	$K_{Li^+/H^+} = 1$ $K_{Li^+/Na^+} = 0.03$ $K_{Li^+/K^+} = 0.007$
NH_4^+	nonactin and monactin in PVC	$K_{NH_4^+/K^+} = 0.12$ $K_{NH_4^+/H^+} = 0.016$ $K_{NH_4^+/Li^+} = 0.0042$ $K_{NH_4^+/Na^+} = 0.002$
ClO_3^-	$Fe(o\text{-phen})_3^{3+}$ in *p*-nitrocymene with porous membrane	$K_{ClO_4^-/OH^-} = 1$ $K_{ClO_4^-/I^-} = 0.012$ $K_{ClO_4^-/NO_3^-} = 0.0015$ $K_{ClO_4^-/Br^-} = 5.6 \times 10^{-4}$ $K_{ClO_4^-/Cl^-} = 2.2 \times 10^{-4}$
NO_3^-	tetradodecyl ammonium nitrate in pVC	$K_{NO_3^-/Cl^-} = 0.006$ $K_{NO_3^-/F^-} = 9 \times 10^{-4}$

Selectivity coefficients are approximate; values found experimentally may vary substantially from the listed values. See Cammann, K. *Working With Ion-Selective Electrodes*, Springer-Verlag: Berlin, 1977.

Gas-Sensing Electrodes

A number of membrane electrodes respond to the concentration of a dissolved gas. The basic design of a ***gas-sensing electrode***, as shown in Figure 5.2.13 , consists of a thin membrane that separates the sample from an inner solution that contains an ion-selective electrode. The membrane is permeable to the gaseous analyte, but impermeable to nonvolatile components in the sample's matrix. The gaseous analyte passes through the membrane where it reacts with the inner solution, producing a species whose concentration is monitored by the ion-selective electrode. For example, in a CO_2 electrode, CO_2 diffuses across the membrane where it reacts in the inner solution to produce H_3O^+.

$$CO_2(aq) + 2H_2O(l) \rightleftharpoons HCO_3^-(aq) + H_3O^+(aq) \tag{5.2.10}$$

The change in the activity of H_3O^+ in the inner solution is monitored with a pH electrode, for which the cell potential is given by Equation 5.2.9. To find the relationship between the activity of H_3O^+ in the inner solution and the activity of CO_2 in the inner solution we rearrange the equilibrium constant expression for reaction 5.2.10; thus

$$a_{H_3O^+} = K_a \times \frac{a_{CO_2}}{a_{HCO_3^-}} \tag{5.2.11}$$

where K_a is the equilibrium constant. If the activity of HCO_3^- in the internal solution is sufficiently large, then its activity is not affected by the small amount of CO_2 that passes through the membrane. Substituting Equation 5.2.11 into Equation 5.2.9 gives

$$E_{cell} = K' + 0.05916 \log a_{co_2}$$

where K′ is a constant that includes the constant for the pH electrode, the equilibrium constant for reaction 5.2.10 and the activity of HCO_3^- in the inner solution.

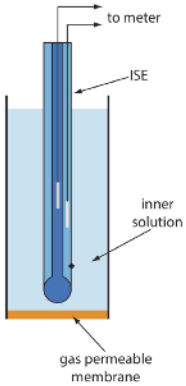


Figure 5.2.13 . Schematic diagram of a gas-sensing membrane electrode.

Table 5.2.4 lists the properties of several gas-sensing electrodes. The composition of the inner solution changes with use, and both the inner solution and the membrane must be replaced periodically. Gas-sensing electrodes are stored in a solution similar to the internal solution to minimize their exposure to atmospheric gases.

Table 5.2.4 . Representative Examples of Gas-Sensing Electrodes

analyte	inner solution	reaction in inner solution	ion-selective electrode
CO_2	10 mM $NaHCO_3$ 10 mM NaCl	$CO_2(aq) + 2H_2O(l) \rightleftharpoons HCO_3^-(aq) + H_3O^+(aq)$	glass pH ISE
HCN	10 mM $KAg(CN)_2$	$HCN(aq) + H_2O(l) \rightleftharpoons CN^-(aq) + H_3O^+(aq)$	Ag_2S solid-state ISE
HF	1 M H_3O^+	$HF(aq) + H_2O(l) \rightleftharpoons F^-(aq) + H_3O^+(aq)$	F^- solid-state ISE
H_2S	pH 5 citrate buffer	$H_2S(aq) + H_2O(l) \rightleftharpoons HS^-(aq) + H_3O^+(aq)$	Ag_2S solid state ISE
NH_3	10 mM NH_4Cl 0.1 M KNO_3	$NH_3(aq) + H_2O(l) \rightleftharpoons NH_4^+(aq) + OH^-(aq)$	glass pH ISE
NO_2	20 mM $NaNO_2$ 0.1 M KNO_3	$2NO_2(aq) + 3H_2O(l) \rightleftharpoons NO_3^-(aq) + NO_2^-(aq) + 2H_3O^+(aq)$	glass pH ISE
SO_2	1 mM $NaHSO_3$ pH 5	$SO_2(aq) + 2H_2O(l) \rightleftharpoons HSO_3^-(aq) + H_3O^+(aq)$	glass pH ISE

Source: Cammann, K. *Working With Ion-Selective Electrodes*, Springer-Verlag: Berlin, 1977.

Potentiometric Biosensors

The approach for developing gas-sensing electrodes can be modified to create potentiometric electrodes that respond to a biochemically important species. The most common class of potentiometric biosensors are ***enzyme electrodes***, in which we trap or immobilize an enzyme at the surface of a potentiometric electrode. The analyte's reaction with the enzyme produces a product whose concentration is monitored by the potentiometric electrode. Potentiometric biosensors also have been designed around other biologically active species, including antibodies, bacterial particles, tissues, and hormone receptors.

One example of an enzyme electrode is the urea electrode, which is based on the catalytic hydrolysis of urea by urease

$$CO(NH_2)_2(aq) + 2H_2O(l) \rightleftharpoons 2NH_4^+(aq) + CO_3^-(aq)$$

Figure 5.2.14 shows one version of the urea electrode, which modifies a gas-sensing NH_3 electrode by adding a dialysis membrane that traps a pH 7.0 buffered solution of urease between the dialysis membrane and the gas permeable membrane [(a) Papastathopoulos, D. S.; Rechnitz, G. A. *Anal. Chim. Acta* **1975**, *79*, 17–26; (b) Riechel, T. L. *J. Chem. Educ*. **1984**, *61*, 640–642].

An NH_3 electrode, as shown in Table 5.2.4 , uses a gas-permeable membrane and a glass pH electrode. The NH_3 diffuses across the membrane where it changes the pH of the internal solution.

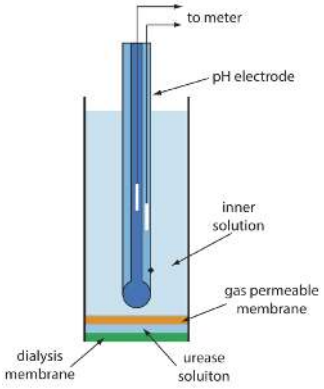


Figure 5.2.14 . Schematic diagram showing an enzyme-based potentiometric biosensor for urea. A solution of the enzyme urease is trapped between a dialysis membrane and a gas permeable membrane. Urea diffuses across the dialysis membrane and reacts with urease, producing NH_3 that diffuses across the gas permeable membrane. The resulting change in the internal solution's pH is measured with the pH electrode.

When immersed in the sample, urea diffuses through the dialysis membrane where it reacts with the enzyme urease to form the ammonium ion, $\mathbf{NH_4^+}$, which is in equilibrium with NH_3.

$$\mathbf{NH_4^+}(aq) + \mathbf{H_2O}(l) \rightleftharpoons \mathbf{H_3O^+}(aq) + \mathbf{NH_3}(aq)$$

The NH_3, in turn, diffuses through the gas permeable membrane where a pH electrode measures the resulting change in pH. The electrode's response to the concentration of urea is

$$E_{\text{cell}} = K - 0.05916 \log a_{\text{urea}} \tag{5.2.12}$$

Another version of the urea electrode (Figure 5.2.15) immobilizes the enzyme urease in a polymer membrane formed directly on the tip of a glass pH electrode [Tor, R.; Freeman, A. *Anal. Chem.* **1986**, *58*, 1042–1046]. In this case the response of the electrode is

$$\text{pH} = Ka_{\text{urea}} \tag{5.2.13}$$

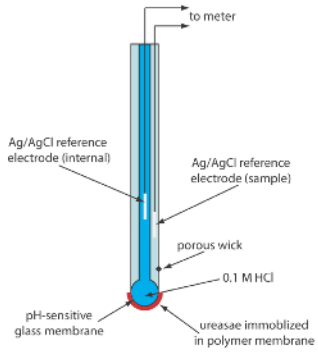


Figure 5.2.15 . Schematic diagram of an enzyme-based potentiometric biosensor for urea in which urease is immobilized in a polymer membrane coated onto the pH-sensitive glass membrane of a pH electrode.

Few potentiometric biosensors are available commercially. As shown in Figure 5.2.14 and Figure 5.2.15 , however, it is possible to convert an ion-selective electrode or a gas-sensing electrode into a biosensor. Several representative examples are described in Table 5.2.5 , and additional examples can be found in this chapter's additional resources.

Table 5.2.5 . Representative Examples of Potentiometric Biosensors

analyte	biologically active phase	substance determined
5′-AMP	AMP-deaminase (E)	NH_3
L-arginine	arginine and urease (E)	NH_3
asparagine	asparaginase (E)	NH_4^+
L-cysteine	*Proteus morganii* (B)	H_2S
L-glutamate	yellow squash (T)	CO_2
L-glutamine	*Sarcina flava* (B)	NH_3
oxalate	oxalate decarboxylase (E)	CO_2
penicillin	penicllinase (E)	H_3O^+
L-phenylalanine	L-amino acid oxidase/horseradish peroxidase (E)	I^-
sugars	bacteria from dental plaque (B)	H_3O^+
urea	urease (E)	NH_3 or H_3O^+

Source: Complied from Cammann, K. *Working With Ion-Selective Electrodes*, Springer-Verlag: Berlin, 1977 and Lunte, C. E.; Heineman, W. R. "Electrochemical techniques in Bioanalysis," in Steckham, E. ed. *Topics in Current Chemistry*, Vol. 143, Springer-Verlag: Berlin, 1988, p.8.
Abbreviations for biologically active phase: E = enzyme; B = bacterial particle; T = tissue.

Quantitative Applications

The potentiometric determination of an analyte's concentration is one of the most common quantitative analytical techniques. Perhaps the most frequent analytical measurement is the determination of a solution's pH, a measurement we will consider in more detail later in this section. Other areas where potentiometry is important are clinical chemistry, environmental chemistry, and potentiometric titrations. Before we consider representative applications, however, we need to examine more closely the relationship between cell potential and the analyte's concentration and methods for standardizing potentiometric measurements.

Activity and Concentration

The Nernst equation relates the cell potential to the analyte's activity. For example, the Nernst equation for a metallic electrode of the first kind is

$$E_{\text{cell}} = K + \frac{0.05916}{n} \log a_{M^{n+}} \tag{5.2.14}$$

where $a_{M^{n+}}$ is the metal ion's activity. When we use a potentiometric electrode, however, our goal is to determine the analyte's concentration. As we learned in Chapter 6, an ion's activity is the product of its concentration, $[M^{n+}]$, and a matrix-dependent activity coefficient, $\gamma_{Mn^{n+}}$.

$$a_{M^{n+}} = [M^{n+}]\,\gamma_{M^{n+}} \tag{5.2.15}$$

Substituting Equation 5.2.15 into Equation 5.2.14 and rearranging, gives

$$E_{\text{cell}} = K + \frac{0.05916}{n} \log \gamma_{M^{n+}} + \frac{0.05916}{n} \log [M^{n+}] \tag{5.2.16}$$

We can solve Equation 5.2.16 for the metal ion's concentration if we know the value for its activity coefficient. Unfortunately, if we do not know the exact ionic composition of the sample's matrix—which is the usual situation—then we cannot calculate the value of $\gamma_{Mn^{n+}}$. There is a solution to this dilemma. If we design our system so that the standards and the samples have an identical matrix, then the value of $\gamma_{Mn^{n+}}$ remains constant and Equation 5.2.16 simplifies to

$$E_{cell} = K' + \frac{0.05916}{n} \log [M^{n+}]$$

where K' includes the activity coefficient.

Quantitative Analysis Using External Standards

Before we can determine the concentration of analyte in a sample, we must standardize the electrode. If the electrode's response obeys the Nernst equation, then we can determine the constant K using a single external standard. Because a small deviation from the ideal slope of $\pm RT/nF$ or $\pm RT/zF$ is not unexpected, we usually use two or more external standards.

> To review the use of external standards, see Chapter 5.3.

In the absence of interferents, a calibration curve of E_{cell} versus $\log a_A$, where A is the analyte, is a straight-line. A plot of E_{cell} versus $\log[A]$, however, may show curvature at higher concentrations of analyte as a result of a matrix-dependent change in the analyte's activity coefficient. To maintain a consistent matrix we add a high concentration of an inert electrolyte to all samples and standards. If the concentration of added electrolyte is sufficient, then the difference between the sample's matrix and the matrix of the standards will not affect the ionic strength and the activity coefficient essentially remains constant. The inert electrolyte added to the sample and the standards is called a ***total ionic strength adjustment buffer*** (TISAB).

Example 5.2.8

The concentration of Ca^{2+} in a water sample is determined using the method of external standards. The ionic strength of the samples and the standards is maintained at a nearly constant level by making each solution 0.5 M in KNO_3. The measured cell potentials for the external standards are shown in the following table.

$[Ca^{2+}]$ (M)	E_{cell} (V)
1.00×10^{-5}	–0.125
5.00×10^{-5}	–0.103
1.00×10^{-4}	–0.093
5.00×10^{-4}	–0.072
1.00×10^{-3}	–0.063
5.00×10^{-3}	–0.043
1.00×10^{-2}	–0.033

What is the concentration of Ca^{2+} in a water sample if its cell potential is found to be –0.084 V?

Solution

Linear regression gives the calibration curve in Figure 5.2.16 , with an equation of

$$E_{cell} = 0.027 + 0.0303 \log [Ca^{2+}]$$

Substituting the sample's cell potential gives the concentration of Ca^{2+} as 2.17×10^{-4} M. Note that the slope of the calibration curve, which is 0.0303, is slightly larger than its ideal value of 0.05916/2 = 0.02958; this is not unusual and is one reason for using multiple standards.

> One reason that it is not unusual to find that the experimental slope deviates from its ideal value of 0.05916/n is that this ideal value assumes that the temperature is 25°C.

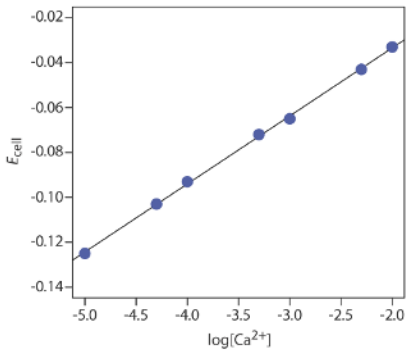


Figure 5.2.16 . Calibration curve for the data in Example 5.2.8 .

Quantitative Analysis Using the Method of Standard Additions

Another approach to calibrating a potentiometric electrode is the method of standard additions. First, we transfer a sample with a volume of V_{samp} and an analyte concentration of C_{samp} into a beaker and measure the potential, $(E_{cell})_{samp}$. Next, we make a standard addition by adding to the sample a small volume, V_{std}, of a standard that contains a known concentration of analyte, C_{std}, and measure the potential, (E_{cell})std. If V_{std} is significantly smaller than V_{samp}, then we can safely ignore the change in the sample's matrix and assume that the analyte's activity coefficient is constant. Example 5.2.9 demonstrates how we can use a one-point standard addition to determine the concentration of analyte in a sample.

> To review the method of standard additions, see Chapter 5.3.

Example 5.2.9

The concentration of Ca^{2+} in a sample of sea water is determined using a Ca ion-selective electrode and a one-point standard addition. A 10.00-mL sample is transferred to a 100-mL volumetric flask and diluted to volume. A 50.00-mL aliquot of the sample is placed in a beaker with the Ca ISE and a reference electrode, and the potential is measured as –0.05290 V. After adding a 1.00-mL aliquot of a 5.00×10^{-2} M standard solution of Ca^{2+} the potential is –0.04417 V. What is the concentration of Ca^{2+} in the sample of sea water?

Solution

To begin, we write the Nernst equation before and after adding the standard addition. The cell potential for the sample is

$$(E_{cell})_{samp} = K + \frac{0.05916}{2} \log C_{samp}$$

and that following the standard addition is

$$(E_{cell})_{std} = K + \frac{0.05916}{2} \log \left\{ \frac{V_{samp}}{V_{tot}} C_{samp} + \frac{V_{std}}{V_{tot}} C_{std} \right\}$$

where V_{tot} is the total volume (V_{samp} + V_{std}) after the standard addition. Subtracting the first equation from the second equation gives

$$\Delta E = (E_{cell})_{std} - (E_{cell})_{samp} = \frac{0.05916}{2} \log \left\{ \frac{V_{samp}}{V_{tot}} C_{samp} + \frac{V_{std}}{V_{tot}} C_{std} \right\} - \frac{0.05916}{2} \log C_{samp}$$

Rearranging this equation leaves us with

$$\frac{2\Delta E_{cell}}{0.05916} = \log \left\{ \frac{V_{samp}}{V_{tot}} + \frac{V_{std} C_{std}}{V_{tot} C_{samp}} \right\}$$

Substituting known values for ΔE, V_{samp}, V_{std}, V_{tot} and C_{std},

$$\frac{2\times\{-0.04417-(-0.05290)\}}{0.05916} = \log\left\{\frac{50.00\text{ mL}}{51.00\text{ mL}} + \frac{(1.00\text{ mL})(5.00\times10^{-2}\text{M})}{(51.00\text{ mL})C_{\text{samp}}}\right\}$$

$$0.2951 = \log\left\{0.9804 + \frac{9.804\times10^{-4}}{C_{\text{samp}}}\right\}$$

and taking the inverse log of both sides gives

$$1.973 = 0.9804 + \frac{9.804 \times 10^{-4}}{C_{\text{samp}}}$$

Finally, solving for C_{samp} gives the concentration of Ca^{2+} as $\mathbf{9.88 \times 10^{-4}}$ M. Because we diluted the original sample of seawater by a factor of 10, the concentration of Ca^{2+} in the seawater sample is $\mathbf{9.88 \times 10^{-3}}$ M.

Free Ions Versus Complexed Ions

Most potentiometric electrodes are selective toward the free, uncomplexed form of the analyte, and do not respond to any of the analyte's complexed forms. This selectivity provides potentiometric electrodes with a significant advantage over other quantitative methods of analysis if we need to determine the concentration of free ions. For example, calcium is present in urine both as free Ca^{2+} ions and as protein-bound Ca^{2+} ions. If we analyze a urine sample using atomic absorption spectroscopy, the signal is proportional to the total concentration of Ca^{2+} because both free and bound calcium are atomized. Analyzing urine with a Ca^{2+} ISE, however, gives a signal that is a function of only free Ca^{2+} ions because the protein-bound Ca^{2+} can not interact with the electrode's membrane.

The best way to appreciate the theoretical and the practical details discussed in this section is to carefully examine a typical analytical method. Although each method is unique, the following description of the determination of F^- in toothpaste provides an instructive example of a typical procedure. The description here is based on Kennedy, J. H. *Analytical Chemistry—Practice*, Harcourt Brace Jaovanovich: San Diego, 1984, p. 117–118.

Representative Method 11.2.1: Determination of Fluoride in Toothpaste

Description of the Method

The concentration of fluoride in toothpastes that contains soluble F^- is determined with a F^- ion-selective electrode using a calibration curve prepared with external standards. Although the F^- ISE is very selective (only OH^- with a K_{F^-/OH^-} of 0.1 is a significant interferent), Fe^{3+} and Al^{3+} interfere with the analysis because they form soluble fluoride complexes that do not interact with the ion-selective electrode's membrane. This interference is minimized by reacting any Fe^{3+} and Al^{3+} with a suitable complexing agent.

Procedure

Prepare 1 L of a standard solution of 1.00% w/v SnF_2 and transfer it to a plastic bottle for storage. Using this solution, prepare 100 mL each of standards that contain 0.32%, 0.36%, 0.40%, 0.44% and 0.48% w/v SnF_2, adding 400 mg of malic acid to each solution as a stabilizer. Transfer the standards to plastic bottles for storage. Prepare a total ionic strength adjustment buffer (TISAB) by mixing 500 mL of water, 57 mL of glacial acetic acid, 58 g of NaCl, and 4 g of disodium DCTA (*trans*-1,2-cyclohexanetetraacetic acid) in a 1-L beaker, stirring until dissolved. Cool the beaker in a water bath and add 5 M NaOH until the pH is between 5–5.5. Transfer the contents of the beaker to a 1-L volumetric flask and dilute to volume. Prepare each external standard by placing approximately 1 g of a fluoride-free toothpaste, 30 mL of distilled water, and 1.00 mL of standard into a 50-mL plastic beaker and mix vigorously for two min with a stir bar. Quantitatively transfer the resulting suspension to a 100-mL volumetric flask along with 50 mL of TISAB and dilute to volume with distilled water. Store the entire external standard in a 250-mL plastic beaker until you are ready to measure the potential. Prepare toothpaste samples by obtaining an approximately 1-g portion and treating in the same manner as the standards. Measure the cell potential for the external standards and the samples using a F^- ion-selective electrode and an appropriate reference electrode. When measuring the potential, stir the solution and allow two to three minutes to reach a stable potential. Report the concentration of F^- in the toothpaste %w/w SnF_2.

Questions

1. The total ionic strength adjustment buffer serves several purposes in this procedure. Identify these purposes.

The composition of the TISAB has three purposes:

(a) The high concentration of NaCl (the final solutions are approximately 1 M NaCl) ensures that the ionic strength of each external standard and each sample is essentially identical. Because the activity coefficient for fluoride is the same in all solutions, we can write the Nernst equation in terms of fluoride's concentration instead of its activity.

(b) The combination of glacial acetic acid and NaOH creates an acetic acid/acetate buffer of pH 5–5.5. As shown in Figure 5.2.17 , the pH of this buffer is high enough to ensure that the predominate form of fluoride is F^- instead of HF. This pH also is sufficiently acidic that it avoids an interference from OH^- (see Example 5.2.8)).

(c) DCTA is added as a complexing agent for Fe^{3+} or Al^{3+}, preventing the formation of $\mathbf{FeF_6^{3-}}$ or $\mathbf{AlF_6^{3-}}$.

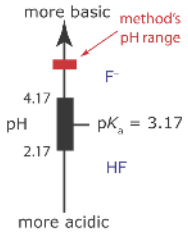


Figure 5.2.17 . Ladder diagram for HF/F^-. Maintaining a pH greater than 4.2 ensures that the only significant form of fluoride is F^-.

2. Why is a fluoride-free toothpaste added to the standard solutions?

Adding a fluoride-free toothpaste protects against any unaccounted for matrix effects that might influence the ion-selective electrode's response. This assumes, of course, that the matrices of the two toothpastes are otherwise similar.

3. The procedure specifies that the standards and the sample should be stored in plastic containers. Why is it a bad idea to store the solutions in glass containers?

The fluoride ion is capable of reacting with glass to form SiF_4.

4. Suppose your calibration curve has a slope of –57.98 mV for each 10-fold change in the concentration of F^-. The ideal slope from the Nernst equation is –59.16 mV per 10-fold change in concentration. What effect does this have on the quantitative analysis for fluoride in toothpaste?

No effect at all! This is why we prepare a calibration curve using multiple standards.

Measurement of pH

With the availability of inexpensive glass pH electrodes and pH meters, the determination of pH is one of the most common quantitative analytical measurements. The potentiometric determination of pH, however, is not without complications, several of which we discuss in this section.

One complication is confusion over the meaning of pH [Kristensen, H. B.; Saloman, A.; Kokholm, G. *Anal. Chem.* **1991**, *63*, 885A–891A]. The conventional definition of pH in most general chemistry textbooks is

$$\mathbf{pH = -\log [H^+]} \tag{5.2.17}$$

As we now know, pH actually is a measure of the activity of H^+.

$$\mathbf{pH = -\log a_{H^+}} \tag{5.2.18}$$

> Try this experiment—find several general chemistry textbooks and look up *pH* in each textbook's index. Turn to the appropriate pages and see how it is defined. Next, look up *activity* or *activity coefficient* in each textbook's index and see if these terms are indexed.

Equation 5.2.17 only approximates the true pH. If we calculate the pH of 0.1 M HCl using Equation 5.2.17, we obtain a value of 1.00; the solution's actual pH, as defined by Equation 5.2.18, is 1.1 [Hawkes, S. J. *J. Chem. Educ.* **1994**, *71*, 747–749]. The activity

and the concentration of H^+ are not the same in 0.1 M HCl because the activity coefficient for H^+ is not 1.00 in this matrix. Figure 5.2.18 shows a more colorful demonstration of the difference between activity and concentration.

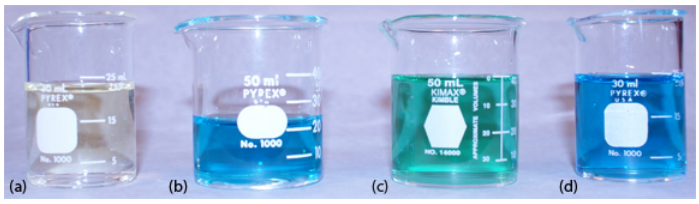


Figure 5.2.18 . A demonstration of the difference between activity and concentration using the indicator methyl green. The indicator is pale yellow in its acid form (beaker a: 1.0 M HCl) and is blue in its base form (beaker d: H_2O). In 10 mM HCl the indicator is in its base form (beaker b: 20 mL of 10 mM HCl with 3 drops of methyl green). Adding 20 mL of 5 M LiCl to this solution shifts the indicator's color to green (beaker c); although the concentration of HCl is cut in half to 5 mM, the activity of H^+ has increased as evidenced by the green color that is intermediate between the indicator's pale yellow, acid form and its blue, base form. The demonstration shown here is adapted from McCarty, C. G.; Vitz, E. "pH Paradoxes: Demonstrating That It Is Not True That pH ≡ –log[H^+]," *J. Chem. Educ.* **2006**, *83*, 752–757. This paper provides several additional demonstrations that illustrate the difference between concentration and activity.

A second complication in measuring pH is the uncertainty in the relationship between potential and activity. For a glass membrane electrode, the cell potential, (E_{cell})samp, for a sample of unknown pH is

$$(E_{cell})_{samp} = K - \frac{RT}{F}\ln\frac{1}{a_{H^+}} = K - \frac{2.303RT}{F}pH_{samp} \tag{5.2.19}$$

where K includes the potential of the reference electrode, the asymmetry potential of the glass membrane, and any junction potentials in the electrochemical cell. All the contributions to K are subject to uncertainty, and may change from day-to-day, as well as from electrode-to-electrode. For this reason, before using a pH electrode we calibrate it using a standard buffer of known pH. The cell potential for the standard, $(E_{cell})_{std}$, is

$$(E_{ccll})_{std} = K - \frac{2.303RT}{F}pH_{std} \tag{5.2.20}$$

where pH_{std} is the standard's pH. Subtracting Equation 5.2.20 from Equation 5.2.19 and solving for pH_{samp} gives

$$pH_{samp} = pH_{std} - \frac{\left\{(E_{cell})_{samp} - (E_{cell})_{std}\right\}F}{2.303RT} \tag{5.2.21}$$

which is the operational definition of pH adopted by the International Union of Pure and Applied Chemistry [Covington, A. K.; Bates, R. B.; Durst, R. A. *Pure & Appl. Chem.* **1985**, *57*, 531–542].

Calibrating a pH electrode presents a third complication because we need a standard with an accurately known activity for H^+. Table 5.2.6 provides pH values for several primary standard buffer solutions accepted by the National Institute of Standards and Technology.

Table 5.2.6 . pH Values for Selected NIST Primary Standard Buffers

temp (°C)	saturated (at 25°C) KHC_4H4O_7 (tartrate)	0.05 m $KH_2C_6H_5O_7$ (citrate)	0.05 m $KHC_8H_4O_4$ (phthlate)	0.025 m KH_2PO_4, 0.025 m $NaHPO_4$	0.008695 m KH_2PO_4, 0.03043 m Na_2HPO_4	0.01 m $Na_4B_4O_7$	0.025 m $NaHCO_3$, 0.025 m Na_2CO_3
0	—	3.863	4.003	6.984	7.534	9.464	10.317
5	—	3.840	3.999	6.951	7.500	9.395	10.245
10	—	3.820	3.998	6.923	7.472	9.332	10.179
15	—	3.802	3.999	6.900	7.448	9.276	10.118
20	—	3.788	4.002	6.881	7.429	9.225	10.062
25	3.557	3.776	4.008	6.865	7.413	9.180	10.012
30	3.552	3.766	4.015	6.854	7.400	9.139	9.966
35	3.549	3.759	4.024	6.844	7.389	9.012	9.925
40	3.547	3.753	4.035	6.838	7.380	9.068	9.889
45	3.547	3.750	4.047	6.834	7.373	9.038	9.856
50	3.549	3.749	4.060	6.833	7.367	9.011	9.828

Source: Values taken from Bates, R. G. *Determination of pH: Theory and Practice*, 2nd ed. Wiley: New York, 1973. See also Buck, R. P., et. al."Measurement of pH. Definition, Standards, and Procedures," *Pure. Appl. Chem.* **2002**, *74*, 2169–2200. All concentrations are molal (m).

To standardize a pH electrode using two buffers, choose one near a pH of 7 and one that is more acidic or basic depending on your sample's expected pH. Rinse your pH electrode in deionized water, blot it dry with a laboratory wipe, and place it in the buffer with the pH closest to 7. Swirl the pH electrode and allow it to equilibrate until you obtain a stable reading. Adjust the "Standardize" or "Calibrate" knob until the meter displays the correct pH. Rinse and dry the electrode, and place it in the second buffer. After the electrode equilibrates, adjust the "Slope" or "Temperature" knob until the meter displays the correct pH.

Some pH meters can compensate for a change in temperature. To use this feature, place a temperature probe in the sample and connect it to the pH meter. Adjust the "Temperature" knob to the solution's temperature and calibrate the pH meter using the "Calibrate" and "Slope" controls. As you are using the pH electrode, the pH meter compensates for any change in the sample's temperature by adjusting the slope of the calibration curve using a Nernstian response of $2.303RT/F$.

Clinical Applications

Because of their selectivity for analytes in complex matricies, ion-selective electrodes are important sensors for clinical samples. The most common analytes are electrolytes, such as Na^+, K^+, Ca^{2+}, H^+, and Cl^-, and dissolved gases such as CO_2. For extracellular fluids, such as blood and urine, the analysis can be made *in vitro*. An *in situ* analysis, however, requires a much smaller electrode that we can insert directly into a cell. Liquid-based membrane microelectrodes with tip diameters smaller than 1 μm are constructed by heating and drawing out a hard-glass capillary tube with an initial diameter of approximately 1–2 mm (Figure 5.2.19). The microelectrode's tip is made hydrophobic by dipping into a solution of dichlorodimethyl silane, and an inner solution appropriate for the analyte and a Ag/AgCl wire reference electrode are placed within the microelectrode. The microelectrode is dipped into a solution of the liquid complexing agent, which through capillary action draws a small volume of the liquid complexing agent into the tip. Potentiometric microelectrodes have been developed for a number of clinically important analytes, including H^+, K^+, Na^+, Ca^{2+}, Cl^-, and I^- [Bakker, E.; Pretsch, E. *Trends Anal. Chem.* **2008**, *27*, 612–618].

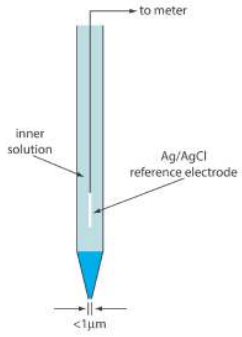


Figure 5.2.19 . Schematic diagram of a liquid-based ion-selective microelectrode.

Environmental Applications

Although ion-selective electrodes are used in environmental analysis, their application is not as widespread as in clinical analysis. Although standard potentiometric methods are available for the analysis of CN^-, F^-, NH_3, and NO_3^- in water and wastewater, other analytical methods generally provide better detection limits. One potential advantage of an ion-selective electrode is the ability to incorporate it into a flow cell for the continuous monitoring of wastewater streams.

Potentiometric Titrations

One method for determining the equivalence point of an acid–base titration is to use a pH electrode to monitor the change in pH during the titration. A potentiometric determination of the equivalence point is possible for acid–base, complexation, redox, and precipitation titrations, as well as for titrations in aqueous and nonaqueous solvents. Acid–base, complexation, and precipitation potentiometric titrations usually are monitored with an ion-selective electrode that responds the analyte, although an electrode that responds to the titrant or a reaction product also can be used. A redox electrode, such as a Pt wire, and a reference electrode are used for potentiometric redox titrations. More details about potentiometric titrations are found in Chapter 9.

Evaluation

Scale of Operation

The working range for most ion-selective electrodes is from a maximum concentration of 0.1–1 M to a minimum concentration of $10^{-5} - 10^{-11}$ M [(a) Bakker, E.; Pretsch, E. *Anal. Chem.* **2002**, *74*, 420A–426A; (b) Bakker, E.; Pretsch, E. *Trends Anal. Chem.* **2005**, *24*, 199–207]. This broad working range extends from major analytes to ultratrace analytes, and is significantly greater than many other analytical techniques. To use a conventional ion-selective electrode we need a minimum sample volume of several mL (a macro sample). Microelectrodes, such as the one shown in Figure 5.2.19 , are used with an ultramicro sample, although care is needed to ensure that the sample is representative of the original sample.

Accuracy

The accuracy of a potentiometric analysis is limited by the error in measuring E_{cell}. Several factors contribute to this measurement error, including the contribution to the potential from interfering ions, the finite current that passes through the cell while we measure the potential, differences between the analyte's activity coefficient in the samples and the standard solutions, and junction potentials. We can limit the effect of an interfering ion by including a separation step before the potentiometric analysis. Modern high impedance potentiometers minimize the amount of current that passes through the electrochemical cell. Finally, we can minimize the errors due to activity coefficients and junction potentials by matching the matrix of the standards to that of the sample. Even in the best circumstances, however, a difference of approximately ±1 mV for samples with equal concentrations of analyte is not unusual.

We can evaluate the effect of uncertainty on the accuracy of a potentiometric measurement by using a propagation of uncertainty. For a membrane ion-selective electrode the general expression for potential is

$$E_{cell} = K + \frac{RT}{zF}\ln[A]$$

where z is the analyte's, A, charge. From Table 4.3.1 in Chapter 4, the uncertainty in the cell potential, ΔE_{cell} is

$$\triangle E_{\text{cell}} = \frac{RT}{zF} \times \frac{\Delta[A]}{[A]}$$

Rearranging and multiplying through by 100 gives the percent relative error in concentration as

$$\%\ \text{relative error} = \frac{\Delta[A]}{[A]} \times 100 = \frac{\triangle E_{\text{cell}}}{RT/zF} \times 100 \tag{5.2.22}$$

The relative error in concentration, therefore, is a function of the measurement error for the electrode's potential, ΔE_{cell}, and the analyte's charge. Table 5.2.7 provides representative values for ions with charges of ±1 and ±2 at a temperature of 25ºC. Accuracies of 1–5% for monovalent ions and 2–10% for divalent ions are typical. Although Equation 5.2.22 applies to membrane electrodes, we can use if for a metallic electrode by replacing *z* with *n*.

Table 5.2.7 . Relationship Between the Uncertainty in Measuring E_{cell} and the Relative Error in the Analyte's Concentration

$\Delta E_{\text{cell}}(\pm\ \text{mV})$	% relative error when $z = \pm 1$	% relative error when $z = \pm 2$
0.1	±0.4	±0.8
0.5	±1.9	±3.9
1.0	±3.0	±7.8
1.5	±5.8	±11.1
2.0	±7.8	±15.6

Precision

Precision in potentiometry is limited by variations in temperature and the sensitivity of the potentiometer. Under most conditions—and when using a simple, general-purpose potentiometer—we can measure the potential with a repeatability of ±0.1 mV. Using Table 5.2.7 , this corresponds to an uncertainty of ±0.4% for monovalent analytes and ±0.8% for divalent analytes. The reproducibility of potentiometric measurements is about a factor of ten poorer.

Sensitivity

The sensitivity of a potentiometric analysis is determined by the term *RT*/*nF* or *RT*/*zF* in the Nernst equation. Sensitivity is best for smaller values of *n* or *z*.

Selectivity

As described earlier, most ion-selective electrodes respond to more than one analyte; the selectivity for the analyte, however, often is significantly greater than the sensitivity for the interfering ions. The manufacturer of an ion-selective usually provides an ISE's selectivity coefficients, which allows us to determine whether a potentiometric analysis is feasible for a given sample.

Time, Cost, and Equipment

In comparison to other techniques, potentiometry provides a rapid, relatively low-cost means for analyzing samples. The limiting factor when analyzing a large number of samples is the need to rinse the electrode between samples. The use of inexpensive, disposable ion-selective electrodes can increase a lab's sample throughput. Figure 5.2.20 shows one example of a disposable ISE for Ag^+ [Tymecki, L.; Zwierkowska, E.; Głąb, S.; Koncki, R. *Sens. Actuators B* **2003**, *96*, 482–488]. Commercial instruments for measuring pH or potential are available in a variety of price ranges, and includes portable models for use in the field.

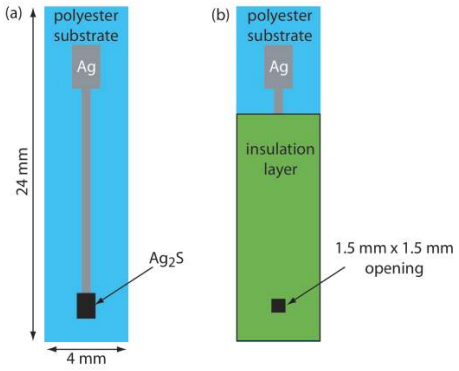


Figure 5.2.20 . Schematic diagram of a disposable ion-selective electrode created by screen-printing. In (a) a thin film of conducting silver is printed on a polyester substrate and a film of Ag_2S overlaid near the bottom. In (b) an insulation layer with a small opening is layered on top exposes a portion of the Ag_2S membrane that is immersed in the sample. The top of the polyester substrate remains uncoated, which allows us to connect the electrode to a potentiometer through the Ag film. The small inset shows the electrode's actual size.

This page titled 5.2: Potentiometric Methods is shared under a CC BY-NC-SA 4.0 license and was authored, remixed, and/or curated by Kathryn Davis.

- **11.2: Potentiometric Methods** by David Harvey is licensed CC BY-NC-SA 4.0.

5.3: Coulometric Methods

In a potentiometric method of analysis we determine an analyte's concentration by measuring the potential of an electrochemical cell under static conditions in which no current flows and the concentrations of species in the electrochemical cell remain fixed. Dynamic techniques, in which current passes through the electrochemical cell and concentrations change, also are important electrochemical methods of analysis. In this section we consider coulometry. Voltammetry and amperometry are covered in Chapter 11.4.

Coulometry is based on an exhaustive electrolysis of the analyte. By exhaustive we mean that the analyte is oxidized or reduced completely at the working electrode, or that it reacts completely with a reagent generated at the working electrode. There are two forms of coulometry: ***controlled-potential coulometry***, in which we apply a constant potential to the electrochemical cell, and ***controlled-current coulometry***, in which we pass a constant current through the electrochemical cell.

During an electrolysis, the total charge, Q, in coulombs, that passes through the electrochemical cell is proportional to the absolute amount of analyte by ***Faraday's law***

$$Q = nFN_A \tag{5.3.1}$$

where n is the number of electrons per mole of analyte, F is Faraday's constant (96 487 C mol^{-1}), and N_A is the moles of analyte. A coulomb is equivalent to an A•sec; thus, for a constant current, i, the total charge is

$$Q = it_e \tag{5.3.2}$$

where t_e is the electrolysis time. If the current varies with time, as it does in controlled-potential coulometry, then the total charge is

$$Q = \int_0^{t_e} i(t)dt \tag{5.3.3}$$

In coulometry, we monitor current as a function of time and use either Equation 5.3.2 or Equation 5.3.3 to calculate Q. Knowing the total charge, we then use Equation 5.3.1 to determine the moles of analyte. To obtain an accurate value for N_A, all the current must oxidize or reduce the analyte; that is, coulometry requires 100% ***current efficiency*** or an accurate measurement of the current efficiency using a standard.

> Current efficiency is the percentage of current that actually leads to the analyte's oxidation or reduction.

Controlled-Potential Coulometry

The easiest way to ensure 100% current efficiency is to hold the working electrode at a constant potential where the analyte is oxidized or reduced completely and where no potential interfering species are oxidized or reduced. As electrolysis progresses, the analyte's concentration and the current decrease. The resulting current-versus-time profile for controlled-potential coulometry is shown in Figure 5.3.1 . Integrating the area under the curve (Equation 5.3.3) from $t = 0$ to $t = t_e$ gives the total charge. In this section we consider the experimental parameters and instrumentation needed to develop a controlled-potential coulometric method of analysis.

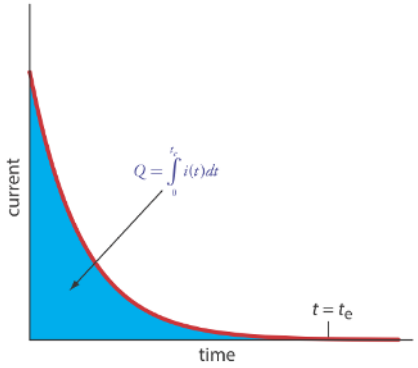


Figure 5.3.1 . Current versus time for a controlled-potential coulometric analysis. The measured current is shown by the red curve. The integrated area under the curve, shown in blue, is the total charge.

Selecting a Constant Potential

To understand how an appropriate potential for the working electrode is selected, let's develop a constant-potential coulometric method for Cu^{2+} based on its reduction to copper metal at a Pt working electrode.

$$Cu^{2+}(aq) + 2e^- \rightleftharpoons Cu(s) \tag{5.3.4}$$

Figure 5.3.2 shows a ladder diagram for an aqueous solution of Cu^{2+}. From the ladder diagram we know that reaction 5.3.4 is favored when the working electrode's potential is more negative than +0.342 V versus the standard hydrogen electrode. To ensure a 100% current efficiency, however, the potential must be sufficiently more positive than +0.000 V so that the reduction of H_3O^+ to H_2 does not contribute significantly to the total current flowing through the electrochemical cell.

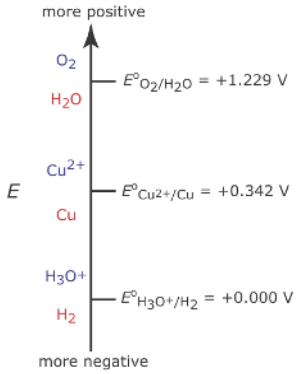


Figure 5.3.2 . Ladder diagram for an aqueous solution of Cu^{2+} showing steps for the reductions of O_2 to H_2O, of Cu^{2+} to Cu, and of H_3O^+ to H_2. For each step, the oxidized species is in blue and the reduced species is in red

We can use the Nernst equation for reaction 5.3.4 to estimate the minimum potential for quantitatively reducing Cu^{2+}.

$$E = E^\circ_{Cu^{2+}/Cu} - \frac{0.05916}{2} \log \frac{1}{[Cu^{2+}]} \tag{5.3.5}$$

So why are we using the concentration of Cu^{2+} in Equation 5.3.5 instead of its activity? In potentiometry we use activity because we use E_{cell} to determine the analyte's concentration. Here we use the Nernst equation to help us select an appropriate potential. Once we identify a potential, we can adjust its value as needed to ensure a quantitative reduction of Cu^{2+}. In addition, in coulometry the analyte's concentration is given by the total charge, not the applied potential.

If we define a quantitative electrolysis as one in which we reduce 99.99% of $^{Cu2+}$ to Cu, then the concentration of Cu^{2+} at t_e is

$$[Cu^{2+}]_{t_e} = 0.0001 \times [Cu^{2+}]_0 \tag{5.3.6}$$

where $[Cu^{2+}]_0$ is the initial concentration of Cu^{2+} in the sample. Substituting Equation 5.3.6 into Equation 5.3.5 allows us to calculate the desired potential.

$$E = E^\circ_{Cu^{2+}/Cu} - \frac{0.05916}{2} \log \frac{1}{0.0001 \times [Cu^{2+}]}$$

If the initial concentration of Cu^{2+} is 1.00×10^{-4} M, for example, then the working electrode's potential must be more negative than +0.105 V to quantitatively reduce Cu^{2+} to Cu. Note that at this potential H_3O^+ is not reduced to H_2, maintaining 100% current efficiency.

> Many controlled-potential coulometric methods for Cu^{2+} use a potential that is negative relative to the standard hydrogen electrode—see, for example, Rechnitz, G. A. *Controlled-Potential Analysis*, Macmillan: New York, 1963, p.49. Based on the ladder diagram in Figure 5.3.2 you might expect that applying a potential <0.000 V will partially reduce H_3O^+ to H_2, resulting in a current efficiency that is less than 100%. The reason we can use such a negative potential is that the reaction rate for the reduction of H_3O^+ to H_2 is very slow at a Pt electrode. This results in a significant ***overpotential***—the need to apply a potential more positive or a more negative than that predicted by thermodynamics—which shifts E^o for the H_3O^+/H_2 redox couple to a more negative value.

Minimizing Electrolysis Time

In controlled-potential coulometry, as shown in Figure 5.3.1 , the current decreases over time. As a result, the rate of electrolysis—recall from Chapter 11.1 that current is a measure of rate—becomes slower and an exhaustive electrolysis of the analyte may require a long time. Because time is an important consideration when designing an analytical method, we need to consider the factors that affect the analysis time.

We can approximate the current's change as a function of time in Figure 5.3.1 as an exponential decay; thus, the current at time t is

$$i_t = i_0 e^{-kt} \tag{5.3.7}$$

where i_0 is the current at t = 0 and k is a rate constant that is directly proportional to the area of the working electrode and the rate of stirring, and that is inversely proportional to the volume of solution. For an exhaustive electrolysis in which we oxidize or reduce 99.99% of the analyte, the current at the end of the analysis, t_e, is

$$i_{t_e} \leq 0.0001 \times i_0 \tag{5.3.8}$$

Substituting Equation 5.3.8 into Equation 5.3.7 and solving for t_e gives the minimum time for an exhaustive electrolysis as

$$t_e = -\frac{1}{k} \times \ln(0.0001) = \frac{9.21}{k}$$

From this equation we see that a larger value for k reduces the analysis time. For this reason we usually carry out a controlled-potential coulometric analysis in a small volume electrochemical cell, using an electrode with a large surface area, and with a high stirring rate. A quantitative electrolysis typically requires approximately 30–60 min, although shorter or longer times are possible.

Instrumentation

A three-electrode potentiostat is used to set the potential in controlled-potential coulometry (see Figure 11.1.5). The working electrodes is usually one of two types: a cylindrical Pt electrode manufactured from platinum-gauze (Figure 5.3.3), or a Hg pool electrode. The large overpotential for the reduction of H_3O^+ at Hg makes it the electrode of choice for an analyte that requires a negative potential. For example, a potential more negative than –1 V versus the SHE is feasible at a Hg electrode—but not at a Pt electrode—even in a very acidic solution. Because mercury is easy to oxidize, it is less useful if we need to maintain a potential that is positive with respect to the SHE. Platinum is the working electrode of choice when we need to apply a positive potential.



Figure 5.3.3 . Example of a cylindrical Pt-gauze electrode used in controlled-potential coulometry. The electrode shown here has a diameter of 13 mm and a height of 48 mm, and was fashioned from Pt wire with a diameter of approximately 0.15 mm. The electrode's surface has 360 openings/cm^2 and a total surface area of approximately 40 cm^2.

The auxiliary electrode, which often is a Pt wire, is separated by a salt bridge from the analytical solution. This is necessary to prevent the electrolysis products generated at the auxiliary electrode from reacting with the analyte and interfering in the analysis. A saturated calomel or Ag/AgCl electrode serves as the reference electrode.

The other essential need for controlled-potential coulometry is a means for determining the total charge. One method is to monitor the current as a function of time and determine the area under the curve, as shown in Figure 5.3.1 . Modern instruments use electronic integration to monitor charge as a function of time. The total charge at the end of the electrolysis is read directly from a digital readout.

Electrogravimetry

If the product of controlled-potential coulometry forms a deposit on the working electrode, then we can use the change in the electrode's mass as the analytical signal. For example, if we apply a potential that reduces Cu^{2+} to Cu at a Pt working electrode, the difference in the electrode's mass before and after electrolysis is a direct measurement of the amount of copper in the sample. As we learned in Chapter 8, we call an analytical technique that uses mass as a signal a gravimetric technique; thus, we call this ***electrogravimetry***.

Controlled-Current Coulometry

A second approach to coulometry is to use a constant current in place of a constant potential, which results in the current-versus-time profile shown in Figure 5.3.4 . Controlled-current coulometry has two advantages over controlled-potential coulometry. First, the analysis time is shorter because the current does not decrease over time. A typical analysis time for controlled-current coulometry is less than 10 min, compared to approximately 30–60 min for controlled-potential coulometry. Second, because the total charge simply is the product of current and time (Equation **5.3.2**), there is no need to integrate the current-time curve in Figure 5.3.4 .

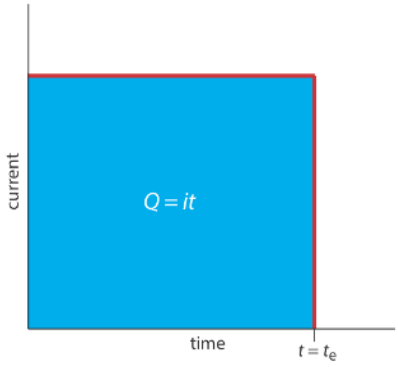


Figure 5.3.4 . Current versus time for a controlled-current coulometric analysis. The measured current is shown by the red curve. The integrated area under the curve, shown in blue, is the total charge.

Using a constant current presents us with two important experimental problems. First, during electrolysis the analyte's concentration—and, therefore, the current that results from its oxidation or reduction—decreases continuously. To maintain a

constant current we must allow the potential to change until another oxidation reaction or reduction reaction occurs at the working electrode. Unless we design the system carefully, this secondary reaction results in a current efficiency that is less than 100%. The second problem is that we need a method to determine when the analyte's electrolysis is complete. As shown in Figure 5.3.1 , in a controlled-potential coulometric analysis we know that electrolysis is complete when the current reaches zero, or when it reaches a constant background or residual current. In a controlled-current coulometric analysis, however, current continues to flow even when the analyte's electrolysis is complete. A suitable method for determining the reaction's endpoint, t_e, is needed.

Maintaining Current Efficiency

To illustrate why a change in the working electrode's potential may result in a current efficiency of less than 100%, let's consider the coulometric analysis for Fe^{2+} based on its oxidation to Fe^{3+} at a Pt working electrode in 1 M H_2SO_4.

$$Fe^{2+}(aq) \rightleftharpoons Fe^{3+}(aq) + e^-$$

Figure 5.3.5 shows the ladder diagram for this system. At the beginning of the analysis, the potential of the working electrode remains nearly constant at a level near its initial value.

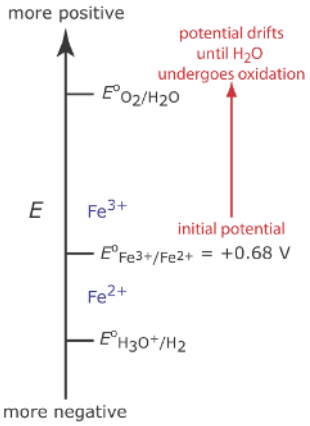


Figure 5.3.5 . Ladder diagram for the constant-current coulometric analysis of Fe^{2+}. The red arrow and text shows how the potential drifts to more positive values, decreasing the current efficiency.

As the concentration of Fe^{2+} decreases and the concentration of Fe^{3+} increases, the working electrode's potential shifts toward more positive values until the oxidation of H_2O begins.

$$2H_2O(l) \rightleftharpoons O_2(g) + 4H^+(aq) + 4e^-$$

Because a portion of the total current comes from the oxidation of H_2O, the current efficiency for the analysis is less than 100% and we cannot use Equation 5.3.1 to determine the amount of Fe^{2+} in the sample.

Although we cannot prevent the potential from drifting until another species undergoes oxidation, we can maintain a 100% current efficiency if the product of that secondary oxidation reaction both rapidly and quantitatively reacts with the remaining Fe^{2+}. To accomplish this we add an excess of Ce^{3+} to the analytical solution. As shown in Figure 5.3.6 , when the potential of the working electrode shifts to a more positive potential, Ce^{3+} begins to oxidize to Ce^{4+}

$$Ce^{3+}(aq) \rightleftharpoons Ce^{4+}(aq) + e^- \quad (5.3.9)$$

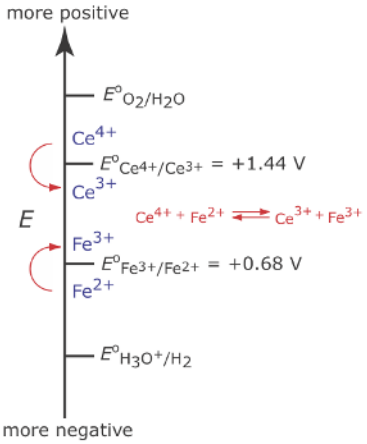


Figure 5.3.6 . Ladder diagram for the constant-current coulometric analysis of Fe^{2+} in the presence of a Ce^{3+} mediator. As the potential drifts to more positive values, we eventually reach a potential where Ce^{3+} undergoes oxidation. Because Ce^{4+}, the product of the oxidation of Ce^{3+}, reacts with Fe^{2+}, we maintain current efficiency.

The Ce^{4+} that forms at the working electrode rapidly mixes with the solution where it reacts with any available Fe^{2+}.

$$Ce^{4+}(aq) + Fe^{2+}(aq) \rightleftharpoons Ce^{3+}(aq) + Fe^{3+}(aq) \tag{5.3.10}$$

Combining reaction 5.3.9 and reaction 5.3.10 shows that the net reaction is the oxidation of Fe^{2+} to Fe^{3+}

$$Fe^{2+}(aq) \rightleftharpoons Fe^{3+}(aq) + e^{-}$$

which maintains a current efficiency of 100%. A species used to maintain 100% current efficiency is called a ***mediator***.

Endpoint Determination

Adding a mediator solves the problem of maintaining 100% current efficiency, but it does not solve the problem of determining when the analyte's electrolysis is complete. Using the analysis for Fe^{2+} in Figure 5.3.6 , when the oxidation of Fe^{2+} is complete current continues to flow from the oxidation of Ce^{3+}, and, eventually, the oxidation of H_2O. What we need is a signal that tells us when no more Fe^{2+} is present in the solution.

For our purposes, it is convenient to treat a controlled-current coulometric analysis as a reaction between the analyte, Fe^{2+}, and the mediator, Ce^{3+}, as shown by reaction 5.3.10. This reaction is identical to a redox titration; thus, we can use the end points for a redox titration—visual indicators and potentiometric or conductometric measurements—to signal the end of a controlled-current coulometric analysis. For example, ferroin provides a useful visual endpoint for the Ce^{3+} mediated coulometric analysis for Fe^{2+}, changing color from red to blue when the electrolysis of Fe^{2+} is complete.

> Reaction 5.3.10 is the same reaction we used in Chapter 9 to develop our understanding of redox titrimetry.

Instrumentation

Controlled-current coulometry normally is carried out using a two-electrode galvanostat, which consists of a working electrode and a counter electrode. The working electrode—often a simple Pt electrode—also is called the generator electrode since it is where the mediator reacts to generate the species that reacts with the analyte. If necessary, the counter electrode is isolated from the analytical solution by a salt bridge or a porous frit to prevent its electrolysis products from reacting with the analyte. Alternatively, we can generate the oxidizing agent or the reducing agent externally, and allow it to flow into the analytical solution. Figure 5.3.7 shows one simple method for accomplishing this. A solution that contains the mediator flows into a small-volume electrochemical cell with the products exiting through separate tubes. Depending upon the analyte, the oxidizing agent or the reducing reagent is delivered to the analytical solution. For example, we can generate Ce^{4+} using an aqueous solution of Ce^{3+}, directing the Ce^{4+} that forms at the anode to our sample.

Figure 11.1.4 shows an example of a manual galvanostat. Although a modern galvanostat uses very different circuitry, you can use Figure 11.1.4 and the accompanying discussion to understand how we can use the working electrode and the counter electrode to control the current. Figure 11.1.4 includes an optional reference electrode, but its presence or absence is not important if we are not interested in monitoring the working electrode's potential.

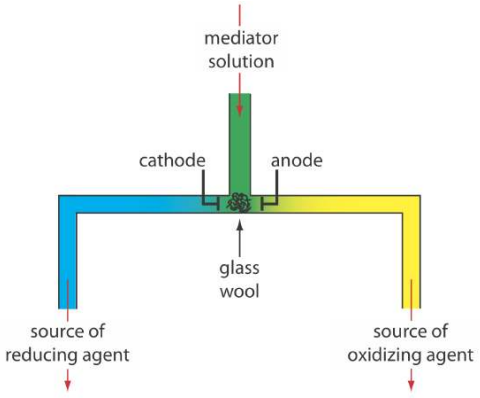


Figure 5.3.7 . One example of a device for the external generation of oxidizing agents and reducing agents for controlled-current coulometry. A solution containing the mediator flows into a small-volume electrochemical cell. The resulting oxidation products, which form at the anode, flow to the right and serve as an oxidizing agent. Reduction at the cathode generates a reducing agent.

There are two other crucial needs for controlled-current coulometry: an accurate clock for measuring the electrolysis time, t_e, and a switch for starting and stopping the electrolysis. An analog clock can record time to the nearest ±0.01 s, but the need to stop and start the electrolysis as we approach the endpoint may result in an overall uncertainty of ±0.1 s. A digital clock allows for a more accurate measurement of time, with an overall uncertainty of ±1 ms. The switch must control both the current and the clock so that we can make an accurate determination of the electrolysis time.

Quantitative Applications

Coulometry is used for the quantitative analysis of both inorganic and organic analytes. Examples of controlled-potential and controlled-current coulometric methods are discussed in the following two sections.

Controlled-Potential Coulometry

The majority of controlled-potential coulometric analyses involve the determination of inorganic cations and anions, including trace metals and halides ions. Table 5.3.1 summarizes several of these methods.

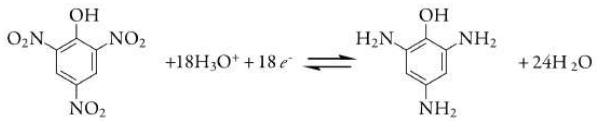
Table 5.3.1 . Representative Controlled-Potential Coulometric Analyses for Inorganic Ions

analyte	electrolytic reaction	electrode
antimony	$Sb(III) + 3e^- \rightleftharpoons Sb$	Pt
arsenic	$As(III) \rightleftharpoons As(V) + 2e^-$	Pt
cadmium	$Cd(II) + 2e^- \rightleftharpoons Cd$	Pt or Hg
cobalt	$Co(II) + 2e^- \rightleftharpoons Co$	Pt or Hg
copper	$Cu(II) + 2e^- \rightleftharpoons Cu$	Pt or Hg
halides (X^-)	$Ag + X^- \rightleftharpoons AgX + e^-$	Ag
iron	$Fe(II) \rightleftharpoons Fe(III) + e^-$	Pt
lead	$Pb(II) + 2e^- \rightleftharpoons Pb$	Pt or Hg
nickel	$Ni(II) + 2e^- \rightleftharpoons Ni$	Pt or Hg
plutonium	$Pu(III) \rightleftharpoons Pu(IV) + e^-$	Pt
silver	$Ag(I) + 1e^- \rightleftharpoons Ag$	Pt
tin	$Sn(II) + 2e^- \rightleftharpoons Sn$	Pt
uranium	$U(VI) + 2e^- \rightleftharpoons U(IV)$	Pt or Hg
zinc	$Zn(II) + 2e^- \rightleftharpoons Zn$	Pt or Hg

Source: Rechnitz, G. A. *Controlled-Potential Analysis*, Macmillan: New York, 1963.
Electrolytic reactions are written in terms of the change in the analyte's oxidation state. The actual species in solution depends on the analyte.

The ability to control selectivity by adjusting the working electrode's potential makes controlled-potential coulometry particularly useful for the analysis of alloys. For example, we can determine the composition of an alloy that contains Ag, Bi, Cd, and Sb by dissolving the sample and placing it in a matrix of 0.2 M H_2SO_4 along with a Pt working electrode and a Pt counter electrode. If we apply a constant potential of +0.40 V versus the SCE, Ag(I) deposits on the electrode as Ag and the other metal ions remain in solution. When electrolysis is complete, we use the total charge to determine the amount of silver in the alloy. Next, we shift the working electrode's potential to –0.08 V versus the SCE, depositing Bi on the working electrode. When the coulometric analysis for bismuth is complete, we determine antimony by shifting the working electrode's potential to –0.33 V versus the SCE, depositing Sb. Finally, we determine cadmium following its electrodeposition on the working electrode at a potential of –0.80 V versus the SCE.

We also can use controlled-potential coulometry for the quantitative analysis of organic compounds, although the number of applications is significantly less than that for inorganic analytes. One example is the six-electron reduction of a nitro group, $–NO_2$, to a primary amine, $–NH_2$, at a mercury electrode. Solutions of picric acid—also known as 2,4,6-trinitrophenol, or TNP, a close relative of TNT—is analyzed by reducing it to triaminophenol.



Another example is the successive reduction of trichloroacetate to dichloroacetate, and of dichloroacetate to monochloroacetate

$$Cl_3CCOO^-(aq) + H_3O^+(aq) + 2e^- \rightleftharpoons Cl_2HCCOO^-(aq) + Cl^-(aq) + H_2O(l)$$

$$Cl_2HCCOO^-(aq) + H_3O^+(aq) + 2e^- \rightleftharpoons ClH_2CCOO^-(aq) + Cl^-(aq) + H_2O(l)$$

We can analyze a mixture of trichloroacetate and dichloroacetate by selecting an initial potential where only the more easily reduced trichloroacetate reacts. When its electrolysis is complete, we can reduce dichloroacetate by adjusting the potential to a more negative potential. The total charge for the first electrolysis gives the amount of trichloroacetate, and the difference in total charge between the first electrolysis and the second electrolysis gives the amount of dichloroacetate.

Controlled-Current Coulometry (Coulometric Titrations)

The use of a mediator makes a coulometric titration a more versatile analytical technique than controlled-potential coulometry. For example, the direct oxidation or reduction of a protein at a working electrode is difficult if the protein's active redox site lies deep within its structure. A coulometric titration of the protein is possible, however, if we use the oxidation or reduction of a mediator to produce a solution species that reacts with the protein. Table 5.3.2 summarizes several controlled-current coulometric methods based on a redox reaction using a mediator.

Table 5.3.2 . Representative Examples of Coulometric Redox Titrations

mediator	electrochemically generated reagent and reaction	representative application
Ag^+	$\mathbf{Ag^+} \rightleftharpoons \mathbf{Ag^{2+}} + e^-$	$\mathbf{H_2C_2O_4}(aq) + 2\mathbf{Ag^{2+}}(aq) + 2\mathbf{H_2O}(l) \rightleftharpoons 2\mathbf{CO_2}(g) + 2\mathbf{Ag^+}(aq) + 2\mathbf{H_3O^+}(aq)$
Br^-	$2\mathbf{Br^-} \rightleftharpoons \mathbf{Br_2} + 2e^-$	$\mathbf{H_2S}(aq) + \mathbf{Br_2}(aq) + 2\mathbf{H_2O}(l) \rightleftharpoons \mathbf{S}(s) + 2\mathbf{Br^-}(aq) + 2\mathbf{H_3O^+}(aq)$
Ce^{3+}	$\mathbf{Ce^{3+}} \rightleftharpoons \mathbf{Ce^{4+}} + e^-$	$\mathbf{Fe(CN)_6^{4-}}(aq) + \mathbf{Ce^{4+}}(aq) \rightleftharpoons \mathbf{Fe(CN)_6^{3-}}(aq) + \mathbf{Ce^{3+}}(aq)$
Cl^-	$2\mathbf{Cl^-} \rightleftharpoons \mathbf{Cl_2} + 2e^-$	$\mathbf{Ti(I)}(aq) + \mathbf{Cl_2}(aq) \rightleftharpoons \mathbf{Ti(III)}(aq) + 2\mathbf{Cl^-}(aq)$
Fe^{3+}	$\mathbf{Fe^{3+}} + e^- \rightleftharpoons \mathbf{Fe^{2+}}$	$\mathbf{Cr_2O_7^{2-}}(aq) + 6\mathbf{Fe^{2+}}(aq) + 14\mathbf{H_3O^+}(aq) \rightleftharpoons 2\mathbf{Cr^{3+}}(aq) + 6\mathbf{Fe^{3+}}(aq) + 21\mathbf{H_2O}(l)$
I^-	$3\mathbf{I^-} \rightleftharpoons \mathbf{I_3^-} + 2e^-$	$2\mathbf{S_2O_3^{2-}}(aq) + \mathbf{I_3^-}(aq) \rightleftharpoons \mathbf{S_4O_6^{2-}}(aq) + 3\mathbf{I^-}(aq)$
Mn^{2+}	$\mathbf{Mn^{2+}} \rightleftharpoons \mathbf{Mn^{3+}} + e^-$	$\mathbf{As(III)}(aq) + 2\mathbf{Mn^{3+}}(aq) \rightleftharpoons \mathbf{As(V)}(aq) + 2\mathbf{Mn^{2+}}(aq)$

Note: The electrochemically generated reagent and the analyte are shown in **bold**.

For an analyte that is not easy to oxidize or reduce, we can complete a coulometric titration by coupling a mediator's oxidation or reduction to an acid–base, precipitation, or complexation reaction that involves the analyte. For example, if we use H_2O as a mediator, we can generate H_3O^+at the anode

$$6\mathbf{H_2O}(l) \rightleftharpoons 4\mathbf{H_3O^+}(aq) + \mathbf{O_2}(g) + 4e^-$$

and generate OH^- at the cathode.

$$2\mathbf{H_2O}(l) + 2e^- \rightleftharpoons 2\mathbf{OH^-}(aq) + \mathbf{H_2}(g)$$

If we carry out the oxidation or reduction of H_2O using the generator cell in Figure 5.3.7 , then we can selectively dispense H_3O^+ or OH^- into a solution that contains the analyte. The resulting reaction is identical to that in an acid–base titration. Coulometric acid–base titrations have been used for the analysis of strong and weak acids and bases, in both aqueous and non-aqueous matrices. Table 5.3.3 summarizes several examples of coulometric titrations that involve acid–base, complexation, and precipitation reactions.

Table 5.3.3 . Representative Coulometric Titrations Using Acid–Base, Complexation, and Precipitation Reactions

type of reaction	mediator	electrochemically generated reagent and reaction	representative application
acid-base	H_2O	$\mathbf{6H_2O \rightleftharpoons 4H_3O^+ + O_2 + e^-}$	$\mathbf{OH^-}(aq) + \mathbf{H_3O^+}(aq) \rightleftharpoons 2\mathbf{H_2O}(l)$
acid-base	H_2O	$\mathbf{2H_2O + 2e^- \rightleftharpoons 2OH^- + H_2}$	$\mathbf{H_3O^+}(aq) + \mathbf{OH^-}(aq) \rightleftharpoons 2\mathbf{H_2O}(l)$
complexation	$HgNH_3Y^{2-}$ (Y = EDTA)	$\mathbf{HgNH_3Y^{2-} + NH_4^+ + 2e^- \rightleftharpoons HY^{3-} + Hg + 2NH_3}$	$\mathbf{Ca^{2+}}(aq) + \mathbf{HY^{3-}}(aq) + \mathbf{H_2O}(l) \rightleftharpoons \mathbf{CaY^{2-}}(aq) + \mathbf{H_3O^+}(aq)$
complexation	Ag	$\mathbf{Ag \rightleftharpoons Ag^+ + e^-}$	$\mathbf{I^-}(aq) + \mathbf{Ag^+}(aq) \rightleftharpoons \mathbf{AgI}(s)$
precipitation	Hg	$\mathbf{2Hg \rightleftharpoons Hg_2^{2+} + 2e^-}$	$2\mathbf{Cl^-}(aq) + \mathbf{Hg_2^{2+}}(aq) \rightleftharpoons \mathbf{Hg_2Cl_2}(s)$
precipitation	$\mathbf{Fe(CN)_6^{3-}}$	$\mathbf{Fe(CN)_6^{3-} + e^- \rightleftharpoons Fe(CN)_6^{4-}}$	$3\mathbf{Zn^{2+}}(aq) + \mathbf{K^+}(aq) + 2\mathbf{Fe(CN)_6^{4-}}(aq) \rightleftharpoons \mathbf{K_2Zn_3[Fe(CN)_6]_2}(s)$

Note: The electrochemically generated reagent and the analyte are shown in **bold**.

In comparison to a conventional titration, a coulometric titration has two important advantages. The first advantage is that electrochemically generating a titrant allows us to use a reagent that is unstable. Although we cannot prepare and store a solution of a highly reactive reagent, such as Ag^{2+} or Mn^{3+}, we can generate them electrochemically and use them in a coulometric titration. Second, because it is relatively easy to measure a small quantity of charge, we can use a coulometric titration to determine an analyte whose concentration is too small for a conventional titration.

Quantitative Calculations

The absolute amount of analyte in a coulometric analysis is determined using Faraday's law (Equation 5.3.1) and the total charge given by Equation 5.3.2 or by Equation 5.3.3. The following example shows the calculations for a typical coulometric analysis.

Example 5.3.1

To determine the purity of a sample of $Na_2S_2O_3$, a sample is titrated coulometrically using I^- as a mediator and $\mathbf{I_3^-}$ as the titrant. A sample weighing 0.1342 g is transferred to a 100-mL volumetric flask and diluted to volume with distilled water. A 10.00-mL portion is transferred to an electrochemical cell along with 25 mL of 1 M KI, 75 mL of a pH 7.0 phosphate buffer, and several drops of a starch indicator solution. Electrolysis at a constant current of 36.45 mA requires 221.8 s to reach the starch indicator endpoint. Determine the sample's purity.

Solution

As shown in Table 5.3.2 , the coulometric titration of $\mathbf{S_2O_3^{2-}}$ with $\mathbf{I_3^-}$ is

$$2\mathbf{S_2O_3^{2-}}(aq) + \mathbf{I_3^-}(aq) \rightleftharpoons \mathbf{S_4O_6^{2-}}(aq) + 3\mathbf{I^-}(aq)$$

The oxidation of $\mathbf{S_2O_3^{2-}}$ to $\mathbf{S_4O_6^{2-}}$ requires one electron per $\mathbf{S_2O_3^{2-}}$ (n = 1). Combining Equation 5.3.1 and Equation 5.3.2, and solving for the moles and grams of $Na_2S_2O_3$ gives

$$N_A = \frac{it_e}{nF} = \frac{(0.03645\ \text{A})(221.8\ \text{s})}{\left(\frac{1\ \text{mol}\ e^-}{\text{mol}\ Na_2S_2O_3}\right)\left(\frac{96487\ \text{C}}{\text{mol}\ e^-}\right)} = 8.379 \times 10^{-5}\ \text{mol}\ Na_2S_2O_3$$

This is the amount of $Na_2S_2O_3$ in a 10.00-mL portion of a 100-mL sample; thus, there are 0.1325 grams of $Na_2S_2O_3$ in the original sample. The sample's purity, therefore, is

$$\frac{0.1325\ \text{g}\ Na_2S_2O_3}{0.1342\ \text{g sample}} \times 100 = 98.73\%\ \text{w/w}\ Na_2S_2O_3$$

Note that for Equation 5.3.1 and Equation 5.3.2 it does not matter whether $S_2O_3^{2-}$ is oxidized at the working electrode or is oxidized by I_3^-.

Exercise 5.3.1

To analyze a brass alloy, a 0.442-g sample is dissolved in acid and diluted to volume in a 500-mL volumetric flask. Electrolysis of a 10.00-mL sample at –0.3 V versus a SCE reduces Cu^{2+} to Cu, requiring a total charge of 16.11 C. Adjusting the potential to –0.6 V versus a SCE and completing the electrolysis requires 0.442 C to reduce Pb^{2+} to Pb. Report the %w/w Cu and Pb in the alloy.

Answer

The reduction of Cu^{2+} to Cu requires two electrons per mole of Cu (n = 2). Using Equation 5.3.1, we calculate the moles and the grams of Cu in the portion of sample being analyzed.

$$N_{Cu} = \frac{Q}{nF} = \frac{16.11\text{ C}}{\frac{2\text{ mol } e^-}{\text{mol Cu}} \times \frac{96487\text{ C}}{\text{mol } e^-}} = 8.348 \times 10^{-5}\text{ mol Cu}$$

$$8.348 \times 10^{-5}\text{ mol Cu} \times \frac{63.55\text{ g Cu}}{\text{mol Cu}} = 5.301 \times 10^{-3}\text{ g Cu}$$

This is the Cu from a 10.00 mL portion of a 500.0 mL sample; thus, the %/w/w copper in the original sample of brass is

$$\frac{5.301 \times 10^{-3}\text{ g Cu} \times \frac{500.0\text{ mL}}{10.00\text{ mL}}}{0.442\text{ g sample}} \times 100 = 60.0\%\text{ w/w Cu}$$

For lead, we follow the same process; thus

$$N_{Pb} = \frac{Q}{nF} = \frac{0.422\text{ C}}{\frac{2\text{ mol } e^-}{\text{mol Pb}} \times \frac{96487\text{ C}}{\text{mol } e^-}} = 2.19 \times 10^{-6}\text{ mol Pb}$$

$$2.19 \times 10^{-6}\text{ mol Pb} \times \frac{207.2\text{ g Pb}}{\text{mol Cu}} = 4.53 \times 10^{-4}\text{ g Pb}$$

$$\frac{4.53 \times 10^{-4}\text{ g Pb} \times \frac{500.0\text{ mL}}{10.00\text{ mL}}}{0.442\text{ g sample}} \times 100 = 5.12\%\text{ w/w Pb}$$

Representative Method 11.3.1: Determination of Dichromate by a Coulometric Redox Titration

The best way to appreciate the theoretical and the practical details discussed in this section is to carefully examine a typical analytical method. Although each method is unique, the following description of the determination of $Cr_2O_7^{2-}$ provides an instructive example of a typical procedure. The description here is based on Bassett, J.; Denney, R. C.; Jeffery, G. H.; Mendham, J. *Vogel's Textbook of Quantitative Inorganic Analysis*, Longman: London, 1978, p. 559–560.

Description of the Method

Thee concentration of $Cr_2O_7^{2-}$ in a sample is determined by a coulometric redox titration using Fe^{3+} as a mediator and electrogenerated Fe^{3+} as the titrant. The endpoint of the titration is determined potentiometrically.

Procedure

The electrochemical cell consists of a Pt working electrode and a Pt counter electrode placed in separate cells connected by a porous glass disk. Fill the counter electrode's cell with 0.2 M Na_2SO_4, keeping the level above that of the solution in the working electrode's cell. Connect a platinum electrode and a tungsten electrode to a potentiometer so that you can measure the working electrode's potential during the analysis. Prepare a mediator solution of approximately 0.3 M $NH_4Fe(SO_4)_2$. Add 5.00 mL of sample, 2 mL of 9 M H_2SO_4, and 10–25 mL of the mediator solution to the working electrode's cell, and add distilled water as needed to cover the electrodes. Bubble pure N_2 through the solution for 15 min to remove any O_2 that is present. Maintain the flow of N_2 during the electrolysis, turning if off momentarily when measuring the potential. Stir the solution using a magnetic stir bar.

Adjust the current to 15–50 mA and begin the titration. Periodically stop the titration and measure the potential. Construct a titration curve of potential versus time and determine the time needed to reach the equivalence point.

Questions

1. Is the platinum working electrode the cathode or the anode?

   Reduction of Fe^{3+} to Fe^{2+} occurs at the working electrode, making it the cathode in this electrochemical cell.

2. Why is it necessary to remove dissolved oxygen by bubbling N_2 through the solution?

   Any dissolved O_2 will oxidize Fe^{2+} back to Fe^{3+}, as shown by the following reaction.

   $$4Fe^{2+}(aq) + O_2 + 4H_3O^+(aq) \rightleftharpoons 4Fe^{3+}(aq) + 6H_2O(l)$$

   To maintain current efficiency, all the Fe^{2+} must react with $Cr_2O_7^{2-}$. The reaction of Fe^{2+} with O_2 means that more of the Fe^{3+} mediator is needed, increasing the time to reach the titration's endpoint. As a result, we report the presence of too much $Cr_2O_7^{2-}$.

3. What is the effect on the analysis if the $NH_4Fe(SO_4)_2$ is contaminated with trace amounts of Fe^{2+}? How can you compensate for this source of Fe^{2+}?

   There are two sources of Fe^{2+}: that generated from the mediator and that present as an impurity. Because the total amount of Fe^{2+} that reacts with $Cr_2O_7^{2-}$ remains unchanged, less Fe^{2+} is needed from the mediator. This decreases the time needed to reach the titration's end point. Because the apparent current efficiency is greater than 100%, the reported concentration of $Cr_2O_7^{2-}$ is too small. We can remove trace amount of Fe^{2+} from the mediator's solution by adding H_2O_2 and heating at 50–70°C until the evolution of O_2 ceases, converting the Fe^{2+} to Fe^{3+}. Alternatively, we can complete a blank titration to correct for any impurities of Fe^{2+} in the mediator.

4. Why is the level of solution in the counter electrode's cell maintained above the solution level in the working electrode's cell?

   This prevents the solution that contains the analyte from entering the counter electrode's cell. The oxidation of H_2O at the counter electrode produces O_2, which can react with the Fe^{2+} generated at the working electrode or the Cr^{3+} resulting from the reaction of Fe^{2+} and $Cr_2O_7^{2-}$. In either case, the result is a positive determinate error.

Characterization Applications

One useful application of coulometry is determining the number of electrons involved in a redox reaction. To make the determination, we complete a controlled-potential coulometric analysis using a known amount of a pure compound. The total charge at the end of the electrolysis is used to determine the value of *n* using Faraday's law (Equation 5.3.1).

Example 5.3.2

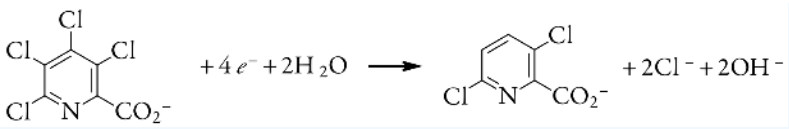
A 0.3619-g sample of tetrachloropicolinic acid, $C_6HNO_2Cl_4$, is dissolved in distilled water, transferred to a 1000-mL volumetric flask, and diluted to volume. An exhaustive controlled-potential electrolysis of a 10.00-mL portion of this solution at a spongy silver cathode requires 5.374 C of charge. What is the value of *n* for this reduction reaction?

Solution

The 10.00-mL portion of sample contains 3.619 mg, or 1.39×10^{-5} mol of tetrachloropicolinic acid. Solving Equation 5.3.1 for *n* and making appropriate substitutions gives

$$n = \frac{Q}{FN_A} = \frac{5.374\ \text{C}}{(96478\ \text{C/mol}\ e^-)\,(1.39 \times 10^{-5}\ \text{mol}\ C_6HNO_2Cl_4)} = 4.01\ \text{mol e}^-/\text{mol}\ C_6HNO_2Cl_4$$

Thus, reducing a molecule of tetrachloropicolinic acid requires four electrons. The overall reaction, which results in the selective formation of 3,6-dichloropicolinic acid, is



Evaluation

Scale of Operation

A coulometric method of analysis can analyze a small absolute amount of an analyte. In controlled-current coulometry, for example, the moles of analyte consumed during an exhaustive electrolysis is given by Equation ???. An electrolysis using a constant current of 100 μA for 100 s, for example, consumes only 1×10^{-7} mol of analyte if n = 1. For an analyte with a molecular weight of 100 g/mol, 1×10^{-7} mol of analyte corresponds to only 10 μg. The concentration of analyte in the electrochemical cell, however, must be sufficient to allow an accurate determination of the endpoint. When using a visual end point, the smallest concentration of analyte that can be determined by a coulometric titration is approximately 10^{-4} M. As is the case for a conventional titration, a coulometric titration using a visual end point is limited to major and minor analytes. A coulometric titration to a preset potentiometric endpoint is feasible even if the analyte's concentration is as small as 10^{-7} M, extending the analysis to trace analytes [Curran, D. J. "Constant-Current Coulometry," in Kissinger, P. T.; Heineman, W. R., eds., *Laboratory Techniques in Electroanalytical Chemistry*, Marcel Dekker Inc.: New York, 1984, pp. 539–568].

Accuracy

In controlled-current coulometry, accuracy is determined by the accuracy with which we can measure current and time, and by the accuracy with which we can identify the end point. The maximum measurement errors for current and time are about ±0.01% and ±0.1%, respectively. The maximum end point error for a coulometric titration is at least as good as that for a conventional titration, and is often better when using small quantities of reagents. Together, these measurement errors suggest that an accuracy of 0.1%–0.3% is feasible. The limiting factor in many analyses, therefore, is current efficiency. A current efficiency of more than 99.5% is fairly routine, and it often exceeds 99.9%.

In controlled-potential coulometry, accuracy is determined by current efficiency and by the determination of charge. If the sample is free of interferents that are easier to oxidize or reduce than the analyte, a current efficiency of greater than 99.9% is routine. When an interferent is present, it can often be eliminated by applying a potential where the exhaustive electrolysis of the interferents is possible without the simultaneous electrolysis of the analyte. Once the interferent is removed the potential is switched to a level where electrolysis of the analyte is feasible. The limiting factor in the accuracy of many controlled-potential coulometric methods of analysis is the determination of charge. With electronic integrators the total charge is determined with an accuracy of better than 0.5%.

If we cannot obtain an acceptable current efficiency, an electrogravimetric analysis is possible if the analyte—and only the analyte—forms a solid deposit on the working electrode. In this case the working electrode is weighed before beginning the electrolysis and reweighed when the electrolysis is complete. The difference in the electrode's weight gives the analyte's mass.

Precision

Precision is determined by the uncertainties in measuring current, time, and the endpoint in controlled-current coulometry or the charge in controlled-potential coulometry. Precisions of ±0.1–0.3% are obtained routinely in coulometric titrations, and precisions of ±0.5% are typical for controlled-potential coulometry.

Sensitivity

For a coulometric method of analysis, the calibration sensitivity is equivalent to nF in Equation 5.3.1. In general, a coulometric method is more sensitive if the analyte's oxidation or reduction involves a larger value of n.

Selectivity

Selectivity in controlled-potential and controlled-current coulometry is improved by adjusting solution conditions and by selecting the electrolysis potential. In controlled-potential coulometry, the potential is fixed by the potentiostat, and in controlled-current coulometry the potential is determined by the redox reaction with the mediator. In either case, the ability to control the electrolysis

potential affords some measure of selectivity. By adjusting pH or by adding a complexing agent, it is possible to shift the potential at which an analyte or interferent undergoes oxidation or reduction. For example, the standard-state reduction potential for Zn^{2+} is –0.762 V versus the SHE. If we add a solution of NH_3, forming $Zn(NH_3)_4^{2+}$, the standard state potential shifts to –1.04 V. This provides an additional means for controlling selectivity when an analyte and an interferent undergo electrolysis at similar potentials.

Time, Cost, and Equipment

Controlled-potential coulometry is a relatively time consuming analysis, with a typical analysis requiring 30–60 min. Coulometric titrations, on the other hand, require only a few minutes, and are easy to adapt to an automated analysis. Commercial instrumentation for both controlled-potential and controlled-current coulometry is available, and is relatively inexpensive. Low cost potentiostats and constant-current sources are available for approximately $1000.

This page titled 5.3: Coulometric Methods is shared under a CC BY-NC-SA 4.0 license and was authored, remixed, and/or curated by Kathryn Davis.

- **11.3: Coulometric Methods** by David Harvey is licensed CC BY-NC-SA 4.0.

5.4: Voltammetric and Amperometric Methods

In ***voltammetry*** we apply a time-dependent potential to an electrochemical cell and measure the resulting current as a function of that potential. We call the resulting plot of current versus applied potential a ***voltammogram***, and it is the electrochemical equivalent of a spectrum in spectroscopy, providing quantitative and qualitative information about the species involved in the oxidation or reduction reaction [Maloy, J. T. *J. Chem. Educ.* **1983**, *60*, 285–289]. The earliest voltammetric technique is polarography, developed by Jaroslav Heyrovsky in the early 1920s—an achievement for which he was awarded the Nobel Prize in Chemistry in 1959. Since then, many different forms of voltammetry have been developed, a few of which are highlighted in Figure 11.1.6. Before examining these techniques and their applications in more detail, we must first consider the basic experimental design for voltammetry and the factors influencing the shape of the resulting voltammogram.

> For an on-line introduction to much of the material in this section, see Analytical Electrochemistry: The Basic Concepts by Richard S. Kelly, a resource that is part of the Analytical Sciences Digital Library.

Voltammetric Measurements

Although early voltammetric methods used only two electrodes, a modern voltammeter makes use of a three-electrode potentiostat. In voltammetry we apply a time-dependent potential excitation signal to the working electrode—changing its potential relative to the fixed potential of the reference electrode—and measure the current that flows between the working electrode and the auxiliary electrode. The auxiliary electrode generally is a platinum wire and the reference electrode usually is a SCE or a Ag/AgCl electrode.

For the working electrode we can choose among several different materials, including mercury (liquid drops), platinum, gold, silver, and carbon. Solid electrodes constructed using platinum, gold, silver, or carbon may be used over a range of potentials, including potentials that are negative and positive with respect to the SCE (Figure 5.4.2). For example, the potential window for a Pt electrode extends from approximately +1.2 V to –0.2 V versus the SCE in acidic solutions, and from +0.7 V to –1 V versus the SCE in basic solutions. A solid electrode can replace a mercury electrode for many voltammetric analyses that require negative potentials, and is the electrode of choice at more positive potentials. Except for the carbon paste electrode, a solid electrode is fashioned into a disk and sealed into the end of an inert support with an electrical lead (Figure 5.4.3). The carbon paste electrode is made by filling the cavity at the end of the inert support with a paste that consists of carbon particles and a viscous oil. Solid electrodes are not without problems, the most important of which is the ease with which the electrode's surface is altered by the adsorption of a solution species or by the formation of an oxide layer. For this reason a solid electrode needs frequent reconditioning, either by applying an appropriate potential or by polishing.

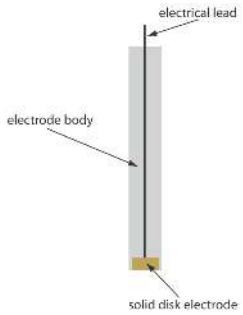


Figure 5.4.3 . Schematic showing a solid electrode. The electrode is fashioned into a disk and sealed in the end of an inert polymer support along with an electrical lead.

A typical arrangement for a voltammetric electrochemical cell is shown in Figure 5.4.4 . In addition to the working electrode, the reference electrode, and the auxiliary electrode, the cell also includes a N_2-purge line for removing dissolved O_2, and an optional stir bar. Electrochemical cells are available in a variety of sizes, allowing the analysis of solution volumes ranging from more than 100 mL to as small as 50 µL.

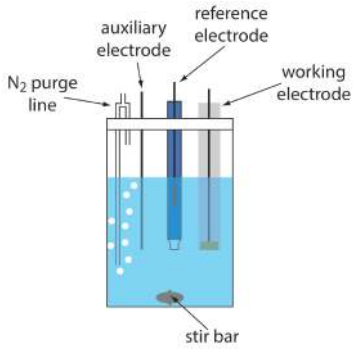


Figure 5.4.4 . Typical electrochemical cell for voltammetry.

Current In Voltammetry

When we oxidize an analyte at the working electrode, the resulting electrons pass through the potentiostat to the auxiliary electrode, reducing the solvent or some other component of the solution matrix. If we reduce the analyte at the working electrode, the current flows from the auxiliary electrode to the cathode. In either case, the current from the redox reactions at the working electrode and the auxiliary electrodes is called a ***faradaic current***. In this section we consider the factors affecting the magnitude of the faradaic current, as well as the sources of any non-faradaic currents.

Sign Conventions

Because the reaction of interest occurs at the working electrode, we describe the faradaic current using this reaction. A faradaic current due to the analyte's reduction is a ***cathodic current***, and its sign is positive. An ***anodic current*** results from the analyte's oxidation at the working electrode, and its sign is negative.

Influence of Applied Potential on the Faradaic Current

As an example, let's consider the faradaic current when we reduce $\mathbf{Fe(CN)_6^{3-}}$ to $\mathbf{Fe(CN)_6^{4-}}$ at the working electrode. The relationship between the concentrations of $\mathbf{Fe(CN)_6^{3-}}$, the concentration of $\mathbf{Fe(CN)_6^{4-}}$, and the potential is given by the Nernst equation

$$E = +0.356\ \text{V} - 0.05916 \log \frac{[\mathbf{Fe(CN)_6^{4-}}]_{x=0}}{[\mathbf{Fe(CN)_6^{3-}}]_{x=0}}$$

where +0.356V is the standard-statepotential for the $\mathbf{Fe(CN)_6^{3-}}$/$\mathbf{Fe(CN)_6^{4-}}$ redox couple, and x = 0 indicates that the concentrations of $\mathbf{Fe(CN)_6^{3-}}$- and $\mathbf{Fe(CN)_6^{4-}}$ are those at the surface of the working electrode. We use surface concentrations instead of bulk concentrations because the equilibrium position for the redox reaction

$$\mathbf{Fe(CN)_6^{3-}}(aq) + e^- \rightleftharpoons \mathbf{Fe(CN)_6^{4-}}(aq)$$

is established at the electrode's surface.

Let's assume we have a solution for which the initial concentration of $\mathbf{Fe(CN)_6^{3-}}$ is 1.0 mM and that $\mathbf{Fe(CN)_6^{4-}}$ is absent. Figure 5.4.5 shows the ladder diagram for this solution.

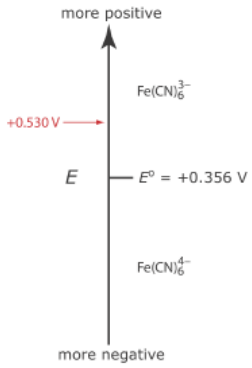


Figure 5.4.5 . Ladder diagram for the $Fe(CN)_6^{3-}/Fe(CN)_6^{4-}$ redox half-reaction.

If we apply a potential of +0.530 V to the working electrode, the concentrations of $Fe(CN)_6^{3-}$ and $Fe(CN)_6^{4-}$ at the surface of the electrode are unaffected, and no faradaic current is observed. If we switch the potential to +0.356 V some of the $Fe(CN)_6^{3-}$ at the electrode's surface is reduced to $Fe(CN)_6^{4-}$until we reach a condition where

$$[Fe(CN)_6^{3-}]_{x=0} = [Fe(CN)_6^{4-}]_{x=0} = 0.50 \text{ mM}$$

This is the first of the five important principles of electrochemistry outlined in Chapter 11.1: the electrode's potential determines the analyte's form at the electrode's surface.

If this is all that happens after we apply the potential, then there would be a brief surge of faradaic current that quickly returns to zero, which is not the most interesting of results. Although the concentrations of $Fe(CN)_6^{3-}$ and $Fe(CN)_6^{4-}$ at the electrode surface are 0.50 mM, their concentrations in bulk solution remains unchanged.

This is the second of the five important principles of electrochemistry outlined in Chapter 11.1: the analyte's concentration at the electrode may not be the same as its concentration in bulk solution.

Because of this difference in concentration, there is a concentration gradient between the solution at the electrode's surface and the bulk solution. This concentration gradient creates a driving force that transports $Fe(CN)_6^{4-}$ away from the electrode and that transports $Fe(CN)_6^{3-}$ to the electrode (Figure 5.4.6). As the $Fe(CN)_6^{3-}$ arrives at the electrode it, too, is reduced to $Fe(CN)_6^{4-}$. A faradaic current continues to flow until there is no difference between the concentrations of $Fe(CN)_6^{3-}$ and $Fe(CN)_6^{4-}$ at the electrode and their concentrations in bulk solution.

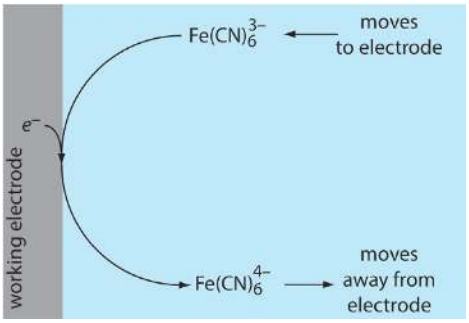


Figure 5.4.6 . Schematic diagram showing the transport of $Fe(CN)_6^{4-}$ away from the electrode's surface and the transport of $Fe(CN)_6^{3-}$ toward the electrode's surface following the reduction of $Fe(CN)_6^{3-}$ to $Fe(CN)_6^{4-}$.

Although the potential at the working electrode determines if a faradaic current flows, the magnitude of the current is determined by the rate of the resulting oxidation or reduction reaction. Two factors contribute to the rate of the electrochemical reaction: the rate at which the reactants and products are transported to and from the electrode—what we call ***mass transport***—and the rate at which electrons pass between the electrode and the reactants and products in solution.

This is the fourth of the five important principles of electrochemistry outlined in Chapter 11.1: current is a measure of rate.

Influence of Mass Transport on the Faradaic Current

There are three modes of mass transport that affect the rate at which reactants and products move toward or away from the electrode surface: diffusion, migration, and convection. ***Diffusion*** occurs whenever the concentration of an ion or a molecule at the surface of the electrode is different from that in bulk solution. If we apply a potential sufficient to completely reduce $\mathbf{Fe(CN)_6^{3-}}$ at the electrode surface, the result is a concentration gradient similar to that shown in Figure 5.4.7 . The region of solution over which diffusion occurs is the ***diffusion layer***. In the absence of other modes of mass transport, the width of the diffusion layer, δ, increases with time as the $\mathbf{Fe(CN)_6^{3-}}$ must diffuse from an increasingly greater distance.

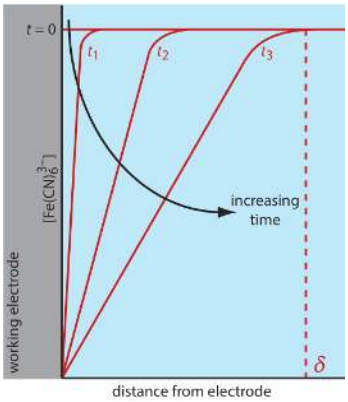


Figure 5.4.7 . Concentration gradients (in red) for $\mathbf{Fe(CN)_6^{3-}}$ following the application of a potential that completely reduces it to $\mathbf{Fe(CN)_6^{4-}}$. Before we apply the potential (t = 0) the concentration of $\mathbf{Fe(CN)_6^{3-}}$ is the same at all distances from the electrode's surface. After we apply the potential, its concentration at the electrode's surface decreases to zero and $\mathbf{Fe(CN)_6^{3-}}$ diffuses to the electrode from bulk solution. The longer we apply the potential, the greater the distance over which diffusion occurs. The dashed red line shows the extent of the diffusion layer at time t_3. These profiles assume that convection and migration do not contribute significantly to the mass transport of $\mathbf{Fe(CN)_6^{3-}}$.

Convection occurs when we mix the solution, which carries reactants toward the electrode and removes products from the electrode. The most common form of convection is stirring the solution with a stir bar; other methods include rotating the electrode and incorporating the electrode into a flow-cell.

The final mode of mass transport is ***migration***, which occurs when a charged particle in solution is attracted to or repelled from an electrode that carries a surface charge. If the electrode carries a positive charge, for example, an anion will move toward the electrode and a cation will move toward the bulk solution. Unlike diffusion and convection, migration affects only the mass transport of charged particles.

The movement of material to and from the electrode surface is a complex function of all three modes of mass transport. In the limit where diffusion is the only significant form of mass transport, the current in a voltammetric cell is equal to

$$i = \frac{nFAD\,(C_{\text{bulk}} - C_{x=0})}{\delta} \tag{5.4.1}$$

where n the number of electrons in the redox reaction, F is Faraday's constant, A is the area of the electrode, D is the diffusion coefficient for the species reacting at the electrode, C_{bulk} and $C_{x\,=\,0}$ are its concentrations in bulk solution and at the electrode surface, and δ is the thickness of the diffusion layer.

For Equation 5.4.1 to be valid, convection and migration must not interfere with the formation of a diffusion layer. We can eliminate migration by adding a high concentration of an inert supporting electrolyte. Because ions of similar charge equally are attracted to or repelled from the surface of the electrode, each has an equal probability of undergoing migration. A large excess of an inert electrolyte ensures that few reactants or products experience migration. Although it is easy to eliminate convection by not stirring the solution, there are experimental designs where we cannot avoid convection, either because we must stir the solution or because we are using an electrochemical flow cell. Fortunately, as shown in Figure 5.4.8 , the dynamics of a fluid moving past an electrode results in a small diffusion layer—typically 1–10 μm in thickness—in which the rate of mass transport by convection drops to zero.

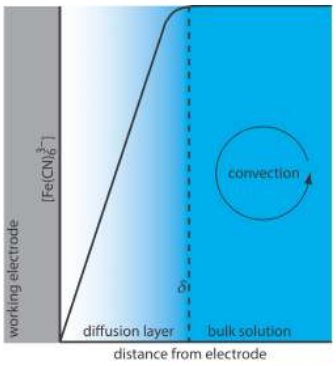


Figure 5.4.8 . Concentration gradient for $Fe(CN)_6^{3-}$ when stirring the solution. Diffusion is the only significant form of mass transport close to the electrode's surface. At distances greater than δ, convection is the only significant form of mass transport, maintaining a homogeneous solution in which the concentration of $Fe(CN)_6^{3-}$ at δ is the same as its concentration in bulk solution.

Effect of Electron Transfer Kinetics on the Faradaic Current

The rate of mass transport is one factor that influences the current in voltammetry. The ease with which electrons move between the electrode and the species that reacts at the electrode also affects the current. When electron transfer kinetics are fast, the redox reaction is at equilibrium. Under these conditions the redox reaction is ***electrochemically reversible*** and the Nernst equation applies. If the electron transfer kinetics are sufficiently slow, the concentration of reactants and products at the electrode surface—and thus the magnitude of the faradaic current—are not what is predicted by the Nernst equation. In this case the system is ***electrochemically irreversible***.

Charging Currents

In addition to the faradaic current from a redox reaction, the current in an electrochemical cell includes other, nonfaradaic sources. Suppose the charge on an electrode is zero and we suddenly change its potential so that the electrode's surface acquires a positive charge. Cations near the electrode's surface will respond to this positive charge by migrating away from the electrode; anions, on the other hand, will migrate toward the electrode. This migration of ions occurs until the electrode's positive surface charge and the negative charge of the solution near the electrode are equal. Because the movement of ions and the movement of electrons are indistinguishable, the result is a small, short-lived ***nonfaradaic current*** that we call the ***charging current***. Every time we change the electrode's potential, a transient charging current flows.

> The migration of ions in response to the electrode's surface charge leads to the formation of a structured electrode-solution interface that we call the ***electrical double layer***, or EDL. When we change an electrode's potential, the charging current is the result of a restructuring of the EDL. The exact structure of the electrical double layer is not important in the context of this text, but you can consult this chapter's additional resources for additional information.

Residual Current

Even in the absence of analyte, a small, measurable current flows through an electrochemical cell. This ***residual current*** has two components: a faradaic current due to the oxidation or reduction of trace impurities and a nonfaradaic charging current. Methods for discriminating between the analyte's faradaic current and the residual current are discussed later in this chapter.

Shape of Voltammograms

The shape of a voltammogram is determined by several experimental factors, the most important of which are how we measure the current and whether convection is included as a means of mass transport. As shown in Figure 5.4.9 , despite an abundance of different voltammetric techniques, several of which are discussed in this chapter, there are only three common shapes for voltammograms.

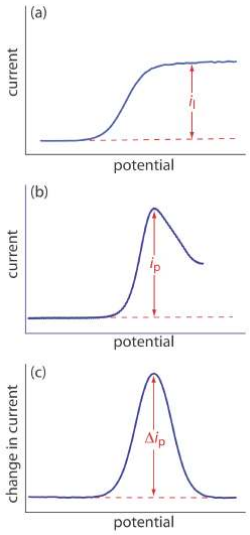


Figure 5.4.9 . The three common shapes for voltammograms. The dashed red line shows the residual current.

For the voltammogram in Figure 5.4.9 a, the current increases from a background residual current to a ***limiting current***, i_l. Because the faradaic current is inversely proportional to δ (Equation 5.4.1), a limiting current occurs only if the thickness of the diffusion layer remains constant because we are stirring the solution (see Figure 5.4.8). In the absence of convection the diffusion layer increases with time (see Figure 5.4.7). As shown in Figure 5.4.9 b, the resulting voltammogram has a ***peak current*** instead of a limiting current.

For the voltammograms in Figure 5.4.9 a and Figure 5.4.9 b, we measure the current as a function of the applied potential. We also can monitor the change in current, Δi, following a change in potential. The resulting voltammogram, shown in Figure 5.4.9 c, also has a peak current.

Quantitative and Qualitative Aspects of Voltammetry

Earlier we described a voltammogram as the electrochemical equivalent of a spectrum in spectroscopy. In this section we consider what quantitative and qualitative information from a voltammogram. We will not work with specific quantitative methods, but we will tour what exists.

Determining Concentration

The limiting current in a voltammogram is a linear function of the concentration of *O* in bulk solution. Therefore, it is possible to generate calibration curves for voltammetric current.

Determining the Standard-State Potential

To extract the standard-state potential from a voltammogram, we need to rewrite the Nernst equation for reaction ???

$$E = E^\circ_{O/R} - \frac{0.05916}{n} \log \frac{[R]_{x=0}}{[O]_{x=0}} \tag{5.4.2}$$

in terms of current instead of the concentrations of *O* and *R*. We will do this in several steps. First, we substitute Equation ??? into Equation ??? and rearrange to give

$$[O]_{x=0} = \frac{i_l - i}{K_O} \tag{5.4.3}$$

Next, we derive a similar equation for $[R]_{x\,=\,0}$, by noting that

$$i = K_R \left([R]_{x=0} - [R]_{\text{bulk}} \right)$$

Because the concentration of $[R]_{\text{bulk}}$ is zero—remember our assumption that the initial solution contains only *O*—we can simplify this equation

$$i = K_R[R]_{x=0}$$

and solve for $[R]_{x = 0}$.

$$[R]_{x=0} = \frac{i}{K_R} \tag{5.4.4}$$

Now we are ready to finish our derivation. Substituting Equation 5.4.4 and Equation 5.4.3 into Equation 5.4.2 and rearranging leaves us with

$$E = E^\circ_{O/R} - \frac{0.05916}{n}\log\frac{K_O}{K_R} - \frac{0.05916}{n}\log\frac{i}{i_l - i} \tag{5.4.5}$$

When the current, i, is half of the limiting current, i_l,

$$i = 0.5 \times i_l$$

we can simplify Equation 5.4.5 to

$$E_{1/2} = E^\circ_{O/R} - \frac{0.05916}{n}\log\frac{K_O}{K_R} \tag{5.4.6}$$

where $E_{1/2}$ is the half-wave potential (Figure 5.4.10). If K_O is approximately equal to K_R, which often is the case, then the half-wave potential is equal to the standard-state potential. Note that Equation 5.4.6 is valid only if the redox reaction is electrochemically reversible.

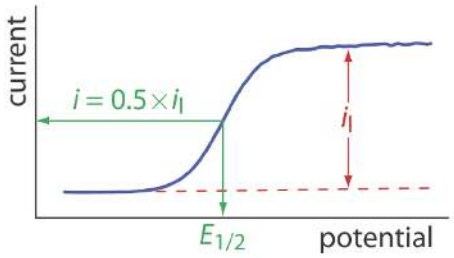


Figure 5.4.10 . Determination of the limiting current, i_l, and the half-wave potential, $E_{1/2}$, for the voltammogram in Figure 5.4.9 a.

Voltammetric Techniques

In voltammetry there are three important experimental parameters under our control: how we change the potential applied to the working electrode, when we choose to measure the current, and whether we choose to stir the solution. Not surprisingly, there are many different voltammetric techniques. In this section we consider several important examples.

Polarography

The chronologically first important voltammetric technique to be developed—***polarography***—uses the dropping mercury electrode shown in Figure 5.4.1 b as the working electrode. As shown in Figure 5.4.11 , the current is measured while applying a linear potential ramp.

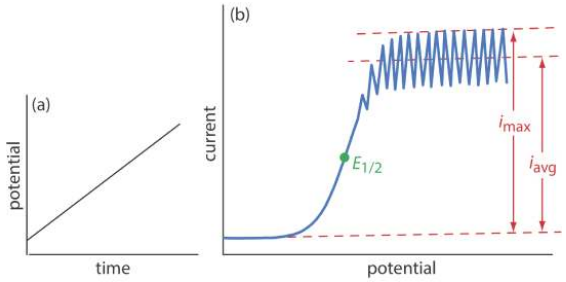


Figure 5.4.11 . Details of normal polarography: (a) the linear potential-excitation signal, and (b) the resulting voltammogram.

Although polarography takes place in an unstirred solution, we obtain a limiting current instead of a peak current. When a Hg drop separates from the glass capillary and falls to the bottom of the electrochemical cell, it mixes the solution. Each new Hg drop,

therefore, grows into a solution whose composition is identical to the bulk solution. The oscillations in the current are a result of the Hg drop's growth, which leads to a time-dependent change in the area of the working electrode. The limiting current—which also is called the diffusion current—is measured using either the maximum current, i_{max}, or from the average current, i_{avg}. The relationship between the analyte's concentration, C_A, and the limiting current is given by the Ilkovic equations

$$i_{max} = 706nD^{1/2}m^{2/3}t^{1/6}C_A = K_{max}C_A$$

$$i_{avg} = 607nD^{1/2}m^{2/3}t^{1/6}C_A = K_{avg}C_A$$

where n is the number of electrons in the redox reaction, D is the analyte's diffusion coefficient, m is the flow rate of Hg, t is the drop's lifetime and K_{max} and K_{avg} are constants. The half-wave potential, $E_{1/2}$, provides qualitative information about the redox reaction.

Normal polarography has been replaced by various forms of ***pulse polarography***, several examples of which are shown in Figure 5.4.12 [Osteryoung, J. *J. Chem. Educ.* **1983**, *60*, 296–298]. Normal pulse polarography (Figure 5.4.12 a), for example, uses a series of potential pulses characterized by a cycle of time τ, a pulse-time of t_p, a pulse potential of ΔE_p, and a scan rate of $\Delta E/\Delta t$. Typical experimental conditions for normal pulse polarography are $\tau \approx 1$ s, $t_p \approx 50$ ms, and $\Delta E/\Delta t \approx 2$ mV/s. The initial value of $\Delta E_p \approx 2$ mV, and it increases by ≈ 2 mV with each pulse. The current is sampled at the end of each potential pulse for approximately 17 ms before returning the potential to its initial value. The shape of the resulting voltammogram is similar to Figure 5.4.11 , but without the current oscillations. Because we apply the potential for only a small portion of the drop's lifetime, there is less time for the analyte to undergo oxidation or reduction and a smaller diffusion layer. As a result, the faradaic current in normal pulse polarography is greater than in the polarography, resulting in better sensitivity and smaller detection limits.

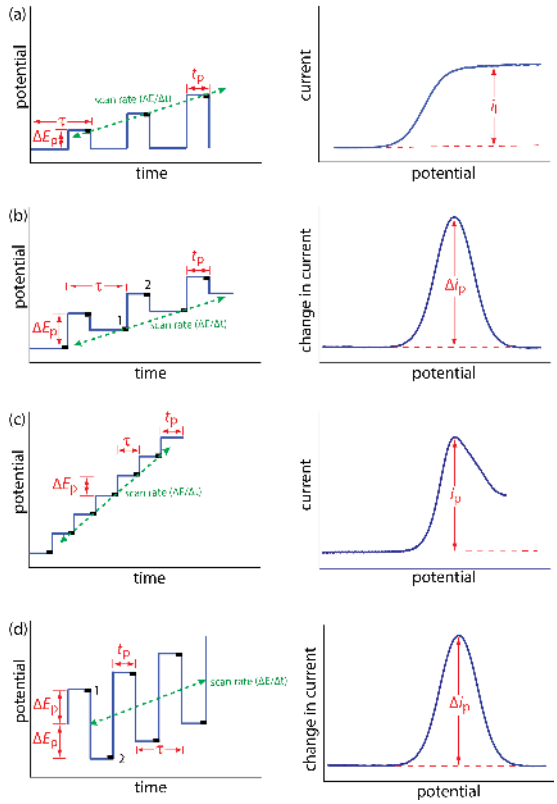


Figure 5.4.12 . Potential-excitation signals and voltammograms for (a) normal pulse polarography, (b) differential pulse polarography, (c) staircase polarography, and (d) square-wave polarography. The current is sampled at the time intervals shown by the black rectangles. When measuring a change in current, Δi, the current at point 1 is subtracted from the current at point 2. The symbols in the diagrams are as follows: τ is the cycle time; ΔE_p is a fixed or variable pulse potential relative to the beginning of the cycle; and t_p is the pulse time. The scan rate (change in potential per unit time) is shown by the dashed arrow.

In differential pulse polarography (Figure 5.4.12 b) the current is measured twice per cycle: for approximately 17 ms before applying the pulse and for approximately 17 ms at the end of the cycle. The difference in the two currents gives rise to the peak-shaped voltammogram. Typical experimental conditions for differential pulse polarography are $\tau \approx 1$ s, $t_p \approx 50$ ms, $\Delta E_p \approx 50$ mV, and $\Delta E/\Delta t \approx 2$ mV/s.

Other forms of pulse polarography include staircase polarography (Figure 5.4.12 c) and square-wave polarography (Figure 5.4.12 d). One advantage of square-wave polarography is that we can make τ very small—perhaps as small as 5 ms, compared to 1 s for other forms of pulse polarography—which significantly decreases analysis time. For example, suppose we need to scan a potential range of 400 mV. If we use normal pulse polarography with a $\Delta E/\Delta t$ of 2 mV/cycle and a τ of 1 s/cycle, then we need 200 s to complete the scan. If we use square-wave polarography with a $\Delta E/\Delta t$ of 2 mV/cycle and a τ of 5 ms/cycle, we can complete the scan in 1 s. At this rate, we can acquire a complete voltammogram using a single drop of Hg!

Polarography is used extensively for the analysis of metal ions and inorganic anions, such as IO_3^- and NO_3^-. We also can use polarography to study organic compounds with easily reducible or oxidizable functional groups, such as carbonyls, carboxylic acids, and carbon-carbon double bonds.

Hydrodynamic Voltammetry

In polarography we obtain a limiting current because each drop of mercury mixes the solution as it falls to the bottom of the electrochemical cell. If we replace the DME with a solid electrode (see Figure 5.4.3), we can still obtain a limiting current if we mechanically stir the solution during the analysis, using either a stir bar or by rotating the electrode. We call this approach ***hydrodynamic voltammetry***.

Hydrodynamic voltammetry uses the same potential profiles as in polarography, such as a linear scan (Figure 5.4.11) or a differential pulse (Figure 5.4.12 b). The resulting voltammograms are identical to those for polarography, except for the lack of current oscillations from the growth of the mercury drops. Because hydrodynamic voltammetry is not limited to Hg electrodes, it is useful for analytes that undergo oxidation or reduction at more positive potentials.

Stripping Voltammetry

Another important voltammetric technique is ***stripping voltammetry***, which consists of three related techniques: anodic stripping voltammetry, cathodic stripping voltammetry, and adsorptive stripping voltammetry. Because anodic stripping voltammetry is the more widely used of these techniques, we will consider it in greatest detail.

Anodic stripping voltammetry consists of two steps (Figure 5.4.13). The first step is a controlled potential electrolysis in which we hold the working electrode—usually a hanging mercury drop or a mercury film electrode—at a cathodic potential sufficient to deposit the metal ion on the electrode. For example, when analyzing Cu^{2+} the deposition reaction is

$$Cu^{2+} + 2e^- \rightleftharpoons Cu(Hg)$$

where Cu(Hg) indicates that the copper is amalgamated with the mercury. This step serves as a means of concentrating the analyte by transferring it from the larger volume of the solution to the smaller volume of the electrode. During most of the electrolysis we stir the solution to increase the rate of deposition. Near the end of the deposition time we stop the stirring—eliminating convection as a mode of mass transport—and allow the solution to become quiescent. Typical deposition times of 1–30 min are common, with analytes at lower concentrations requiring longer times.

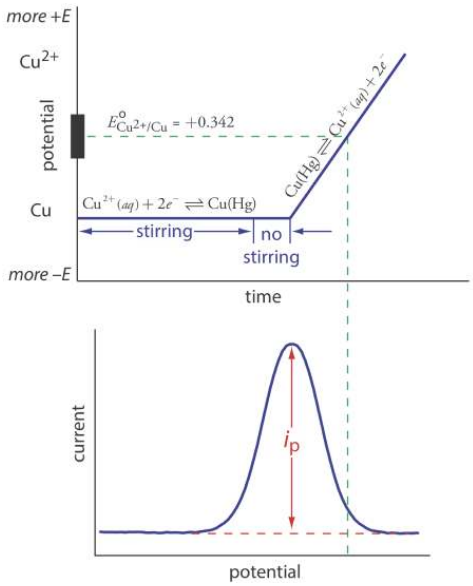


Figure 5.4.13 . Potential-excitation signal and voltammogram for anodic stripping voltammetry at a hanging mercury drop electrode or a mercury film electrode. Note the ladder diagram for copper in the upper figure.

In the second step, we scan the potential anodically—that is, toward a more positive potential. When the working electrode's potential is sufficiently positive, the analyte is stripped from the electrode, returning to solution in its oxidized form.

$$\mathbf{Cu(Hg) \rightleftharpoons Cu^{2+} + 2e^-}$$

Monitoring the current during the stripping step gives a peak-shaped voltammogram, as shown in Figure 5.4.13 . The peak current is proportional to the analyte's concentration in the solution. Because we are concentrating the analyte in the electrode, detection limits are much smaller than other electrochemical techniques. An improvement of three orders of magnitude—the equivalent of parts per billion instead of parts per million—is routine.

Anodic stripping voltammetry is very sensitive to experimental conditions, which we must carefully control to obtain results that are accurate and precise. Key variables include the area of the mercury film or the size of the hanging Hg drop, the deposition time, the rest time, the rate of stirring, and the scan rate during the stripping step. Anodic stripping voltammetry is particularly useful for metals that form amalgams with mercury, several examples of which are listed in Table 5.4.1 .

Table 5.4.1 . Representative Examples of Analytes Determined by Stripping Voltammetry

anodic stripping voltammetry	cathodic stripping voltammetry	adsorptive stripping voltammetry
Bi^{3+}	Br^-	bilirubin
Cd^{2+}	Cl^-	codeine
Cu^{2+}	I^-	cocaine
Ga^{3+}	mercaptans (RSH)	digitoxin
In^{3+}	S^{2-}	dopamine
Pb^{2+}	SCN^-	heme
Tl^+		monesin
Sn^{2+}		testosterone
Zn^{2+}		

Source: Compiled from Peterson, W. M.; Wong, R. V. *Am. Lab.* November 1981, 116–128; Wang, J. *Am. Lab.* May 1985, 41–50.

The experimental design for cathodic stripping voltammetry is similar to anodic stripping voltammetry with two exceptions. First, the deposition step involves the oxidation of the Hg electrode to Hg_2^{2+}, which then reacts with the analyte to form an insoluble film at the surface of the electrode. For example, when Cl^- is the analyte the deposition step is

$$2Hg(l) + 2Cl^-(aq) \rightleftharpoons Hg_2Cl_2(s) + 2e^-$$

Second, stripping is accomplished by scanning cathodically toward a more negative potential, reducing Hg_2^{2+} back to Hg and returning the analyte to solution.

$$Hg_2Cl_2(s) + 2e^- \rightleftharpoons 2Hg(l) + 2Cl^-(aq)$$

Table 5.4.1 lists several analytes analyzed successfully by cathodic stripping voltammetry.

In adsorptive stripping voltammetry, the deposition step occurs without electrolysis. Instead, the analyte adsorbs to the electrode's surface. During deposition we maintain the electrode at a potential that enhances adsorption. For example, we can adsorb a neutral molecule on a Hg drop if we apply a potential of –0.4 V versus the SCE, a potential where the surface charge of mercury is approximately zero. When deposition is complete, we scan the potential in an anodic or a cathodic direction, depending on whether we are oxidizing or reducing the analyte. Examples of compounds that have been analyzed by absorptive stripping voltammetry also are listed in Table 5.4.1 .

Cyclic Voltammetry

In the voltammetric techniques consider to this point we scan the potential in one direction, either to more positive potentials or to more negative potentials. In ***cyclic voltammetry*** we complete a scan in both directions. Figure 5.4.14 a shows a typical potential-excitation signal. In this example, we first scan the potential to more positive values, resulting in the following oxidation reaction for the species *R*.

$$R \rightleftharpoons O + ne^-$$

When the potential reaches a predetermined switching potential, we reverse the direction of the scan toward more negative potentials. Because we generated the species *O* on the forward scan, during the reverse scan it reduces back to *R*.

$$O + ne^- \rightleftharpoons R$$

Cyclic voltammetry is carried out in an unstirred solution, which, as shown in Figure 5.4.14 b, results in peak currents instead of limiting currents. The voltammogram has separate peaks for the oxidation reaction and for the reduction reaction, each characterized by a peak potential and a peak current.

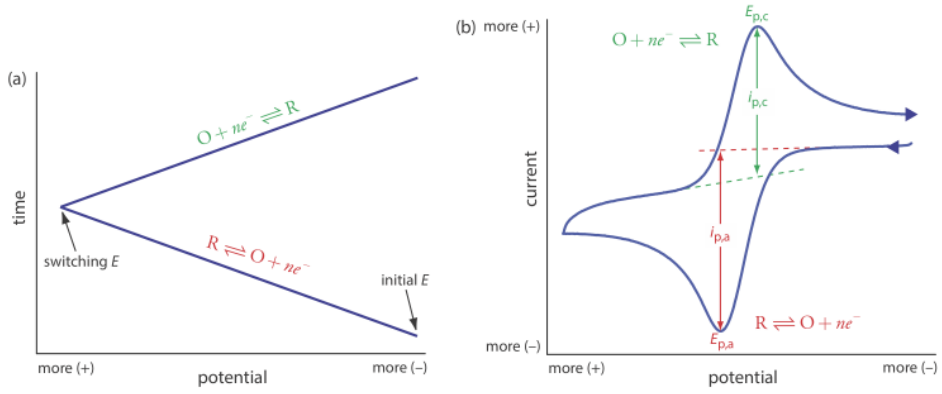


Figure 5.4.14 . Details for cyclic voltammetry. (a) One cycle of the triangular potential-excitation signal showing the initial potential and the switching potential. A cyclic voltammetry experiment can consist of one cycle or many cycles. Although the initial potential in this example is the negative switching potential, the cycle can begin with an intermediate initial potential and cycle between two limits. (b) The resulting cyclic voltammogram showing the measurement of the peak currents and peak potentials.

The peak current in cyclic voltammetry is given by the Randles-Sevcik equation

$$i_p = \left(2.69 \times 10^5\right) n^{3/2} A D^{1/2} \nu^{1/2} C_A$$

where n is the number of electrons in the redox reaction, A is the area of the working electrode, D is the diffusion coefficient for the electroactive species, ν is the scan rate, and C_A is the concentration of the electroactive species at the electrode. For a well-behaved system, the anodic and the cathodic peak currents are equal, and the ratio $i_{p,a}/i_{p,c}$ is 1.00. The half-wave potential, $E_{1/2}$, is midway between the anodic and cathodic peak potentials.

$$E_{1/2} = \frac{E_{p,a} + E_{p,c}}{2}$$

Scanning the potential in both directions provides an opportunity to explore the electrochemical behavior of species generated at the electrode. This is a distinct advantage of cyclic voltammetry over other voltammetric techniques. Figure 5.4.15 shows the cyclic voltammogram for the same redox couple at both a faster and a slower scan rate. At the faster scan rate, 5.4.15 a, we see two peaks. At the slower scan rate in Figure 5.4.15 b, however, the peak on the reverse scan disappears. One explanation for this is that the products from the reduction of R on the forward scan have sufficient time to participate in a chemical reaction whose products are not electroactive.

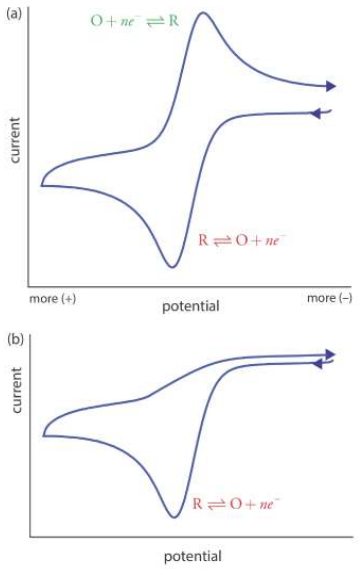


Figure 5.4.15 . Cyclic voltammograms for R obtained at (a) a faster scan rate and at (b) a slower scan rate. One of the principal uses of cyclic voltammetry is to study the chemical and electrochemical behavior of compounds. See this chapter's additional resources for further information.

Amperometry

The final voltammetric technique we will consider is ***amperometry***, in which we apply a constant potential to the working electrode and measure current as a function of time. Because we do not vary the potential, amperometry does not result in a voltammogram.

One important application of amperometry is in the construction of chemical sensors. One of the first amperometric sensors was developed in 1956 by L. C. Clark to measure dissolved O_2 in blood. Figure 5.4.16 shows the sensor's design, which is similar to a potentiometric membrane electrode. A thin, gas-permeable membrane is stretched across the end of the sensor and is separated from the working electrode and the counter electrode by a thin solution of KCl. The working electrode is a Pt disk cathode, and a Ag ring anode serves as the counter electrode. Although several gases can diffuse across the membrane, including O_2, N_2, and CO_2, only oxygen undergoes reduction at the cathode

$$O_2(g) + 4H_3O^+(aq) + 4e^- \rightleftharpoons 6H_2O(l)$$

with its concentration at the electrode's surface quickly reaching zero. The concentration of O_2 at the membrane's inner surface is fixed by its diffusion through the membrane, which creates a diffusion profile similar to that in Figure 5.4.8 . The result is a steady-state current that is proportional to the concentration of dissolved oxygen. Because the electrode consumes oxygen,the sample is stirred to prevent the depletion of O_2 at the membrane's outer surface.

> The oxidation of the Ag anode is the other half-reaction.

$$Ag(s) + Cl^-(aq) \rightleftharpoons AgCl(s) + e^-$$

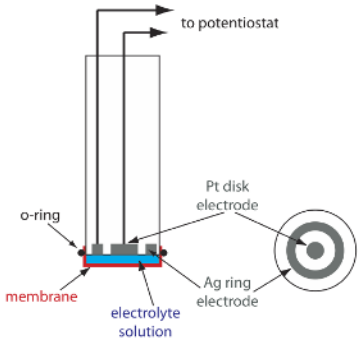


Figure 5.4.16 . Clark amperometric sensor for determining dissolved O_2. The diagram on the right is a cross-section through the electrode, which shows the Ag ring electrode and the Pt disk electrode.

Another example of an amperometric sensor is a glucose sensor. In this sensor the single membrane in Figure 5.4.16 is replaced with three membranes. The outermost membrane of polycarbonate is permeable to glucose and O_2. The second membrane contains an immobilized preparation of glucose oxidase that catalyzes the oxidation of glucose to gluconolactone and hydrogen peroxide.

$$\beta - D - \text{glucose}\ (aq) + O_2(aq) + H_2O(l) \rightleftharpoons \text{gluconolactone}\ (aq) + H_2O_2(aq)$$

The hydrogen peroxide diffuses through the innermost membrane of cellulose acetate where it undergoes oxidation at a Pt anode.

$$H_2O_2(aq) + 2OH^-(aq) \rightleftharpoons O_2(aq) + 2H_2O(l) + 2e^-$$

Figure 5.4.17 summarizes the reactions that take place in this amperometric sensor. FAD is the oxidized form of flavin adenine nucleotide—the active site of the enzyme glucose oxidase—and $FADH_2$ is the active site's reduced form. Note that O_2 serves a mediator, carrying electrons to the electrode.

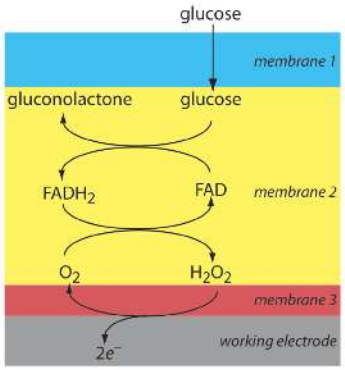


Figure 5.4.17 . Schematic showing the reactions by which an amperometric biosensor responds to glucose.

By changing the enzyme and mediator, it is easy to extend to the amperometric sensor in Figure 5.4.17 to the analysis of other analytes. For example, a CO_2 sensor has been developed using an amperometric O_2 sensor with a two-layer membrane, one of which contains an immobilized preparation of autotrophic bacteria [Karube, I.; Nomura, Y.; Arikawa, Y. *Trends in Anal. Chem.* **1995**, *14*, 295–299]. As CO_2 diffuses through the membranes it is converted to O_2 by the bacteria, increasing the concentration of O_2 at the Pt cathode.

Quantitative Applications

Voltammetry has been used for the quantitative analysis of a wide variety of samples, including environmental samples, clinical samples, pharmaceutical formulations, steels, gasoline, and oil.

Selecting the Voltammetric Technique

The choice of which voltammetric technique to use depends on the sample's characteristics, including the analyte's expected concentration and the sample's location. For example, amperometry is ideally suited for detecting analytes in flow systems,

including the *in vivo* analysis of a patient's blood or as a selective sensor for the rapid analysis of a single analyte. The portability of amperometric sensors, which are similar to potentiometric sensors, also make them ideal for field studies. Although cyclic voltammetry is used to determine an analyte's concentration, other methods described in this chapter are better suited for quantitative work.

Pulse polarography and stripping voltammetry frequently are interchangeable. The choice of which technique to use often depends on the analyte's concentration and the desired accuracy and precision. Detection limits for normal pulse polarography generally are on the order of 10^{-6} M to 10^{-7} M, and those for differential pulse polarography, staircase, and square wave polarography are between 10^{-7} M and 10^{-9} M. Because we concentrate the analyte in stripping voltammetry, the detection limit for many analytes is as little as 10^{-10} M to 10^{-12} M. On the other hand, the current in stripping voltammetry is much more sensitive than pulse polarography to changes in experimental conditions, which may lead to poorer precision and accuracy. We also can use pulse polarography to analyze a wider range of inorganic and organic analytes because there is no need to first deposit the analyte at the electrode surface.

Stripping voltammetry also suffers from occasional interferences when two metals, such as Cu and Zn, combine to form an intermetallic compound in the mercury amalgam. The deposition potential for Zn . is sufficiently negative that any Cu^{2+} in the sample also deposits into the mercury drop or film, leading to the formation of intermetallic compounds such as CuZn and $CuZn_2$. During the stripping step, zinc in the intermetallic compounds strips at potentials near that of copper, decreasing the current for zinc at its usual potential and increasing the apparent current for copper. It is possible to overcome this problem by adding an element that forms a stronger intermetallic compound with the interfering metal. Thus, adding Ga^{3+} minimizes the interference of Cu when analyzing for Zn by forming an intermetallic compound of Cu and Ga.

Correcting the Residual Current

In any quantitative analysis we must correct the analyte's signal for signals that arise from other sources. The total current, i_{tot}, in voltammetry consists of two parts: the current from the analyte's oxidation or reduction, i_A, and a background or residual current, i_r.

$$i_{tot} = i_A + i_r$$

The residual current, in turn, has two sources. One source is a faradaic current from the oxidation or reduction of trace interferents in the sample, i_{int}. The other source is the charging current, i_{ch}, that accompanies a change in the working electrode's potential.

$$i_r = i_{\text{int}} + i_{ch}$$

We can minimize the faradaic current due to impurities by carefully preparing the sample. For example, one important impurity is dissolved O_2, which undergoes a two-step reduction: first to H_2O_2 at a potential of –0.1 V versus the SCE, and then to H_2O at a potential of –0.9 V versus the SCE. Removing dissolved O_2 by bubbling an inert gas such as N_2 through the sample eliminates this interference. After removing the dissolved O_2, maintaining a blanket of N_2 over the top of the solution prevents O_2 from reentering the solution.

> The cell in Figure 5.4.4 shows a typical N_2 purge line.

There are two methods to compensate for the residual current. One method is to measure the total current at potentials where the analyte's faradaic current is zero and extrapolate it to other potentials. This is the method shown in Figure 5.4.9 . One advantage of extrapolating is that we do not need to acquire additional data. An important disadvantage is that an extrapolation assumes that any change in the residual current with potential is predictable, which may not be the case. A second, and more rigorous approach, is to obtain a voltammogram for an appropriate blank. The blank's residual current is then subtracted from the sample's total current.

Analysis for Single Components

The analysis of a sample with a single analyte is straightforward using any of the standardization methods discussed in Chapter 5.

Example 5.4.1

The concentration of As(III) in water is determined by differential pulse polarography in 1 M HCl. The initial potential is set to –0.1 V versus the SCE and is scanned toward more negative potentials at a rate of 5 mV/s. Reduction of As(III) to As(0) occurs

at a potential of approximately –0.44 V versus the SCE. The peak currents for a set of standard solutions, corrected for the residual current, are shown in the following table.

[As(III)] (μM)	i_p (μM)
1.00	0.298
3.00	0.947
6.00	1.83
9.00	2.72

What is the concentration of As(III) in a sample of water if its peak current is 1.37 μA?

Solution

Linear regression gives the calibration curve shown in Figure 5.4.18 , with an equation of

$$i_p = 0.0176 + 3.01 \times [\text{As(III)}]$$

Substituting the sample's peak current into the regression equation gives the concentration of As(III) as 4.49 μM.

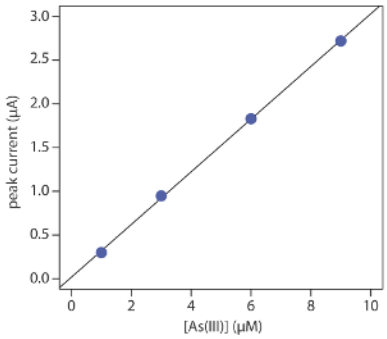


Figure 5.4.18 . Calibration curve for the data in Example 5.4.1 .

Exercise 5.4.1

The concentration of copper in a sample of sea water is determined by anodic stripping voltammetry using the method of standard additions. The analysis of a 50.0-mL sample gives a peak current of 0.886 μA. After adding a 5.00-μL spike of 10.0 mg/L Cu^{2+}, the peak current increases to 2.52 μA. Calculate the μg/L copper in the sample of sea water.

Answer

For anodic stripping voltammetry, the peak current, i_p, is a linear function of the analyte's concentration

$$i_p = K \times C_{\text{Cu}}$$

where K is a constant that accounts for experimental parameters such as the electrode's area, the diffusion coefficient for Cu^{2+}, the deposition time, and the rate of stirring. For the analysis of the sample before the standard addition we know that the current is

$$i_p = 0.886\ \mu\text{A} = K \times C_{\text{Cu}}$$

and after the standard addition the current is

$$i_p = 2.52\ \mu\text{A} = K\left\{C_{\text{Cu}} \times \frac{50.00\ \text{mL}}{50.005\ \text{mL}} + \frac{10.00\text{mgCu}}{\text{L}} \times \frac{0.005\ \text{mL}}{50.005\ \text{mL}}\right\}$$

where 50.005 mL is the total volume after we add the 5.00 μL spike. Solving each equation for K and combining leaves us with the following equation.

$$\frac{0.886\ \mu A}{C_{Cu}} = K = \frac{2.52\ \mu A}{C_{Cu} \times \frac{50.00\ mL}{50.005\ mL} + \frac{10.00\ mg\ Cu}{L} \times \frac{0.005\ mL}{50.005\ mL}}$$

Solving this equation for C_{Cu} gives its value as 5.42×10^{-4} mg Cu^{2+}/L, or 0.542 μg Cu^{2+}/L.

Multicomponent Analysis

Voltammetry is a particularly attractive technique for the analysis of samples that contain two or more analytes. Provided that the analytes behave independently, the voltammogram of a multicomponent mixture is a summation of each analyte's individual voltammograms. As shown in Figure 5.4.19 , if the separation between the half-wave potentials or between the peak potentials is sufficient, we can determine the presence of each analyte as if it is the only analyte in the sample. The minimum separation between the half-wave potentials or peak potentials for two analytes depends on several factors, including the type of electrode and the potential-excitation signal. For normal polarography the separation is at least ±0.2–0.3 V, and differential pulse voltammetry requires a minimum separation of ±0.04–0.05 V.

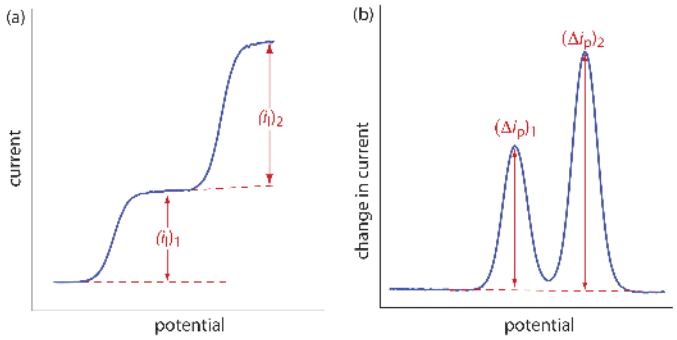


Figure 5.4.19 . Voltammograms for a sample that contains two analytes showing the measurement of (a) limiting currents, and (b) peak currents.

If the voltammograms for two analytes are not sufficiently separated, a simultaneous analysis may be possible. An example of this approach is outlined the following example.

Example 5.4.2

The differential pulse polarographic analysis of a mixture of indium and cadmium in 0.1 M HCl is complicated by the overlap of their respective voltammograms [Lanza P. *J. Chem. Educ.* **1990**, *67*, 704–705]. The peak potential for indium is at –0.557 V and that for cadmium is at –0.597 V. When a 0.800-ppm indium standard is analyzed, Δi_p (in arbitrary units) is 200.5 at –0.557 V and 87.5 at –0.597 V relative to a saturated Ag/AgCl reference electorde. A standard solution of 0.793 ppm cadmium has a Δi_p of 58.5 at –0.557 V and 128.5 at –0.597 V. What is the concentration of indium and cadmium in a sample if Δi_p is 167.0 at a potential of –0.557 V and 99.5 at a potential of –0.597V.

Solution

The change in current, Δi_p, in differential pulse polarography is a linear function of the analyte's concentration

$$\Delta i_p = k_A C_A$$

where k_A is a constant that depends on the analyte and the applied potential, and C_A is the analyte's concentration. To determine the concentrations of indium and cadmium in the sample we must first find the value of k_A for each analyte at each potential. For simplicity we will identify the potential of –0.557 V as E_1, and that for –0.597 V as E_2. The values of k_A are

$$k_{In,E_1} = \frac{200.5}{0.800\ ppm} = 250.6\ ppm^{-1}$$
$$k_{In,E_2} = \frac{87.5}{0.800\ ppm} = 109.4\ ppm^{-1}$$
$$k_{Cd E_1} = \frac{58.5}{0.793\ ppm} = 73.8\ ppm^{-1}$$
$$k_{Cd E_2} = \frac{128.5}{0.793\ ppm} = 162.0\ ppm^{-1}$$

Next, we write simultaneous equations for the current at the two potentials.

$$\Delta i_{E_1} = 167.0 = 250.6 \text{ ppm}^{-1} \times C_{\text{In}} + 73.8 \text{ ppm}^{-1} \times C_{\text{Cd}}$$
$$\Delta i_{E_2} = 99.5 = 109.4 \text{ ppm}^{-1} \times C_{\text{In}} + 162.0 \text{ ppm}^{-1} \times C_{\text{Cd}}$$

Solving the simultaneous equations, which is left as an exercise, gives the concentration of indium as 0.606 ppm and the concentration of cadmium as 0.205 ppm.

Environmental Samples

Voltammetry is one of several important analytical techniques for the analysis of trace metals in environmental samples, including groundwater, lakes, rivers and streams, seawater, rain, and snow. Detection limits at the parts-per-billion level are routine for many trace metals using differential pulse polarography, with anodic stripping voltammetry providing parts-per-trillion detection limits for some trace metals.

One interesting environmental application of anodic stripping voltammetry is the determination of a trace metal's chemical form within a water sample. Speciation is important because a trace metal's bioavailability, toxicity, and ease of transport through the environment often depends on its chemical form. For example, a trace metal that is strongly bound to colloidal particles generally is not toxic because it is not available to aquatic lifeforms. Unfortunately, anodic stripping voltammetry can not distinguish a trace metal's exact chemical form because closely related species, such as Pb^{2+} and $PbCl^{+}$, produce a single stripping peak. Instead, trace metals are divided into "operationally defined" categories that have environmental significance.

Operationally defined means that an analyte is divided into categories by the specific methods used to isolate it from the sample. There are many examples of operational definitions in the environmental literature. The distribution of trace metals in soils and sediments, for example, often is defined in terms of the reagents used to extract them; thus, you might find an operational definition for Zn^{2+} in a lake sediment as that extracted using 1.0 M sodium acetate, or that extracted using 1.0 M HCl.

Although there are many speciation schemes in the environmental literature, we will consider one proposed by Batley and Florence [see (a) Batley, G. E.; Florence, T. M. *Anal. Lett.* **1976**, *9*, 379–388; (b) Batley, G. E.; Florence, T. M. *Talanta* **1977**, *24*, 151–158; (c) Batley, G. E.; Florence, T. M. *Anal. Chem.* **1980**, *52*, 1962–1963; (d) Florence, T. M., Batley, G. E.; *CRC Crit. Rev. Anal. Chem.* **1980**, *9*, 219–296]. This scheme, which is outlined in Table 5.4.2 , combines anodic stripping voltammetry with ion-exchange and UV irradiation, dividing soluble trace metals into seven groups. In the first step, anodic stripping voltammetry in a pH 4.8 acetic acid buffer differentiates between labile metals and nonlabile metals. Only labile metals—those present as hydrated ions, weakly bound complexes, or weakly adsorbed on colloidal surfaces—deposit at the electrode and give rise to a signal. Total metal concentration are determined by ASV after digesting the sample in 2 M HNO_3 for 5 min, which converts all metals into an ASV-labile form.

Table 5.4.2 . Operational Speciation of Soluble Trace Metals

method	speciation of soluble metals						
ASV	labile metals			nonlabile or bound metals			
Ion-Exchange	removed	not removed		removed		not removed	
UV Irradiation		released	not released	released	not released	released	not released
Groups	I	II	III	IV	V	VI	VII
Group I: free metal ions; weaker labile organic complexes and inorganic complexes							
Group II: stronger labile organic complexes; labile metals absorbed on organic solids							
Group III: stronger labile inorganic complexes; labile metals absorbed on inorganic solids							
Group IV: weaker nonlabile organic complexes							
Group V: weaker nonlabile inorganic complexes							
Group VI: stronger nonlabile organic complexes; nonlabile metals absorbed on organic solids							
Group VII: stronger nonlabile inorganic complexes; nonlabile metals absorbed on inorganic solids							
Operational definitions of speciation from (a)Batley,G.E.;Florence,T.M.*Anal.Lett.***1976**,*9*,379–388; (b)Batley,G.E.;Florence,T.M.*Talanta***1977**,*24*,151–158; (c) Batley, G. E.; Florence, T. M. *Anal. Chem.* **1980**, *52*, 1962–1963; (d) Florence, T. M., Batley, G. E.; *CRC Crit. Rev. Anal. Chem.* **1980**, *9*, 219–296.							

A Chelex-100 ion-exchange resin further differentiates between strongly bound metals—usually metals bound to inorganic and organic solids, but also those tightly bound to chelating ligands—and more loosely bound metals. Finally, UV radiation differentiates between metals bound to organic phases and inorganic phases. The analysis of seawater samples, for example, suggests that cadmium, copper, and lead are present primarily as labile organic complexes or as labile adsorbates on organic colloids (Group II in Table 5.4.2).

Differential pulse polarography and stripping voltammetry are used to determine trace metals in airborne particulates, incinerator fly ash, rocks, minerals, and sediments. The trace metals, of course, are first brought into solution using a digestion or an extraction.

Amperometric sensors also are used to analyze environmental samples. For example, the dissolved O_2 sensor described earlier is used to determine the level of dissolved oxygen and the biochemical oxygen demand, or BOD, of waters and wastewaters. The latter test—which is a measure of the amount of oxygen required by aquatic bacteria as they decompose organic matter—is important when evaluating the efficiency of a wastewater treatment plant and for monitoring organic pollution in natural waters. A high BOD suggests that the water has a high concentration of organic matter. Decomposition of this organic matter may seriously deplete the level of dissolved oxygen in the water, adversely affecting aquatic life. Other amperometric sensors are available to monitor anionic surfactants in water, and CO_2, H_2SO_4, and NH_3 in atmospheric gases.

Clinical Samples

Differential pulse polarography and stripping voltammetry are used to determine the concentration of trace metals in a variety of clinical samples, including blood, urine, and tissue. The determination of lead in blood is of considerable interest due to concerns about lead poisoning. Because the concentration of lead in blood is so small, anodic stripping voltammetry frequently is the more appropriate technique. The analysis is complicated, however, by the presence of proteins that may adsorb to the mercury electrode, inhibiting either the deposition or stripping of lead. In addition, proteins may prevent the electrodeposition of lead through the formation of stable, nonlabile complexes. Digesting and ashing the blood sample mini- mizes this problem. Differential pulse polarography is useful for the routine quantitative analysis of drugs in biological fluids, at concentrations of less than 10^{-6} M [Brooks, M. A. “Application of Electrochemistry to Pharmaceutical Analysis,” Chapter 21 in Kissinger, P. T.; Heinemann, W. R., eds. *Laboratory Techniques in Electroanalytical Chemistry*, Marcel Dekker, Inc.: New York, 1984, pp 539–568.]. Amperometric sensors using enzyme catalysts also have many clinical uses, several examples of which are shown in Table 5.4.3 .

Table 5.4.3 . Representative Amperometric Biosensors

analyte	enzyme	species detected
choline	choline oxidase	H_2O_2
ethanol	alcohol oxidase	H_2O_2
formaldehyde	formaldehyde dehydrogenase	NADH
glucose	glucose oxidase	H_2O_2
glutamine	glutaminase, glutamine oxidase	H_2O_2
glycerol	glycerol dehydrogenase	NADH, O_2
lactate	lactate oxidase	H_2O_2
phenol	polyphenol oxidase	quinone
inorganic phosphorous	nucleoside phosphoylase	O_2

Source: Cammann, K.; Lemke, U.; Rohen, A.; Sander, J.; Wilken, H.; Winter, B. *Angew. Chem. Int. Ed. Engl.* **1991**, *30*, 516–539.

Miscellaneous Samples

In addition to environmental samples and clinical samples, differential pulse polarography and stripping voltammetry are used for the analysis of trace metals in other sample, including food, steels and other alloys, gasoline, gunpowder residues, and pharmaceuticals. Voltammetry is an important technique for the quantitative analysis of organics, particularly in the pharmaceutical industry where it is used to determine the concentration of drugs and vitamins in formulations. For example, voltammetric methods are available for the quantitative analysis of vitamin A, niacinamide, and riboflavin. When the compound of interest is not electroactive, it often can be derivatized to an electroactive form. One example is the differential pulse polarographic determination of sulfanilamide, which is converted into an electroactive azo dye by coupling with sulfamic acid and 1-napthol.

Representative Method 11.4.1: Determination of Chloropromazine in a Pharmaceutical Product

The best way to appreciate the theoretical and the practical details discussed in this section is to carefully examine a typical analytical method. Although each method is unique, the following description of the determination of chloropromazine in a pharmaceutical product provides an instructive example of a typical procedure. The description here is based on a method from Pungor, E. *A Practical Guide to Instrumental Analysis*, CRC Press: Boca Raton, FL, 1995, pp. 34–37.

Description of Method

Chlorpromazine, also is known by its trade name Thorazine, is an antipsychotic drug used in the treatment of schizophrenia. The amount of chlorpromazine in a pharmaceutical product is determined voltammetrically at a graphite working electrode in a unstirred solution, with calibration by the method of standard additions.

Procedure

Add 10.00 mL of an electrolyte solution consisting of 0.01 M HCl and 0.1 M KCl to the electrochemical cell. Place a graphite working electrode, a Pt auxiliary electrode, and a SCE reference electrode in the cell, and record the voltammogram from 0.2 V to 2.0 V at a scan rate of 50 mV/s. Weigh out an appropriate amount of the pharmaceutical product and dissolve it in a small amount of the electrolyte. Transfer the solution to a 100-mL volumetric flask and dilute to volume with the electrolyte. Filter a small amount of the diluted solution and transfer 1.00 mL of the filtrate to the voltammetric cell. Mix the contents of the voltammetric cell and allow the solution to sit for 10 s before recording the voltammogram. Return the potential to 0.2 V, add 1.00 mL of a chlorpromazine standard and record the voltammogram. Report the %w/w chlorpromazine in the formulation.

Questions

1. Is chlorpromazine undergoing oxidation or reduction at the graphite working electrode?

    Because we are scanning toward more positive potentials, we are oxidizing chlorpromazine.

2. Why does this procedure use a graphite electrode instead of a Hg electrode?

As shown in Figure 5.4.2 , the potential window for a Hg electrode extends from approximately –0.3 V to between –1V and –2 V, de- pending on the pH. Because we are scanning the potential from 0.2 V to 2.0 V, we cannot use a Hg electrode.

3. Many voltammetric procedures require that we first remove dissolved O_2 by bubbling N_2 through the solution. Why is this not necessary for this analysis?

Dissolved O_2 is a problem when we scan toward more negative potentials, because its reduction may produce a significant cathodic current. In this procedure we are scanning toward more positive potentials and generating anodic currents; thus, dissolved O_2 is not an interferent and does not need to be removed.

4. What is the purpose of recording a voltammogram in the absence of chlorpromazine?

This voltammogram serves as a blank, which provides a measurement of the residual current due to the electrolyte. Because the potential window for a graphite working electrode (see Figure 5.4.2) does not extend to 2.0 V, there is a measurable anodic residual current due to the solvent's oxidation. Having measured this residual current, we can subtract it from the total current in the presence of chlorpromazine.

5. Based on the description of this procedure, what is the shape of the resulting voltammogram. You may wish to review the three common shapes shown in Figure 5.4.9 .

Because the solution is unstirred, the voltammogram will have a peak current similar to that shown in Figure 5.4.9 b.

Characterization Applications

In the previous section we learned how to use voltammetry to determine an analyte's concentration in a variety of different samples. We also can use voltammetry to characterize an analyte's properties, including verifying its electrochemical reversibility, determining the number of electrons transferred during its oxidation or reduction, and determining its equilibrium constant in a coupled chemical reaction.

Electrochemical Reversibility and Determination of *n*

Earlier in this chapter we derived a relationship between $E_{1/2}$ and the standard-state potential for a redox couple (Equation 5.4.6), noting that a redox reaction must be electrochemically reversible. How can we tell if a redox reaction is reversible by looking at its voltammogram? For a reversible redox reaction Equation 5.4.5, which we repeat here, describes the relationship between potential and current for a voltammetric experiment with a limiting current.

$$E = E^{\circ}_{O/R} - \frac{0.05916}{n}\log\frac{K_O}{K_R} - \frac{0.05916}{n}\log\frac{i}{i_l - i}$$

If a reaction is electrochemically reversible, a plot of E versus $\log(i/i_l - i)$ is a straight line with a slope of $-0.05916/n$. In addition, the slope should yield an integer value for n.

Example 5.4.3

The following data were obtained from a linear scan hydrodynamic voltammogram of a reversible reduction reaction.

E (V vs. SCE)	current (μA)
–0.358	0.37
–0.372	0.95
–0.382	1.71
–0.400	3.48
–0.410	4.20
–0.435	4.97

The limiting current is 5.15 μA. Show that the reduction reaction is reversible, and determine values for n and for $E_{1/2}$.

Solution

Figure 5.4.20 shows a plot of E versus $\log(i/i_l–i)$. Because the result is a straight-line, we know the reaction is electrochemically reversible under the conditions of the experiment. A linear regression analysis gives the equation for the straight line as

$$E = -0.391\text{V} - 0.0300 \log \frac{i}{i_l - i}$$

From Equation 5.4.5, the slope is equivalent to –0.05916/n; solving for n gives a value of 1.97, or 2 electrons. From Equation 5.4.5 and Equation 5.4.6, we know that $E_{1/2}$ is the y-intercept for a plot of E versus $\log(i/i_l - i)$; thus, $E_{1/2}$ for the data in this example is –0.391 V versus the SCE.

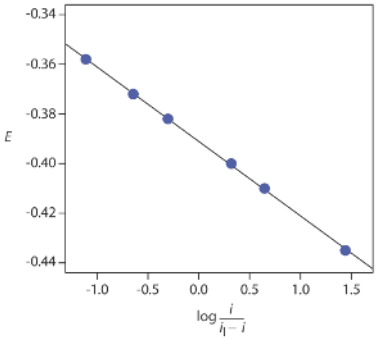


Figure 5.4.20 . Determination of electrochemical reversibility for the data in Example 5.4.3 .

We also can use cyclic voltammetry to evaluate electrochemical reversibility by looking at the difference between the peak potentials for the anodic and the cathodic scans. For an electrochemically reversible reaction, the following equation holds true.

$$\Delta E_p = E_{p,a} - E_{p,c} = \frac{0.05916\ \text{V}}{n}$$

As an example, for a two-electron reduction we expect a ΔE_p of approximately 29.6 mV. For an electrochemically irreversible reaction the value of ΔE_p is larger than expected.

Determining Equilibrium Constants for Coupled Chemical Reactions

Another important application of voltammetry is determining the equilibrium constant for a solution reaction that is coupled to a redox reaction. The presence of the solution reaction affects the ease of electron transfer in the redox reaction, shifting $E_{1/2}$ to a more negative or to a more positive potential. Consider, for example, the reduction of O to R

$$O + ne^- \rightleftharpoons R$$

the voltammogram for which is shown in Figure 5.4.21 . If we introduce a ligand, L, that forms a strong complex with O, then we also must consider the reaction

$$O + pL \rightleftharpoons OL_p$$

In the presence of the ligand, the overall redox reaction is

$$OL_p + ne^- \rightleftharpoons R + pL$$

Because of its stability, the reduction of the OL_p complex is less favorable than the reduction of O. As shown in Figure 5.4.21 , the resulting voltammogram shifts to a potential that is more negative than that for O. Furthermore, the shift in the voltammogram increases as we increase the ligand's concentration.

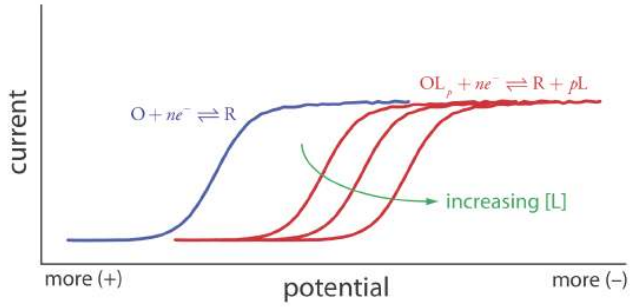


Figure 5.4.21 . Effect of a metal-ligand complexation reaction on a voltammogram. The voltammogram in blue is for the reduction of *O* in the absence of ligand. Adding the ligand shifts the potentials to more negative potentials, as shown by the voltammograms in red.

We can use this shift in the value of $E_{1/2}$ to determine both the stoichiometry and the formation constant for a metal-ligand complex. To derive a relationship between the relevant variables we begin with two equations: the Nernst equation for the reduction of *O*

$$E = E^\circ_{O/R} - \frac{0.05916}{n} \log \frac{[R]_{x=0}}{[O]_{x=0}} \tag{5.4.7}$$

and the stability constant, β_p for the metal-ligand complex at the electrode surface.

$$\beta_p = \frac{[OL_p]_{x=0}}{[O]_{x=0}[L]^p_{x=0}} \tag{5.4.8}$$

In the absence of ligand the half-wave potential occurs when $[R]_{x\,=\,0}$ and $[O]_{x\,=\,0}$ are equal; thus, from the Nernst equation we have

$$(E_{1/2})_{nc} = E^\circ_{O/R} \tag{5.4.9}$$

where the subscript "*nc*" signifies that the complex is not present.
When ligand is present we must account for its effect on the concentration of *O*. Solving Equation 5.4.1 for $[O]_{x\,=\,0}$ and substituting into the Equation 5.4.7 gives

$$E = E^\circ_{O/R} - \frac{0.05916}{n} \log \frac{[R]_{x=0}[L]^p_{x=0}\beta_p}{[OL_p]_{x=0}} \tag{5.4.10}$$

If the formation constant is sufficiently large, such that essentially all *O* is present as the complex OL_p, then $[R]_{x\,=\,0}$ and $[OL_p]_{x\,=\,0}$ are equal at the half-wave potential, and Equation 5.4.10 simplifies to

$$(E_{1/2})_c = E^\circ_{O/R} - \frac{0.05916}{n} \log [L]^p_{x=0}\beta_p \tag{5.4.11}$$

where the subscript "*c*" indicates that the complex is present. Defining $\Delta E_{1/2}$ as

$$\triangle E_{1/2} = (E_{1/2})_c - (E_{1/2})_{nc} \tag{5.4.12}$$

and substituting Equation 5.4.9 and Equation 5.4.11 and expanding the log term leaves us with the following equation.

$$\Delta E_{1/2} = -\frac{0.05916}{n} \log \beta_p - \frac{0.05916p}{n} \log [L] \tag{5.4.13}$$

A plot of $\Delta E_{1/2}$ versus log[*L*] is a straight-line, with a slope that is a function of the metal-ligand complex's stoichiometric coefficient, *p*, and a *y*-intercept that is a function of its formation constant β_p.

Example 5.4.4

A voltammogram for the two-electron reduction (n = 2) of a metal, *M*, has a half-wave potential of –0.226 V versus the SCE. In the presence of an excess of ligand, *L*, the following half-wave potentials are recorded.

[L] (M)	$(E_{1/2})_c$ (V vs. SCE)
0.020	–0.494
0.040	–0.512
0.060	–0.523
0.080	–0.530
0.100	–0.536

Determine the stoichiometry of the metal-ligand complex and its formation constant.

Solution

We begin by calculating values of $\Delta E_{1/2}$ using Equation 5.4.12, obtaining the values in the following table.

[L] (M)	$\Delta E_{1/2}$ (V vs. SCE)
0.020	–0.268
0.040	–0.286
0.060	–0.297
0.080	–0.304
0.100	–0.310

Figure 5.4.22 shows the resulting plot of $\Delta E_{1/2}$ as a function of log[L]. A linear regression analysis gives the equation for the straight line as

$$\Delta E_{1/2} = -0.370\text{V} - 0.0601 \log [L]$$

From Equation 5.4.13 we know that the slope is equal to –0.05916p/n. Using the slope and n = 2, we solve for p obtaining a value of 2.03 ≈ 2. The complex's stoichiometry, therefore, is ML_2. We also know, from Equation 5.4.13, that the y-intercept is equivalent to –(0.05916/n)logβ_p. Solving for β_2 gives a formation constant of 3.2×10^{12}.

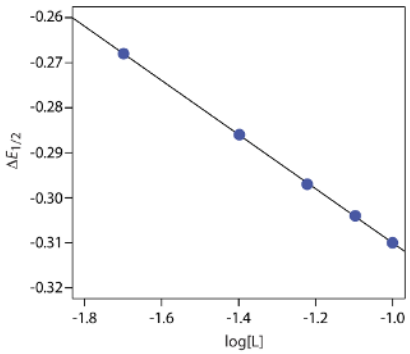


Figure 5.4.22 . Determination of the stoichiometry and formation constant for a metal-ligand complex using the data in Example 5.4.4 .

? Exercise 5.4.2

The voltammogram for 0.50 mM Cd^{2+} has an $E_{1/2}$ of –0.565 V versus an SCE. After making the solution 0.115 M in ethylenediamine, $E_{1/2}$ is –0.845 V, and $E_{1/2}$ is –0.873 V when the solution is 0.231 M in ethylenediamine. Determine the stoichiometry of the Cd^{2+}–ethylenediamine complex and its formation constant. The data in this problem comes from

Morinaga, K. "Polarographic Studies of Metal Complexes. V. Ethylenediamine Complexes of Cadmium, Nickel, and Zinc," *Bull. Chem. Soc. Japan* **1956**, *29*, 793–799.

Answer

For simplicity, we will use *en* as a shorthand notation for ethylenediamine. From the three half-wave potentials we have a $\Delta E_{1/2}$ of –0.280 V for 0.115 M en and a $\Delta E_{1/2}$ of –0.308 V for 0.231 M en. Using Equation 5.4.13 we write the following two equations.

$$-0.280 = -\frac{0.05916}{2}\log\beta_p - \frac{0.05916p}{2}\log(0.115)$$
$$-0.308 = -\frac{0.05916}{2}\log\beta_p - \frac{0.05916p}{2}\log(0.231)$$

To solve for the value of *p*, we first subtract the second equation from the first equation

$$0.028 = -\frac{0.05916p}{2}\log(0.115) - \left\{-\frac{0.05916p}{2}\log(0.231)\right\}$$

which eliminates the term with β_p. Next we solve this equation for *p*

$$0.028 = \left(2.778 \times 10^{-2}\right) \times p - \left(1.882 \times 10^{-2}\right) \times p = \left(8.96 \times 10^{-3}\right) \times p$$

obtaining a value of 3.1, or $p \approx 3$. Thus, the complex is $Cd(en)_3$. To find the formation complex, β_3, we return to Equation 5.4.13, using our value for *p*. Using the data for an en concentration of 0.115 M

$$-0.280 = -\frac{0.05916}{2}\log\beta_3 - \frac{0.05916 \times 3}{2}\log(0.115)$$
$$-0.363 = -\frac{0.05916}{2}\log\beta_3$$

gives a value for β_3 of 1.92×10^{12}. Using the data for an en concentration of 0.231 M gives a value of 2.10×10^{12}.

As suggested by Figure 5.4.15 , cyclic voltammetry is one of the most powerful electrochemical techniques for exploring the mechanism of coupled electrochemical and chemical reactions. The treatment of this aspect of cyclic voltammetry is beyond the level of this text, although you can consult this chapter's additional resources for additional information.

Evaluation

Scale of Operation

Detection levels at the parts-per-million level are routine. For some analytes and for some voltammetric techniques, lower detection limits are possible. Detection limits at the parts-per-billion and the part-per-trillion level are possible with stripping voltammetry. Although most analyses are carried out in conventional electrochemical cells using macro samples, the availability of microelectrodes with diameters as small as 2 μm, allows for the analysis of samples with volumes under 50 μL. For example, the concentration of glucose in 200-μm pond snail neurons was monitored successfully using an amperometric glucose electrode with a 2 mm tip [Abe, T.; Lauw, L. L.; Ewing, A. G. *J. Am. Chem. Soc.* **1991**, *113*, 7421–7423].

Accuracy

The accuracy of a voltammetric analysis usually is limited by our ability to correct for residual currents, particularly those due to charging. For an analyte at the parts-per-million level, an accuracy of ±1–3% is routine. Accuracy decreases for samples with significantly smaller concentrations of analyte.

Precision

Precision generally is limited by the uncertainty in measuring the limiting current or the peak current. Under most conditions, a precision of ±1–3% is reasonable. One exception is the analysis of ultratrace analytes in complex matrices by stripping voltammetry, in which the precision may be as poor as ±25%.

Sensitivity

In many voltammetric experiments, we can improve the sensitivity by adjusting the experimental conditions. For example, in stripping voltammetry we can improve sensitivity by increasing the deposition time, by increasing the rate of the linear potential scan, or by using a differential-pulse technique. One reason that potential pulse techniques are popular is that they provide an improvement in current relative to a linear potential scan.

Selectivity

Selectivity in voltammetry is determined by the difference between half-wave potentials or peak potentials, with a minimum difference of ±0.2–0.3 V for a linear potential scan and ±0.04–0.05 V for differential pulse voltammetry. We often can improve selectivity by adjusting solution conditions. The addition of a complexing ligand, for example, can substantially shift the potential where a species is oxidized or reduced to a potential where it no longer interferes with the determination of an analyte. Other solution parameters, such as pH, also can be used to improve selectivity.

Time, Cost, and Equipment

Commercial instrumentation for voltammetry ranges from <$1000 for simple instruments to >$20,000 for a more sophisticated instrument. In general, less expensive instrumentation is limited to linear potential scans. More expensive instruments provide for more complex potential-excitation signals using potential pulses. Except for stripping voltammetry, which needs a long deposition time, voltammetric analyses are relatively rapid.

This page titled 5.4: Voltammetric and Amperometric Methods is shared under a CC BY-NC-SA 4.0 license and was authored, remixed, and/or curated by Kathryn Davis.

- **11.4: Voltammetric and Amperometric Methods** by David Harvey is licensed CC BY-NC-SA 4.0.

CHAPTER OVERVIEW

6: Beyond Beer's Law- Quantitative Spectroscopic Analysis

6.1: Overview of Spectroscopy
6.2: Spectroscopy Based on Absorption
6.3: UV/Vis and IR Spectroscopy
6.4: Atomic Absorption Spectroscopy
6.5: Photoluminescent Spectroscopy
6.6: Atomic Emission Spectroscopy

This page titled 6: Beyond Beer's Law- Quantitative Spectroscopic Analysis is shared under a not declared license and was authored, remixed, and/or curated by Kathryn Davis.

6.1: Overview of Spectroscopy

The focus of this chapter is on the interaction of ultraviolet, visible, and infrared radiation with matter. Because these techniques use optical materials to disperse and focus the radiation, they often are identified as optical spectroscopies. For convenience we will use the simpler term spectroscopy in place of optical ***spectroscopy***; however, you should understand we will consider only a limited piece of what is a much broader area of analytical techniques.

Despite the difference in instrumentation, all spectroscopic techniques share several common features. Before we consider individual examples in greater detail, let's take a moment to consider some of these similarities. As you work through the chapter, this overview will help you focus on the similarities between different spectroscopic methods of analysis. You will find it easier to understand a new analytical method when you can see its relationship to other similar methods.

What is Electromagnetic Radiation?

Electromagnetic radiation—light—is a form of energy whose behavior is described by the properties of both waves and particles. Some properties of electromagnetic radiation, such as its refraction when it passes from one medium to another (Figure 6.1.1), are explained best when we describe light as a wave. Other properties, such as absorption and emission, are better described by treating light as a particle. The exact nature of electromagnetic radiation remains unclear, as it has since the development of quantum mechanics in the first quarter of the 20th century [Home, D.; Gribbin, J. *New Scientist* 1991, 2 Nov. 30–33]. Nevertheless, this dual model of wave and particle behavior provide a useful description for electromagnetic radiation.



Figure 6.1.1 . The Golden Gate bridge as seen through rain drops. Refraction of light by the rain drops produces the distorted images. Source: Brocken Inaglory (commons. Wikipedia.org).

Wave Properties of Electromagnetic Radiation

Electromagnetic radiation consists of oscillating electric and magnetic fields that propagate through space along a linear path and with a constant velocity. In a vacuum, electromagnetic radiation travels at the speed of light, c, which is 2.99792×10^8 m/s. When electromagnetic radiation moves through a medium other than a vacuum, its velocity, v, is less than the speed of light in a vacuum. The difference between v and c is sufficiently small (<0.1%) that the speed of light to three significant figures, 3.00×10^8 m/s, is accurate enough for most purposes.

The oscillations in the electric field and the magnetic field are perpendicular to each other and to the direction of the wave's propagation. Figure 6.1.2 shows an example of plane-polarized electromagnetic radiation, which consists of a single oscillating electric field and a single oscillating magnetic field.

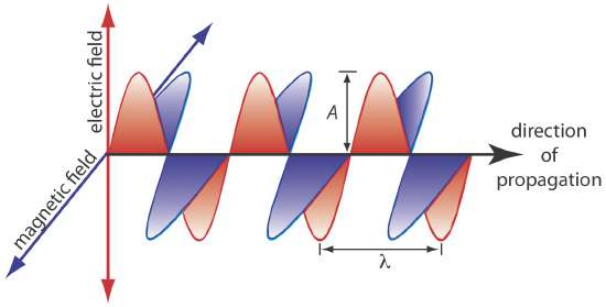


Figure 6.1.2 . Plane-polarized electromagnetic radiation showing the oscillating electric field in blue and the oscillating magnetic field in red. The radiation's amplitude, A, and its wavelength, λ, are shown. Normally, electromagnetic radiation is unpolarized, with oscillating electric and magnetic fields present in all possible planes perpendicular to the direction of propagation.

An electromagnetic wave is characterized by several fundamental properties, including its velocity, amplitude, frequency, phase angle, polarization, and direction of propagation [Ball, D. W. *Spectroscopy* **1994**, *9(5)*, 24–25]. For example, the amplitude of the oscillating electric field at any point along the propagating wave is

$$A_t = A_e \sin(2\pi\nu t + \Phi)$$

where A_t is the magnitude of the electric field at time t, A_e is the electric field's maximum ***amplitude***, ν is the wave's ***frequency***—the number of oscillations in the electric field per unit time—and Φ is a ***phase angle*** that accounts for the fact that A_t need not have a value of zero at $t = 0$. The identical equation for the magnetic field is

$$A_t = A_m \sin(2\pi\nu t + \Phi)$$

where A_m is the magnetic field's maximum amplitude.

Other properties also are useful for characterizing the wave behavior of electromagnetic radiation. The ***wavelength***, λ, is defined as the distance between successive maxima (see Figure 6.1.2). For ultraviolet and visible electromagnetic radiation the wavelength usually is expressed in nanometers (1 nm = 10^{-9} m), and for infrared radiation it is expressed in microns (1 mm = 10^{-6} m). The relationship between wavelength and frequency is

$$\lambda = \frac{c}{\nu}$$

Another unit useful unit is the ***wavenumber***, $\bar{\nu}$, which is the reciprocal of wavelength

$$\bar{\nu} = \frac{1}{\lambda}$$

Wavenumbers frequently are used to characterize infrared radiation, with the units given in cm^{-1}.

When electromagnetic radiation moves between different media—for example, when it moves from air into water—its frequency, ν, remains constant. Because its velocity depends upon the medium in which it is traveling, the electromagnetic radiation's wavelength, λ, changes. If we replace the speed of light in a vacuum, c, with its speed in the medium, v, then the wavelength is

$$\lambda = \frac{v}{\nu}$$

This change in wavelength as light passes between two media explains the refraction of electromagnetic radiation shown in Figure 6.1.1 .

Particle Properties of Electromagnetic Radiation

When matter absorbs electromagnetic radiation it undergoes a change in energy. The interaction between matter and electromagnetic radiation is easiest to understand if we assume that radiation consists of a beam of energetic particles called photons. When a ***photon*** is absorbed by a sample it is "destroyed" and its energy acquired by the sample [Ball, D. W. *Spectroscopy*

1994, *9(6)* 20–21]. The energy of a photon, in joules, is related to its frequency, wavelength, and wavenumber by the following equalities

$$E = h\nu = \frac{hc}{\lambda} = hc\bar{\nu}$$

where *h* is Planck's constant, which has a value of 6.626×10^{-34} Js.

The Electromagnetic Spectrum

The frequency and the wavelength of electromagnetic radiation vary over many orders of magnitude. For convenience, we divide electromagnetic radiation into different regions—the ***electromagnetic spectrum***—based on the type of atomic or molecular transitions that gives rise to the absorption or emission of photons (Figure 6.1.3). The boundaries between the regions of the electromagnetic spectrum are not rigid and overlap between spectral regions is possible.

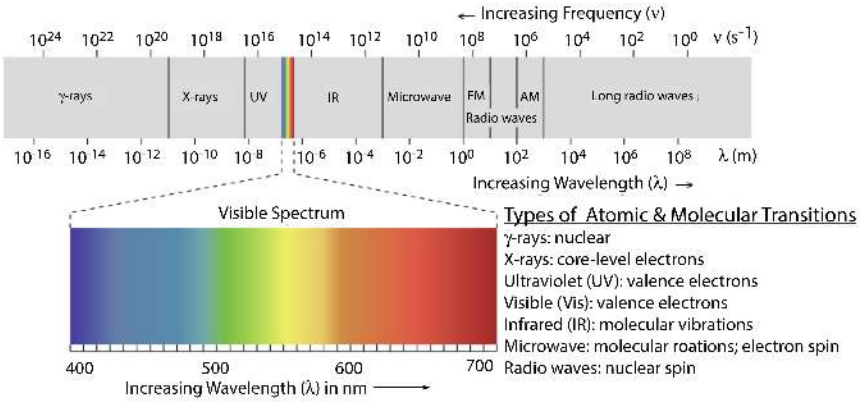


Figure 6.1.3 . The electromagnetic spectrum showing the boundaries between different regions and the type of atomic or molecular transitions responsible for the change in energy. The colored inset shows the visible spectrum. Source: modified from Zedh (www.commons.Wikipedia.org).

Photons as a Signal Source

In the previous section we defined several characteristic properties of electromagnetic radiation, including its energy, velocity, amplitude, frequency, phase angle, polarization, and direction of propagation. A spectroscopic measurement is possible only if the photon's interaction with the sample leads to a change in one or more of these characteristic properties.

We will divide spectroscopy into two broad classes of techniques. In one class of techniques there is a transfer of energy between the photon and the sample. Table 6.1.1 provides a list of several representative examples.

Table 6.1.1 . Examples of Spectroscopic Techniques That Involve an Exchange of Energy Between a Photon and the Sample

type of energy transfer	region of electromagnetic spectrum	spectroscopic technique
absorption	γ-ray	Mossbauer spectroscopy
	X-ray	X-ray absorption spectroscopy
	UV/Vis	*UV/Vis spectroscopy*
	IR	*infrared spectroscopy*
	microwave	raman spectroscopy
	radio wave	electron spin resonance nuclear magnetic resonance
emission (thermal excitation)	UV/Vis	*atomic emission spectroscopy*
photoluminescence	X-ray	X-ray fluorescence
	UV/Vis	*fluorescence spectroscopy* *phosphorescence spectroscopy* atomic fluorescence spectroscopy
chemiluminescence	UV/Vis	chemiluminescence spectroscopy
techniques discussed in this chapter are shown in *italics*		

In absorption spectroscopy a photon is absorbed by an atom or molecule, which undergoes a transition from a lower-energy state to a higher-energy, or excited state (Figure 6.1.4). The type of transition depends on the photon's energy. The electromagnetic spectrum in Figure 6.1.3 , for example, shows that absorbing a photon of visible light promotes one of the atom's or molecule's valence electrons to a higher-energy level. When an molecule absorbs infrared radiation, on the other hand, one of its chemical bonds experiences a change in vibrational energy.

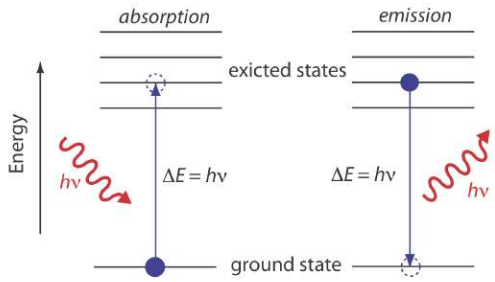


Figure 6.1.4 . A simplified energy diagram that shows the absorption and emission of a photon by an atom or a molecule. When a photon of energy $h\nu$ strikes the atom or molecule, absorption may occur if the difference in energy, ΔE, between the ground state and the excited state is equal to the photon's energy. An atom or molecule in an excited state may emit a photon and return to the ground state. The photon's energy, $h\nu$, equals the difference in energy, ΔE, between the two states.

When it absorbs electromagnetic radiation the number of photons passing through a sample decreases. The measurement of this decrease in photons, which we call ***absorbance***, is a useful analytical signal. Note that each energy level in Figure 6.1.4 has a well-defined value because each is quantized. Absorption occurs only when the photon's energy, $h\nu$, matches the difference in energy, ΔE, between two energy levels. A plot of absorbance as a function of the photon's energy is called an ***absorbance spectrum***. Figure 6.1.5 , for example, shows the absorbance spectrum of cranberry juice.

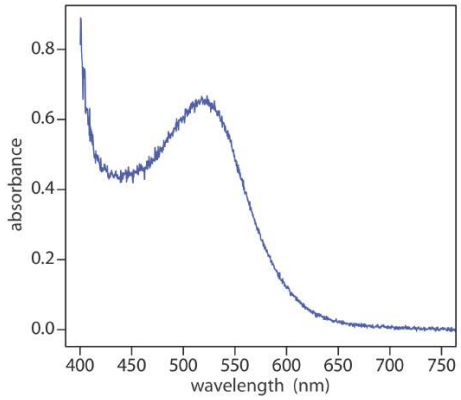


Figure 6.1.5 . Visible absorbance spectrum for cranberry juice. The anthocyanin dyes in cranberry juice absorb visible light with blue, green, and yellow wavelengths (see Figure 6.1.3). As a result, the juice appears red.

When an atom or molecule in an excited state returns to a lower energy state, the excess energy often is released as a photon, a process we call ***emission*** (Figure 6.1.4). There are several ways in which an atom or a molecule may end up in an excited state, including thermal energy, absorption of a photon, or as the result of a chemical reaction. Emission following the absorption of a photon is also called ***photoluminescence***, and that following a chemical reaction is called ***chemiluminescence***. A typical emission spectrum is shown in Figure 6.1.6 .

> Molecules also can release energy in the form of heat. We will return to this point later in the chapter.

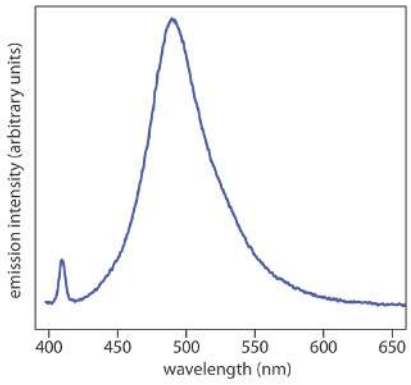


Figure 6.1.6 . Photoluminescence spectrum of the dye coumarin 343, which is incorporated in a reverse micelle suspended in cyclohexanol. The dye's absorbance spectrum (not shown) has a broad peak around 400 nm. The sharp peak at 409 nm is from the laser source used to excite coumarin 343. The broad band centered at approximately 500 nm is the dye's emission band. Because the dye absorbs blue light, a solution of coumarin 343 appears yellow in the absence of photoluminescence. Its photoluminescent emission is blue-green. Source: data from Bridget Gourley, Department of Chemistry & Biochemistry, DePauw University.

In the second broad class of spectroscopic techniques, the electromagnetic radiation undergoes a change in amplitude, phase angle, polarization, or direction of propagation as a result of its refraction, reflection, scattering, diffraction, or dispersion by the sample. Several representative spectroscopic techniques are listed in Table 6.1.2 .

Table 6.1.2 . Examples of Spectroscopic Techniques That Do Not Involve an Exchange of Energy Between a Photon and the Sample

region of electromagnetic spectrum	type of interaction	spectroscopic technique
X-ray	diffraction	X-ray diffraction
UV/Vis	refraction	refractrometry
	scattering	*nephelometry* *turbidimetry*
	dispersion	optical rotary dispersion
techniques discussed in this chapter are shown in *italics*		

Basic Components of Spectroscopic Instruments

The spectroscopic techniques in Table 6.1.1 and Table 6.1.2 use instruments that share several common basic components, including a source of energy, a means for isolating a narrow range of wavelengths, a detector for measuring the signal, and a signal processor that displays the signal in a form convenient for the analyst. In this section we introduce these basic components. Specific instrument designs are considered in later sections.

> You will find a more detailed treatment of these components in the additional resources for this chapter.

Sources of Energy

All forms of spectroscopy require a source of energy. In absorption and scattering spectroscopy this energy is supplied by photons. Emission and photoluminescence spectroscopy use thermal, radiant (photon), or chemical energy to promote the analyte to a suitable excited state.

Sources of Electromagnetic Radiation. A source of electromagnetic radiation must provide an output that is both intense and stable. Sources of electromagnetic radiation are classified as either continuum or line sources. A ***continuum source*** emits radiation over a broad range of wavelengths, with a relatively smooth variation in intensity (Figure 6.1.7). A ***line source***, on the other hand, emits radiation at selected wavelengths (Figure 6.1.8). Table 6.1.3 provides a list of the most common sources of electromagnetic radiation.

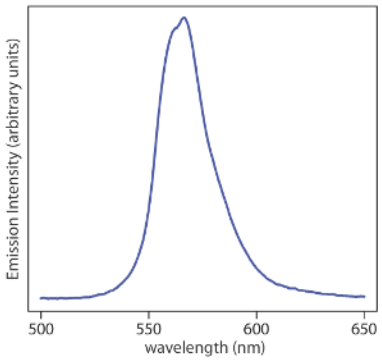


Figure 6.1.7 . Spectrum showing the emission from a green LED, which provides continuous emission over a wavelength range of approximately 530–640 nm.

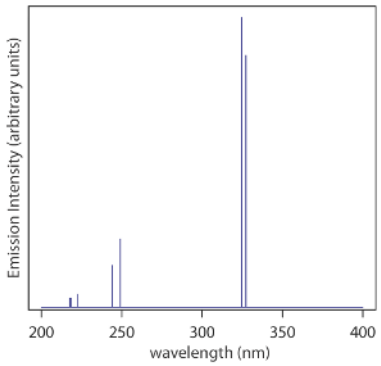


Figure 6.1.8 . Emission spectrum from a Cu hollow cathode lamp. This spectrum consists of seven distinct emission lines (the first two differ by only 0.4 nm and are not resolved at the scale shown in this spectrum). Each emission line has a width of approximately 0.01 nm at 1⁄2 of its maximum intensity.

Table 6.1.3 . Common Source of Electromagnetic Radiation

source	wavelength region	useful for...
H_2 and D_2 lamp	continuum source from 160–380 nm	molecular absorption
tungsten lamp	continuum source from 320–2400 nm	molecular absorption
Xe arc lamp	continuum source from 200–1000 nm	molecular fluorescence
nernst glower	continuum source from 0.4–20 μm	molecular absorption
globar	continuum source from 1–40 μm	molecular absorption
nichrome wire	continuum source from 0.75–20 μm	molecular absorption
hollow cathode lamp	line source in UV/Vis	atomic absorption
Hg vapor lamp	line source in UV/Vis	molecular fluorescence
laser	line source in UV/Vis/Ir	atomic and molecular absorption, fluorescence, and scattering

Sources of Thermal Radiation. The most common sources of thermal energy are flames and plasmas. A flame source uses a combustion of a fuel and an oxidant to achieve temperatures of 2000–3400 K. Plasmas, which are hot, ionized gases, provide temperatures of 6000–10000 K.

Chemical Sources of Energy. Exothermic reactions also may serve as a source of energy. In chemiluminescence the analyte is raised to a higher-energy state by means of a chemical reaction, emitting characteristic radiation when it returns to a lower-energy state. When the chemical reaction results from a biological or enzymatic reaction, the emission of radiation is called bioluminescence. Commercially available “light sticks” and the flash of light from a firefly are examples of chemiluminescence and bioluminescence.

Wavelength Selection

In Nessler’s original colorimetric method for ammonia, which was described at the beginning of the chapter, the sample and several standard solutions of ammonia are placed in separate tall, flat-bottomed tubes. As shown in Figure 6.1.9 , after adding the reagents and allowing the color to develop, the analyst evaluates the color by passing ambient light through the bottom of the tubes and looking down through the solutions. By matching the sample’s color to that of a standard, the analyst is able to determine the concentration of ammonia in the sample.

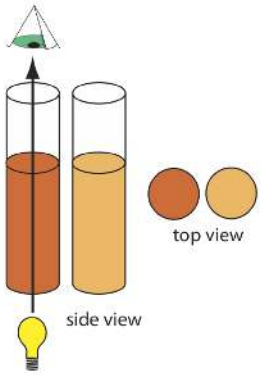


Figure 6.1.9 . Nessler's original method for comparing the color of two solutions. Natural light passes upwards through the samples and standards and the analyst views the solutions by looking down toward the light source. The top view, shown on the right, is what the analyst sees. To determine the analyte's concentration, the analyst exchanges standards until the two colors match.

In Figure 6.1.9 every wavelength of light from the source passes through the sample. This is not a problem if there is only one absorbing species in the sample. If the sample contains two components, then a quantitative analysis using Nessler's original method is impossible unless the standards contains the second component at the same concentration it has in the sample.

To overcome this problem, we want to select a wavelength that only the analyte absorbs. Unfortunately, we can not isolate a single wavelength of radiation from a continuum source, although we can narrow the range of wavelengths that reach the sample. As seen in Figure 6.1.10 , a wavelength selector always passes a narrow band of radiation characterized by a ***nominal wavelength***, an ***effective bandwidth***, and a maximum throughput of radiation. The effective bandwidth is defined as the width of the radiation at half of its maximum throughput.

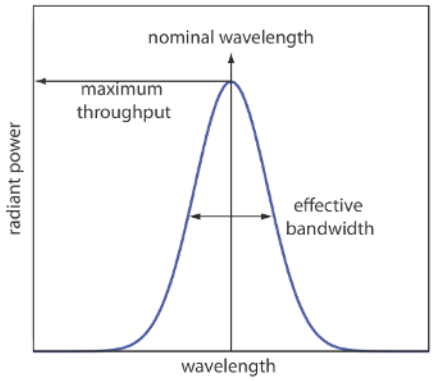


Figure 6.1.10 . Radiation exiting a wavelength selector showing the band's nominal wavelength and its effective bandwidth.

The ideal wavelength selector has a high throughput of radiation and a narrow effective bandwidth. A high throughput is desirable because the more photons that pass through the wavelength selector, the stronger the signal and the smaller the background noise. A narrow effective bandwidth provides a higher ***resolution***, with spectral features separated by more than twice the effective bandwidth being resolved. As shown in Figure 6.1.11 , these two features of a wavelength selector often are in opposition. A larger effective bandwidth favors a higher throughput of radiation, but provide less resolution. Decreasing the effective bandwidth improves resolution, but at the cost of a noisier signal [Jiang, S.; Parker, G. A. *Am. Lab.* **1981**, October, 38–43]. For a qualitative analysis, resolution usually is more important than noise and a smaller effective bandwidth is desirable; however, in a quantitative analysis less noise usually is desirable.

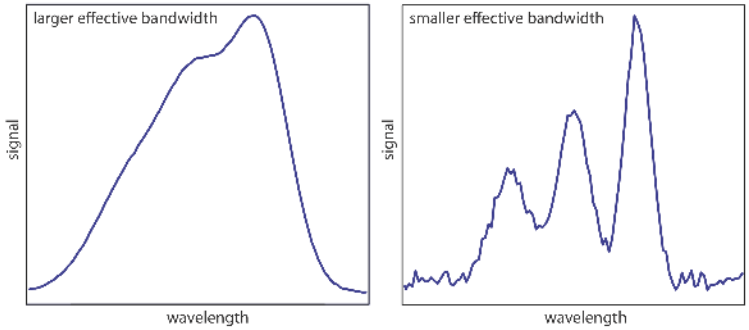


Figure 6.1.11 . Example showing the effect of the wavelength selector's effective bandwidth on resolution and noise. The spectrum with the smaller effective bandwidth (on the right) has a better resolution, allowing us to see the presence of three peaks, but at the expense of a noisier signal. The spectrum with the larger effective bandwidth (on the left) has less noise, but at the expense of less resolution between the three peaks.

Wavelength Selection Using Filters. The simplest method for isolating a narrow band of radiation is to use an absorption or interference ***filter***. Absorption filters work by selectively absorbing radiation from a narrow region of the electromagnetic spectrum. Interference filters use constructive and destructive interference to isolate a narrow range of wavelengths. A simple example of an absorption filter is a piece of colored glass. A purple filter, for example, removes the complementary color green from 500–560 nm.

Commercially available absorption filters provide effective bandwidths of 30–250 nm, although the throughput at the low end of this range often is only 10% of the source's emission intensity. Interference filters are more expensive than absorption filters, but have narrower effective bandwidths, typically 10–20 nm, with maximum throughputs of at least 40%.

Wavelength Selection Using Monochromators. A filter has one significant limitation—because a filter has a fixed nominal wavelength, if we need to make measurements at two different wavelengths, then we must use two different filters. A ***monochromator*** is an alternative method for selecting a narrow band of radiation that also allows us to continuously adjust the band's nominal wavelength.

The construction of a typical monochromator is shown in Figure 6.1.12 . Radiation from the source enters the monochromator through an entrance slit. The radiation is collected by a collimating mirror, which reflects a parallel beam of radiation to a diffraction grating. The diffraction grating is an optically reflecting surface with a large number of parallel grooves (see insert to Figure 6.1.12). The diffraction grating disperses the radiation and a second mirror focuses the radiation onto a planar surface that contains an exit slit. In some monochromators a prism is used in place of the diffraction grating.

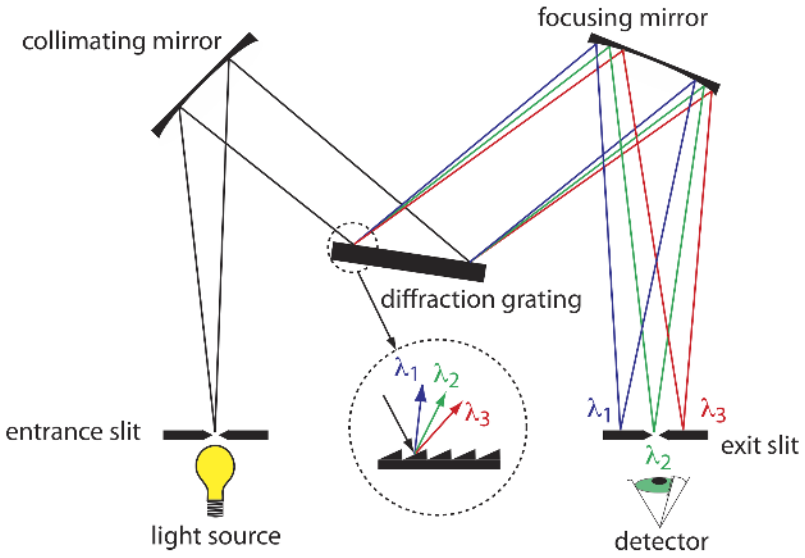


Figure 6.1.12 . Schematic diagram of a monochromator that uses a diffraction grating to disperse the radiation.

Radiation exits the monochromator and passes to the detector. As shown in Figure 6.1.12 , a monochromator converts a ***polychromatic*** source of radiation at the entrance slit to a ***monochromatic*** source of finite effective bandwidth at the exit slit. The

choice of which wavelength exits the monochromator is determined by rotating the diffraction grating. A narrower exit slit provides a smaller effective bandwidth and better resolution than does a wider exit slit, but at the cost of a smaller throughput of radiation.

> Polychromatic means many colored. Polychromatic radiation contains many different wavelengths of light. Monochromatic means one color, or one wavelength. Although the light exiting a monochromator is not strictly of a single wavelength, its narrow effective bandwidth allows us to think of it as monochromatic.

Monochromators are classified as either fixed-wavelength or scanning. In a fixed-wavelength monochromator we manually select the wavelength by rotating the grating. Normally a fixed-wavelength monochromator is used for a quantitative analysis where measurements are made at one or two wavelengths. A scanning monochromator includes a drive mechanism that continuously rotates the grating, which allows successive wavelengths of light to exit from the monochromator. A scanning monochromator is used to acquire spectra, and, when operated in a fixed-wavelength mode, for a quantitative analysis.

Interferometers. An ***interferometer*** provides an alternative approach for wavelength selection. Instead of filtering or dispersing the electromagnetic radiation, an interferometer allows source radiation of all wavelengths to reach the detector simultaneously (Figure 6.1.13). Radiation from the source is focused on a beam splitter that reflects half of the radiation to a fixed mirror and transmits the other half to a moving mirror. The radiation recombines at the beam splitter, where constructive and destructive interference determines, for each wavelength, the intensity of light that reaches the detector. As the moving mirror changes position, the wavelength of light that experiences maximum constructive interference and maximum destructive interference also changes. The signal at the detector shows intensity as a function of the moving mirror's position, expressed in units of distance or time. The result is called an ***interferogram*** or a time domain spectrum. The time domain spectrum is converted mathematically, by a process called a Fourier transform, to a spectrum (a frequency domain spectrum) that shows intensity as a function of the radiation's energy.

> The mathematical details of the Fourier transform are beyond the level of this textbook. You can consult the chapter's additional resources for additional information.

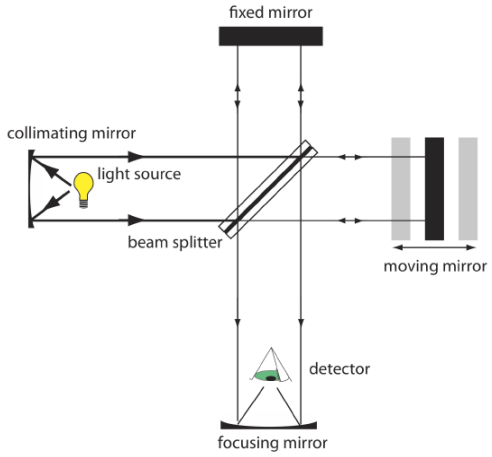


Figure 6.1.13 . Schematic diagram of an interferometers.

In comparison to a monochromator, an interferometer has two significant advantages. The first advantage, which is termed ***Jacquinot's advantage***, is the greater throughput of source radiation. Because an interferometer does not use slits and has fewer optical components from which radiation is scattered and lost, the throughput of radiation reaching the detector is $80 - 200\times$ greater than that for a monochromator. The result is less noise. The second advantage, which is called ***Fellgett's advantage***, is a savings in the time needed to obtain a spectrum. Because the detector monitors all frequencies simultaneously, a spectrum takes approximately one second to record, as compared to 10–15 minutes when using a scanning monochromator.

Detectors

In Nessler's original method for determining ammonia (Figure 6.1.9) the analyst's eye serves as the detector, matching the sample's color to that of a standard. The human eye, of course, has a poor range—it responds only to visible light—and it is not particularly sensitive or accurate. Modern detectors use a sensitive ***transducer*** to convert a signal consisting of photons into an easily measured electrical signal. Ideally the detector's signal, *S*, is a linear function of the electromagnetic radiation's power, *P*,

$$S = kP + D$$

where *k* is the detector's sensitivity, and *D* is the detector's ***dark current***, or the background current when we prevent the source's radiation from reaching the detector.

There are two broad classes of spectroscopic transducers: thermal transducers and photon transducers. Table 6.1.4 provides several representative examples of each class of transducers.

> Transducer is a general term that refers to any device that converts a chemical or a physical property into an easily measured electrical signal. The retina in your eye, for example, is a transducer that converts photons into an electrical nerve impulse; your eardrum is a transducer that converts sound waves into a different electrical nerve impulse.

Table 6.1.4 . Examples of Transducers for Spectroscopy

transducer	class	wavelength range	output signal
phototube	photon	200–1000 nm	current
photomultiplier	photon	110–1000 nm	current
Si photodiode	photon	250–1100 nm	current
photoconductor	photon	750–6000 nm	change in resistance
photovoltaic cell	photon	400–5000 nm	current or voltage
thermocouple	thermal	0.8–40 μm	voltage
thermistor	thermal	0.8–40 μm	change in resistance
pneumatic	thermal	0.8–1000 μm	membrane displacement
pyroelectric	thermal	0.3–1000 μm	current

Photon Transducers. Phototubes and photomultipliers use a photosensitive surface that absorbs radiation in the ultraviolet, visible, or near IR to produce an electrical current that is proportional to the number of photons reaching the transducer (Figure 6.1.14). Other photon detectors use a semiconductor as the photosensitive surface. When the semiconductor absorbs photons, valence electrons move to the semiconductor's conduction band, producing a measurable current. One advantage of the Si photodiode is that it is easy to miniaturize. Groups of photodiodes are gathered together in a linear array that contains 64–4096 individual photodiodes. With a width of 25 μm per diode, a linear array of 2048 photodiodes requires only 51.2 mm of linear space. By placing a ***photodiode array*** along the monochromator's focal plane, it is possible to monitor simultaneously an entire range of wavelengths.

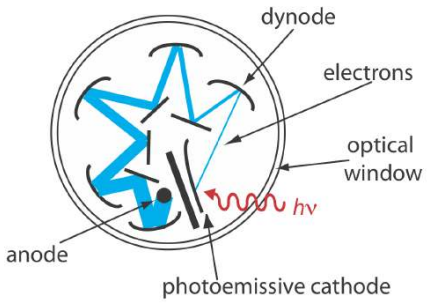


Figure 6.1.14 . Schematic of a photomultiplier. A photon strikes the photoemissive cathode producing electrons, which accelerate toward a positively charged dynode. Collision of these electrons with the dynode generates additional electrons, which accelerate toward the next dynode. A total of 10^6–10^7 electrons per photon eventually reach the anode, generating an electrical current.

Thermal Transducers. Infrared photons do not have enough energy to produce a measurable current with a photon transducer. A thermal transducer, therefore, is used for infrared spectroscopy. The absorption of infrared photons increases a thermal transducer's temperature, changing one or more of its characteristic properties. A pneumatic transducer, for example, is a small tube of xenon gas with an IR transparent window at one end and a flexible membrane at the other end. Photons enter the tube and are absorbed by a blackened surface, increasing the temperature of the gas. As the temperature inside the tube fluctuates, the gas expands and contracts and the flexible membrane moves in and out. Monitoring the membrane's displacement produces an electrical signal.

Signal Processors

A transducer's electrical signal is sent to a ***signal processor*** where it is displayed in a form that is more convenient for the analyst. Examples of signal processors include analog or digital meters, recorders, and computers equipped with digital acquisition boards. A signal processor also is used to calibrate the detector's response, to amplify the transducer's signal, to remove noise by filtering, or to mathematically transform the signal.

> If the retina in your eye and the eardrum in your ear are transducers, then your brain is the signal processor.

This page titled 6.1: Overview of Spectroscopy is shared under a CC BY-NC-SA 4.0 license and was authored, remixed, and/or curated by Kathryn Davis.

- **10.1: Overview of Spectroscopy** by David Harvey is licensed CC BY-NC-SA 4.0.

6.2: Spectroscopy Based on Absorption

In absorption spectroscopy a beam of electromagnetic radiation passes through a sample. Much of the radiation passes through the sample without a loss in intensity. At selected wavelengths, however, the radiation's intensity is attenuated. This process of attenuation is called absorption.

Absorption Spectra

There are two general requirements for an analyte's absorption of electromagnetic radiation. First, there must be a mechanism by which the radiation's electric field or magnetic field interacts with the analyte. For ultraviolet and visible radiation, absorption of a photon changes the energy of the analyte's valence electrons. A bond's vibrational energy is altered by the absorption of infrared radiation.

> Figure 10.1.3 provides a list of the types of atomic and molecular transitions associated with different types of electromagnetic radiation.

The second requirement is that the photon's energy, $h\nu$, must exactly equal the difference in energy, ΔE, between two of the analyte's quantized energy states. Figure 10.1.4 shows a simplified view of a photon's absorption, which is useful because it emphasizes that the photon's energy must match the difference in energy between a lower-energy state and a higher-energy state. What is missing, however, is information about what types of energy states are involved, which transitions between energy states are likely to occur, and the appearance of the resulting spectrum.

We can use the energy level diagram in Figure 6.2.1 to explain an absorbance spectrum. The lines labeled E_0 and E_1 represent the analyte's ground (lowest) electronic state and its first electronic excited state. Superimposed on each electronic energy level is a series of lines representing vibrational energy levels.

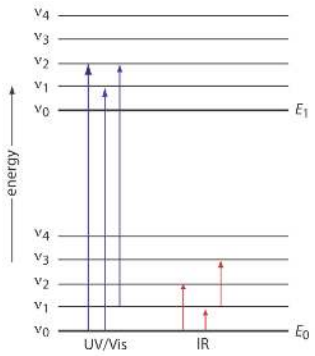


Figure 6.2.1 . Diagram showing two electronic energy levels (E_0 and E_1), each with five vibrational energy levels ν_{0-4}. Absorption of ultraviolet and visible radiation (shown by the blue arrows) leads to a change in the analyte's electronic energy levels and, possibly, a change in vibrational energy as well. A change in vibrational energy without a change in electronic energy levels occurs with the absorption of infrared radiation (shown by the red arrows).

Infrared Spectra for Molecules and Polyatomic Ions

The energy of infrared radiation produces a change in a molecule's or a polyatomic ion's vibrational energy, but is not sufficient to effect a change in its electronic energy. Looked at another way, electronic spectroscopy like UV-Vis involves promoting electrons to higher energy levels (HOMO to LUMO, pi to pi*, etc.), while vibrational spectroscopy like IR or Raman causes the nuclear positions to move as specific vibrational motions (stretches or bends) are stimulated. The resulting spectrum is unique to each molecule as it involves the different spatial positions of each atom in the molecule or polyatomic ion.

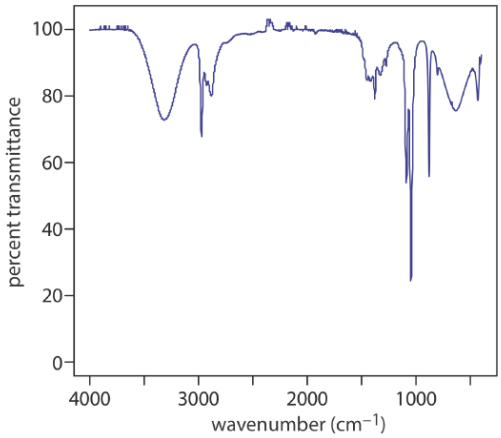


Figure 6.2.2 . Infrared spectrum of ethanol.

UV/Vis Spectra for Molecules and Ions

In contrast to vibrational spectra, electronic spectra like UV/Vis involve stimulation of the valence electrons in organic molecules and polyatomic ions. These valence electrons, such as those in CO_3^{2-}, occupy quantized sigma bonding (σ), pi bonding (π), and non-bonding (n) molecular orbitals (MOs). Unoccupied sigma antibonding (σ^*) and pi antibonding (π^*) molecular orbitals are slightly higher in energy. Because the difference in energy between the highest-energy occupied MOs and the lowest-energy unoccupied MOs corresponds to ultraviolet and visible radiation, absorption of a photon is possible.

Four types of transitions between quantized energy levels account for most molecular UV/Vis spectra. Table 6.2.1 lists the approximate wavelength ranges for these transitions, as well as a partial list of bonds, functional groups, or molecules responsible for these transitions. Of these transitions, the most important are $n \rightarrow \pi^*$ and $\pi \rightarrow \pi^*$ because they involve important functional groups that are characteristic of many analytes and because the wavelengths are easily accessible. The bonds and functional groups that give rise to the absorption of ultraviolet and visible radiation are called ***chromophores***. Note that double bonds, particularly conjugated double bonds, are chromophores that respond in the UV/Vis region of the electromagnetic spectrum. Single bonds only absorb very short wavelength UV light and are not typically good for UV/Vis analysis.

Table 6.2.1 . Electronic Transitions Involving n, σ, and π Molecular Orbitals

transition	wavelength range	examples
$\sigma \rightarrow \sigma^*$	<200 nm	C—C, C—H
$n \rightarrow \sigma^*$	160–260 nm	H_2O, CH_3OH, CH_3Cl
$\pi \rightarrow \pi^*$	200–500 nm	C=C, C=O, C=N, C≡C
$n \rightarrow \pi^*$	250–600 nm	C=O, C=N, N=N, N=O

Many transition metal ions, such as Cu^{2+} and Co^{2+}, form colorful solutions because the metal ion absorbs visible light. This makes them good chromophores for UV/Vis as well. The transitions that give rise to this absorption are valence electrons in the metal ion's *d*-orbitals. For a free metal ion, the five *d*-orbitals are of equal energy. In the presence of a complexing ligand or solvent molecule, however, the *d*-orbitals split into two or more groups that differ in energy. For example, in an octahedral complex of $Cu(H_2O)_6^{2+}$ the six water molecules perturb the *d*-orbitals into the two groups shown in Figure 6.2.3 . The resulting $d \rightarrow d$ transitions for transition metal ions are relatively weak.

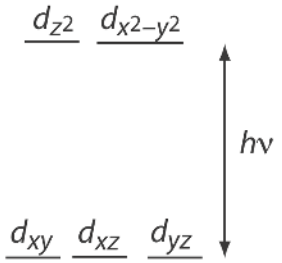


Figure 6.2.3 . Splitting of the *d*-orbitals in an octahedral field.

Inorganic metal-ligand complexes are even better chromophores for UV/Vis absorption. This is because they undergo charge transfer, in which absorption of a photon produces an excited state in which there is transfer of an electron from the metal, *M*, to the ligand, *L*.

$$M - L + h\nu \rightarrow (M^{+} - L^{-})^{*}$$

Charge-transfer absorption produces very large absorbances and therefore very large molar absorptivities in Beer's Law.. One important example of a charge-transfer complex is that of *o*-phenanthroline with Fe^{2+}, the UV/Vis spectrum for which is shown in Figure 6.2.4 . Charge-transfer absorption in which an electron moves from the ligand to the metal also is possible.

Why is a larger absorbance desirable? An analytical method is more sensitive if a smaller concentration of analyte gives a larger signal.

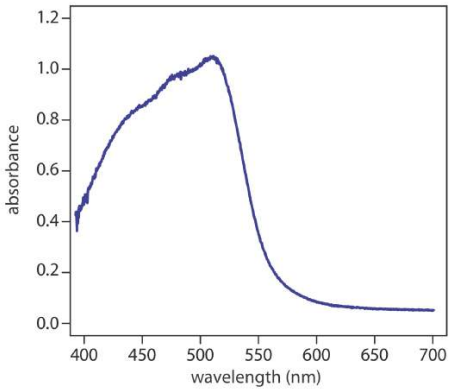


Figure 6.2.4 . UV/Vis spectrum for the metal–ligand complex $\mathbf{Fe(phen)_3^{2+}}$, where phen is the ligand *o*-phenanthroline.

Comparing the IR spectrum in Figure 6.2.2 to the UV/Vis spectrum in Figure 6.2.4 shows us that UV/Vis absorption bands are often significantly broader than those for IR absorption. We can use Figure 6.2.1 to explain why this is true. When a species absorbs UV/Vis radiation, the transition between electronic energy levels may also include a transition between vibrational energy levels. The result is a number of closely spaced absorption bands that merge together to form a single broad absorption band.

UV/Vis Spectra for Atoms

The energy of ultraviolet and visible electromagnetic radiation is sufficient to cause a change in an atom's valence electron configuration. Sodium, for example, has a single valence electron in its 3*s* atomic orbital. As shown in Figure 6.2.5 , unoccupied, higher energy atomic orbitals also exist.

The valence shell energy level diagram in Figure 6.2.5 might strike you as odd because it shows that the 3*p* orbitals are split into two groups of slightly different energy. The reasons for this splitting are unimportant in the context of our treatment of atomic absorption. For further information about the reasons for this splitting, consult the chapter's additional resources.

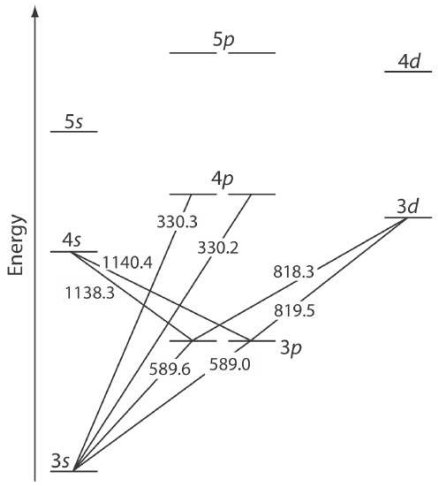


Figure 6.2.5 . Valence shell energy level diagram for sodium. The wavelengths (in wavenumbers) corresponding to several transitions are shown.

Absorption of a photon is accompanied by the excitation of an electron from a lower-energy atomic orbital to an atomic orbital of higher energy. Not all possible transitions between atomic orbitals are allowed. For sodium the only allowed transitions are those in which there is a change of ±1 in the orbital quantum number (l); thus transitions from $s \rightarrow p$ orbitals are allowed, but transitions from $s \rightarrow s$ and from $s \rightarrow d$ orbitals are forbidden.

The atomic absorption spectrum for Na is shown in Figure 6.2.6 , and is typical of that found for most atoms. The most obvious feature of this spectrum is that it consists of a small number of discrete absorption lines that correspond to transitions between the ground state (the 3*s* atomic orbital) and the 3*p* and the 4*p* atomic orbitals. Absorption from excited states, such as the $3p \rightarrow 4s$ and the $3p \rightarrow 3d$ transitions included in Figure 6.2.5 , are too weak to detect. Because an excited state's lifetime is short—an excited state atom typically returns to a lower energy state in 10^{-7} to 10^{-8} seconds—an atom in the exited state is likely to return to the ground state before it has an opportunity to absorb a photon.

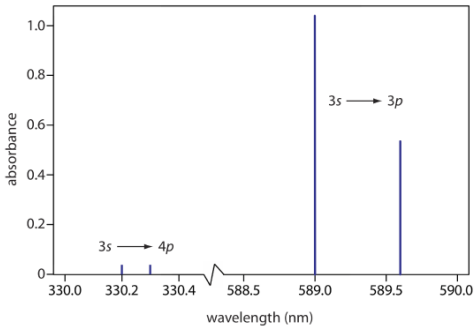


Figure 6.2.6 . Atomic absorption spectrum for sodium. Note that the scale on the *x*-axis includes a break.

Another feature of the atomic absorption spectrum in Figure 6.2.6 is the narrow width of the absorption lines, which is a consequence of the fixed difference in energy between the ground state and the excited state, and the lack of vibrational and rotational energy levels. Natural line widths for atomic absorption, which are governed by the uncertainty principle, are approximately 10^{-5} nm. Other contributions to broadening increase this line width to approximately 10^{-3} nm.

Quantitative Descriptions of Transmittance and Absorbance

As light passes through a sample, its power decreases as some of it is absorbed. This attenuation of radiation is described quantitatively by two separate, but related terms: transmittance and absorbance. As shown in Figure 6.2.7 a, transmittance is the ratio of the source radiation's power as it exits the sample, P_T, to that incident on the sample, P_0.

$$T = \frac{P_T}{P_0} \tag{6.2.1}$$

Multiplying the transmittance by 100 gives the percent transmittance, %T, which varies between 100% (no absorption) and 0% (complete absorption). All methods of detecting photons—including the human eye and modern photoelectric transducers—measure the transmittance of electromagnetic radiation.

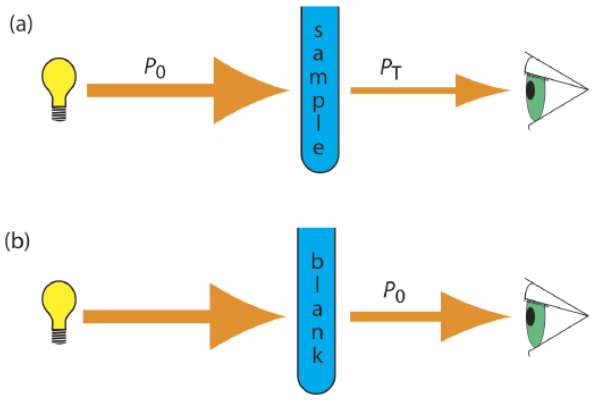


Figure 6.2.7 . (a) Schematic diagram showing the attenuation of radiation passing through a sample; P_0 is the source's radiant power and P_T is the radiant power transmitted by the sample. (b) Schematic diagram showing how we redefine P_0 as the radiant power transmitted by the blank. Redefining P_0 in this way corrects the transmittance in (a) for the loss of radiation due to scattering, reflection, absorption by the sample's container, and absorption by the sample's matrix.

Equation 6.2.1 does not distinguish between different mechanisms that prevent a photon emitted by the source from reaching the detector. In addition to absorption by the analyte, several additional phenomena contribute to the attenuation of radiation, including reflection and absorption by the sample's container, absorption by other components in the sample's matrix, and the scattering of radiation. To compensate for this loss of the radiation's power, we use a method blank. As shown in Figure 6.2.7 b, we redefine P_0 as the power exiting the method blank.

An alternative method for expressing the attenuation of electromagnetic radiation is absorbance, A, which we define as

$$A = -\log T = -\log \frac{P_T}{P_0} \tag{6.2.2}$$

Absorbance is the more common unit for expressing the attenuation of radiation because it is a linear function of the analyte's concentration.

> We will show that this is true in the next section when we introduce Beer's law.

Example 6.2.1

A sample has a percent transmittance of 50%. What is its absorbance?

Solution

A percent transmittance of 50.0% is the same as a transmittance of 0.500. Substituting into Equation 6.2.2 gives

$$A = -\log T = -\log(0.500) = 0.301$$

Exercise 6.2.1

What is the %T for a sample if its absorbance is 1.27?

Answer

To find the transmittance, T, we begin by noting that

$$A = 1.27 = -\log T$$

Solving for T

$$-1.27 = \log T$$
$$10^{-1.27} = T$$

gives a transmittance of 0.054, or a %T of 5.4%.

Equation 6.2.1 has an important consequence for atomic absorption. As we learned from Figure 6.2.6 , atomic absorption lines are very narrow. Even with a high quality monochromator, the effective bandwidth for a continuum source is $100 - 1000\times$ greater than the width of an atomic absorption line. As a result, little radiation from a continuum source is absorbed when it passes through a sample of atoms; because $P_0 \approx P_T$ the measured absorbance effectively is zero. For this reason, atomic absorption requires that we use a line source instead of a continuum source.

Absorbance and Concentration: Beer's Law

When monochromatic electromagnetic radiation passes through an infinitesimally thin layer of sample of thickness *dx*, it experiences a decrease in its power of *dP* (Figure 6.2.8).

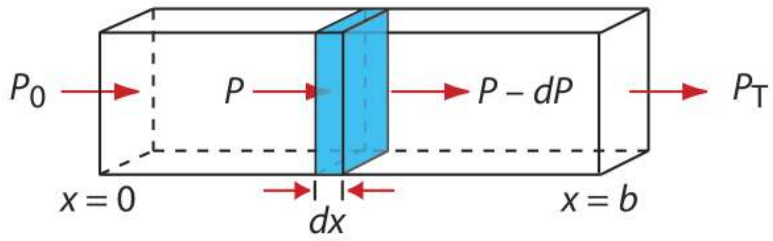


Figure 6.2.8 . Factors used to derive the Beer's law.

This fractional decrease in power is proportional to the sample's thickness and to the analyte's concentration, *C*; thus

$$-\frac{dP}{P} = \alpha C dx \tag{6.2.3}$$

where *P* is the power incident on the thin layer of sample and α is a proportionality constant. Integrating the left side of Equation 6.2.3 over the sample's full thickness

$$-\int_{P=P_0}^{P=P_t} \frac{dP}{P} = \alpha C \int_{x=0}^{x=b} dx$$

$$\ln \frac{P_0}{P_T} = \alpha b C$$

converting from ln to log, and substituting into Equation 6.2.2, gives

$$A = abC \tag{6.2.4}$$

where *a* is the analyte's ***absorptivity*** with units of cm^{-1} $conc^{-1}$. If we express the concentration using molarity, then we replace *a* with the ***molar absorptivity***, ε, which has units of cm^{-1} M^{-1}.

$$A = \varepsilon b C \tag{6.2.5}$$

The absorptivity and the molar absorptivity are proportional to the probability that the analyte absorbs a photon of a given energy. As a result, values for both *a* and ε depend on the wavelength of the absorbed photon.

Example 6.2.2

A 5.00×10^{-4} M solution of analyte is placed in a sample cell that has a pathlength of 1.00 cm. At a wavelength of 490 nm, the solution's absorbance is 0.338. What is the analyte's molar absorptivity at this wavelength?

Solution

Solving Equation 6.2.5 for ϵ and making appropriate substitutions gives

$$\varepsilon = \frac{A}{bC} = \frac{0.338}{(1.00\ \text{cm})\left(5.00 \times 10^{-4}\ \text{M}\right)} = 676\ \text{cm}^{-1}\ \text{M}^{-1}$$

? Exercise 6.2.2

A solution of the analyte from Example 6.2.2 has an absorbance of 0.228 in a 1.00-cm sample cell. What is the analyte's concentration?

Answer

Making appropriate substitutions into Beer's law

$$A = 0.228 = \varepsilon b C = \left(676\ \text{M}^{-1}\ \text{cm}^{-1}\right)(1\ \text{cm})C$$

and solving for C gives a concentration of 3.37×10^{-4} M.

Equation 6.2.4 and Equation 6.2.5, which establish the linear relationship between absorbance and concentration, are known as Beer's law. Calibration curves based on Beer's law are common in quantitative analyses.

As is often the case, the formulation of a law is more complicated than its name suggests. This is the case, for example, with Beer's law, which also is known as the Beer-Lambert law or the Beer-Lambert-Bouguer law. Pierre Bouguer, in 1729, and Johann Lambert, in 1760, noted that the transmittance of light decreases exponentially with an increase in the sample's thickness.

$$T \propto e^{-b}$$

Later, in 1852, August Beer noted that the transmittance of light decreases exponentially as the concentration of the absorbing species increases.

$$T \propto e^{-C}$$

Together, and when written in terms of absorbance instead of transmittance, these two relationships make up what we know as Beer's law.

Limitations to Beer's Law

Beer's law suggests that a plot of absorbance vs. concentration—we will call this a Beer's law plot—is a straight line with a *y*-intercept of zero and a slope of ab or εb. In some cases a Beer's law plot deviates from this ideal behavior (see Figure 6.2.9), and such deviations from linearity are divided into three categories: fundamental, chemical, and instrumental.

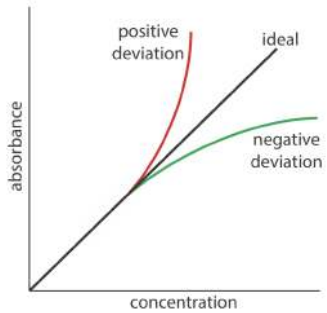


Figure 6.2.9 . Plots of absorbance vs. concentration showing positive and negative deviations from the ideal Beer's law relationship, which is a straight line.

Fundamental Limitations to Beer's Law

Beer's law is a limiting law that is valid only for low concentrations of analyte. There are two contributions to this fundamental limitation to Beer's law. At higher concentrations the individual particles of analyte no longer are independent of each other. The

resulting interaction between particles of analyte may change the analyte's absorptivity. A second contribution is that an analyte's absorptivity depends on the solution's refractive index. Because a solution's refractive index varies with the analyte's concentration, values of a and ε may change. For sufficiently low concentrations of analyte, the refractive index essentially is constant and a Beer's law plot is linear.

Chemical Limitations to Beer's Law

A chemical deviation from Beer's law may occur if the analyte is involved in an equilibrium reaction. Consider, for example, the weak acid, HA. To construct a Beer's law plot we prepare a series of standard solutions—each of which contains a known total concentration of HA—and then measure each solution's absorbance at the same wavelength. Because HA is a weak acid, it is in equilibrium with its conjugate weak base, A^-.

> In the equations that follow, the conjugate weak base A^- is written as A as it is easy to mistake the symbol for anionic charge as a minus sign.

$$\mathrm{HA}(aq) + \mathrm{H_2O}(l) \rightleftharpoons \mathrm{H_3O^+}(aq) + \mathrm{A^-}(aq)$$

If both HA and A^- absorb at the selected wavelength, then Beer's law is

$$A = \varepsilon_{\mathrm{HA}} b C_{\mathrm{HA}} + \varepsilon_{\mathrm{A}} b C_{\mathrm{A}} \tag{6.2.6}$$

Because the weak acid's total concentration, C_{total}, is

$$C_{\text{total}} = C_{\mathrm{HA}} + C_{\mathrm{A}}$$

we can write the concentrations of HA and A^- as

$$C_{\mathrm{HA}} = \alpha_{\mathrm{HA}} C_{\text{total}} \tag{6.2.7}$$

$$C_{\mathrm{A}} = (1 - \alpha_{\mathrm{HA}}) C_{\text{total}} \tag{6.2.8}$$

where α_{HA} is the fraction of weak acid present as HA. Substituting Equation 6.2.7 and Equation 6.2.8 into Equation 6.2.6 and rearranging, gives

$$A = \left(\varepsilon_{\mathrm{HA}} \alpha_{\mathrm{HA}} + \varepsilon_{\mathrm{A}} - \varepsilon_{\mathrm{A}} \alpha_{\mathrm{A}}\right) b C_{\text{total}} \tag{6.2.9}$$

To obtain a linear Beer's law plot, we must satisfy one of two conditions. If $\varepsilon_{\mathrm{HA}}$ and ε_{A} have the same value at the selected wavelength, then Equation 6.2.9 simplifies to

$$A = \varepsilon_{\mathrm{A}} b C_{\text{total}} = \varepsilon_{\mathrm{HA}} b C_{\text{total}}$$

Alternatively, if α_{HA} has the same value for all standard solutions, then each term within the parentheses of Equation 6.2.9 is constant—which we replace with k—and a linear calibration curve is obtained at any wavelength.

$$A = k b C_{\text{total}}$$

Because HA is a weak acid, the value of α_{HA} varies with pH. To hold α_{HA} constant we buffer each standard solution to the same pH. Depending on the relative values of α_{HA} and α_{A}, the calibration curve has a positive or a negative deviation from Beer's law if we do not buffer the standards to the same pH.

Instrumental Limitations to Beer's Law

There are two principal instrumental limitations to Beer's law. The first limitation is that Beer's law assumes that radiation reaching the sample is of a single wavelength—that is, it assumes a purely monochromatic source of radiation. As shown in Figure 10.1.10, even the best wavelength selector passes radiation with a small, but finite effective bandwidth. Polychromatic radiation always gives a negative deviation from Beer's law, but the effect is smaller if the value of ε essentially is constant over the wavelength range passed by the wavelength selector. For this reason, as shown in Figure 6.2.10 , it is better to make absorbance measurements at the top of a broad absorption peak. In addition, the deviation from Beer's law is less serious if the source's effective bandwidth is less than one-tenth of the absorbing species' natural bandwidth [(a) Strong, F. C., III *Anal. Chem.* **1984**, *56*, 16A–34A; Gilbert, D.

D. *J. Chem. Educ.* **1991**, *68*, A278–A281]. When measurements must be made on a slope, linearity is improved by using a narrower effective bandwidth.

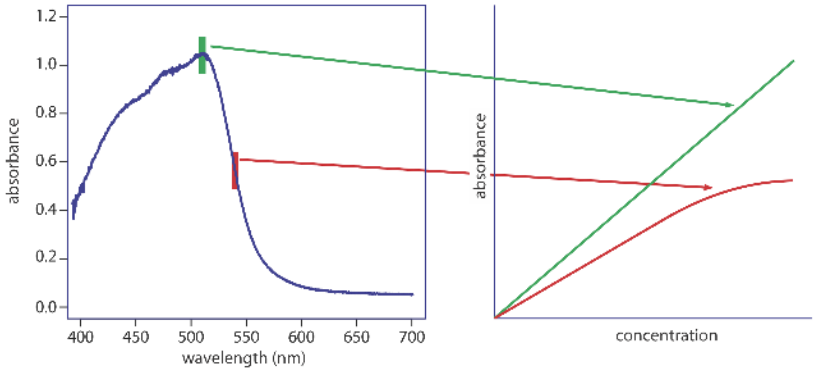


Figure 6.2.10 . Effect of wavelength selection on the linearity of a Beer's law plot. Another reason for measuring absorbance at the top of an absorbance peak is that it provides for a more sensitive analysis. Note that the green Beer's law plot has a steeper slope—and, therefore, a greater sensitivity—than the red Beer's law plot. A Beer's law plot, of course, is equivalent to a calibration curve.

Stray radiation is the second contribution to instrumental deviations from Beer's law. Stray radiation arises from imperfections in the wavelength selector that allow light to enter the instrument and to reach the detector without passing through the sample. Stray radiation adds an additional contribution, P_{stray}, to the radiant power that reaches the detector; thus

$$A = -\log \frac{P_T + P_{\text{stray}}}{P_0 + P_{\text{stray}}}$$

For a small concentration of analyte, P_{stray} is significantly smaller than P_0 and P_T, and the absorbance is unaffected by the stray radiation. For higher concentrations of analyte, less light passes through the sample and P_T and P_{stray} become similar in magnitude. This results is an absorbance that is smaller than expected, and a negative deviation from Beer's law.

This page titled 6.2: Spectroscopy Based on Absorption is shared under a CC BY-NC-SA 4.0 license and was authored, remixed, and/or curated by Kathryn Davis.

- **10.2: Spectroscopy Based on Absorption** by David Harvey is licensed CC BY-NC-SA 4.0.

6.3: UV/Vis and IR Spectroscopy

In Figure 10.1.9 we examined Nessler's original method for matching the color of a sample to the color of a standard. Matching colors is a labor intensive process for the analyst and, not surprisingly, spectroscopic methods of analysis were slow to find favor. The 1930s and 1940s saw the introduction of photoelectric transducers for ultraviolet and visible radiation, and thermocouples for infrared radiation. As a result, modern instrumentation for absorption spectroscopy routinely became available in the 1940s—further progress has been rapid ever since.

Instrumentation

Frequently an analyst must select from among several instruments of different design, the one instrument best suited for a particular analysis. In this section we examine several different instruments for molecular absorption spectroscopy, with an emphasis on their advantages and limitations. Methods of sample introduction also are covered in this section.

Instrument Designs for Molecular UV/Vis Absorption

Single-Beam Spectrophotometer. An instrument that uses a monochromator for wavelength selection is called a ***spectrophotometer***. The simplest spectrophotometer is a single-beam instrument equipped with a fixed-wavelength monochromator (Figure 6.3.2). Single-beam spectrophotometers are calibrated and used in the same manner as a photometer. One example of a single-beam spectrophotometer is Thermo Scientific's Spectronic 20D+, which is shown in the photographic insert to Figure 6.3.2 . The Spectronic 20D+ has a wavelength range of 340–625 nm (950 nm when using a red-sensitive detector), and a fixed effective bandwidth of 20 nm. Battery-operated, hand-held single-beam spectrophotometers are available, which are easy to transport into the field. Other single-beam spectrophotometers also are available with effective bandwidths of 2–8 nm. Fixed wavelength single-beam spectrophotometers are not practical for recording spectra because manually adjusting the wavelength and recalibrating the spectrophotometer is awkward and time-consuming. The accuracy of a single-beam spectrophotometer is limited by the stability of its source and detector over time.

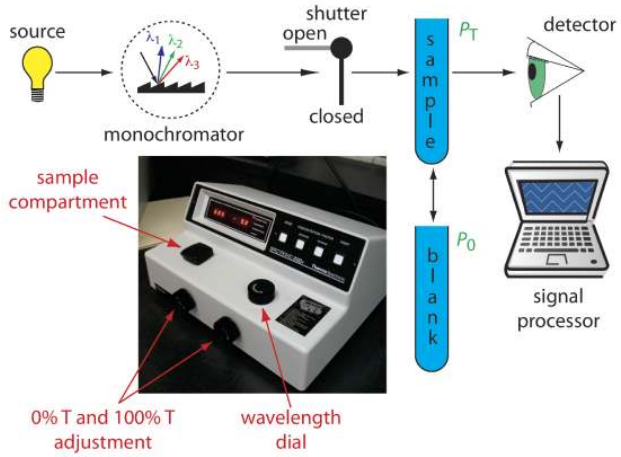


Figure 6.3.2 . Schematic diagram of a fixed-wavelength, single-beam spectrophotometer. The photographic inset shows a typical instrument. The shutter remains closed until the sample or blank is placed in the sample compartment. The analyst manually selects the wavelength by adjusting the wavelength dial. Inset photo modified from: Adi (www.commons.Wikipedia.org).

Double-Beam Spectrophotometer. The limitations of a fixed-wavelength, single-beam spectrophotometer is minimized by using a ***double-beam*** spectrophotometer (Figure 6.3.3). A chopper controls the radiation's path, alternating it between the sample, the blank, and a shutter. The signal processor uses the chopper's speed of rotation to resolve the signal that reaches the detector into the transmission of the blank, P_0, and the sample, P_T. By including an opaque surface as a shutter, it also is possible to continuously adjust 0%T. The effective bandwidth of a double-beam spectrophotometer is controlled by adjusting the monochromator's entrance and exit slits. Effective bandwidths of 0.2–3.0 nm are common. A scanning monochromator allows for the automated recording of spectra. Double-beam instruments are more versatile than single-beam instruments, being useful for both quantitative and qualitative analyses, but also are more expensive and not particularly portable.

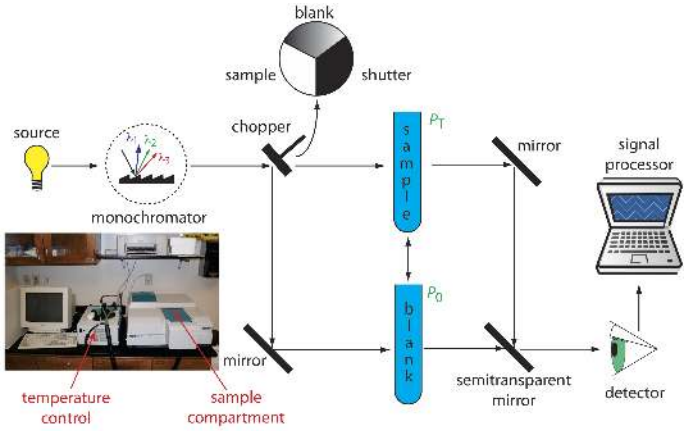


Figure 6.3.3 . Schematic diagram of a scanning, double-beam spectrophotometer. A chopper directs the source's radiation, using a transparent window to pass radiation to the sample and a mirror to reflect radiation to the blank. The chopper's opaque surface serves as a shutter, which allows for a constant adjustment of the spectrophotometer's 0%T. The photographic insert shows a typical instrument. The module in the middle of the photo is a temperature control unit that makes it possible to heat or cool the sample to a constant temperature.

Diode Array Spectrometer. An instrument with a single detector can monitor only one wavelength at a time. If we replace a single photomultiplier with an array of photodiodes, we can use the resulting detector to record a full spectrum in as little as 0.1 s. In a diode array spectrometer the source radiation passes through the sample and is dispersed by a grating (Figure 6.3.4). The photodiode array detector is situated at the grating's focal plane, with each diode recording the radiant power over a narrow range of wavelengths. Because we replace a full monochromator with just a grating, a diode array spectrometer is small and compact.

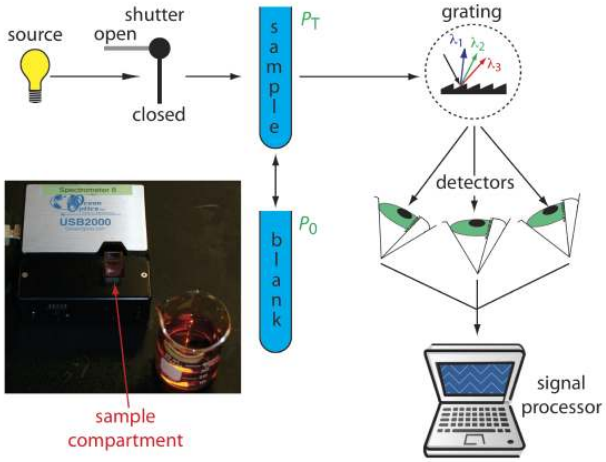


Figure 6.3.4 . Schematic diagram of a diode array spectrophotometer. The photographic insert shows a typical instrument. Note that the 50-mL beaker provides a sense of scale. Because the spectrometer is small and compact, it is easy to transport into the field.

Sample Cells. The sample compartment provides a light-tight environment that limits stray radiation. Samples normally are in a liquid or solution state, and are placed in cells constructed with UV/Vis transparent materials, such as quartz, glass, and plastic (Figure 6.3.6). A quartz or fused-silica cell is required when working at a wavelength <300 nm where other materials show a significant absorption. The most common pathlength is 1 cm (10 mm), although cells with shorter (as little as 0.1 cm) and longer pathlengths (up to 10 cm) are available. Longer pathlength cells are useful when analyzing a very dilute solution or for gas samples. The highest quality cells allow the radiation to strike a flat surface at a 90^o angle, minimizing the loss of radiation to reflection. A test tube often is used as a sample cell with simple, single-beam instruments, although differences in the cell's pathlength and optical properties add an additional source of error to the analysis.

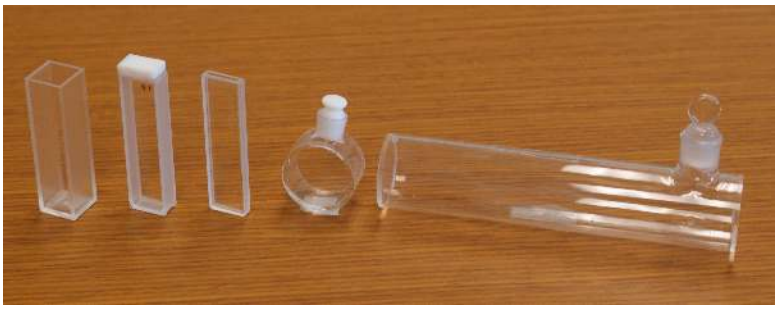


Figure 6.3.6 . Examples of sample cells for UV/Vis spectroscopy. From left to right (with path lengths in parentheses): rectangular plastic cuvette (10.0 mm), rectangular quartz cuvette (5.000 mm), rectangular quartz cuvette (1.000 mm), cylindrical quartz cuvette (10.00 mm), cylindrical glass cuvette with quartz windows (100.0 mm). Cells often are available as a matched pair, which is important when using a double-beam instrument.

If we need to monitor an analyte's concentration over time, it may not be possible to remove samples for analysis. This often is the case, for example, when monitoring an industrial production line or waste line, when monitoring a patient's blood, or when monitoring an environmental system, such as stream. With a ***fiber-optic probe*** we can analyze samples *in situ*. An example of a remote sensing fiber-optic probe is shown in Figure 6.3.7 . The probe consists of two bundles of fiber-optic cable. One bundle transmits radiation from the source to the probe's tip, which is designed to allow the sample to flow through the sample cell. Radiation from the source passes through the solution and is reflected back by a mirror. The second bundle of fiber-optic cable transmits the nonabsorbed radiation to the wavelength selector. Another design replaces the flow cell shown in Figure 6.3.7 with a membrane that contains a reagent that reacts with the analyte. When the analyte diffuses into the membrane it reacts with the reagent, producing a product that absorbs UV or visible radiation. The nonabsorbed radiation from the source is reflected or scattered back to the detector. Fiber optic probes that show chemical selectivity are called optrodes [(a) Seitz, W. R. *Anal. Chem.* **1984**, *56*, 16A–34A; (b) Angel, S. M. *Spectroscopy* **1987**, *2(2)*, 38–48].

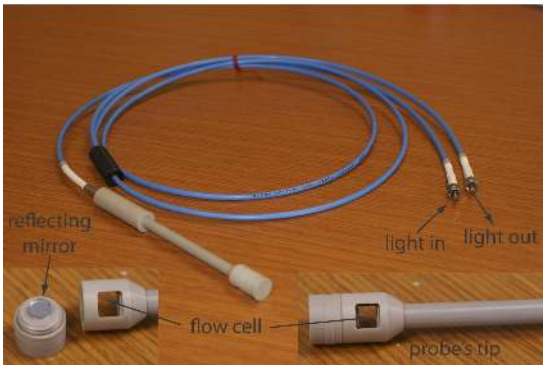


Figure 6.3.7 . Example of a fiber-optic probe. The inset photographs at the bottom of the figure provide close-up views of the probe's flow cell and the reflecting mirror.

Quantitative Applications of UV/Vis Spectrophotometry

The determination of an analyte's concentration based on its absorption of ultraviolet or visible radiation is one of the most frequently encountered quantitative analytical methods. One reason for its popularity is that many organic and inorganic compounds have strong absorption bands in the UV/Vis region of the electromagnetic spectrum. In addition, if an analyte does not absorb UV/Vis radiation—or if its absorbance is too weak—we often can react it with another species that is strongly absorbing. For example, a dilute solution of Fe^{2+} does not absorb visible light. Reacting Fe^{2+} with *o*-phenanthroline, however, forms an orange–red complex of $\mathbf{Fe(phen)_3^{2+}}$ that has a strong, broad absorbance band near 500 nm. An additional advantage to UV/Vis absorption is that in most cases it is relatively easy to adjust experimental and instrumental conditions so that Beer's law is obeyed.

A quantitative analysis based on the absorption of infrared radiation, although important, is encountered less frequently than with UV/Vis absorption. One reason is the greater tendency for instrumental deviations from Beer's law when using infrared radiation. Because an infrared absorption band is relatively narrow, any deviation due to the lack of monochromatic radiation is more pronounced. In addition, infrared sources are less intense than UV/Vis sources, which makes stray radiation more of a problem. Differences between the pathlengths for samples and for standards when using thin liquid films or KBr pellets are a problem,

although an internal standard can correct for any difference in pathlength. Finally, establishing a 100%T (A = 0) baseline often is difficult because the optical properties of NaCl sample cells may change significantly with wavelength due to contamination and degradation. We can minimize this problem by measuring absorbance relative to a baseline established for the absorption band. Figure 6.3.10 shows how this is accomplished.

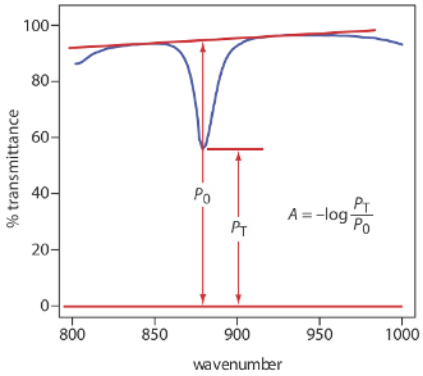


Figure 6.3.10 . Method for determining absorbance from an IR spectrum.

> Another approach is to use a cell with a fixed pathlength, such as that shown in Figure 6.3.8 b.

Environmental Applications

The analysis of waters and wastewaters often relies on the absorption of ultraviolet and visible radiation. Many of these methods are outlined in Table 6.3.1 . Several of these methods are described here in more detail.

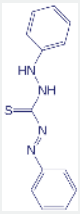
Table 6.3.1 . Examples of Molecular UV/Vis Analysis of Waters and Wastewaters

analyte	method	γ (nm)
trace metals		
aluminum	react with Eriochrome cyanide R dye at pH 6; forms red to pink complex	535
arsenic	reduce to AsH_3 using Zn and react with silver diethyldithiocarbamate; forms red complex	535
cadmium	extract into $CHCl_3$ containing dithizone from a sample made basic with NaOH; forms pink to red complex	518
chromium	oxidize to Cr(VI) and react with diphenylcarbazide; forms 540 red-violet product	540
copper	react with neocuprine in neutral to slightly acid solution and extract into $CHCl_3/CH_3OH$; forms yellow complex	457
iron	reduce to Fe^{2+} and react with *o*-phenanthroline; forms orange-red complex	510
lead	extract into $CHCl_3$ containing dithizone from sample made basic with NH_3/ NH_4^+ buffer; forms cherry red complex	510
manganese	oxidize to MnO_4^- with persulfate; forms purple solution	525
mercury	extract into $CHCl_3$ containing dithizone from acidic sample; forms orange complex	492
zinc	react with zincon at pH 9; forms blue complex	620
inorganic nonmetals		
ammonia	reaction with hypochlorite and phenol using a manganous 630 salt catalyst; forms blue indophenol as product	630
cyanide	react with chloroamine-T to form CNCl and then with a pyridine-barbituric acid; forms a red-blue dye	578
fluoride	react with red Zr-SPADNS lake; formation of ZrF_6^{2-} decreases color of the red lake	570
chlorine (residual)	react with leuco crystal violet; forms blue product	592
nitrate	react with Cd to form NO_2^- and then react with sulfanilamide and *N*-(1-napthyl)-ethylenediamine; forms red azo 543 dye	543
phosphate	react with ammonium molybdate and then	690

analyte	method	λ (nm)
	reduce with $SnCl_2$; forms molybdenum blue	
organics		
phenol	react with 4-aminoantipyrine and $K_3Fe(CN)_6$; forms yellow antipyrine dye	460
anionic surfactants	react with cationic methylene blue dye and extract into $CHCl_3$; forms blue ion pair	652

Although the quantitative analysis of metals in waters and wastewaters is accomplished primarily by atomic absorption or atomic emission spectroscopy, many metals also can be analyzed following the formation of a colored metal–ligand complex. One advantage to these spectroscopic methods is that they easily are adapted to the analysis of samples in the field using a filter photometer. One ligand used for the analysis of several metals is diphenylthiocarbazone, also known as dithizone. Dithizone is not soluble in water, but when a solution of dithizone in $CHCl_3$ is shaken with an aqueous solution that contains an appropriate metal ion, a colored metal–dithizonate complex forms that is soluble in $CHCl_3$. The selectivity of dithizone is controlled by adjusting the sample's pH. For example, Cd^{2+} is extracted from solutions made strongly basic with NaOH, Pb^{2+} from solutions made basic with an NH_3/ NH_4^+ buffer, and Hg^{2+} from solutions that are slightly acidic.

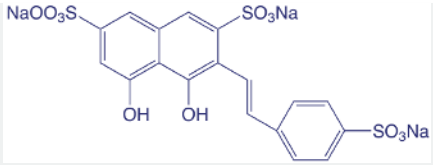
The structure of dithizone is shown below. See Chapter 7 for a discussion of extracting metal ions using dithizone.



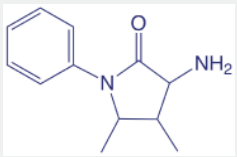
When chlorine is added to water the portion available for disinfection is called the chlorine residual. There are two forms of chlorine residual. The free chlorine residual includes Cl_2, HOCl, and OCl^-. The combined chlorine residual, which forms from the reaction of NH_3 with HOCl, consists of monochloramine, NH_2Cl, dichloramine, $NHCl_2$, and trichloramine, NCl_3. Because the free chlorine residual is more efficient as a disinfectant, there is an interest in methods that can distinguish between the total chlorine residual's different forms. One such method is the leuco crystal violet method. The free residual chlorine is determined by adding leuco crystal violet to the sample, which instantaneously oxidizes to give a blue-colored compound that is monitored at 592 nm. Completing the analysis in less than five minutes prevents a possible interference from the combined chlorine residual. The total chlorine residual (free + combined) is determined by reacting a separate sample with iodide, which reacts with both chlorine residuals to form HOI. When the reaction is complete, leuco crystal violet is added and oxidized by HOI, giving the same blue-colored product. The combined chlorine residual is determined by difference.

The concentration of fluoride in drinking water is determined indirectly by its ability to form a complex with zirconium. In the presence of the dye SPADNS, a solution of zirconium forms a red colored compound, called a lake, that absorbs at 570 nm. When fluoride is added, the formation of the stable ZrF_6^{2-} complex causes a portion of the lake to dissociate, decreasing the absorbance. A plot of absorbance versus the concentration of fluoride, therefore, has a negative slope.

SPADNS, the structure of which is shown below, is an abbreviation for the sodium salt of 2-(4-sulfophenylazo)-1,8-dihydroxy-3,6-napthalenedisulfonic acid, which is a mouthful to say.



Spectroscopic methods also are used to determine organic constituents in water. For example, the combined concentrations of phenol and ortho- and meta-substituted phenols are determined by using steam distillation to separate the phenols from nonvolatile impurities. The distillate reacts with 4-aminoantipyrine at pH 7.9 ± 0.1 in the presence of $K_3Fe(CN)_6$ to a yellow colored antipyrine dye. After extracting the dye into $CHCl_3$, its absorbance is monitored at 460 nm. A calibration curve is prepared using only the unsubstituted phenol, C_6H_5OH. Because the molar absorptivity of substituted phenols generally are less than that for phenol, the reported concentration represents the minimum concentration of phenolic compounds.



4-aminoantipyrene

Molecular absorption also is used for the analysis of environmentally significant airborne pollutants. In many cases the analysis is carried out by collecting the sample in water, converting the analyte to an aqueous form that can be analyzed by methods such as those described in Table 6.3.1 . For example, the concentration of NO_2 is determined by oxidizing NO_2 to $\mathbf{NO_3^-}$. The concentration of $\mathbf{NO_3^-}$ is then determined by first reducing it to $\mathbf{NO_2^-}$ with Cd, and then reacting $\mathbf{NO_2^-}$ with sulfanilamide and *N*-(1-naphthyl)-ethylenediamine to form a red azo dye. Another important application is the analysis for SO_2, which is determined by collecting the sample in an aqueous solution of $\mathbf{HgCl_4^{2-}}$ where it reacts to form $\mathbf{Hg(SO_3)_2^{2-}}$. Addition of *p*-rosaniline and formaldehyde produces a purple complex that is monitored at 569 nm. Infrared absorption is useful for the analysis of organic vapors, including HCN, SO_2, nitrobenzene, methyl mercaptan, and vinyl chloride. Frequently, these analyses are accomplished using portable, dedicated infrared photometers.

Clinical Applications

The analysis of clinical samples often is complicated by the complexity of the sample's matrix, which may contribute a significant background absorption at the desired wavelength. The determination of serum barbiturates provides one example of how this problem is overcome. The barbiturates are first extracted from a sample of serum with $CHCl_3$ and then extracted from the $CHCl_3$ into 0.45 M NaOH (pH ≈ 13). The absorbance of the aqueous extract is measured at 260 nm, and includes contributions from the barbiturates as well as other components extracted from the serum sample. The pH of the sample is then lowered to approximately 10 by adding NH_4Cl and the absorbance remeasured. Because the barbiturates do not absorb at this pH, we can use the absorbance at pH 10, $A_{\text{pH 10}}$, to correct the absor-ance at pH 13, $A_{\text{pH 13}}$

$$\mathbf{A_{barb} = A_{pH\ 13} - \frac{V_{samp} + V_{NH_4Cl}}{V_{samp}} \times A_{pH\ 10}}$$

where A_{barb} is the absorbance due to the serum barbiturates and V_{samp} and $\mathbf{V_{NH_4Cl}}$ are the volumes of sample and NH_4Cl, respectively. Table 6.3.2 provides a summary of several other methods for analyzing clinical samples.

Table 6.3.2 . Examples of the Molecular UV/Vis Analysis of Clinical Samples

analyte	method	λ (nm)
total serum protein	react with NaOH and Cu^{2+}; forms blue-violet complex	540
serum cholesterol	react with Fe^{3+} in presence of isopropanol, acetic acid, and H_2SO_4; forms blue-violet complex	540
uric acid	react with phosphotungstic acid; forms tungsten blue	710
serum barbituates	extract into $CHCl_3$ to isolate from interferents and then extract into 0.45 M NaOH	260
glucose	react with *o*-toludine at 100°C; forms blue-green complex	630
protein-bound iodine	decompose protein to release iodide, which catalyzes redox reaction between Ce^{3+} and As^{3+}; forms yellow colored Ce^{4+}	420

Industrial Applications

UV/Vis molecular absorption is used for the analysis of a diverse array of industrial samples including pharmaceuticals, food, paint, glass, and metals. In many cases the methods are similar to those described in Table 6.3.1 and in Table 6.3.2 . For example, the amount of iron in food is determined by bringing the iron into solution and analyzing using the *o*-phenanthroline method listed in Table 6.3.1 .

Many pharmaceutical compounds contain chromophores that make them suitable for analysis by UV/Vis absorption. Products analyzed in this fashion include antibiotics, hormones, vitamins, and analgesics. One example of the use of UV absorption is in determining the purity of aspirin tablets, for which the active ingredient is acetylsalicylic acid. Salicylic acid, which is produced by the hydrolysis of acetylsalicylic acid, is an undesirable impurity in aspirin tablets, and should not be present at more than 0.01% w/w. Samples are screened for unacceptable levels of salicylic acid by monitoring the absorbance at a wavelength of 312 nm. Acetylsalicylic acid absorbs at 280 nm, but absorbs poorly at 312 nm. Conditions for preparing the sample are chosen such that an absorbance of greater than 0.02 signifies an unacceptable level of salicylic acid.

Forensic Applications

UV/Vis molecular absorption routinely is used for the analysis of narcotics and for drug testing. One interesting forensic application is the determination of blood alcohol using the Breathalyzer test. In this test a 52.5-mL breath sample is bubbled through an acidified solution of $K_2Cr_2O_7$, which oxidizes ethanol to acetic acid. The concentration of ethanol in the breath sample is determined by a decrease in the absorbance at 440 nm where the dichromate ion absorbs. A blood alcohol content of 0.10%, which is above the legal limit, corresponds to 0.025 mg of ethanol in the breath sample.

Quantitative Analysis for a Single Sample

To determine the concentration of an analyte we measure its absorbance and apply Beer's law. The most common methods are a normal calibration curve using external standards and the method of standard additions. A single point standardization also is possible, although we must first verify that Beer's law holds for the concentration of analyte in the samples and the standard.

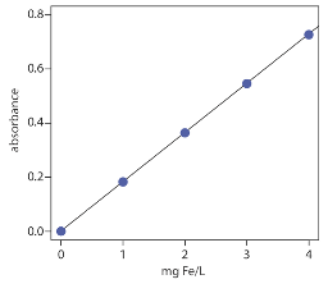
Example 6.3.1

The determination of iron in an industrial waste stream is carried out by the *o*-phenanthroline described in Representative Method 10.3.1. Using the data in the following table, determine the mg Fe/L in the waste stream.

mg Fe/L	absorbance
0.00	0.000
1.00	0.183
2.00	0.364
3.00	0.546
4.00	0.727
sample	0.269

Solution

Linear regression of absorbance versus the concentration of Fe in the standards gives the calibration curve and calibration equation shown here



$$A = 0.0006 + \left(0.1817\ \text{mg}^{-1}\text{L}\right) \times (\text{mgFe/L})$$

Substituting the sample's absorbance into the calibration equation gives the concentration of Fe in the waste stream as 1.48 mg Fe/L

Exercise 6.3.1

The concentration of Cu^{2+} in a sample is determined by reacting it with the ligand cuprizone and measuring its absorbance at 606 nm in a 1.00-cm cell. When a 5.00-mL sample is treated with cuprizone and diluted to 10.00 mL, the resulting solution has an absorbance of 0.118. A second 5.00-mL sample is mixed with 1.00 mL of a 20.00 mg/L standard of Cu^{2+}, treated with cuprizone and diluted to 10.00 mL, giving an absorbance of 0.162. Report the mg Cu^{2+}/L in the sample.

Answer

For this standard addition we write equations that relate absorbance to the concentration of Cu^{2+} in the sample before the standard addition

$$0.118 = \varepsilon b \left[C_{\text{Cu}} \times \frac{5.00\ \text{mL}}{10.00\ \text{mL}}\right]$$

and after the standard addition

$$0.162 = \varepsilon b \left(C_{\text{Cu}} \times \frac{5.00\ \text{mL}}{10.00\ \text{mL}} + \frac{20.00\ \text{mg Cu}}{\text{L}} \times \frac{1.00\ \text{mL}}{10.00\ \text{mL}}\right)$$

in each case accounting for the dilution of the original sample and for the standard. The value of εb is the same in both equation. Solving each equation for εb and equating

$$\frac{0.162}{C_{\text{Cu}} \times \frac{5.00\ \text{mL}}{10.00\ \text{mL}} + \frac{20.00\ \text{mg Cu}}{\text{L}} \times \frac{1.00\ \text{mL}}{10.00\ \text{mL}}} = \frac{0.118}{C_{\text{Cu}} \times \frac{5.00\ \text{mL}}{10.00\ \text{mL}}}$$

leaves us with an equation in which C_{Cu} is the only variable. Solving for C_{Cu} gives its value as

$$\frac{0.162}{0.500 \times C_{Cu} + 2.00 \text{ mg Cu/L}} = \frac{0.118}{0.500 \times C_{Cu}}$$

$$0.0810 \times C_{Cu} = 0.0590 \times C_{Ca} + 0.236 \text{ mg Cu/L}$$

$$0.0220 \times C_{Cu} = 0.236 \text{ mg Cu/L}$$

$$C_{Cu} = 10.7 \text{ mg Cu/L}$$

Characterization Applications

Molecular absorption, particularly in the UV/Vis range, has been used for a variety of different characterization studies, including determining the stoichiometry of metal–ligand complexes and determining equilibrium constants. Both of these examples are examined in this section.

Stoichiometry of a Metal-Ligand Complex

We can determine the stoichiometry of the metal–ligand complexation reaction

$$M + yL \rightleftharpoons ML_y$$

using several methods. Of these approaches, the ***method of continuous variations***, also called Job's method, is the most popular. In this method a series of solutions is prepared such that the total moles of metal and of ligand, n_{total}, in each solution is the same. If $(n_M)_i$ and $(n_L)_i$ are, respectively, the moles of metal and ligand in solution i, then

$$n_{\text{total}} = (n_M)_i + (n_L)_i$$

The relative amount of ligand and metal in each solution is expressed as the mole fraction of ligand, $(X_L)i$, and the mole fraction of metal, $(X_M)_i$,

$$(X_L)_i = \frac{(n_L)_i}{n_{total}}$$

$$(X_M)_i = 1 - \frac{(n_L)_i}{n_{\text{total}}} = \frac{(n_M)_i}{n_{\text{total}}}$$

The concentration of the metal–ligand complex in any solution is determined by the limiting reagent, with the greatest concentration occurring when the metal and the ligand are mixed stoichiometrically. If we monitor the complexation reaction at a wavelength where only the metal–ligand complex absorbs, a graph of absorbance versus the mole fraction of ligand has two linear branches—one when the ligand is the limiting reagent and a second when the metal is the limiting reagent. The intersection of the two branches represents a stoichiometric mixing of the metal and the ligand. We use the mole fraction of ligand at the intersection to determine the value of y for the metal–ligand complex ML_y.

$$y = \frac{n_L}{n_M} = \frac{X_L}{X_M} = \frac{X_L}{1 - X_L}$$

You also can plot the data as absorbance versus the mole fraction of metal. In this case, y is equal to $(1 - X_M)/X_M$.

Example 6.3.4

To determine the formula for the complex between Fe^{2+} and *o*-phenanthroline, a series of solutions is prepared in which the total concentration of metal and ligand is held constant at 3.15×10^{-4} M. The absorbance of each solution is measured at a wavelength of 510 nm. Using the following data, determine the formula for the complex.

X_L	absorbance	X_L	absorbance
0.000	0.000	0.600	0.693
0.100	0.116	0.700	0.809
0.200	0.231	0.800	0.693
0.300	0.347	0.900	0.347
0.400	0.462	1.000	0.000
0.500	0.578		

Solution

A plot of absorbance versus the mole fraction of ligand is shown in Figure 6.3.14 . To find the maximum absorbance, we extrapolate the two linear portions of the plot. The two lines intersect at a mole fraction of ligand of 0.75. Solving for *y* gives

$$y = \frac{X_L}{1 - X_L} = \frac{0.75}{1 - 0.75} = 3$$

The formula for the metal–ligand complex is $\mathbf{Fe(phen)_3^{2+}}$.

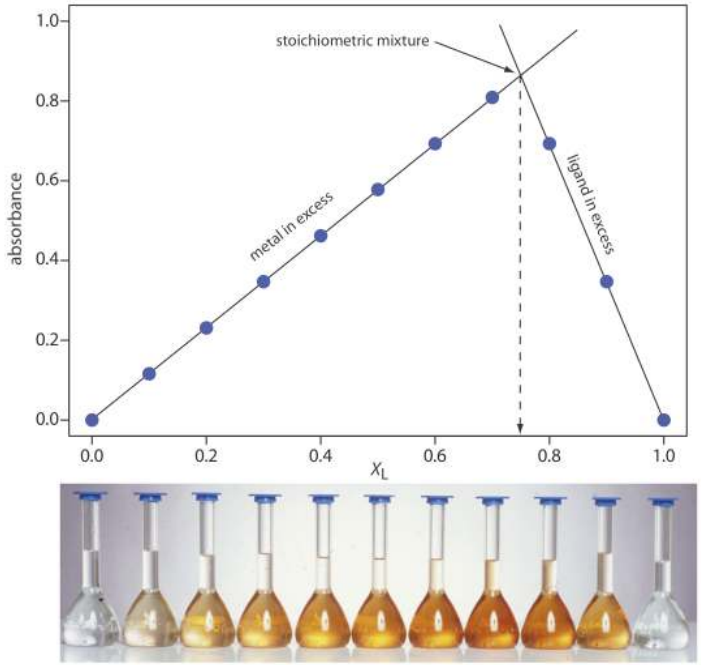


Figure 6.3.14 . Continuous variations plot for Example 6.3.4 . The photo shows the solutions used to gather the data. Each solution is displayed directly below its coresponding point on the continuous variations plot. To prepare these solutions I first prepared a solution of $\mathbf{3.15 \times 10^{-4}}$ M Fe^{2+} and a solution of $\mathbf{3.15 \times 10^{-4}}$ M *o*-phenanthroline. Because the two stock solutions have the same concentration, diluting a portion of one solution with the other solution gives a mixture in which the combined concentration of *o*-phenanthroline and Fe^{2+} is $\mathbf{3.15 \times 10^{-4}}$ M. Because each solution has the same volume, each solution also contains the same total moles of metal and ligand.

Determination of Equilibrium Constants

Another important application of molecular absorption spectroscopy is the determination of equilibrium constants. Let's consider, as a simple example, an acid–base reaction of the general form

$$\mathbf{HIn}(aq) + \mathbf{H_2O}(l) \rightleftharpoons \mathbf{H_3O^+}(aq) + \mathbf{In^-}(aq)$$

where HIn and In^- are the conjugate weak acid and weak base forms of an acid–base indicator. The equilibrium constant for this reaction is

$$K_a = \frac{[H_3O^+]\,[A^-]}{[HA]}$$

To determine the equilibrium constant's value, we prepare a solution in which the reaction is in a state of equilibrium and determine the equilibrium concentration for H_3O^+, HIn, and In^-. The concentration of H_3O^+ is easy to determine by measuring the solution's pH. To determine the concentration of HIn and In^- we can measure the solution's absorbance.

If both HIn and In^- absorb at the selected wavelength, then, from Beer's law, we know that

$$A = \varepsilon_{HIn} b[HIn] + \varepsilon_{In} b[In^-] \tag{6.3.1}$$

where ε_{HIn} and ε_{In} are the molar absorptivities for HIn and In^-. The indicator's total concentration, C, is given by a mass balance equation

$$C = [HIn] + [In^-] \tag{6.3.2}$$

Solving Equation 6.3.2 for [HIn] and substituting into Equation 6.3.1 gives

$$A = \varepsilon_{HIn} b\,(C - [In^-]) + \varepsilon_{In} b\,[In^-]$$

which we simplify to

$$A = \varepsilon_{HIn} bC - \varepsilon_{HIn} b\,[In^-] + \varepsilon_{In} b\,[In^-]$$

$$A = A_{HIn} + b\,[In^-]\,(\varepsilon_{In} - \varepsilon_{HIn}) \tag{6.3.3}$$

where A_{HIn}, which is equal to $\varepsilon_{HIn} bC$, is the absorbance when the pH is acidic enough that essentially all the indicator is present as HIn. Solving Equation 6.3.3 for the concentration of In^- gives

$$[In^-] = \frac{A - A_{HIn}}{b\,(\varepsilon_{In} - \varepsilon_{HIn})} \tag{6.3.4}$$

Proceeding in the same fashion, we derive a similar equation for the concentration of HIn

$$[HIn] = \frac{A_{In} - A}{b\,(\varepsilon_{In} - \varepsilon_{HIn})} \tag{6.3.5}$$

where A_{In}, which is equal to $\varepsilon_{In} bC$, is the absorbance when the pH is basic enough that only In^- contributes to the absorbance. Substituting Equation 6.3.4 and Equation 6.3.5 into the equilibrium constant expression for HIn gives

$$K_a = \frac{[H_3O^+][In^-]}{[HIn]} = [H_3O^+] \times \frac{A - A_{HIn}}{A_{In} - A} \tag{6.3.6}$$

We can use Equation 6.3.6 to determine K_a in one of two ways. The simplest approach is to prepare three solutions, each of which contains the same amount, C, of indicator. The pH of one solution is made sufficiently acidic such that [HIn] >> [In^-]. The absorbance of this solution gives A_{HIn}. The value of A_{In} is determined by adjusting the pH of the second solution such that [In^-] >> [HIn]. Finally, the pH of the third solution is adjusted to an intermediate value, and the pH and absorbance, A, recorded. The value of K_a is calculated using Equation 6.3.6.

Example 6.3.5

The acidity constant for an acid–base indicator is determined by preparing three solutions, each of which has a total concentration of indicator equal to 5.00×10^{-5} M. The first solution is made strongly acidic with HCl and has an absorbance of 0.250. The second solution is made strongly basic and has an absorbance of 1.40. The pH of the third solution is 2.91 and has an absorbance of 0.662. What is the value of K_a for the indicator?

Solution

The value of K_a is determined by making appropriate substitutions into 10.20 where [H_3O^+] is 1.23×10^{-3}; thus

$$K_a = (1.23 \times 10^{-3}) \times \frac{0.662 - 0.250}{1.40 - 0.662} = 6.87 \times 10^{-4}$$

Exercise 6.3.5

To determine the K_a of a merocyanine dye, the absorbance of a solution of 3.5×10^{-4} M dye was measured at a pH of 2.00, a pH of 6.00, and a pH of 12.00, yielding absorbances of 0.000, 0.225, and 0.680, respectively. What is the value of K_a for this dye? The data for this problem is adapted from Lu, H.; Rutan, S. C. *Anal. Chem.*, **1996**, *68*, 1381–1386.

Answer

The value of K_a is

$$K_a = (1.00 \times 10^{-6}) \times \frac{0.225 - 0.000}{0.680 - 0.225} = 4.95 \times 10^{-7}$$

A second approach for determining K_a is to prepare a series of solutions, each of which contains the same amount of indicator. Two solutions are used to determine values for A_{HIn} and A_{In}. Taking the log of both sides of Equation 6.3.6 and rearranging leave us with the following equation.

$$\log \frac{A - A_{HIn}}{A_{In^-} - A} = pH - pK_a \tag{6.3.7}$$

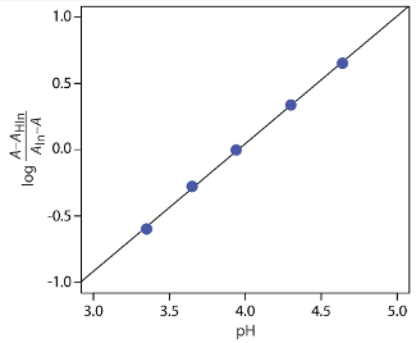
A plot of $\log[(A - A_{HIn})/(A_{In} - A)]$ versus pH is a straight-line with a slope of +1 and a *y*-intercept of $-pK_a$.

Exercise 6.3.6

To determine the K_a for the indicator bromothymol blue, the absorbance of each a series of solutions that contain the same concentration of bromothymol blue is measured at pH levels of 3.35, 3.65, 3.94, 4.30, and 4.64, yielding absorbance values of 0.170, 0.287, 0.411, 0.562, and 0.670, respectively. Acidifying the first solution to a pH of 2 changes its absorbance to 0.006, and adjusting the pH of the last solution to 12 changes its absorbance to 0.818. What is the value of K_a for bromothymol blue? The data for this problem is from Patterson, G. S. *J. Chem. Educ.*, **1999**, *76*, 395–398.

Answer

To determine K_a we use Equation 6.3.7, plotting $\log[(A - A_{HIn})/(A_{In} - A)]$ versus pH, as shown below.



Fitting a straight-line to the data gives a regression model of

$$\log \frac{A - A_{HIn}}{A_{In} - A} = -3.80 + 0.962pH$$

The *y*-intercept is $-pK_a$; thus, the pK_a is 3.80 and the K_a is 1.58×10^{-4}.

In developing these approaches for determining K_a we considered a relatively simple system in which the absorbance of HIn and In^- are easy to measure and for which it is easy to determine the concentration of H_3O^+. In addition to acid–base reactions, we can

adapt these approaches to any reaction of the general form

$$X(aq) + Y(aq) \rightleftharpoons Z(aq)$$

including metal–ligand complexation reactions and redox reactions, provided we can determine spectrophotometrically the concentration of the product, *Z*, and one of the reactants, either *X* or *Y*, and that we can determine the concentration of the other reactant by some other method. With appropriate modifications, a more complicated system in which we cannot determine the concentration of one or more of the reactants or products also is possible [Ramette, R. W. *Chemical Equilibrium and Analysis*, Addison-Wesley: Reading, MA, 1981, Chapter 13].

Evaluation of UV/Vis and IR Spectroscopy

Scale of Operations

Molecular UV/Vis absorption routinely is used for the analysis of trace analytes in macro and meso samples. Major and minor analytes are determined by diluting the sample before analysis, and concentrating a sample may allow for the analysis of ultratrace analytes. The scale of operations for infrared absorption is generally poorer than that for UV/Vis absorption.

Accuracy

Under normal conditions a relative error of 1–5% is easy to obtained with UV/Vis absorption. Accuracy usually is limited by the quality of the blank. Examples of the type of problems that are encountered include the pres- ence of particulates in the sample that scatter radiation, and the presence of interferents that react with analytical reagents. In the latter case the interferent may react to form an absorbing species, which leads to a positive determinate error. Interferents also may prevent the analyte from reacting, which leads to a negative determinate error. With care, it is possible to improve the accuracy of an analysis by as much as an order of magnitude.

Precision

In absorption spectroscopy, precision is limited by indeterminate errors—primarily instrumental noise—which are introduced when we measure absorbance. Precision generally is worse for low absorbances where $P_0 \approx P_T$, and for high absorbances where P_T approaches 0. We might expect, therefore, that precision will vary with transmittance.

We can derive an expression between precision and transmittance by applying the propagation of uncertainty as described in Chapter 4. To do so we rewrite Beer's law as

$$C = -\frac{1}{\varepsilon b}\log T \tag{6.3.8}$$

Table 4.3.1 in Chapter 4 helps us complete the propagation of uncertainty for Equation 6.3.8; thus, the absolute uncertainty in the concentration, s_C, is

$$s_c = -\frac{0.4343}{\varepsilon b} \times \frac{s_T}{T} \tag{6.3.9}$$

where s_T is the absolute uncertainty in the transmittance. Dividing Equation 6.3.9 by Equation 6.3.8 gives the relative uncertainty in concentration, s_C/C, as

$$\frac{s_c}{C} = \frac{0.4343 s_T}{T \log T}$$

If we know the transmittance's absolute uncertainty, then we can determine the relative uncertainty in concentration for any measured transmittance.

Determining the relative uncertainty in concentration is complicated because s_T is a function of the transmittance. As shown in Table 6.3.3 , three categories of indeterminate instrumental error are observed [Rothman, L. D.; Crouch, S. R.; Ingle, J. D. Jr. *Anal. Chem.* **1975**, *47*, 1226–1233]. A constant s_T is observed for the uncertainty associated with reading %*T* on a meter's analog or digital scale. Typical values are ±0.2–0.3% (a k_1 of ±0.002–0.003) for an analog scale and ±0.001% a (k_1 of ±0.00001) for a digital scale.

Table 6.3.3 . Effect of Indeterminate Errors on Relative Uncertainty in Concentration

category	sources of indeterminate error	relative uncertainty in concentration
$s_T = k_1$	%T readout resolution noise in thermal detectors	$\frac{s_C}{C} = \frac{0.4343k_1}{T \log T}$
$s_T = k_2\sqrt{T^2 + T}$	noise in photon detectors	$\frac{s_C}{C} = \frac{0.4343k_2}{\log T}\sqrt{1 + \frac{1}{T}}$
$s_T = k_3 T$	positioning of sample cell fluctuations in source intensity	$\frac{s_C}{C} = \frac{0.4343k_3}{\log T}$

A constant s_T also is observed for the thermal transducers used in infrared spectrophotometers. The effect of a constant s_T on the relative uncertainty in concentration is shown by curve A in Figure 6.3.16 . Note that the relative uncertainty is very large for both high absorbances and low absorbances, reaching a minimum when the absorbance is 0.4343. This source of indeterminate error is important for infrared spectrophotometers and for inexpensive UV/Vis spectrophotometers. To obtain a relative uncertainty in concentration of ±1–2%, the absorbance is kept within the range 0.1–1.

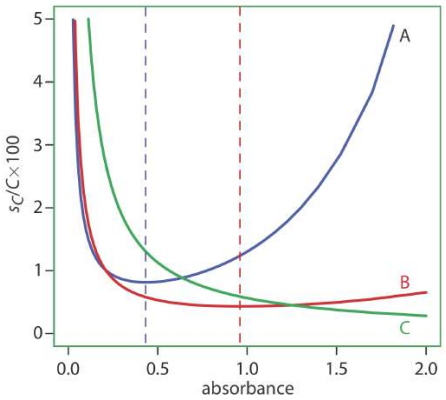


Figure 6.3.16 . Percent relative uncertainty in concentration as a function of absorbance for the categories of indeterminate errors in Table **6.3.10.3**. A: k_1 = ±0.0030; B: k_2 = ±0.0030; and C: k_3= ±0.0130. The dashed lines correspond to the minimum uncertainty for curve A (absorbance of 0.4343) and for curve B (absorbance of 0.963).

Values of s_T are a complex function of transmittance when indeterminate errors are dominated by the noise associated with photon detectors. Curve B in Figure 6.3.16 shows that the relative uncertainty in concentration is very large for low absorbances, but is smaller at higher absorbances. Although the relative uncertainty reaches a minimum when the absorbance is 0.963, there is little change in the relative uncertainty for absorbances between 0.5 and 2. This source of indeterminate error generally limits the precision of high quality UV/Vis spectrophotometers for mid-to-high absorbances.

Finally, the value of s_T is directly proportional to transmittance for indeterminate errors that result from fluctuations in the source's intensity and from uncertainty in positioning the sample within the spectrometer. The latter is particularly important because the optical properties of a sample cell are not uniform. As a result, repositioning the sample cell may lead to a change in the intensity of transmitted radiation. As shown by curve C in Figure 6.3.16 , the effect is important only at low absorbances. This source of indeterminate errors usually is the limiting factor for high quality UV/Vis spectrophotometers when the absorbance is relatively small.

When the relative uncertainty in concentration is limited by the %T readout resolution, it is possible to improve the precision of the analysis by redefining 100% T and 0% T. Normally 100% T is established using a blank and 0% T is established while preventing the source's radiation from reaching the detector. If the absorbance is too high, precision is improved by resetting 100% T using a standard solution of analyte whose concentration is less than that of the sample (Figure 6.3.17 a). For a sample whose absorbance is too low, precision is improved by redefining 0% T using a standard solution of the analyte whose concentration is greater than that of the analyte (Figure 6.3.17 b). In this case a calibration curve is required because a linear relationship between absorbance and concentration no longer exists. Precision is further increased by combining these two methods (Figure 6.3.17 c). Again, a calibration curve is necessary since the relation- ship between absorbance and concentration is no longer linear.

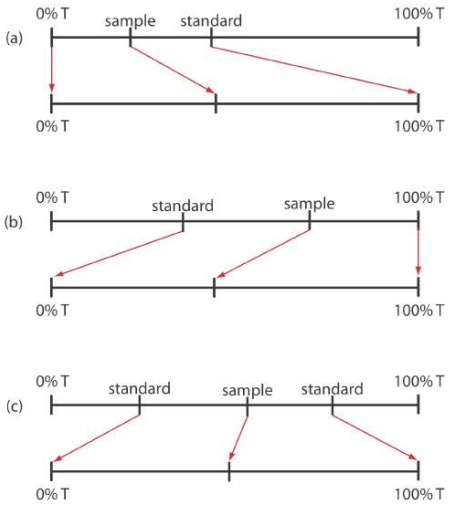


Figure 6.3.17 . Methods for improving the precision of absorption methods: (a) high-absorbance method; (b) low-absorbance method; (c) maximum precision method.

Sensitivity

The sensitivity of a molecular absorption method, which is the slope of a Beer's law calibration curve, is the product of the analyte's absorptivity and the pathlength of the sample cell (εb). You can improve a method's sensitivity by selecting a wavelength where absorbance is at a maximum or by increasing pathlength.

> See Figure 10.2.10 for an example of how the choice of wavelength affects a calibration curve's sensitivity.

Selectivity

Selectivity rarely is a problem in molecular absorption spectrophotometry. In many cases it is possible to find a wavelength where only the analyte absorbs. When two or more species do contribute to the measured absorbance, a multicomponent analysis is still possible, as shown in Example 6.3.2 and Example 6.3.3 .

Time, Cost, and Equipment

The analysis of a sample by molecular absorption spectroscopy is relatively rapid, although additional time is required if we need to convert a nonabsorbing analyte into an absorbing form. The cost of UV/Vis instrumentation ranges from several hundred dollars for a simple filter photometer, to more than $50,000 for a computer-controlled, high-resolution double-beam instrument equipped with variable slit widths, and operating over an extended range of wavelengths. Fourier transform infrared spectrometers can be obtained for as little as $15,000–$20,000, although more expensive models are available.

This page titled 6.3: UV/Vis and IR Spectroscopy is shared under a CC BY-NC-SA 4.0 license and was authored, remixed, and/or curated by Kathryn Davis.

- **10.3: UV/Vis and IR Spectroscopy** by David Harvey is licensed CC BY-NC-SA 4.0.

6.4: Atomic Absorption Spectroscopy

Guystav Kirchoff and Robert Bunsen first used atomic absorption—along with atomic emission—in 1859 and 1860 as a means for identify atoms in flames and hot gases. Although atomic emission continued to develop as an analytical technique, progress in atomic absorption languished for almost a century. Modern atomic absorption spectroscopy has its beginnings in 1955 as a result of the independent work of A. C. Walsh and C. T. J. Alkemade [(a) Walsh, A. *Anal. Chem.* **1991**, *63*, 933A–941A; (b) Koirtyohann, S. R. *Anal. Chem.* **1991**, *63*, 1024A–1031A; (c) Slavin, W. *Anal. Chem.* **1991**, *63*, 1033A–1038A]. Commercial instruments were in place by the early 1960s, and the importance of atomic absorption as an analytical technique soon was evident.

Instrumentation

Atomic absorption spectrophotometers use the same single-beam or double-beam optics described earlier for molecular absorption spectrophotometers (see Figure 10.3.2 and Figure 10.3.3). There is, however, an important additional need in atomic absorption spectroscopy: we first must covert the analyte into free atoms. In most cases the analyte is in solution form. If the sample is a solid, then we must bring the analyte into solution before the analysis. When analyzing a lake sediment for Cu, Zn, and Fe, for example, we bring the analytes into solution as Cu^{2+}, Zn^{2+}, and Fe^{3+} by extracting them with a suitable reagent. For this reason, only the introduction of solution samples is considered in this chapter.

> What reagent we choose to use to bring an analyte into solution depends on our research goals. If we need to know the total amount of metal in the sediment, then we might try a microwave digestion using a mixture of concentrated acids, such as HNO_3, HCl, and HF. This destroys the sediment's matrix and brings everything into solution. On the other hand, if our interest is biologically available metals, we might extract the sample under milder conditions using, for example, a dilute solution of HCl or CH_3COOH at room temperature.

Atomization

The process of converting an analyte to a free gaseous atom is called ***atomization***. Converting an aqueous analyte into a free atom requires that we strip away the solvent, volatilize the analyte, and, if necessary, dissociate the analyte into free atoms. Desolvating an aqueous solution of $CuCl_2$, for example, leaves us with solid particulates of $CuCl_2$. Converting the particulate $CuCl_2$ to gas phases atoms of Cu and Cl requires thermal energy.

$$\mathrm{CuCl_2}(aq) \rightarrow \mathrm{CuCl_2}(s) \rightarrow \mathrm{Cu}(g) + 2\mathrm{Cl}(g)$$

There are two common atomization methods: flame atomization and electrothermal atomization, although a few elements are atomized using other methods.

Flame Atomizer

Figure 10.4.1 shows a typical flame atomization assembly with close-up views of several key components. In the unit shown here, the aqueous sample is drawn into the assembly by passing a high-pressure stream of compressed air past the end of a capillary tube immersed in the sample. When the sample exits the nebulizer it strikes a glass impact bead, which converts it into a fine aerosol mist within the spray chamber. The aerosol mist is swept through the spray chamber by the combustion gases—compressed air and acetylene in this case—to the burner head where the flame's thermal energy desolvates the aerosol mist to a dry aerosol of small, solid particulates. The flame's thermal energy then volatilizes the particles, producing a vapor that consists of molecular species, ionic species, and free atoms.

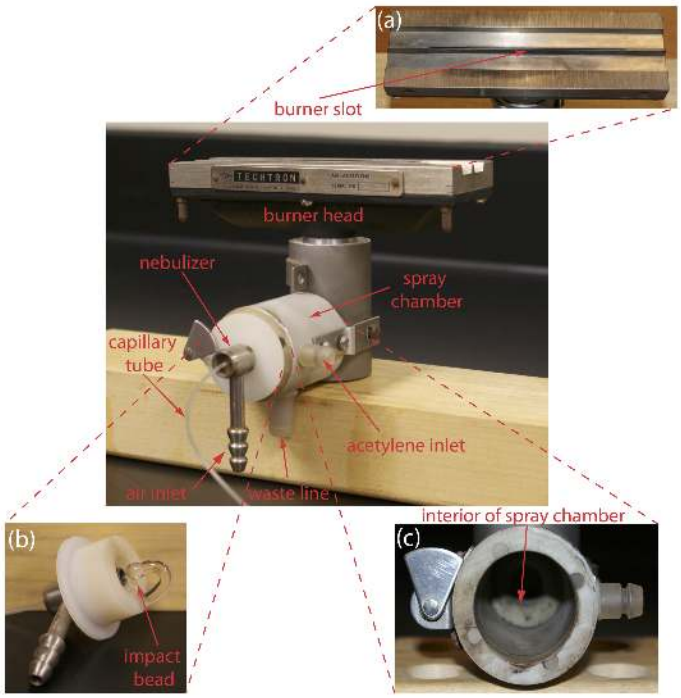


Figure 10.4.1 . Flame atomization assembly with expanded views of (a) the burner head showing the burner slot where the flame is located; (b) the nebulizer's impact bead; and (c) the interior of the spray chamber. Although the unit shown here is from an instrument dating to the 1970s, the basic components of a modern flame AA spectrometer are the same.

Burner. The slot burner in Figure 10.4.1 a provides a long optical pathlength and a stable flame. Because absorbance is directly proportional to pathlength, a long pathlength provides greater sensitivity. A stable flame minimizes uncertainty due to fluctuations in the flame.

The burner is mounted on an adjustable stage that allows the entire assembly to move horizontally and vertically. Horizontal adjustments ensure the flame is aligned with the instrument's optical path. Vertical adjustments change the height within the flame from which absorbance is monitored. This is important because two competing processes affect the concentration of free atoms in the flame. The more time an analyte spends in the flame the greater the atomization efficiency; thus, the production of free atoms increases with height. On the other hand, a longer residence time allows more opportunity for the free atoms to combine with oxygen to form a molecular oxide. As seen in Figure 10.4.2 , for a metal this is easy to oxidize, such as Cr, the concentration of free atoms is greatest just above the burner head. For a metal, such as Ag, which is difficult to oxidize, the concentration of free atoms increases steadily with height.

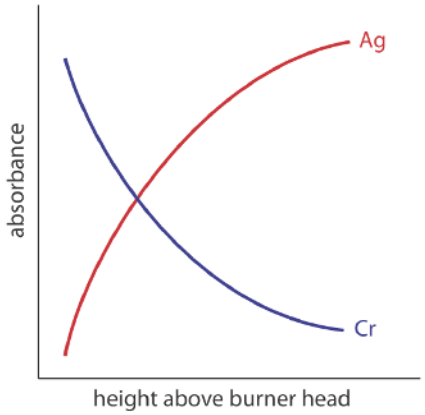


Figure 10.4.2 . Absorbance versus height profiles for Ag and Cr in flame atomic absorption spectroscopy.

Flame. The flame's temperature, which affects the efficiency of atomization, depends on the fuel–oxidant mixture, several examples of which are listed in Table 10.4.1 . Of these, the air–acetylene and the nitrous oxide–acetylene flames are the most

popular. Normally the fuel and oxidant are mixed in an approximately stoichiometric ratio; however, a fuel-rich mixture may be necessary for easily oxidized analytes.

Table 10.4.1 . Fuels and Oxidants Used for Flame Combustion

fuel	oxidant	temperature range (^{o}C)
natural gas	air	1700–1900
hydrogen	air	2000–2100
acetylene	air	2100–2400
acetylene	nitrous oxide	2600–2800
acetylene	oxygen	3050–3150

Figure 10.4.3 shows a cross-section through the flame, looking down the source radiation's optical path. The primary combustion zone usually is rich in gas combustion products that emit radiation, limiting is useful- ness for atomic absorption. The interzonal region generally is rich in free atoms and provides the best location for measuring atomic absorption. The hottest part of the flame typically is 2–3 cm above the primary combustion zone. As atoms approach the flame's secondary combustion zone, the decrease in temperature allows for formation of stable molecular species.

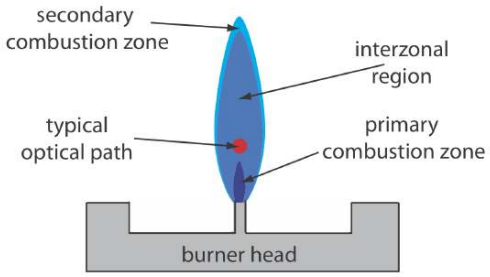


Figure 10.4.3 . Profile of typical flame using a slot burner. The relative size of each zone depends on many factors, including the choice of fuel and oxidant, and their relative proportions.

Sample Introduction. The most common means for introducing a sample into a flame atomizer is a continuous aspiration in which the sample flows through the burner while we monitor absorbance. Continuous aspiration is sample intensive, typically requiring from 2–5 mL of sample.

Flame microsampling allows us to introduce a discrete sample of fixed volume, and is useful if we have a limited amount of sample or when the sample's matrix is incompatible with the flame atomizer. For example, continuously aspirating a sample that has a high concentration of dissolved solids—sea water, for example, comes to mind—may build-up a solid de- posit on the burner head that obstructs the flame and that lowers the absorbance. Flame microsampling is accomplished using a micropipet to place 50–250 µL of sample in a Teflon funnel connected to the nebulizer, or by dipping the nebulizer tubing into the sample for a short time. Dip sampling usually is accomplished with an automatic sampler. The signal for flame microsampling is a transitory peak whose height or area is proportional to the amount of analyte that is injected.

Advantages and Disadvantages of Flame Atomization. The principal advantage of flame atomization is the reproducibility with which the sample is introduced into the spectrophotometer; a significant disadvantage is that the efficiency of atomization is quite poor. There are two reasons for poor atomization efficiency. First, the majority of the aerosol droplets produced during nebulization are too large to be carried to the flame by the combustion gases. Consequently, as much as 95% of the sample never reaches the flame, which is the reason for the waste line shown at the bottom of the spray chamber in Figure 10.4.1 . A second reason for poor atomization efficiency is that the large volume of combustion gases significantly dilutes the sample. Together, these contributions to the efficiency of atomization reduce sensitivity because the analyte's concentration in the flame may be a factor of 2.5×10^{-6} less than that in solution [Ingle, J. D.; Crouch, S. R. *Spectrochemical Analysis*, Prentice-Hall: Englewood Cliffs, NJ, 1988; p. 275].

Electrothermal Atomizers

A significant improvement in sensitivity is achieved by using the resistive heating of a graphite tube in place of a flame. A typical electrothermal atomizer, also known as a ***graphite furnace***, consists of a cylindrical graphite tube approximately 1–3 cm in length and 3–8 mm in diameter. As shown in Figure 10.4.4 , the graphite tube is housed in an sealed assembly that has an optically transparent window at each end. A continuous stream of inert gas is passed through the furnace, which protects the graphite tube from oxidation and removes the gaseous products produced during atomization. A power supply is used to pass a current through the graphite tube, resulting in resistive heating.

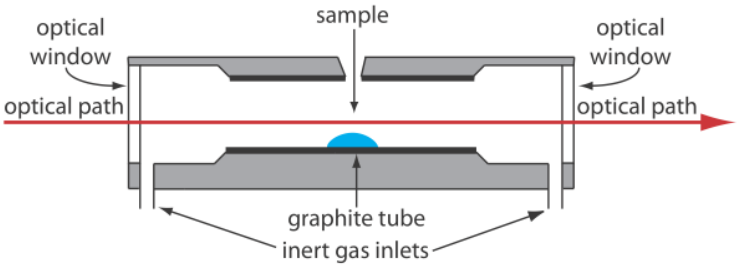


Figure 10.4.4 . Diagram showing a cross-section of an electrothermal analyzer.

Samples of between 5–50 μL are injected into the graphite tube through a small hole at the top of the tube. Atomization is achieved in three stages. In the first stage the sample is dried to a solid residue using a current that raises the temperature of the graphite tube to about 110°C. In the second stage, which is called ashing, the temperature is increased to between 350–1200°C. At these temperatures organic material in the sample is converted to CO_2 and H_2O, and volatile inorganic materials are vaporized. These gases are removed by the inert gas flow. In the final stage the sample is atomized by rapidly increasing the temperature to between 2000–3000°C. The result is a transient absorbance peak whose height or area is proportional to the absolute amount of analyte injected into the graphite tube. Together, the three stages take approximately 45–90 s, with most of this time used for drying and ashing the sample.

Electrothermal atomization provides a significant improvement in sensitivity by trapping the gaseous analyte in the small volume within the graphite tube. The analyte's concentration in the resulting vapor phase is as much as **1000 ×** greater than in a flame atomization [Parsons, M. L.; Major, S.; Forster, A. R. *Appl. Spectrosc.* **1983**, *37*, 411–418]. This improvement in sensitivity—and the resulting improvement in detection limits—is offset by a significant decrease in precision. Atomization efficiency is influenced strongly by the sample's contact with the graphite tube, which is difficult to control reproducibly.

Miscellaneous Atomization Methods

A few elements are atomized by using a chemical reaction to produce a volatile product. Elements such as As, Se, Sb, Bi, Ge, Sn, Te, and Pb, for example, form volatile hydrides when they react with $NaBH_4$ in the presence of acid. An inert gas carries the volatile hydride to either a flame or to a heated quartz observation tube situated in the optical path. Mercury is determined by the cold-vapor method in which it is reduced to elemental mercury with $SnCl_2$. The volatile Hg is carried by an inert gas to an unheated observation tube situated in the instrument's optical path.

Quantitative Applications

Atomic absorption is used widely for the analysis of trace metals in a variety of sample matrices. Using Zn as an example, there are standard atomic absorption methods for its determination in samples as diverse as water and wastewater, air, blood, urine, muscle tissue, hair, milk, breakfast cereals, shampoos, alloys, industrial plating baths, gasoline, oil, sediments, and rocks.

Developing a quantitative atomic absorption method requires several considerations, including choosing a method of atomization, selecting the wavelength and slit width, preparing the sample for analysis, minimizing spectral and chemical interferences, and selecting a method of standardization. Each of these topics is considered in this section.

Developing a Quantitative Method

Flame or Electrothermal Atomization? The most important factor in choosing a method of atomization is the analyte's concentration. Because of its greater sensitivity, it takes less analyte to achieve a given absorbance when using electrothermal atomization. Table 10.4.2 , which compares the amount of analyte needed to achieve an absorbance of 0.20 when using flame

atomization and electrothermal atomization, is useful when selecting an atomization method. For example, flame atomization is the method of choice if our samples contain 1–10 mg Zn^{2+}/L, but electrothermal atomization is the best choice for samples that contain 1–10 μg Zn^{2+}/L.

Table 10.4.2 . Concentration of Analyte (in mg/L) That Yields an Absorbance of 0.20

element	flame atomization	electrothermal atomization
Ag	1.5	0.0035
Al	40	0.015
As	40	0.050
Ca	0.8	0.003
Cd	0.6	0.001
Co	2.5	0.021
Cr	2.5	0.0075
Cu	1.5	0.012
Fe	2.5	0.006
Hg	70	0.52
Mg	0.15	0.00075
Mn	1	0.003
Na	0.3	0.00023
Ni	2	0.024
Pb	5	0.080
Pt	70	0.29
Sn	50	0.023
Zn	0.3	0.00071

Source: Varian Cookbook, SpectraAA Software Version 4.00 Pro.
As: 10 mg/L by hydride vaporization; Hg: 11.5 mg/L by cold-vapor; and Sn:18 mg/L by hydride vaporization

Selecting the Wavelength and Slit Width. The source for atomic absorption is a hollow cathode lamp that consists of a cathode and anode enclosed within a glass tube filled with a low pressure of an inert gas, such as Ne or Ar (Figure 10.4.5). Applying a potential across the electrodes ionizes the filler gas. The positively charged gas ions collide with the negatively charged cathode, sputtering atoms from the cathode's surface. Some of the sputtered atoms are in the excited state and emit radiation characteristic of the metal(s) from which the cathode is manufactured. By fashioning the cathode from the metallic analyte, a hollow cathode lamp provides emission lines that correspond to the analyte's absorption spectrum.

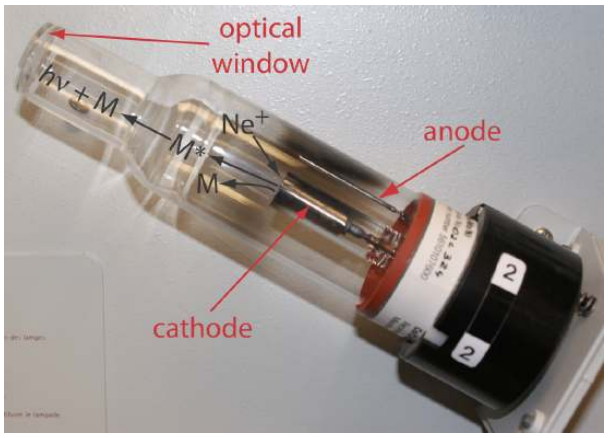


Figure 10.4.5 . Photo of a typical multielemental hollow cathode lamp. The cathode in this lamp is fashioned from an alloy of Co, Cr, Cu, Fe, Mn, and Ni, and is surrounded by a glass shield that isolates it from the anode. The lamp is filled with Ne gas. Also shown is the process that leads to atomic emission. Note the black deposit of sputtered metal on the outer wall of the hollow cathode lamp. See the text for additional details.

Because atomic absorption lines are narrow, we need to use a line source instead of a continuum source (compare, for example, Figure 10.2.4 with Figure 10.2.6). The effective bandwidth when using a continuum source is roughly 1000× larger than an atomic absorption line; thus, $P_T \approx P_0$, $\%T \approx 100$, and $A \approx 0$. Because a hollow cathode lamp is a line source, P_T and P_0 have different values giving a $\%T < 100$ and $A > 0$.

Each element in a hollow cathode lamp provides several atomic emission lines that we can use for atomic absorption. Usually the wavelength that provides the best sensitivity is the one we choose to use, although a less sensitive wavelength may be more appropriate for a sample that has higher concentration of analyte. For the Cr hollow cathode lamp in Table 10.4.3 , the best sensitivity is obtained using a wavelength of 357.9 nm.

Table 10.4.3 . Atomic Emission Lines for a Cr Hollow Cathode Lamp

wavelength (nm)	slit width (nm)	mg Cr/L giving $A = 0.20$	P_0 (relative)
357.9	0.2	2.5	40
425.4	0.2	12	85
429.0	0.5	20	100
520.5	0.2	1500	15
520.8	0.2	500	20

Another consideration is the emission line's intensity. If several emission lines meet our requirements for sensitivity, we may wish to use the emission line with the largest relative P_0 because there is less uncertainty in measuring P_0 and P_T. When analyzing a sample that is ≈10 mg Cr/L, for example, the first three wavelengths in Table 10.4.3 provide an appropriate sensitivity; the wavelengths of 425.4 nm and 429.0 nm, however, have a greater P_0 and will provide less uncertainty in the measured absorbance.

The emission spectrum for a hollow cathode lamp includes, in addition to the analyte's emission lines, additional emission lines from impurities present in the metallic cathode and from the filler gas. These additional lines are a potential source of stray radiation that could result in an instrumental deviation from Beer's law. The monochromator's slit width is set as wide as possible to improve the throughput of radiation and narrow enough to eliminate these sources of stray radiation.

Preparing the Sample. Flame and electrothermal atomization require that the analyte is in solution. Solid samples are brought into solution by dissolving in an appropriate solvent. If the sample is not soluble it is digested, either on a hot-plate or by microwave, using HNO_3, H_2SO_4, or $HClO_4$. Alternatively, we can extract the analyte using a Soxhlet extractor. Liquid samples are analyzed directly or the analytes extracted if the matrix is in- compatible with the method of atomization. A serum sample, for instance, is

difficult to aspirate when using flame atomization and may produce an unacceptably high background absorbance when using electrothermal atomization. A liquid–liquid extraction using an organic solvent and a chelating agent frequently is used to concentrate analytes. Dilute solutions of Cd^{2+}, Co^{2+}, Cu^{2+}, Fe^{3+}, Pb^{2+}, Ni^{2+}, and Zn^{2+}, for example, are concentrated by extracting with a solution of ammonium pyrrolidine dithiocarbamate in methyl isobutyl ketone.

Minimizing Spectral Interference. A spectral interference occurs when an analyte's absorption line overlaps with an interferent's absorption line or band. Because they are so narrow, the overlap of two atomic absorption lines seldom is a problem. On the other hand, a molecule's broad absorption band or the scattering of source radiation is a potentially serious spectral interference.

An important consideration when using a flame as an atomization source is its effect on the measured absorbance. Among the products of combustion are molecular species that exhibit broad absorption bands and particulates that scatter radiation from the source. If we fail to compensate for these spectral interferences, then the intensity of transmitted radiation is smaller than expected. The result is an apparent increase in the sample's absorbance. Fortunately, absorption and scattering of radiation by the flame are corrected by analyzing a blank.

Spectral interferences also occur when components of the sample's matrix other than the analyte react to form molecular species, such as oxides and hydroxides. The resulting absorption and scattering constitutes the sample's background and may present a significant problem, particularly at wavelengths below 300 nm where the scattering of radiation becomes more important. If we know the composition of the sample's matrix, then we can prepare our samples using an identical matrix. In this case the background absorption is the same for both the samples and the standards. Alternatively, if the background is due to a known matrix component, then we can add that component in excess to all samples and standards so that the contribution of the naturally occurring interferent is insignificant. Finally, many interferences due to the sample's matrix are eliminated by increasing the atomization temperature. For example, switching to a higher temperature flame helps prevents the formation of interfering oxides and hydroxides.

If the identity of the matrix interference is unknown, or if it is not possible to adjust the flame or furnace conditions to eliminate the interference, then we must find another method to compensate for the background interference. Several methods have been developed to compensate for matrix interferences, and most atomic absorption spectrophotometers include one or more of these methods.

One of the most common methods for ***background correction*** is to use a continuum source, such as a D_2 lamp. Because a D_2 lamp is a continuum source, absorbance of its radiation by the analyte's narrow absorption line is negligible. Only the background, therefore, absorbs radiation from the D_2 lamp. Both the analyte and the background, on the other hand, absorb the hollow cathode's radiation. Subtracting the absorbance for the D_2 lamp from that for the hollow cathode lamp gives a corrected absorbance that compensates for the background interference. Although this method of background correction is effective, it does assume that the background absorbance is constant over the range of wavelengths passed by the monochromator. If this is not true, then subtracting the two absorbances underestimates or overestimates the background.

> Other methods of background correction have been developed, including Zeeman effect background correction and Smith–Hieftje background correction, both of which are included in some commercially available atomic absorption spectrophotometers. Consult the chapter's additional resources for additional information.

Minimizing Chemical Interferences. The quantitative analysis of some elements is complicated by chemical interferences that occur during atomization. The most common chemical interferences are the formation of nonvolatile compounds that contain the analyte and ionization of the analyte.

One example of the formation of a nonvolatile compound is the effect of $\mathbf{PO_4^{3-}}$ or Al^{3+} on the flame atomic absorption analysis of Ca^{2+}. In one study, for example, adding 100 ppm Al^{3+} to a solution of 5 ppm Ca^{2+} decreased calcium ion's absorbance from 0.50 to 0.14, while adding 500 ppm $\mathbf{PO_4^{3-}}$ to a similar solution of Ca^{2+} decreased the absorbance from 0.50 to 0.38. These interferences are attributed to the formation of nonvolatile particles of $Ca_3(PO_4)_2$ and an Al–Ca–O oxide [Hosking, J. W.; Snell, N. B.; Sturman, B. T. *J. Chem. Educ.* **1977**, *54*, 128–130].

When using flame atomization, we can minimize the formation of non-volatile compounds by increasing the flame's temperature by changing the fuel-to-oxidant ratio or by switching to a different combination of fuel and oxidant. Another approach is to add a

releasing agent or a protecting agent to the sample. A ***releasing agent*** is a species that reacts preferentially with the interferent, releasing the analyte during atomization. For example, Sr^{2+} and La^{3+} serve as releasing agents for the analysis of Ca^{2+} in the presence of PO_4^{3-} or Al^{3+}. Adding 2000 ppm $SrCl_2$ to the Ca^{2+}/ PO_4^{3-} and to the Ca^{2+}/Al^{3+} mixtures described in the previous paragraph increased the absorbance to 0.48. A ***protecting agent*** reacts with the analyte to form a stable volatile complex. Adding 1% w/w EDTA to the Ca^{2+}/ PO_4^{3-} solution described in the previous paragraph increased the absorbance to 0.52.

An ionization interference occurs when thermal energy from the flame or the electrothermal atomizer is sufficient to ionize the analyte

$$M(s) \rightleftharpoons M^+(aq) + e^- \tag{6.4.1}$$

where M is the analyte. Because the absorption spectra for M and M^+ are different, the position of the equilibrium in reaction 6.4.1 affects the absorbance at wavelengths where M absorbs. To limit ionization we add a high concentration of an ***ionization suppressor***, which is a species that ionizes more easily than the analyte. If the ionization suppressor's concentration is sufficient, then the increased concentration of electrons in the flame pushes reaction 6.4.1 to the left, preventing the analyte's ionization. Potassium and cesium frequently are used as an ionization suppressor because of their low ionization energy.

Standardizing the Method. Because Beer's law also applies to atomic absorption, we might expect atomic absorption calibration curves to be linear. In practice, however, most atomic absorption calibration curves are nonlinear or linear over a limited range of concentrations. Nonlinearity in atomic absorption is a consequence of instrumental limitations, including stray radiation from the hollow cathode lamp and the variation in molar absorptivity across the absorption line. Accurate quantitative work, therefore, requires a suitable means for computing the calibration curve from a set of standards.

When possible, a quantitative analysis is best conducted using external standards. Unfortunately, matrix interferences are a frequent problem, particularly when using electrothermal atomization. For this reason the method of standard additions often is used. One limitation to this method of standardization, however, is the requirement of a linear relationship between absorbance and concentration.

> Most instruments include several different algorithms for computing the calibration curve. The instrument in my lab, for example, includes five algorithms. Three of the algorithms fit absorbance data using linear, quadratic, or cubic polynomial functions of the analyte's concentration. It also includes two algorithms that fit the concentrations of the standards to quadratic functions of the absorbance.

Representative Method 10.4.1: Determination of Cu and Zn in Tissue Samples

The best way to appreciate the theoretical and the practical details discussed in this section is to carefully examine a typical analytical method. Although each method is unique, the following description of the determination of Cu and Zn in biological tissues provides an instructive example of a typical procedure. The description here is based on Bhattacharya, S. K.; Goodwin, T. G.; Crawford, A. J. *Anal. Lett.* **1984**, *17*, 1567–1593, and Crawford, A. J.; Bhattacharya, S. K. Varian Instruments at Work, Number AA–46, April 1985.

Description of Method.

Copper and zinc are isolated from tissue samples by digesting the sample with HNO_3 after first removing any fatty tissue. The concentration of copper and zinc in the supernatant are determined by atomic absorption using an air-acetylene flame.

Procedure.

Tissue samples are obtained by a muscle needle biopsy and dried for 24–30 h at 105°C to remove all traces of moisture. The fatty tissue in a dried sample is removed by extracting overnight with anhydrous ether. After removing the ether, the sample is dried to obtain the fat-free dry tissue weight (FFDT). The sample is digested at 68°C for 20–24 h using 3 mL of 0.75 M HNO_3. After centrifuging at 2500 rpm for 10 minutes, the supernatant is transferred to a 5-mL volumetric flask. The digestion is repeated two more times, for 2–4 hours each, using 0.9-mL aliquots of 0.75 M HNO_3. These supernatants are added to the 5-mL volumetric flask, which is diluted to volume with 0.75 M HNO_3. The concentrations of Cu and Zn in the diluted supernatant are determined by flame atomic absorption spectroscopy using an air-acetylene flame and external standards. Copper is analyzed at a wavelength of

324.8 nm with a slit width of 0.5 nm, and zinc is analyzed at 213.9 nm with a slit width of 1.0 nm. Background correction using a D_2 lamp is necessary for zinc. Results are reported as µg of Cu or Zn per gram of FFDT.

Questions.

1. Describe the appropriate matrix for the external standards and for the blank?

    The matrix for the standards and the blank should match the matrix of the samples; thus, an appropriate matrix is 0.75 M HNO_3. Any interferences from other components of the sample matrix are minimized by background correction.

2. Why is a background correction necessary for the analysis of Zn, but not for the analysis of Cu?

    Background correction compensates for background absorption and scattering due to interferents in the sample. Such interferences are most severe when using a wavelength less than 300 nm. This is the case for Zn, but not for Cu.

3. A Cu hollow cathode lamp has several emission lines, the properties of which are shown in the following table. Explain why this method uses the line at 324.8 nm.

wavelength (nm)	slit width (nm)	mg Cu/L for A = 0.20	P_0 (relative)
217.9	0.2	15	3
218.2	0.2	15	3
222.6	0.2	60	5
244.2	0.2	400	15
249.2	0.5	200	24
324.8	0.5	1.5	100
327.4	0.5	3	87

    With 1.5 mg Cu/L giving an absorbance of 0.20, the emission line at 324.8 nm has the best sensitivity. In addition, it is the most intense emission line, which decreases the uncertainty in the measured absorbance.

Example 10.4.1

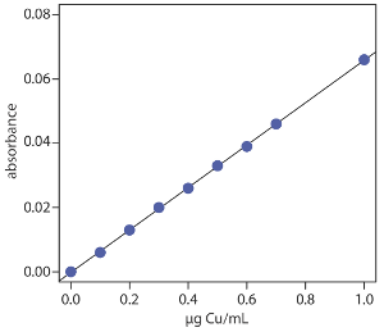
To evaluate the method described in Representative Method 10.4.1, a series of external standard is prepared and analyzed, providing the results shown here [Crawford, A. J.; Bhattacharya, S. K. “Microanalysis of Copper and Zinc in Biopsy-Sized Tissue Specimens by Atomic Absorption Spectroscopy Using a Stoichiometric Air-Acetylene Flame,” Varian Instruments at Work, Number AA–46, April 1985].

µg Cu/mL	absorbance	µg Cu/mL	absorbance
0.000	0.000	0.500	0.033
0.100	0.006	0.600	0.039
0.200	0.013	0.700	0.046
0.300	0.020	1.00	0.066
0.400	0.026		

A bovine liver standard reference material is used to evaluate the method’s accuracy. After drying and extracting the sample, a 11.23-mg FFDT tissue sample gives an absorbance of 0.023. Report the amount of copper in the sample as µg Cu/g FFDT.

Solution

Linear regression of absorbance versus the concentration of Cu in the standards gives the calibration curve shown below and the following calibration equation.



$$A = -0.0002 + 0.0661 \times \frac{\mu g\ Cu}{mL}$$

Substituting the sample's absorbance into the calibration equation gives the concentration of copper as 0.351 µg/mL. The concentration of copper in the tissue sample, therefore, is

$$\frac{\frac{0.351 \mu g\ Cu}{mL} \times 5.000\ mL}{0.01123\ g\ sample} = 156\ \mu g\ Cu/g\ FDT$$

Evaluation of Atomic Absorption Spectroscopy

Scale of Operation

Atomic absorption spectroscopy is ideally suited for the analysis of trace and ultratrace analytes, particularly when using electrothermal atomization. For minor and major analytes, sample are diluted before the analysis. Most analyses use a macro or a meso sample. The small volume requirement for electrothermal atomization or for flame microsampling, however, makes practical the analysis of micro and ultramicro samples.

Accuracy

If spectral and chemical interferences are minimized, an accuracy of 0.5–5% is routinely attainable. When the calibration curve is nonlinear, accuracy is improved by using a pair of standards whose absorbances closely bracket the sample's absorbance and assuming that the change in absorbance is linear over this limited concentration range. Determinate errors for electrothermal atomization often are greater than those obtained with flame atomization due to more serious matrix interferences.

Precision

For an absorbance greater than 0.1–0.2, the relative standard deviation for atomic absorption is 0.3–1% for flame atomization and 1–5% for electrothermal atomization. The principle limitation is the uncertainty in the concentration of free analyte atoms that result from variations in the rate of aspiration, nebulization, and atomization for a flame atomizer, and the consistency of injecting samples for electrothermal atomization.

Sensitivity

The sensitivity of a flame atomic absorption analysis is influenced by the flame's composition and by the position in the flame from which we monitor the absorbance. Normally the sensitivity of an analysis is optimized by aspirating a standard solution of analyte and adjusting the fuel-to-oxidant ratio, the nebulizer flow rate, and the height of the burner, to give the greatest absorbance. With electrothermal atomization, sensitivity is influenced by the drying and ashing stages that precede atomization. The temperature and time at each stage is optimized for each type of sample.

Sensitivity also is influenced by the sample's matrix. We already noted, for example, that sensitivity is decreased by a chemical interference. An increase in sensitivity may be realized by adding a low molecular weight alcohol, ester, or ketone to the solution, or by using an organic solvent.

Selectivity

Due to the narrow width of absorption lines, atomic absorption provides excellent selectivity. Atomic absorption is used for the analysis of over 60 elements at concentrations at or below the level of μg/L.

Time, Cost, and Equipment

The analysis time when using flame atomization is short, with sample throughputs of 250–350 determinations per hour when using a fully automated system. Electrothermal atomization requires substantially more time per analysis, with maximum sample throughputs of 20–30 determinations per hour. The cost of a new instrument ranges from between $10,000– $50,000 for flame atomization, and from $18,000–$70,000 for electrothermal atomization. The more expensive instruments in each price range include double-beam optics, automatic samplers, and can be programmed for multielemental analysis by allowing the wavelength and hollow cathode lamp to be changed automatically.

This page titled 6.4: Atomic Absorption Spectroscopy is shared under a CC BY-NC-SA 4.0 license and was authored, remixed, and/or curated by Kathryn Davis.

- **10.4: Atomic Absorption Spectroscopy** by David Harvey is licensed CC BY-NC-SA 4.0.

6.5: Photoluminescent Spectroscopy

Photoluminescence is divided into two categories: fluorescence and phosphorescence. A pair of electrons that occupy the same electronic ground state have opposite spins and are in a singlet spin state (Figure 10.6.1 a).

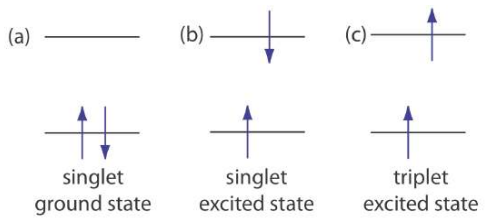


Figure 10.6.1 . Electron configurations for (a) a singlet ground state; (b) a singlet excited state; and (c) a triplet excited state.

When an analyte absorbs an ultraviolet or a visible photon, one of its valence electrons moves from the ground state to an excited state with a conservation of the electron's spin (Figure 10.6.1 b). Emission of a photon from a ***singlet excited state*** to the singlet ground state—or between any two energy levels with the same spin—is called ***fluorescence***. The probability of fluorescence is very high and the average lifetime of an electron in the excited state is only 10^{-5}–10^{-8} s. Fluorescence, therefore, rapidly decays once the source of excitation is removed.

In some cases an electron in a singlet excited state is transformed to a ***triplet excited state*** (Figure 10.6.1 c) in which its spin no is longer paired with the ground state. Emission between a triplet excited state and a singlet ground state—or between any two energy levels that differ in their respective spin states–is called ***phosphorescence***. Because the average lifetime for phosphorescence ranges from 10^{-4}–10^{4} s, phosphorescence may continue for some time after we remove the excitation source.

The use of molecular fluorescence for qualitative analysis and for semi-quantitative analysis dates to the early to mid 1800s, with more accurate quantitative methods appearing in the 1920s. Instrumentation for fluorescence spectroscopy using a filter or a monochromator for wavelength selection appeared in, respectively, the 1930s and 1950s. Although the discovery of phosphorescence preceded that of fluorescence by almost 200 years, qualitative and quantitative applications of molecular phosphorescence did not receive much attention until after the development of fluorescence instrumentation.

> As you might expect, the persistence of long-lived phosphorescence made it more noticeable.

Fluorescence and Phosphorescence Spectra

To appreciate the origin of fluorescence and phosphorescence we must consider what happens to a molecule following the absorption of a photon. Let's assume the molecule initially occupies the lowest vibrational energy level of its electronic ground state, which is the singlet state labeled S_0 in Figure 10.6.2 . Absorption of a photon excites the molecule to one of several vibrational energy levels in the first excited electronic state, S_1, or the second electronic excited state, S_2, both of which are singlet states. Relaxation to the ground state occurs by a number of mechanisms, some of which result in the emission of a photon and others that occur without the emission of a photon. These relaxation mechanisms are shown in Figure 10.6.2 . The most likely relaxation pathway from any excited state is the one with the shortest lifetime.

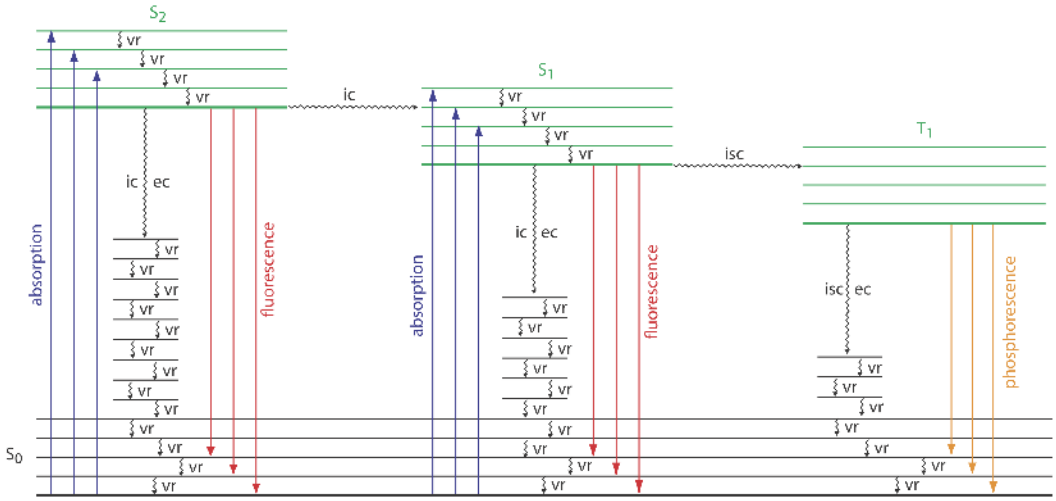


Figure 10.6.2 . Energy level diagram for a molecule that shows pathways for the deactivation of an excited state: ***vr*** is vibrational relaxation; ***ic*** is internal conversion; ***ec*** is external conversion; and ***isc*** is an intersystem crossing. The lowest vibrational energy for each electronic state is indicated by the thicker line. The electronic ground state is shown in black and the three electronic excited states are shown in green. The absorption, fluorescence, and phosphorescence of photons also are shown.

Radiationless Deactivation

When a molecule relaxes without emitting a photon we call the process ***radiationless deactivation***. One example of radiationless deactivation is ***vibrational relaxation***, in which a molecule in an excited vibrational energy level loses energy by moving to a lower vibrational energy level in the same electronic state. Vibrational relaxation is very rapid, with an average lifetime of $<10^{-12}$ s. Because vibrational relaxation is so efficient, a molecule in one of its excited state's higher vibrational energy levels quickly returns to the excited state's lowest vibrational energy level.

Another form of radiationless deactivation is an ***internal conversion*** in which a molecule in the ground vibrational level of an excited state passes directly into a higher vibrational energy level of a lower energy electronic state of the same spin state. By a combination of internal conversions and vibrational relaxations, a molecule in an excited electronic state may return to the ground electronic state without emitting a photon. A related form of radiationless deactivation is an ***external conversion*** in which excess energy is transferred to the solvent or to another component of the sample's matrix.

> Let's use Figure 10.6.2 to illustrate how a molecule can relax back to its ground state without emitting a photon. Suppose our molecule is in the highest vibrational energy level of the second electronic excited state. After a series of vibrational relaxations brings the molecule to the lowest vibrational energy level of S_2, it undergoes an internal conversion into a higher vibrational energy level of the first excited electronic state. Vibrational relaxations bring the molecule to the lowest vibrational energy level of S_1. Following an internal conversion into a higher vibrational energy level of the ground state, the molecule continues to undergo vibrational relaxation until it reaches the lowest vibrational energy level of S_0.

A final form of radiationless deactivation is an ***intersystem crossing*** in which a molecule in the ground vibrational energy level of an excited electronic state passes into one of the higher vibrational energy levels of a lower energy electronic state with a different spin state. For example, an intersystem crossing is shown in Figure 10.6.2 between the singlet excited state S_1 and the triplet excited state T_1.

Relaxation by Fluorescence

Fluorescence occurs when a molecule in an excited state's lowest vibrational energy level returns to a lower energy electronic state by emitting a photon. Because molecules return to their ground state by the fastest mechanism, fluorescence is observed only if it is a more efficient means of relaxation than a combination of internal conversions and vibrational relaxations.

A quantitative expression of fluorescence efficiency is the fluorescent ***quantum yield***, Φ_f, which is the fraction of excited state molecules that return to the ground state by fluorescence. The fluorescent quantum yields range from 1 when every molecule in an excited state undergoes fluorescence, to 0 when fluorescence does not occur.

The intensity of fluorescence, I_f, is proportional to the amount of radiation absorbed by the sample, $P_0 - P_T$, and the fluorescent quantum yield

$$I_f = k\Phi_f (P_0 - P_T) \tag{6.5.1}$$

where k is a constant that accounts for the efficiency of collecting and detecting the fluorescent emission. From Beer's law we know that

$$\frac{P_T}{P_0} = 10^{-\varepsilon bC} \tag{6.5.2}$$

where C is the concentration of the fluorescing species. Solving Equation 6.5.2 for P_T and substituting into Equation 6.5.1 gives, after simplifying

$$I_f = k\Phi_f P_0 \left(1 - 10^{-\varepsilon bC}\right) \tag{6.5.3}$$

When $\varepsilon bC < 0.01$, which often is the case when the analyte's concentration is small, Equation 6.5.3 simplifies to

$$I_f = 2.303 k\Phi_f \varepsilon bC P_0 = k' P_0 \tag{6.5.4}$$

where k' is a collection of constants. The intensity of fluorescence, therefore, increases with an increase in the quantum efficiency, the source's incident power, and the molar absorptivity and the concentration of the fluorescing species.

Fluorescence generally is observed when the molecule's lowest energy absorption is a $\pi \rightarrow \pi^*$ transition, although some $n \rightarrow \pi^*$ transitions show weak fluorescence. Many unsubstituted, nonheterocyclic aromatic compounds have a favorable fluorescence quantum yield, although substitutions on the aromatic ring can effect Φ_f significantly. For example, the presence of an electron-withdrawing group, such as $-NO_2$, decreases Φ_f, while adding an electron-donating group, such as –OH, increases Φ_f. Fluorrescence also increases for aromatic ring systems and for aromatic molecules with rigid planar structures. Figure 10.6.3 shows the fluorescence of quinine under a UV lamp.



Figure 10.6.3 . Tonic water, which contains quinine, is fluorescent when placed under a UV lamp. Source: Splarka (commons.Wikipedia.org).

A molecule's fluorescent quantum yield also is influenced by external variables, such as temperature and solvent. Increasing the temperature generally decreases Φ_f because more frequent collisions between the molecule and the solvent increases external conversion. A decrease in the solvent's viscosity decreases Φ_f for similar reasons. For an analyte with acidic or basic functional groups, a change in pH may change the analyte's structure and its fluorescent properties.

As shown in Figure 10.6.2 , fluorescence may return the molecule to any of several vibrational energy levels in the ground electronic state. Fluorescence, therefore, occurs over a range of wavelengths. Because the change in energy for fluorescent emission generally is less than that for absorption, a molecule's fluorescence spectrum is shifted to higher wavelengths than its absorption spectrum.

Relaxation by Phosphorescence

A molecule in a triplet electronic excited state's lowest vibrational energy level normally relaxes to the ground state by an intersystem crossing to a singlet state or by an external conversion. Phosphorescence occurs when the molecule relaxes by emitting a photon. As shown in Figure 10.6.2 , phosphorescence occurs over a range of wavelengths, all of which are at lower energies than the molecule's absorption band. The intensity of phosphorescence, I_p, is given by an equation similar to Equation 6.5.4 for fluorescence

$$I_P = 2.303k\Phi_P\varepsilon bCP_0 \tag{6.5.5}$$

$$= k'P_0 \tag{6.5.6}$$

where Φ_p is the ***phosphorescent quantum yield***.

Phosphorescence is most favorable for molecules with $n \rightarrow \pi^*$ transitions, which have a higher probability for an intersystem crossing than $\pi \rightarrow \pi^*$ transitions. For example, phosphorescence is observed with aromatic molecules that contain carbonyl groups or heteroatoms. Aromatic compounds that contain halide atoms also have a higher efficiency for phosphorescence. In general, an increase in phosphorescence corresponds to a decrease in fluorescence.

Because the average lifetime for phosphorescence can be quite long, ranging from 10^{-4}–10^4 s, the phosphorescent quantum yield usually is quite small. An improvement in Φ_p is realized by decreasing the efficiency of external conversion. This is accomplished in several ways, including lowering the temperature, using a more viscous solvent, depositing the sample on a solid substrate, or trapping the molecule in solution. Figure 10.6.4 shows an example of phosphorescence.

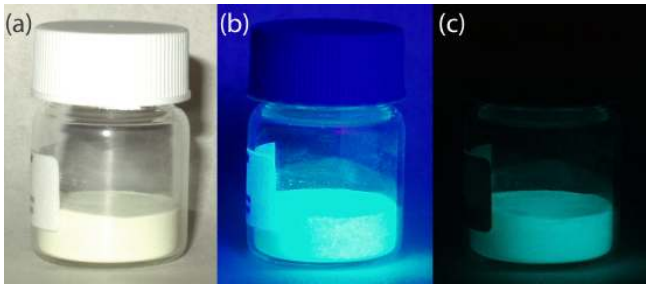


Figure 10.6.4 . An europium doped strontium silicate-aluminum oxide powder under (a) natural light, (b) a long-wave UV lamp, and (c) in total darkness. The photo taken in total darkness shows the phosphorescent emission. Source: modified from Splarka (commons.Wikipedia.org).

Excitation Versus Emission Spectra

Photoluminescence spectra are recorded by measuring the intensity of emitted radiation as a function of either the excitation wavelength or the emission wavelength. An ***excitation spectrum*** is obtained by monitoring emission at a fixed wavelength while varying the excitation wavelength. When corrected for variations in the source's intensity and the detector's response, a sample's excitation spectrum is nearly identical to its absorbance spectrum. The excitation spectrum provides a convenient means for selecting the best excitation wavelength for a quantitative or qualitative analysis.

In an ***emission spectrum*** a fixed wavelength is used to excite the sample and the intensity of emitted radiation is monitored as function of wavelength. Although a molecule has a single excitation spectrum, it has two emission spectra, one for fluorescence and one for phosphorescence. Figure 10.6.5 shows the UV absorption spectrum and the UV fluorescence emission spectrum for quinine.

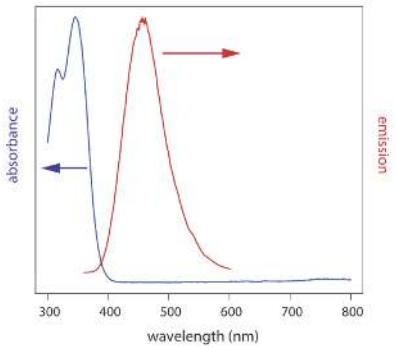


Figure 10.6.5 . Absorbance spectrum and fluorescence emission spectrum for quinine in 0.05 M H_2SO_4. The emission spectrum uses an excitation wavelength of 350 nm with a bandwidth of 20 nm. Both spectra are normalized so that the maximum absorbance is 1.00 and the maximum emission is 1.00. The actual maximum absorbance is 0.444 and the actual maximum emission is 126747. Source: data from Daniel Scott, Department of Chemistry & Biochemistry, DePauw University.

Instrumentation

The basic instrumentation for monitoring fluorescence and phosphorescence—a source of radiation, a means of selecting a narrow band of radiation, and a detector—are the same as those for absorption spectroscopy. The unique demands of fluorescence and phosphorescence, however, require some modifications to the instrument designs seen earlier in Figure 10.3.1 (filter photometer), Figure 10.3.2 (single-beam spectrophotometer), Figure 10.3.3 (double-beam spectrophotometer), and Figure 10.3.4 (diode array spectrometer). The most important difference is that the detector cannot be placed directly across from the source. Figure 10.6.6 shows why this is the case. If we place the detector along the source's axis it receives both the transmitted source radiation, P_T, and the fluorescent, I_f, or phosphorescent, I_p, radiation. Instead, we rotate the director and place it at 90º to the source.

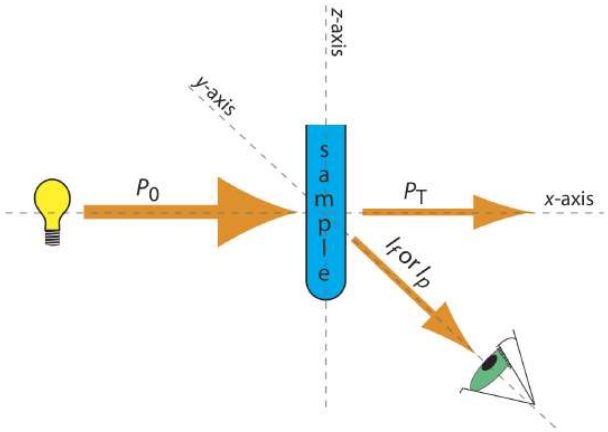


Figure 10.6.6 . Schematic diagram showing the orientation of the source and the detector when measuring fluorescence and phosphorescence. Contrast this to Figure 10.2.7, which shows the orientation for absorption spectroscopy.

Instruments for Measuring Fluorescence

Figure 10.6.7 shows the basic design of an instrument for measuring fluorescence, which includes two wavelength selectors, one for selecting the source's excitation wavelength and one for selecting the analyte's emission wavelength. In a ***fluorimeter*** the excitation and emission wavelengths are selected using absorption or interference filters. The excitation source for a fluorimeter usually is a low-pressure Hg vapor lamp that provides intense emission lines distributed throughout the ultraviolet and visible region. When a monochromator is used to select the excitation and the emission wavelengths, the instrument is called a ***spectrofluorometer***. With a monochromator the excitation source usually is a high-pressure Xe arc lamp, which has a continuous emission spectrum. Either instrumental design is appropriate for quantitative work, although only a spectrofluorometer can record an excitation or emission spectrum.

> A Hg vapor lamp has emission lines at 254, 312, 365, 405, 436, 546, 577, 691, and 773 nm.

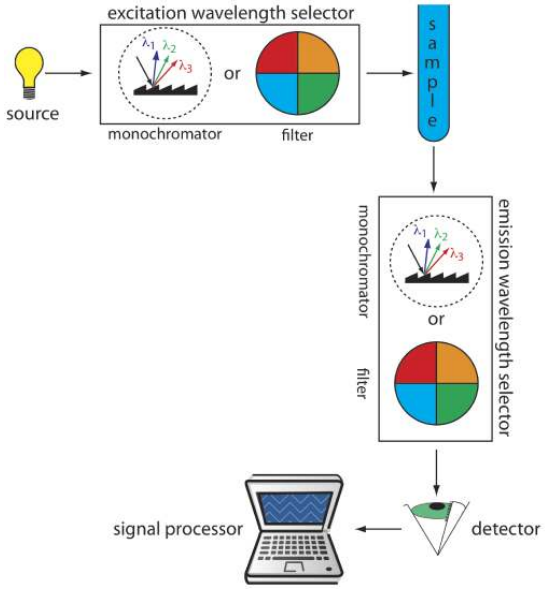


Figure 10.6.7 . Schematic diagram for measuring fluorescence showing the placement of the wavelength selectors for excitation and emission. When a filter is used the instrument is called a fluorimeter and when a monochromator is used the instrument is called a spectrofluorimeter.

The sample cells for molecular fluorescence are similar to those for molecular absorption (see Figure 10.3.6). Remote sensing using a fiber optic probe (see Figure 10.3.7) is possible using with either a fluorimeter or spectrofluorometer. An analyte that is fluorescent is monitored directly. For an analyte that is not fluorescent, a suitable fluorescent probe molecule is incorporated into the tip of the fiber optic probe. The analyte's reaction with the probe molecule leads to an increase or decrease in fluorescence.

Instruments for Measuring Phosphorescence

An instrument for molecular phosphorescence must discriminate between phosphorescence and fluorescence. Because the lifetime for fluorescence is shorter than that for phosphorescence, discrimination is achieved by incorporating a delay between exciting the sample and measuring the phosphorescent emission. Figure 10.6.8 shows how two out-of-phase choppers allow us to block fluorescent emission from reaching the detector when the sample is being excited and to prevent the source radiation from causing fluorescence when we are measuring the phosphorescent emission.

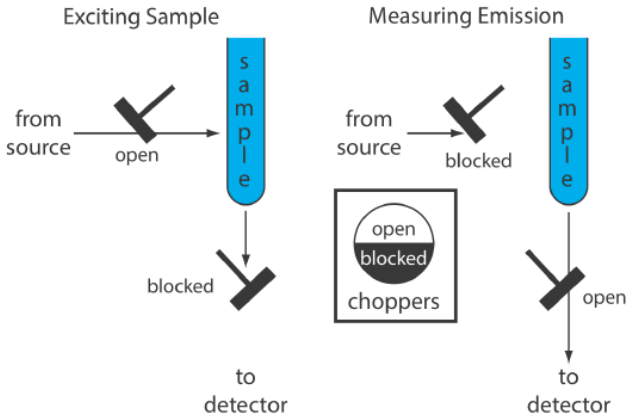


Figure 10.6.8 . Schematic diagram showing how choppers are used to prevent fluorescent emission from interfering with the measurement of phosphorescent emission.

Because phosphorescence is such a slow process, we must prevent the excited state from relaxing by external conversion. One way this is accomplished is by dissolving the sample in a suitable organic solvent, usually a mixture of ethanol, isopentane, and diethylether. The resulting solution is frozen at liquid-N_2 temperatures to form an optically clear solid. The solid matrix minimizes external conversion due to collisions between the analyte and the solvent. External conversion also is minimized by immobilizing the sample on a solid substrate, making possible room temperature measurements. One approach is to place a drop of a solution

that contains the analyte on a small disc of filter paper. After drying the sample under a heat lamp, the sample is placed in the spectrofluorometer for analysis. Other solid substrates include silica gel, alumina, sodium acetate, and sucrose. This approach is particularly useful for the analysis of thin layer chromatography plates.

Quantitative Applications

Molecular fluorescence and, to a lesser extent, phosphorescence are used for the direct or indirect quantitative analysis of analytes in a variety of matrices. A direct quantitative analysis is possible when the analyte's fluorescent or phosphorescent quantum yield is favorable. If the analyte is not fluorescent or phosphorescent, or if the quantum yield is unfavorable, then an indirect analysis may be feasible. One approach is to react the analyte with a reagent to form a product that is fluorescent or phosphorescent. Another approach is to measure a decrease in fluorescence or phosphores- cence when the analyte is added to a solution that contains a fluorescent or phosphorescent probe molecule. A decrease in emission is observed when the reaction between the analyte and the probe molecule enhances radiationless deactivation or results in a nonemitting product. The application of fluorescence and phosphorescence to inorganic and organic analytes are considered in this section.

Inorganic Analytes

Except for a few metal ions, most notably UO_2^+, most inorganic ions are not sufficiently fluorescent for a direct analysis. Many metal ions are determined indirectly by reacting with an organic ligand to form a fluorescent or, less commonly, a phosphorescent metal–ligand complex. One example is the reaction of Al^{3+} with the sodium salt of 2, 4, 3′-trihydroxyazobenzene-5′-sulfonic acid —also known as alizarin garnet R—which forms a fluorescent metal–ligand complex (Figure 10.6.9). The analysis is carried out using an excitation wavelength of 470 nm, with fluorescence monitored at 500 nm. Table 10.6.1 provides additional examples of chelating reagents that form fluorescent metal–ligand complexes with metal ions. A few inorganic nonmetals are determined by their ability to decrease, or quench, the fluorescence of another species. One example is the analysis for F^- based on its ability to quench the fluorescence of the Al^{3+}–alizarin garnet R complex.

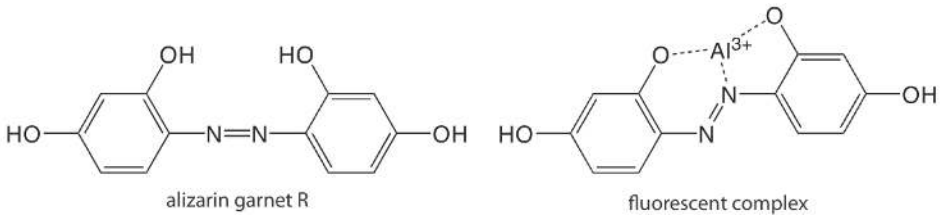


Figure 10.6.9 . Structure of alizarin garnet R and its metal–ligand complex with Al^{3+}.

Table 10.6.1 . Chelating Agents for the Fluorescent Analysis of Metal Ions

chelating agent	metal ions
8-hydroxyquinoline	Al^{3+}, Be^{2+}, Zn^{2+}, Li^+, Mg^{2+} (and others)
flavonal	Zr^{2+}, Sn^{4+}
benzoin	$B_4O_6^{2-}$, Zn^{2+}
2′, 3′, 4′, 5, 7 – pentahydroxylflavone	Be^{2+}
2-(*o*-hydroxyphenyl) benzoxazole	Cd^{2+}

Organic Analytes

As noted earlier, organic compounds that contain aromatic rings generally are fluorescent and aromatic heterocycles often are phosphorescent. Table 10.6.2 provides examples of several important biochemical, pharmaceutical, and environmental compounds that are analyzed quantitatively by fluorimetry or phosphorimetry. If an organic analyte is not naturally fluorescent or phosphorescent, it may be possible to incorporate it into a chemical reaction that produces a fluorescent or phosphorescent product. For example, the enzyme creatine phosphokinase is determined by using it to catalyze the formation of creatine from phosphocreatine. Reacting the creatine with ninhydrin produces a fluorescent product of unknown structure.

Table 10.6.2 . Examples of Naturally Photoluminescent Organic Analytes

class	compounds (F = fluorescence, P = phosphorescence)
aromatic amino acids	phenylalanine (F) tyrosine (F) tryptophan (F, P)
vitamins	vitamin A (F) vitamin B2 (F) vitamin B6 (F) vitamin B12 (F) vitamin E (F) folic acid (F)
catecholamines	dopamine (F) norepinephrine (F)
pharmaceuticals and drugs	quinine (F) salicylic acid (F, P) morphine (F) barbiturates (F) LSD (F) codeine (P) caffeine (P) sulfanilamide (P)
environmental pollutants	pyrene (F) benzo[a]pyrene (F) organothiophosphorous pesticides (F) carbamate insecticides (F) DDT (P)

Standardizing the Method

From Equation 6.5.4 and Equation 6.5.6 we know that the intensity of fluorescence or phosphorescence is a linear function of the analyte's concentration provided that the sample's absorbance of source radiation ($A = \varepsilon bC$) is less than approximately 0.01. Calibration curves often are linear over four to six orders of magnitude for fluorescence and over two to four orders of magnitude for phosphorescence. For higher concentrations of analyte the calibration curve becomes nonlinear because the assumptions that led to Equation 6.5.4 and Equation 6.5.6 no longer apply. Nonlinearity may be observed for smaller concentrations of analyte fluorescent or phosphorescent contaminants are present. As discussed earlier, quantum efficiency is sensitive to temperature and sample matrix, both of which must be con- trolled when using external standards. In addition, emission intensity depends on the molar absorptivity of the photoluminescent species, which is sensitive to the sample matrix.

Representative Method 10.6.1: Determination of Quinine in Urine

The best way to appreciate the theoretical and the practical details discussed in this section is to carefully examine a typical analytical method. Although each method is unique, the following description of the determination of quinine in urine provides an instructive example of a typical procedure. The description here is based on Mule, S. J.; Hushin, P. L. *Anal. Chem.* **1971**, *43*, 708–711, and O'Reilly, J. E.; *J. Chem. Educ.* **1975**, *52*, 610–612. Figure 10.6.3 shows the fluorescence of the quinine in tonic water.

Description of the Method

Quinine is an alkaloid used to treat malaria. It is a strongly fluorescent compound in dilute solutions of H_2SO_4 ($\Phi_f = 0.55$). Quinine's excitation spectrum has absorption bands at 250 nm and 350 nm and its emission spectrum has a single emission band at 450 nm. Quinine is excreted rapidly from the body in urine and is determined by measuring its fluorescence following its extraction from the urine sample.

Procedure

Transfer a 2.00-mL sample of urine to a 15-mL test tube and use 3.7 M NaOH to adjust its pH to between 9 and 10. Add 4 mL of a 3:1 (v/v) mixture of chloroform and isopropanol and shake the contents of the test tube for one minute. Allow the organic and the aqueous (urine) layers to separate and transfer the organic phase to a clean test tube. Add 2.00 mL of 0.05 M H_2SO_4 to the organic phase and shake the contents for one minute. Allow the organic and the aqueous layers to separate and transfer the aqueous phase to the sample cell. Measure the fluorescent emission at 450 nm using an excitation wavelength of 350 nm. Determine the concentration of quinine in the urine sample using a set of external standards in 0.05 M H_2SO_4, prepared from a 100.0 ppm solution of quinine in 0.05 M H_2SO_4. Use distilled water as a blank.

Questions

1. Chloride ion quenches the intensity of quinine's fluorescent emission. For example, in the presence of 100 ppm NaCl (61 ppm Cl^-) quinine's emission intensity is only 83% of its emission intensity in the absence of chloride. The presence of 1000 ppm NaCl (610 ppm Cl^-) further reduces quinine's fluorescent emission to less than 30% of its emission intensity in the absence of chloride. The concentration of chloride in urine typically ranges from 4600–6700 ppm Cl^-. Explain how this procedure prevents an interference from chloride.

> The procedure uses two extractions. In the first of these extractions, quinine is separated from urine by extracting it into a mixture of chloroform and isopropanol, leaving the chloride ion behind in the original sample.

2. Samples of urine may contain small amounts of other fluorescent compounds, which will interfere with the analysis if they are carried through the two extractions. Explain how you can modify the procedure to take this into account?

> One approach is to prepare a blank that uses a sample of urine known to be free of quinine. Subtracting the blank's fluorescent signal from the measured fluorescence from urine samples corrects for the interfering compounds.

The fluorescent emission for quinine at 450 nm can be induced using an excitation frequency of either 250 nm or 350 nm. The fluorescent quantum efficiency is the same for either excitation wavelength. Quinine's absorption spectrum shows that ε_{250} is greater than ε_{350}. Given that quinine has a stronger absorbance at 250 nm, explain why its fluorescent emission intensity is greater when using 350 nm as the excitation wavelength.

> From Equation 6.5.4 we know that I_f is a function of the following terms: k, Φ_f, P_0, ε, b, and C. We know that Φ_f, b, and C are the same for both excitation wavelengths and that ε is larger for a wavelength of 250 nm; we can, therefore, ignore these terms. The greater emission intensity when using an excitation wavelength of 350 nm must be due to a larger value for P_0 or k . In fact, P_0 at 350 nm for a high-pressure Xe arc lamp is about 170% of that at 250 nm. In addition, the sensitivity of a typical photomultiplier detector (which contributes to the value of k) at 350 nm is about 140% of that at 250 nm.

Example 10.6.1

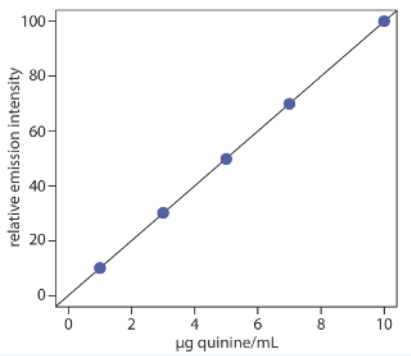
To evaluate the method described in Representative Method 10.6.1, a series of external standard are prepared and analyzed, providing the results shown in the following table. All fluorescent intensities are corrected using a blank prepared from a quinine-free sample of urine. The fluorescent intensities are normalized by setting I_f for the highest concentration standard to 100.

[quinine] (µg/mL)	I_f
1.00	10.11
3.00	30.20
5.00	49.84
7.00	69.89
10.00	100.0

After ingesting 10.0 mg of quinine, a volunteer provides a urine sample 24-h later. Analysis of the urine sample gives a relative emission intensity of 28.16. Report the concentration of quinine in the sample in mg/L and the percent recovery for the ingested quinine.

Solution

Linear regression of the relative emission intensity versus the concentration of quinine in the standards gives the calibration curve shown below and the following calibration equation.



$$I_f = 0.122 + 9.978 \times \frac{\text{g quinine}}{\text{mL}}$$

Substituting the sample's relative emission intensity into the calibration equation gives the concentration of quinine as 2.81 μg/mL. Because the volume of urine taken, 2.00 mL, is the same as the volume of 0.05 M H_2SO_4 used to extract the quinine, the concentration of quinine in the urine also is 2.81 μg/mL. The recovery of the ingested quinine is

$$\frac{\frac{2.81\ \mu\text{g quinine}}{\text{mL urine}} \times 2.00\ \text{mL urine} \times \frac{1\text{mg}}{1000\ \mu\text{g}}}{10.0\ \text{mg quinine ingested}} \times 100 = 0.0562\%$$

It can take 10–11 days for the body to completely excrete quinine so it is not surprising that such a small amount of quinine is recovered from this sample of urine.

Evaluation of Photoluminescence Spectroscopy

Scale of Operation

Photoluminescence spectroscopy is used for the routine analysis of trace and ultratrace analytes in macro and meso samples. Detection limits for fluorescence spectroscopy are influenced by the analyte's quantum yield. For an analyte with $\Phi_f > 0.5$, a picomolar detection limit is possible when using a high quality spectrofluorometer. For example, the detection limit for quinine sulfate, for which Φ is 0.55, generally is between 1 part per billion and 1 part per trillion. Detection limits for phosphorescence are somewhat higher, with typical values in the nanomolar range for low-temperature phosphorimetry and in the micromolar range for room-temperature phosphorimetry using a solid substrate.

Accuracy

The accuracy of a fluorescence method generally is between 1–5% when spectral and chemical interferences are insignificant. Accuracy is limited by the same types of problems that affect other optical spectroscopic methods. In addition, accuracy is affected by interferences that affect the fluorescent quantum yield. The accuracy of phosphorescence is somewhat greater than that for fluorescence.

Precision

The relative standard deviation for fluorescence usually is between 0.5–2% when the analyte's concentration is well above its detection limit. Precision usually is limited by the stability of the excitation source. The precision for phosphorescence often is limited by reproducibility in preparing samples for analysis, with relative standard deviations of 5–10% being common.

Sensitivity

From Equation 6.5.4 and Equation 6.5.6 we know that the sensitivity of a fluorescent or a phosphorescent method is affected by a number of parameters. We already have considered the importance of quantum yield and the effect of temperature and solution composition on Φ_f and Φ_p. Besides quantum yield, sensitivity is improved by using an excitation source that has a greater emission

intensity, P_0, at the desired wavelength, and by selecting an excitation wavelength for which the analyte has a greater molar absorptivity, ε. Another approach for improving sensitivity is to increase the volume from which emission is monitored. Figure 10.6.10 shows how rotating a monochromator's slits from their usual vertical orientation to a horizontal orientation increases the sampling volume. The result can in- crease the emission from the sample by $5-30\times$.

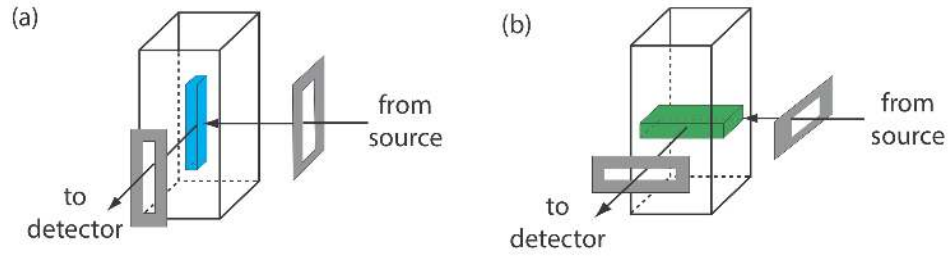


Figure 10.6.10 . Use of slit orientation to change the volume from which fluorescence is measured: (a) vertical slit orientation; (b) horizontal slit orientation. Suppose the slit's dimensions are 0.1 mm × 3 mm. In (a) the dimensions of the sampling volume are 0.1 mm × 0.1 mm × 3 mm, or 0.03 mm^3. For (b) the dimensions of the sampling volume are 0.1 mm × 3 mm × 3 mm, or 0.9 mm^3, a 30-fold increase in the sampling volume.

Selectivity

The selectivity of fluorescence and phosphorescence is superior to that of absorption spectrophotometry for two reasons: first, not every compound that absorbs radiation is fluorescent or phosphorescent; and, second, selectivity between an analyte and an interferent is possible if there is a difference in either their excitation or their emission spectra. The total emission intensity is a linear sum of that from each fluorescent or phosphorescent species. The analysis of a sample that contains *n* analytes, therefore, is accomplished by measuring the total emission intensity at *n* wavelengths.

Time, Cost, and Equipment

As with other optical spectroscopic methods, fluorescent and phosphorescent methods provide a rapid means for analyzing samples and are capable of automation. Fluorimeters are relatively inexpensive, ranging from several hundred to several thousand dollars, and often are satisfactory for quantitative work. Spectrofluorometers are more expensive, with models often exceeding $50,000.

This page titled 6.5: Photoluminescent Spectroscopy is shared under a CC BY-NC-SA 4.0 license and was authored, remixed, and/or curated by Kathryn Davis.

- **10.6: Photoluminescent Spectroscopy** by David Harvey is licensed CC BY-NC-SA 4.0.

6.6: Atomic Emission Spectroscopy

The focus of this section is on the emission of ultraviolet and visible radiation following the thermal excitation of atoms. Atomic emission spectroscopy has a long history. Qualitative applications based on the color of flames were used in the smelting of ores as early as 1550 and were more fully developed around 1830 with the observation of atomic spectra generated by flame emission and spark emission [Dawson, J. B. *J. Anal. At. Spectrosc.* **1991**, *6*, 93–98]. Quantitative applications based on the atomic emission from electric sparks were developed by Lockyer in the early 1870 and quantitative applications based on flame emission were pioneered by Lundegardh in 1930. Atomic emission based on emission from a plasma was introduced in 1964.

> For an on-line introduction to much of the material in this section, see Atomic Emission Spectroscopy (AES) by Tomas Spudich and Alexander Scheeline, a resource that is part of the Analytical Sciences Digital Library.

Atomic Emission Spectra

Atomic emission occurs when a valence electron in a higher energy atomic orbital returns to a lower energy atomic orbital. Figure 10.7.1 shows a portion of the energy level diagram for sodium, which consists of a series of discrete lines at wavelengths that correspond to the difference in energy between two atomic orbitals.

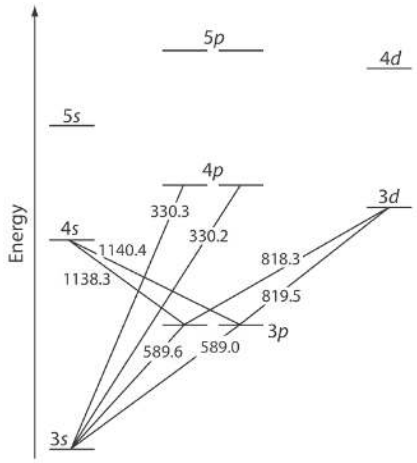


Figure 10.7.1 . Valence shell energy level diagram for sodium. The wavelengths corresponding to several transitions are shown. Note that this is the same energy level diagram as Figure 10.2.5.

The intensity of an atomic emission line, I_e, is proportional to the number of atoms, N^*, that populate the excited state,

$$I_e = kN^* \tag{6.6.1}$$

where k is a constant that accounts for the efficiency of the transition. If a system of atoms is in thermal equilibrium, the population of excited state i is related to the total concentration of atoms, N, by the Boltzmann distribution. For many elements at temperatures of less than 5000 K the Boltzmann distribution is approximated as

$$N^* = N\left(\frac{g_i}{g_0}\right)e^{-E_i/kT} \tag{6.6.2}$$

where g_i and g_0 are statistical factors that account for the number of equivalent energy levels for the excited state and the ground state, E_i is the energy of the excited state relative to a ground state energy, E_0, k is Boltzmann's constant (1.3807×10^{-23} J/K), and T is the temperature in Kelvin. From Equation 6.6.2 we expect that excited states with lower energies have larger populations and more intense emission lines. We also expect emission intensity to increase with temperature.

Equipment

An atomic emission spectrometer is similar in design to the instrumentation for atomic absorption. In fact, it is easy to adapt most flame atomic absorption spectrometers for atomic emission by turning off the hollow cathode lamp and monitoring the difference between the emission intensity when aspirating the sample and when aspirating a blank. Many atomic emission spectrometers,

however, are dedicated instruments designed to take advantage of features unique to atomic emission, including the use of plasmas, arcs, sparks, and lasers as atomization and excitation sources, and an enhanced capability for multielemental analysis.

Atomization and Excitation

Atomic emission requires a means for converting into a free gaseous atom an analyte that is present in a solid, liquid, or solution sample. The same source of thermal energy used for atomization usually serves as the excitation source. The most common methods are flames and plasmas, both of which are useful for liquid or solution samples. Solid samples are analyzed by dissolving in a solvent and using a flame or plasma atomizer.

Flame Sources

Atomization and excitation in flame atomic emission is accomplished with the same nebulization and spray chamber assembly used in atomic absorption (Figure 10.4.1). The burner head consists of a single or multiple slots, or a Meker-style burner. Older atomic emission instruments often used a total consumption burner in which the sample is drawn through a capillary tube and injected directly into the flame.

> A Meker burner is similar to the more common Bunsen burner found in most laboratories; it is designed to allow for higher temperatures and for a larger diameter flame.

Plasma Sources

A ***plasma*** is a hot, partially ionized gas that contains an abundant concentration of cations and electrons. The plasma used in atomic emission is formed by ionizing a flowing stream of argon gas, producing argon ions and electrons. A plasma's high temperature results from resistive heating as the electrons and argon ions move through the gas. Because a plasma operates at a much higher temperature than a flame, it provides for a better atomization efficiency and a higher population of excited states.

A schematic diagram of the inductively coupled plasma source (ICP) is shown in Figure 10.7.2 . The ICP torch consists of three concentric quartz tubes, surrounded at the top by a radio-frequency induction coil. The sample is mixed with a stream of Ar using a nebulizer, and is carried to the plasma through the torch's central capillary tube. Plasma formation is initiated by a spark from a Tesla coil. An alternating radio-frequency current in the induction coil creates a fluctuating magnetic field that induces the argon ions and the electrons to move in a circular path. The resulting collisions with the abundant unionized gas give rise to resistive heating, providing temperatures as high as 10000 K at the base of the plasma, and between 6000 and 8000 K at a height of 15–20 mm above the coil, where emission usually is measured. At these high temperatures the outer quartz tube must be thermally isolated from the plasma. This is accomplished by the tangential flow of argon shown in the schematic diagram.

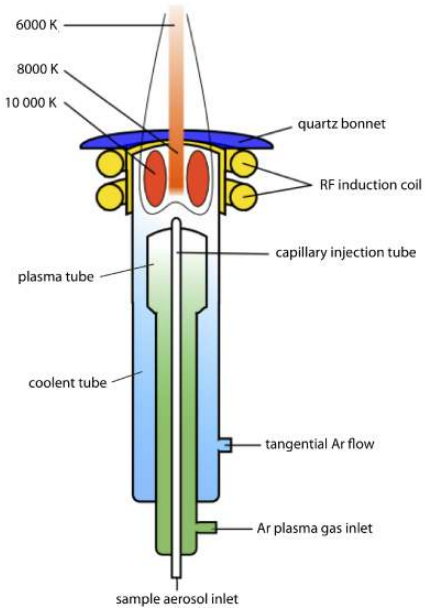


Figure 10.7.2 . Schematic diagram of an inductively coupled plasma torch.

Multielemental Analysis

Atomic emission spectroscopy is ideally suited for a multielemental analysis because all analytes in a sample are excited simultaneously. If the instrument includes a scanning monochromator, we can program it to move rapidly to an analyte's desired wavelength, pause to record its emission intensity, and then move to the next analyte's wavelength. This sequential analysis allows for a sampling rate of 3–4 analytes per minute.

Another approach to a multielemental analysis is to use a multichannel instrument that allows us to monitor simultaneously many analytes. A simple design for a multichannel spectrometer, shown in Figure 10.7.3 , couples a monochromator with multiple detectors that are positioned in a semicircular array around the monochromator at positions that correspond to the wavelengths for the analytes.

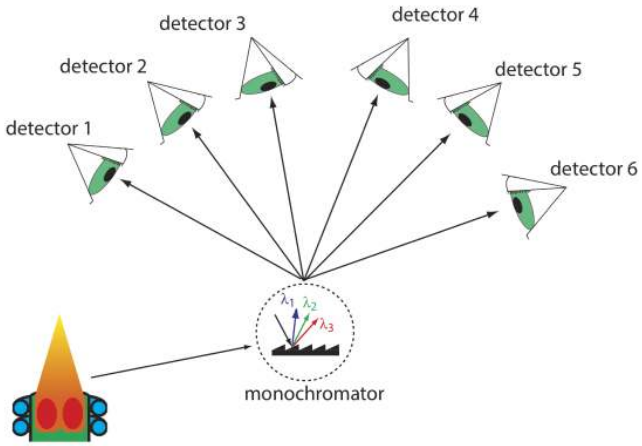


Figure 10.7.3 . Schematic diagram of a multichannel atomic emission spectrometer for the simultaneous analysis of several elements. Instruments may contain as many as 48–60 detectors.

Quantitative Applications

Atomic emission is used widely for the analysis of trace metals in a variety of sample matrices. The development of a quantitative atomic emission method requires several considerations, including choosing a source for atomization and excitation, selecting a wavelength and slit width, preparing the sample for analysis, minimizing spectral and chemical interferences, and selecting a method of standardization.

Choice of Atomization and Excitation Source

Except for the alkali metals, detection limits when using an ICP are significantly better than those obtained with flame emission (Table 10.7.1). Plasmas also are subject to fewer spectral and chemical interferences. For these reasons a plasma emission source is usually the better choice.

Table \(\PageIndex{1}). Detection Limits for Atomic Emission

element	detection limit (µg/mL): flame emission	detection limit (µg/mL): ICP
Ag	2	0.2
Al	3	0.2
As	2000	2
Ca	0.1	0.0001
Cd	300	0.07
Co	5	0.1
Cr	1	0.08
Fe	10	0.09
Hg	150	1
K	0.01	30
Li	0.001	0.02
Mg	1	0.02
Mn	1	0.01
Na	0.01	0.1
Ni	10	0.2
Pb	0.2	1
Pt	2000	0.9
Sn	100	3
Zn	1000	0.1

Source: Parsons, M. L.; Major, S.; Forster, A. R.; App. Spectrosc. 1983, 37, 411–418.

Selecting the Wavelength and Slit Width

The choice of wavelength is dictated by the need for sensitivity and the need to avoid interferences from the emission lines of other constituents in the sample. Because an analyte's atomic emission spectrum has an abundance of emission lines—particularly when using a high temperature plasma source—it is inevitable that there will be some overlap between emission lines. For example, an analysis for Ni using the atomic emission line at 349.30 nm is complicated by the atomic emission line for Fe at 349.06 nm.

A narrower slit width provides better resolution, but at the cost of less radiation reaching the detector. The easiest approach to selecting a wavelength is to record the sample's emission spectrum and look for an emission line that provides an intense signal and is resolved from other emission lines.

Preparing the Sample

Flame and plasma sources are best suited for samples in solution and in liquid form. Although a solid sample can be analyzed by directly inserting it into the flame or plasma, they usually are first brought into solution by digestion or extraction.

Minimizing Spectral Interferences

The most important spectral interference is broad, background emission from the flame or plasma and emission bands from molecular species. This background emission is particularly severe for flames because the temperature is insufficient to break down refractory compounds, such as oxides and hydroxides. Background corrections for flame emission are made by scanning over the emission line and drawing a baseline (Figure 10.7.4). Because a plasma's temperature is much higher, a background interference

due to molecular emission is less of a problem. Although emission from the plasma's core is strong, it is insignificant at a height of 10–30 mm above the core where measurements normally are made.

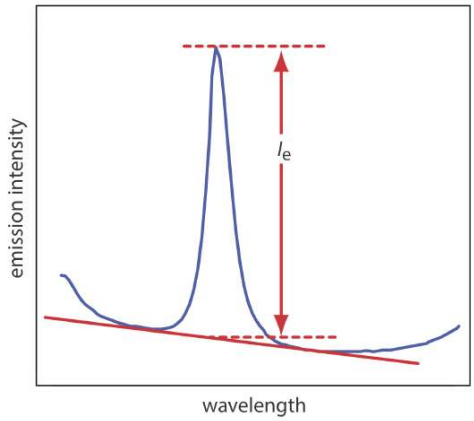


Figure 10.7.4 . Method for correcting an analyte's emission for the flame's background emission.

Minimizing Chemical Interferences

Flame emission is subject to the same types of chemical interferences as atomic absorption; they are minimized using the same methods: by adjusting the flame's composition and by adding protecting agents, releasing agents, or ionization suppressors. An additional chemical interference results from ***self-absorption***. Because the flame's temperature is greatest at its center, the concentration of analyte atoms in an excited state is greater at the flame's center than at its outer edges. If an excited state atom in the flame's center emits a photon, then a ground state atom in the cooler, outer regions of the flame may absorb the photon, which decreases the emission intensity. For higher concentrations of analyte self-absorption may invert the center of the emission band (Figure 10.7.5).

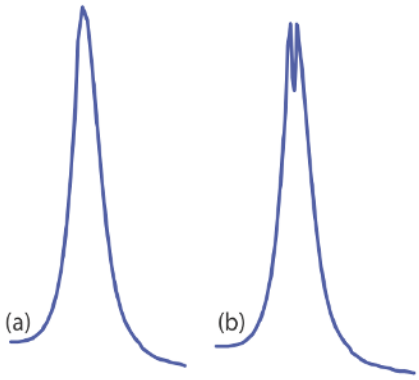


Figure 10.7.5 . Atomic emission lines for (a) a low concentration of analyte, and (b) a high concentration of analyte showing the effect of self-absorption.

Chemical interferences when using a plasma source generally are not significant because the plasma's higher temperature limits the formation of nonvolatile species. For example, $\mathbf{PO_4^{3-}}$ is a significant interferent when analyzing samples for Ca^{2+} by flame emission, but has a negligible effect when using a plasma source. In addition, the high concentration of electrons from the ionization of argon minimizes ionization interferences.

Standardizing the Method

From Equation **6.6.1** we know that emission intensity is proportional to the population of the analyte's excited state, N^*. If the flame or plasma is in thermal equilibrium, then the excited state population is proportional to the analyte's total population, N, through the Boltzmann distribution (Equation **6.6.2**).

A calibration curve for flame emission usually is linear over two to three orders of magnitude, with ionization limiting linearity when the analyte's concentrations is small and self-absorption limiting linearity at higher concentrations of analyte. When using a

plasma, which suffers from fewer chemical interferences, the calibration curve often is linear over four to five orders of magnitude and is not affected significantly by changes in the matrix of the standards.

Emission intensity is affected significantly by many parameters, including the temperature of the excitation source and the efficiency of atomization. An increase in temperature of 10 K, for example, produces a 4% increase in the fraction of Na atoms in the 3*p* excited state, an uncertainty in the signal that may limit the use of external standards. The method of internal standards is used when the variations in source parameters are difficult to control. To compensate for changes in the temperature of the excitation source, the internal standard is selected so that its emission line is close to the analyte's emission line. In addition, the internal standard should be subject to the same chemical interferences to compensate for changes in atomization efficiency. To accurately correct for these errors the analyte and internal standard emission lines are monitored simultaneously.

Representative Method 10.7.1: Determination of Sodium in a Salt Substitute

The best way to appreciate the theoretical and the practical details discussed in this section is to carefully examine a typical analytical method. Although each method is unique, the following description of the determination of sodium in salt substitutes provides an instructive example of a typical procedure. The description here is based on Goodney, D. E. *J. Chem. Educ.* **1982**, *59*, 875–876.

Description of Method

Salt substitutes, which are used in place of table salt for individuals on low-sodium diets, replaces NaCl with KCl. Depending on the brand, fumaric acid, calcium hydrogen phosphate, or potassium tartrate also are present. Although intended to be sodium-free, salt substitutes contain small amounts of NaCl as an impurity. Typically, the concentration of sodium in a salt substitute is about 100 μg/g The exact concentration of sodium is determined by flame atomic emission. Because it is difficult to match the matrix of the standards to that of the sample, the analysis is accomplished by the method of standard additions.

Procedure

A sample is prepared by placing an approximately 10-g portion of the salt substitute in 10 mL of 3 M HCl and 100 mL of distilled water. After the sample has dissolved, it is transferred to a 250-mL volumetric flask and diluted to volume with distilled water. A series of standard additions is prepared by placing 25-mL portions of the diluted sample into separate 50-mL volumetric flasks, spiking each with a known amount of an approximately 10 mg/L standard solution of Na^+, and diluting to volume. After zeroing the instrument with an appropriate blank, the instrument is optimized at a wavelength of 589.0 nm while aspirating a standard solution of Na^+. The emission intensity is measured for each of the standard addition samples and the concentration of sodium in the salt substitute is reported in μg/g.

Questions

1. Potassium ionizes more easily than sodium. What problem might this present if you use external standards prepared from a stock solution of 10 mg Na/L instead of using a set of standard additions?

> Because potassium is present at a much higher concentration than is sodium, its ionization suppresses the ionization of sodium. Normally suppressing ionization is a good thing because it increases emission intensity. In this case, however, the difference between the standard's matrix and the sample's matrix means that the sodium in a standard experiences more ionization than an equivalent amount of sodium in a sample. The result is a determinate error.

2. One way to avoid a determinate error when using external standards is to match the matrix of the standards to that of the sample. We could, for example, prepare external standards using reagent grade KCl to match the matrix to that of the sample. Why is this not a good idea for this analysis?

> Sodium is a common contaminant in many chemicals. Reagent grade KCl, for example, may contain 40–50 μg Na/g. This is a significant source of sodium, given that the salt substitute contains approximately 100 μg Na/g.

3. Suppose you decide to use an external standardization. Given the previous questions, is the result of your analysis likely to underestimate or to overestimate the amount of sodium in the salt substitute?

> The solid black line in Figure 10.7.6 shows the ideal calibration curve, assuming we match the standard's matrix to the sample's matrix, and that we do so without adding any additional sodium. If we prepare the external standards without adding KCl, the emission for each standard decreases due to increased ionization. This is shown by the lower of the two

dashed red lines. Preparing the standards by adding reagent grade KCl increases the concentration of sodium due to its contamination. Because we underestimate the actual concentration of sodium in the standards, the resulting calibration curve is shown by the other dashed red line. In both cases, the sample's emission results in our overestimating the concentration of sodium in the sample.

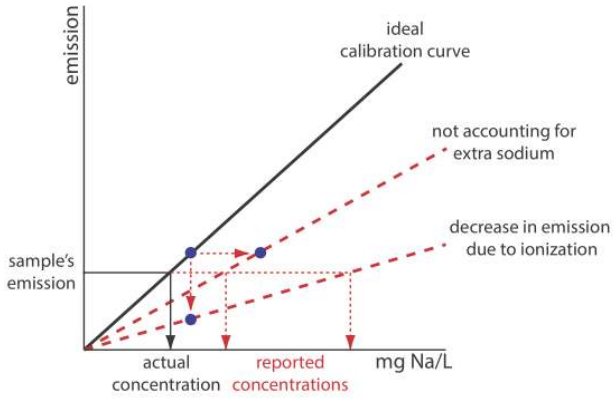


Figure 10.7.6 . External standards calibration curves for the flame atomic emission analysis of Na in a salt substitute. The solid black line shows the ideal calibration curve assuming we match the matrix of the samples and the standards using pure KCl. The lower of the two dashed red lines shows the effect of failing to add KCl to the external standards, which decreases emission. The other dashed red line shows the effect of using KCl that is contaminated with NaCl, which causes us to underestimate the concentration of Na in the standards. In both cases, the result is a positive determinate error in the analysis of samples.

4. One problem with analyzing salt samples is their tendency to clog the aspirator and burner assembly. What effect does this have on the analysis?

Clogging the aspirator and burner assembly decreases the rate of aspiration, which decreases the analyte's concentration in the flame. The result is a decrease in the emission intensity and a negative determinate error.

Example 10.7.1

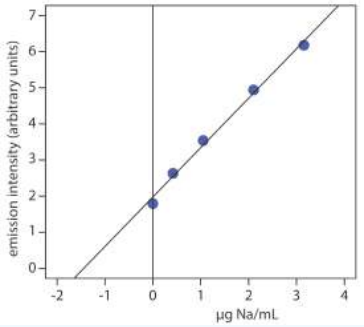
To evaluate the method described in Representative Method 10.7.1, a series of standard additions is prepared using a 10.0077-g sample of a salt substitute. The results of a flame atomic emission analysis of the standards is shown here [Goodney, D. E. *J. Chem. Educ.* **1982**, *59*, 875–876].

added Na (µg/mL)	I_e (arb. units)
0.000	1.79
0.420	2.63
1.051	3.54
2.102	4.94
3.153	6.18

What is the concentration of sodium, in µg/g, in the salt substitute.

Solution

Linear regression of emission intensity versus the concentration of added Na gives the standard additions calibration curve shown below, which has the following calibration equation.



$$I_e = 1.97 + 1.37 \times \frac{\mu g\ Na}{mL}$$

The concentration of sodium in the sample is the absolute value of the calibration curve's *x*-intercept. Substituting zero for the emission intensity and solving for sodium's concentration gives a result of 1.44 μgNa/mL. The concentration of sodium in the salt substitute is

$$\frac{\frac{1.44\ \mu g\ Na}{mL} \times \frac{50.00\ mL}{25.00\ mL} \times 250.0\ mL}{10.0077\ g\ sample} = 71.9\ \mu g\ Na/g$$

Evaluation of Atomic Emission Spectroscopy

Scale of Operation

The scale of operations for atomic emission is ideal for the direct analysis of trace and ultratrace analytes in macro and meso samples. With appropriate dilutions, atomic emission can be applied to major and minor analytes.

Accuracy

When spectral and chemical interferences are insignificant, atomic emission can achieve quantitative results with accuracies of 1–5%. For flame emission, accuracy frequently is limited by chemical interferences. Because the higher temperature of a plasma source gives rise to more emission lines, accuracy when using plasma emission often is limited by stray radiation from overlapping emission lines.

Precision

For samples and standards in which the analyte's concentration exceeds the detection limit by at least a factor of 50, the relative standard deviation for both flame and plasma emission is about 1–5%. Perhaps the most important factor that affect precision is the stability of the flame's or the plasma's temperature. For example, in a 2500 K flame a temperature fluctuation of ± 2.5 K gives a relative standard deviation of 1% in emission intensity. Significant improvements in precision are realized when using internal standards.

Sensitivity

Sensitivity is influenced by the temperature of the excitation source and the composition of the sample matrix. Sensitivity is optimized by aspirating a standard solution of analyte and maximizing the emission by adjusting the flame's composition and the height from which we monitor the emission. Chemical interferences, when present, decrease the sensitivity of the analysis. Because the sensitivity of plasma emission is less affected by the sample matrix, a calibration curve prepared using standards in a matrix of distilled water is possible even for samples that have more complex matrices.

Selectivity

The selectivity of atomic emission is similar to that of atomic absorption. Atomic emission has the further advantage of rapid sequential or simultaneous analysis of multiple analytes.

Time, Cost, and Equipment

Sample throughput with atomic emission is rapid when using an automated system that can analyze multiple analytes. For example, sampling rates of 3000 determinations per hour are possible using a multichannel ICP, and sampling rates of 300 determinations per hour when using a sequential ICP. Flame emission often is accomplished using an atomic absorption spectrometer, which typically costs between $10,000–$50,000. Sequential ICP's range in price from $55,000–$150,000, while an ICP capable of simultaneous multielemental analysis costs between $80,000–$200,000. Combination ICP's that are capable of both sequential and simultaneous analysis range in price from $150,000–$300,000. The cost of Ar, which is consumed in significant quantities, can not be overlooked when considering the expense of operating an ICP.

This page titled 6.6: Atomic Emission Spectroscopy is shared under a CC BY-NC-SA 4.0 license and was authored, remixed, and/or curated by Kathryn Davis.

- **10.7: Atomic Emission Spectroscopy** by David Harvey is licensed CC BY-NC-SA 4.0.

CHAPTER OVERVIEW

7: Mass Spectrometry

7.1: Mass Spectrometers
7.2: Inductively Coupled Plasma Mass Spectrometer
7.3: Molecular Mass Spectra
7.4: Mass Spectrometers
7.5: Ion Sources
7.6: Applications of Molecular Mass Spectrometry

This page titled 7: Mass Spectrometry is shared under a not declared license and was authored, remixed, and/or curated by Kathryn Davis.

7.1: Mass Spectrometers

A mass spectrometer has three essential needs: a means for producing ions, in this case (mostly) singly charged atoms; a means for separating these ions in space or in time by their mass-to-charge ratios; and a means for counting the number of ions for each mass-to-charge ratio. Figure **7.1.1** provides a general view of a mass spectrometer in the same way that we first introduced optical instruments in Chapter 7. The ionization of the sample is analagous to the source of photons in optical spectroscopy as it generates the particles (ions, instead of photons) that ultimately make up the measured signal. The separation of the resulting ions by their mass-to-charge ratios, which is accomplished using a mass analyzer, is analagous to the role of a monochromator in optical spectroscopy. The means for counting ions serves the same role as, for example, a photomultiplier tube in optical spectroscopy. Note that the mass spectrometer is held under vacuum as this allows the ions to travel great distances without undergoing collisions that might alter their charge or energy.

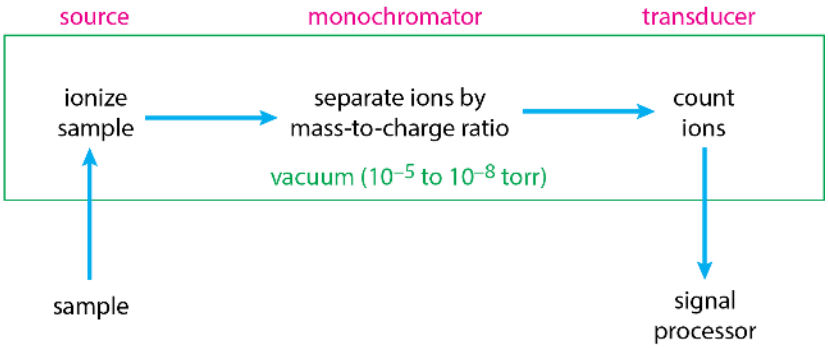


Figure **7.1.1**: The basic components of a mass spectrometer. The blue arrows show the direction of sample-to-signal in which the sample is ionized, the ions separated by their mass-to-charge ratio, and ions with the same mass-to-charge ratio counted. The text in red at the top of the figure relates these components to their equivalent in optical spectroscopy.

Sources of Ionization

The most common means for generating ions are plasmas of various sorts, lasers, electrical sparks, and other ions. We will give greater attention to these in the next several sections as we consider specific examples of atomic mass spectrometry.

Transducers for Counting Ions

The transducer for mass spectrometry must be able to report the number of ions that emerge from the mass analyzer. Here we consider two common types of transducers.

Electron Multipliers

In Chapter 7 we introduced the photomultiplier tube as a way to convert photons into electrons, amplifying the signal so that a single photon produces 10^6 to 10^7 electrons, which generates a measurable current. An electron multiplier serves the same role in mass spectrometry. Figure **7.1.2** shows two versions of this transducer. The electron multiplier in Figure **7.1.2*a*** uses a set of individual dynodes. When an ion strikes the first dynode, it generates several electrons, each of which is passed along to the next dynode before arriving at a collecting plate where the current is measured. The result is an amplification, or gain, in the signal of approximately $\mathbf{10^7\times}$. The electron multiplier in Figure **7.1.2*b*** uses a horn-shaped cylinder—typically made from glass coated with a thin layer of a semiconducting material—whose surface acts as a single, continuous dynode. When an ion strikes the continuous dynode it generates several electrons that are reflected toward the collector plate where the current is measured. The result is an amplification of $\mathbf{10^5}$ **to** $\mathbf{10^8\times}$.

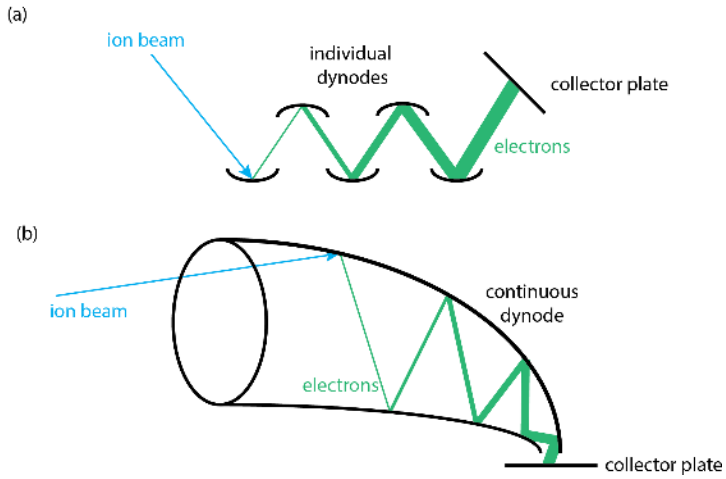


Figure **7.1.2**: Electron multipliers using (a) individual, or discrete dynodes, and (b) a single, continuous dynode. The ion beam is represented by the blue arrows and the electrons are represented by the green lines. The increasing thickness of the green lines shows the amplification of the signal.

Faraday Cup

A Faraday cup, as its name suggests, is a simple device shaped like a cup. Ions enter the cup where they strike a collector electrode. A current is directed to the collector plate that is sufficient to neutralize the charge of the ions. The magnitude of this current is proportional to the number of ions. A Faraday cup has the advantage of simplicity, but is less sensitive than an electron multiplier because it lacks the amplification provided by the dynodes.

Separating Ions

Before we can detect the ions, we need to separate them so that we can generate a spectrum that shows the intensity of ions as a function of their mass-to-charge ratio. In this section we consider the three most common mass analyzers for atomic mass spectrometry.

Quadrupole Mass Analyzers

The quadrupole mass analyzer is the most important of the mass analyzers included in this chapter: it is compact in size, low in cost, easy to use, and easy to maintain. As shown in Figure **7.1.3**, a quadrapole mass analyzer consists of four cylindrical rods, two of which are connected to the positive terminal of a variable direct current (dc) power supply and two of which are connected to the power supply's negative terminal; the two positive rods are positioned opposite of each other and the two negative rods are positioned opposite of each other. Each pair of rods is also connected to a variable alternating current (ac) source operated such that the alternating currents are 180° out-of-phase with each other. An ion beam from the source is drawn into the channel between the quadrupoles and, depending on the applied dc and ac voltages, ions with only one mass-to-charge ratio successfully travel the length of the mass analyzer and reach the transducer; all other ions collide with one of the four rods and are destroyed.

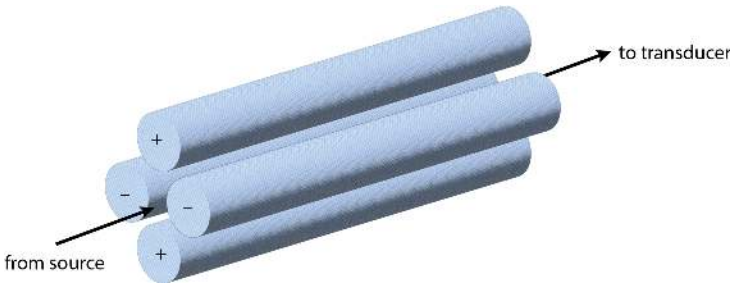


Figure **7.1.3**: Basic arrangement of the quadrupole mass analyzer. The plus and the minus signs on each rod indicate which are connected to the positive terminal of the dc power supply. Not shown here is the circuitry for applying the alternating current. The ion beam enters the channel between the quadrupoles. Depending on the applied dc and ac voltages, some of the ions emerge from this channel and reach the transducer.

To understand how a quadrupole mass analyzer achieves this separation of ions, it helps to consider the movement of an ion relative to just two of the four rods, as shown in Figure **7.1.4** for the poles that carry a positive dc voltage. When the ion beam

enters the channel between the rods, the ac voltage causes the ion to begin to oscillate. If, as in the top diagram, the ion is able to maintain a stable oscillation, it will pass through the mass analyzer and reach the transducer. If, as in the middle diagram, the ion is unable to maintain a stable oscillation, then the ion eventually collides with one of the rods and is destroyed. When the rods have a positive dc voltage, as they do here, ions with larger mass-to-charge ratios will be slow to respond to the alternating ac voltage and will pass through the transducer. The result is shown in the figure at the bottom (and repeated in Figure **7.1.5*a***) where we see that ions with a sufficiently large mass-to-charge ratios successfully pass through the transducer; ions with smaller mass-to-charge ratios do not. In this case, the quadrupole mass analyzer acts as a high-pass filter.

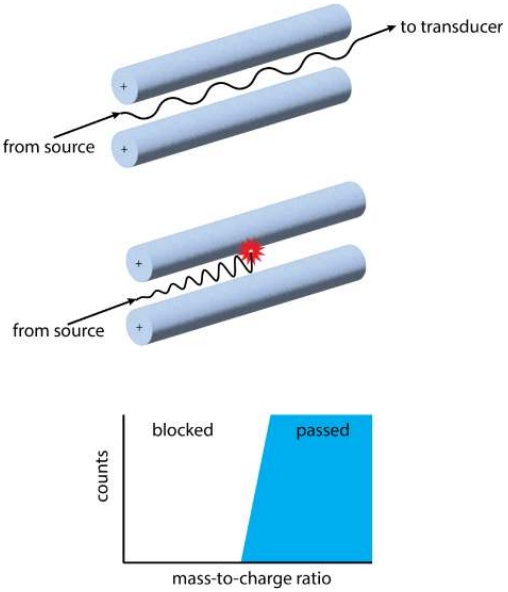


Figure **7.1.4**: Illustration of how a quadrupole mass analyzer achieves separation of ions by their mass-to-charge ratio. See the text for additional details.

We can extend this to the behavior of the ions when they interact with rods that carry a negative dc voltage. In this case, the ions are attracted to the rods, but those ions that have a sufficiently small mass-to-charge ratio are able to respond to the alternating current's voltage and remain in the channel between the rods. The ions with larger mass-to-charge ratios move more sluggishly and eventually collide with one of the rods. As shown in Figure **7.1.5*b***, in this case, the quadrupole mass analyzer acts as a low-pass filter. Together, as we see in Figure **7.1.5*c***, a quadrupole mass analyzer operates as both a high-pass and a low-pass filter, allowing a narrow band of mass-to-charge ratios to pass through the transducer. By varying the applied dc voltage and the applied ac voltage, we can obtain a full mass spectrum.

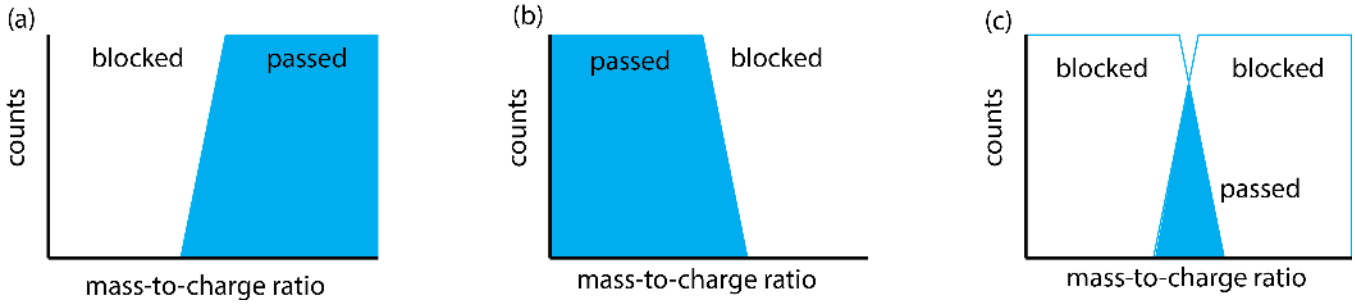


Figure **7.1.5**: Illustration that shows how a quadrupole mass analyzer acts as both (a) a high-pass filter and (b) a low pass filter, with the result that it passes only ions with a narrow range of mass-to-charge ratios.

Quadrupole mass analyzers provide a modest mass-to-charge resolution of about 1 amu and extend to m/z ratios of approximately 2000. Quadrupole mass analyzers are particularly useful for sources based on plasmas.

Time-of-Flight (TOF) Mass Analyzers

In a time-of-flight mass analyzers, ions are created in small clusters by applying a periodic pulse of energy to the sample using a laser beam or a beam of energetic particles to ionize the sample. The small cluster of ions are then drawn into a tube by applying an

electric field and then allowed to drift through the tube in the absence of any additional applied field; the tube, for obvious reasons, is called a drift tube. All of the ions in the cluster enter the drift tube with the same kinetic energy, KE, which means, given

$$\mathrm{KE} = \frac{1}{2}mv^2 \tag{7.1.1}$$

that the square of an ion's velocity is inversely proportional to the ion's mass. As a result, lighter ions move more quickly than heavier ions. Flight times are typically less than 30 μs. A time-of-flight mass analyzer provide better resolution than a quadrupole mass analyzer, but is limited to sources that can be pulsed.

Double-Focusing Mass Analyzers

In a double-focusing mass analyzer, two mechanisms are used to focus a beam of ions onto the transducer. One of the mechanisms is an electrotatic analyzer that serves to confine the kinetic energy of the ions to a narrow range of energies. The second mechanism is a magnetic sector analyzer that uses an applied magnetic field to separate the ions by their mass-to-charge ratio. The combination of two analyzers allows for a significant resolution. More details on this type of mass analyzer is included in Chapter 20.

This page titled 7.1: Mass Spectrometers is shared under a CC BY-NC-SA 4.0 license and was authored, remixed, and/or curated by Kathryn Davis.

- **11.2: Mass Spectrometers** by David Harvey is licensed CC BY-NC-SA 4.0.

7.2: Inductively Coupled Plasma Mass Spectrometer

In Chapter 10 we introduced the inductively coupled plasma (ICP) as a source for atomic emission. The plasma in ICP is formed by ionizing a flowing stream of argon gas, producing argon ions and electrons. The sample is introduced into the plasma where the high operating temperature of 6000–8000 K is sufficient to atomize and ionize the sample. In optical ICP we measure the emission of photons from the atoms and ions that are in excited states. In ICP-MS we use the plasma as a source of ions that we can send to a mass spectrometer for analysis.

Instrumentation for ICP-MS

An ICP torch operates at room pressure and at an elevated temperature, and a mass spectrometer, as noted in Section 11.2, operates under a vacuum and at room temperature. This difference in pressure and temperature means that a coupling together of these two instrument requires an interface than can bring the pressure and temprature in line with the demands of the mass spectrometer. Figure **7.2.1** provides a schematic diagram of a typical ICP-MS instrument with the ICP torch on the right and the mass spectrometer's quadrupole mass analyzer and a continuous electron multiplier on the left. In between the two is a two-stage interface. Note that none of the components in Figure **7.2.1** are drawn to scale.

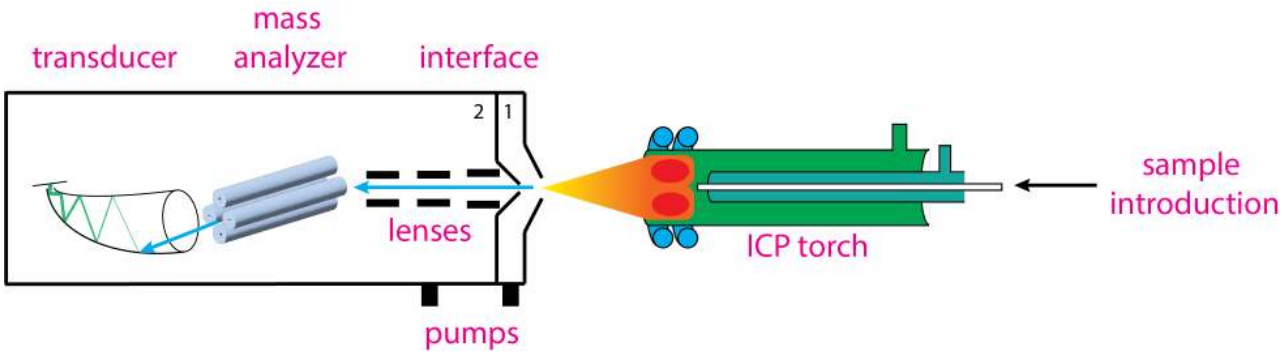


Figure **7.2.1**. Schematic diagram of an instrument for an inductively coupled plasma mass spectrometer (ICP-MS), showing the torch and the sample nebulizer that make up the ICP on the right, and the mass analyzer and the transducer that make up the MS on the left. Also shown is the interface between the two. The first stage of the interface (1) samples the plasma from the ICP torch and then further reduces the number of particles that are passed along to the second stage (2) a set of ion lenses are used to remove electrons, neutral species, and photons and to focus the ion beam onto the quadrupole.

The first stage of the interface consists of two cone-shaped openings: a sampler cone and a skimmer cone. The hot plasma from the ICP torch enters the first stage of the interface through the sampler cone, which is a pin-hole with a diameter of approximately 1 mm. Samples in solution form are drawn directly into the ICP torch using a nebulizer. Solid samples are vaporized using a laser (a process called laser ablation) and the vapor drawn directly into the ICP torch.

A pump is used to drop the pressure in the first stage to approximately 1 torr. The expansion of the plasma as it enters the first stage results in some cooling of the plasma. The skimmer cone allows a small portion of the plasma in the first stage to pass into the second stage, which is held at the mass spectrometer's operating pressure of approximately 10^{-5} torr. A series of ion lenses are used to narrow the conical dispersion of the plasma, to isolate positive ions from electrons, neutral species, and photons—all of which will generate a signal if they reach the transducer—and to focus the ion beam onto the quadrupole's entrance.

Atomic Mass Spectra and Interferences

Figure **7.2.2** shows an example of an ICP-MS spectrum for the analysis of a metal coating using laser ablation to volatilize the sample. The quadrupole mass analyzer operates over a mass-to-charge range of approximately 3 to 300 and can resolve lines that differ by ± 1 m/z. Data are collected either by scanning the quadrupole to provide a survey spectrum of all ions generated in the plasma, as is the case in Figure **7.2.2**, or by peak hopping in which we gather data for just a few discrete mass-to-charge ratios,

adjusting the quadrupole so that it passes only a single mass-to-charge ratio and count the ions for a set period of time before moving to the next mass-to-charge ratio.

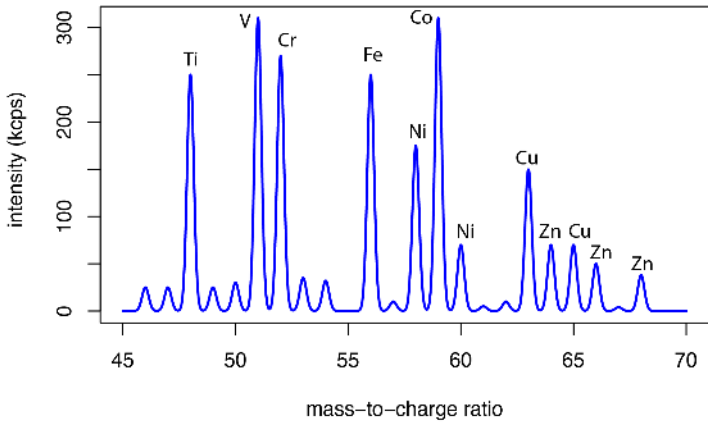


Figure **7.2.2**. Example of an ICP-MS spectrum of a metal coating using laser ablation to vaporize the sample before drawing it into the ICP torch. The intensity of ions is reported in kilocounts per seconds. The major peaks are identified by element. The data used to construct this figure were extrapolated from the source linked to here.

Spectroscopic Interferences

An ICP-MS spectrum is much simpler than the corresponding ICP atomic emission spectrum because each element in the latter has many emission lines and because the plasma itself has many emission lines. Still, an ICP-MS is not free from interferences, the two most important of which are isobaric ions and polyatomic ions.

Isobaric Ions. Iso- means same and -baric means weight; thus, isobaric means same weight and refers to two (or more) species that have—within the resolution of the mass spectrometer—identical weights and that both contribute to the same peak in the mass spectrum. The source of this interference is the existence of isotopes. For example, the most abundant ions for argon and for calcium are ^{40}Ar and ^{40}Ca, and, given the resolving power of a quadrupole mass analyzer, the two ions appear as a single peak at $m/z = 40$ even though the mass of ^{40}Ar is 39.962383 amu and the mass of ^{40}Ca is 39.962591 amu. We can correct for this interference because the second most abundant isotope of calcium, ^{44}Ca, does not share a m/z with argon (or with another element). Figure **7.2.3** shows the ICP-MS spectrum for a sample that contains calcium and argon, and Example **7.2.1** shows how we can use this spectrum to determine the contribution of each element.

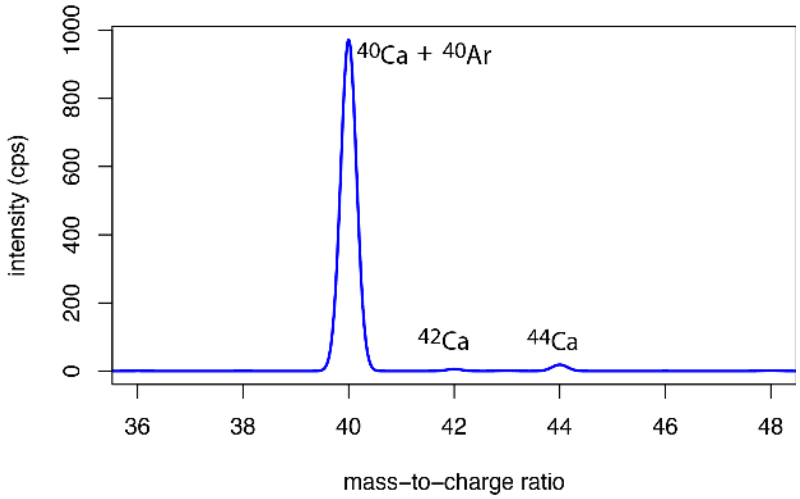


Figure **7.2.3**: ICP-MS spectrum for a mixture of calcium and argon. The peak at $m/z = 40$ includes contributions from both ^{40}Ca and ^{40}Ar. The other two peaks are for ^{42}Ca and for ^{44}Ca and do not include contributions from argon. The peaks for ^{36}Ar, ^{38}Ar, ^{43}Ca, ^{46}Ca, and ^{48}Ca are too small to appear as peaks in this spectrum.

Example 7.2.1

For the spectrum in Figure **7.2.3**, the intensity at $m/z = 40$ is 972.07 cps and the intensity at $m/z = 44$ is 18.77 cps. Given that the istopic abundance of ^{40}Ca is 96.941% and the isotopic abundance of ^{44}Ca is 2.086%, what is the counts-per-second at $m/z = 40$ for Ca and for Ar.

Solution

Given that only ^{44}Ca contributes to the peak at $m/z = 44$ we can use the relative abundances of ^{40}Ca and ^{44}Ca to determine the expected contribution of ^{40}Ca to the total intensity at $m/z = 40$.

$$18.77 \text{ cps} \times \frac{96.941}{2.086} = 872.28 \text{ cps}$$

Subtracting this result from the total intensity gives the intensity at $m/z = 40$ for argon as

$$972.07 \text{ cps} - 872.28 \text{ cps} = 99.79 \text{ cps}$$

Polyatomic Ions. Compensating for isobaric ions is relatively straightforward because we can rely on the known isotopic abundances of the elements. A more difficult problem is an interference between the isotope of an elemental analyte and a polyatomic ion that has the same mass. Such polyatomic ions may arise from the sample's matrix or from the plasma. For example, the ion $^{40}Ar^{16}O^{+}$ has a mass-to-charge ratio of 56, which overlaps with peak for ^{56}Fe, the most abundant isotope of iron. Although we could choose to monitor iron at a different mass-to-charge ratio, we will lose sensitivity as we are using a less abundant isotope. Corrections can be made using the method outlined in Example **7.2.1**, although it may require using multiple peaks, which increases the uncertainty of the final result.

Matrix Effects

A matrix effect occurs when the sample's matrix affects the relationship between the signal and the concentration of the analyte. Matrix effects are common in ICP-MS and may lead to either a suppression or an enhancement in the signal. Although not always well understood, matrix effects likely result from how easily an ionizable element affects the ability to ionize other elements. Matrix matching, using the method of standard additions, or using an internal standard can help minimize matrix effects for quantitative work.

Applications of ICP-MS

ICP-MS finds application for analytes in a wide variety of matrices, including both solutions and solids. Solution samples with high concentrations of dissolved ions may present problems due to the deposition of the salts onto the sampler and skimmer cones, which reduces the size of the pinhole that provides entry into the interface between the ICP torch and the mass spectrometer. The use of laser ablation makes it possible to analyzer surfaces—such as glasses, metals, and ceramics—without additional sample preparation.

Qualitative and Semiquantitative Applications. One of the strengths of ICP-MS is its ability to provide a survey scan, such as that in Figure **7.2.1**, that allows for the identification of the elements present in a sample. Analysis of a single sample that contains known concentrations of these elements is suitable for providing a rough estimate of their concentration in the sample.

Quantitative Analysis. For a more accurate and precise quantitative analysis, one can prepare multiple external standards and prepare a calibration curve. Linearly across approximately six orders of magnitude with detection limits of less than 1 ppb. Including an internal standard in the external standards can help reduce matrix effects. The ideal internal standard will not produce isobaric ions and its primary ionization potential should be similar to that for the analyte; when working with several analytes, it may be necessary to choose a different internal standard for each analyte.

Isotope Ratios. An important advantage of ICP-MS over other analytical methods is its ability to monitor multiple isotopes for a single element.

This page titled 7.2: Inductively Coupled Plasma Mass Spectrometer is shared under a CC BY-NC-SA 4.0 license and was authored, remixed, and/or curated by Kathryn Davis.

- **11.3: Inductively Coupled Plasma Mass Spectrometer** by David Harvey is licensed CC BY-NC-SA 4.0.

7.3: Molecular Mass Spectra

Figure **7.3.1** shows a mass spectrum for *p*-nitrophenol, $C_6H_5NO_3$, which has a nominal (integer) mass of 139 daltons. If we send a beam of energetic electrons through a gas phase sample of *p*-nitrophenol, it loses an electron, which we write as the reaction

$$C_6H_5NO_3 + e^- \rightarrow C_6H_5NO_3^{+\bullet} + 2e^- \tag{7.3.1}$$

where the product is a radical cation that has a charge of **+1** and that retains the nominal mass of 139 daltons. We call this the molecular ion—highlighted here in green—and it has a mass-to-charge ratio (*m*/*z*) of 139.

Note

Some of the terminology in this chapter was covered earlier in Chapter 11 on atomic mass spectrometry. See the first section of that chapter for a discussion of atomic mass units (amu) and daltons (Da), and of mass-to-charge ratios.

If reaction 7.3.1 is all that happens when *p*-nitrophenol interacts with an energetic electron, then it would not provide much in the way of useful information. The radical cation $C_6H_5NO_3^{+\bullet}$, however, retains sufficient excess energy from the initial electron-molecule collision that it is in an excited state. In returning to its ground state, the molecular ion undergoes a series of fragmentations that result in the formation of ions—called daughter ions—with different mass-to-charge ratios. A plot that shows the relative intensity of these ions as a function of their mass-to-charge ratios is called a mass spectrum. The most abundant fragment in the spectrum—shown here in red and which is called the base peak—is assigned a relative intensity of 100; the intensity of all other ions is reported relative to the base perk.

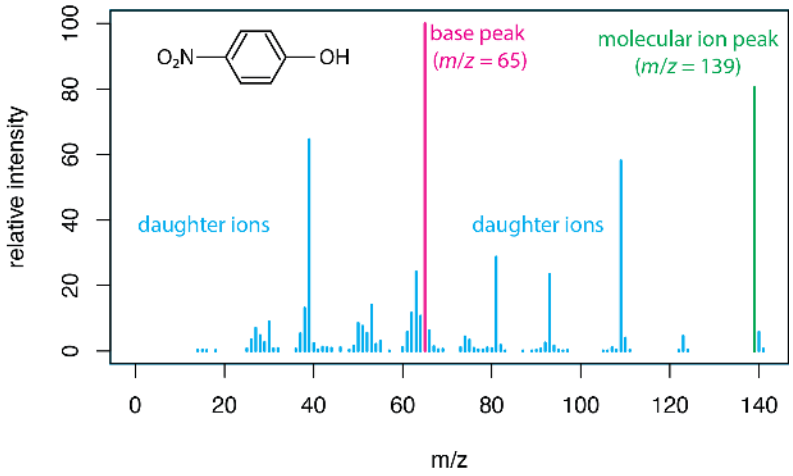


Figure **7.3.1**: The mass spectrum for *p*-nitrophenol showing the molecular ion at a m/z of 139 (in green) and the daughter ions (in blue) formed through fragmentation. The most abundant fragment is the base peak at a m/z of 65 (in red). The original data is available here. This particular spectrum was collected using an electron impact source; more on that in Section 20.2.

A molecule's fragmentation patterns provides rich information about its structure. Figure **7.3.2** compares the mass spectra for *o*-nitrophenol, *m*-nitrophenol, and *p*-nitrophenol. All three molecules have clusters of fragment ions at similar mass-to-charge ratios, but the relative abundance of the ions in these clusters varies quite a bit from molecule-to-molecule. For example, the pink rectangle in each spectrum highlights peaks with mass-to-charge ratios from approximately 104 *m*/*z* to 115 *m*/*z*. All three molecules share the property of producing fragment ions with these mass-to-charge ratios; the relative abundance of the fragment ions, however, varies substantially between the three molecules with *o*-nitrophenol and *p*-nitrophenol having a major peak at 109 *m*/*z*, but *m*-nitrophenol showing no more than a trace peak at 109 *m*/*z*. We will return to the use of mass spectrometry for determining structure information later in this chapter.

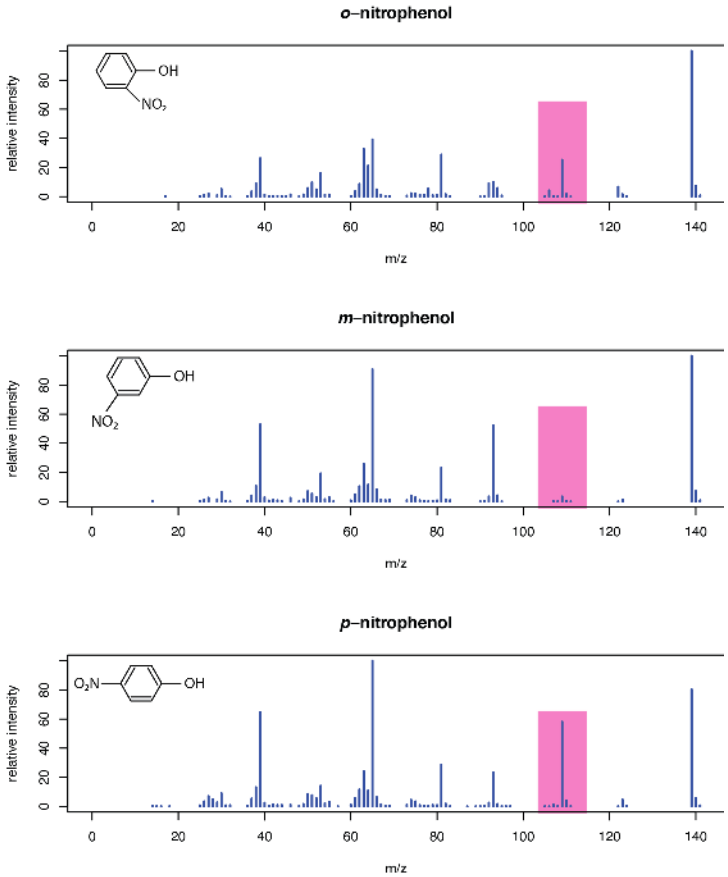


Figure 7.3.2: The mass spectra for *o*-nitrophenol (top), *m*-nitrophenol (middle), and *p*-nitrophenol (bottom). All three molecules show the same pattern of the mass-to-charge ratios where clusters of fragment ions appear; however, the relative abundance of each cluster varies from molecule-to-molecule. The pink rectangle highlights the *m*/*z* values of 104–115. The original data for these spectra are here, here, and here from top-to-bottom.

This page titled 7.3: Molecular Mass Spectra is shared under a CC BY-NC-SA 4.0 license and was authored, remixed, and/or curated by Kathryn Davis.

- **20.1: Molecular Mass Spectra** by David Harvey is licensed CC BY-NC-SA 4.0.

7.4: Mass Spectrometers

A mass spectrometer has four essential elements: a means for introducing the sample to the instrument, a means for generating a mixture of ions, a means for separating the ions, and a means for counting the ions. In Chapter 20.2 we introduced some of the most important ways to generate ions. In this section we turn our attention to sample inlet systems and to separating and counting ions. You may wish to review Chapter 11 where we considered these topics in the context of atomic mass spectrometry. As we noted in Chapter 11, a mass spectrometer must operate under a vacuum to ensure that ions can travel long distances without undergoing undesired collisions that affect their ion energy.

Sample Inlet Systems

When the sample is a gas or a volatile liquid, it is easy to transfer a portion of the sample into a reservoir as a gas maintained at a relatively small pressure. The sample is then allowed to enter into the mass spectrometer's ion source through a diaphragm that contains a pin-hole, drawn in by holding the ion source at lower pressure.

Solid and non-volatile liquids are sampled by inserting them directly into the ion source through a vacuum lock that allows the mass spectrometer to remain under vacuum except for the ion source where the sample is inserted. The sample is placed in a capillary tube or a small cup at the end of a sample probe, and then moved into the ion source. The sample probe includes a heating coil that is used, along with the instrument's vacuum, to help volatilize the sample.

Of particular importance are inlet systems that couple a chromatographic or an electrophoretic instrument to a mass spectrometer, providing a way to separate a complex mixture into its individual components and then using the mass spectrometer to determine the composition of those components. The interface between a gas chromatograph and a mass spectrometer (GC-MS) must account for the significant drop in pressure from atmospheric pressure to a pressure of 10^{-8} torr; the interface for LC-MS and for EC-MS must provide a way to remove the liquid eluent, to volatilize the samples, and to account for the drop in pressure. See Chapters 27, 28, and 30 for more details.

Mass Analyzers

The purpose of the mass analyzer is to separate the ions by their mass-to-charge ratios. Ideally we want the mass analyzer to allow us to distinguish between small differences in mass and to do so with a strong signal-to-noise ratio. As we learned in Chapter 7 when introducing optical spectroscopy, these two desires usually are in tension with each other, with improvements in resolution often coming with an increase in noise.

Resolution

The resolution between two peaks, R, in mass spectrometry is defined as the ratio of their average mass to the difference in their masses

$$R = \frac{\overline{m}}{\Delta m} \tag{7.4.1}$$

The following table shows how resolution varies as a function of the average mass and the difference in mass. A resolution of 1,000, for example is sufficient to resolve two ions with an average mass of 100 amu that differ by 0.1 amu, or two ions that have an average mass of 1,000 amu that differ by 1 amu.

Table **7.4.1**. Resolution for stated values of $\overline{m}$ and Δm.

$\overline{m} \rightarrow$ $\Delta m \downarrow$	100 amu	1000 amu	10,000 amu
0.1 amu	1,000	10,000	100,000
1 amu	100	1,000	10,000
10 amu	10	100	1,000

Magnetic Sector Mass Analyzers

When a beam of ions passes through a magnetic field, its path is altered, as we see in Figure **7.4.1**. The ions experience an acceleration as they exit the ion source and enter the mass analyzer with a kinetic energy that is given by the equations

$$\mathrm{KE} = zeV \tag{7.4.2}$$

$$\mathrm{KE} = \frac{1}{2}mv^2 \tag{7.4.3}$$

where z is the ion's charge (usually +1), e is the electronic charge in Coulombs, V is the applied voltage responsible for the acceleration, m is the ion's mass, and v is the ion's velocity after acceleration. Equation 7.4.2 shows us that all ions with the same charge have the same kinetic energy. Equation 7.4.3, then, tells us that ions with a greater mass will move more slowly.

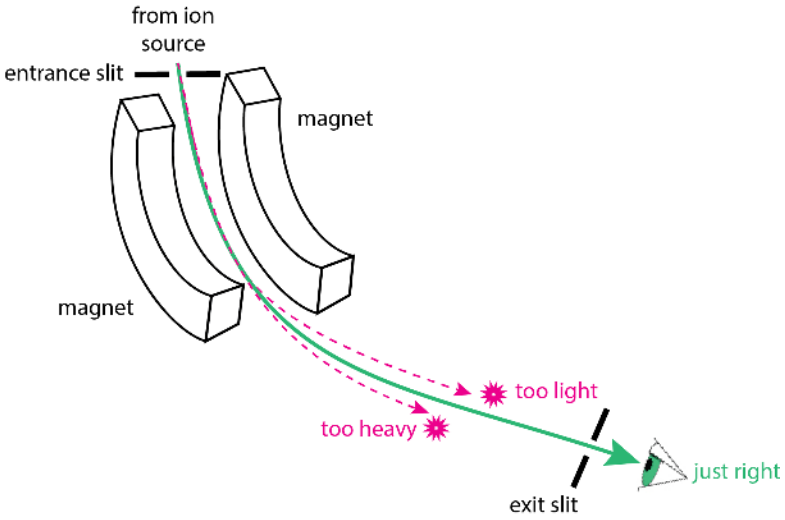


Figure **7.4.1**: Illustration of a magnetic sector analyzer for mass spectrometry. Ions from the ion source enter into the mass analyzer. The magnets in the mass analyzer bend the path followed by the ions. For any combination of magnetic field strength and accelerating voltage, only ions with a compatible mass-to-charge ratio are able to leave the mass analyzer through the exit slit; ions that are too heavy or too light, fail to exit the mass analyzer.

An ion's path through the magnetic field is determined by two forces. The first of these forces is the magnetic force, F_M, that acts on the ion, which is

$$F_M = Bzev \tag{7.4.4}$$

where B is the magnetic field strength. The second of these forces is the centripetal force, F_C, that acts on the ion as it moves along its curved path, which is

$$F_C = \frac{mv^2}{r} \tag{7.4.5}$$

where r is the magnet's radius of curvature. An ion can only navigate these opposing forces if F_M and F_C are equal to each other. This requires that

$$Bzev = \frac{mv^2}{r} \tag{7.4.6}$$

Solving for v gives

$$v = \frac{Bzer}{m} \tag{7.4.7}$$

Substituting back into Equation 7.4.3 and solving for the mass-to-charge ratio gives

$$\frac{m}{z} = \frac{B^2r^2e}{2V} \tag{7.4.8}$$

Equation 7.4.8 tells us that for any combinaton of magnetic field strength, B, and accelerating voltage, V, only one mass-to-charge ratio has the correct value of r to reach the director. Ions that are too heavy or ions that are too light, will collide with the sides of the mass analyzer before they reach the detector. The mass spectrum is recorded by holding V and r constant and varying the magnetic field strength, B. The resolution of a magnetic sector instrument is usually less than 2000.

Double-Focusing Mass Analyzers

The resolution of a magnetic sector instrument suffers from limitations that affect its ability to narrow the range of kinetic energies —and, thus, velocities—possessed by the ions when they exit the ion source and enter the mass analyzer. The double-focusing mass analyzer in Figure 7.4.2 compensates for this by placing an electrostatic analyzer before the magnetic analyzer, separating the two by a slit. The electrostatic analyzer consists of two curved metal plates, one of which is held at a positive potential and one at a negative potential. As ions pass betweeen the plates, those ions that have too much energy and those that have too little energy fail to pass through the slit that separates the electrostatic analyzer from the magnetic analyzer. In this way, the distribution of energies —and, thus, velocities—is tightened, improving the resolution achieved by the magnetic sector analyzer. Depending on its design, a double-focusing analyzer can achieve a resolution as large as 100,000.

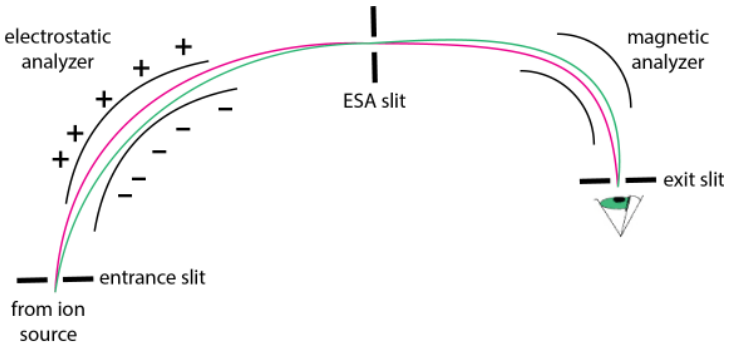


Figure 7.4.2: Illustration of a double-focusing mass analyzer that consists of an electrostatic mass analyzer and a magnetic mass analyzer. Ions that make it through the slit that separates the two analyzers have a smaller range of kinetic energies than the ions in a magnetic sector mass analyzer, which improves resolution.

Quadrupole Mass Analyzers

The quadrupole mass analyzer was introduced in Chapter 11 and the treatment here is largely the same. A quadupole mass analyzer is compact in size, low in cost, easy to use, and easy to maintain. As shown in Figure 7.4.3, it consists of four cylindrical rods, two of which are connected to the positive terminal of a variable direct current (dc) power supply and two of which are connected to the power supply's negative terminal; the two positive rods are positioned opposite of each other and the two negative rods are positioned opposite of each other. Each pair of rods is also connected to a variable alternating current (ac) source operated such that the alternating currents are 180° out-of-phase with each other. An ion beam from the source is drawn into the channel between the quadrupoles and, depending on the applied dc and ac voltages, ions with only one mass-to-charge ratio successfully travel the length of the mass analyzer and reach the transducer; all other ions collide with one of the four rods and are destroyed.

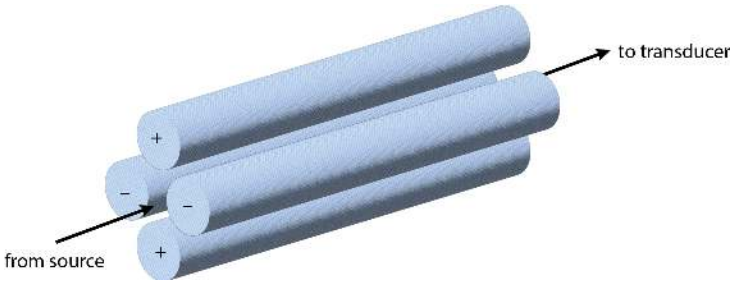


Figure 7.4.3: Basic arrangement of the quadrupole mass analyzer. The plus and the minus signs on each rod indicate which are connected to the positive terminal of the dc power supply. Not shown here is the circuitry for applying the alternating current. The ion beam enters the channel between the quadrupoles. Depending on the applied dc and ac voltages, some of the ions emerge from this channel and reach the transducer.

To understand how a quadrupole mass analyzer achieves this separation of ions, it helps to consider the movement of an ion relative to just two of the four rods, as shown in Figure 7.4.4 for the poles that carry a positive dc voltage. When the ion beam

enters the channel between the rods, the ac voltage causes the ion to begin to oscillate. If, as in the top diagram, the ion is able to maintain a stable oscillation, it will pass through the mass analyzer and reach the transducer. If, as in the middle diagram, the ion is unable to maintain a stable oscillation, then the ion eventually collides with one of the rods and is destroyed. When the rods have a positive dc voltage, as they do here, ions with larger mass-to-charge ratios will be slow to respond to the alternating ac voltage and will pass through the transducer. The result is shown in the figure at the bottom (and repeated in Figure **7.4.5*a***) where we see that ions with a sufficiently large mass-to-charge ratios successfully pass through the transducer; ions with smaller mass-to-charge ratios do not. In this case, the quadrupole mass analyzer acts as a high-pass filter.

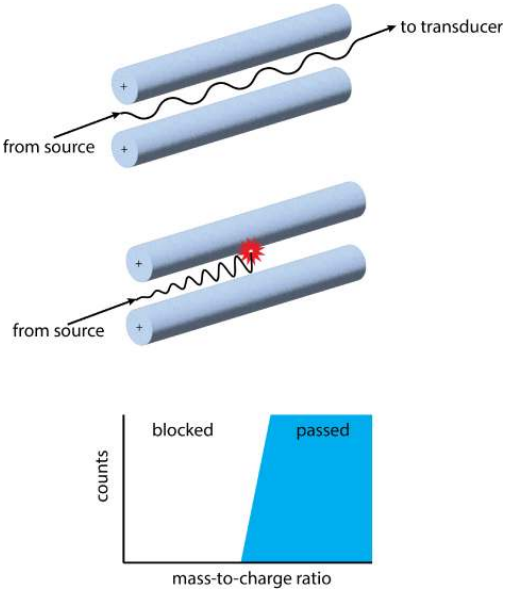


Figure **7.4.4**: Illustration of how a quadrupole mass analyzer achieves separation of ions by their mass-to-charge ratio. See the text for additional details.

We can extend this to the behavior of the ions when they interact with rods that carry a negative dc voltage. In this case, the ions are attracted to the rods, but those ions that have a sufficiently small mass-to-charge ratio are able to respond to the alternating current's voltage and remain in the channel between the rods. The ions with larger mass-to-charge ratios move more sluggishly and eventually collide with one of the rods. As shown in Figure **7.4.5*b***, in this case, the quadrupole mass analyzer acts as a low-pass filter. Together, as we see in Figure **7.4.5*c***, a quadrupole mass analyzer operates as both a high-pass and a low-pass filter, allowing a narrow band of mass-to-charge ratios to pass through the transducer. By varying the applied dc voltage and the applied ac voltage, we can obtain a full mass spectrum.

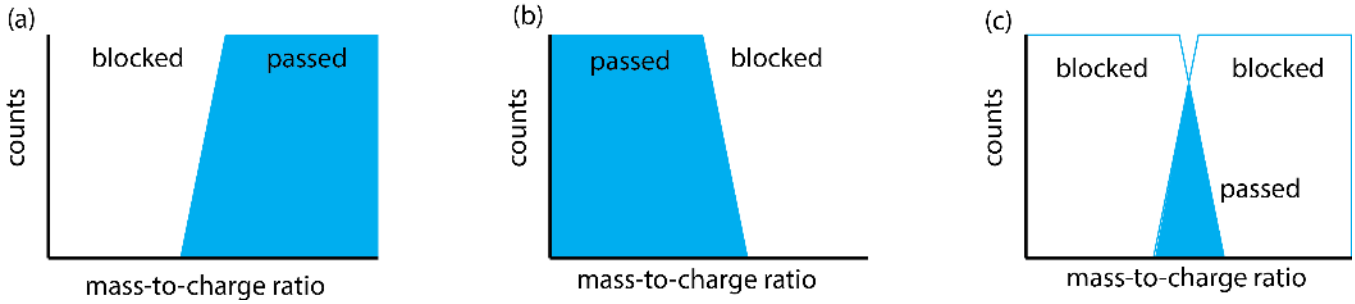


Figure **7.4.5**: Illustration that shows how a quadrupole mass analyzer acts as both (a) a high-pass filter and (b) a low pass filter, with the result that it passes only ions with a narrow range of mass-to-charge ratios.

Quadrupole mass analyzers provide a modest mass-to-charge resolution of about 1 amu and extend to m/z ratios of approximately 2000.

Time-Of-Flight Mass Analyzers

In a time-of-flight mass analyzers, Figure **7.4.6**, ions are created in small clusters by applying a periodic pulse of energy to the sample using a laser beam or a beam of energetic particles to ionize the sample. The small cluster of ions are then drawn into a tube

by applying an electric field and then allowed to drift through the tube in the absence of any additional applied field; the tube, for obvious reasons, is called a drift tube. All of the ions in the cluster enter the drift tube with the same kinetic energy, KE, which we define as

$$\text{KE} = \frac{1}{2}mv^2 = zeV \tag{7.4.9}$$

The time, T, that it takes the ion to travel the distance, L, to the detector is

$$T = \frac{L}{v} \tag{7.4.10}$$

Substituting Equation 7.4.10 into Equation 7.4.9

$$T = \sqrt{\frac{m}{z}} \times \sqrt{\frac{1}{2eV}} \tag{7.4.11}$$

shows us that the time it takes an ion to travel through the drift tube is proportional to the square rate of its mass-to-charge ratio. As a result, lighter ions move more quickly than heavier ions. Flight times are typically less than 30 μs. A time-of-flight mass analyzer provide better resolution than a quadrupole mass analyzer, but is limited to sources that can be pulsed. A linear time-of-flight analyzer, such as that in Figure **7.4.6**, provide a resolution of approximately 4,000; other configurations can achieve resolutions of 10,000 or better. The time-of-flight analyzer is well-suited for MALDI ionization as the time between pulses of the laser provides the time needed for detection to occur.

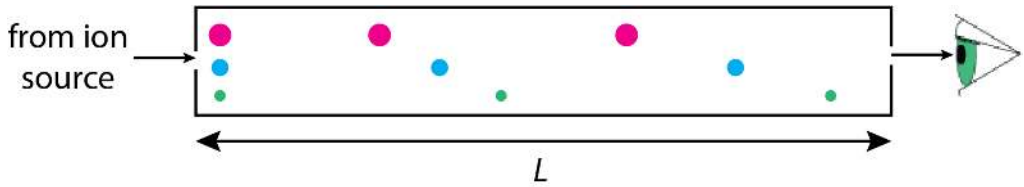


Figure **7.4.6**: Illustration of a linear time-of-flight mass analyzer showing three views of the relative positions of three ions with a small (green), medium (blue), and large (red) mass-to-charge ratios as they migrate through the drift tube.

Ion Trap Mass Analyzers

Figure **7.4.7** provides an illustration of an ion trap mass analyzer, which consists of three electrodes—a central ring electrode and two conical end cap electrodes—that create a cavity into which ions are drawn. The ions in the cavity experience stabilizing and destabilizing forces that affect their movement within the cavity. Ions that adopt stable orbits remain in the cavity. By varying the potentials applied to the electrodes, ions with different mass-to-charge ratios enter into destabilizing orbits and exit through a small hole at the bottom of the trap. An ion trap typcially provides a resolution of 1,000.

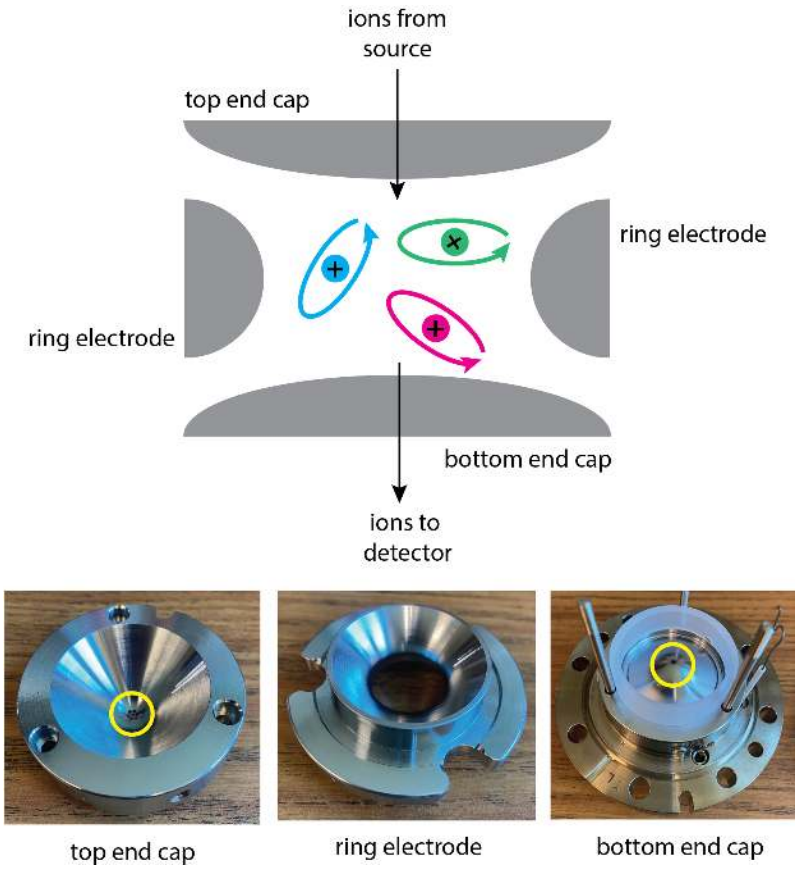


Figure 7.4.7: Illustration of the ion trap mass analyzer showing the cavity defined by the top end cap, the ring electrode, and the bottom end cap. The photographs on the bottom show the conical-shaped top end cap with small holes (inside the yellow circle) that allows ions to enter into the cavity, the ring electrode, and the conical-shaped bottom end cap, which has a small hole (inside the yellow circle) that allows ions to exit the cavity and reach the detector.

Ion Cyclotron Resonance Mass Analyzer

The ion cyclotron resonance (ICR) analyzer is a form of an ion trap but operates in a way that retains all ions within the trap. When a gas phase ion is placed within an applied magnetic field, the ions move in a circular orbit that is perpendicular to the applied field (Figure 7.4.8). In discussing the magnetric sector analyzer, we showed that the velocity, v, of an ion in an applied magnetic field with a strength of B is a function of the radius of the ion's motion, r, and its charge

$$v = \frac{Bzer}{m} \tag{7.4.12}$$

Solving for the ratio v/r gives the ion's cyclotron frequency, w_c, as

$$w_c = \frac{v}{r} = \frac{zeB}{m} \tag{7.4.13}$$

When an ion moving in a circular orbit, as shown by the smaller of the two circular orbits in Figure 7.4.8*a*, absorbs energy equal to its cyclotron frequency, w_c, its velocity, v, and the radius of its orbit, r both increase to maintain a constant value for w_c; the result is an ion that moves in a circular orbit of greater radius. As w_c depends on the mass-to-charge ratio, all ions of equal m/z experience the same change in their orbit, while ions with other mass-to-charge ratios are unaffected. Ions in the larger orbits eventually return to their original circular orbit as a result of collisions in which they lose energy.

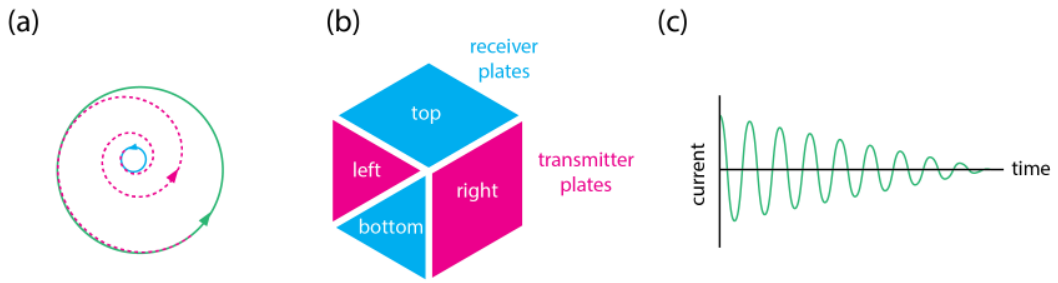


Figure 7.4.8: Illustration of how an ICR mass analyzer works. In (a) an ion originally in a circular orbit with a small radius, shown in blue moves into a circular orbit with a larger radius, shown in green when it absorbs energy equal to its cyclotron frequency, w_c, following the path shown in pink. The ICR cell in (b) consists of two transmitter plates that apply the potential that alters each ion's orbit, and two receiver plates that measure the current generated by the ions; there are two additional plates, one in front and one in back, that provide an entrance for bringing ions into the ICR cell from the ion source and for removing the ions in preparation for the next sample. The signal in (c) decays with time as the ions lose energy through collisions.

The trap itself, as seen in Figure 7.4.8*b*, is defined by two pairs of plates (four in all). The transmitter plates are used to apply the potential that alters the orbits of the ions. Movement of the ions generates a current in the receiver plates that serves as the signal, as seen in Figure 7.4.8*c*, that is positive when the ion is closer to one receiver plate and negative when it is closer to the other receiver plate. The initial magnitude of the current is proportional to the number of ions with the mass-to-charge ratio.

The ion cyclotron resonance analyzer is usually operated by applying a short pulse of energy that varies linearly in its frequency. This sets all ions into motion, with each mass-to-charge ratio yielding a current response similar to that in Figure 7.4.8*c*. Collectively, these individual current-time curves gives a time domain spectrum that we can covert into a frequency domain spectrum by taking the Fourier transform. The frequency domain spectrum yields the mass spectrum through Equation 7.4.13. FT-ICR instruments are capable of achieving resolutions of 1,000,000.

This page titled 7.4: Mass Spectrometers is shared under a CC BY-NC-SA 4.0 license and was authored, remixed, and/or curated by Kathryn Davis.

- **20.3: Mass Spectrometers** by David Harvey is licensed CC BY-NC-SA 4.0.

7.5: Ion Sources

Since a mass spectrum shows the relative abundance of ions with different mass-to-charge ratios, a mass spectrometer must include a way to generate ions. More specifically, it needs a method that generates the initial ion as it, once formed, will undergo fragmentation without additional help from the analyst (which does not mean the analyst cannot assist in that fragmentation; see discussion of tandem mass spectrometry in Section 20.4). In this section we consider several common ion sources. We can describe these sources using two characteristic properties: (a) the physical state of the species that is initially ionized (gas, liquid, or solid phase), and (b) whether ionization favors the formation of fragment ions or the formation of molecular ions (hard sources or soft sources).

Electron Ionization Sources (gas phase/hard source)

The electron ionization (EI) source, also known as an electron impact source, uses a beam of energetic electrons to ionize the analyte. As shown in **7.5.1**, the sample is volatilized prior to entering the ion source as gas phase molecules, M(g). A heated tungsten filament is used to generate electrons, which are pulled toward a positively charged anode. This electron beam intersects with the gas phase molecules at 90° where ionization occurs

$$\mathrm{M}(g) + e^- \rightarrow \mathrm{M}^{+\bullet}(g) + 2e^- \tag{7.5.1}$$

The molecular ions, $\mathrm{M}^{+\bullet}(g)$, are then swept into the mass analyzer using a set of accelerating plates (not shown here).

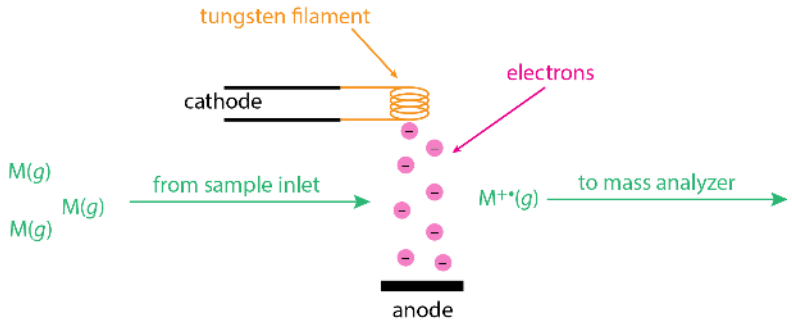


Figure **7.5.1**: Illustration of an electron ionization source. The sample is volatilized and brought into the ion source where it intersects with an electron beam, forming the molecular ion, $\mathrm{M}^{+\bullet}$, which is carried on into the mass analyzer.

The electron beam in Figure **7.5.1** has a lot of energy due to the significant potential difference between the cathode and the anode, which may be as much as 70 V. The kinetic energy of these electrons is equivalent to the product of the electron's charge in Coulombs, the applied potential in volts, and Avogadro's number

$$e \times V \times N_A = 1.6 \times 10^{-19} \times 6.022 \times 10^{-23} = 6.7 \times 10^{6}\ \mathrm{J/mol}$$

or 6,700 kJ/mol. This energy is much greater than typical bond energies, which range from approximately 150–600 kJ/mol for single bonds, from approximately 500–750 kJ/mol for double bonds, and from approximately 800–1100 kJ/mol for triple bonds. The significant difference between the energy of the electrons and bond energies explains why electron ionization spectra are rich in fragment ions, as we saw earlier in Section 20.1 for *o*-nitrophenol, *m*-nitrophenol, and *p*-nitrophenol. This extensive fragmentation is useful in determining an analyte's structure—which is an advantage of a hard ionization method—but at the possible cost of the loss of the molecular ion peak for some analytes. For example, Figure **7.5.2** shows the electron ionization mass spectrum from 1-decanol, $C_{10}H_{22}O$, which has a nominal mass of 158 daltons. The small peak at m/z = 157 is for the fragment ion $C_{10}H_{21}O^+$; the molecular ion is not observed in this spectrum.

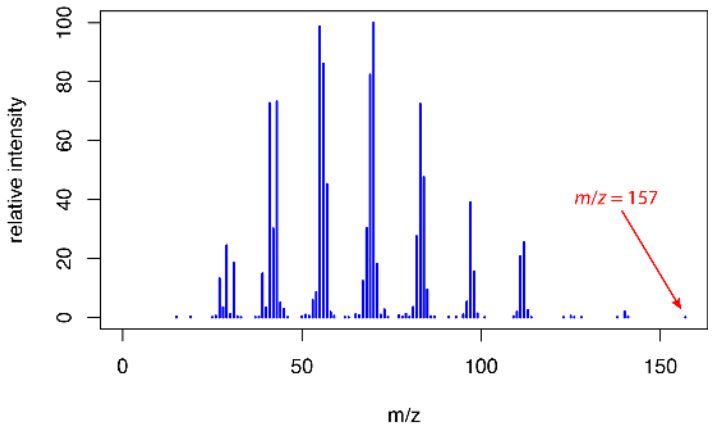


Figure 7.5.2: Mass spectrum for 1-decanol, $C_{10}H_{22}O$, using electron ionization. The peak furthest to the right (m/z = 157 amu) is one atomic mass unit less than the expected peak for the molecular ion, which does not appear in the spectrum. The original data is available here.

Chemical Ionization Sources (gas phase/soft source)

Electron ionization is a hard source because the electron beam's energy results in easy fragmentation. In chemical ionization, we introduced a reagent molecule, such as methane, into the electron ionization (CI) source so that it is present at level that is $1000\times$ to $10,000\times$ greater than the analyte. At this higher concentration, it is the reagent molecule that is ionized; for example, when using CH_4 as the reagent gas, ions such as CH_4^+ and CH_3^+ form. These ions then react with additional methane molecules

$$CH_4^+(g) + CH_4(g) \rightarrow CH_5^+(g) + CH_3(g) \tag{7.5.2}$$

$$CH_3^+(g) + CH_4(g) \rightarrow C_2H_5^+(g) + H_2(g) \tag{7.5.3}$$

to form CH_5^+ and $C_2H_5^+$, species that are sufficiently reactive that they easily transfer a hydrogen to a molecule of the analyte, MH

$$CH_5^+(g) + MH(g) \rightarrow MH_2^+(g) + CH_4(g) \tag{7.5.4}$$

to give a molecular ion that we identify as $[M + H]^+$ and that has a mass that is one amu unit greater than that for M. Alternatively, they can easily remove a hydrogen from a molecule of the analyte, MH

$$C_2H_5^+(g) + MH(g) \rightarrow M^+(g) + C_2H_6(g) \tag{7.5.5}$$

to give a molecular ion that we identify as $[M - H]^-$ and that has a mass that is one amu less than that for M. Because formation of the molecular ion occurs indirectly and less energetically, fragmentation is suppressed, leading to a mass spectrum with a molecular ion peak and with only a small number of other ions. Figure 7.5.2 shows the mass spectrum for 1-decanol when using chemical ionization with CH_4 as the reagent gas.

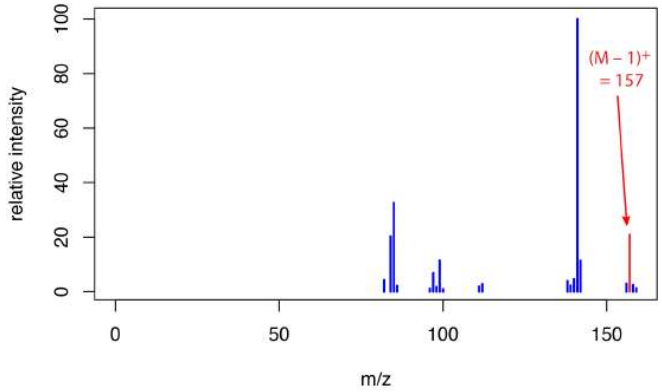


Figure 7.5.3: Mass spectrum for 1-decanol, $C_{10}H_{22}O$, using chemical ionization. The peak highlighted in red is the molecular ion, which has a m/z ratio of $158 - 1 = 157$ amu. The original data is available here.

Electrospray Ionization Sources (liquid phase/soft source)

Electron impact and chemical ionization are gas phase sources because the sample is volatilized before it enters the mass spectrometer's inlet. In electrospray ionization (ESI), the sample is a liquid and ions desorb from that matrix in the mass spectrometer's inlet system. The liquid sample is pulled into the spectrometer's inlet through a capillary needle, forming a mist of droplets. The application of a large potential across this inlet assures that the droplets carry positive charges. These charged droplets then enter a chamber where they undergo desolvation, which decreases the size of the droplet and increases their charge density (see Figure **7.5.4**). As this charge density increases, the droplets eventually become unstable, for reasons that are not fully understood, and ionized gas-phase ions desorb from the droplets and enter into the mass analyzer.

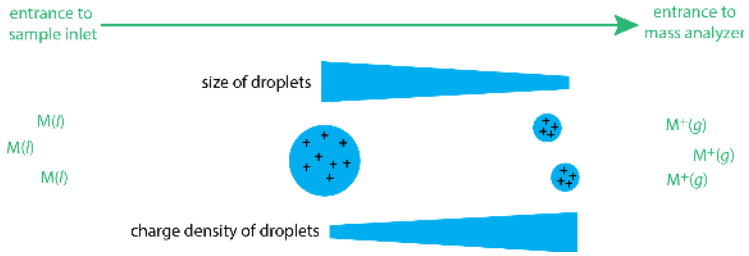


Figure **7.5.4**: Illustration showing the change in the size of droplets and the charge density of droplets during electrospray ionization.

A typical electrospray ionization mass spectrum for a small molecule is shown in Figure **7.5.5** for the compound (4-aminophenyl)arsonic acid. As we saw in Figure **7.5.3** for chemical ionization, a soft ionization source results in a limited amount of fragmentation and a strong peak for the molecular ion, which here includes a proton transfer to give the $[M + H]^+$ peak at a *m*/*z* of 218 amu.

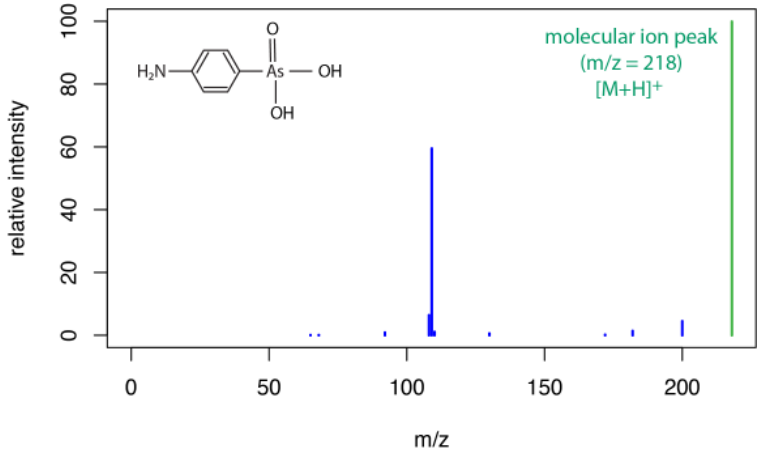


Figure **7.5.5**: Mass spectrum for (4-aminophenyl)arsonic acid obtained using electrospray ionization. The spectrum contains only two majors peak: the molecular ion at $m/z = 218$ amu and a fragment at $m/z = 109$ amu. The original data is available here.

Electrospray ionization is particularly useful for biological molecules, such as peptides and proteins, because the soft ionization ensures that molecular weight information is retained. Because these molecules are large, they readily pick up multiple protons, forming multiply charged ions of the general form $[M + zH]^{z+}$ where *z* is the number of protons added. Figure **7.5.6** shows a hypothetical spectrum for the molecule M and Table **7.5.1** provides the corresponding *m*/*z* values for the mass spectrum's peaks.

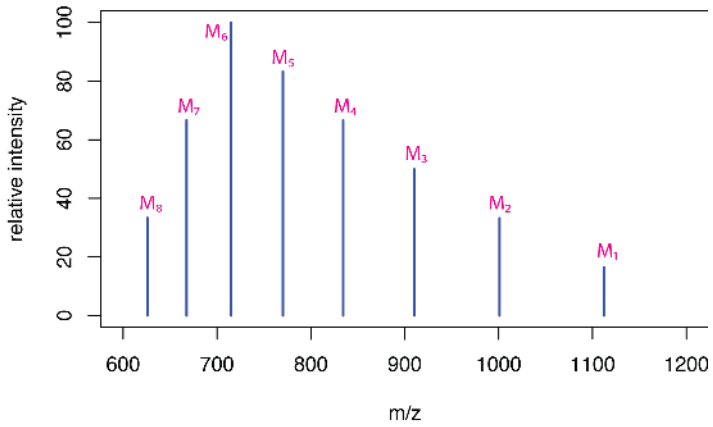


Figure **7.5.6**: Simulated electrospray ionization mass spectrum for a molecule, M, that shows eight peaks with mass-to-charge ratios between 600 amu and 1200 amu. The subscripts in the symbols M_i serve to identify the peaks; they are not an indication of charge.

Table **7.5.1**. Mass-to-charge ratios for the peaks in Figure **7.5.6**.

peak	*m*/*z*
M_1	1112
M_2	1001
M_3	910
M_4	834
M_5	770
M_6	715
M_7	667
M_8	626

If we take the mass-to-charge ratios for any two adjacent peaks, M_i and M_j, where the peak M_i has the greater value for *m*/*z*, and if we assume that M_j has one additional hydrogen atom, giving it a charge that is one unit higher, then

$$Z_i = \frac{M_j - 1}{M_i - M_j} \tag{7.5.6}$$

where Z_i is the charge on the ion M_i. Table **7.5.2** shows the calculated charges for the ions M_1 to M_7.

Note

Here is a derivation for Equation 7.5.6. Suppose the molecule of interest has a molecular weight of m. If the charge on the ion responsible for peak M_i is Z, then it must be the case that the peak's mass is equal to m + Z as it has Z extra hydrogens and it must be the case that its mass-to-charge ratio is

$$M_i = \frac{m + Z}{Z}$$

and its molecular weight, m, is

$$m = (M_i \times Z) - Z$$

In the same way, the peak M_j has a charge of $Z + 1$ and

$$M_j = \frac{m + Z + 1}{Z + 1}$$

$$m = (M_j \times Z) + M_j - Z - 1$$

Setting the two equations for m equal to each other and solving for Z gives

$$(M_i \times Z) - Z = (M_j \times Z) + M_j - Z - 1$$

$$(M_i \times Z) = (M_j \times Z) + M_j - 1$$

$$(M_i \times Z) - (M_j \times Z) = M_j - 1$$

$$Z = \frac{M_j - 1}{M_i - M_j}$$

Table 7.5.2. Calculated charges on the ions for peaks M_1 to M_7

peak	*m*/*z*	Z
M_1	1112	9
M_2	1001	10
M_3	910	11
M_4	834	12
M_5	770	13
M_6	715	14
M_7	667	15
M_8	626	—

The molecular weight, m, is given by the equation

$$m = (M_i \times Z) - Z \tag{7.5.7}$$

Table 7.5.3 shows the molecular weights for the ions M_1 to M_7 and their average value. The simulated mass spectrum was created by setting the molecular weight to 10,000 amu and with charges ranging from +9 to +16.

Table 7.5.3. Calculated molecular weights for the ions M_1 to M_7.

peak	*m*/*z*	Z	m
M_1	1112	9	9,999
M_2	1001	10	10,000
M_3	910	11	9,999
M_4	834	12	9,996
M_5	770	13	9,997
M_6	715	14	9,996
M_7	667	15	10,005
M_8	626	—	—
		average molecular weight	9,999

Matrix-Assisted Laser Desorption/Ionization Sources (solid phase/soft source)

Matrix-assisted laser desorption ionization (MALDI) is a soft ionization source for obtaining the mass spectrum for biologically important molecules, such as proteins and peptides. Figure 7.5.7 illustrates the basic steps in obtaining a MALDI spectrum. The sample is first mixed with a small molecule—which is called the matrix—to form a solution; the matrix usually is present in a 10:1

ratio. A drop of this mixture is placed on a sample probe and allowed to dry, leaving the sample in a solid form. A pulsed laser beam ($\lambda = 237$ nm is typical) is focused on the solid sample–matrix mixture. The matrix absorbs the laser pulse and the absorption of the laser's energy volatilizes both the matrix and the sample. Ionization of the sample forms molecular ions, usually $[M + H]^+$ ions, which are then swept into the mass analyzer.

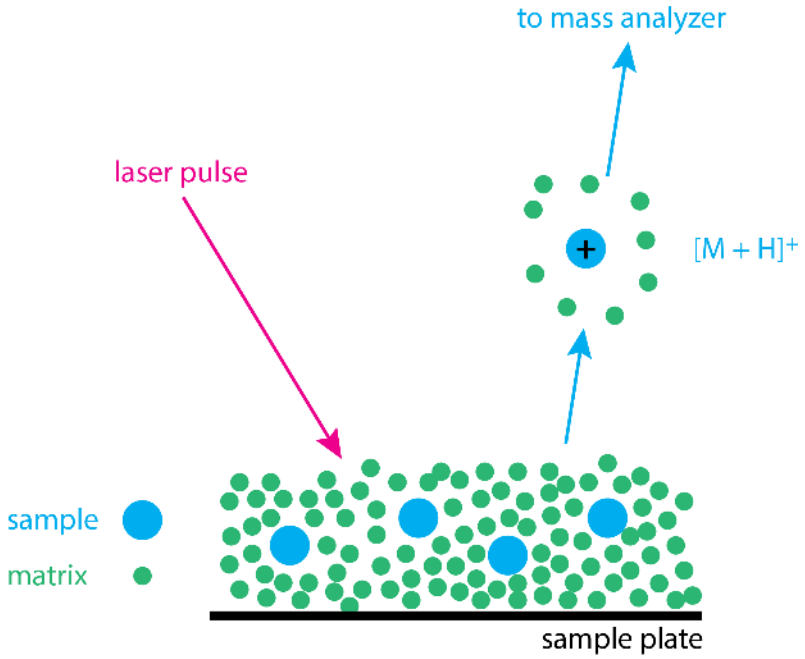


Figure 7.5.7: Illustration of matrix-assisted laser desorption ionization. The sample is dispersed in a liquid matrix and then allowed to dry. A pulsed laser beam is used to vaporize and ionize the sample.

When the sample is a digestion of a protein, then it is a mixture of peptides, each of which appeara as a $[M + H]^+$ peak in the resulting mass spectrum. For example, a peptide with the sequence AWSVAR (alanine–tryptophan–serine–valine–alanine–arginine) will appear as a peak with a mass of 689.8 daltons. To find this value we add together the molecular weights of the amino acids, account for the loss of a molecule of water for each peptide bond that forms, and then account for the hydrogen that gives the $[M + H]^+$ ion. In this case we have

$$[M + H]^+ = 89.1 + 204.2 + 105.1 + 117.1 + 89.1 + 174.2 - (5 \times 18.0) + 1 = 689.8 \text{ amu}$$

where the term 5×18.0 accounts for the loss of five molecules of H_2O when forming the five peptide bonds.

Fast Atom Bombardment Sources (liquid phase/soft source)

Fast atom bombardment (FAB) bears some similarity to MALDI: the sample is mixed with a liquid matrix (often glycerol) and bombarded with a beam of xenon or argon atoms (instead of a laser). Desorption of the sample from its matrix forms gas phase ions that are swept into the mass analyzer. Spectra usually contain both a molecular ion and fragmentation patterns.

This page titled 7.5: Ion Sources is shared under a CC BY-NC-SA 4.0 license and was authored, remixed, and/or curated by Kathryn Davis.

- **20.2: Ion Sources** by David Harvey is licensed CC BY-NC-SA 4.0.

7.6: Applications of Molecular Mass Spectrometry

Qualitative Applications

In a qualitative analysis our interest is in determining the identity of a substance of interest to us. By itself, mass spectrometry is a powerful tool for determining the identity of pure compounds. The analysis of mixtures, however, is possible if we use a mass spectrometer as the detector for a separation technique, such as gas chromatography, or if we string together two or more mass analyzers in sequence.

Identification of Pure Compounds

There are several ways to use a mass spectrum to identify a compound, including identifying its molecular weight, using isotopic ratios, examining fragmentation patterns, and by searching through data bases.

Using Molecular Weight Information. A molecular ion peak, $M^{+\bullet}$, when it is present, a $[M + H]^+$ peak or a $[M – H]^+$ peak, provides information about the compound's molecular weight. When using a low resolution mass analyzer, this may be sufficient to distinguish between molecular ions with, for example, a nominal mass of 95 amu and a nominal mass of 96 amu, but insufficient to distinguish between molecular ions with a more precise mass of 96.0399 amu and 96.0575 amu. When using a high resolution mass analyzer, the difference between the last pair of molecular ions may be feasible.

Using Isotopic Ratios. The molecule cycloheptene has the formula C_7H_{12} and a nominal mass of 96 amu, and the molecule cyclohexenone has the formula C_6H_8O and a nominal mass of 96 amu. Although both molecules will produce a molecular ion with the same nominal mass-to-charge ratio, each will also have a peak with a nominal mass of M + 1 due to the presence of isotopes of carbon, hydrogen, and oxygen. Because cycloheptene and cyclohexenone have different chemical formulas, the relative heights of their M + 1 peaks are different. Here is how we can work this out.

For every 100 atoms of ^{12}C there are 1.08 atoms of ^{13}C (that is, 1.08% of the carbon atoms are ^{13}C), for every 100 atoms of ^{1}H there are 0.015 atoms of ^{2}H, and for every 100 atoms of ^{16}O there are 0.04 atoms of ^{17}O. For cycloheptene, this means that the relative height of its M + 1 peak to its M peak is

$$(7 \times 1.08) + (12 \times 0.015) = 7.74$$

and for cyclohexenone we have

$$(6 \times 1.08) + (8 \times 0.015) + (1 \times 0.04) = 6.64$$

Here we see that a careful examination of the relative height of the M + 1 peak provides a way to distinguish between C_7H_{12} and C_6H_8O even though they have the same nominal masses. On-line calculators are available—this link provides one example—that you can use to calculate the full isotopic abundance patterns, including M + 2, M + 3, and other peaks. Isotopic patterns are particularly useful for identifying the presence of chlorine and bromine in a molecule because each has one isotope with a significant abundance: for chlorine, ^{37}Cl has an abundance of 32.5% relative to ^{35}Cl, and for bromine, ^{81}Br has an abundance of 98.0% of ^{79}Br.

Using Fragmentation Patterns. Figure **7.6.1** shows the mass spectrum of *p*-nitrophenol, which we first considered in Section 20.1. A molecule's mass spectrum is unique and contains information that we can use to deduce its structure. Interpretation of a mass spectrum relies on identifying possible sources for the loss of mass, such as the a Δm of 30 amu corresponding to the loss of NO, or a Δm of 46 amu corresponding to the loss of NO_2. Some mass-to-charge ratios are recognized as evidence for a particular ion, such as $C_5H_5^+$ at a mass-to-charge ratio of 65. The interpretation of fragmentation patterns is covered elsewhere in the curriculum, particularly in organic chemistry, and is not given more consideration here.

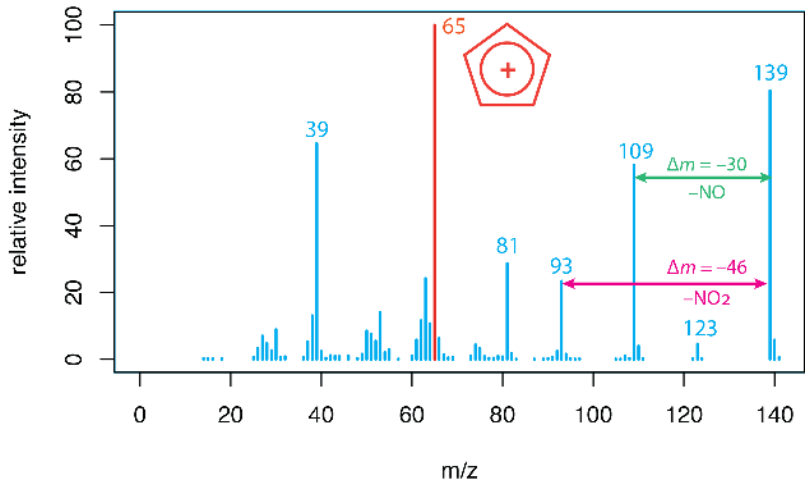


Figure **7.6.1**: Mass spectrum of *p*-nitrophenol.

Using Computer Searching. Large databases of mass spectra are available (see here for a source from NIST). A peak table of mass-to-charge ratios and peak intensities for a sample is entered into an algorithm that searches the database and identifies the most likely matches.

Analysis of Mixtures Using MS as a Detector for a GC or LC Separation

Mass spectrometry is a powerful analytical technique when the sample we are analyzing is pure (or if impurities are of sufficiently low concentration that they have little effect on the mass spectrum). For a mixture of two or more analytes, the interpretation of the mass spectrum is difficult, if not impossible. To analyze such a mixture, we need a means of separating the analytes from each other. One approach is to interface a mass spectrometer to a gas chromatograph or a liquid chromatograph. The GC, or LC separates the mixture into its component parts with the mass spectrometer serving as the detector. See Chapter 27 and Chapter 28 for further details about GC-MS and LC-MS.

Analysis of Mixtures Using Tandem Mass Spectrometry

Another approach to working with a complex sample is to use two or more mass analyzers in what is called tandem mass spectrometry. For example, if we place three quadrupole mass analyzers in a sequence, we can use a soft ionization source to generate mostly molecular ions of the form $[M + H]^+$ for each of the sample's analytes, and then let the first quadrupole separate these molecular ions by the differences in their mass-to-charge ratio. The $[M + H]^+$ molecular ions for one of the analytes is then selectively passed into the second quadrupole where it is allowed to undergo fragmentation by collision with a gas, such as He. Finally, these fragment ions are passed along to the third quadrupole where the mass spectrum is obtained. By sequentially passing each of the molecular ions from the first quadrupole through the second and third quadrupoles, we are able to obtain mass spectra for each molecule in the mixture.

Quantitative Applications

As a detector for other instrumental methods, such as gas chromatography and liquid chromatography, mass spectrometry provides for a quantitative analysis by monitoring either the total ion count or by monitoring ions of a single mass-to-charge ratio, which is known as selective ion monitoring. As an Independent method for determining an analyte's concentration, mass spectrometry is less attractive due to the difficulty of controlling the amount of sample or standard introduced into the instrument and the affect of the sample's matrix on fragmentation. The use of an internal standard improves precision and accuracy.

This page titled 7.6: Applications of Molecular Mass Spectrometry is shared under a CC BY-NC-SA 4.0 license and was authored, remixed, and/or curated by Kathryn Davis.

- **20.4: Applications of Molecular Mass Spectrometry** by David Harvey is licensed CC BY-NC-SA 4.0.

CHAPTER OVERVIEW

8: Analysis and Separation of Mixtures

8.1: UV/Vis Analysis of Two-Component Mixtures
8.2: Classifying Separation Techniques
8.3: Liquid-Liquid Extractions
8.4: Overview of Analytical Separations
8.5: General Theory of Column Chromatography
8.6: Optimizing Chromatographic Separations
8.7: Gas Chromatography
8.8: High-Performance Liquid Chromatography
8.9: Other Forms of Chromatography
8.10: Electrophoresis

This page titled 8: Analysis and Separation of Mixtures is shared under a not declared license and was authored, remixed, and/or curated by Kathryn Davis.

8.1: UV/Vis Analysis of Two-Component Mixtures

In Figure 10.1.9 we examined Nessler's original method for matching the color of a sample to the color of a standard. Matching colors is a labor intensive process for the analyst and, not surprisingly, spectroscopic methods of analysis were slow to find favor. The 1930s and 1940s saw the introduction of photoelectric transducers for ultraviolet and visible radiation, and thermocouples for infrared radiation. As a result, modern instrumentation for absorption spectroscopy routinely became available in the 1940s—further progress has been rapid ever since.

Quantitative Analysis of Mixtures

Suppose we need to determine the concentration of two analytes, *X* and *Y*, in a sample. If each analyte has a wavelength where the other analyte does not absorb, then we can proceed using the approach in Example 8.1.5 . Unfortunately, UV/Vis absorption bands are so broad that frequently it is not possible to find suitable wavelengths. Because Beer's law is additive the mixture's absorbance, A_{mix}, is

$$(A_{mix})_{\lambda_1} = (\varepsilon_x)_{\lambda_1} bC_X + (\varepsilon_Y)_{\lambda_1} bC_Y \tag{8.1.1}$$

where λ_1 is the wavelength at which we measure the absorbance. Because Equation 8.1.1 includes terms for the concentration of both *X* and *Y*, the absorbance at one wavelength does not provide enough information to determine either C_X or C_Y. If we measure the absorbance at a second wavelength

$$(A_{mix})_{\lambda_2} = (\varepsilon_x)_{\lambda_2} bC_X + (\varepsilon_Y)_{\lambda_2} bC_Y \tag{8.1.2}$$

then we can determine C_X and C_Y by solving simultaneously Equation 8.1.1 and Equation 8.1.2. Of course, we also must determine the value for ε_X and ε_Y at each wavelength. For a mixture of *n* components, we must measure the absorbance at *n* different wavelengths.

Example 8.1.2

The concentrations of Fe^{3+} and Cu^{2+} in a mixture are determined following their reaction with hexacyanoruthenate (II), $Ru(CN)_6^{4-}$, which forms a purple-blue complex with Fe^{3+} (λ_{max} = 550 nm) and a pale-green complex with Cu^{2+} (λ_{max} = 396 nm) [DiTusa, M. R.; Schlit, A. A. *J. Chem. Educ.* **1985**, *62*, 541–542]. The molar absorptivities (M^{-1} cm^{-1}) for the metal complexes at the two wavelengths are summarized in the following table.

analyte	ε_{550}	ε_{396}
Fe^{3+}	9970	84
Cu^{2+}	34	856

When a sample that contains Fe^{3+} and Cu^{2+} is analyzed in a cell with a pathlength of 1.00 cm, the absorbance at 550 nm is 0.183 and the absorbance at 396 nm is 0.109. What are the molar concentrations of Fe^{3+} and Cu^{2+} in the sample?

Solution

Substituting known values into Equation 8.1.1 and Equation 8.1.2 gives

$$A_{550} = 0.183 = 9970C_{Fe} + 34C_{Cu}$$
$$A_{396} = 0.109 = 84C_{Fe} + 856C_{Cu}$$

To determine C_{Fe} and C_{Cu} we solve the first equation for C_{Cu}

$$C_{Cu} = \frac{0.183 - 9970C_{Fe}}{34}$$

and substitute the result into the second equation.

$$0.109 = 84C_{Fe} + 856 \times \frac{0.183 - 9970C_{Fe}}{34}$$
$$= 4.607 - \left(2.51 \times 10^5\right) C_{Fe}$$

Solving for C_{Fe} gives the concentration of Fe^{3+} as 1.8×10^{-5} M. Substituting this concentration back into the equation for the mixture's absorbance at 396 nm gives the concentration of Cu^{2+} as 1.3×10^{-4} M.

Another approach to solving Example 8.1.2 is to multiply the first equation by 856/34 giving

$$4.607 = 251009C_{Fe} + 856C_{Cu}$$

Subtracting the second equation from this equation

$$4.607 = 251009C_{Fe} + 856C_{Cu}$$
$$-0.109 = 84C_{Fe} + 856C_{Cu}$$

gives

$$4.498 = 250925C_{Fe}$$

and we find that C_{Fe} is 1.8×10^{-5}. Having determined C_{Fe} we can substitute back into one of the other equations to solve for C_{Cu}, which is 1.3×10^{-5}.

? Exercise 8.1.2

The absorbance spectra for Cr^{3+} and Co^{2+} overlap significantly. To determine the concentration of these analytes in a mixture, its absorbance is measured at 400 nm and at 505 nm, yielding values of 0.336 and 0.187, respectively. The individual molar absorptivities (M^{-1} cm^{-1}) for $Cr3^{+}$ are 15.2 at 400 nm and 0.533 at 505 nm; the values for Co^{2+} are 5.60 at 400 nm and 5.07 at 505 nm.

Answer

Substituting into Equation 8.1.1 and Equation 8.1.2 gives

$$A_{400} = 0.336 = 15.2C_{Cr} + 5.60C_{Co}$$

$$A_{400} = 0187 = 0.533C_{Cr} + 5.07C_{Co}$$

To determine C_{Cr} and C_{Co} we solve the first equation for C_{Co}

$$C_{Co} = \frac{0.336 - 15.2C_{Co}}{5.60}$$

and substitute the result into the second equation.

$$0.187 = 0.533C_{Cr} + 5.07 \times \frac{0.336 - 15.2C_{Co}}{5.60}$$

$$0.187 = 0.3042 - 13.23C_{Cr}$$

Solving for C_{Cr} gives the concentration of Cr^{3+} as 8.86×10^{-3} M. Substituting this concentration back into the equation for the mixture's absorbance at 400 nm gives the concentration of Co^{2+} as 3.60×10^{-2} M.

To obtain results with good accuracy and precision the two wavelengths should be selected so that $\varepsilon_X > \varepsilon_Y$ at one wavelength and $\varepsilon_X < \varepsilon_Y$ at the other wavelength. It is easy to appreciate why this is true. Because the absorbance at each wavelength is dominated by one analyte, any uncertainty in the concentration of the other analyte has less of an impact. Figure 8.1.11 shows that the choice of wavelengths for Practice Exercise 8.1.2 are reasonable. When the choice of wavelengths is not obvious, one method for locating the optimum wavelengths is to plot $\varepsilon_X/\varepsilon_y$ as function of wavelength, and determine the wavelengths where $\varepsilon_X/\varepsilon_y$ reaches maximum and minimum values [Mehra, M. C.; Rioux, J. *J. Chem. Educ.* **1982**, *59*, 688–689].

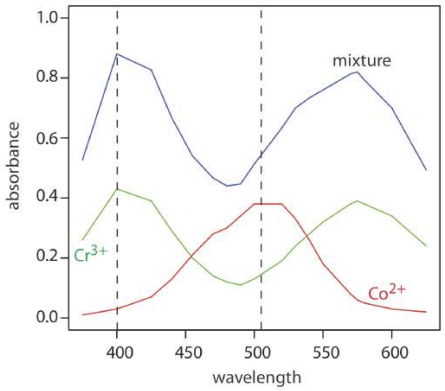


Figure 8.1.11 . Visible absorption spectra for 0.0250 M Cr^{3+}, 0.0750 M Co^{2+}, and for a mixture of Cr^{3+} and Co^{2+}. The two wavelengths used to analyze the mixture of Cr^{3+} and Co^{2+} are shown by the dashed lines. The data for the two standards are from Brewer, S. *Solving Problems in Analytical Chemistry*, John Wiley & Sons: New York, 1980.

When the analyte's spectra overlap severely, such that $\varepsilon_X \approx \varepsilon_Y$ at all wavelengths, other computational methods may provide better accuracy and precision. In a multiwavelength linear regression analysis, for example, a mixture's absorbance is compared to that for a set of standard solutions at several wavelengths [Blanco, M.; Iturriaga, H.; Maspoch, S.; Tarin, P. *J. Chem. Educ.* **1989**, *66*, 178–180]. If A_{SX} and A_{SY} are the absorbance values for standard solutions of components *X* and *Y* at any wavelength, then

$$A_{SX} = \varepsilon_X b C_{SX} \tag{8.1.3}$$

$$A_{SY} = \varepsilon_Y b C_{SY} \tag{8.1.4}$$

where C_{SX} and C_{SY} are the known concentrations of *X* and *Y* in the standard solutions. Solving Equation 8.1.3 and Equation 8.1.4 for ε_X and for ε_Y, substituting into Equation 8.1.1, and rearranging, gives

$$\frac{A_{mix}}{A_{SX}} = \frac{C_X}{C_{SX}} + \frac{C_Y}{C_{SY}} \times \frac{A_{SY}}{A_{SX}}$$

To determine C_X and C_Y the mixture's absorbance and the absorbances of the standard solutions are measured at several wavelengths. Graphing A_{mix}/A_{SX} versus A_{SY}/A_{SX} gives a straight line with a slope of C_Y/C_{SY} and a *y*-intercept of C_X/C_{SX}. This approach is particularly helpful when it is not possible to find wavelengths where $\varepsilon_X > \varepsilon_Y$ and $\varepsilon_X < \varepsilon_Y$.

The approach outlined here for a multiwavelength linear regression uses a single standard solution for each analyte. A more rigorous approach uses multiple standards for each analyte. The math behind the analysis of such data—which we call a multiple linear regression—is beyond the level of this text. For more details about multiple linear regression see Brereton, R. G. *Chemometrics: Data Analysis for the Laboratory and Chemical Plant*, Wiley: Chichester, England, 2003.

Example 8.1.3

Figure ***PageIndex*10.11** shows visible absorbance spectra for a standard solution of 0.0250 M Cr^{3+}, a standard solution of 0.0750 M Co^{2+}, and a mixture that contains unknown concentrations of each ion. The data for these spectra are shown here.

λ (nm)	A_{Cr}	A_{Cu}	A_{mix}	λ (nm)	A_{Cr}	A_{Cu}	A_{mix}
375	0.26	0.01	0.53	520	0.19	0.38	0.63
400	0.43	0.03	0.88	530	0.24	0.33	0.70
425	0.39	0.07	0.83	540	0.28	0.26	0.73
440	0.29	0.13	0.67	550	0.32	0.18	0.76
455	0.20	0.21	0.54	570	0.38	0.08	0.81
470	0.14	0.28	0.47	575	0.39	0.06	0.82
480	0.12	0.30	0.44	580	0.38	0.05	0.79
490	0.11	0.34	0.45	600	0.34	0.03	0.70
500	0.13	0.38	0.51	625	0.24	0.02	0.49

Use a multiwavelength regression analysis to determine the composition of the unknown.

Solution

First we need to calculate values for A_{mix}/A_{SX} and for A_{SY}/A_{SX}. Let's define X as Co^{2+} and Y as Cr^{3+}. For example, at a wavelength of 375 nm A_{mix}/A_{SX} is 0.53/0.01, or 53 and A_{SY}/A_{SX} is 0.26/0.01, or 26. Completing the calculation for all wavelengths and graphing A_{mix}/A_{SX} versus A_{SY}/A_{SX} gives the calibration curve shown in Figure 8.1.12 . Fitting a straight-line to the data gives a regression model of

$$\frac{A_{mix}}{A_{SX}} = 0.636 + 2.01 \times \frac{A_{SY}}{A_{SX}}$$

Using the *y*-intercept, the concentration of Co^{2+} is

$$\frac{C_X}{C_{SX}} = \frac{[Co^{2+}]}{0.0750 M} = 0.636$$

or $[Co^{2+}]$ = 0.048 M; using the slope the concentration of Cr^{3+} is

$$\frac{C_Y}{C_{SY}} = \frac{[Cr^{3+}]}{0.0250 M} = 2.01$$

or $[Cr^{3+}]$ = 0.050 M.

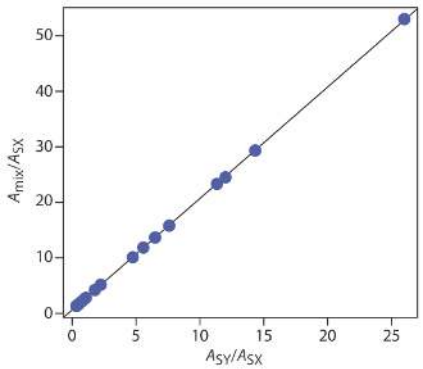


Figure 8.1.12 . Multiwavelength linear regression analysis for the data in Example 8.1.3 .

Exercise 8.1.3

A mixture of MnO_4^- and $Cr_2O_7^{2-}$, and standards of 0.10 mM $KMnO_4$ and of 0.10 mM $K_2Cr_2O_7$ give the results shown in the following table. Determine the composition of the mixture. The data for this problem is from Blanco, M. C.; Iturriaga, H.; Maspoch, S.; Tarin, P. *J. Chem. Educ.* **1989**, *66*, 178–180.

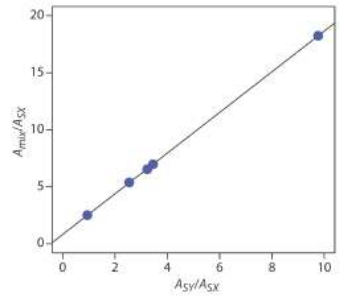
λ (nm)	A_{Mn}	A_{Cr}	A_{mix}
266	0.042	0.410	0.766
288	0.082	0.283	0.571
320	0.168	0.158	0.422
350	0.125	0.318	0.672
360	0.036	0.181	0.366

Answer

Letting *X* represent MnO_4^- and letting *Y* represent $Cr_2O_7^{2-}$, we plot the equation

$$\frac{A_{mix}}{A_{SX}} = \frac{C_X}{C_{SX}} + \frac{C_Y}{C_{SY}} \times \frac{A_{SY}}{A_{SX}}$$

placing A_{mix}/A_{SX} on the *y*-axis and A_{SY}/A_{SX} on the *x*-axis. For example, at a wavelength of 266 nm the value A_{mix}/A_{SX} of is 0.766/0.042, or 18.2, and the value of A_{SY}/A_{SX} is 0.410/0.042, or 9.76. Completing the calculations for all wavelengths and plotting the data gives the result shown here



Fitting a straight-line to the data gives a regression model of

$$\frac{A_{mix}}{A_{SX}} = 0.8147 + 1.7839 \times \frac{A_{SY}}{A_{SX}}$$

Using the *y*-intercept, the concentration of MnO_4^- is

$$\frac{C_X}{C_{SX}} = 0.8147 = \frac{[MnO_4^-]}{1.0 \times 10^{-4}\ \text{M}\ MnO_4^-}$$

or 8.15×10^{-5} M MnO_4^-, and using the slope, the concentration of $Cr_2O_7^{2-}$ is

$$\frac{C_Y}{C_{SY}} = 1.7839 = \frac{[Cr_2O_7^{2-}]}{1.00 \times 10^{-4}\ \text{M}\ Cr_2O_7^{2-}}$$

or 1.78×10^{-4} M $Cr_2O_7^{2-}$.

This page titled 8.1: UV/Vis Analysis of Two-Component Mixtures is shared under a CC BY-NC-SA 4.0 license and was authored, remixed, and/or curated by Kathryn Davis.

- **10.3: UV/Vis and IR Spectroscopy** by David Harvey is licensed CC BY-NC-SA 4.0.

8.2: Classifying Separation Techniques

We can separate an analyte and an interferent if there is a significant difference in at least one of their chemical or physical properties. Table 7.6.1 provides a partial list of separation techniques, organized by the chemical or physical property affecting the separation.

Table 7.6.1 . Classification of Separation Techniques

basis of separation	separation technique(s)
size	filtration; dialysis; size-exclusion chromatography
mass or density	centrifugation
complex formation	masking
change in physical state	distillation; sublimation; recrystalization
change in chemical state	precipitation; electrodeposition; volatilization
partitioning between phases	extraction; chromatography

Separations Based on Size

Size is the simplest physical property we can exploit in a separation. To accomplish the separation we use a porous medium through which only the analyte or the interferent can pass. Examples of size-based separations include filtration, dialysis, and size-exclusion.

In a ***filtration*** we separate a particulate interferent from soluble analytes using a filter with a pore size that will retain the interferent. The solution that passes through the filter is called the ***filtrate***, and the material retained by the filter is the ***retentate***. Gravity filtration and suction filtration using filter paper are techniques with which you should already be familiar. A membrane filter is the method of choice for particulates that are too small to be retained by filter paper. Figure 7.6.1 provides information about three types of membrane filters. For applications of gravity filtration and suction filtration in gravimetric methods of analysis, see Chapter 8.

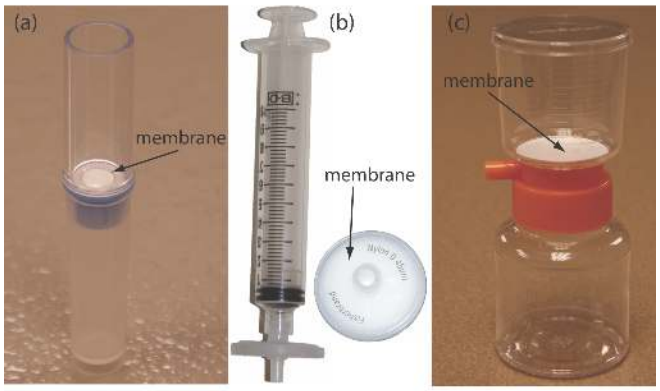


Figure 7.6.1 . Examples of three types of membrane filters for separating analytes and interferents. (a) A centrifugal filter for concentrating and desalting macromolecular solutions. The membrane has a nominal molecular weight cut-off of 1×10^6 g/mol. The sample is placed in the upper reservoir and the unit is placed in a centrifuge. Upon spinning the unit at $2000 \times g - 5000 \times g$, the filtrate collects in the bottom reservoir and the retentate remains in the upper reservoir. (b) A 0.45 µm membrane syringe filter. The photo on the right shows the membrane filter in its casing. In the photo on the left, the filter is attached to a syringe. Samples are placed in the syringe and pushed through the filter. The filtrate is collected in a test tube or other suitable container. (c) A disposable filter system with a 0.22 µm cellulose acetate membrane filter. The sample is added to the upper unit and vacuum suction is used to draw the filtrate through the membrane and into the lower unit. To store the filtrate, the top half of the unit is removed and a cap placed on the lower unit. The filter unit shown here has a capacity of 150 mL.

Dialysis is another example of a separation technique in which size is used to separate the analyte and the interferent. A dialysis membrane usually is made using cellulose and fashioned into tubing, bags, or cassettes. Figure 7.6.2 shows an example of a

commercially available dialysis cassette. The sample is injected into the dialysis membrane, which is sealed tightly by a gasket, and the unit is placed in a container filled with a solution with a composition different from the sample. If there is a difference in a species' concentration on the membrane's two sides, the resulting concentration gradient provides a driving force for its diffusion across the membrane. While small species freely pass through the membrane, larger species are unable to pass. Dialysis frequently is used to purify proteins, hormones, and enzymes. During kidney dialysis, metabolic waste products, such as urea, uric acid, and creatinine, are removed from blood by passing it over a dialysis membrane.



Figure 7.6.2 . Example of a dialysis cassette. The dialysis membrane in this unit has a molecular weight cut-off of 10000 g/mol. Two sheets of the membrane are separated by a gasket and held in place by the plastic frame. Four ports, one of which is labeled, provide a means for injecting the sample between the dialysis membranes. The cassette is inverted and submerged in a beaker that contains the external solution. A foam buoy, used as a stand in the photo, serves as a float so that the unit remains suspended in the external solution. The external solution is stirred using a stir bar, and usually replaced several time during dialysis. When dialysis is complete, the solution in the cassette is removed through an injection port.

Size-exclusion chromatography is a third example of a separation technique that uses size as a means to effect a separation. In this technique a column is packed with small, approximately 10-µm, porous polymer beads of cross-linked dextrin or polyacrylamide. The pore size of the particles is controlled by the degree of cross-linking, with more cross-linking producing smaller pore sizes. The sample is placed into a stream of solvent that is pumped through the column at a fixed flow rate. Those species too large to enter the pores pass through the column at the same rate as the solvent. Species that enter into the pores take longer to pass through the column, with smaller species requiring more time to pass through the column. Size-exclusion chromatography is widely used in the analysis of polymers, and in biochemistry, where it is used for the separation of proteins. A more detailed treatment of size-exclusion chromatography, which also is called gel permeation chromatography, is in Chapter 12.

Separations Based on Mass or Density

If the analyte and the interferent have different masses or densities, then a separation using ***centrifugation*** may be possible. The sample is placed in a centrifuge tube and spun at a high angular velocity, measured in revolutions per minute (rpm). The sample's constituents experience a centrifugal force that pulls them toward the bottom of the centrifuge tube. Those species that experience the greatest centrifugal force have the fastest sedimentation rate and are the first to reach the bottom of the centrifuge tube. If two species have the same density, their separation is based on a difference in mass, with the heavier species having the greater sedimentation rate. If the species are of equal mass, then the species with the larger density has the greatest sedimentation rate.

Centrifugation is an important separation technique in biochemistry. Table 7.6.2 , for example, lists conditions for separating selected cellular components. We can separate lysosomes from other cellular components by several differential centrifugations, in which we divide the sample into a solid residue and a supernatant solution. After destroying the cells, the solution is centrifuged for 20 minutes at $15000 \times g$ (a centrifugal force that is 15 000 times the earth's gravitational force), leaving a solid residue of cell membranes and mitochondria. The supernatant, which contains the lysosomes, is isolated by decanting it from the residue and then centrifuged for 30 minutes at $30000 \times g$, leaving a solid residue of lysosomes. Figure 7.6.3 shows a typical centrifuge capable of producing the centrifugal forces needed for biochemical separations.

Table 7.6.2 . Conditions for Separating Selected Cellular Components by Centrifugation

components	centrifugal force ($\times g$)	time (min)
eukaryotic cells	1000	5
cell membranes; nuclei	4000	10
mitochondria, bacterial cells	15000	20
lysosomes; bacterial membranes	30000	30
ribosomes	100000	180

Source: Adapted from Zubay, G. *Biochemistry*, 2nd ed. Macmillan: New York, 1988, p.120.



Figure 7.6.3 . Bench-top centrifuge capable of reaching speeds up to 14000 rpm and centrifugal forces of $20800 \times g$. This particular centrifuge is refrigerated, allowing samples to be cooled to temperatures as low as –4°C.

An alternative approach to differential centrifugation is a density gradient centrifugation. To prepare a sucrose density gradient, for example, a solution with a smaller concentration of sucrose—and, thus, of lower density—is gently layered upon a solution with a higher concentration of sucrose. Repeating this process several times, fills the centrifuge tube with a multi-layer density gradient. The sample is placed on top of the density gradient and centrifuged using a force greater than $150000 \times g$. During centrifugation, each of the sample's components moves through the gradient until it reaches a position where its density matches the surrounding sucrose solution. Each component is isolated as a separate band positioned where its density is equal to that of the local density within the gradient. Figure 7.6.4 provides an example of a typical sucrose density centrifugation for separating plant thylakoid membranes.

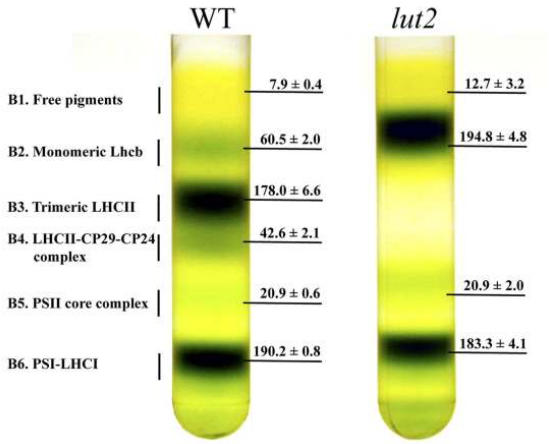


Figure 7.6.4 . Example of a sucrose density gradient centrifugation of thylakoid membranes from wild type (WT) and *lut2* plants. The thylakoid membranes were extracted from the plant's leaves and separated by centrifuging in a 0.1–1 M sucrose gradient for 22 h at $280000 \times g$ and at 4°C. Six bands and their chlorophyll contents are shown. Adapted from Dall'Osto, L.; Lico, C.; Alric, J.; Giuliano, G.; Havaux, M.; Bassi, R. *BMC Plant Biology* **2006**, *6:32*.

Separations Based on Complexation Reactions (Masking)

One widely used technique for preventing an interference is to bind the interferent in a strong, soluble complex that prevents it from interfering in the analyte's determination. This process is known as ***masking***. As shown in Table 7.6.3 , a wide variety of ions and molecules are useful ***masking agents***, and, as a result, selectivity is usually not a problem.

> Technically, masking is not a separation technique because we do not physically separate the analyte and the interferent. We do, however, chemically isolate the interferent from the analyte, resulting in a pseudo-separation.

Table 7.6.3 . Selected Inorganic and Organic Masking Agents for Metal Ions

masking agent	elements whose ions are masked
CN^-	Ag, Au, Cd, Co, Cu, Fe, Hg, Mn, Ni, Pd, Pt, Zn
SCN^-	Ag, Cd, Co, Cu, Fe, Ni, Pd, Pt, Zn
NH_3	Ag, Co, Ni, Cu, Zn
F^-	Al, Co, Cr, Mg, Mn, Sn, Zn
$S_2O_3^{2-}$	Au, Ce, Co, Cu, Fe, Hg, Mn, Pb, Pd, Pt, Sb, Sn, Zn
tartrate	Al, Ba, Bi, Ca, Ce, Co, Cr, Cu, Fe, Hg, Mn, Pb, Pd, Pt, Sb, Sn, Zn
oxalate	Al, Fe, Mg, Mn
thioglycolic acid	Cu, Fe, Sn

Source: Meites, L. *Handbook of Analytical Chemistry*, McGraw-Hill: New York, 1963.

✔ Example 7.6.1

Using Table 7.6.3 , suggest a masking agent for the analysis of aluminum in the presence of iron.

Solution

A suitable masking agent must form a complex with the interferent, but not with the analyte. Oxalate, for example, is not a suitable masking agent because it binds both Al and Fe. Thioglycolic acid, on the other hand, is a selective masking agent for Fe in the presence of Al. Other acceptable masking agents are cyanide (CN^-) thiocyanate (SCN^-), and thiosulfate ($S_2O_3^{2-}$).

Exercise 7.6.1

Using Table 7.6, suggest a masking agent for the analysis of Fe in the presence of Al.

Answer

The fluoride ion, F^-, is a suitable masking agent as it binds with Al^{3+} to form the stable $\mathbf{AlF_6^{3-}}$ complex, leaving iron in solution.

As shown in Example 7.6.2 , we can judge a masking agent's effectiveness by considering the relevant equilibrium constants.

Example 7.6.2

Show that CN^- is an appropriate masking agent for Ni^{2+} in a method where nickel's complexation with EDTA is an interference.

Solution

The relevant reactions and formation constants are

$$\mathbf{Ni^{2+}}(aq) + \mathbf{Y^{4-}}(aq) \rightleftharpoons \mathbf{NiY^{2-}}(aq) \quad K_1 = 4.2 \times 10^{18}$$

$$\mathbf{Ni^{2+}}(aq) + 4\mathbf{CN^-}(aq) \rightleftharpoons \mathbf{Ni(CN)_4^{2-}}(aq) \quad \beta_4 = 1.7 \times 10^{30}$$

where Y^{4-} is an abbreviation for EDTA. Cyanide is an appropriate masking agent because the formation constant for $\mathbf{Ni(CN)_4^{2-}}$ is greater than that for the Ni–EDTA complex. In fact, the equilibrium constant for the reaction in which EDTA displaces the masking agent

$$\mathbf{Ni(CN)_4^{2-}}(aq) + \mathbf{Y^{4-}}(aq) \rightleftharpoons \mathbf{NiY^{2-}}(aq) + 4\mathbf{CN^-}(aq)$$

$$K = \frac{K_1}{\beta_4} = \frac{4.2 \times 10^{18}}{1.7 \times 10^{30}} = 2.5 \times 10^{-12}$$

is sufficiently small that $\mathbf{Ni(CN)_4^{2-}}$ is relatively inert in the presence of EDTA.

Exercise 7.6.2

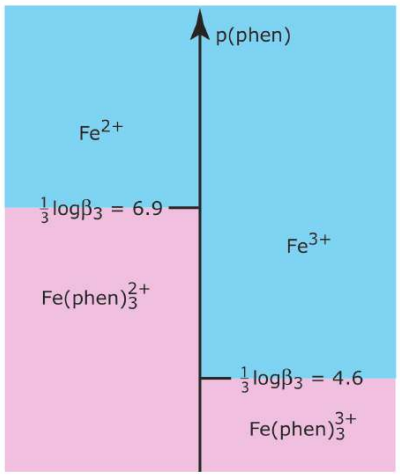
Use the formation constants in Appendix 12 to show that 1,10-phenanthroline is a suitable masking agent for Fe^{2+} in the presence of Fe^{3+}. Use a ladder diagram to define any limitations on using 1,10-phenanthroline as a masking agent. See Chapter 6 for a review of ladder diagrams.

Answer

The relevant reactions and equilibrium constants are

$$\mathbf{Fe^{2+}}(aq) + 3\mathbf{phen}(aq) \rightleftharpoons \mathbf{Fe(phen)_3^{2+}}(aq) \quad \beta_3 = 5 \times 10^{20}$$
$$\mathbf{Fe^{3+}}(aq) + 3\mathbf{phen}(aq) \rightleftharpoons \mathbf{Fe(phen)_3^{3+}}(aq) \quad \beta_3 = 6 \times 10^{13}$$

where phen is an abbreviation for 1,10-phenanthroline. Because β_3 is larger for the complex with Fe^{2+} than it is for the complex with Fe^{3+},1,10-phenanthroline will bind Fe^{2+} before it binds Fe^{3+}. A ladder diagram for this system (as shown below) suggests that an equilibrium p(phen) between 5.6 and 5.9 will fully complex Fe^{2+} without any significant formation of the $\mathbf{Fe(phen)_3^{3+}}$ complex. Adding a stoichiometrically equivalent amount of 1,10-phenanthroline to a solution of Fe^{2+} is sufficient to mask Fe^{2+} in the presence of Fe^{3+}. A large excess of 1,10-phenanthroline, however, decreases p(phen) and allows for the formation of both metal–ligand complexes.



Separations Based on a Change of State

Because an analyte and its interferent are usually in the same phase, we can achieve a separation if one of them undergoes a change in its physical state or its chemical state.

Changes in Physical State

When the analyte and the interferent are miscible liquids, separation by ***distillation*** is possible if their boiling points are significantly different. Figure 7.6.5 shows the progress of a distillation as a plot of temperature versus the composition of mixture's vapor-phase and liquid-phase. The initial liquid mixture (point A), contains more interferent than analyte. When this solution is brought to its boiling point, the vapor phase in equilibrium with the liquid phase is enriched in analyte (point B). The horizontal line that connects points A and B represents this vaporization equilibrium. Condensing the vapor phase at point B, by lowering the temperature, creates a new liquid phase with a composition identical to that in the vapor phase (point C). The vertical line that connects points B and C represents this condensation equilibrium. The liquid phase at point C has a lower boiling point than the original mixture, and is in equilibrium with the vapor phase at point D. This process of repeated vaporization and condensation gradually separates the analyte and the interferent.

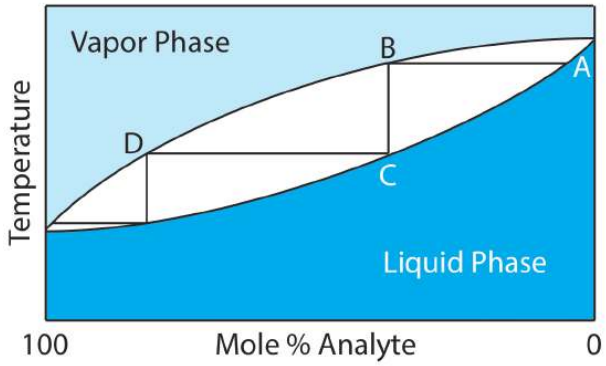


Figure 7.6.5 . Boiling point versus composition diagram for a near-ideal solution consisting of a low-boiling analyte and a high-boiling interferent. The horizontal lines represent vaporization equilibria and the vertical lines represent condensation equilibria. See the text for additional details.

Two experimental set-ups for distillations are shown in Figure 7.6.6 . The simple distillation apparatus shown in Figure 7.6.6 a is useful only for separating a volatile analyte (or interferent) from a non-volatile interferent (or analyte), or for separating an analyte and an interferent whose boiling points differ by more than 150ºC. A more efficient separation is achieved using the fractional distillation apparatus in Figure 7.6.6 b. Packing the fractionating column with a high surface area material, such as a steel sponge or glass beads, provides more opportunity for the repeated process of vaporization and condensation necessary to effect a complete separation.

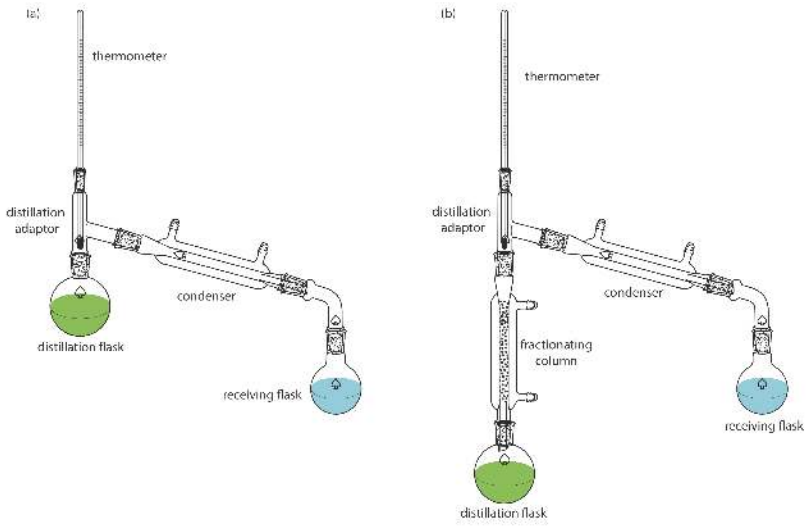


Figure 7.6.6 . Typical experimental set-up for (a) a simple distillation, and (b) a fractional distillation.

When the sample is a solid, ***sublimation*** may provide a useful separation of the analyte and the interferent. The sample is heated at a temperature and pressure below the analyte's triple point, allowing it to vaporize without passing through a liquid state. Condensing the vapor recovers the purified analyte (Figure 7.6.7). A useful analytical example of sublimation is the isolation of amino acids from fossil mollusk shells and deep-sea sediments [Glavin, D. P.; Bada, J. L. *Anal. Chem.* **1998**, *70*, 3119–3122].

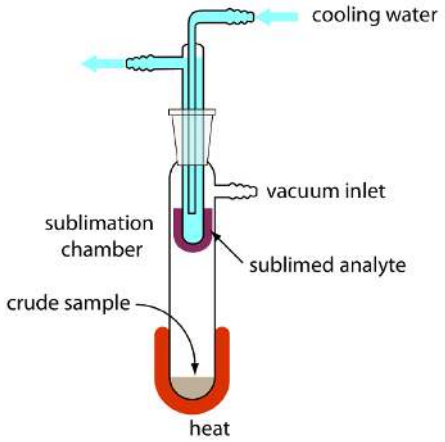


Figure 7.6.7 . Typical experimental set-up for a sublimation. The sample is placed in the sublimation chamber, which can be evacuated. Heating the sample causes the analyte to vaporize and sublime onto the cold finger, which is cooled using cold water.

Recrystallization is another method for purifying a solid. A solvent is chosen in which the analyte's solubility is significant when the solvent is hot and minimal when the solvent is cold. The interferents must be less soluble in the hot solvent than the analyte or present in much smaller amounts. After heating a portion of the solvent in an Erlenmeyer flask, small amounts of sample are added until undissolved sample is visible. Additional hot solvent is added until the sample redissolves, or until only insoluble impurities remain. This process of adding sample and solvent is repeated until the entire sample is added to the Erlenmeyer flask. Any insoluble impurities are removed by filtering the hot solution. The solution is allowed to cool slowly, which promotes the growth of large, pure crystals, and then cooled in an ice bath to minimize solubility losses. The purified sample is isolated by filtration and rinsed to remove any soluble impurities. Finally, the sample is dried to remove any remaining traces of the solvent. Further purification, if necessary, is accomplished by additional recrystallizations.

Changes in Chemical State

Distillation, sublimation, and recrystallization use a change in physical state to effect a separation. Chemical reactivity also is a useful tool for separating analytes and interferents. For example, we can separate SiO_2 from a sample by reacting it with HF to form SiF_4. Because SiF_4 is volatile, it is easy to remove by evaporation. If we wish to collect the reaction's volatile product, then a

distillation is possible. For example, we can isolate the NH_4^+ in a sample by making the solution basic and converting it to NH_3. The ammonia is then removed by distillation. Table 7.6.4 provides additional examples of this approach for isolating inorganic ions.

Table 7.6.4 . Examples of Using a Chemical Reaction and a Distillation to Separate an Inorganic Analyte From Interferents

analyte	treatment	isolated species
CO_3^{2-}	$CO_3^{2-}(aq) + 2H_3O^+(aq) \rightarrow CO_2(g) + 3H_2O(l)$	CO_2
NH_4^+	$NH_4^+(aq) + OH^-(aq) \rightarrow NH_3(aq) + H_2O(l)$	NH_3
SO_3^-	$SO_3^{2-}(aq) + 2H_3O^+(aq) \rightarrow SO_2(g) + 3H_2O(l)$	SO_2
S^{2-}	$S^{2-}(aq) + 2H_3O^+(aq) \rightarrow H_2S(g) + 2H_2O(l)$	H_2S

Another reaction for separating analytes and interferents is precipitation. Two important examples of using a precipitation reaction in a separation are the pH-dependent solubility of metal oxides and hydroxides, and the pH-dependent solubility of metal sulfides.

Separations based on the pH-dependent solubility of oxides and hydroxides usually use a strong acid, a strong base, or an NH_3/NH_4Cl buffer to adjust the pH. Most metal oxides and hydroxides are soluble in hot concentrated HNO_3, although a few oxides, such as WO_3, SiO_2, and SnO_2 remain insoluble even under these harsh conditions. To determine the amount of Cu in brass, for example, we can avoid an interference from Sn by dissolving the sample with a strong acid and filtering to remove the solid residue of SnO_2.

Most metals form a hydroxide precipitate in the presence of concentrated NaOH. Those metals that form amphoteric hydroxides, however, do not precipitate because they react to form higher-order hydroxo-complexes. For example, Zn^{2+} and Al^{3+} do not precipitate in concentrated NaOH because they form the soluble complexes $Zn(OH)_3^-$ and $Al(OH)_4^-$. The solubility of Al^{3+} in concentrated NaOH allows us to isolate aluminum from impure samples of bauxite, an ore of Al_2O_3. After crushing the ore, we place it in a solution of concentrated NaOH, dissolving the Al_2O_3 and forming $Al(OH)_4^-$. Other oxides in the ore, such as Fe_2O_3 and SiO_2, remain insoluble. After filtering, we recover the aluminum as a precipitate of $Al(OH)_3$ by neutralizing some of the OH^- with acid.

The pH of an NH_3/NH_4Cl buffer (pK_a = 9.26) is sufficient to precipitate most metals as the hydroxide. The alkaline earths and alkaline metals, however, do not precipitate at this pH. In addition, metal ions that form soluble complexes with NH_3, such as Cu^{2+}, Zn^{2+}, Ni^{2+}, and Co^{2+} also do not precipitate under these conditions.

The use of S^{2-} as a precipitating reagent is one of the earliest examples of a separation technique. In Fresenius's 1881 text *A System of Instruction in Quantitative Chemical Analysis*, sulfide frequently is used to separate metal ions from the remainder of the sample's matrix [Fresenius. C. R. *A System of Instruction in Quantitative Chemical Analysis*, John Wiley and Sons: New York, 1881]. Sulfide is a useful reagent for separating metal ions for two reasons: (1) most metal ions, except for the alkaline earths and alkaline metals, form insoluble sulfides; and (2) these metal sulfides show a substantial variation in solubility. Because the concentration of S^{2-} is pH-dependent, we can control which metal ions precipitate by adjusting the pH. For example, in Fresenius's gravimetric procedure for the determination of Ni in ore samples (see Figure 1.1.1 for a schematic diagram of this procedure), sulfide is used three times to separate Co^{2+} and Ni^{2+} from Cu^{2+} and, to a lesser extent, from Pb^{2+}.

Separations Based on a Partitioning Between Phases

The most important group of separation techniques uses a selective partitioning of the analyte or interferent between two immiscible phases. If we bring a phase that contains the solute, *S*, into contact with a second phase, the solute will partition itself between the two phases, as shown by the following equilibrium reaction.

$$S_{\text{phase 1}} \rightleftharpoons S_{\text{phase 2}} \tag{8.2.1}$$

The equilibrium constant for reaction 8.2.1

$$K_D = \frac{[S_{\text{phase 2}}]}{[S_{\text{phase 1}}]}$$

is called the distribution constant or the ***partition coefficient***. If K_D is sufficiently large, then the solute moves from phase 1 to phase 2. The solute will remain in phase 1 if the partition coefficient is sufficiently small. When we bring a phase that contains two solutes into contact with a second phase, a separation of the solutes is possible if K_D is favorable for only one of the solutes. The physical states of the phases are identified when we describe the separation process, with the phase that contains the sample listed first. For example, if the sample is in a liquid phase and the second phase is a solid, then the separation involves liquid–solid partitioning.

Extraction Between Two Phases

We call the process of moving a species from one phase to another phase an ***extraction***. Simple extractions are particularly useful for separations where only one component has a favorable partition coefficient. Several important separation techniques are based on a simple extraction, including liquid–liquid, liquid–solid, solid–liquid, and gas–solid extractions.

Liquid-Liquid Extractions

A liquid–liquid extraction usually is accomplished using a separatory funnel (Figure 7.6.8). After placing the two liquids in the separatory funnel, we shake the funnel to increase the surface area between the phases. When the extraction is complete, we allow the liquids to separate. The stopcock at the bottom of the separatory funnel allows us to remove the two phases.

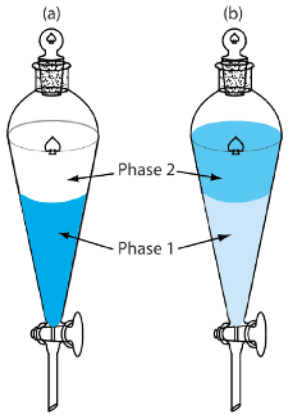


Figure 7.6.8 . Example of a liquid–liquid extraction using a separatory funnel. (a) Before the extraction, 100% of the analyte is in phase 1. (b) After the extraction, most of the analyte is in phase 2, although some analyte remains in phase 1. Although one liquid–liquid extraction can result in the complete transfer of analyte, a single extraction usually is not sufficient. See Chapter7.7 for a discussion of extraction efficiency and multiple extractions.

We also can carry out a liquid–liquid extraction without a separatory funnel by adding the extracting solvent to the sample's container. Pesticides in water, for example, are preserved in the field by extracting them into a small volume of hexane. A liquid–liquid microextraction, in which the extracting phase is a 1-µL drop suspended from a microsyringe (Figure 7.6.9), also has been described [Jeannot, M. A.; Cantwell, F. F. *Anal. Chem.* **1997**, *69*, 235–239]. Because of its importance, a more thorough discussion of liquid–liquid extractions is in Chapter7.7.

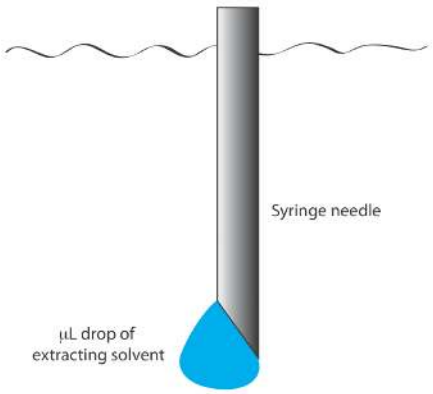


Figure 7.6.9 . Schematic of a liquid–liquid microextraction showing a syringe needle with a µL drop of the extracting solvent.

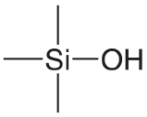
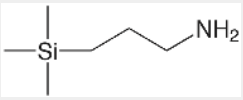
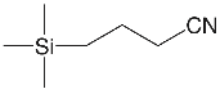
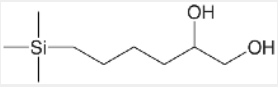
Solid Phase Extractions

In a solid phase extraction of a liquid sample, we pass the sample through a cartridge that contains a solid adsorbent, several examples of which are shown in Figure 7.6.10 . The choice of adsorbent is determined by the species we wish to separate. Table 7.6.5 provides several representative examples of solid adsorbents and their applications.



Figure 7.6.10 . Selection of solid phase extraction cartridges for liquid samples. The solid adsorbent is the white or black material in each cartridge. From left-to-right, the absorbent materials are octadecylsilane, carbon, octadecylsilane, polyamide resin, and diol; see Table 7.6.5 for additional details. The size of the cartridges dictates the volume of sample used; from left-to-right, these cartridges use samples of 1 mL, 3 mL, 6 mL, 3 mL, and 1 mL.

Table 7.6.5 . Representative Adsorbents for the Solid Phase Extraction of Liquid Samples

absorbent	structure	properties and uses
silica		• retains low to moderate polarity species from organic matrices • fat soluble vitamins, steroids
aminopropyl		• retains polar compounds • carbohydrates, organic acids
cyanopropyl		• retains wide variety of species from aqueous and organic matrices • pesticides, hydrophobic peptides
diol		• retains wide variety of species from aqueous and organic matrices • proteins, peptides, fungicides
octadecyl (C–18)	—$C_{18}H_{37}$	• retains hydrophobic species from aqueous matrices • caffeine, sedatives, polyaromatic hydrocarbons, carbohydrates, pesticides
octyl (C–8)	—C_8H_{17}	• similar to C-18

As an example, let's examine a procedure for isolating the sedatives secobarbital and phenobarbital from serum samples using a C-18 solid adsorbent [Alltech Associates *Extract-Clean SPE Sample Preparation Guide*, Bulletin 83]. Before adding the sample, the solid phase cartridge is rinsed with 6 mL each of methanol and water. Next, a 500-µL sample of serum is pulled through the cartridge, with the sedatives and matrix interferents retained following a liquid–solid extraction (Figure 7.6.11 a). Washing the cartridge with distilled water removes any interferents (Figure 7.6.11 b). Finally, we elute the sedatives using 500 µL of acetone (Figure 7.6.11 c). In comparison to a liquid–liquid extraction, a solid phase extraction has the advantage of being easier, faster, and requires less solvent.

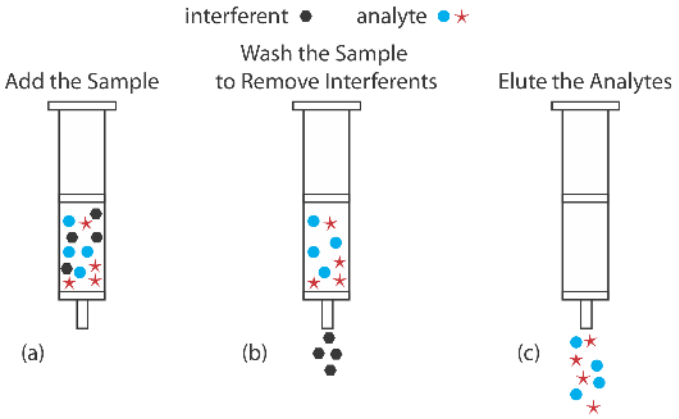


Figure 7.6.11 . Steps in a typical solid phase extraction. After preconditioning the solid phase cartridge with solvent, (a) the sample is added to the cartridge, (b) the sample is washed to remove interferents, and (c) the analytes are eluted.

Continuous Extractions

An extraction is possible even if the analyte has an unfavorable partition coefficient, provided that the sample's other components have significantly smaller partition coefficients. Because the analyte's partition coefficient is unfavorable, a single extraction will not recover all the analyte. Instead we continuously pass the extracting phase through the sample until we achieve a quantitative extraction.

A continuous extraction of a solid sample is carried out using a ***Soxhlet extractor*** (Figure 7.6.12). The extracting solvent is placed in the lower reservoir and heated to its boiling point. Solvent in the vapor phase moves upward through the tube on the far right side of the apparatus, reaching the condenser where it condenses back to the liquid state. The solvent then passes through the sample, which is held in a porous cellulose filter thimble, collecting in the upper reservoir. When the solvent in the upper reservoir reaches the return tube's upper bend, the solvent and extracted analyte are siphoned back to the lower reservoir. Over time the analyte's concentration in the lower reservoir increases.

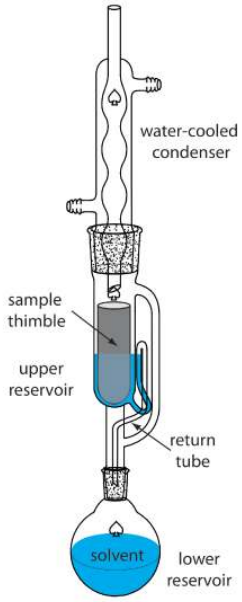


Figure 7.6.12 . Soxhlet extractor. See text for details.

Microwave-assisted extractions have replaced Soxhlet extractions in some applications [Renoe, B. W. *Am. Lab* August **1994**, 34–40]. The process is the same as that described earlier for a microwave digestion. After placing the sample and the solvent in a sealed digestion vessel, a microwave oven is used to heat the mixture. Using a sealed digestion vessel allows the extraction to take place at a higher temperature and pressure, reducing the amount of time needed for a quantitative extraction. In a Soxhlet extraction

the temperature is limited by the solvent's boiling point at atmospheric pressure. When acetone is the solvent, for example, a Soxhlet extraction is limited to 56°C, but a microwave extraction can reach 150°C.

Two other continuous extractions deserve mention. Volatile organic compounds (VOCs) can be quantitatively removed from a liquid sample by a liquid–gas extraction. As shown in Figure 7.6.13 , an inert purging gas, such as He, is passed through the sample. The purge gas removes the VOCs, which are swept to a primary trap where they collect on a solid absorbent. When the extraction is complete, the VOCs are removed from the primary trap by rapidly heating the tube while flushing with He. This technique is known as a ***purge-and-trap***. Because the analyte's recovery may not be reproducible, an internal standard is required for quantitative work.

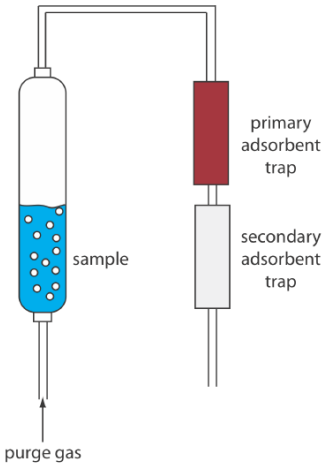


Figure 7.6.13 . Schematic diagram of a purge-and-trap system for extracting volatile analytes. The purge gas releases the analytes, which subsequently collect in the primary adsorbent trap. The secondary adsorption trap is monitored for evidence that the primary trap's capacity to absorb analyte is exceeded.

Continuous extractions also can be accomplished using supercritical fluids [McNally, M. E. *Anal. Chem.* **1995**, *67*, 308A–315A]. If we heat a substance above its critical temperature and pressure it forms a ***supercritical fluid*** whose properties are between those of a gas and a liquid. A supercritical fluid is a better solvent than a gas, which makes it a better reagent for extractions. In addition, a supercritical fluid's viscosity is significantly less than that of a liquid, which makes it easier to push it through a particulate sample. One example of a supercritical fluid extraction is the determination of total petroleum hydrocarbons (TPHs) in soils, sediments, and sludges using supercritical CO_2 ["TPH Extraction by SFE," ISCO, Inc. Lincoln, NE, Revised Nov. 1992]. An approximately 3-g sample is placed in a 10-mL stainless steel cartridge and supercritical CO_2 at a pressure of 340 atm and a temperature of 80°C is passed through the cartridge for 30 minutes at flow rate of 1–2 mL/min. To collect the TPHs, the effluent from the cartridge is passed through 3 mL of tetrachloroethylene at room temperature. At this temperature the CO_2 reverts to the gas phase and is released to the atmosphere.

Chromatographic Separations

In an extraction, the sample originally is in one phase and we extract the analyte or the interferent into a second phase. We also can separate the analyte and interferents by continuously passing one sample-free phase, called the mobile phase, over a second sample-free phase that remains fixed or stationary. The sample is injected into the mobile phase and the sample's components partition themselves between the mobile phase and the stationary phase. Those components with larger partition coefficients are more likely to move into the stationary phase and take longer time to pass through the system. This is the basis of all chromatographic separations. Chromatography provides both a separation of analytes and interferents, and a means for performing a qualitative or quantitative analysis for the analyte. For this reason a more thorough treatment of chromatography is found in Chapter 12.

This page titled 8.2: Classifying Separation Techniques is shared under a CC BY-NC-SA 4.0 license and was authored, remixed, and/or curated by Kathryn Davis.

- **7.6: Classifying Separation Techniques** by David Harvey is licensed CC BY-NC-SA 4.0.

8.3: Liquid-Liquid Extractions

A liquid–liquid extraction is an important separation technique for environmental, clinical, and industrial laboratories. A standard environmental analytical method illustrates the importance of liquid–liquid extractions. Municipal water departments routinely monitor public water supplies for trihalomethanes ($CHCl_3$, $CHBrCl_2$, $CHBr_2Cl$, and $CHBr_3$) because they are known or suspected carcinogens. Before their analysis by gas chromatography, trihalomethanes are separated from their aqueous matrix using a liquid–liquid extraction with pentane ["The Analysis of Trihalomethanes in Drinking Water by Liquid Extraction,"EPAMethod501.2 (EPA 500-Series, November 1979)].

> The Environmental Protection Agency (EPA) also publishes two additional methods for trihalomethanes. Method 501.1 and Method 501.3 use a purge-and-trap to collect the trihalomethanes prior to a gas chromatographic analysis with a halide-specific detector (Method 501.1) or a mass spectrometer as the detector (Method 501.3). You will find more details about gas chromatography, including detectors, in Chapter 12.

In a simple liquid–liquid extraction the solute partitions itself between two immiscible phases. One phase usually is an aqueous solvent and the other phase is an organic solvent, such as the pentane used to extract trihalomethanes from water. Because the phases are immiscible they form two layers, with the denser phase on the bottom. The solute initially is present in one of the two phases; after the extraction it is present in both phases. ***Extraction efficiency***—that is, the percentage of solute that moves from one phase to the other—is determined by the equilibrium constant for the solute's partitioning between the phases and any other side reactions that involve the solute. Examples of other reactions that affect extraction efficiency include acid–base reactions and complexation reactions.

Partition Coefficients and Distribution Ratios

As we learned earlier in this chapter, a solute's partitioning between two phases is described by a partition coefficient, K_D. If we extract a solute from an aqueous phase into an organic phase

$$S_{aq} \rightleftharpoons S_{org}$$

then the partition coefficient is

$$K_D = \frac{[S_{org}]}{[S_{aq}]}$$

A large value for K_D indicates that extraction of solute into the organic phase is favorable.

To evaluate an extraction's efficiency we must consider the solute's total concentration in each phase, which we define as a ***distribution ratio***, D.

$$D = \frac{[S_{org}]_{\text{total}}}{[S_{aq}]_{\text{total}}}$$

The partition coefficient and the distribution ratio are identical if the solute has only one chemical form in each phase; however, if the solute exists in more than one chemical form in either phase, then K_D and D usually have different values. For example, if the solute exists in two forms in the aqueous phase, A and B, only one of which, A, partitions between the two phases, then

$$D = \frac{[S_{org}]_A}{[S_{aq}]_A + [S_{aq}]_B} \leq K_D = \frac{[S_{org}]_A}{[S_{aq}]_A}$$

This distinction between K_D and D is important. The partition coefficient is a thermodynamic equilibrium constant and has a fixed value for the solute's partitioning between the two phases. The distribution ratio's value, however, changes with solution conditions if the relative amounts of A and B change. If we know the solute's equilibrium reactions within each phase and between the two phases, we can derive an algebraic relationship between K_D and D.

Liquid-Liquid Extraction With No Secondary Reactions

In a simple liquid–liquid extraction, the only reaction that affects the extraction efficiency is the solute's partitioning between the two phases (Figure 7.7.1).

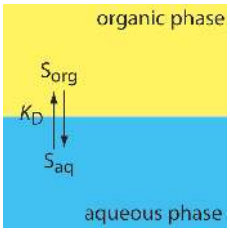


Figure 7.7.1 . Scheme for a simple liquid–liquid extraction in which the solute's partitioning depends only on the K_D equilibrium.

In this case the distribution ratio and the partition coefficient are equal.

$$D = \frac{[S_{org}]_{\text{total}}}{[S_{aq}]_{\text{total}}} = K_D = \frac{[S_{org}]}{[S_{aq}]} \tag{8.3.1}$$

Let's assume the solute initially is present in the aqueous phase and that we wish to extract it into the organic phase. A conservation of mass requires that the moles of solute initially present in the aqueous phase equal the combined moles of solute in the aqueous phase and the organic phase after the extraction.

$$(\text{mol } S_{aq})_0 = (\text{mol } S_{aq})_1 + (\text{mol } S_{org})_1 \tag{8.3.2}$$

where the subscripts indicate the extraction number with 0 representing the system before the extraction and 1 the system following the first extraction. After the extraction, the solute's concentration in the aqueous phase is

$$[S_{aq}]_1 = \frac{(\text{mol } S_{aq})_1}{V_{aq}} \tag{8.3.3}$$

and its concentration in the organic phase is

$$[S_{org}]_1 = \frac{(\text{mol } S_{org})_1}{V_{org}} \tag{8.3.4}$$

where V_{aq} and V_{org} are the volumes of the aqueous phase and the organic phase. Solving Equation 8.3.2 for (mol S_{org})$_1$ and substituting into Equation 8.3.4 leave us with

$$[S_{org}]_1 = \frac{(\text{mol } S_{aq})_0 - (\text{mol } S_{aq})_1}{V_{org}} \tag{8.3.5}$$

Substituting Equation 8.3.3 and Equation 8.3.5 into Equation 8.3.1 gives

$$D = \frac{\frac{(\text{mol } S_{aq})_0 - (\text{mol } S_{aq})_1}{V_{org}}}{\frac{(\text{mol } S_{aq})_1}{V_{aq}}} = \frac{(\text{mol } S_{aq})_0 \times V_{aq} - (\text{mol } S_{aq})_1 \times V_{aq}}{(\text{mol } S_{aq})_1 \times V_{org}}$$

Rearranging and solving for the fraction of solute that remains in the aqueous phase after one extraction, (q_{aq})$_1$, gives

$$(q_{aq})_1 = \frac{(\text{mol } S_{aq})_1}{(\text{mol } S_{aq})_0} = \frac{V_{aq}}{DV_{org} + V_{aq}} \tag{8.3.6}$$

The fraction present in the organic phase after one extraction, (q_{org})$_1$, is

$$(q_{org})_1 = \frac{(\text{mol} S_{org})_1}{(\text{mol} S_{aq})_0} = 1 - (q_{aq})_1 = \frac{DV_{org}}{DV_{org} + V_{aq}}$$

Example 7.7.1 shows how we can use Equation 8.3.6 to calculate the efficiency of a simple liquid-liquid extraction.

Example 7.7.1

A solute has a K_D between water and chloroform of 5.00. Suppose we extract a 50.00-mL sample of a 0.050 M aqueous solution of the solute using 15.00 mL of chloroform. (a) What is the separation's extraction efficiency? (b) What volume of chloroform do we need if we wish to extract 99.9% of the solute?

Solution

For a simple liquid–liquid extraction the distribution ratio, D, and the partition coefficient, K_D, are identical.

(a) The fraction of solute that remains in the aqueous phase after the extraction is given by Equation 8.3.6.

$$(q_{aq})_1 = \frac{V_{aq}}{DV_{org} + V_{aq}} = \frac{50.00\ \text{mL}}{(5.00)(15.00\ \text{mL}) + 50.00\ \text{mL}} = 0.400$$

The fraction of solute in the organic phase is 1–0.400, or 0.600. Extraction efficiency is the percentage of solute that moves into the extracting phase; thus, the extraction efficiency is 60.0%.

(b) To extract 99.9% of the solute $(q_{aq})_1$ must be 0.001. Solving Equation 8.3.6 for V_{org}, and making appropriate substitutions for $(q_{aq})_1$ and V_{aq} gives

$$V_{org} = \frac{V_{aq} - (q_{aq})_1 V_{aq}}{(q_{aq})_1 D} = \frac{50.00\ \text{mL} - (0.001)(50.00\ \text{mL})}{(0.001)(5.00\ \text{mL})} = 999\ \text{mL}$$

This is large volume of chloroform. Clearly, a single extraction is not reasonable under these conditions.

In Example 7.7.1 , a single extraction provides an extraction efficiency of only 60%. If we carry out a second extraction, the fraction of solute remaining in the aqueous phase, $(q_{aq})_2$, is

$$(q_{aq})_2 = \frac{(\text{mol } S_{aq})_2}{(\text{mol } S_{aq})_1} = \frac{V_{aq}}{DV_{org} + V_{aq}}$$

If V_{aq} and V_{org} are the same for both extractions, then the cumulative fraction of solute that remains in the aqueous layer after two extractions, $(Q_{aq})_2$, is the product of $(q_{aq})_1$ and $(q_{aq})_2$, or

$$(Q_{aq})_2 = \frac{(\text{mol } S_{aq})_2}{(\text{mol } S_{aq})_0} = (q_{aq})_1 \times (q_{aq})_2 = \left(\frac{V_{aq}}{DV_{org}+V_{aq}}\right)^2$$

In general, for a series of n identical extractions, the fraction of analyte that remains in the aqueous phase after the last extraction is

$$(Q_{aq})_n = \left(\frac{V_{aq}}{DV_{org}+V_{aq}}\right)^n \tag{8.3.7}$$

Example 7.7.2

For the extraction described in Example 7.7.1 , determine (a) the extraction efficiency for two identical extractions and for three identical extractions; and (b) the number of extractions required to ensure that we extract 99.9% of the solute.

Solution

(a) The fraction of solute remaining in the aqueous phase after two extractions and three extractions is

$$(Q_{aq})_2 = \left(\frac{50.00\ \text{mL}}{(5.00)(15.00\ \text{mL})+50.00\ \text{mL}}\right)^2 = 0.160$$

$$(Q_{aq})_3 = \left(\frac{50.0\ \text{mL}}{(5.00)(15.00\ \text{mL})+50.00\ \text{mL}}\right)^3 = 0.0640$$

The extraction efficiencies are 84.0% for two extractions and 93.6% for three extractions.

(b) To determine the minimum number of extractions for an efficiency of 99.9%, we set $(Q_{aq})_n$ to 0.001 and solve for n using Equation 8.3.7.

$$0.001 = \left(\frac{50.00\ \text{mL}}{(5.00)(15.00\ \text{mL})+50.00\ \text{mL}}\right)^n = (0.400)^n$$

Taking the log of both sides and solving for n

$$\log(0.001) = n\log(0.400)$$
$$n = 7.54$$

we find that a minimum of eight extractions is necessary.

The last two examples provide us with an important observation—for any extraction efficiency, we need less solvent if we complete several extractions using smaller portions of solvent instead of one extraction using a larger volume of solvent. For the conditions in Example 7.7.1 and Example 7.7.2 , an extraction efficiency of 99.9% requires one extraction with 9990 mL of chloroform, or 120 mL when using eight 15-mL portions of chloroform. Although extraction efficiency increases dramatically with the first few multiple, the effect diminishes quickly as we increase the number of extractions (Figure 7.7.2). In most cases there is little improvement in extraction efficiency after five or six extractions. For the conditions in Example 7.7.2 , we reach an extraction efficiency of 99% after five extractions and need three additional extractions to obtain the extra 0.9% increase in extraction efficiency.

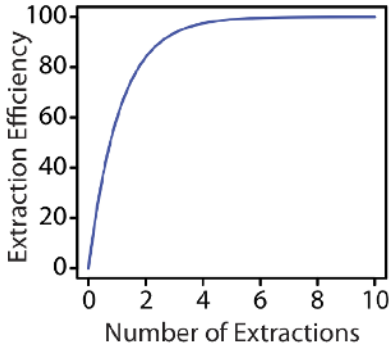


Figure 7.7.2 . Plot of extraction efficiency versus the number of extractions for the liquid–liquid extraction in Example 7.7.2 .

Exercise 7.7.1

To plan a liquid–liquid extraction we need to know the solute's distribution ratio between the two phases. One approach is to carry out the extraction on a solution that contains a known amount of solute. After the extraction, we isolate the organic phase and allow it to evaporate, leaving behind the solute. In one such experiment, 1.235 g of a solute with a molar mass of 117.3 g/mol is dissolved in 10.00 mL of water. After extracting with 5.00 mL of toluene, 0.889 g of the solute is recovered in the organic phase. (a) What is the solute's distribution ratio between water and toluene? (b) If we extract 20.00 mL of an aqueous solution that contains the solute using 10.00 mL of toluene, what is the extraction efficiency? (c) How many extractions will we need to recover 99.9% of the solute?

Answer

(a) The solute's distribution ratio between water and toluene is

$$D = \frac{[S_{org}]}{[S_{aq}]} = \frac{0.889\ \text{g} \times \frac{1\ \text{mol}}{117.3\ \text{g}} \times \frac{1}{0.00500\ \text{L}}}{(1.235\ \text{g} - 0.889\ \text{g}) \times \frac{1\ \text{mol}}{117.3\ \text{g}} \times \frac{1}{0.01000\ \text{L}}} = 5.14$$

(b) The fraction of solute remaining in the aqueous phase after one extraction is

$$(q_{aq})_1 = \frac{V_{aq}}{DV_{org} + V_{aq}} = \frac{20.00\ \text{mL}}{(5.14)(10.00\ \text{mL}) + 20.00\ \text{mL}} = 0.280$$

The extraction efficiency, therefore, is 72.0%.

(c) To extract 99.9% of the solute requires

$$(Q_{aq})_n = 0.001 = \left(\frac{20.00\ \text{mL}}{(5.14)(10.00\ \text{mL})+20.00\ \text{mL}}\right)^n = (0.280)^n$$

$$\log(0.001) = n\log(0.280)$$
$$n = 5.4$$

a minimum of six extractions.

Liquid-Liquid Extractions Involving Acid-Base Equilibria

As we see in Equation 8.3.1, in a simple liquid–liquid extraction the distribution ratio and the partition coefficient are identical. As a result, the distribution ratio does not depend on the composition of the aqueous phase or the organic phase. A change in the pH of the aqueous phase, for example, will not affect the solute's extraction efficiency when K_D and D have the same value.

If the solute participates in one or more additional equilibrium reactions within a phase, then the distribution ratio and the partition coefficient may not be the same. For example, Figure 7.7.3 shows the equilibrium reactions that affect the extraction of the weak acid, HA, by an organic phase in which ionic species are not soluble.

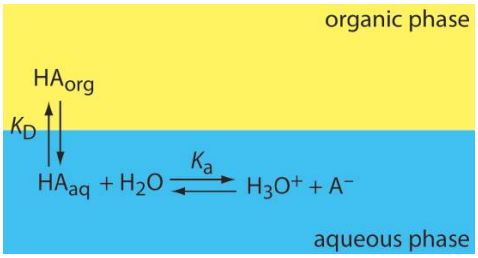


Figure 7.7.3 . Scheme for the liquid–liquid extraction of a weak acid, HA. Although the weak acid is soluble in both phases, its conjugate weak base, A^-, is soluble in the aqueous phase only. The K_a reaction for HA, which is called a ***secondary equilibrium reaction***, affects weak acid's extraction efficiency because it determines the relative abundance of HA in solution.

In this case the partition coefficient and the distribution ratio are

$$K_D = \frac{[HA_{org}]}{[HA_{aq}]} \tag{8.3.8}$$

$$D = \frac{[HA_{org}]_{\text{total}}}{[HA_{aq}]_{\text{total}}} = \frac{[HA_{org}]}{[HA_{aq}] + [A^-_{aq}]} \tag{8.3.9}$$

Because the position of an acid–base equilibrium depends on pH, the distribution ratio, D, is pH-dependent. To derive an equation for D that shows this dependence, we begin with the acid dissociation constant for HA.

$$K_a = \frac{[H_3O^+_{aq}]\,[A^-_{aq}]}{[HA_{aq}]} \tag{8.3.10}$$

Solving Equation 8.3.10 for the concentration of A^- in the aqueous phase

$$[A^-_{aq}] = \frac{K_a \times [HA_{aq}]}{[H_3O^+_{aq}]}$$

and substituting into Equation 8.3.9 gives

$$D = \frac{[HA_{org}]}{[HA_{aq}] + \frac{K_a \times [HA_{aq}]}{[H_3O^+_{aq}]}}$$

Factoring $[HA_{aq}]$ from the denominator, replacing $[HA_{org}]/[HA_{aq}]$ with K_D (Equation 8.3.8), and simplifying leaves us with the following relationship between the distribution ratio, D, and the pH of the aqueous solution.

$$D = \frac{K_D\,[H_3O^+_{aq}]}{[H_3O^+_{aq}] + K_a} \tag{8.3.11}$$

Example 7.7.3

An acidic solute, HA, has a K_a of 1.00×10^{-5} and a K_D between water and hexane of 3.00. Calculate the extraction efficiency if we extract a 50.00 mL sample of a 0.025 M aqueous solution of HA, buffered to a pH of 3.00, with 50.00 mL of hexane. Repeat for pH levels of 5.00 and 7.00.

Solution

When the pH is 3.00, $[H_3O^+_{aq}]$ is 1.0×10^{-3} and the distribution ratio is

$$D = \frac{(3.00)\,(1.0 \times 10^{-3})}{1.0 \times 10^{-3} + 1.00 \times 10^{-5}} = 2.97$$

The fraction of solute that remains in the aqueous phase is

$$(Q_{aq})_1 = \frac{50.00\ \text{mL}}{(2.97)(50.00\ \text{mL}) + 50.00\ \text{mL}} = 0.252$$

The extraction efficiency, therefore, is almost 75%. The same calculation at a pH of 5.00 gives the extraction efficiency as 60%. At a pH of 7.00 the extraction efficiency is just 3% .

The extraction efficiency in Example 7.7.3 is greater at more acidic pH levels because HA is the solute's predominate form in the aqueous phase. At a more basic pH, where A^- is the solute's predominate form, the extraction efficiency is smaller. A graph of extraction efficiency versus pH is shown in Figure 7.7.4 . Note that extraction efficiency essentially is independent of pH for pH levels more acidic than the HA's pK_a, and that it is essentially zero for pH levels more basic than HA's pK_a. The greatest change in extraction efficiency occurs at pH levels where both HA and A^- are predominate species. The ladder diagram for HA along the graph's *x*-axis helps illustrate this effect.

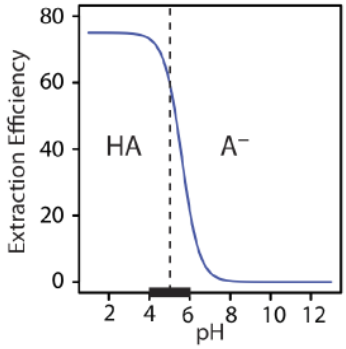


Figure 7.7.4 . Plot of extraction efficiency versus pH of the aqueous phase for the extraction in Example 7.7.3 . A ladder diagram for HA is superimposed along the *x*-axis, which divides the pH scale into regions where HA and A^- are the predominate aqueous phase species. The greatest change in extraction efficiency occurs as the pH moves through HA's buffer region.

Exercise 7.7.2

The liquid–liquid extraction of the weak base B is governed by the following equilibrium reactions:

$$B(aq) \rightleftharpoons B(org) \quad K_D = 5.00$$
$$B(aq) + H_2O(l) \rightleftharpoons OH^-(aq) + HB^+(aq) \quad K_b = 1.0 \times 10^{-4}$$

Derive an equation for the distribution ratio, *D*, and calculate the extraction efficiency if 25.0 mL of a 0.025 M solution of B, buffered to a pH of 9.00, is extracted with 50.0 mL of the organic solvent.

Answer

Because the weak base exists in two forms, only one of which extracts into the organic phase, the partition coefficient, K_D, and the distribution ratio, *D*, are not identical.

$$K_D = \frac{[B_{org}]}{[B_{aq}]}$$

$$D = \frac{[B_{org}]}{[B_{aq}]} = \frac{[B_{org}]}{[B_{aq}] + [HB^+_{aq}]}$$

Using the K_b expression for the weak base

$$K_b = \frac{[OH^-_{aq}]\,[HB^+_{aq}]}{[B_{aq}]}$$

we solve for the concentration of HB^+ and substitute back into the equation for D, obtaining

$$D = \frac{[B_{org}]}{[B_{aq}] + \frac{K_b \times [B_{aq}]}{[OH^-_{aq}]}} = \frac{[B_{org}]}{[B_{aq}]\left(1 + \frac{K_b}{[OH^+_{aq}]}\right)} = \frac{K_D\,[OH^-_{aq}]}{[OH^-_{aq}] + K_b}$$

At a pH of 9.0, the $[OH^-]$ is 1×10^{-5} M and the distribution ratio has a value of

$$D = \frac{K_D\,[OH^-_{aq}]}{[OH^-_{aq}] + K_b} = \frac{(5.00)\,(1.0 \times 10^{-5})}{1.0 \times 10^{-5} + 1.0 \times 10^{-4}} = 0.455$$

After one extraction, the fraction of B remaining in the aqueous phase is

$$(q_{aq})_1 = \frac{25.00\ \text{mL}}{(0.455)(50.00\ \text{mL}) + 25.00\ \text{mL}} = 0.524$$

The extraction efficiency, therefore, is 47.6%. At a pH of 9, most of the weak base is present as HB^+, which explains why the overall extraction efficiency is so poor.

Liquid-Liquid Extraction of a Metal-Ligand Complex

One important application of a liquid–liquid extraction is the selective extraction of metal ions using an organic ligand. Unfortunately, many organic ligands are not very soluble in water or undergo hydrolysis or oxidation reactions in aqueous solutions. For these reasons the ligand is added to the organic solvent instead of the aqueous phase. Figure 7.7.5 shows the relevant equilibrium reactions (and equilibrium constants) for the extraction of M^{n+} by the ligand HL, including the ligand's extraction into the aqueous phase ($K_{D,HL}$), the ligand's acid dissociation reaction (K_a), the formation of the metal–ligand complex (β_n), and the complex's extraction into the organic phase ($K_{D,c}$).

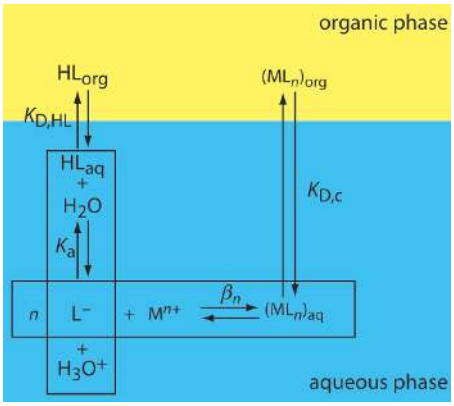


Figure 7.7.5 . Scheme for the liquid–liquid extraction of a metal ion, M^{n+}, by the ligand L^-. The ligand initially is present in the organic phase as HL. Four equilibrium reactions are needed to explain the extraction efficiency.

If the ligand's concentration is much greater than the metal ion's concentration, then the distribution ratio is

$$D = \frac{\beta_n K_{D,c}\,(K_a)^n\,(C_{HL})^n}{(K_{D,HL})^n\,[H_3O^+]^n + \beta_n\,(K_a)^n\,(C_{HL})^n} \qquad (8.3.12)$$

where C_{HL} is the ligand's initial concentration in the organic phase. As shown in Example 7.7.4 , the extraction efficiency for metal ions shows a marked pH dependency.

Example 7.7.4

A liquid–liquid extraction of the divalent metal ion, M^{2+}, uses the scheme outlined in Figure 7.7.5 . The partition coefficients for the ligand, $K_{D,HL}$, and for the metal–ligand complex, $K_{D,c}$, are 1.0×10^4 and 7.0×10^4, respectively. The ligand's acid dissociation constant, K_a, is 5.0×10^{-5}, and the formation constant for the metal–ligand complex, β_2, is 2.5×10^{16}. What is the extraction efficiency if we extract 100.0 mL of a 1.0×10^{-6} M aqueous solution of M^{2+}, buffered to a pH of 1.00, with 10.00 mL of an organic solvent that is 0.1 mM in the chelating agent? Repeat the calculation at a pH of 3.00.

Solution

When the pH is 1.00 the distribution ratio is

$$D = \frac{(2.5 \times 10^{16})(7.0 \times 10^4)(5.0 \times 10^{-5})^2 (1.0 \times 10^{-4})^2}{(1.0 \times 10^4)^2 (0.10)^2 + (2.5 \times 10^{16})(5.0 \times 10^{-5})^2 (1.0 \times 10^{-4})^2}$$

or a D of 0.0438. The fraction of metal ion that remains in the aqueous phase is

$$(Q_{aq})_1 = \frac{100.0 \text{ mL}}{(0.0438)(10.00 \text{ mL}) + 100.0 \text{ mL}} = 0.996$$

At a pH of 1.00, we extract only 0.40% of the metal into the organic phase. Changing the pH to 3.00, however, increases the extraction efficiency to 97.8%. Figure 7.7.6 shows how the pH of the aqueous phase affects the extraction efficiency for M^{2+}.

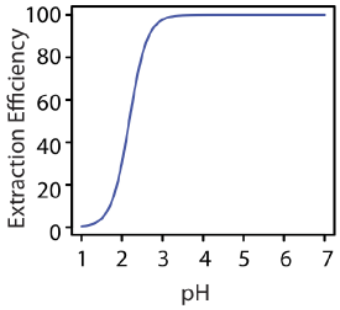


Figure 7.7.6 . Plot of extraction efficiency versus pH for the extraction of the metal ion, M^{2+}, in Example 7.7.4 .

One advantage of using a ligand to extract a metal ion is the high degree of selectivity that it brings to a liquid–liquid extraction. As seen in Figure 7.7.6 , a divalent metal ion's extraction efficiency increases from approximately 0% to 100% over a range of 2 pH units. Because a ligand's ability to form a metal–ligand complex varies substantially from metal ion to metal ion, significant selectivity is possible if we carefully control the pH. Table 7.7.1 shows the minimum pH for extracting 99% of a metal ion from an aqueous solution using an equal volume of 4 mM dithizone in CCl_4.

Table 7.7.1 . Minimum pH for Extracting 99% of an Aqueous Metal Ion Using 4.0 mM Dithizone in CCl_4 $V_{aq} = V_{org}$

metal ion	minimum pH
Hg^{2+}	–8.7
Ag^{+}	–1.7
Cu^{2+}	–0.8
Bi^{3+}	0.9
Zn^{2+}	2.3
Cd^{2+}	3.6
Co^{2+}	3.6
Pb^{2+}	4.1
Ni^{2+}	6.0
Tl^{+}	8.7

Example 7.7.5

Using Table 7.7.1 , explain how we can separate the metal ions in an aqueous mixture of Cu^{2+}, Cd^{2+}, and Ni^{2+} by extracting with an equal volume of dithizone in CCl_4.

Solution

From Table 7.7.1 , a quantitative separation of Cu^{2+} from Cd^{2+} and from Ni^{2+} is possible if we acidify the aqueous phase to a pH of less than 1. This pH is greater than the minimum pH for extracting Cu^{2+} and significantly less than the minimum pH for extracting either Cd^{2+} or Ni^{2+}. After the extraction of Cu^{2+} is complete, we shift the pH of the aqueous phase to 4.0, which allows us to extract Cd^{2+} while leaving Ni^{2+} in the aqueous phase.

This page titled 8.3: Liquid-Liquid Extractions is shared under a CC BY-NC-SA 4.0 license and was authored, remixed, and/or curated by Kathryn Davis.

- **7.7: Liquid-Liquid Extractions** by David Harvey is licensed CC BY-NC-SA 4.0.

8.4: Overview of Analytical Separations

In Chapter 7 we examined several methods for separating an analyte from potential interferents. For example, in a liquid–liquid extraction the analyte and interferent initially are present in a single liquid phase. We add a second, immiscible liquid phase and thoroughly mix them by shaking. During this process the analyte and interferents partition between the two phases to different extents, effecting their separation. After allowing the phases to separate, we draw off the phase enriched in analyte. Despite the power of liquid–liquid extractions, there are significant limitations.

A Better Way to Separate Mixtures

The problem with a liquid–liquid extraction is that the separation occurs in one direction only: from the sample to the extracting phase. Let's take a closer look at the liquid–liquid extraction of an analyte and an interferent with distribution ratios of, respectively, 5 and 0.5. Figure 8.4.1 shows that a single extraction using equal volumes of sample and extractant transfers 83% of the analyte and 33% of the interferent to the extracting phase. If the original concentrations of A and I are identical, then their concentration ratio in the extracting phase after one extraction is

$$\frac{[A]}{[I]} = \frac{0.83}{0.33} = 2.5$$

A single extraction, therefore, enriches the analyte by a factor of $2.5\times$. After completing a second extraction (Figure 8.4.1) and combining the two extracting phases, the separation of the analyte and the interferent, surprisingly, is less efficient.

$$\frac{[A]}{[I]} = \frac{0.97}{0.55} = 1.8$$

Figure 8.4.1 makes it clear why the second extraction results in a poorer overall separation: the second extraction actually favors the interferent!

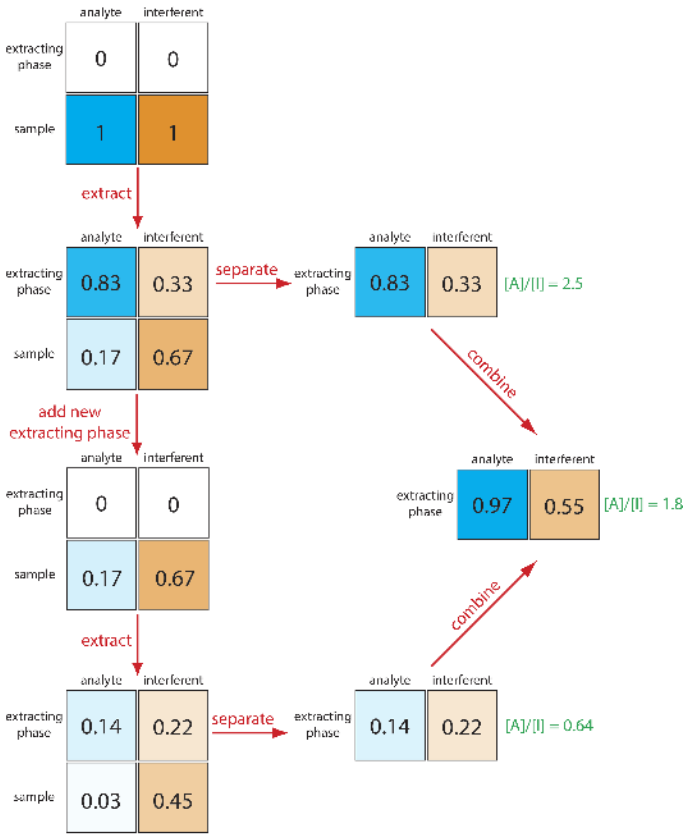


Figure 8.4.1 . Progress of a traditional liquid–liquid extraction using two identical extractions of a single sample using fresh portions of the extractant. The numbers give the fraction of analyte and interferent in each phase assuming equal volumes of sample and extractant and distribution ratios of 5 and 0.5 for the analyte and the interferent, respectively. The opacity of the colors equals the fraction of analyte and interferent present.

We can improve the separation by first extracting the solutes from the sample into the extracting phase and then extracting them back into a fresh portion of solvent that matches the sample's matrix (Figure 8.4.2). Because the analyte has the larger distribution ratio, more of it moves into the extractant during the first extraction and less of it moves back to the sample phase during the second extraction. In this case the concentration ratio in the extracting phase after two extractions is significantly greater.

$$\frac{[A]}{[I]} = \frac{0.69}{0.11} = 6.3$$

https://chem.libretexts.org/@go/page/556150

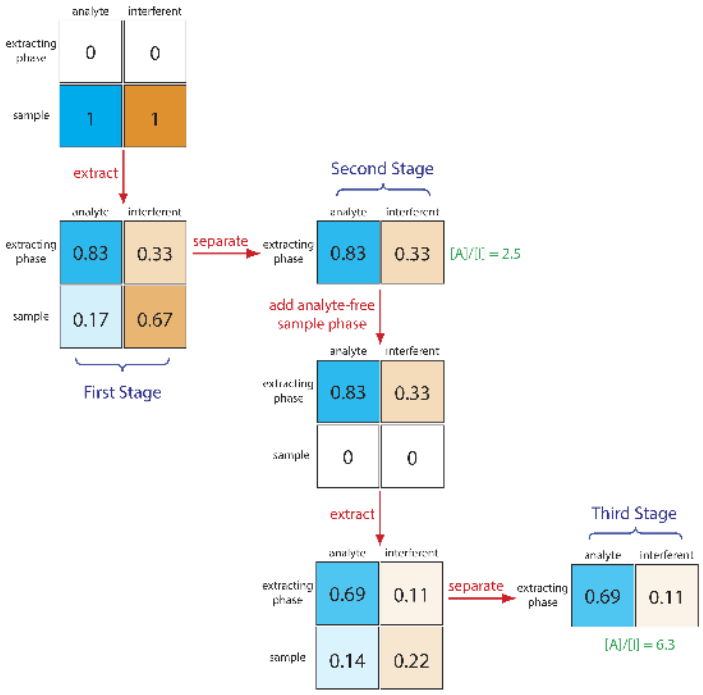


Figure 8.4.2 . Progress of a liquid–liquid extraction in which we first extract the solutes into the extracting phase and then extract them back into an analyte-free portion of the sample's phase. The numbers give the fraction of analyte and interferent in each phase assuming equal volumes of sample and extractant and distribution ratios of 5 and 0.5 for the analyte and the interferent, respectively. The opacity of the colors equals the fraction of analyte and interferent present.

Not shown above is that we can add a fresh portion of the extracting phase to the sample that remains after the first extraction (the bottom row of the first stage in Figure 12.2, beginning the process anew. As we increase the number of extractions, the analyte and the interferent each spread out in space over a series of stages. Because the interferent's distribution ratio is smaller than the analyte's, the interferent lags behind the analyte. With a sufficient number of extractions—that is, a sufficient number of stages—a complete separation of the analyte and interferent is possible. This process of extracting the solutes back and forth between fresh portions of the two phases, which we call a ***countercurrent extraction***, was developed by Craig in the 1940s [Craig, L. C. *J. Biol. Chem.* **1944**, *155*, 519–534]. The same phenomenon forms the basis of modern chromatography.

Chromatographic Separations

In ***chromatography*** we pass a sample-free phase, which we call the ***mobile phase***, over a second sample-free ***stationary phase*** that remains fixed in space (Figure 8.4.3). We inject or place the sample into the mobile phase. As the sample moves with the mobile phase, its components partition between the mobile phase and the stationary phase. A component whose distribution ratio favors the stationary phase requires more time to pass through the system. Given sufficient time and sufficient stationary and mobile phase, we can separate solutes even if they have similar distribution ratios.

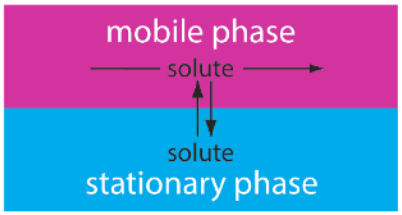


Figure 8.4.3 . In chromatography we pass a mobile phase over a stationary phase. When we inject a sample into the mobile phase, the sample's components both move with the mobile phase and partition into the stationary phase. The solute that spends the most time in the stationary phase takes the longest time to move through the system.

There are many ways in which we can identify a chromatographic separation: by describing the physical state of the mobile phase and the stationary phase; by describing how we bring the stationary phase and the mobile phase into contact with each other; or by

describing the chemical or physical interactions between the solute and the stationary phase. Let's briefly consider how we might use each of these classifications.

> We can trace the history of chromatography to the turn of the century when the Russian botanist Mikhail Tswett used a column packed with calcium carbonate and a mobile phase of petroleum ether to separate colored pigments from plant extracts. As the sample moved through the column, the plant's pigments separated into individual colored bands. After effecting the separation, the calcium carbonate was removed from the column, sectioned, and the pigments recovered. Tswett named the technique chromatography, combining the Greek words for "color" and "to write." There was little interest in Tswett's technique until Martin and Synge's pioneering development of a theory of chromatography (see Martin, A. J. P.; Synge, R. L. M. "A New Form of Chromatogram Employing Two Liquid Phases," *Biochem. J.* **1941**, *35*, 1358–1366). Martin and Synge were awarded the 1952 Nobel Prize in Chemistry for this work.

Types of Mobile Phases and Stationary Phases

The mobile phase is a liquid or a gas, and the stationary phase is a solid or a liquid film coated on a solid substrate. We often name chromatographic techniques by listing the type of mobile phase followed by the type of stationary phase. In gas–liquid chromatography, for example, the mobile phase is a gas and the stationary phase is a liquid film coated on a solid substrate. If a technique's name includes only one phase, as in gas chromatography, it is the mobile phase.

Contact Between the Mobile Phase and the Stationary Phase

There are two common methods for bringing the mobile phase and the stationary phase into contact. In ***column chromatography*** we pack the stationary phase into a narrow column and pass the mobile phase through the column using gravity or by applying pressure. The stationary phase is a solid particle or a thin liquid film coated on either a solid particulate packing material or on the column's walls.

In ***planar chromatography*** the stationary phase is coated on a flat surface—typically, a glass, metal, or plastic plate. One end of the plate is placed in a reservoir that contains the mobile phase, which moves through the stationary phase by capillary action. In paper chromatography, for example, paper is the stationary phase.

Interaction Between the Solute and the Stationary Phase

The interaction between the solute and the stationary phase provides a third method for describing a separation (Figure 8.4.4). In ***adsorption chromatography***, solutes separate based on their ability to adsorb to a solid stationary phase. In ***partition chromatography***, the stationary phase is a thin liquid film on a solid support. Separation occurs because there is a difference in the equilibrium partitioning of solutes between the stationary phase and the mobile phase. A stationary phase that consists of a solid support with covalently attached anionic (e.g., $-\mathrm{SO_3^-}$) or cationic (e.g., $-\mathrm{N(CH_3)_3^+}$) functional groups is the basis for ion-exchange chromatography in which ionic solutes are attracted to the stationary phase by electrostatic forces. In size-exclusion chromatography the stationary phase is a porous particle or gel, with separation based on the size of the solutes. Larger solutes are unable to penetrate as deeply into the porous stationary phase and pass more quickly through the column.

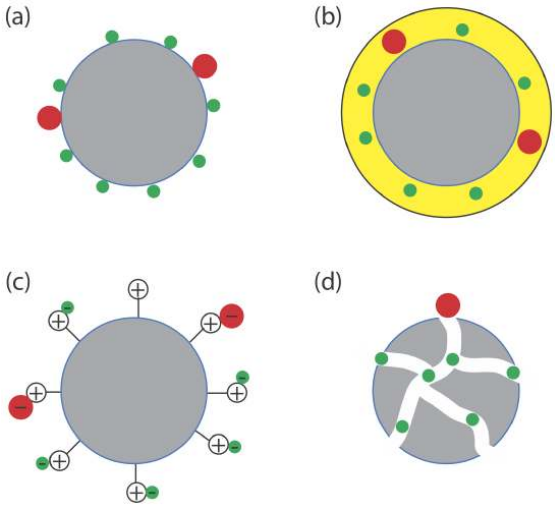


Figure 8.4.4 . Four examples of interactions between a solute and the stationary phase: (a) adsorption on a solid surface, (b) partitioning into a liquid phase, (c) ion-exchange, and (d) size exclusion. For each example, the smaller, green solute is more strongly retained than the larger, red solute.

There are other interactions that can serve as the basis of a separation. In affinity chromatography the interaction between an antigen and an antibody, between an enzyme and a substrate, or between a receptor and a ligand forms the basis of a separation. See this chapter's additional resources for some suggested readings.

Electrophoretic Separations

In chromatography, a separation occurs because there is a difference in the equilibrium partitioning of solutes between the mobile phase and the stationary phase. Equilibrium partitioning, however, is not the only basis for effecting a separation. In an electrophoretic separation, for example, charged solutes migrate under the influence of an applied potential. A separation occurs because of differences in the charges and the sizes of the solutes (Figure 8.4.5).

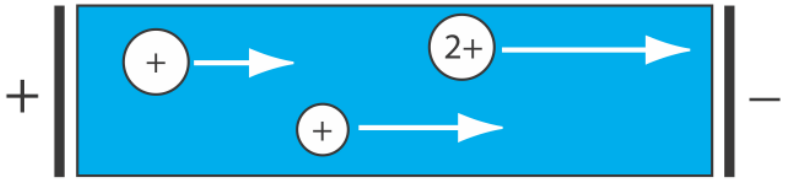


Figure 8.4.5 . Movement of charged solutes under the influence of an applied potential. The lengths of the arrows indicate the relative speed of the solutes. In general, a larger solute moves more slowly than a smaller solute of equal charge, and a solute with a larger charge move more quickly than a solute with a smaller charge.

This page titled 8.4: Overview of Analytical Separations is shared under a CC BY-NC-SA 4.0 license and was authored, remixed, and/or curated by Kathryn Davis.

- **12.1: Overview of Analytical Separations** by David Harvey is licensed CC BY-NC-SA 4.0.

8.5: General Theory of Column Chromatography

Of the two methods for bringing the stationary phase and the mobile phases into contact, the most important is column chromatography. In this section we develop a general theory that we may apply to any form of column chromatography.

Figure 12.2.1 provides a simple view of a liquid–solid column chromatography experiment. The sample is introduced as a narrow band at the top of the column. Ideally, the solute's initial concentration profile is rectangular (Figure 12.2.2 a). As the sample moves down the column, the solutes begin to separate (Figure 12.2.1 b,c) and the individual solute bands begin to broaden and develop a Gaussian profile (Figure 12.2.2 b,c). If the strength of each solute's interaction with the stationary phase is sufficiently different, then the solutes separate into individual bands (Figure 12.2.1 d and Figure 12.2.2 d).

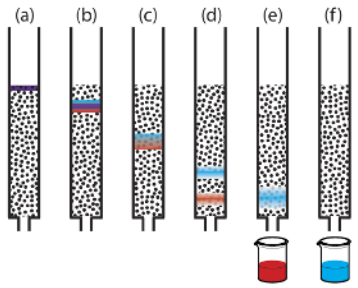


Figure 12.2.1 . Progress of a column chromatographic separation of a two-component mixture. In (a) the sample is layered on top of the stationary phase. As mobile phase passes through the column, the sample separates into two solute bands (b–d). In (e) and (f), we collect each solute as it elutes from the column.

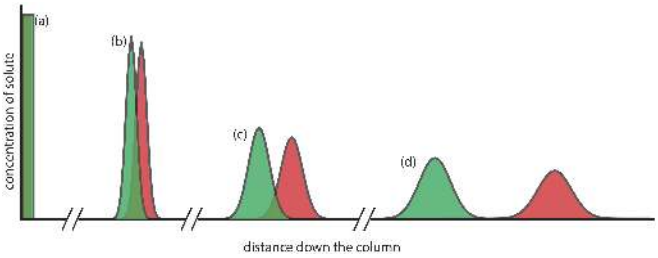


Figure 12.2.2 . An alternative view of the separation in Figure 12.2.1 showing the concentration of each solute as a function of distance down the column.

We can follow the progress of the separation by collecting fractions as they elute from the column (Figure 12.2.1 e,f), or by placing a suitable detector at the end of the column. A plot of the detector's response as a function of elution time, or as a function of the volume of mobile phase, is known as a ***chromatogram*** (Figure 12.2.3), and consists of a peak for each solute.

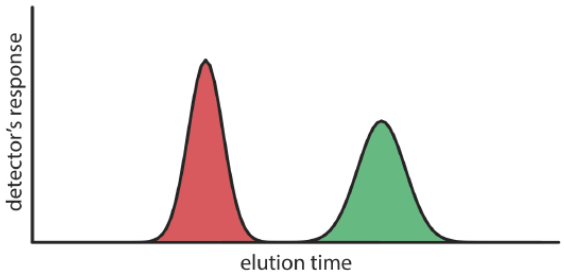


Figure 12.2.3 . Chromatogram for the separation shown in Figure 12.2.1 and Figure 12.2.2 , showing the detector's response as a function of the elution time.

> There are many possible detectors that we can use to monitor the separation. Later sections of this chapter describe some of the most popular.

We can characterize a chromatographic peak's properties in several ways, two of which are shown in Figure 12.2.4 . ***Retention time***, t_r, is the time between the sample's injection and the maximum response for the solute's peak. A chromatographic peak's ***baseline width***, w, as shown in Figure 12.2.4 , is determined by extending tangent lines from the inflection points on either side of the peak through the baseline. Although usually we report t_r and w using units of time, we can report them using units of volume by multiplying each by the mobile phase's velocity, or report them in linear units by measuring distances with a ruler.

> For example, a solute's retention volume, V_r, is $\boldsymbol{t_r \times u}$ where u is the mobile phase's velocity through the column.

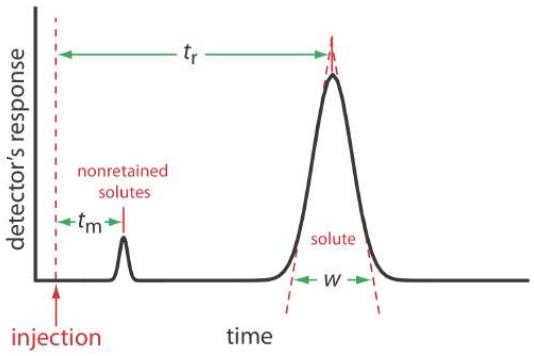


Figure 12.2.4 . Chromatogram showing a solute's retention time, t_r, and baseline width, w, and the column's void time, t_m, for nonretained solutes.

In addition to the solute's peak, Figure 12.2.4 also shows a small peak that elutes shortly after the sample is injected into the mobile phase. This peak contains all ***nonretained solutes***, which move through the column at the same rate as the mobile phase. The time required to elute the nonretained solutes is called the column's ***void time***, t_m.

Chromatographic Resolution

The goal of chromatography is to separate a mixture into a series of chromatographic peaks, each of which constitutes a single component of the mixture. The ***resolution*** between two chromatographic peaks, R_{AB}, is a quantitative measure of their separation, and is defined as

$$R_{AB} = \frac{t_{t,B} - t_{t,A}}{0.5\,(w_B + w_A)} = \frac{2\Delta t_r}{w_B + w_A} \tag{8.5.1}$$

where B is the later eluting of the two solutes. As shown in Figure 12.2.5 , the separation of two chromatographic peaks improves with an increase in R_{AB}. If the areas under the two peaks are identical—as is the case in Figure 12.2.5 —then a resolution of 1.50 corresponds to an overlap of only 0.13% for the two elution profiles. Because resolution is a quantitative measure of a separation's success, it is a useful way to determine if a change in experimental conditions leads to a better separation.

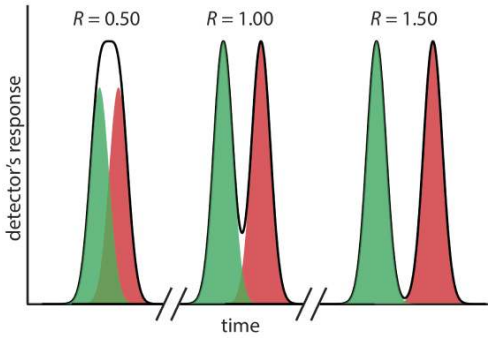


Figure 12.2.5 . Three examples that show the relationship between resolution and the separation of a two component mixture. The green peak and the red peak are the elution profiles for the two components. The chromatographic peak— which is the sum of the two elution profiles—is shown by the solid black line.

Example 12.2.1

In a chromatographic analysis of lemon oil a peak for limonene has a retention time of 8.36 min with a baseline width of 0.96 min. γ-Terpinene elutes at 9.54 min with a baseline width of 0.64 min. What is the resolution between the two peaks?

Solution

Using Equation 8.5.1 we find that the resolution is

$$R_{AB} = \frac{2\Delta t_r}{w_B + w_A} = \frac{2(9.54\text{ min} - 8.36\text{ min})}{0.64\text{ min} + 0.96\text{ min}} = 1.48$$

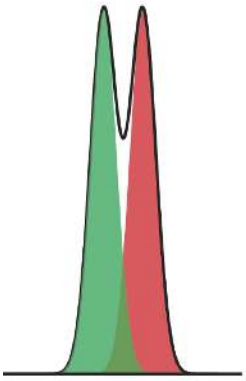


Figure 12.2.6 . Chromatogram for Exercise 12.2.1 .

Exercise 12.2.1

Figure 12.2.6 shows the separation of a two-component mixture. What is the resolution between the two components? Use a ruler to measure Δt_r, w_A, and w_B in millimeters.

Answer

Because the relationship between elution time and distance is proportional, we can measure Δt_r, w_A, and w_B using a ruler. My measurements are 8.5 mm for Δt_r, and 12.0 mm each for w_A and w_B. Using these values, the resolution is

$$R_{AB} = \frac{2\Delta t_t}{w_A + w_B} = \frac{2(8.5\text{ mm})}{12.0\text{ mm} + 12.0\text{ mm}} = 0.70$$

Your measurements for Δt_r, w_A, and w_B will depend on the relative size of your monitor or printout; however, your value for the resolution should be similar to the answer above.

Equation 8.5.1 suggests that we can improve resolution by increasing Δt_r, or by decreasing w_A and w_B (Figure 12.2.7). To increase Δt_r we can use one of two strategies. One approach is to adjust the separation conditions so that both solutes spend less time in the mobile phase—that is, we increase each *solute's retention factor*—which provides more time to effect a separation. A second approach is to increase *selectivity* by adjusting conditions so that only one solute experiences a significant change in its retention time. The baseline width of a solute's peak depends on the solutes movement within and between the mobile phase and the stationary phase, and is governed by several factors that collectively we call *column efficiency*. We will consider each of these approaches for improving resolution in more detail, but first we must define some terms.

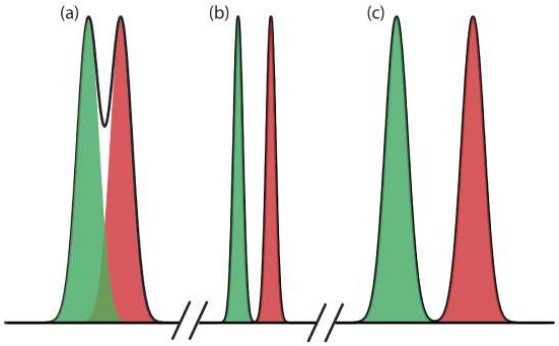


Figure 12.2.7 . Two method for improving chromatographic resolution: (a) original chromatogram; (b) chromatogram after decreasing w_A and w_B by 4×; and (c) chromatogram after increasing Δt_r by 2×.

Solute Retention Factor

Let's assume we can describe a solute's distribution between the mobile phase and stationary phase using the following equilibrium reaction

$$S_m \rightleftharpoons S_s$$

where S_m is the solute in the mobile phase and S_s is the solute in the stationary phase. Following the same approach we used in Chapter 7.7 for liquid–liquid extractions, the equilibrium constant for this reaction is an equilibrium partition coefficient, K_D.

$$K_D = \frac{[S_s]}{[S_m]}$$

This is not a trivial assumption. In this section we are, in effect, treating the solute's equilibrium between the mobile phase and the stationary phase as if it is identical to the equilibrium in a liquid–liquid extraction. You might question whether this is a reasonable assumption. There is an important difference between the two experiments that we need to consider. In a liquid–liquid extraction, which takes place in a separatory funnel, the two phases remain in contact with each other at all times, allowing for a true equilibrium. In chromatography, however, the mobile phase is in constant motion. A solute that moves into the stationary phase from the mobile phase will equilibrate back into a different portion of the mobile phase; this does not describe a true equilibrium.

So, we ask again: Can we treat a solute's distribution between the mobile phase and the stationary phase as an equilibrium process? The answer is yes, if the mobile phase velocity is slow relative to the kinetics of the solute's movement back and forth between the two phase. In general, this is a reasonable assumption.

In the absence of any additional equilibrium reactions in the mobile phase or the stationary phase, K_D is equivalent to the distribution ratio, D,

$$D = \frac{[S_0]}{[S_m]} = \frac{(\text{mol S})_s/V_s}{(\text{mol S})_m/V_m} = K_D \tag{8.5.2}$$

where V_s and V_m are the volumes of the stationary phase and the mobile phase, respectively.

A conservation of mass requires that the total moles of solute remain constant throughout the separation; thus, we know that the following equation is true.

$$(\text{mol S})_{tot} = (\text{mol S})_m + (\text{mol S})_s \tag{8.5.3}$$

Solving Equation 8.5.3 for the moles of solute in the stationary phase and substituting into Equation 8.5.2 leaves us with

$$D = \frac{\{(\text{mol S})_{tot} - (\text{mol S})_m\}/V_s}{(\text{mol S})_m/V_m}$$

Rearranging this equation and solving for the fraction of solute in the mobile phase, f_m, gives

$$f_m = \frac{(\text{mol S})_m}{(\text{mol S})_{tot}} = \frac{V_m}{DV_s + V_m} \tag{8.5.4}$$

which is identical to the result for a liquid-liquid extraction (see Chapter 7). Because we may not know the exact volumes of the stationary phase and the mobile phase, we simplify Equation 8.5.4 by dividing both the numerator and the denominator by V_m; thus

$$f_m = \frac{V_m/V_m}{DV_s/V_m + V_m/V_m} = \frac{1}{DV_s/V_m + 1} = \frac{1}{1+k} \tag{8.5.5}$$

where k

$$k = D \times \frac{V_s}{V_m} \tag{8.5.6}$$

is the solute's ***retention factor***. Note that the larger the retention factor, the more the distribution ratio favors the stationary phase, leading to a more strongly retained solute and a longer retention time.

Other (older) names for the retention factor are capacity factor, capacity ratio, and partition ratio, and it sometimes is given the symbol k'. Keep this in mind if you are using other resources. Retention factor is the approved name from the IUPAC Gold

Book.

We can determine a solute's retention factor from a chromatogram by measuring the column's void time, t_m, and the solute's retention time, t_r (see Figure 12.2.4). Solving Equation 8.5.5 for k, we find that

$$k = \frac{1 - f_m}{f_m} \tag{8.5.7}$$

Earlier we defined f_m as the fraction of solute in the mobile phase. Assuming a constant mobile phase velocity, we also can define f_m as

$$f_m = \frac{\text{time spent in the mobile phase}}{\text{time spent in the stationary phase}} = \frac{t_m}{t_r}$$

Substituting back into Equation 8.5.7 and rearranging leaves us with

$$k = \frac{1 - \frac{t_m}{t_t}}{\frac{t_m}{t_r}} = \frac{t_t - t_m}{t_m} = \frac{t'_r}{t_m} \tag{8.5.8}$$

where t'_r is the ***adjusted retention time***.

Example 12.2.2

In a chromatographic analysis of low molecular weight acids, butyric acid elutes with a retention time of 7.63 min. The column's void time is 0.31 min. Calculate the retention factor for butyric acid.

Solution

$$k_{but} = \frac{t_r - t_m}{t_m} = \frac{7.63 \text{ min} - 0.31 \text{ min}}{0.31 \text{ min}} = 23.6$$

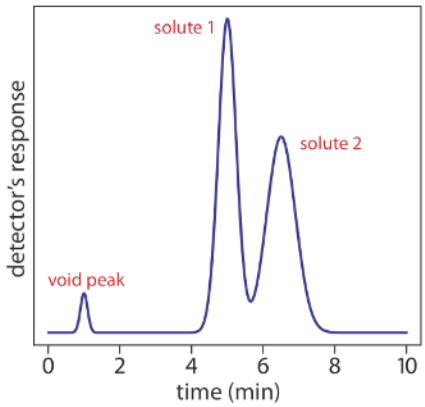


Figure 12.2.8 . Chromatogram for Exercise 12.2.2 .

Exercise 12.2.2

Figure 12.2.8 is the chromatogram for a two-component mixture. Determine the retention factor for each solute assuming the sample was injected at time t = 0.

Answer

Because the relationship between elution time and distance is proportional, we can measure t_m, $t_{r,1}$, and $t_{r,2}$ using a ruler. My measurements are 7.8 mm, 40.2 mm, and 51.5 mm, respectively. Using these values, the retention factors for solute A and solute B are

$$k_1 = \frac{t_{r1} - t_m}{t_m} = \frac{40.2 \text{ mm} - 7.8 \text{ mm}}{7.8 \text{ mm}} = 4.15$$

$$k_2 = \frac{t_{r2} - t_m}{t_m} = \frac{51.5 \text{ mm} - 7.8 \text{ mm}}{7.8 \text{ mm}} = 5.60$$

Your measurements for t_m, $t_{r,1}$, and $t_{r,2}$ will depend on the relative size of your monitor or printout; however, your value for the resolution should be similar to the answer above.

Selectivity

Selectivity is a relative measure of the retention of two solutes, which we define using a selectivity factor, α

$$\alpha = \frac{k_B}{k_A} = \frac{t_{r,B} - t_m}{t_{r,A} - t_m} \tag{8.5.9}$$

where solute A has the smaller retention time. When two solutes elute with identical retention time, $\alpha = 1.00$; for all other conditions $\alpha > 1.00$.

Example 12.2.3

In the chromatographic analysis for low molecular weight acids described in Example 12.2.2 , the retention time for isobutyric acid is 5.98 min. What is the selectivity factor for isobutyric acid and butyric acid?

Solution

First we must calculate the retention factor for isobutyric acid. Using the void time from Example 12.2.2 we have

$$k_{iso} = \frac{t_r - t_m}{t_m} = \frac{5.98 \text{ min} - 0.31 \text{ min}}{0.31 \text{ min}} = 18.3$$

The selectivity factor, therefore, is

$$\alpha = \frac{k_{but}}{k_{iso}} = \frac{23.6}{18.3} = 1.29$$

Exercise 12.2.3

Determine the selectivity factor for the chromatogram in Exercise 12.2.2 .

Answer

Using the results from Exercise 12.2.2 , the selectivity factor is

$$\alpha = \frac{k_2}{k_1} = \frac{5.60}{4.15} = 1.35$$

Your answer may differ slightly due to differences in your values for the two retention factors.

Column Efficiency

Suppose we inject a sample that has a single component. At the moment we inject the sample it is a narrow band of finite width. As the sample passes through the column, the width of this band continually increases in a process we call ***band broadening***. Column efficiency is a quantitative measure of the extent of band broadening.

See Figure 12.2.1 and Figure 12.2.2 . When we inject the sample it has a uniform, or rectangular concentration profile with respect to distance down the column. As it passes through the column, the band broadens and takes on a Gaussian concentration profile.

In their original theoretical model of chromatography, Martin and Synge divided the chromatographic column into discrete sections, which they called theoretical plates. Within each theoretical plate there is an equilibrium between the solute present in the

stationary phase and the solute present in the mobile phase [Martin, A. J. P.; Synge, R. L. M. *Biochem. J.* **1941**, *35*, 1358–1366]. They described column efficiency in terms of the number of ***theoretical plates***, *N*,

$$N = \frac{L}{H} \tag{8.5.10}$$

where *L* is the column's length and *H* is the height of a theoretical plate. For any given column, the column efficiency improves—and chromatographic peaks become narrower—when there are more theoretical plates.

If we assume that a chromatographic peak has a Gaussian profile, then the extent of band broadening is given by the peak's variance or standard deviation. The height of a theoretical plate is the peak's variance per unit length of the column

$$H = \frac{\sigma^2}{L} \tag{8.5.11}$$

where the standard deviation, σ, has units of distance. Because retention times and peak widths usually are measured in seconds or minutes, it is more convenient to express the standard deviation in units of time, τ, by dividing σ by the solute's average linear velocity, $\overline{u}$, which is equivalent to dividing the distance it travels, *L*, by its retention time, t_r.

$$\tau = \frac{\sigma}{\overline{u}} = \frac{\sigma t_r}{L} \tag{8.5.12}$$

For a Gaussian peak shape, the width at the baseline, *w*, is four times its standard deviation, τ.

$$w = 4\tau \tag{8.5.13}$$

Combining Equation 8.5.11, Equation 8.5.12, and Equation 8.5.13 defines the height of a theoretical plate in terms of the easily measured chromatographic parameters t_r and *w*.

$$H = \frac{Lw^2}{16t_r^2} \tag{8.5.14}$$

Combing Equation 8.5.14 and Equation 8.5.10 gives the number of theoretical plates.

$$N = 16\frac{t_r^2}{w^2} = 16\left(\frac{t_r}{w}\right)^2 \tag{8.5.15}$$

Example 12.2.4

A chromatographic analysis for the chlorinated pesticide Dieldrin gives a peak with a retention time of 8.68 min and a baseline width of 0.29 min. Calculate the number of theoretical plates? Given that the column is 2.0 m long, what is the height of a theoretical plate in mm?

Solution

Using Equation 8.5.15, the number of theoretical plates is

$$N = 16\frac{t_r^2}{w^2} = 16 \times \frac{(8.68\text{ min})^2}{(0.29\text{ min})^2} = 14300\text{ plates}$$

Solving Equation 8.5.10 for *H* gives the average height of a theoretical plate as

$$H = \frac{L}{N} = \frac{2.00\text{ m}}{14300\text{ plates}} \times \frac{1000\text{ mm}}{\text{m}} = 0.14\text{ mm/plate}$$

Exercise 12.2.4

For each solute in the chromatogram for Exercise 12.2.2 , calculate the number of theoretical plates and the average height of a theoretical plate. The column is 0.5 m long.

Answer

Because the relationship between elution time and distance is proportional, we can measure $t_{r,1}$, $t_{r,2}$, w_1, and w_2 using a ruler. My measurements are 40.2 mm, 51.5 mm, 8.0 mm, and 13.5 mm, respectively. Using these values, the number of theoretical plates for each solute is

$$N_1 = 16\frac{t_{r,1}^2}{w_1^2} = 16 \times \frac{(40.2\text{ mm})^2}{(8.0\text{ mm})^2} = 400\text{ theoretical plates}$$

$$N_2 = 16\frac{t_{r,2}^2}{w_2^2} = 16 \times \frac{(51.5\text{ mm})^2}{(13.5\text{ mm})^2} = 233\text{ theoretical plates}$$

The height of a theoretical plate for each solute is

$$H_1 = \frac{L}{N_1} = \frac{0.500\text{ m}}{400\text{ plates}} \times \frac{1000\text{ mm}}{\text{m}} = 1.2\text{ mm/plate}$$

$$H_2 = \frac{L}{N_2} = \frac{0.500\text{ m}}{233\text{ plates}} \times \frac{1000\text{ mm}}{\text{m}} = 2.15\text{ mm/plate}$$

Your measurements for $t_{r,1}$, $t_{r,2}$, w_1, and w_2 will depend on the relative size of your monitor or printout; however, your values for N and for H should be similar to the answer above.

It is important to remember that a theoretical plate is an artificial construct and that a chromatographic column does not contain physical plates. In fact, the number of theoretical plates depends on both the properties of the column and the solute. As a result, the number of theoretical plates for a column may vary from solute to solute.

Peak Capacity

One advantage of improving column efficiency is that we can separate more solutes with baseline resolution. One estimate of the number of solutes that we can separate is

$$n_c = 1 + \frac{\sqrt{N}}{4}\ln\frac{V_{max}}{V_{min}} \tag{8.5.16}$$

where n_c is the column's ***peak capacity***, and V_{min} and V_{max} are the smallest and the largest volumes of mobile phase in which we can elute and detect a solute [Giddings, J. C. *Unified Separation Science*, Wiley-Interscience: New York, 1991]. A column with 10 000 theoretical plates, for example, can resolve no more than

$$n_c = 1 + \frac{\sqrt{10000}}{4}\ln\frac{30\text{mL}}{1\text{mL}} = 86\text{ solutes}$$

if V_{min} and V_{max} are 1 mL and 30 mL, respectively. This estimate provides an upper bound on the number of solutes and may help us exclude from consideration a column that does not have enough theoretical plates to separate a complex mixture. Just because a column's theoretical peak capacity is larger than the number of solutes, however, does not mean that a separation is feasible. In most situations the practical peak capacity is less than the theoretical peak capacity because the retention characteristics of some solutes are so similar that a separation is impossible. Nevertheless, columns with more theoretical plates, or with a greater range of possible elution volumes, are more likely to separate a complex mixture.

The smallest volume we can use is the column's void volume. The largest volume is determined either by our patience—the maximum analysis time we can tolerate—or by our inability to detect solutes because there is too much band broadening.

Asymmetric Peaks

Our treatment of chromatography in this section assumes that a solute elutes as a symmetrical Gaussian peak, such as that shown in Figure 12.2.4 . This ideal behavior occurs when the solute's partition coefficient, K_D

$$K_D = \frac{[S_s]}{[S_m]}$$

is the same for all concentrations of solute. If this is not the case, then the chromatographic peak has an asymmetric peak shape similar to those shown in Figure 12.2.9 . The chromatographic peak in Figure 12.2.9 a is an example of ***peak tailing***, which occurs when some sites on the stationary phase retain the solute more strongly than other sites. Figure 12.2.9 b, which is an example of ***peak fronting*** most often is the result of overloading the column with sample.

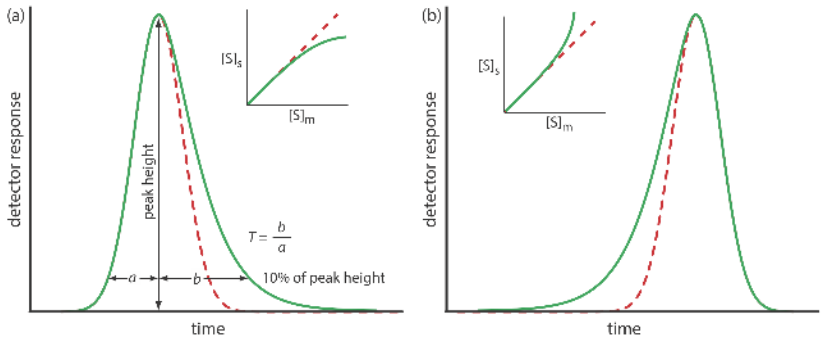


Figure 12.2.9 . Examples of asymmetric chromatographic peaks showing (a) peak tailing and (b) peak fronting. For both (a) and (b) the green chromatogram is the asymmetric peak and the red dashed chromatogram shows the ideal, Gaussian peak shape. The insets show the relationship between the concentration of solute in the stationary phase, $[S]_s$, and its concentration in the mobile phase, $[S]_m$. The dashed red lines show ideal behavior (K_D is constant for all conditions) and the green lines show nonideal behavior (K_D decreases or increases for higher total concentrations of solute). A quantitative measure of peak tailing, T, is shown in (a).

As shown in Figure 12.2.9 a, we can report a peak's asymmetry by drawing a horizontal line at 10% of the peak's maximum height and measuring the distance from each side of the peak to a line drawn vertically through the peak's maximum. The asymmetry factor, T, is defined as

$$T = \frac{b}{a}$$

The number of theoretical plates for an asymmetric peak shape is approximately

$$N \approx \frac{41.7 \times \frac{t_r^2}{(w_{0.1})^2}}{T + 1.25} = \frac{41.7 \times \frac{t_r^2}{(a+b)^2}}{T + 1.25}$$

where $w_{0.1}$ is the width at 10% of the peak's height [Foley, J. P.; Dorsey, J. G. *Anal. Chem.* **1983**, *55*, 730–737].

Asymmetric peaks have fewer theoretical plates, and the more asymmetric the peak the smaller the number of theoretical plates. For example, the following table gives values for N for a solute eluting with a retention time of 10.0 min and a peak width of 1.00 min.

b	a	T	N
0.5	0.5	1.00	1850
0.6	0.4	1.50	1520
0.7	0.3	2.33	1160
0.8	0.2	4.00	790

This page titled 8.5: General Theory of Column Chromatography is shared under a CC BY-NC-SA 4.0 license and was authored, remixed, and/or curated by Kathryn Davis.

- **12.2: General Theory of Column Chromatography** by David Harvey is licensed CC BY-NC-SA 4.0.

8.6: Optimizing Chromatographic Separations

Now that we have defined the solute retention factor, selectivity, and column efficiency we are able to consider how they affect the resolution of two closely eluting peaks. Because the two peaks have similar retention times, it is reasonable to assume that their peak widths are nearly identical. If the number of theoretical plates is the same for all solutes—not strictly true, but not a bad assumption—then from equation 12.2.15, the ratio t_r/w is a constant. If two solutes have similar retention times, then their peak widths must be similar. Equation 12.2.1, therefore, becomes

$$R_{AB} = \frac{t_{r,B} - t_{r,A}}{0.5\,(w_B + w_A)} \approx \frac{t_{r,B} - t_{r,A}}{0.5\,(2w_B)} = \frac{t_{r,B} - t_{r,A}}{w_B} \tag{8.6.1}$$

where B is the later eluting of the two solutes. Solving equation 12.2.15 for w_B and substituting into Equation 8.6.1 leaves us with the following result.

$$R_{AB} = \frac{\sqrt{N_B}}{4} \times \frac{t_{r,B} - t_{r,A}}{t_{r,B}} \tag{8.6.2}$$

Rearranging equation 12.2.8 provides us with the following equations for the retention times of solutes A and B.

$$t_{r,A} = k_A t_m + t_m \quad \text{and} \quad t_{r,B} = k_B t_m + t_m$$

After substituting these equations into Equation 8.6.2 and simplifying, we have

$$R_{AB} = \frac{\sqrt{N_B}}{4} \times \frac{k_B - k_A}{1 + k_B}$$

Finally, we can eliminate solute A's retention factor by substituting in equation 12.2.9. After rearranging, we end up with the following equation for the resolution between the chromatographic peaks for solutes A and B.

$$R_{AB} = \frac{\sqrt{N_B}}{4} \times \frac{\alpha - 1}{\alpha} \times \frac{k_B}{1 + k_B} \tag{8.6.3}$$

In addition to resolution, another important factor in chromatography is the amount of time needed to elute a pair of solutes, which we can approximate using the retention time for solute B.

$$t_{r,s} = \frac{16 R_{AB}^2 H}{u} \times \left(\frac{\alpha}{\alpha - 1}\right)^2 \times \frac{(1 + k_B)^3}{k_B^2} \tag{8.6.4}$$

where u is the mobile phase's velocity.

> Although Equation 8.6.3 is useful for considering how a change in N, α, or k qualitatively affects resolution—which suits our purpose here—it is less useful for making accurate quantitative predictions of resolution, particularly for smaller values of N and for larger values of R. For more accurate predictions use the equation
>
> $$R_{AB} = \frac{\sqrt{N}}{4} \times (\alpha - 1) \times \frac{k_B}{1 + k_{avg}}$$
>
> where k_{avg} is $(k_A + k_B)/2$. For a derivation of this equation and for a deeper discussion of resolution in column chromatography, see Foley, J. P. "Resolution Equations for Column Chromatography," *Analyst*, **1991**, *116*, 1275-1279.

Equation 8.6.3 and Equation 8.6.4 contain terms that correspond to column efficiency, selectivity, and the solute retention factor. We can vary these terms, more or less independently, to improve resolution and analysis time. The first term, which is a function of the number of theoretical plates (for Equation 8.6.3) or the height of a theoretical plate (for Equation 8.6.4), accounts for the effect of column efficiency. The second term is a function of α and accounts for the influence of column selectivity. Finally, the third term in both equations is a function of k_B and accounts for the effect of solute B's retention factor. A discussion of how we can use these parameters to improve resolution is the subject of the remainder of this section.

Using the Retention Factor to Optimize Resolution

One of the simplest ways to improve resolution is to adjust the retention factor for solute *B*. If all other terms in Equation 8.6.3 remain constant, an increase in k_B will improve resolution. As shown by the green curve in Figure 8.6.1 , however, the improvement is greatest if the initial value of k_B is small. Once k_B exceeds a value of approximately 10, a further increase produces only a marginal improvement in resolution. For example, if the original value of k_B is 1, increasing its value to 10 gives an 82% improvement in resolution; a further increase to 15 provides a net improvement in resolution of only 87.5%.

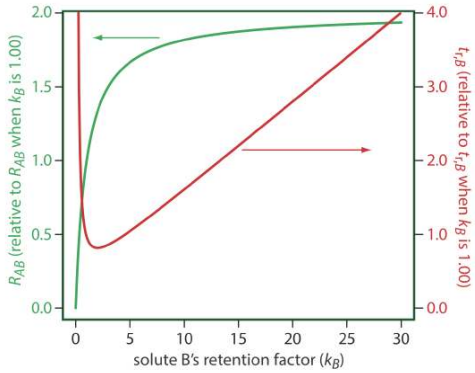


Figure 8.6.1 . Effect of k_B on the resolution for a pair of solutes, R_{AB}, and the retention time for the later eluting solute, $t_{r,B}$. The *y*-axes display the resolution and retention time relative to their respective values when k_B is 1.00.

Any improvement in resolution from increasing the value of k_B generally comes at the cost of a longer analysis time. The red curve in Figure 8.6.1 shows the relative change in the retention time for solute *B* as a function of its retention factor. Note that the minimum retention time is for $k_B = 2$. Increasing k_B from 2 to 10, for example, approximately doubles solute B's retention time.

> The relationship between retention factor and analysis time in Figure 8.6.1 works to our advantage if a separation produces an acceptable resolution with a large k_B. In this case we may be able to decrease k_B with little loss in resolution and with a significantly shorter analysis time.

To increase k_B without changing selectivity, α, any change to the chromatographic conditions must result in a general, nonselective increase in the retention factor for both solutes. In gas chromatography, we can accomplish this by decreasing the column's temperature. Because a solute's vapor pressure is smaller at lower temperatures, it spends more time in the stationary phase and takes longer to elute. In liquid chromatography, the easiest way to increase a solute's retention factor is to use a mobile phase that is a weaker solvent. When the mobile phase has a lower solvent strength, solutes spend proportionally more time in the stationary phase and take longer to elute.

Adjusting the retention factor to improve the resolution between one pair of solutes may lead to unacceptably long retention times for other solutes. For example, suppose we need to analyze a four-component mixture with baseline resolution and with a run-time of less than 20 min. Our initial choice of conditions gives the chromatogram in Figure 8.6.2 a. Although we successfully separate components 3 and 4 within 15 min, we fail to separate components 1 and 2. Adjusting conditions to improve the resolution for the first two components by increasing k_2 provides a good separation of all four components, but the run-time is too long (Figure 8.6.2 b). This problem of finding a single set of acceptable operating conditions is known as the ***general elution problem***.

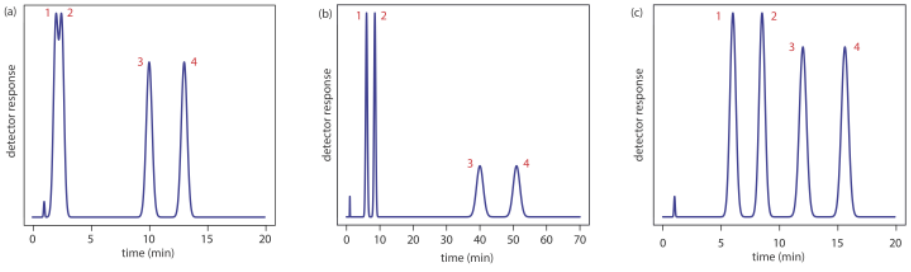


Figure 8.6.2 . Example showing the general elution problem in chromatography. See text for details.

https://chem.libretexts.org/@go/page/556152

One solution to the general elution problem is to make incremental adjustments to the retention factor as the separation takes place. At the beginning of the separation we set the initial chromatographic conditions to optimize the resolution for early eluting solutes. As the separation progresses, we adjust the chromatographic conditions to decrease the retention factor—and, therefore, to decrease the retention time—for each of the later eluting solutes (Figure 8.6.2 c). In gas chromatography this is accomplished by temperature programming. The column's initial temperature is selected such that the first solutes to elute are resolved fully. The temperature is then increased, either continuously or in steps, to bring off later eluting components with both an acceptable resolution and a reasonable analysis time. In liquid chromatography the same effect is obtained by increasing the solvent's eluting strength. This is known as a gradient elution. We will have more to say about each of these in later sections of this chapter.

Using Selectivity to Optimize Resolution

A second approach to improving resolution is to adjust the selectivity, α. In fact, for $\alpha \approx 1$ usually it is not possible to improve resolution by adjusting the solute retention factor, k_B, or the column efficiency, N. A change in α often has a more dramatic effect on resolution than a change in k_B. For example, changing α from 1.1 to 1.5, while holding constant all other terms, improves resolution by 267%. In gas chromatography, we adjust α by changing the stationary phase; in liquid chromatography, we change the composition of the mobile phase to adjust α.

To change α we need to selectively adjust individual solute retention factors. Figure 8.6.3 shows one possible approach for the liquid chromatographic separation of a mixture of substituted benzoic acids. Because the retention time of a compound's weak acid form and its weak base form are different, its retention time will vary with the pH of the mobile phase, as shown in Figure 8.6.3 a. The intersections of the curves in Figure 8.6.3 a show pH values where two solutes co-elute. For example, at a pH of 3.8 terephthalic acid and *p*-hydroxybenzoic acid elute as a single chromatographic peak.

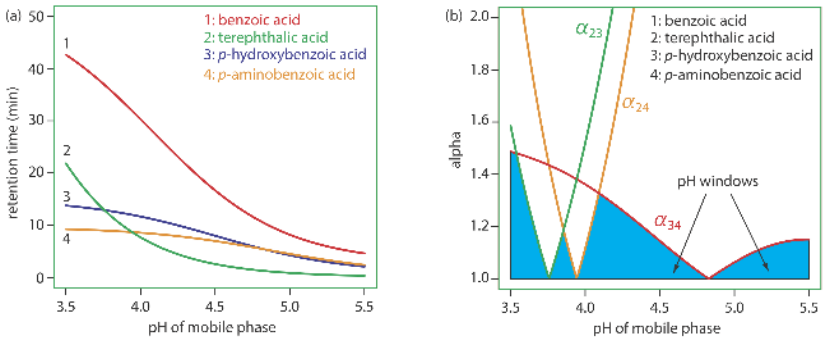


Figure 8.6.3 . Example showing how the mobile phase pH in liquid chromatography affects selectivity: (a) retention times for four substituted benzoic acids as a function of the mobile phase's pH; (b) alpha values for three pairs of solutes that are difficult to separate. See text for details. The mobile phase is an acetic acid/sodium acetate buffer and the stationary phase is a nonpolar hydrocarbon. Data from Harvey, D. T.; Byerly, S.; Bowman, A.; Tomlin, J. "Optimization of HPLC and GC Separations Using Response Surfaces," *J. Chem. Educ.* **1991**, *68*, 162–168.

Figure 8.6.3 a shows that there are many pH values where some separation is possible. To find the optimum separation, we plot a for each pair of solutes. The red, green, and orange curves in Figure 8.6.3 b show the variation in a with pH for the three pairs of solutes that are hardest to separate (for all other pairs of solutes, $\alpha > 2$ at all pH levels). The blue shading shows windows of pH values in which at least a partial separation is possible—this figure is sometimes called a window diagram—and the highest point in each window gives the optimum pH within that range. The best overall separation is the highest point in any window, which, for this example, is a pH of 3.5. Because the analysis time at this pH is more than 40 min (Figure 8.6.3 a), choosing a pH between 4.1–4.4 might produce an acceptable separation with a much shorter analysis time.

Let's use benzoic acid, C_6H_5COOH, to explain why pH can affect a solute's retention time. The separation uses an aqueous mobile phase and a nonpolar stationary phase. At lower pHs, benzoic acid predominately is in its weak acid form, C_6H_5COOH, and partitions easily into the nonpolar stationary phase. At more basic pHs, however, benzoic acid is in its weak base form, $C_6H_5COO^-$. Because it now carries a charge, its solubility in the mobile phase increases and its solubility in the nonpolar stationary phase decreases. As a result, it spends more time in the mobile phase and has a shorter retention time.

Although the usual way to adjust pH is to change the concentration of buffering agents, it also is possible to adjust pH by changing the column's temperature because a solute's pK_a value is pH-dependent; for a review, see Gagliardi, L. G.; Tascon, M.; Castells, C. B. "Effect of Temperature on Acid–Base Equilibria in Separation Techniques: A Review," *Anal. Chim. Acta*, **2015**, *889*, 35–57.

Using Column Efficiency to Optimize Resolution

A third approach to improving resolution is to adjust the column's efficiency by increasing the number of theoretical plates, *N*. If we have values for k_B and α, then we can use Equation 8.6.3 to calculate the number of theoretical plates for any resolution. Table 8.6.1 provides some representative values. For example, if α = 1.05 and k_B = 2.0, a resolution of 1.25 requires approximately 24 800 theoretical plates. If our column provides only 12 400 plates, half of what is needed, then a separation is not possible. How can we double the number of theoretical plates? The easiest way is to double the length of the column, although this also doubles the analysis time. A better approach is to cut the height of a theoretical plate, *H*, in half, providing the desired resolution without changing the analysis time. Even better, if we can decrease *H* by more than 50%, it may be possible to achieve the desired resolution with an even shorter analysis time by also decreasing k_B or α.

Table 8.6.1 . Minimum Number of Theoretical Plates to Achieve Desired Resolution for Selected Values of k_B and α

	R_{AB} = 1.00		R_{AB} = 1.25		R_{AB} = 1.50	
k_B	$\alpha = 1.05$	$\alpha = 1.10$	$\alpha = 1.05$	$\alpha = 1.10$	$\alpha = 1.05$	$\alpha = 1.10$
0.5	63500	17400	99200	27200	143000	39200
1.0	28200	7740	44100	12100	63500	17400
1.5	19600	5380	30600	8400	44100	12100
2.0	15900	4360	24800	6810	35700	9800
3.0	12500	3440	19600	5380	28200	7740
5.0	10200	2790	15900	4360	22900	6270
10.0	8540	2340	13300	3660	19200	5270

To decrease the height of a theoretical plate we need to understand the experimental factors that affect band broadening. There are several theoretical treatments of band broadening. We will consider one approach that considers four contributions: variations in path lengths, longitudinal diffusion, mass transfer in the stationary phase, and mass transfer in the mobile phase.

Multiple Paths: Variations in Path Length

As solute molecules pass through the column they travel paths that differ in length. Because of this difference in path length, two solute molecules that enter the column at the same time will exit the column at different times. The result, as shown in Figure 8.6.4 , is a broadening of the solute's profile on the column. The contribution of ***multiple paths*** to the height of a theoretical plate, H_p, is

$$H_p = 2\lambda d_p \tag{8.6.5}$$

where d_p is the average diameter of the particulate packing material and λ is a constant that accounts for the consistency of the packing. A smaller range of particle sizes and a more consistent packing produce a smaller value for λ. For a column without packing material, H_p is zero and there is no contribution to band broadening from multiple paths.

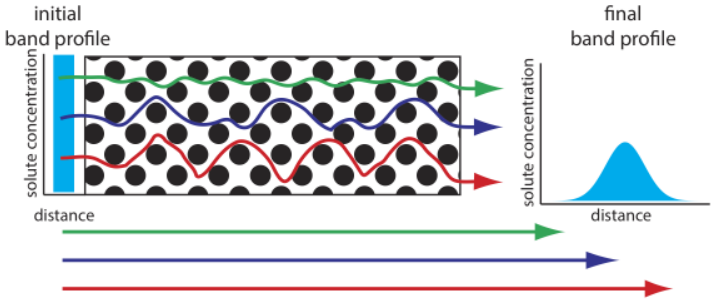


Figure 8.6.4 . The effect of multiple paths on a solute's band broadening. The solute's initial band profile is rectangular. As this band travels through the column, individual solute molecules travel different paths, three of which are shown by the meandering colored paths (the actual lengths of these paths are shown by the straight arrows at the bottom of the figure). Most solute molecules travel paths with lengths similar to that shown in blue, with a few traveling much shorter paths (green) or much longer paths (red). As a result, the solute's band profile at the end of the column is broader and Gaussian in shape.

An inconsistent packing creates channels that allow some solute molecules to travel quickly through the column. It also can creates pockets that temporarily trap some solute molecules, slowing their progress through the column. A more uniform packing minimizes these problems.

Longitudinal Diffusion

The second contribution to band broadening is the result of the solute's ***longitudinal diffusion*** in the mobile phase. Solute molecules are in constant motion, diffusing from regions of higher solute concentration to regions where the concentration of solute is smaller. The result is an increase in the solute's band width (Figure 8.6.5). The contribution of longitudinal diffusion to the height of a theoretical plate, H_d, is

$$H_d = \frac{2\gamma D_m}{u} \tag{8.6.6}$$

where D_m is the solute's diffusion coefficient in the mobile phase, u is the mobile phase's velocity, and γ is a constant related to the efficiency of column packing. Note that the effect of H_d on band broadening is inversely proportional to the mobile phase velocity: a higher velocity provides less time for longitudinal diffusion. Because a solute's diffusion coefficient is larger in the gas phase than in a liquid phase, longitudinal diffusion is a more serious problem in gas chromatography.

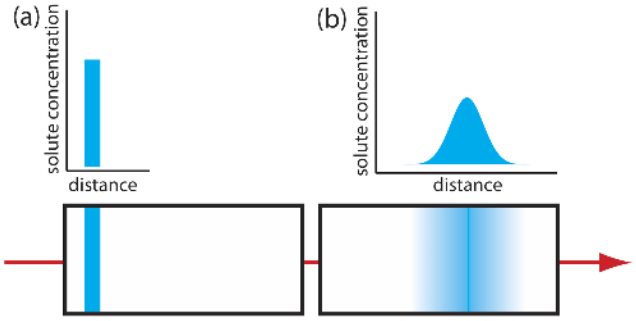


Figure 8.6.5 . The effect of longitudinal diffusion on a solute's band broadening. Two horizontal cross-sections through the column and the corresponding concentration versus distance profiles are shown, with (a) being earlier in time. The red arrow shows the direction in which the mobile phase is moving.

Mass Transfer

As the solute passes through the column it moves between the mobile phase and the stationary phase. We call this movement between phases ***mass transfer***. As shown in Figure 8.6.6 , band broadening occurs if the solute's movement within the mobile phase or within the stationary phase is not fast enough to maintain an equilibrium in its concentration between the two phases. On average, a solute molecule in the mobile phase moves down the column before it passes into the stationary phase. A solute molecule in the stationary phase, on the other hand, takes longer than expected to move back into the mobile phase. The

contributions of mass transfer in the stationary phase, H_s, and mass transfer in the mobile phase, H_m, are given by the following equations

$$H_s = \frac{qkd_f^2}{(1+k)^2 D_s} u \tag{8.6.7}$$

$$H_m = \frac{fn\left(d_p^2, d_c^2\right)}{D_m} u \tag{8.6.8}$$

where d_f is the thickness of the stationary phase, d_c is the diameter of the column, D_s and D_m are the diffusion coefficients for the solute in the stationary phase and the mobile phase, k is the solute's retention factor, and q is a constant related to the column packing material. Although the exact form of H_m is not known, it is a function of particle size and column diameter. Note that the effect of H_s and H_m on band broadening is directly proportional to the mobile phase velocity because a smaller velocity provides more time for mass transfer.

> The abbreviation *fn* in Equation 8.6.7 means "is a function of."

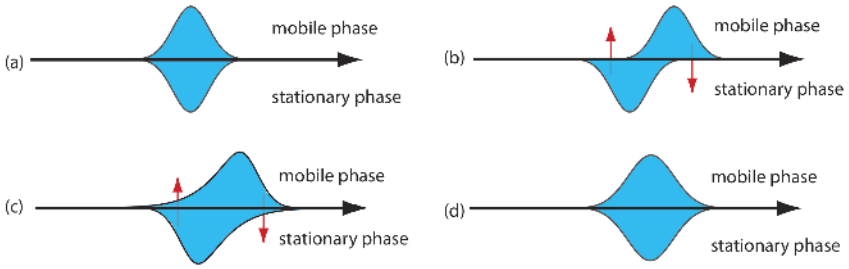


Figure 8.6.6 . Effect of mass transfer on band broadening: (a) Ideal equilibrium Gaussian profiles for the solute in the mobile phase and in the stationary phase. (b, c) If we allow the solute's band to move a small distance down the column, an equilibrium between the two phases no longer exits. The red arrows show the movement of solute—what we call the mass transfer of solute—from the stationary phase to the mobile phase, and from the mobile phase to the stationary phase. (d) Once equilibrium is reestablished, the solute's band is now broader.

Putting It All Together

The height of a theoretical plate is a summation of the contributions from each of the terms affecting band broadening.

$$H = H_p + H_d + H_s + H_m \tag{8.6.9}$$

An alternative form of this equation is the ***van Deemter equation***

$$H = A + \frac{B}{u} + Cu \tag{8.6.10}$$

which emphasizes the importance of the mobile phase's velocity. In the van Deemter equation, A accounts for the contribution of multiple paths (H_p), B/u accounts for the contribution of longitudinal diffusion (H_d), and Cu accounts for the combined contribution of mass transfer in the stationary phase and in the mobile phase (H_s and H_m).

There is some disagreement on the best equation for describing the relationship between plate height and mobile phase velocity [Hawkes, S. J. *J. Chem. Educ.* **1983**, *60*, 393–398]. In addition to the van Deemter equation, other equations include

$$H = \frac{B}{u} + (C_s + C_m)\, u$$

where C_s and C_m are the mass transfer terms for the stationary phase and the mobile phase and

$$H = Au^{1/3} + \frac{B}{u} + Cu$$

All three equations, and others, have been used to characterize chromatographic systems, with no single equation providing the best explanation in every case [Kennedy, R. T.; Jorgenson, J. W. *Anal. Chem.* **1989**, *61*, 1128–1135].

To increase the number of theoretical plates without increasing the length of the column, we need to decrease one or more of the terms in Equation 8.6.9. The easiest way to decrease H is to adjust the velocity of the mobile phase. For smaller mobile phase velocities, column efficiency is limited by longitudinal diffusion, and for higher mobile phase velocities efficiency is limited by the two mass transfer terms. As shown in Figure 8.6.7 —which uses the van Deemter equation—the optimum mobile phase velocity is the minimum in a plot of H as a function of u.

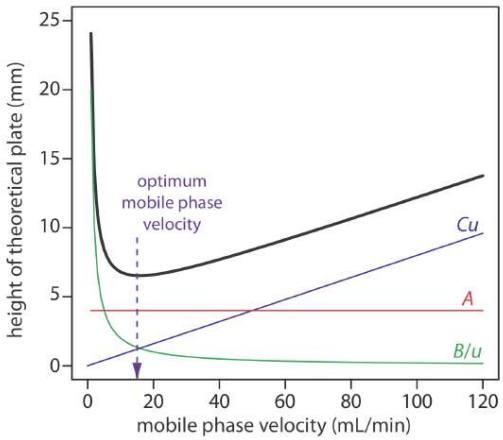


Figure 8.6.7 . Plot showing the relationship between the height of a theoretical plate, H, and the mobile phase's velocity, u, based on the van Deemter equation.

The remaining parameters that affect the terms in Equation 8.6.9 are functions of the column's properties and suggest other possible approaches to improving column efficiency. For example, both H_p and H_m are a function of the size of the particles used to pack the column. Decreasing particle size, therefore, is another useful method for improving efficiency.

> For a more detailed discussion of ways to assess the quality of a column, see Desmet, G.; Caooter, D.; Broeckhaven, K. "Graphical Data Represenation Methods to Assess the Quality of LC Columns," *Anal. Chem.* **2015**, *87*, 8593–8602.

Perhaps the most important advancement in chromatography columns is the development of open-tubular, or ***capillary columns***. These columns have very small diameters ($d_c \approx$ 50–500 μm) and contain no packing material ($d_p = 0$). Instead, the capillary column's interior wall is coated with a thin film of the stationary phase. Plate height is reduced because the contribution to H from H_p (Equation 8.6.5) disappears and the contribution from H_m (Equation 8.6.8) becomes smaller. Because the column does not contain any solid packing material, it takes less pressure to move the mobile phase through the column, which allows for longer columns. The combination of a longer column and a smaller height for a theoretical plate increases the number of theoretical plates by approximately $100\times$. Capillary columns are not without disadvantages. Because they are much narrower than packed columns, they require a significantly smaller amount of sample, which may be difficult to inject reproducibly. Another approach to improving resolution is to use thin films of stationary phase, which decreases the contribution to H from H_s (Equation 8.6.7).

> The smaller the particles, the more pressure is needed to push the mobile phase through the column. As a result, for any form of chromatography there is a practical limit to particle size.

This page titled 8.6: Optimizing Chromatographic Separations is shared under a CC BY-NC-SA 4.0 license and was authored, remixed, and/or curated by Kathryn Davis.

- **12.3: Optimizing Chromatographic Separations** by David Harvey is licensed CC BY-NC-SA 4.0.

8.7: Gas Chromatography

In ***gas chromatography*** (GC) we inject the sample, which may be a gas or a liquid, into an gaseous mobile phase (often called the carrier gas). The mobile phase carries the sample through a packed or a capillary column that separates the sample's components based on their ability to partition between the mobile phase and the stationary phase. Figure 8.7.1 shows an example of a typical gas chromatograph, which consists of several key components: a supply of compressed gas for the mobile phase; a heated injector, which rapidly volatilizes the components in a liquid sample; a column, which is placed within an oven whose temperature we can control during the separation; and a detector to monitor the eluent as it comes off the column. Let's consider each of these components.



Figure 8.7.1 . Example of a typical gas chromatograph with insets showing the heated injection ports—note the symbol indicating that it is hot—and the oven that houses the column. This particular instrument is equipped with an autosampler for injecting samples, a capillary column, and a mass spectrometer (MS) as the detector. Note that the carrier gas is supplied by a tank of compressed gas.

Mobile Phase

The most common mobile phases for gas chromatography are He, Ar, and N_2, which have the advantage of being chemically inert toward both the sample and the stationary phase. The choice of carrier gas often is determined by the needs of instrument's detector. For a packed column the mobile phase velocity usually is 25–150 mL/min. The typical flow rate for a capillary column is 1–25 mL/min.

Chromatographic Columns

There are two broad classes of chromatographic columns: packed columns and capillary columns. In general, a packed column can handle larger samples and a capillary column can separate more complex mixtures.

Packed Columns

Packed columns are constructed from glass, stainless steel, copper, or aluminum, and typically are 2–6 m in length with internal diameters of 2–4 mm. The column is filled with a particulate solid support, with particle diameters ranging from 37–44 μm to 250–354 μm. Figure 8.7.2 shows a typical example of a packed column.

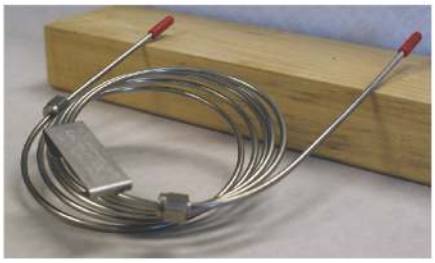


Figure 8.7.2 . Typical example of a packed column for gas chromatography. This column is made from stainless steel and is 2 m long with an internal diameter of 3.2 mm. The packing material in this column has a particle diameter of 149–177 μm. To put this in perspective, beach sand has a typical diameter of 700 μm and the diameter of fine grained sand is 250 μm.

The most widely used particulate support is diatomaceous earth, which is composed of the silica skeletons of diatoms. These particles are very porous, with surface areas ranging from 0.5–7.5 m^2/g, which provides ample contact between the mobile phase and the stationary phase. When hydrolyzed, the surface of a diatomaceous earth contains silanol groups (–SiOH), that serve as active sites for absorbing solute molecules in gas-solid chromatography (GSC).

In ***gas-liquid chromatography*** (GLC), we coat the packing material with a liquid mobile phase. To prevent uncoated packing material from adsorbing solutes, which degrades the quality of the separation, surface silanols are deactivated by reacting them with dimethyldichlorosilane and rinsing with an alcohol—typically methanol—before coating the particles with stationary phase.

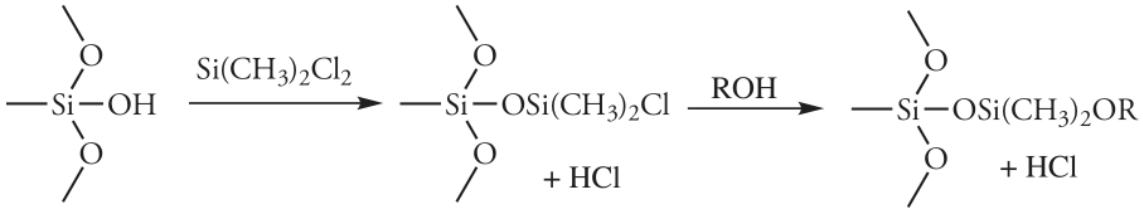


Figure 8.7.2 , for example, has approximately 1800 plates/m, or a total of approximately 3600 theoretical plates. If we assume a $V_{max}/V_{min} \approx 50$, then it has a peak capacity (equation 12.2.16) of

$$n_c = 1 + \frac{\sqrt{3600}}{4}\ln(50) \approx 60$$

Capillary Columns

A capillary, or ***open tubular column*** is constructed from fused silica and is coated with a protective polymer coating. Columns range from 15–100 m in length with an internal diameter of approximately 150–300 μm. Figure 8.7.3 shows an example of a typical capillary column.



Figure 8.7.3 . Typical example of a capillary column for gas chromatography. This column is 30 m long with an internal diameter of 247 μm. The interior surface of the capillary has a 0.25 μm coating of the liquid phase.

Capillary columns are of three principal types. In a ***wall-coated open tubular column*** (WCOT) a thin layer of stationary phase, typically 0.25 nm thick, is coated on the capillary's inner wall. In a ***porous-layer open tubular column*** (PLOT), a porous solid support—alumina, silica gel, and molecular sieves are typical examples—is attached to the capillary's inner wall. A ***support-coated open tubular column*** (SCOT) is a PLOT column that includes a liquid stationary phase. Figure 8.7.4 shows the differences between these types of capillary columns.

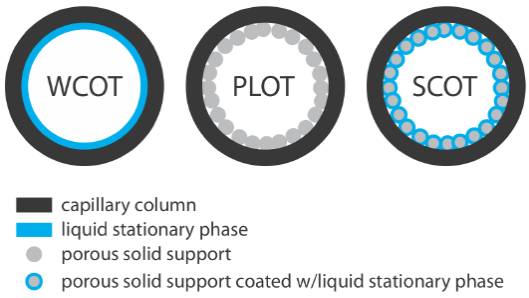


Figure 8.7.4 . Cross sections through the three types of capillary columns.

A capillary column provides a significant improvement in separation efficiency because it has more theoretical plates per meter and is longer than a packed column. For example, the capillary column in Figure 8.7.3 has almost 4300 plates/m, or a total of 129 000 theoretical plates. If we assume a $V_{max}/V_{min} \approx 50$, then it has a peak capacity of approximately 350. On the other hand, a packed column can handle a larger sample. Because of its smaller diameter, a capillary column requires a smaller sample, typically less than 10^{-2} μL.

Stationary Phases for Gas-Liquid Chromatography

Elution order in gas–liquid chromatography depends on two factors: the boiling point of the solutes, and the interaction between the solutes and the stationary phase. If a mixture's components have significantly different boiling points, then the choice of stationary phase is less critical. If two solutes have similar boiling points, then a separation is possible only if the stationary phase selectively interacts with one of the solutes. As a general rule, nonpolar solutes are separated more easily when using a nonpolar stationary phase, and polar solutes are easier to separate when using a polar stationary phase.

There are several important criteria for choosing a stationary phase: it must not react with the solutes, it must be thermally stable, it must have a low volatility, and it must have a polarity that is appropriate for the sample's components. Table 8.7.1 summarizes the properties of several popular stationary phases.

Table 8.7.1 . Selected Examples of Stationary Phases for Gas-Liquid Chromatography

stationary phase	polarity	trade name	temperature limit (°C)	representative applications
squalane	nonpolar	Squalane	150	low-boiling aliphatics hydrocarbons
Apezion L	nonpolar	Apezion L	300	amides, fatty acid methyl esters, terpenoids
polydimethyl siloxane	slightly polar	SE-30	300–350	alkaloids, amino acid derivatives, drugs, pesticides, phenols, steroids
phenylmethyl polysiloxane (50% phenyl, 50% methyl)	moderately polar	OV-17	375	alkaloids, drugs, pesticides, polyaromatic hydrocarbons, polychlorinated biphenyls
trifluoropropylmethyl polysiloxane (50% trifluoropropyl, 50% methyl)	moderately polar	OV-210	275	alkaloids, amino acid derivatives, drugs, halogenated compounds, ketones
cyanopropylphenylmethyl polysiloxane (50%cyanopropyl, 50% phenylmethyl)	polar	OV-225	275	nitriles, pesticides, steroids
polyethylene glycol	polar	Carbowax 20M	225	aldehydes, esters, ethers, phenols

Many stationary phases have the general structure shown in Figure 8.7.5 a. A stationary phase of polydimethyl siloxane, in which all the –R groups are methyl groups, $–CH_3$, is nonpolar and often makes a good first choice for a new separation. The order of elution when using polydimethyl siloxane usually follows the boiling points of the solutes, with lower boiling solutes eluting first. Replacing some of the methyl groups with other substituents increases the stationary phase's polarity and provides greater selectivity. For example, replacing 50% of the $–CH_3$ groups with phenyl groups, $–C_6H_5$, produces a slightly polar stationary phase. Increasing polarity is provided by substituting trifluoropropyl, $–C_3H_6CF$, and cyanopropyl, $–C_3H_6CN$, functional groups, or by using a stationary phase of polyethylene glycol (Figure 8.7.5 b).

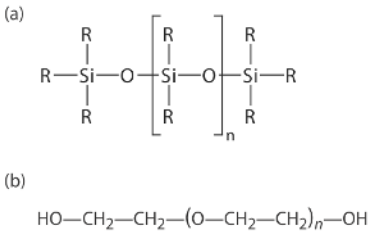


Figure 8.7.5 . General structures of common stationary phases: (a) substituted polysiloxane; (b) polyethylene glycol.

An important problem with all liquid stationary phases is their tendency to elute, or ***bleed*** from the column when it is heated. The temperature limits in Table 8.7.1 minimize this loss of stationary phase. Capillary columns with bonded or cross-linked stationary phases provide superior stability. A bonded stationary phase is attached chemically to the capillary's silica surface. Cross-linking, which is done after the stationary phase is in the capillary column, links together separate polymer chains to provide greater stability.

Another important consideration is the thickness of the stationary phase. From equation 12.3.7 we know that separation efficiency improves with thinner films of stationary phase. The most common thickness is 0.25 μm, although a thicker films is useful for highly volatile solutes, such as gases, because it has a greater capacity for retaining such solutes. Thinner films are used when separating low volatility solutes, such as steroids.

A few stationary phases take advantage of chemical selectivity. The most notable are stationary phases that contain chiral functional groups, which are used to separate enantiomers [Hinshaw, J. V. *LC*.*GC* **1993**, *11*, 644–648].

Sample Introduction

Three factors determine how we introduce a sample to the gas chromatograph. First, all of the sample's constituents must be volatile. Second, the analytes must be present at an appropriate concentration. Finally, the physical process of injecting the sample must not degrade the separation. Each of these needs is considered in this section.

Preparing a Volatile Sample

Not every sample can be injected directly into a gas chromatograph. To move through the column, the sample's constituents must be sufficiently volatile. A solute of low volatility, for example, may be retained by the column and continue to elute during the analysis of subsequent samples. A nonvolatile solute will condense at the top of the column, degrading the column's performance.

We can separate a sample's volatile analytes from its nonvolatile components using any of the extraction techniques described in Chapter 7. A liquid–liquid extraction of analytes from an aqueous matrix into methylene chloride or another organic solvent is a common choice. Solid-phase extractions also are used to remove a sample's nonvolatile components.

An attractive approach to isolating analytes is a ***solid-phase microextraction*** (SPME). In one approach, which is illustrated in Figure 8.7.6 , a fused-silica fiber is placed inside a syringe needle. The fiber, which is coated with a thin film of an adsorbent material, such as polydimethyl siloxane, is lowered into the sample by depressing a plunger and is exposed to the sample for a predetermined time. After withdrawing the fiber into the needle, it is transferred to the gas chromatograph for analysis.

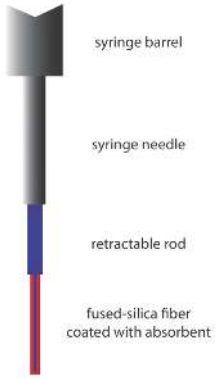


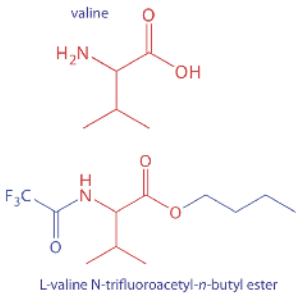
Figure 8.7.6 . Schematic diagram of a solid-phase microextraction device. The absorbent is shown in red.

Two additional methods for isolating volatile analytes are a purge-and-trap and headspace sampling. In a ***purge-and-trap***, we bubble an inert gas, such as He or N_2, through the sample, releasing—or purging—the volatile compounds. These compounds are carried by the purge gas through a trap that contains an absorbent material, such as Tenax, where they are retained. Heating the trap and back-flushing with carrier gas transfers the volatile compounds to the gas chromatograph. In ***headspace sampling*** we place the sample in a closed vial with an overlying air space. After allowing time for the volatile analytes to equilibrate between the sample and the overlying air, we use a syringe to extract a portion of the vapor phase and inject it into the gas chromatograph. Alternatively, we can sample the headspace with an SPME.

Thermal desorption is a useful method for releasing volatile analytes from solids. We place a portion of the solid in a glass-lined, stainless steel tube. After purging with carrier gas to remove any O_2 that might be present, we heat the sample. Volatile analytes are swept from the tube by an inert gas and carried to the GC. Because volatilization is not a rapid process, the volatile analytes often are concentrated at the top of the column by cooling the column inlet below room temperature, a process known as ***cryogenic focusing***. Once volatilization is complete, the column inlet is heated rapidly, releasing the analytes to travel through the column.

> The reason for removing O_2 is to prevent the sample from undergoing an oxidation reaction when it is heated.

To analyze a nonvolatile analyte we must convert it to a volatile form. For example, amino acids are not sufficiently volatile to analyze directly by gas chromatography. Reacting an amino acid, such as valine, with 1-butanol and acetyl chloride produces an esterified amino acid. Subsequent treatment with trifluoroacetic acid gives the amino acid's volatile N-trifluoroacetyl-*n*-butyl ester derivative.



Adjusting the Analyte's Concentration

In an analyte's concentration is too small to give an adequate signal, then we must concentrate the analyte before we inject the sample into the gas chromatograph. A side benefit of many extraction methods is that they often concentrate the analytes. Volatile organic materials isolated from an aqueous sample by a purge-and-trap, for example, are concentrated by as much as 1000×.

If an analyte is too concentrated, it is easy to overload the column, resulting in peak fronting (see Figure 12.2.7) and a poor separation. In addition, the analyte's concentration may exceed the detector's linear response. Injecting less sample or diluting the sample with a volatile solvent, such as methylene chloride, are two possible solutions to this problem.

Injecting the Sample

In Chapter 12.3 we examined several explanations for why a solute's band increases in width as it passes through the column, a process we called band broadening. We also introduce an additional source of band broadening if we fail to inject the sample into the minimum possible volume of mobile phase. There are two principal sources of this precolumn band broadening: injecting the sample into a moving stream of mobile phase and injecting a liquid sample instead of a gaseous sample. The design of a gas chromatograph's injector helps minimize these problems.

An example of a simple injection port for a packed column is shown in Figure 8.7.7 . The top of the column fits within a heated injector block, with carrier gas entering from the bottom. The sample is injected through a rubber septum using a microliter syringe, such as the one shown in in Figure 8.7.8 . Injecting the sample directly into the column minimizes band broadening because it mixes the sample with the smallest possible amount of carrier gas. The injector block is heated to a temperature at least 50°C above the boiling point of the least volatile solute, which ensures a rapid vaporization of the sample's components.

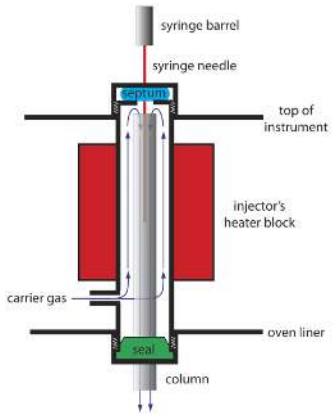


Figure 8.7.7 . Schematic diagram of a heated GC injector port for use with packed columns. The needle pierces a rubber septum and enters into the top of the column, which is located within a heater block.



Figure 8.7.8 . Example of a syringe for injecting samples into a gas chromatograph. This syringe has a maximum capacity of 10 µL with graduations every 0.1 µL.

Because a capillary column's volume is significantly smaller than that for a packed column, it requires a different style of injector to avoid overloading the column with sample. Figure 8.7.9 shows a schematic diagram of a typical split/splitless injector for use with a capillary column.

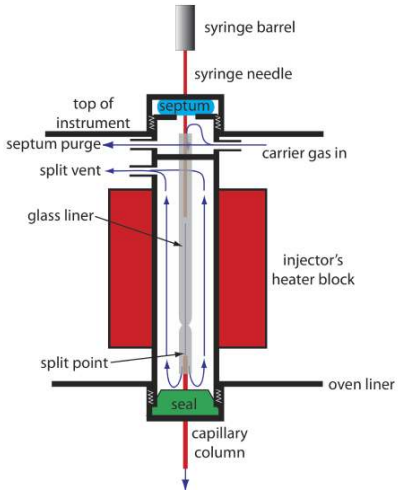


Figure 8.7.9 . Schematic diagram of a split/splitless injection port for use with capillary columns. The needle pierces a rubber septum and enters into a glass liner, which is located within a heater block. In a split injection the split vent is open; the split vent is closed for a splitless injection.

In a ***split injection*** we inject the sample through a rubber septum using a microliter syringe. Instead of injecting the sample directly into the column, it is injected into a glass liner where it mixes with the carrier gas. At the split point, a small fraction of the carrier gas and sample enters the capillary column with the remainder exiting through the split vent. By controlling the flow rate of the carrier gas as it enters the injector, and its flow rate through the septum purge and the split vent, we can control the fraction of sample that enters the capillary column, typically 0.1–10%.

> For example, if the carrier gas flow rate is 50 mL/min, and the flow rates for the septum purge and the split vent are 2 mL/min and 47 mL/min, respectively, then the flow rate through the column is 1 mL/min (= 50 – 2 – 47). The ratio of sample entering the column is 1/50, or 2%.

In a ***splitless injection***, which is useful for trace analysis, we close the split vent and allow all the carrier gas that passes through the glass liner to enter the column—this allows virtually all the sample to enters the column. Because the flow rate through the injector is low, significant precolumn band broadening is a problem. Holding the column's temperature approximately 20–25°C below the solvent's boiling point allows the solvent to condense at the entry to the capillary column, forming a barrier that traps the solutes. After allowing the solutes to concentrate, the column's temperature is increased and the separation begins.

For samples that decompose easily, an ***on-column injection*** may be necessary. In this method the sample is injected directly into the column without heating. The column temperature is then increased, volatilizing the sample with as low a temperature as is practical.

Temperature Control

Control of the column's temperature is critical to attaining a good separation when using gas chromatography. For this reason the column is placed inside a thermostated oven (see Figure 8.7.1). In an ***isothermal*** separation we maintain the column at a constant temperature. To increase the interaction between the solutes and the stationary phase, the temperature usually is set slightly below that of the lowest-boiling solute.

One difficulty with an isothermal separation is that a temperature that favors the separation of a low-boiling solute may lead to an unacceptably long retention time for a higher-boiling solute. ***Temperature programming*** provides a solution to this problem. At the beginning of the analysis we set the column's initial temperature below that for the lowest-boiling solute. As the separation progresses, we slowly increase the temperature at either a uniform rate or in a series of steps.

Detectors for Gas Chromatography

The final part of a gas chromatograph is the detector. The ideal detector has several desirable features: a low detection limit, a linear response over a wide range of solute concentrations (which makes quantitative work easier), sensitivity for all solutes or selectivity for a specific class of solutes, and an insensitivity to a change in flow rate or temperature.

Thermal Conductivity Detector (TCD)

One of the earliest gas chromatography detectors takes advantage of the mobile phase's thermal conductivity. As the mobile phase exits the column it passes over a tungsten-rhenium wire filament (see Figure 8.7.10 . The filament's electrical resistance depends on its temperature, which, in turn, depends on the thermal conductivity of the mobile phase. Because of its high thermal conductivity, helium is the mobile phase of choice when using a ***thermal conductivity detector*** (TCD).

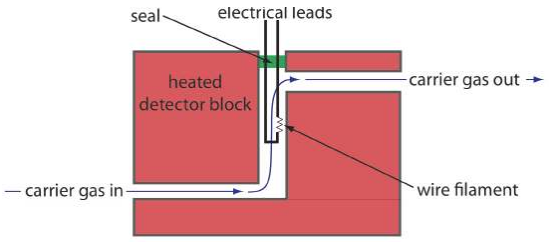


Figure 8.7.10 . Schematic diagram of a thermal conductivity detector showing one cell of a matched pair. The sample cell takes the carrier gas as it elutes from the column. A source of carrier gas that bypasses the column passes through a reference cell.

> Thermal conductivity, as the name suggests, is a measure of how easily a substance conducts heat. A gas with a high thermal conductivity moves heat away from the filament—and, thus, cools the filament—more quickly than does a gas with a low thermal conductivity.

When a solute elutes from the column, the thermal conductivity of the mobile phase in the TCD cell decreases and the temperature of the wire filament, and thus it resistance, increases. A reference cell, through which only the mobile phase passes, corrects for any time-dependent variations in flow rate, pressure, or electrical power, all of which affect the filament's resistance.

Because all solutes affect the mobile phase's thermal conductivity, the thermal conductivity detector is a universal detector. Another advantage is the TCD's linear response over a concentration range spanning 10^4–10^5 orders of magnitude. The detector also is non-

destructive, which allows us to recover analytes using a postdetector cold trap. One significant disadvantage of the TCD detector is its poor detection limit for most analytes.

Flame Ionization Detector (FID)

The combustion of an organic compound in an H_2/air flame results in a flame that contains electrons and organic cations, presumably CHO^+. Applying a potential of approximately 300 volts across the flame creates a small current of roughly 10^{-9} to 10^{-12} amps. When amplified, this current provides a useful analytical signal. This is the basis of the popular ***flame ionization detector,*** a schematic diagram of which is shown in Figure 8.7.11 .

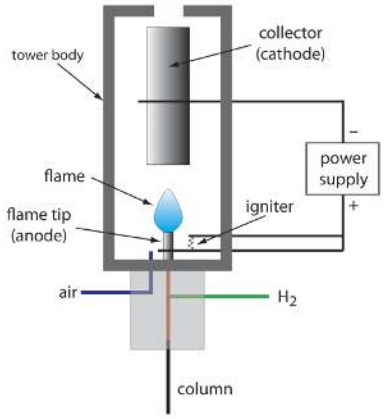


Figure 8.7.11 . Schematic diagram of a flame ionization detector. The eluent from the column mixes with H_2 and is burned in the presence of excess air. Combustion produces a flame that contains electrons and the cation $CHO^{+\cdot}$ Applying a potential between the flame's tip and the collector gives a current that is proportional to the concentration of cations in the flame.

Most carbon atoms—except those in carbonyl and carboxylic groups—generate a signal, which makes the FID an almost universal detector for organic compounds. Most inorganic compounds and many gases, such as H_2O and CO_2, are not detected, which makes the FID detector a useful detector for the analysis of organic analytes in atmospheric and aqueous environmental samples. Advantages of the FID include a detection limit that is approximately two to three orders of magnitude smaller than that for a thermal conductivity detector, and a linear response over 10^6–10^7 orders of magnitude in the amount of analyte injected. The sample, of course, is destroyed when using a flame ionization detector.

Electron Capture Detector (ECD)

The ***electron capture detector*** is an example of a selective detector. As shown in Figure 8.7.12 , the detector consists of a β-emitter, such as ^{63}Ni. The emitted electrons ionize the mobile phase, usually N_2, generating a standing current between a pair of electrodes. When a solute with a high affinity for capturing electrons elutes from the column, the current decreases, which serves as the signal. The ECD is highly selective toward solutes with electronegative functional groups, such as halogens and nitro groups, and is relatively insensitive to amines, alcohols, and hydrocarbons. Although its detection limit is excellent, its linear range extends over only about two orders of magnitude.

> A β-particle is an electron.

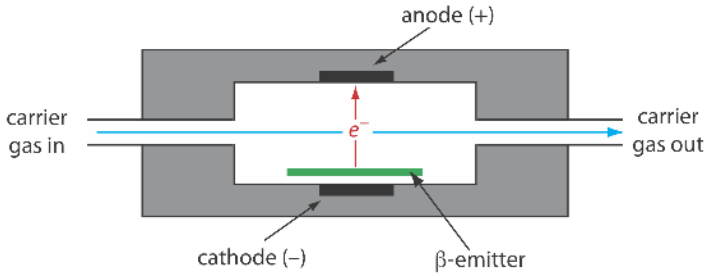


Figure 8.7.12 . Schematic diagram showing an electron capture detector.

https://chem.libretexts.org/@go/page/556153

Mass Spectrometer (MS)

A ***mass spectrometer*** is an instrument that ionizes a gaseous molecule using sufficient energy that the resulting ion breaks apart into smaller ions. Because these ions have different mass-to-charge ratios, it is possible to separate them using a magnetic field or an electrical field. The resulting mass spectrum contains both quantitative and qualitative information about the analyte. Figure 8.7.13 shows a mass spectrum for toluene.

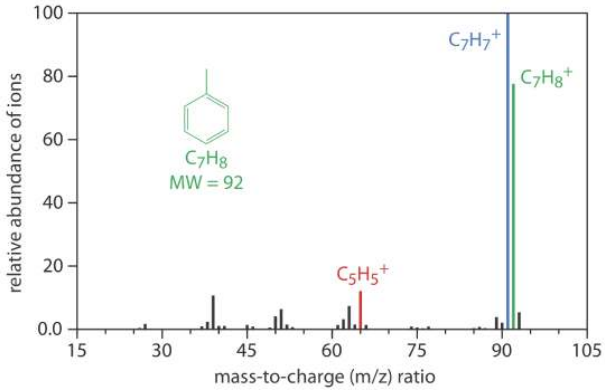


Figure 8.7.13 . Mass spectrum for toluene highlighting the molecular ion in green (m/z=92), and two fragment ions in blue (m/z=91) and in red (m/z= 65). A mass spectrum provides both quantitative and qualitative information: the height of any peak is proportional to the amount of toluene in the mass spectrometer and the fragmentation pattern is unique to toluene.

Figure 8.7.14 shows a block diagram of a typical gas chromatography-mass spectrometer (GC–MS) instrument. The effluent from the column enters the mass spectrometer's ion source in a manner that eliminates the majority of the carrier gas. In the ionization chamber the remaining molecules—a mixture of carrier gas, solvent, and solutes—undergo ionization and fragmentation. The mass spectrometer's mass analyzer separates the ions by their mass-to-charge ratio and a detector counts the ions and displays the mass spectrum.

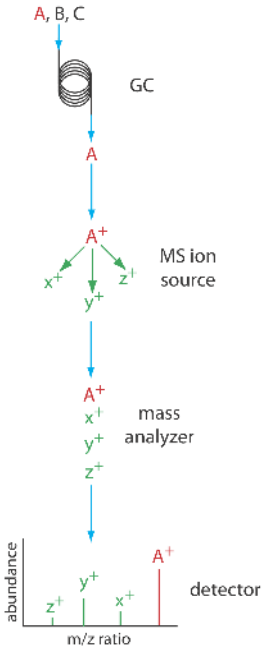


Figure 8.7.14 . Block diagram of GC– MS. A three component mixture enters the GC. When component A elutes from the column, it enters the MS ion source and ionizes to form the parent ion and several fragment ions. The ions enter the mass analyzer, which separates them by their mass-to-charge ratio, providing the mass spectrum shown at the detector.

There are several options for monitoring a chromatogram when using a mass spectrometer as the detector. The most common method is to continuously scan the entire mass spectrum and report the total signal for all ions that reach the detector during each scan. This total ion scan provides universal detection for all analytes. We can achieve some degree of selectivity by monitoring one

or more specific mass-to-charge ratios, a process called selective-ion monitoring. A mass spectrometer provides excellent detection limits, typically 25 fg to 100 pg, with a linear range of 10^5 orders of magnitude. Because we continuously record the mass spectrum of the column's eluent, we can go back and examine the mass spectrum for any time increment. This is a distinct advantage for GC–MS because we can use the mass spectrum to help identify a mixture's components.

> For more details on mass spectrometry see Introduction to Mass Spectrometry by Michael Samide and Olujide Akinbo, a resource that is part of the Analytical Sciences Digital Library.

Other Detectors

Two additional detectors are similar in design to a flame ionization detector. In the flame photometric detector, optical emission from phosphorous and sulfur provides a detector selective for compounds that contain these elements. The thermionic detector responds to compounds that contain nitrogen or phosphorous.

A Fourier transform infrared spectrophotometer (FT–IR) also can serve as a detector. In GC–FT–IR, effluent from the column flows through an optical cell constructed from a 10–40 cm Pyrex tube with an internal diameter of 1–3 mm. The cell's interior surface is coated with a reflecting layer of gold. Multiple reflections of the source radiation as it is transmit- ted through the cell increase the optical path length through the sample. As is the case with GC–MS, an FT–IR detector continuously records the column eluent's spectrum, which allows us to examine the IR spectrum for any time increment.

> See Section 10.3 for a discussion of FT-IR spectroscopy and instrumentation.

Quantitative Applications

Gas chromatography is widely used for the analysis of a diverse array of samples in environmental, clinical, pharmaceutical, biochemical, forensic, food science and petrochemical laboratories. Table 8.7.2 provides some representative examples of applications.

Table 8.7.2 . Representative Applications of Gas Chromatography

area	applications
environmental analysis	green house gases (CO_2, CH_4, NO_x) in air pesticides in water, wastewater, and soil vehicle emissions trihalomethanes in drinking water
clinical analysis	drugs blood alcohols
forensic analysis	analysis of arson accelerants detection of explosives
consumer products	volatile organics in spices and fragrances trace organics in whiskey monomers in latex paint
petrochemical and chemical industry	purity of solvents refinery gas composition of gasoline

Quantitative Calculations

In a GC analysis the area under the peak is proportional to the amount of analyte injected onto the column. A peak's area is determined by integration, which usually is handled by the instrument's computer or by an electronic integrating recorder. If two peak are resolved fully, the determination of their respective areas is straightforward.

Before electronic integrating recorders and computers, two methods were used to find the area under a curve. One method used a manual planimeter; as you use the planimeter to trace an object's perimeter, it records the area. A second approach for finding a peak's area is the cut-and-weigh method. The chromatogram is recorded on a piece of paper and each peak of interest is cut out and weighed. Assuming the paper is uniform in thickness and density of fibers, the ratio of weights for two peaks is the same as the ratio of areas. Of course, this approach destroys your chromatogram.

Overlapping peaks, however, require a choice between one of several options for dividing up the area shared by the two peaks (Figure 8.7.15). Which method we use depends on the relative size of the two peaks and their resolution. In some cases, the use of peak heights provides more accurate results [(a) Bicking, M. K. L. Chromatography Online, April 2006; (b) Bicking, M. K. L. Chromatography Online, June 2006].

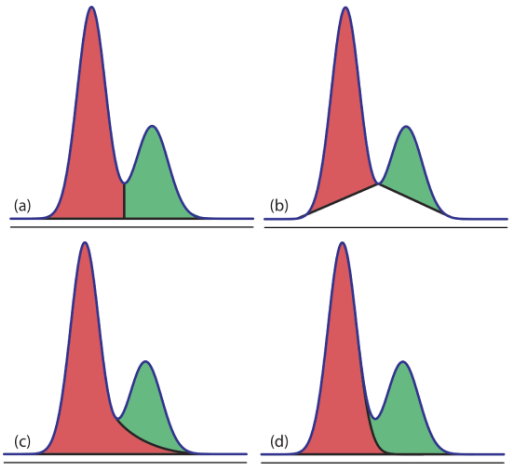


Figure 8.7.15 . Four methods for determining the areas under two overlapping chromatographic peaks: (a) the drop method; (b) the valley method; (c) the exponential skim method; and (d) the Gaussian skim method. Other methods for determining areas also are available.

For quantitative work we need to establish a calibration curve that relates the detector's response to the analyte's concentration. If the injection volume is identical for every standard and sample, then an external standardization provides both accurate and precise results. Unfortunately,even under the best conditions the relative precision for replicate injections may differ by 5%; often it is substantially worse. For quantitative work that requires high accuracy and precision, the use of internal standards is recommended.

To review the method of internal standards, see Chapter 5.3.

Example 8.7.1

Marriott and Carpenter report the following data for five replicate injections of a mixture that contains 1% v/v methyl isobutyl ketone and 1% v/v *p*-xylene in dichloromethane [Marriott, P. J.; Carpenter, P. D. *J. Chem. Educ.* **1996**, *73*, 96–99].

injection	peak	peak area (arb. units)
I	1	48075
	2	78112
II	1	85829
	2	135404
III	1	84136
	2	132332
IV	1	71681
	2	112889
V	1	58054
	2	91287

Assume that *p*-xylene (peak 2) is the analyte, and that methyl isobutyl ketone (peak 1) is the internal standard. Determine the 95% confidence interval for a single-point standardization with and without using the internal standard.

Solution

For a single-point external standardization we ignore the internal standard and determine the relationship between the peak area for *p*-xylene, A_2, and the concentration, C_2, of *p*-xylene.

$$A_2 = kC_2$$

Substituting the known concentration for *p*-xylene (1% v/v) and the appropriate peak areas, gives the following values for the constant *k*.

$$78112 \quad 135404 \quad 132332 \quad 112889 \quad 91287$$

The average value for *k* is 110 000 with a standard deviation of 25 100 (a relative standard deviation of 22.8%). The 95% confidence interval is

$$\mu = \overline{X} \pm \frac{ts}{\sqrt{n}} = 111000 \pm \frac{(2.78)(25100)}{\sqrt{5}} = 111000 \pm 31200$$

For an internal standardization, the relationship between the analyte's peak area, A_2, the internal standard's peak area, A_1, and their respective concentrations, C_2 and C_1, is

$$\frac{A_2}{A_1} = k\frac{C_2}{C_1}$$

Substituting in the known concentrations and the appropriate peak areas gives the following values for the constant *k*.

$$1.5917 \quad 1.5776 \quad 1.5728 \quad 1.5749 \quad 1.5724$$

The average value for *k* is 1.5779 with a standard deviation of 0.0080 (a relative standard deviation of 0.507%). The 95% confidence interval is

$$\mu = \overline{X} \pm \frac{ts}{\sqrt{n}} = 1.5779 \pm \frac{(2.78)(0.0080)}{\sqrt{5}} = 1.5779 \pm 0.0099$$

Although there is a substantial variation in the individual peak areas for this set of replicate injections, the internal standard compensates for these variations, providing a more accurate and precise calibration.

? Exercise 8.7.1

Figure 8.7.16 shows chromatograms for five standards and for one sample. Each standard and sample contains the same concentration of an internal standard, which is 2.50 mg/mL. For the five standards, the concentrations of analyte are 0.20 mg/mL, 0.40 mg/mL, 0.60 mg/mL, 0.80 mg/mL, and 1.00 mg/mL, respectively. Determine the concentration of analyte in the sample by (a) ignoring the internal standards and creating an external standards calibration curve, and by (b) creating an internal standard calibration curve. For each approach, report the analyte's concentration and the 95% confidence interval. Use peak heights instead of peak areas.

Answer

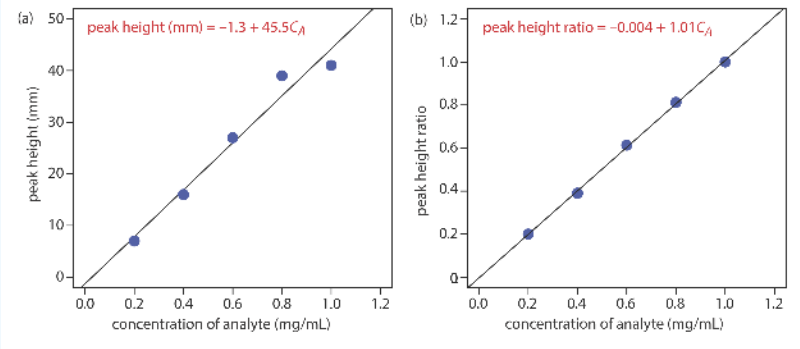
The following table summarizes my measurements of the peak heights for each standard and the sample, and their ratio (although your absolute values for peak heights will differ from mine, depending on the size of your monitor or printout, your relative peak height ratios should be similar to mine).

[standard] (mg/mL)	peak height of standard (mm)	peak height of analyte (mm)	peak height ratio
0.20	35	7	0.20
0.40	41	16	0.39
0.60	44	27	0.61
0.80	48	39	0.81
1.00	41	41	1.00
sample	39	21	0.54

Figure (a) shows the calibration curve and the calibration equation when we ignore the internal standard. Substituting the sample's peak height into the calibration equation gives the analyte's concentration in the sample as 0.49 mg/mL. The 95% confidence interval is ±0.24 mg/mL. The calibration curve shows quite a bit of scatter in the data because of uncertainty in the injection volumes.

Figure (b) shows the calibration curve and the calibration equation when we include the internal standard. Substituting the sample's peak height ratio into the calibration equation gives the analyte's concentration in the sample as 0.54 mg/mL. The 95% confidence interval is ±0.04 mg/mL.

To review the use of Excel or R for regression calculations and confidence intervals, see Chapter 5.5.



The data for this exercise were created so that the analyte's actual concentration is 0.55 mg/mL. Given the resolution of my ruler's scale, my answer is pretty reasonable. Your measurements may be slightly different, but your answers should be close to the actual values.

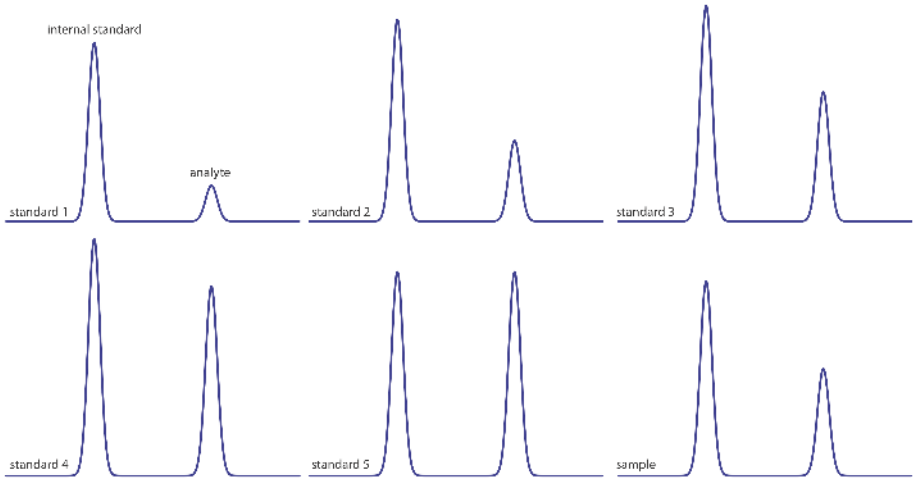


Figure 8.7.16 . Chromatograms for Practice Exercise 12.5.

Qualitative Applications

In addition to a quantitative analysis, we also can use chromatography to identify the components of a mixture. As noted earlier, when using an FT–IR or a mass spectrometer as the detector we have access to the eluent's full spectrum for any retention time. By interpreting the spectrum or by searching against a library of spectra, we can identify the analyte responsible for each chromatographic peak.

> In addition to identifying the component responsible for a particular chromatographic peak, we also can use the saved spectra to evaluate peak purity. If only one component is responsible for a chromatographic peak, then the spectra should be identical throughout the peak's elution. If a spectrum at the beginning of the peak's elution is different from a spectrum taken near the end of the peak's elution, then at least two components are co-eluting.

Evaluation

Scale of Operation

Gas chromatography is used to analyze analytes present at levels ranging from major to ultratrace components. Depending on the detector, samples with major and minor analytes may need to be diluted before analysis. The thermal conductivity and flame ionization detectors can handle larger amounts of analyte; other detectors, such as an electron capture detector or a mass spectrometer, require substantially smaller amounts of analyte. Although the injection volume for gas chromatography is quite small—typically about a microliter—the amount of available sample must be sufficient that the injection is a representative subsample. For a trace analyte, the actual amount of injected analyte is often in the picogram range. Using Representative Method 12.4.1 as an example, a 3.0-μL injection of 1 μg/L $CHCl_3$ is equivalent to 15 pg of $CHCl_3$, assuming a 100% extraction efficiency.

Accuracy

The accuracy of a gas chromatographic method varies substantially from sample-to-sample. For routine samples, accuracies of 1–5% are common. For analytes present at very low concentration levels, for samples with complex matrices, or for samples that require significant processing before analysis, accuracy may be substantially poorer. In the analysis for trihalomethanes described in Representative Method 12.4.1, for example, determinate errors as large as ±25% are possible.

Precision

The precision of a gas chromatographic analysis includes contributions from sampling, sample preparation, and the instrument. The relative standard deviation due to the instrument typically is 1–5%, although it can be significantly higher. The principal limitations are detector noise, which affects the determination of peak area, and the reproducibility of injection volumes. In quantitative work, the use of an internal standard compensates for any variability in injection volumes.

Sensitivity

In a gas chromatographic analysis, sensitivity is determined by the detector's characteristics. Of particular importance for quantitative work is the detector's linear range; that is, the range of concentrations over which a calibration curve is linear. Detectors with a wide linear range, such as the thermal conductivity detector and the flame ionization detector, can be used to analyze samples over a wide range of concentrations without adjusting operating conditions. Other detectors, such as the electron capture detector, have a much narrower linear range.

Selectivity

Because it combines separation with analysis, chromatographic methods provide excellent selectivity. By adjusting conditions it usually is possible to design a separation so that the analytes elute by themselves, even when the mixture is complex. Additional selectivity is obtained by using a detector, such as the electron capture detector, that does not respond to all compounds.

Time, Cost, and Equipment

Analysis time can vary from several minutes for samples that contain only a few constituents, to more than an hour for more complex samples. Preliminary sample preparation may substantially increase the analysis time. Instrumentation for gas chromatography ranges in price from inexpensive (a few thousand dollars) to expensive (>$50,000). The more expensive models are designed for capillary columns, include a variety of injection options, and use more sophisticated detectors, such as a mass spectrometer, or include multiple detectors. Packed columns typically cost <$200, and the cost of a capillary column is typically $300–$1000.

This page titled 8.7: Gas Chromatography is shared under a CC BY-NC-SA 4.0 license and was authored, remixed, and/or curated by Kathryn Davis.

- **12.4: Gas Chromatography** by David Harvey is licensed CC BY-NC-SA 4.0.

8.8: High-Performance Liquid Chromatography

In ***high-performance liquid chromatography*** (HPLC) we inject the sample, which is in solution form, into a liquid mobile phase. The mobile phase carries the sample through a packed or capillary column that separates the sample's components based on their ability to partition between the mobile phase and the stationary phase. Figure 8.8.1 shows an example of a typical HPLC instrument, which has several key components: reservoirs that store the mobile phase; a pump for pushing the mobile phase through the system; an injector for introducing the sample; a column for separating the sample into its component parts; and a detector for monitoring the eluent as it comes off the column. Let's consider each of these components.

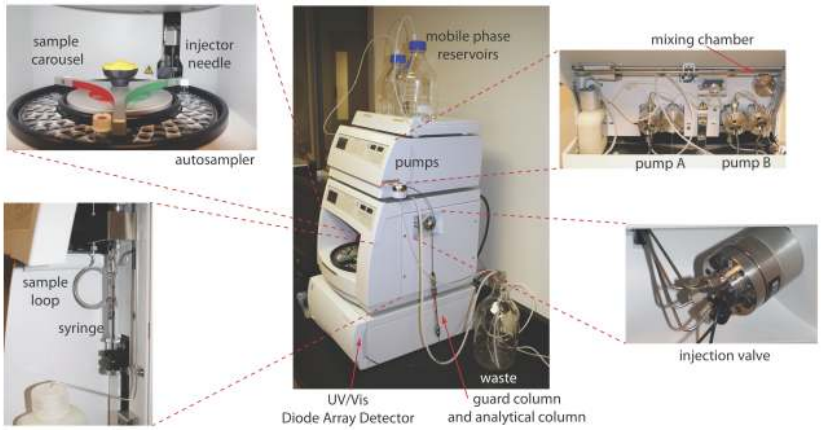


Figure 8.8.1 . Example of a typical high-performance liquid chromatograph with insets showing the pumps that move the mobile phase through the system and the plumbing used to inject the sample into the mobile phase. This particular instrument includes an autosampler. An instrument in which samples are injected manually does not include the features shown in the two left-most insets, and has a different style of loop injection valve.

A solute's retention time in HPLC is determined by its interaction with the stationary phase and the mobile phase. There are several different types of solute/stationary phase interactions, including liquid–solid adsorption, liquid–liquid partitioning, ion-exchange, and size-exclusion. This chapter deals exclusively with HPLC separations based on liquid–liquid partitioning. Other forms of liquid chromatography receive consideration in Chapter 12.6.

HPLC Columns

An HPLC typically includes two columns: an analytical column, which is responsible for the separation, and a guard column that is placed before the analytical column to protect it from contamination.

Analytical Columns

The most common type of HPLC column is a stainless steel tube with an internal diameter between 2.1 mm and 4.6 mm and a length between 30 mm and 300 mm (Figure 8.8.2). The column is packed with 3–10 μm porous silica particles with either an irregular or a spherical shape. Typical column efficiencies are 40000–60000 theoretical plates/m. Assuming a V_{max}/V_{min} of approximately 50, a 25-cm column with 50 000 plates/m has 12 500 theoretical plates and a peak capacity of 110.



Figure 8.8.2 . Typical packed column for HPLC. This particular column has an internal diameter of 4.6 mm and a length of 150 mm, and is packed with 5 μm particles coated with stationary phase.

Capillary columns use less solvent and, because the sample is diluted to a lesser extent, produce larger signals at the detector. These columns are made from fused silica capillaries with internal diameters from 44–200 μm and lengths of 50–250 mm. Capillary columns packed with 3–5 μm particles have been prepared with column efficiencies of up to 250 000 theoretical plates [Novotony, M. *Science*, **1989**, *246*, 51–57].

One limitation to a packed capillary column is the back pressure that develops when pumping the mobile phase through the small interstitial spaces between the particulate micron-sized packing material (Figure 8.8.3). Because the tubing and fittings that carry the mobile phase have pressure limits, a higher back pressure requires a lower flow rate and a longer analysis time. Monolithic columns, in which the solid support is a single, porous rod, offer column efficiencies equivalent to a packed capillary column while allowing for faster flow rates. A monolithic column—which usually is similar in size to a conventional packed column, although smaller, capillary columns also are available—is prepared by forming the mono- lithic rod in a mold and covering it with PTFE tubing or a polymer resin. Monolithic rods made of a silica-gel polymer typically have macropores with diameters of approximately 2 μm and mesopores—pores within the macropores—with diameters of approximately 13 nm [Cabrera, K. Chromatography Online, April 1, 2008].

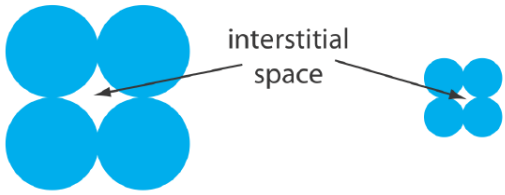


Figure 8.8.3 . The packing of smaller particles creates smaller interstitial spaces than the packing of larger particles. Although reducing particle size by **2×** increases efficiency by a factor of 1.4, it also produces a 4-fold increase in back pressure.

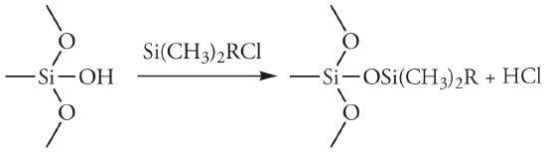
Guard Columns

Two problems tend to shorten the lifetime of an analytical column. First, solutes that bind irreversibly to the stationary phase degrade the column's performance by decreasing the amount of stationary phase available for effecting a separation. Second, particulate material injected with the sample may clog the analytical column. To minimize these problems we place a guard column before the analytical column. A Guard column usually contains the same particulate packing material and stationary phase as the analytical column, but is significantly shorter and less expensive—a length of 7.5 mm and a cost one-tenth of that for the corresponding analytical column is typical. Because they are intended to be sacrificial, guard columns are replaced regularly.

> If you look closely at Figure 8.8.1 , you will see the small guard column just above the analytical column.

Stationary Phases for Liquid-Liquid Chromatography

In liquid–liquid chromatography the stationary phase is a liquid film coated on a packing material, typically 3–10 μm porous silica particles. Because the stationary phase may be partially soluble in the mobile phase, it may elute, or bleed from the column over time. To prevent the loss of stationary phase, which shortens the column's lifetime, it is bound covalently to the silica particles. ***Bonded stationary phases*** are created by reacting the silica particles with an organochlorosilane of the general form $Si(CH_3)_2RCl$, where R is an alkyl or substituted alkyl group.



To prevent unwanted interactions between the solutes and any remaining –SiOH groups, $Si(CH_3)_3Cl$ is used to convert unreacted sites to $\mathbf{-SiOSi(CH_3)_3}$; such columns are designated as end-capped.

The properties of a stationary phase depend on the organosilane's alkyl group. If R is a polar functional group, then the stationary phase is polar. Examples of polar stationary phases include those where R contains a cyano ($-C_2H_4CN$), a diol ($-C_3H_6OCH_2CHOHCH_2OH$), or an amino ($-C_3H_6NH_2$) functional group. Because the stationary phase is polar, the mobile phase is a nonpolar or a moderately polar solvent. The combination of a polar stationary phase and a nonpolar mobile phase is called ***normal-phase chromatography***.

In ***reversed-phase chromatography***, which is the more common form of HPLC, the stationary phase is nonpolar and the mobile phase is polar. The most common nonpolar stationary phases use an organochlorosilane where the R group is an *n*-octyl (C_8) or *n*-

octyldecyl (C_{18}) hydrocarbon chain. Most reversed-phase separations are carried out using a buffered aqueous solution as a polar mobile phase, or using other polar solvents, such as methanol and acetonitrile. Because the silica substrate may undergo hydrolysis in basic solutions, the pH of the mobile phase must be less than 7.5.

> It seems odd that the more common form of liquid chromatography is identified as reverse-phase instead of normal phase. You might recall that one of the earliest examples of chromatography was Mikhail Tswett's separation of plant pigments using a polar column of calcium carbonate and a nonpolar mobile phase of petroleum ether. The assignment of normal and reversed, therefore, is all about precedence.

Mobile Phases

The elution order of solutes in HPLC is governed by polarity. For a normal-phase separation, a solute of lower polarity spends proportionally less time in the polar stationary phase and elutes before a solute that is more polar. Given a particular stationary phase, retention times in normal-phase HPLC are controlled by adjusting the mobile phase's properties. For example, if the resolution between two solutes is poor, switching to a less polar mobile phase keeps the solutes on the column for a longer time and provides more opportunity for their separation. In reversed-phase HPLC the order of elution is the opposite that in a normal-phase separation, with more polar solutes eluting first. Increasing the polarity of the mobile phase leads to longer retention times. Shorter retention times require a mobile phase of lower polarity.

Choosing a Mobile Phase: Using the Polarity Index

There are several indices that help in selecting a mobile phase, one of which is the polarity index [Snyder, L. R.; Glajch, J. L.; Kirkland, J. J. *Practical HPLC Method Development*, Wiley-Inter- science: New York, 1988]. Table 8.8.1 provides values of the polarity index, P', for several common mobile phases, where larger values of P' correspond to more polar solvents. Mixing together two or more mobile phases—assuming they are miscible—creates a mobile phase of intermediate polarity. For example, a binary mobile phase made by combining solvent *A* and solvent *B* has a polarity index, P'_{AB}, of

$$P'_{AB} = \Phi_A P'_A + \Phi_B P'_B \tag{8.8.1}$$

where P'_A and P'_B are the polarity indices for solvents *A* and *B*, and Φ_A and Φ_B are the volume fractions for the two solvents.

Table 8.8.1 . Properties of HPLC Mobile Phases

mobile phase	polarity index (P')	UV cutoff (nm)
cyclohexane	0.04	210
n-hexane	0.1	210
carbon tetrachloride	1.6	265
i-propyl ether	2.4	220
toluene	2.4	286
diethyl ether	2.8	218
tetrahydrofuran	4.0	220
ethanol	4.3	210
ethyl acetate	4.4	255
dioxane	4.8	215
methanol	5.1	210
acetonitrile	5.8	190
water	10.2	—

Example 8.8.1

A reversed-phase HPLC separation is carried out using a mobile phase of 60% v/v water and 40% v/v methanol. What is the mobile phase's polarity index?

Solution

Using Equation 8.8.1 and the values in Table 8.8.1 , the polarity index for a 60:40 water–methanol mixture is

$$P'_{AB} = \Phi_{\text{water}} P'_{\text{water}} + \Phi_{\text{methanol}} P'_{\text{methanol}}$$

$$P'_{AB} = 0.60 \times 10.2 + 0.40 \times 5.1 = 8.2$$

Exercise 8.8.1

Suppose you need a mobile phase with a polarity index of 7.5. Explain how you can prepare this mobile phase using methanol and water.

Answer

If we let x be the fraction of water in the mobile phase, then $1 - x$ is the fraction of methanol. Substituting these values into Equation 8.8.1 and solving for x

$$7.5 = 10.2x + 5.1(1 - x)$$

$$7.5 = 10.2x + 5.1 - 5.1x$$

$$2.4 = 5.1x$$

gives x as 0.47. The mobile phase is 47% v/v water and 53% v/v methanol.

As a general rule, a two unit change in the polarity index corresponds to an approximately 10-fold change in a solute's retention factor. Here is a simple example. If a solute's retention factor, k, is 22 when using water as a mobile phase (P' = 10.2), then switching to a mobile phase of 60:40 water–methanol (P' = 8.2) decreases k to approximately 2.2. Note that the retention factor becomes smaller because we are switching from a more polar mobile phase to a less polar mobile phase in a reversed-phase separation.

Choosing a Mobile Phase: Adjusting Selectivity

Changing the mobile phase's polarity index changes a solute's retention factor. As we learned in Chapter 12.3, however, a change in k is not an effective way to improve resolution when the initial value of k is greater than 10. To effect a better separation between two solutes we must improve the selectivity factor, α. There are two common methods for increasing α: adding a reagent to the mobile phase that reacts with the solutes in a secondary equilibrium reaction or switching to a different mobile phase.

Taking advantage of a secondary equilibrium reaction is a useful strategy for improving a separation [(a) Foley, J. P. *Chromatography*, **1987**, *7*, 118–128; (b) Foley, J. P.; May, W. E. Anal. Chem. 1987, 59, 102–109; (c) Foley, J. P.; May, W. E. Anal. Chem. 1987, 59, 110–115]. Figure 12.3.3, which we considered earlier in this chapter, shows the reversed-phase separation of four weak acids—benzoic acid, terephthalic acid, *p*-aminobenzoic acid, and *p*-hydroxybenzoic acid—on a nonpolar C_{18} column using an aqueous buffer of acetic acid and sodium acetate as the mobile phase. The retention times for these weak acids are shorter when using a less acidic mobile phase because each solute is present in an anionic, weak base form that is less soluble in the nonpolar stationary phase. If the mobile phase's pH is sufficiently acidic, the solutes are present as neutral weak acids that are more soluble in the stationary phase and take longer to elute. Because the weak acid solutes do not have identical pK_a values, the pH of the mobile phase has a different effect on each solute's retention time, allowing us to find the optimum pH for effecting a complete separation of the four solutes.

> Acid–base chemistry is not the only example of a secondary equilibrium reaction. Other examples include ion-pairing, complexation, and the interaction of solutes with micelles. We will consider the last of these in Chapter 12.7 when we discuss

micellar electrokinetic capillary chromatography.

In Example 8.8.1 we learned how to adjust the mobile phase's polarity by blending together two solvents. A polarity index, however, is just a guide, and binary mobile phase mixtures with identical polarity indices may not resolve equally a pair of solutes. Table 8.8.2 , for example, shows retention times for four weak acids in two mobile phases with nearly identical values for P'. Although the order of elution is the same for both mobile phases, each solute's retention time is affected differently by the choice of organic solvent. If we switch from using acetonitrile to tetrahydrofuran, for example, we find that benzoic acid elutes more quickly and that *p*-hydroxybenzoic acid elutes more slowly. Although we can resolve fully these two solutes using mobile phase that is 16% v/v acetonitrile, we cannot resolve them if the mobile phase is 10% tetrahydrofuran.

Table 8.8.2 . Retention Times for Four Weak Acids in Mobile Phases With Similar Polarity Indexes

retention time (min)	16% acetonitrile (CH_3CN) 84% pH 4.11 aqueous buffer (P' = 9.5)	10% tetrahydrofuran (THF) 90% pH 4.11 aqueous buffer (P' = 9.6)
$t_{r,\,BA}$	5.18	4.01
$t_{r,\,PH}$	1.67	2.91
$t_{r,\,PA}$	1.21	1.05
$t_{r,\,TP}$	0.23	0.54

Key: BA is benzoic acid; PH is *p*-hydroxybenzoic acid; PA is *p*-aminobenzoic acid; TP is terephthalic acid
Source: Harvey, D. T.; Byerly, S.; Bowman, A.; Tomlin, J. "Optimization of HPLC and GC Separations Using Re- sponse Surfaces," *J. Chem. Educ.* **1991**, *68*, 162–168.

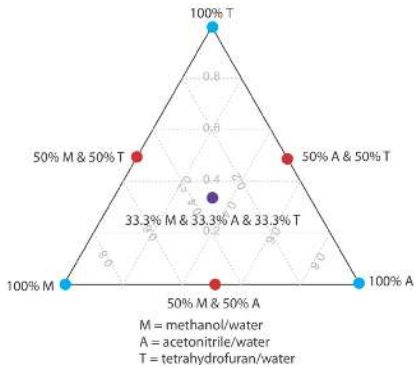


Figure 8.8.4 . Solvent triangle for optimizing a reversed-phase HPLC separation. The three blue circles show mobile phases consisting of an organic solvent and water. The three red circles are binary mobile phases created by combining equal volumes of the pure mobile phases. The ternary mobile phase shown by the purple circle contains all three of the pure mobile phases.

One strategy for finding the best mobile phase is to use the solvent triangle shown in Figure 8.8.4 , which allows us to explore a broad range of mobile phases with only seven experiments. We begin by adjusting the amount of acetonitrile in the mobile phase to produce the best possible separation within the desired analysis time. Next, we use Table 8.8.3 to estimate the composition of methanol/H_2O and tetrahydrofuran/H_2O mobile phases that will produce similar analysis times. Four additional mobile phases are prepared using the binary and ternary mobile phases shown in Figure 8.8.4 . When we examine the chromatograms from these seven mobile phases we may find that one or more provides an adequate separation, or we may identify a region within the solvent triangle where a separation is feasible. Figure 8.8.5 shows a resolution map for the reversed-phase separation of benzoic acid, terephthalic acid, *p*-aminobenzoic acid, and *p*-hydroxybenzoic acid on a nonpolar C_{18} column in which the maximum desired analysis time is set to 6 min [Harvey, D. T.; Byerly, S.; Bowman, A.; Tomlin, J. *J. Chem. Educ.* **1991**, *68*, 162–168]. The areas in blue, green, and red show mobile phase compositions that do not provide baseline resolution. The unshaded area represents mobile phase compositions where a separation is possible.

The choice to start with acetonitrile is arbitrary—we can just as easily choose to begin with methanol or with tetrahydrofuran.

Table 8.8.3 . Composition of Mobile Phases With Approximately Equal Solvent Strengths

%v/v CH_3OH	% v/v CH_3CN	%v/v THF
0	0	0
10	6	4
20	14	10
30	22	16
40	32	24
50	40	30
6	50	36
70	60	44
80	72	52
90	87	62
100	99	71

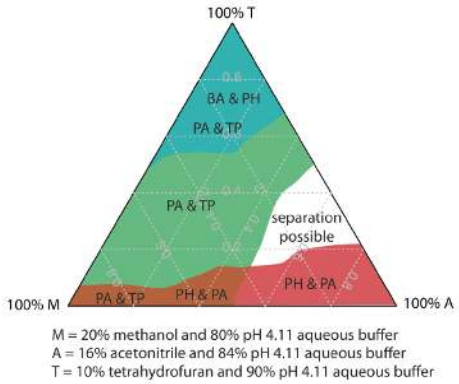


Figure 8.8.5 . Resolution map for the separation of benzoic acid (BA), terephthalic acid (TP), *p*-aminobenzoic acid (PA), and *p*-hydroxybenzoic acid (PH) on a nonpolar C_{18} column subject to a maximum analysis time of 6 min. The shaded areas represent regions where a separation is not possible, with the unresolved solutes identified. A separation is possible in the unshaded area. See Harvey, D. T.; Byerly, S.; Bowman, A.; Tomlin, J. "Optimization of HPLC and GC Separations Using Response Surfaces," *J. Chem. Educ.* **1991**, *68*, 162–168 for details on the mathematical model used to generate the resolution map.

Choosing a Mobile Phase: Isocratic and Gradient Elutions

A separation using a mobile phase that has a fixed composition is an ***isocratic elution***. One difficulty with an isocratic elution is that an appropriate mobile phase strength for resolving early-eluting solutes may lead to unacceptably long retention times for late-eluting solutes. Optimizing the mobile phase for late-eluting solutes, on the other hand, may provide an inadequate separation of early-eluting solutes. Changing the mobile phase's composition as the separation progresses is one solution to this problem. For a reversed-phase separation we use an initial mobile phase that is more polar. As the separation progresses, we adjust the composition of mobile phase so that it becomes less polar (see Figure 8.8.6). Such separations are called ***gradient elutions***.

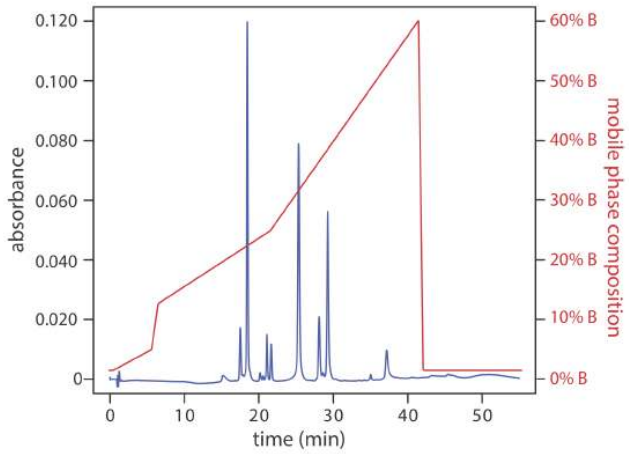


Figure 8.8.6 . Gradient elution separation of a mixture of flavonoids. Mobile phase A is an aqueous solution of 0.1% formic acid and mobile phase B is 0.1% formic acid in acetonitrile. The initial mobile phase is 98% A and 2% B. The percentage of mobile phase B increases in four steps: from 2% to 5% over 5 min, beginning at 0.5 min; from 5% to 12% over 1 min, beginning at 5.5 min; from 12% to 25% over 15 min, beginning at 6.5 min; and from 25% to 60% over 20 min, beginning at 21.5 min. Data provided by Christopher Schardon, Kyle Meinhardt, and Michelle Bushey, Department of Chemistry, Trinty University.

HPLC Plumbing

In a gas chromatograph the pressure from a compressed gas cylinder is sufficient to push the mobile phase through the column. Pushing a liquid mobile phase through a column, however, takes a great deal more effort, generating pressures in excess of several hundred atmospheres. In this section we consider the basic plumbing needed to move the mobile phase through the column and to inject the sample into the mobile phase.

Moving the Mobile Phase

A typical HPLC includes between 1–4 reservoirs for storing mobile phase solvents. The instrument in Figure 8.8.1 , for example, has two mobile phase reservoirs that are used for an isocratic elution or a gradient elution by drawing solvents from one or both reservoirs.

Before using a mobile phase solvent we must remove dissolved gases, such as N_2 and O_2, and small particulate matter, such as dust. Because there is a large drop in pressure across the column—the pressure at the column's entrance is as much as several hundred atmospheres, but it is atmospheric pressure at the column's exit—gases dissolved in the mobile phase are released as gas bubbles that may interfere with the detector's response. Degassing is accomplished in several ways, but the most common are the use of a vacuum pump or sparging with an inert gas, such as He, which has a low solubility in the mobile phase. Particulate materials, which may clog the HPLC tubing or column, are removed by filtering the solvents.

> Bubbling an inert gas through the mobile phase releases volatile dissolved gases. This process is called sparging.

The mobile phase solvents are pulled from their reservoirs by the action of one or more pumps. Figure 8.8.7 shows a close-up view of the pumps for the instrument in Figure 8.8.1 . The working pump and the equilibrating pump each have a piston whose back and forth movement maintains a constant flow rate of up to several mL/min and provides the high output pressure needed to push the mobile phase through the chromatographic column. In this particular instrument, each pump sends its mobile phase to a mixing chamber where they combine to form the final mobile phase. The relative speed of the two pumps determines the mobile phase's final composition.

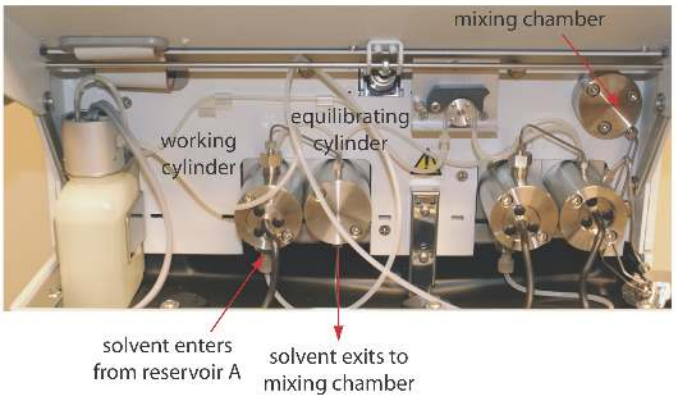


Figure 8.8.7 . Close-up view of the pumps for the instrument shown in Figure 8.8.1 . The working cylinder and the equilibrating cylinder for the pump on the left take solvent from reservoir A and send it to the mixing chamber. The pump on the right moves solvent from reservoir B to the mixing chamber. The mobile phase's flow rate is determined by the combined speeds of the two pumps. By changing the relative speeds of the two pumps, different binary mobile phases can be prepared.

The back and forth movement of a reciprocating pump creates a pulsed flow that contributes noise to the chromatogram. To minimize these pulses, each pump in Figure 8.8.7 has two cylinders. During the working cylinder's forward stoke it fills the equilibrating cylinder and establishes flow through the column. When the working cylinder is on its reverse stroke, the flow is maintained by the piston in the equilibrating cylinder. The result is a pulse-free flow.

There are other possible ways to control the mobile phase's composition and flow rate. For example, instead of the two pumps in Figure 8.8.7 , we can place a solvent proportioning valve before a single pump. The solvent proportioning value connects two or more solvent reservoirs to the pump and determines how much of each solvent is pulled during each of the pump's cycles. Another approach for eliminating a pulsed flow is to include a pulse damper between the pump and the column. A pulse damper is a chamber filled with an easily compressed fluid and a flexible diaphragm. During the piston's forward stroke the fluid in the pulse damper is compressed. When the piston withdraws to refill the pump, pressure from the expanding fluid in the pulse damper maintains the flow rate.

Injecting the Sample

The operating pressure within an HPLC is sufficiently high that we cannot inject the sample into the mobile phase by inserting a syringe through a septum, as is possible in gas chromatography. Instead, we inject the sample using a ***loop injector***, a diagram of which is shown in Figure 8.8.8 . In the load position a sample loop—which is available in a variety of sizes ranging from 0.5 µL to 5 mL—is isolated from the mobile phase and open to the atmosphere. The sample loop is filled using a syringe with a capacity several times that of the sample loop, with excess sample exiting through the waste line. After loading the sample, the injector is turned to the inject position, which redirects the mobile phase through the sample loop and onto the column.

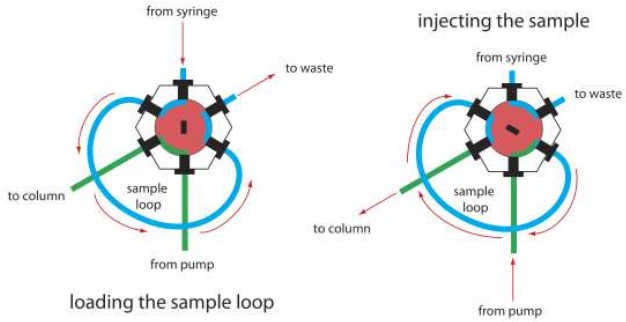


Figure 8.8.8 . Schematic diagram of a manual loop injector. In the load position the flow of mobile phase from the pump to the column (shown in green) is isolated from the sample loop, which is filled using a syringe (shown in blue). Rotating the inner valve (shown in red) to the inject position directs the mobile phase through the sample loop and onto the column.

The instrument in Figure 8.8.1 uses an autosampler to inject samples. Instead of using a syringe to push the sample into the sample loop, the syringe draws sample into the sample loop.

Detectors for HPLC

Many different types of detectors have been use to monitor HPLC separations, most of which use the spectroscopic techniques from Chapter 10 or the electrochemical techniques from Chapter 11.

Spectroscopic Detectors

The most popular HPLC detectors take advantage of an analyte's UV/Vis absorption spectrum. These detectors range from simple designs, in which the analytical wavelength is selected using appropriate filters, to a modified spectrophotometer in which the sample compartment includes a flow cell. Figure 8.8.9 shows the design of a typical flow cell when using a diode array spectrometer as the detector. The flow cell has a volume of 1–10 μL and a path length of 0.2–1 cm.

To review the details of how we measure absorbance, see Chapter 10.2. More information about different types of instruments, including the diode array spectrometer, is in Chapter 10.3.

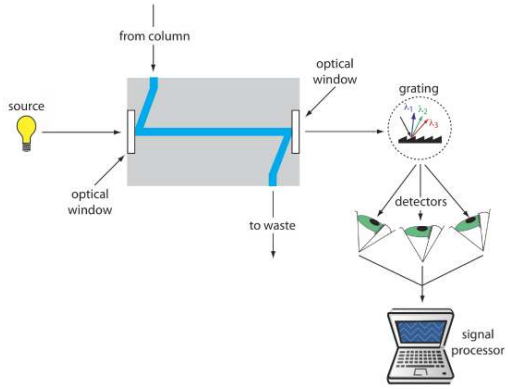


Figure 8.8.9 . Schematic diagram of a flow cell for a detector equipped with a diode array spectrometer.

When using a UV/Vis detector the resulting chromatogram is a plot of absorbance as a function of elution time (see Figure 8.8.10). If the detector is a diode array spectrometer, then we also can display the result as a three-dimensional chromatogram that shows absorbance as a function of wavelength and elution time. One limitation to using absorbance is that the mobile phase cannot absorb at the wavelengths we wish to monitor. Table 8.8.1 lists the minimum useful UV wavelength for several common HPLC solvents. Absorbance detectors provide detection limits of as little as 100 pg–1 ng of injected analyte.

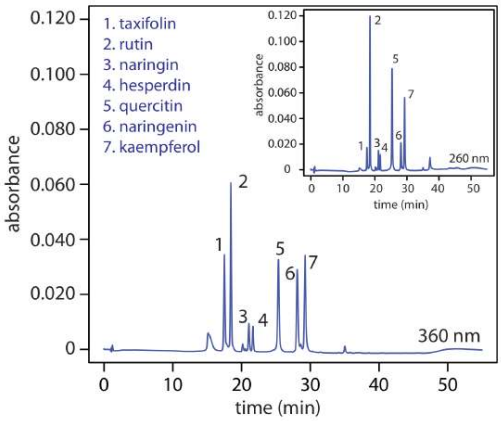


Figure 8.8.10 . HPLC separation of a mixture of flavonoids with UV/Vis detection at 360 nm and, in the inset, at 260 nm. The choice of wavelength affects each analyte's signal. By carefully choosing the wavelength, we can enhance the signal for the analytes of greatest interest. Data provided by Christopher Schardon, Kyle Meinhardt, and Michelle Bushey, Department of Chemistry, Trinty University.

If an analyte is fluorescent, we can place the flow cell in a spectrofluorimeter. As shown in Figure 8.8.11 , a fluorescence detector provides additional selectivity because only a few of a sample's components are fluorescent. Detection limits are as little as 1–10 pg of injected analyte.

> See Chapter 10.6 for a review of fluorescence spectroscopy and spectrofluorimeters.

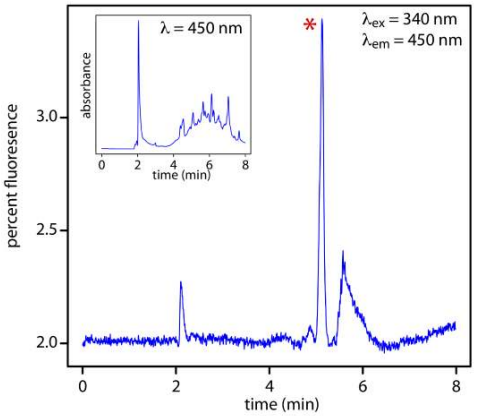


Figure 8.8.11 . HPLC chromatogram for the determination of riboflavin in urine using fluorescence detection with exci-tation at a wavelength of 340 nm and detection at 450 nm. The peak corresponding to riboflavin is marked with a red asterisk (*). The inset shows the same chromatogram when using a less-selective UV/Vis detector at a wavelength of 450 nm. Data provided by Jason Schultz, Jonna Berry, Kaelene Lundstrom, and Dwight Stoll, Department of Chemistry, Gustavus Adolphus College.

Electrochemical Detectors

Another common group of HPLC detectors are those based on electrochemical measurements such as amperometry, voltammetry, coulometry, and conductivity. Figure 8.8.12 , for example, shows an amperometric flow cell. Effluent from the column passes over the working electrode—held at a constant potential relative to a downstream reference electrode—that completely oxidizes or reduces the analytes. The current flowing between the working electrode and the auxiliary electrode serves as the analytical signal. Detection limits for amperometric electrochemical detection are from 10 pg–1 ng of injected analyte.

> See Chapter 11.4 for a review of amperometry.

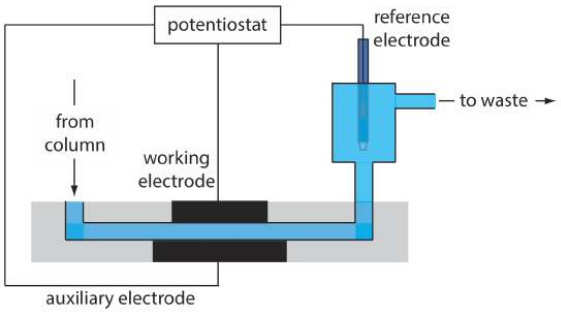


Figure 8.8.12 . Schematic diagram showing a flow cell for an amperometric electrochemical detector.

Other Detectors

Several other detectors have been used in HPLC. Measuring a change in the mobile phase's refractive index is analogous to monitoring the mobile phase's thermal conductivity in gas chromatography. A refractive index detector is nearly universal, responding to almost all compounds, but has a relatively poor detection limit of 0.1–1 μg of injected analyte. An additional limitation of a refractive index detector is that it cannot be used for a gradient elution unless the mobile phase components have identical refractive indexes.

Another useful detector is a mass spectrometer. Figure 8.8.13 shows a block diagram of a typical HPLC–MS instrument. The effluent from the column enters the mass spectrometer's ion source using an interface the removes most of the mobile phase, an essential need because of the incompatibility between the liquid mobile phase and the mass spectrometer's high vacuum environment. In the ionization chamber the remaining molecules—a mixture of the mobile phase components and solutes—undergo ionization and fragmentation. The mass spectrometer's mass analyzer separates the ions by their mass-to-charge ratio (m/z). A detector counts the ions and displays the mass spectrum.

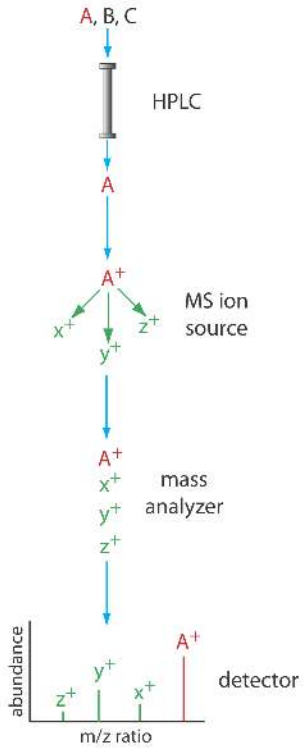


Figure 8.8.13 . Block diagram of an HPLC–MS. A three component mixture enters the HPLC. When component A elutes from the column, it enters the MS ion source and ionizes to form the parent ion and several fragment ions. The ions enter the mass analyzer, which separates them by their mass-to-charge ratio, providing the mass spectrum shown at the detector.

There are several options for monitoring the chromatogram when using a mass spectrometer as the detector. The most common method is to continuously scan the entire mass spectrum and report the total signal for all ions reaching the detector during each scan. This total ion scan provides universal detection for all analytes. As seen in Figure 8.8.14 , we can achieve some degree of selectivity by monitoring only specific mass-to-charge ratios, a process called selective-ion monitoring.

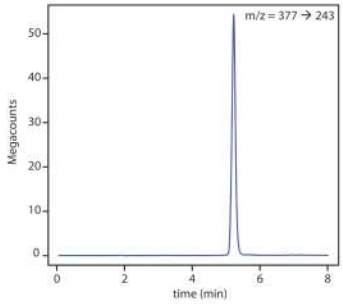


Figure 8.8.14 . HPLC–MS/MS chromatogram for the determination of riboflavin in urine. An initial parent ion with an m/z ratio of 377 enters a second mass spectrometer where it undergoes additional 20 ionization; the fragment ion with an m/z ratio of 243 provides the signal. The selectivity of this detector is evident when you compare this chromatogram to the one in Figure 8.8.11 , which uses fluoresence deterction. Data provided by Jason Schultz, Jonna Berry, Kaelene Lundstrom, and Dwight Stoll, Department of Chemistry, Gustavus Adolphus College.

The advantages of using a mass spectrometer in HPLC are the same as for gas chromatography. Detection limits are very good, typically 0.1–1 ng of injected analyte, with values as low as 1–10 pg for some samples. In addition, a mass spectrometer provides

qualitative, structural information that can help to identify the analytes. The interface between the HPLC and the mass spectrometer is technically more difficult than that in a GC–MS because of the incompatibility of a liquid mobile phase with the mass spectrometer's high vacuum requirement.

> For more details on mass spectrometry see Introduction to Mass Spectrometry by Michael Samide and Olujide Akinbo, a resource that is part of the Analytical Sciences Digital Library.

Quantitative Applications

High-performance liquid chromatography is used routinely for both qualitative and quantitative analyses of environmental, pharmaceutical, industrial, forensic, clinical, and consumer product samples.

Preparing Samples for Analysis

Samples in liquid form are injected into the HPLC after a suitable clean-up to remove any particulate materials, or after a suitable extraction to remove matrix interferents. In determining polyaromatic hydrocarbons (PAH) in wastewater, for example, an extraction with CH_2Cl_2 serves the dual purpose of concentrating the analytes and isolating them from matrix interferents. Solid samples are first dissolved in a suitable solvent or the analytes of interest brought into solution by extraction. For example, an HPLC analysis for the active ingredients and the degradation products in a pharmaceutical tablet often begins by extracting the powdered tablet with a portion of mobile phase. Gas samples are collected by bubbling them through a trap that contains a suitable solvent. Organic isocyanates in industrial atmospheres are collected by bubbling the air through a solution of 1-(2-methoxyphenyl)piperazine in toluene. The reaction between the isocyanates and 1-(2-methoxyphenyl)piperazine both stabilizes them against degradation before the HPLC analysis and converts them to a chemical form that can be monitored by UV absorption.

Quantitative Calculations

A quantitative HPLC analysis is often easier than a quantitative GC analysis because a fixed volume sample loop provides a more precise and accurate injection. As a result, most quantitative HPLC methods do not need an internal standard and, instead, use external standards and a normal calibration curve.

> An internal standard is necessary when using HPLC–MS because the interface between the HPLC and the mass spectrometer does not allow for a reproducible transfer of the column's eluent into the MS's ionization chamber.

Example 8.8.2

The concentration of polynuclear aromatic hydrocarbons (PAH) in soil is determined by first extracting the PAHs with methylene chloride. The extract is diluted, if necessary, and the PAHs separated by HPLC using a UV/Vis or fluorescence detector. Calibration is achieved using one or more external standards. In a typical analysis a 2.013-g sample of dried soil is extracted with 20.00 mL of methylene chloride. After filtering to remove the soil, a 1.00-mL portion of the extract is removed and diluted to 10.00 mL with acetonitrile. Injecting 5 μL of the diluted extract into an HPLC gives a signal of 0.217 (arbitrary units) for the PAH fluoranthene. When 5 μL of a 20.0-ppm fluoranthene standard is analyzed using the same conditions, a signal of 0.258 is measured. Report the parts per million of fluoranthene in the soil.

Solution

For a single-point external standard, the relationship between the signal, S, and the concentration, C, of fluoranthene is

$$S = kC$$

Substituting in values for the standard's signal and concentration gives the value of k as

$$k = \frac{S}{C} = \frac{0.258}{20.0 \text{ ppm}} = 0.0129 \text{ ppm}^{-1}$$

Using this value for k and the sample's HPLC signal gives a fluoranthene concentration of

$$C = \frac{S}{k} = \frac{0.217}{0.0129\ \text{ppm}^{-1}} = 16.8\ \text{ppm}$$

for the extracted and diluted soil sample. The concentration of fluoranthene in the soil is

$$\frac{16.8\ \text{g/mL} \times \frac{10.00\ \text{mL}}{1.00\ \text{mL}} \times 20.00\ \text{mL}}{2.013\ \text{g sample}} = 1670\ \text{ppm fluoranthene}$$

? Exercise 8.8.2

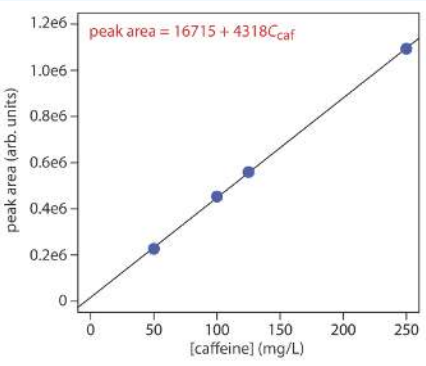
The concentration of caffeine in beverages is determined by a reversed-phase HPLC separation using a mobile phase of 20% acetonitrile and 80% water, and using a nonpolar C_8 column. Results for a series of 10-µL injections of caffeine standards are in the following table.

[caffeine] (mg/L)	peak area (arb. units)
50.0	226724
100.0	453762
125.0	559443
250.0	1093637

What is the concentration of caffeine in a sample if a 10-µL injection gives a peak area of 424195? The data in this problem comes from Kusch, P.; Knupp, G. "Simultaneous Determination of Caffeine in Cola Drinks and Other Beverages by Reversed-Phase HPTLC and Reversed-Phase HPLC," *Chem. Educator*, **2003**, *8*, 201–205.

Answer

The figure below shows the calibration curve and calibration equation for the set of external standards. Substituting the sample's peak area into the calibration equation gives the concentration of caffeine in the sample as 94.4 mg/L.



The best way to appreciate the theoretical and the practical details discussed in this section is to carefully examine a typical analytical method. Although each method is unique, the following description of the determination of fluoxetine in serum provides an instructive example of a typical procedure. The description here is based on Smyth, W. F. *Analytical Chemistry of Complex Matricies*, Wiley Teubner: Chichester, England, 1996, pp. 187–189.

Evaluation

With a few exceptions, the scale of operation, accuracy, precision, sensitivity, selectivity, analysis time, and cost for an HPLC method are similar to GC methods. Injection volumes for an HPLC method usually are larger than for a GC method because HPLC columns have a greater capacity. Because it uses a loop injection, the precision of an HPLC method often is better than a GC

method. HPLC is not limited to volatile analytes, which means we can analyze a broader range of compounds. Capillary GC columns, on the other hand, have more theoretical plates, and can separate more complex mixtures.

This page titled 8.8: High-Performance Liquid Chromatography is shared under a CC BY-NC-SA 4.0 license and was authored, remixed, and/or curated by Kathryn Davis.

- **12.5: High-Performance Liquid Chromatography** by David Harvey is licensed CC BY-NC-SA 4.0.

8.9: Other Forms of Chromatography

At the beginning of Section 12.5, we noted that there are several different types of solute/stationary phase interactions in liquid chromatography, but limited our discussion to liquid–liquid chromatography. In this section we turn our attention to liquid chromatography techniques in which partitioning occurs by liquid–solid adsorption, ion-exchange, and size exclusion.

Liquid-Solid Chromatography

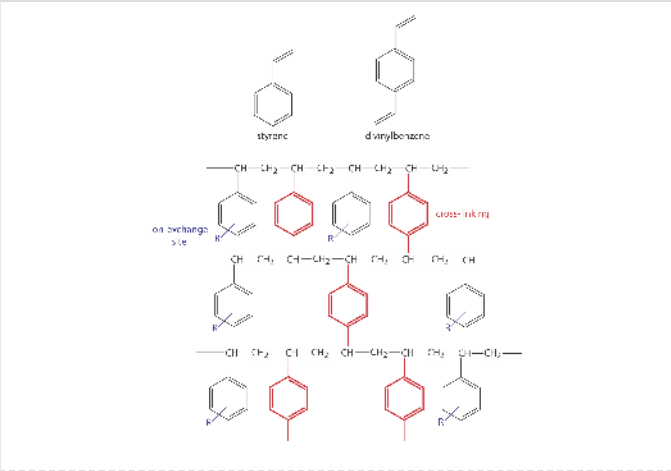
In ***liquid–solid adsorption chromatography*** (LSC) the column packing also serves as the stationary phase. In Tswett's original work the stationary phase was finely divided $CaCO_3$, but modern columns employ porous 3–10 μm particles of silica or alumina. Because the stationary phase is polar, the mobile phase usually is a nonpolar or a moderately polar solvent. Typical mobile phases include hexane, isooctane, and methylene chloride. The usual order of elution—from shorter to longer retention times—is

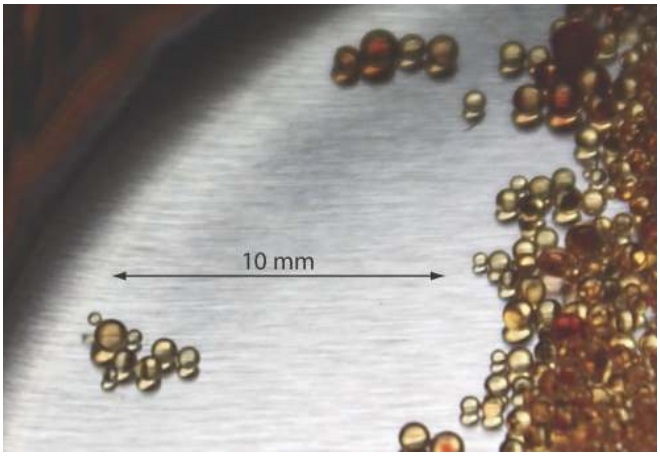
olefins < aromatic hydrocarbons < ethers < esters, aldehydes, ketones < alcohols, amines < amide < carboxylic acids

Nonpolar stationary phases, such as charcoal-based absorbents, also are used. For most samples, liquid–solid chromatography does not offer any special advantages over liquid–liquid chromatography. One exception is the analysis of isomers, where LSC excels.

Ion-Exchange Chromatography

In ***ion-exchange chromatography*** (IEC) the stationary phase is a cross-linked polymer resin, usually divinylbenzene cross-linked polystyrene, with covalently attached ionic functional groups (see Figure 8.9.1 and Table 8.9.1). The counterions to these fixed charges are mobile and are displaced by ions that compete more favorably for the exchange sites. Ion-exchange resins are divided into four categories: strong acid cation exchangers; weak acid cation exchangers; strong base anion exchangers; and weak base anion exchangers.





Size-Exclusion Chromatography

We have considered two classes of micron-sized stationary phases in this section: silica particles and cross-linked polymer resin beads. Both materials are porous, with pore sizes ranging from approximately 5–400 nm for silica particles, and from 5 nm to 100 μm for divinylbenzene cross-linked polystyrene resins. In ***size-exclusion chromatography***—which also is known by the terms molecular-exclusion or gel permeation chromatography—the separation of solutes depends upon their ability to enter into the pores of the stationary phase. Smaller solutes spend proportionally more time within the pores and take longer to elute from the column.

Size-exclusion chromatography provides a rapid means for separating larger molecules, including polymers and biomolecules. It is also capable of providing an estimation of a solute's molecular weight (MW). Calibration curves are prepared using a series of standards of known molecular weight and measuring each standard's retention volume. As shown in Figure 8.9.3 , a plot of log(MW) versus V_r is roughly linear between the column parameters called the exclusion limit and the inclusion limit. Because a solute's retention volume is influenced by both its size and its shape, a reasonably accurate estimation of molecular weight is possible only if the standards are chosen carefully to minimize the effect of shape.

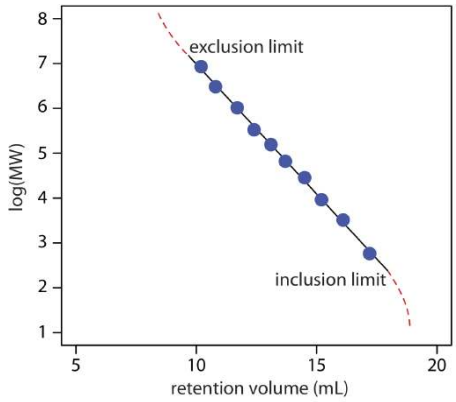


Figure 8.9.3 . Calibration curve for the determination of molecular weight by size-exclusion chromatography. The data shown here are adapted from Rouessac, F.; Rouessac, A. *Chemical Analysis: Modern Instrumentation Methods and Techniques*, Wiley: Chichester, England, 2004, p 141.

Size-exclusion chromatography is carried out using conventional HPLC instrumentation, replacing the HPLC column with an appropriate size-exclusion column. A UV/Vis detector is the most common means for obtaining the chromatogram.

Supercritical Fluid Chromatography

Although there are many analytical applications of gas chromatography and liquid chromatography, they can not separate and analyze all types of samples. Capillary column GC separates complex mixtures with excellent resolution and short analysis times. Its application is limited, however, to volatile analytes or to analytes made volatile by a suitable derivatization reaction. Liquid chromatography separates a wider range of solutes than GC, but the most common detectors—UV, fluorescence, and electrochemical— have poorer detection limits and smaller linear ranges than GC detectors, and are not as universal in their selectivity.

For some samples, ***supercritical fluid chromatography*** (SFC) provides a useful alternative to gas chromatography and liquid chromatography. The mobile phase in supercritical fluid chromatography is a gas held at a temperature and pressure that exceeds its critical point (Figure 8.9.4). Under these conditions the mobile phase is neither a gas nor a liquid. Instead, the mobile phase is a supercritical fluid.

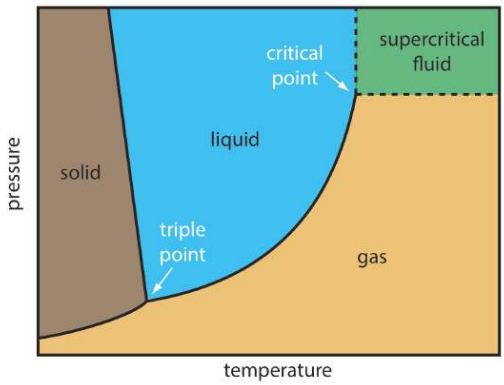


Figure 8.9.4 . Phase diagram showing the combinations of temperature and pres- sure for which a compound is in its solid state, its liquid state, and its gas state. For pressures and temperatures above the critical point, the compound is a supercritical fluid with properties intermediate between a gas and a liquid. Click here to see an interesting video demonstration of supercritical fluids from Nottingham Science City at the University of Nottingham.

Analysis time and resolution, although not as good as in GC, usually are better than in conventional HPLC. The density of a supercritical fluid, on the other hand, is much closer to that of a liquid, which explains why supercritical fluids are good solvents. In terms of its separation power, a mobile phase in SFC behaves more like the liquid mobile phase in HPLC than the gaseous mobile phase in GC.

The most common mobile phase for supercritical fluid chromatography is CO_2. Its low critical temperature of 31.1°C and its low critical pressure of 72.9 atm are relatively easy to achieve and maintain. Although supercritical CO_2 is a good solvent for nonpolar organics, it is less useful for polar solutes. The addition of an organic modifier, such as methanol, improves the mobile phase's elution strength. The instrumentation for supercritical fluid chromatography essentially is the same as that for a standard HPLC. The only important additions are a heated oven for the column and a pressure restrictor downstream from the column to maintain the critical pressure. Gradient elutions are accomplished by changing the applied pressure over time. The resulting change in the mobile phase's density affects its solvent strength. Detection is accomplished using standard GC detectors or HPLC detectors. Supercritical fluid chromatography has many applications in the analysis of polymers, fossil fuels, waxes, drugs, and food products.

This page titled 8.9: Other Forms of Chromatography is shared under a CC BY-NC-SA 4.0 license and was authored, remixed, and/or curated by Kathryn Davis.

- **12.6: Other Forms of Chromatography** by David Harvey is licensed CC BY-NC-SA 4.0.

8.10: Electrophoresis

Electrophoresis is a class of separation techniques in which we separate analytes by their ability to move through a conductive medium—usually an aqueous buffer—in response to an applied electric field. In the absence of other effects, cations migrate toward the electric field's negatively charged cathode. Cations with larger charge-to-size ratios—which favors ions of greater charge and of smaller size—migrate at a faster rate than larger cat- ions with smaller charges. Anions migrate toward the positively charged anode and neutral species do not experience the electrical field and remain stationary.

> As we will see shortly, under normal conditions even neutral species and anions migrate toward the cathode.

There are several forms of electrophoresis. In slab gel electrophoresis the conducting buffer is retained within a porous gel of agarose or polyacrylamide. Slabs are formed by pouring the gel between two glass plates separated by spacers. Typical thicknesses are 0.25–1 mm. Gel electrophoresis is an important technique in biochemistry where it frequently is used to separate DNA fragments and proteins. Although it is a powerful tool for the qualitative analysis of complex mixtures, it is less useful for quantitative work.

In ***capillary electrophoresis*** the conducting buffer is retained within a capillary tube with an inner diameter that typically is 25–75 μm. The sample is injected into one end of the capillary tube, and as it migrates through the capillary the sample's components separate and elute from the column at different times. The resulting ***electropherogram*** looks similar to a GC or an HPLC chromatogram, and provides both qualitative and quantitative information. Only capillary electrophoretic methods receive further consideration in this section.

Theory of Electrophoresis

In capillary electrophoresis we inject the sample into a buffered solution retained within a capillary tube. When an electric field is applied across the capillary tube, the sample's components migrate as the result of two types of actions: electrophoretic mobility and electroosmotic mobility. ***Electrophoretic mobility*** is the solute's response to the applied electrical field in which cations move toward the negatively charged cathode, anions move toward the positively charged anode, and neutral species remain stationary. The other contribution to a solute's migration is ***electroosmotic flow***, which occurs when the buffer moves through the capillary in response to the applied electrical field. Under normal conditions the buffer moves toward the cathode, sweeping most solutes, including the anions and neutral species, toward the negatively charged cathode.

Electrophoretic Mobility

The velocity with which a solute moves in response to the applied electric field is called its ***electrophoretic velocity***, ν_{ep}; it is defined as

$$\nu_{ep} = \mu_{ep} E \tag{8.10.1}$$

where μ_{ep} is the solute's electrophoretic mobility, and E is the magnitude of the applied electrical field. A solute's electrophoretic mobility is defined as

$$\mu_{ep} = \frac{q}{6\pi\eta r} \tag{8.10.2}$$

where q is the solute's charge, η is the buffer's viscosity, and r is the solute's radius. Using Equation 8.10.1 and Equation 8.10.2 we can make several important conclusions about a solute's electrophoretic velocity. Electrophoretic mobility and, therefore, electrophoretic velocity, increases for more highly charged solutes and for solutes of smaller size. Because q is positive for a cation and negative for an anion, these species migrate in opposite directions. A neutral species, for which q is zero, has an electrophoretic velocity of zero.

Electroosmotic Mobility

When an electric field is applied to a capillary filled with an aqueous buffer we expect the buffer's ions to migrate in response to their electrophoretic mobility. Because the solvent, H_2O, is neutral we might reasonably expect it to remain stationary. What we

observe under normal conditions, however, is that the buffer moves toward the cathode. This phenomenon is called the electroosmotic flow.

Electroosmotic flow occurs because the walls of the capillary tubing carry a charge. The surface of a silica capillary contains large numbers of silanol groups (–SiOH). At a pH level greater than approximately 2 or 3, the silanol groups ionize to form negatively charged silanate ions ($–SiO^-$). Cations from the buffer are attracted to the silanate ions. As shown in Figure 12.7.1 , some of these cations bind tightly to the silanate ions, forming a fixed layer. Because the cations in the fixed layer only partially neutralize the negative charge on the capillary walls, the solution adjacent to the fixed layer—which is called the diffuse layer—contains more cations than anions. Together these two layers are known as the double layer. Cations in the diffuse layer migrate toward the cathode. Because these cations are solvated, the solution also is pulled along, producing the electroosmotic flow.

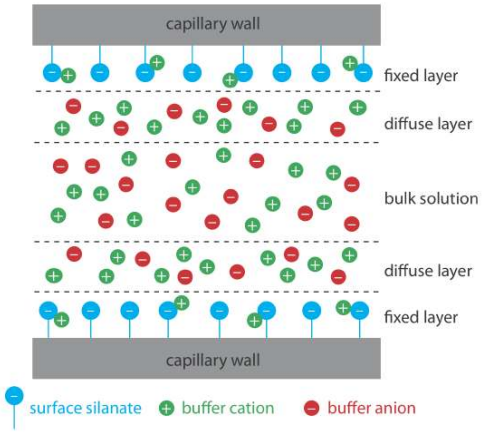


Figure 12.7.1 . Schematic diagram showing the origin of the double layer within a capillary tube. Although the net charge within the capillary is zero, the distribution of charge is not. The walls of the capillary have an excess of negative charge, which decreases across the fixed layer and the diffuse layer, reaching a value of zero in bulk solution.

> The anions in the diffuse layer, which also are solvated, try to move toward the anode. Because there are more cations than anions, however, the cations win out and the electroosmotic flow moves in the direction of the cathode.

The rate at which the buffer moves through the capillary, what we call its ***electroosmotic flow velocity***, ν_{eof}, is a function of the applied electric field, E, and the buffer's electroosmotic mobility, μ_{eof}.

$$\nu_{eof} = \mu_{eof} E \tag{8.10.3}$$

Electroosmotic mobility is defined as

$$\mu_{eof} = \frac{\varepsilon \zeta}{4\pi\eta} \tag{8.10.4}$$

where ϵ is the buffer dielectric constant, ζ is the zeta potential, and η is the buffer's viscosity.

The ***zeta potential***—the potential of the diffuse layer at a finite distance from the capillary wall—plays an important role in determining the electroosmotic flow velocity. Two factors determine the zeta potential's value. First, the zeta potential is directly proportional to the charge on the capillary walls, with a greater density of silanate ions corresponding to a larger zeta potential. Below a pH of 2 there are few silanate ions and the zeta potential and the electroosmotic flow velocity approach zero. As the pH increases, both the zeta potential and the electroosmotic flow velocity increase. Second, the zeta potential is directly proportional to the thickness of the double layer. Increasing the buffer's ionic strength provides a higher concentration of cations, which decreases the thickness of the double layer and decreases the electroosmotic flow.

> The definition of zeta potential given here admittedly is a bit fuzzy. For a more detailed explanation see Delgado, A. V.; González-Caballero, F.; Hunter, R. J.; Koopal, L. K.; Lyklema, J. "Measurement and Interpretation of Electrokinetic Phenomena," *Pure. Appl. Chem.* **2005**, *77*, 1753–1805. Although this is a very technical report, Sections 1.3–1.5 provide a good introduction to the difficulty of defining the zeta potential and of measuring its value.

The electroosmotic flow profile is very different from that of a fluid moving under forced pressure. Figure 12.7.2 compares the electroosmotic flow profile with the hydrodynamic flow profile in gas chromatography and liquid chromatography. The uniform, flat profile for electroosmosis helps minimize band broadening in capillary electrophoresis, improving separation efficiency.

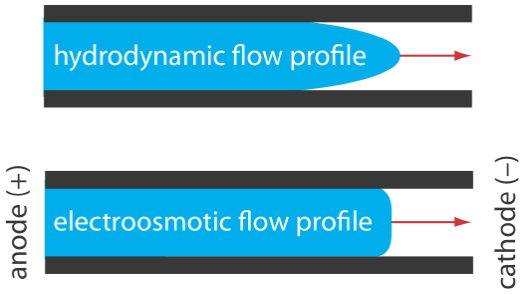


Figure 12.7.2 . Comparison of hydrodynamic flow and electroosmotic flow. The nearly uniform electroosmotic flow profile means that the electroosmotic flow velocity is nearly constant across the capillary.

Total Mobility

A solute's total velocity, ν_{tot}, as it moves through the capillary is the sum of its electrophoretic velocity and the electroosmotic flow velocity.

$$\nu_{tot} = \nu_{ep} + \nu_{eof}$$

As shown in Figure 12.7.3 , under normal conditions the following general relationships hold true.

$$(\nu_{tot})_{cations} > \nu_{eof}$$

$$(\nu_{tot})_{neutrals} = \nu_{eof}$$

$$(\nu_{tot})_{anions} < \nu_{eof}$$

Cations elute first in an order that corresponds to their electrophoretic mobilities, with small, highly charged cations eluting before larger cations of lower charge. Neutral species elute as a single band with an elution rate equal to the electroosmotic flow velocity. Finally, anions are the last components to elute, with smaller, highly charged anions having the longest elution time.

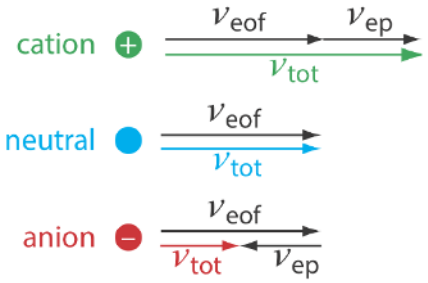


Figure 12.7.3 . Visual explanation for the general elution order in capillary electrophoresis. Each species has the same electroosmotic flow, ν_{eof}. Cations elute first because they have a positive electrophoretic velocity, ν_{ep}. Anions elute last because their negative electrophoretic velocity partially offsets the electroosmotic flow velocity. Neutrals elute with a velocity equal to the electroosmotic flow.

Migration Time

Another way to express a solute's velocity is to divide the distance it travels by the elapsed time

$$\nu_{tot} = \frac{l}{t_m} \tag{8.10.5}$$

where l is the distance between the point of injection and the detector, and t_m is the solute's migration time. To understand the experimental variables that affect migration time, we begin by noting that

$$\nu_{tot} = \mu_{tot} E = (\mu_{ep} + \mu_{eof}) E \tag{8.10.6}$$

Combining Equation 8.10.5 and Equation 8.10.6 and solving for t_m leaves us with

$$t_m = \frac{l}{(\mu_{ep} + \mu_{eof})\, E} \tag{8.10.7}$$

The magnitude of the electrical field is

$$E = \frac{V}{L} \tag{8.10.8}$$

where V is the applied potential and L is the length of the capillary tube. Finally, substituting Equation 8.10.8 into Equation 8.10.7 leaves us with the following equation for a solute's migration time.

$$t_m = \frac{lL}{(\mu_{ep} + \mu_{eof})\, V} \tag{8.10.9}$$

To decrease a solute's migration time—which shortens the analysis time—we can apply a higher voltage or use a shorter capillary tube. We can also shorten the migration time by increasing the electroosmotic flow, although this decreases resolution.

Efficiency

As we learned in Chapter 12.2, the efficiency of a separation is given by the number of theoretical plates, N. In capillary electrophoresis the number of theoretic plates is

$$N = \frac{l^2}{2Dt_m} = \frac{(\mu_{ep} + \mu_{eof})\, El}{2DL} \tag{8.10.10}$$

where D is the solute's diffusion coefficient. From Equation 8.10.10, the efficiency of a capillary electrophoretic separation increases with higher voltages. Increasing the electroosmotic flow velocity improves efficiency, but at the expense of resolution. Two additional observations deserve comment. First, solutes with larger electrophoretic mobilities—in the same direction as the electroosmotic flow—have greater efficiencies; thus, smaller, more highly charged cations are not only the first solutes to elute, but do so with greater efficiency. Second, efficiency in capillary electrophoresis is independent of the capillary's length. Theoretical plate counts of approximately 100 000–200 000 are not unusual.

> It is possible to design an electrophoretic experiment so that anions elute before cations—more about this later—in which smaller, more highly charged anions elute with greater efficiencies.

Selectivity

In chromatography we defined the selectivity between two solutes as the ratio of their retention factors. In capillary electrophoresis the analogous expression for selectivity is

$$\alpha = \frac{\mu_{ep,1}}{\mu_{ep,2}}$$

where $\mu_{ep,1}$ and $\mu_{ep,2}$ are the electrophoretic mobilities for the two solutes, chosen such that $\alpha \geq 1$. We can often improve selectivity by adjusting the pH of the buffer solution. For example, NH_4^+ is a weak acid with a pK_a of 9.75. At a pH of 9.75 the concentrations of NH_4^+ and NH_3 are equal. Decreasing the pH below 9.75 increases its electrophoretic mobility because a greater fraction of the solute is present as the cation NH_4^+. On the other hand, raising the pH above 9.75 increases the proportion of neutral NH_3, decreasing its electrophoretic mobility.

Resolution

The resolution between two solutes is

$$R = \frac{0.177(\mu_{ep,2} - \mu_{ep,1})\sqrt{V}}{\sqrt{D(\mu_{avg} + \mu_{eof}}} \tag{8.10.11}$$

where μ_{avg} is the average electrophoretic mobility for the two solutes. Increasing the applied voltage and decreasing the electroosmotic flow velocity improves resolution. The latter effect is particularly important. Although increasing electroosmotic

flow improves analysis time and efficiency, it de- creases resolution.

Instrumentation

The basic instrumentation for capillary electrophoresis is shown in Figure 12.7.4 and includes a power supply for applying the electric field, anode and cathode compartments that contain reservoirs of the buffer solution, a sample vial that contains the sample, the capillary tube, and a detector. Each part of the instrument receives further consideration in this section.

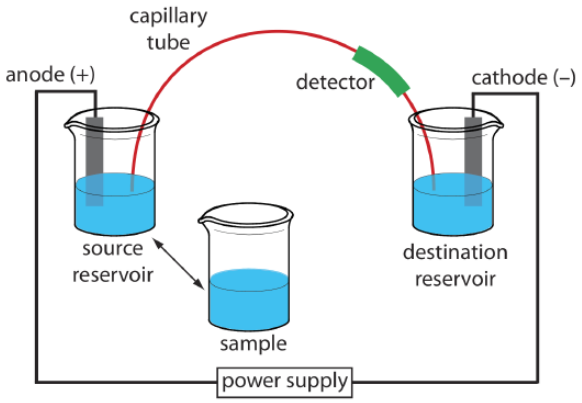


Figure 12.7.4 . Schematic diagram of the basic instrumentation for capillary electrophoresis. The sample and the source reservoir are switched when making injections.

Capillary Tubes

Figure 12.7.5 shows a cross-section of a typical capillary tube. Most capillary tubes are made from fused silica coated with a 15–35 μm layer of polyimide to give it mechanical strength. The inner diameter is typically 25–75 μm, which is smaller than the internal diameter of a capillary GC column, with an outer diameter of 200–375 μm.

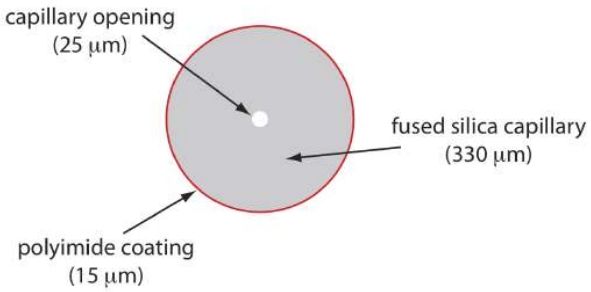


Figure 12.7.5 . Cross section of a capillary column for capillary electrophoresis. The dimensions shown here are typical and are scaled proportionally in this figure.

The capillary column's narrow opening and the thickness of its walls are important. When an electric field is applied to the buffer solution, current flows through the capillary. This current leads to the release of heat, which we call ***Joule heating***. The amount of heat released is proportional to the capillary's radius and to the magnitude of the electrical field. Joule heating is a problem because it changes the buffer's viscosity, with the solution at the center of the capillary being less viscous than that near the capillary walls. Because a solute's electrophoretic mobility depends on its viscosity (see Equation 8.10.2), solute species in the center of the capillary migrate at a faster rate than those near the capillary walls. The result is an additional source of band broadening that degrades the separation. Capillaries with smaller inner diameters generate less Joule heating, and capillaries with larger outer diameters are more effective at dissipating the heat. Placing the capillary tube inside a thermostated jacket is another method for minimizing the effect of Joule heating; in this case a smaller outer diameter allows for a more rapid dissipation of thermal energy.

Injecting the Sample

There are two common methods for injecting a sample into a capillary electrophoresis column: hydrodynamic injection and electrokinetic injection. In both methods the capillary tube is filled with the buffer solution. One end of the capillary tube is placed in the destination reservoir and the other end is placed in the sample vial.

Hydrodynamic injection uses pressure to force a small portion of sample into the capillary tubing. A difference in pressure is applied across the capillary either by pressurizing the sample vial or by applying a vacuum to the destination reservoir. The volume of sample injected, in liters, is given by the following equation

$$V_{\text{inj}} = \frac{\Delta P d^4 \pi t}{128 \eta L} \times 10^3 \tag{8.10.12}$$

where ΔP is the difference in pressure across the capillary in pascals, d is the capillary's inner diameter in meters, t is the amount of time the pressure is applied in seconds, η is the buffer's viscosity in kg m^{-1} s^{-1}, and L is the length of the capillary tubing in meters. The factor of 10^3 changes the units from cubic meters to liters.

For a hydrodynamic injection we move the capillary from the source reservoir to the sample. The anode remains in the source reservoir. A hydrodynamic injection also is possible if we raise the sample vial above the destination reservoir and briefly insert the filled capillary.

Example 12.7.1

In a hydrodynamic injection we apply a pressure difference of 2.5×10^3 Pa (a $\Delta P \approx 0.02$ atm) for 2 s to a 75-cm long capillary tube with an internal diameter of 50 μm. Assuming the buffer's viscosity is 10^{-3} kg m^{-1} s^{-1}, what volume and length of sample did we inject?

Solution

Making appropriate substitutions into Equation 8.10.12 gives the sample's volume as

$$V_{inj} = \frac{\left(2.5 \times 10^3 \text{ kg m}^{-1} \text{ s}^{-2}\right)\left(50 \times 10^{-6} \text{ m}\right)^4 (3.14)(2 \text{ s})}{(128)\left(0.001 \text{ kg m}^{-1} \text{ s}^{-1}\right)(0.75 \text{ m})} \times 10^3 \text{L/m}^3$$

$$V_{inj} = 1 \times 10^{-9} \text{ L} = 1 \text{ nL}$$

Because the interior of the capillary is cylindrical, the length of the sample, l, is easy to calculate using the equation for the volume of a cylinder; thus

$$l = \frac{V_{\text{inj}}}{\pi r^2} = \frac{\left(1 \times 10^{-9} \text{ L}\right)\left(10^{-3} \text{ m}^3/\text{L}\right)}{(3.14)\left(25 \times 10^{-6} \text{ m}\right)^2} = 5 \times 10^{-4} \text{ m} = 0.5 \text{ mm}$$

Exercise 12.7.1

Suppose you need to limit your injection to less than 0.20% of the capillary's length. Using the information from Example 12.7.1 , what is the maximum injection time for a hydrodynamic injection?

Answer

The capillary is 75 cm long, which means that 0.20% of that sample's maximum length is 0.15 cm. To convert this to the maximum volume of sample we use the equation for the volume of a cylinder.

$$V_{inj} = l \pi r^2 = (0.15 \text{ cm})(3.14)\left(25 \times 10^{-4} \text{ cm}\right)^2 = 2.94 \times 10^{-6} \text{ cm}^3$$

Given that 1 cm^3 is equivalent to 1 mL, the maximum volume is 2.94×10^{-6} mL or 2.94×10^{-9} L. To find the maximum injection time, we first solve Equation 8.10.12 for t

$$t = \frac{128 V_{inj} \eta L}{P d^4 \pi} \times 10^{-3} \text{ m}^3/\text{L}$$

and then make appropriate substitutions.

$$t = \frac{(128)\left(2.94 \times 10^{-9}\ \text{L}\right)\left(0.001\ \text{kg m}^{-1}\ \text{s}^{-1}\right)(0.75\ \text{m})}{\left(2.5 \times 10^{3}\ \text{kg m}^{-1}\ \text{s}^{-2}\right)\left(50 \times 10^{-6}\ \text{m}\right)^{4}(3.14)} \times \frac{10^{-3}\ \text{m}^{3}}{\text{L}} = 5.8\ \text{s}$$

The maximum injection time, therefore, is 5.8 s.

In an ***electrokinetic injection*** we place both the capillary and the anode into the sample and briefly apply an potential. The volume of injected sample is the product of the capillary's cross sectional area and the length of the capillary occupied by the sample. In turn, this length is the product of the solute's velocity (see Equation 8.10.6) and time; thus

$$V_{inj} = \pi r^2 L = \pi r^2 (\mu_{ep} + \mu_{eof}) E' t \tag{8.10.13}$$

where r is the capillary's radius, L is the capillary's length, and E' is the effective electric field in the sample. An important consequence of Equation 8.10.13 is that an electrokinetic injection is biased toward solutes with larger electrophoretic mobilities. If two solutes have equal concentrations in a sample, we inject a larger volume—and thus more moles—of the solute with the larger μ_{ep}.

The electric field in the sample is different that the electric field in the rest of the capillary because the sample and the buffer have different ionic compositions. In general, the sample's ionic strength is smaller, which makes its conductivity smaller. The effective electric field is

$$E' = E \times \frac{\chi_{\text{buffer}}}{\chi_{\text{sample}}}$$

where χ_{buffer} and χ_{sample} are the conductivities of the buffer and the sample, respectively.

When an analyte's concentration is too small to detect reliably, it maybe possible to inject it in a manner that increases its concentration. This method of injection is called ***stacking***. Stacking is accomplished by placing the sample in a solution whose ionic strength is significantly less than that of the buffer in the capillary tube. Because the sample plug has a lower concentration of buffer ions, the effective field strength across the sample plug, E', is larger than that in the rest of the capillary.

We know from Equation 8.10.1 that electrophoretic velocity is directly proportional to the electrical field. As a result, the cations in the sample plug migrate toward the cathode with a greater velocity, and the anions migrate more slowly—neutral species are unaffected and move with the electroosmotic flow. When the ions reach their respective boundaries between the sample plug and the buffer, the electrical field decreases and the electrophoretic velocity of the cations decreases and that for the anions increases. As shown in Figure 12.7.6 , the result is a stacking of cations and anions into separate, smaller sampling zones. Over time, the buffer within the capillary becomes more homogeneous and the separation proceeds without additional stacking.

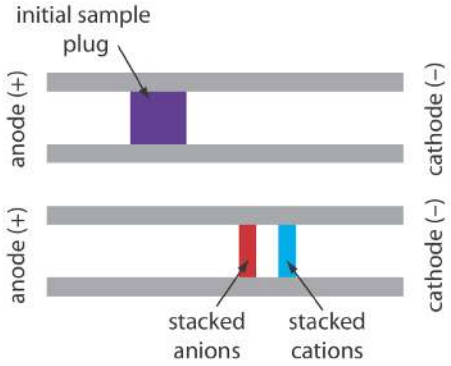


Figure 12.7.6 . The stacking of cations and anions. The top diagram shows the initial sample plug and the bottom diagram shows how the cations and anions are concentrated at opposite sides of the sample plug.

Applying the Electrical Field

Migration in electrophoresis occurs in response to an applied electric field. The ability to apply a large electric field is important because higher voltages lead to shorter analysis times (Equation 8.10.9), more efficient separations (Equation 8.10.10), and better

resolution (Equation 8.10.11). Because narrow bored capillary tubes dissipate Joule heating so efficiently, voltages of up to 40 kV are possible.

> Because of the high voltages, be sure to follow your instrument's safety guidelines.

Detectors

Most of the detectors used in HPLC also find use in capillary electrophoresis. Among the more common detectors are those based on the absorption of UV/Vis radiation, fluorescence, conductivity, amperometry, and mass spectrometry. Whenever possible, detection is done "on-column" before the solutes elute from the capillary tube and additional band broadening occurs.

UV/Vis detectors are among the most popular. Because absorbance is directly proportional to path length, the capillary tubing's small diameter leads to signals that are smaller than those obtained in HPLC. Several approaches have been used to increase the pathlength, including a Z-shaped sample cell and multiple reflections (see Figure 12.7.7). Detection limits are about 10^{-7} M.

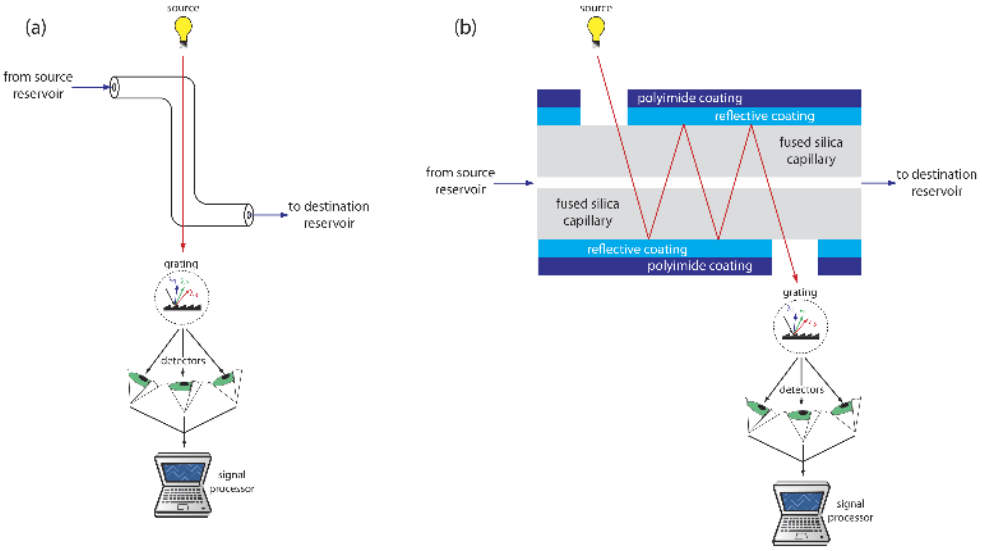


Figure 12.7.7 . Two approaches to on-column detection in capillary electrophoresis using a UV/Vis diode array spectrometer: (a) Z-shaped bend in capillary, and (b) multiple reflections.

Better detection limits are obtained using fluorescence, particularly when using a laser as an excitation source. When using fluorescence detection a small portion of the capillary's protective coating is removed and the laser beam is focused on the inner portion of the capillary tubing. Emission is measured at an angle of 90^{o} to the laser. Because the laser provides an intense source of radiation that can be focused to a narrow spot, detection limits are as low as 10^{-16} M.

Solutes that do not absorb UV/Vis radiation or that do not undergo fluorescence can be detected by other detectors. Table 12.7.1 provides a list of detectors for capillary electrophoresis along with some of their important characteristics.

Table 12.7.1 . Characteristics of Detectors for Capillary Electrophoresis

detector	selectivity (universal or analyte must ...)	detection limited (moles injected)	detection limit (molarity)	on-column detection?
UV/Vis absorbance	have a UV/Vis chromophore	$10^{-13} - 10^{-16}$	$10^{-5} - 10^{-7}$	yes
indirect absorbancd	universal	$10^{-12} - 10^{-15}$	$10^{-4} - 10^{-6}$	yes
fluoresence	have a favorable quantum yield	$10^{-13} - 10^{-17}$	$10^{-7} - 10^{-9}$	yes
laser fluorescence	have a favorable quantum yield	$10^{-18} - 10^{-20}$	$10^{-13} - 10^{-16}$	yes
mass spectrometer	universal (total ion) selective (single ion)	$10^{-16} - 10^{-17}$	$10^{-8} - 10^{-10}$	no
amperometry	undergo oxidation or reduction	$10^{-18} - 10^{-19}$	$10^{-7} - 10^{-10}$	no
conductivity	universal	$10^{-15} - 10^{-16}$	$10^{-7} - 10^{-9}$	no
radiometric	be radioactive	$10^{-17} - 10^{-19}$	$10^{-10} - 10^{-12}$	yes

Capillary Electrophoresis Methods

There are several different forms of capillary electrophoresis, each of which has its particular advantages. Four of these methods are described briefly in this section.

Capillary Zone Electrophoresis (CZE)

The simplest form of capillary electrophoresis is ***capillary zone electrophoresis***. In CZE we fill the capillary tube with a buffer and, after loading the sample, place the ends of the capillary tube in reservoirs that contain additional buffer. Usually the end of the capillary containing the sample is the anode and solutes migrate toward the cathode at a velocity determined by their respective electrophoretic mobilities and the electroosmotic flow. Cations elute first, with smaller, more highly charged cations eluting before larger cations with smaller charges. Neutral species elute as a single band. Anions are the last species to elute, with smaller, more negatively charged anions being the last to elute.

We can reverse the direction of electroosmotic flow by adding an alkylammonium salt to the buffer solution. As shown in Figure 12.7.8 , the positively charged end of the alkyl ammonium ions bind to the negatively charged silanate ions on the capillary's walls. The tail of the alkyl ammonium ion is hydrophobic and associates with the tail of another alkyl ammonium ion. The result is a layer of positive charges that attract anions in the buffer. The migration of these solvated anions toward the anode reverses the electroosmotic flow's direction. The order of elution is exactly opposite that observed under normal conditions.

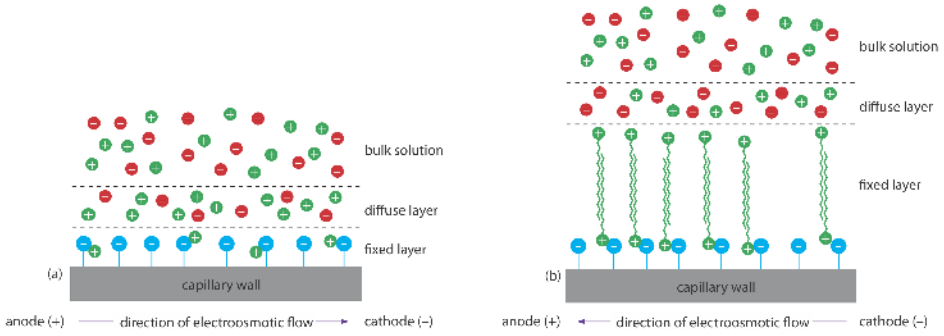


Figure 12.7.8 . Two modes of capillary zone electrophoresis showing (a) normal migration with electroosmotic flow toward the cathode and (b) reversed migration in which the electroosmotic flow is toward the anode.

Coating the capillary's walls with a nonionic reagent eliminates the electroosmotic flow. In this form of CZE the cations migrate from the anode to the cathode. Anions elute into the source reservoir and neutral species remain stationary.

Capillary zone electrophoresis provides effective separations of charged species, including inorganic anions and cations, organic acids and amines, and large biomolecules such as proteins. For example, CZE was used to separate a mixture of 36 inorganic and organic ions in less than three minutes [Jones, W. R.; Jandik, P. *J. Chromatog.* **1992**, *608*, 385–393]. A mixture of neutral species, of course, can not be resolved.

Micellar Electrokinetic Capillary Chromatography (MEKC)

One limitation to CZE is its inability to separate neutral species. ***Micellar electrokinetic capillary chromatography*** overcomes this limitation by adding a surfactant, such as sodium dodecylsulfate (Figure 12.7.9 a) to the buffer solution. Sodium dodecylsulfate, or SDS, consists of a long-chain hydrophobic tail and a negatively charged ionic functional group at its head. When the concentration of SDS is sufficiently large a micelle forms. A micelle consists of a spherical agglomeration of 40–100 surfactant molecules in which the hydrocarbon tails point inward and the negatively charged heads point outward (Figure 12.7.9 b).

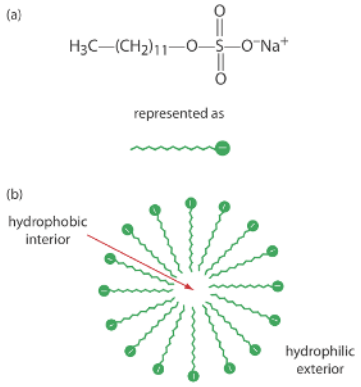


Figure 12.7.9 . (a) Structure of sodium dodecylsulfate and (b) cross section through a micelle showing its hydrophobic interior and its hydrophilic exterior.

Because micelles have a negative charge, they migrate toward the cathode with a velocity less than the electroosmotic flow velocity. Neutral species partition themselves between the micelles and the buffer solution in a manner similar to the partitioning of solutes between the two liquid phases in HPLC. Because there is a partitioning between two phases, we include the descriptive term chromatography in the techniques name. Note that in MEKC both phases are mobile.

The elution order for neutral species in MEKC depends on the extent to which each species partitions into the micelles. Hydrophilic neutrals are insoluble in the micelle's hydrophobic inner environment and elute as a single band, as they would in CZE. Neutral solutes that are extremely hy- drophobic are completely soluble in the micelle, eluting with the micelles as a single band. Those neutral species that exist in a partition equilibrium between the buffer and the micelles elute between the completely hydro- philic and completely hydrophobic neutral species. Those neutral species that favor the buffer elute before those favoring the micelles. Micellar electrokinetic chromatography is used to separate a wide variety of samples, including mixtures of pharmaceutical compounds, vitamins, and explosives.

Capillary Gel Electrophoresis (CGE)

In ***capillary gel electrophoresis*** the capillary tubing is filled with a polymeric gel. Because the gel is porous, a solute migrates through the gel with a velocity determined both by its electrophoretic mobility and by its size. The ability to effect a separation using size is helpful when the solutes have similar electrophoretic mobilities. For example, fragments of DNA of varying length have similar charge-to-size ratios, making their separation by CZE difficult. Because the DNA fragments are of different size, a CGE separation is possible.

The capillary used for CGE usually is treated to eliminate electroosmotic flow to prevent the gel from extruding from the capillary tubing. Samples are injected electrokinetically because the gel provides too much resistance for hydrodynamic sampling. The primary application of CGE is the separation of large biomolecules, including DNA fragments, proteins, and oligonucleotides.

Capillary Electrochromatography (CEC)

Another approach to separating neutral species is ***capillary electrochromatography***. In CEC the capillary tubing is packed with 1.5–3 μm particles coated with a bonded stationary phase. Neutral species separate based on their ability to partition between the stationary phase and the buffer, which is moving as a result of the electroosmotic flow; Figure 12.7.10 provides a representative example for the separation of a mixture of hydrocarbons. A CEC separation is similar to the analogous HPLC separation, but without the need for high pressure pumps. Efficiency in CEC is better than in HPLC, and analysis times are shorter.

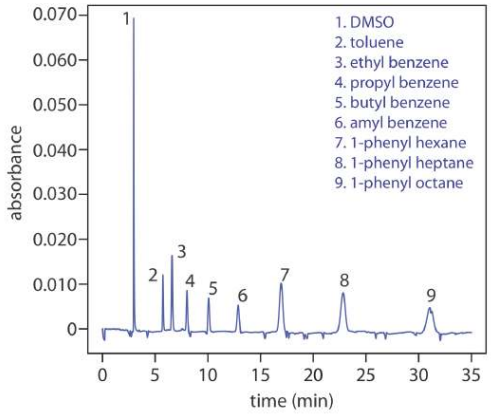


Figure 12.7.10 . Capillary electrochromatographic separation of a mixture of hydrocarbons in DMSO. The column contains a porous polymer of butyl methacrylate and lauryl acrylate (25%:75% mol:mol) with butane dioldacrylate as a crosslinker. Data provided by Zoe LaPier and Michelle Bushey, Department of Chemistry, Trinity University.

The best way to appreciate the theoretical and the practical details discussed in this section is to carefully examine a typical analytical method. Although each method is unique, the following description of the determination of a vitamin B complex by capillary zone electrophoresis or by micellar electrokinetic capillary chromatography provides an instructive example of a typical procedure. The description here is based on Smyth, W. F. *Analytical Chemistry of Complex Matrices*, Wiley Teubner: Chichester, England, 1996, pp. 154–156.

Representative Method 12.7.1: Determination of Vitamin B Complex by CZE or MEKC

Description of Method

The water soluble vitamins B_1 (thiamine hydrochloride), B_2 (riboflavin), B_3 (niacinamide), and B_6 (pyridoxine hydrochloride) are determined by CZE using a pH 9 sodium tetraborate-sodium dihydrogen phosphate buffer, or by MEKC using the same buffer with the addition of sodium dodecyl sulfate. Detection is by UV absorption at 200 nm. An internal standard of *o*-ethoxybenzamide is used to standardize the method.

Procedure

Crush a vitamin B complex tablet and place it in a beaker with 20.00 mL of a 50 % v/v methanol solution that is 20 mM in sodium tetraborate and 100.0 ppm in *o*-ethoxybenzamide. After mixing for 2 min to ensure that the B vitamins are dissolved, pass a 5.00-mL portion through a 0.45-μm filter to remove insoluble binders. Load an approximately 4 nL sample into a capillary column with an inner diameter of a 50 μm. For CZE the capillary column contains a 20 mM pH 9 sodium tetraborate-sodium dihydrogen phosphate buffer. For MEKC the buffer is also 150 mM in sodium dodecyl sulfate. Apply a 40 kV/m electrical field to effect both the CZE and MEKC separations.

Questions

1. Methanol, which elutes at 4.69 min, is included as a neutral species to indicate the electroosmotic flow. When using standard solutions of each vitamin, CZE peaks are found at 3.41 min, 4.69 min, 6.31 min, and 8.31 min. Examine the structures and pK_a information in Figure 12.7.11 and identify the order in which the four B vitamins elute.

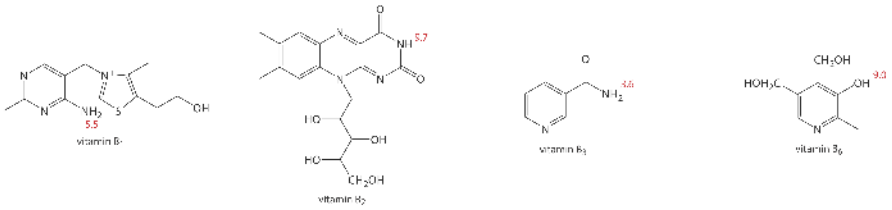


Figure 12.7.11 . Structures of the four water soluble B vitamins in their predominate forms at a pH of 9; pK_a values are shown in red.

At a pH of 9, vitamin B_1 is a cation and elutes before the neutral species methanol; thus it is the compound that elutes at 3.41 min. Vitamin B_3 is a neutral species at a pH of 9 and elutes with methanol at 4.69 min. The remaining two B vitamins are weak acids that partially ionize to weak base anions at a pH of 9. Of the two, vitamin B_6 is the stronger acid (a pK_a of 9.0 versus a pK_a of 9.7) and is present to a greater extent in its anionic form. Vitamin B_6, therefore, is the last of the vitamins to elute.

2. The order of elution when using MEKC is vitamin B_3 (5.58 min), vitamin B_6 (6.59 min), vitamin B_2 (8.81 min), and vitamin B_1 (11.21 min). What conclusions can you make about the solubility of the B vitamins in the sodium dodecylsulfate micelles? The micelles elute at 17.7 min.

The elution time for vitamin B_1 shows the greatest change, increasing from 3.41 min to 11.21 minutes. Clearly vitamin B_1 has the greatest solubility in the micelles. Vitamin B_2 and vitamin B3 have a more limited solubility in the micelles, and show only slightly longer elution times in the presence of the micelles. Interestingly, the elution time for vitamin B_6 decreases in the presence of the micelles.

3. For quantitative work an internal standard of *o*-ethoxybenzamide is added to all samples and standards. Why is an internal standard necessary?

Although the method of injection is not specified, neither a hydrodynamic injection nor an electrokinetic injection is particularly reproducible. The use of an internal standard compensates for this limitation.

Evaluation

When compared to GC and HPLC, capillary electrophoresis provides similar levels of accuracy, precision, and sensitivity, and it provides a comparable degree of selectivity. The amount of material injected into a capillary electrophoretic column is significantly smaller than that for GC and HPLC—typically 1 nL versus 0.1 µL for capillary GC and 1–100 µL for HPLC. Detection limits for capillary electrophoresis, however, are 100–1000 times poorer than that for GC and HPLC. The most significant advantages of capillary electrophoresis are improvements in separation efficiency, time, and cost. Capillary electrophoretic columns contain substantially more theoretical plates ($\approx 10^6$ plates/m) than that found in HPLC ($\approx 10^5$ plates/m) and capillary GC columns ($\approx 10^3$ plates/m), providing unparalleled resolution and peak capacity. Separations in capillary electrophoresis are fast and efficient. Furthermore, the capillary column's small volume means that a capillary electrophoresis separation requires only a few microliters of buffer, compared to 20–30 mL of mobile phase for a typical HPLC separation.

This page titled 8.10: Electrophoresis is shared under a CC BY-NC-SA 4.0 license and was authored, remixed, and/or curated by Kathryn Davis.

- **12.7: Electrophoresis** by David Harvey is licensed CC BY-NC-SA 4.0.

CHAPTER OVERVIEW

9: Solubility Equilibria

9.1: Ladder Diagrams

9.2: Solving Equilibrium Problems

9.3: Activity Effects

9.4: Precipitation Gravimetry

This page titled 9: Solubility Equilibria is shared under a not declared license and was authored, remixed, and/or curated by Kathryn Davis.

9.1: Ladder Diagrams

When we develop or evaluate an analytical method, we often need to understand how the chemistry that takes place affects our results. Suppose we wish to isolate Ag^+ by precipitating it as AgCl. If we also need to control pH, then we must use a reagent that does not adversely affect the solubility of AgCl. It is a mistake to use NH_3 to adjust the pH, for example, because it increases the solubility of AgCl (see reaction 6.5.4). One of the primary sources of determinate errors in many analytical methods is failing to account for potential chemical interferences.

In this section we introduce the ladder diagram as a simple graphical tool for visualizing equilibrium chemistry. We will use ladder diagrams to determine what reactions occur when we combine several reagents, to estimate the approximate composition of a system at equilibrium, and to evaluate how a change to solution conditions might affect an analytical method.

> Although not specifically on the topic of ladder diagrams as developed in this section, the following papers provide appropriate background information: (a) Runo, J. R.; Peters, D. G. *J. Chem. Educ.* **1993**, *70*, 708–713; (b) Vale, J.; Fernández-Pereira, C.; Alcalde, M. *J. Chem. Educ.* **1993**, *70*, 790–795; (c) Fernández-Pereira, C.; Vale, J. *Chem. Educator* **1996**, *6*, 1–18; (d) Fernández- Pereira, C.; Vale, J.; Alcalde, M. *Chem. Educator* **2003**, *8*, 15–21; (e) Fernández-Pereira, C.; Alcalde, M.; Villegas, R.; Vale, J. *J. Chem. Educ.* **2007**, *84*, 520–525. Ladder diagrams are a great tool for helping you to think intuitively about analytical chemistry. We will make frequent use of them in the chapters to follow.

Ladder Diagrams for Acid–Base Equilibria

Let's use acetic acid, CH_3COOH, to illustrate the process we will use to draw and to interpret an acid–base ladder diagram. Before we draw the diagram, however, let's consider the equilibrium reaction in more detail. Acetic acid's acid dissociation reaction and equilibrium constant expression are

$$CH_3COOH(aq) + H_2O(l) \rightleftharpoons H_3O^+(aq) + CH_3COO^-(aq)$$

$$K_a = \frac{[CH_3COO^-]\,[H_3O^+]}{[CH_3COOH]} = 1.75 \times 10^{-5}$$

First, let's take the logarithm of each term in this equation and multiply through by –1

$$-\log K_a = 4.76 = -\log [H_3O^+] - \log \frac{[CH_3COO^-]}{[CH_3COOH]}$$

Now, let's replace $-\log[H_3O^+]$ with pH and rearrange the equation to obtain the result shown here.

$$pH = 4.76 + \log \frac{[CH_3COO^-]}{[CH_3COOH]} \tag{9.1.1}$$

Equation 9.1.1 tells us a great deal about the relationship between pH and the relative amounts of acetic acid and acetate at equilibrium. If the concentrations of CH_3COOH and CH_3COO^- are equal, then Equation 9.1.1 reduces to

$$pH = 4.76 + \log(1) = 4.76 + 0 = 4.76$$

If the concentration of CH_3COO^- is greater than that of CH_3COOH, then the log term in Equation 9.1.1 is positive and the pH is greater than 4.76. This is a reasonable result because we expect the concentration of the conjugate base, CH_3COO^-, to increase as the pH increases. Similar reasoning will convince you that the pH is less than 4.76 when the concentration of CH_3COOH exceeds that of CH_3COO^-.

Now we are ready to construct acetic acid's ladder diagram (Figure 6.6.1). First, we draw a vertical arrow that represents the solution's pH, with smaller (more acidic) pH levels at the bottom and larger (more basic) pH levels at the top. Second, we draw a horizontal line at a pH equal to acetic acid's pK_a value. This line, or step on the ladder, divides the pH axis into regions where either CH_3COOH or CH_3COO^- is the predominate species. This completes the ladder diagram.

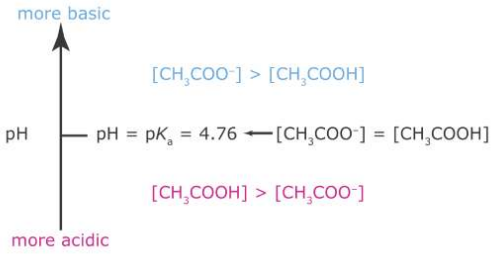


Figure 6.6.1 . Acid–base ladder diagram for acetic acid showing the relative concentrations of CH_3COOH and CH_3COO^-. A simpler version of this ladder diagram dispenses with the equalities and inequalities and shows only the predominate species in each region.

Using the ladder diagram, it is easy to identify the predominate form of acetic acid at any pH. At a pH of 3.5, for example, acetic acid exists primarily as CH_3COOH. If we add sufficient base to the solution such that the pH increases to 6.5, the predominate form of acetic acid is CH_3COO^-.

Example 6.6.1

Draw a ladder diagram for the weak base *p*-nitrophenolate and identify its predominate form at a pH of 6.00.

Solution

To draw a ladder diagram for a weak base, we simply draw the ladder diagram for its conjugate weak acid. From Appendix 11, the pK_a for *p*-nitrophenol is 7.15. The resulting ladder diagram is shown in Figure 6.6.2 . At a pH of 6.00, *p*-nitrophenolate is present primarily in its weak acid form.

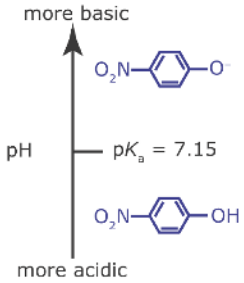


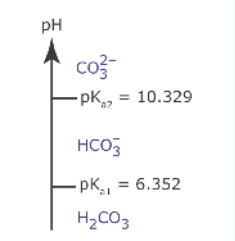
Figure 6.6.2 . Acid–base ladder diagram for *p*-nitrophenolate.

Exercise 6.6.1

Draw a ladder diagram for carbonic acid, H_2CO_3. Because H_2CO_3 is a diprotic weak acid, your ladder diagram will have two steps. What is the predominate form of carbonic acid when the pH is 7.00? Relevant equilibrium constants are in Appendix 11.

Answer

From Appendix 11, the pK_a values for H_2CO_3 are 6.352 and 10.329. The ladder diagram for H_2CO_3 is shown below. The predominate form at a pH of 7.00 is $\mathbf{HCO_3^-}$.



A ladder diagram is particularly useful for evaluating the reactivity between a weak acid and a weak base. Figure 6.6.3 , for example, shows a single ladder diagram for acetic acid/acetate and for *p*-nitrophenol/*p*-nitrophenolate. An acid and a base can not co-exist if their respective areas of predominance do not overlap. If we mix together solutions of acetic acid and sodium *p*-nitrophenolate, the reaction

$$\mathrm{C_6H_4NO_2^-}(aq) + \mathrm{CH_3COOH}(aq) \rightleftharpoons \mathrm{CH_3COO^-}(aq) + \mathrm{C_6H_4NO_2H}(aq) \tag{9.1.2}$$

occurs because the areas of predominance for acetic acid and *p*-nitrophenolate do not overlap. The solution's final composition depends on which species is the limiting reagent. The following example shows how we can use the ladder diagram in Figure 6.6.3 to evaluate the result of mixing together solutions of acetic acid and *p*-nitrophenolate.

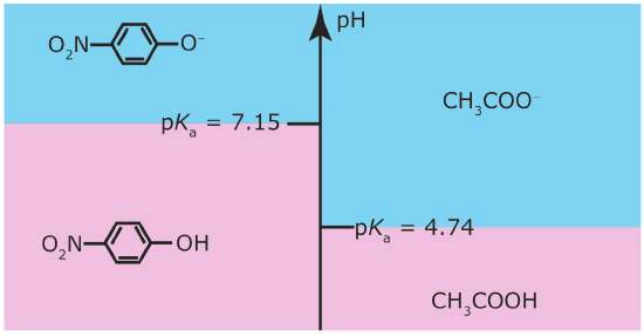


Figure 6.6.3 . Acid–base ladder diagram showing the areas of predominance for acetic acid/acetate and for *p*-nitrophenol/*p*-nitrophenolate. The areas shaded in blue shows the pH range where the weak bases are the predominate species; the weak acid forms are the predominate species in the areas shaded in pink.

Example 6.6.2

Predict the approximate pH and the final composition after mixing together 0.090 moles of acetic acid and 0.040 moles of *p*-nitrophenolate.

Solution

The ladder diagram in Figure 6.6.3 indicates that the reaction between acetic acid and *p*-nitrophenolate is favorable. Because acetic acid is in excess, we assume the reaction of *p*-nitrophenolate to *p*-nitrophenol is complete. At equilibrium essentially no *p*-nitrophenolate remains and there are 0.040 mol of *p*-nitrophenol. Converting *p*-nitrophenolate to *p*-nitrophenol consumes 0.040 moles of acetic acid; thus

$$\text{moles } \mathrm{CH_3COOH} = 0.090 - 0.040 = 0.050 \text{ mol}$$
$$\text{moles } \mathrm{CH_3COO^-} = 0.040 \text{ mol}$$

According to the ladder diagram, the pH is 4.74 when there are equal amounts of CH_3COOH and CH_3COO^-. Because we have slightly more CH_3COOH than CH_3COO^-, the pH is slightly less than 4.74.

Exercise 6.6.2

Using Figure 6.6.3 , predict the approximate pH and the composition of the solution formed by mixing together 0.090 moles of *p*-nitrophenolate and 0.040 moles of acetic acid.

Answer

The ladder diagram in Figure 6.6.3 indicates that the reaction between acetic acid and *p*-nitrophenolate is favorable. Because *p*-nitrophenolate is in excess, we assume the reaction of acetic acid to acetate is complete. At equilibrium essentially no acetic acid remains and there are 0.040 moles of acetate. Converting acetic acid to acetate consumes 0.040 moles of *p*-nitrophenolate; thus

$$\text{moles } p\text{-nitrophenolate } = 0.090 - 0.040 = 0.050 \text{ mol}$$

$$\text{moles } p\text{-nitrophenol } = 0.040 \text{ mol}$$

According to the ladder diagram for this system, the pH is 7.15 when there are equal concentrations of *p*-nitrophenol and *p*-nitrophenolate. Because we have slightly more *p*-nitrophenolate than we have *p*-nitrophenol, the pH is slightly greater than 7.15.

If the areas of predominance for an acid and a base overlap, then we do not expect that much of a reaction will occur. For example, if we mix together solutions of CH_3COO^- and *p*-nitrophenol, we do not expect a significant change in the moles of either reagent. Furthermore, the pH of the mixture must be between 4.76 and 7.15, with the exact pH depending upon the relative amounts of CH_3COO^- and *p*-nitrophenol.

We also can use an acid–base ladder diagram to evaluate the effect of pH on other equilibria. For example, the solubility of CaF_2

$$CaF_2(s) \rightleftharpoons Ca^{2+}(aq) + 2F^-(aq)$$

is affected by pH because F^- is a weak base. From Le Châtelier's principle, we know that converting F^- to HF will increase the solubility of CaF_2. To minimize the solubility of CaF_2 we need to maintain the solution's pH so that F^- is the predominate species. The ladder diagram for HF (Figure 6.6.4) shows us that maintaining a pH of more than 3.17 will minimize solubility losses.

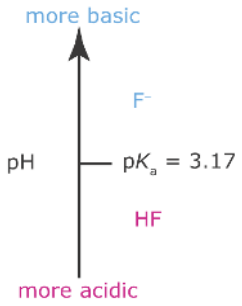


Figure 6.6.4 . Acid–base ladder diagram for HF. To minimize the solubility of CaF_2, we need to keep the pH above 3.17, with more basic pH levels leading to smaller solubility losses. See Chapter 8 for a more detailed discussion.

Ladder Diagrams for Complexation Equilibria

We can apply the same principles for constructing and interpreting an acid–base ladder diagram to equilibria that involve metal–ligand complexes. For a complexation reaction we define the ladder diagram's scale using the concentration of uncomplexed, or free ligand, pL. Using the formation of $Cd(NH_3)^{2+}$ as an example

$$Cd^{2+}(aq) + NH_3(aq) \rightleftharpoons Cd(NH_3)^{2+}(aq)$$

we can show that log K_1 is the dividing line between the areas of predominance for Cd^{2+} and for $Cd(NH_3)^{2+}$.

$$K_1 = 3.55 \times 10^2 = \frac{[Cd(NH_3)^{2+}]}{[Cd^{2+}]\,[NH_3]}$$

$$\log K_1 = \log\left(3.55 \times 10^2\right) = \log \frac{[Cd(NH_3)^{2+}]}{[Cd^{2+}]} - \log [NH_3]$$

$$\log K_1 = 2.55 = \log \frac{[Cd(NH_3)^{2+}]}{[Cd^{2+}]} + pNH_3$$

$$pNH_3 = \log K_1 + \log \frac{[Cd^{2+}]}{[Cd(NH_3)^{2+}]} = 2.55 + \log \frac{[Cd^{2+}]}{[Cd(NH_3)^{2+}]}$$

Thus, Cd^{2+} is the predominate species when pNH_3 is greater than 2.55 (a concentration of NH_3 smaller than 2.82×10^{-3} M) and for a pNH_3 value less than 2.55, $Cd(NH_3)^{2+}$ is the predominate species. Figure 6.6.5 shows a complete metal–ligand ladder diagram for Cd^{2+} and NH_3 that includes additional Cd–NH_3 complexes.

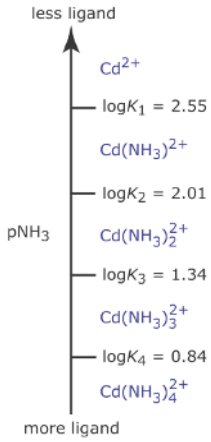


Figure 6.6.5 . Metal–ligand ladder diagram for Cd^{2+}–NH_3 complexation reactions. Note that higher-order complexes form when pNH_3 is smaller (which corresponds to larger concentrations of NH_3).

Example 6.6.3

Draw a single ladder diagram for the $Ca(EDTA)^{2-}$ and the $Mg(EDTA)^{2-}$ metal–ligand complexes. Use your ladder diagram to predict the result of adding 0.080 moles of Ca^{2+} to 0.060 moles of $Mg(EDTA)^{2-}$. EDTA is an abbreviation for the ligand ethylenediaminetetraacetic acid.

Solution

Figure 6.6.6 shows the ladder diagram for this system of metal–ligand complexes. Because the predominance regions for Ca^{2+} and $Mg(EDTA)^{2-}$ do not overlap, the reaction

$$\mathbf{Ca^{2+}}(aq) + \mathbf{Mg(EDTA)^{2-}}(aq) \rightleftharpoons \mathbf{Ca(EDTA)^{2-}}(aq) + \mathbf{Mg^{2+}}(aq)$$

proceeds essentially to completion. Because Ca^{2+} is the excess reagent, the composition of the final solution is approximately

$$\text{moles } \mathbf{Ca^{2+}} = 0.080 - 0.060 = 0.020 \text{ mol}$$

$$\text{moles } \mathbf{Ca(EDTA)^{2-}} = 0.060 \text{ mol}$$

$$\text{moles } \mathbf{Mg^{2+}} = 0.060 \text{ mol}$$

$$\text{moles } \mathbf{Mg(EDTA)^{2-}} = 0 \text{ mol}$$

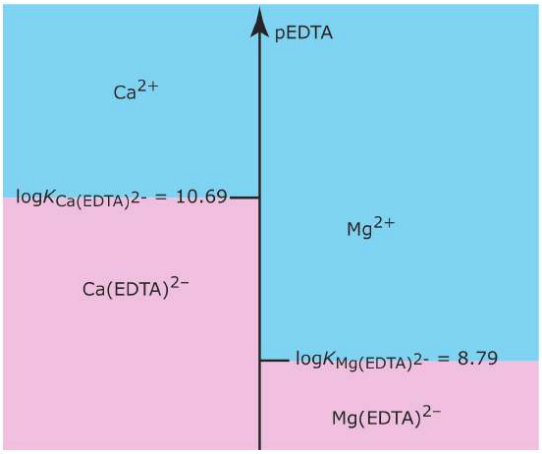


Figure 6.6.6 . Metal–ligand ladder diagram for $Ca(EDTA)^{2-}$ and for $Mg(EDTA)^{2-}$. The areas shaded in blue show the pEDTA range where the free metal ions are the predominate species; the metal–ligand complexes are the predominate species in the areas shaded in pink.

The metal–ligand ladder diagram in Figure 6.6.5 uses stepwise formation constants. We also can construct a ladder diagram using cumulative formation constants. For example, the first three stepwise formation constants for the reaction of Zn^{2+} with NH_3

$$Zn^{2+}(aq) + NH_3(aq) \rightleftharpoons Zn(NH_3)^{2+}(aq) \quad K_1 = 1.6 \times 10^2$$

$$Zn(NH_3)^{2+}(aq) + NH_3(aq) \rightleftharpoons Zn(NH_3)_2^{2+}(aq) \quad K_2 = 1.95 \times 10^2$$

$$Zn(NH_3)_2^{2+}(aq) + NH_3(aq) = Zn(NH_3)_3^{2+}(aq) \quad K_3 = 2.3 \times 10^2$$

suggests that the formation of $Zn(NH_3)_3^{2+}$ is more favorable than the formation of $Zn(NH_3)^{2+}$ or $Zn(NH_3)_2^{2+}$. For this reason, the equilibrium is best represented by the cumulative formation reaction shown here.

$$Zn^{2+}(aq) + 3NH_3(aq) \rightleftharpoons Zn(NH_3)_3^{2+}(aq) \quad \beta_3 = 7.2 \times 10^6$$

> Because K_3 is greater than K_2, which is greater than K_1, the formation of the metal-ligand complex $Zn(NH_3)_3^{2+}$ is more favorable than the formation of the other metal ligand complexes. For this reason, at lower values of pNH_3 the concentration of $Zn(NH_3)_3^{2+}$ is larger than the concentrations of $Zn(NH_3)^{2+}$ or $Zn(NH_3)_2^{2+}$. The value of β_3 is
>
> $$\beta_3 = K_1 \times K_2 \times K_3$$

To see how we incorporate this cumulative formation constant into a ladder diagram, we begin with the reaction's equilibrium constant expression.

$$\beta_3 = \frac{[Zn(NH_3)_3^{2+}]}{[Zn^{2+}][NH_3]^3}$$

Taking the log of each side

$$\log \beta_3 = \log \frac{[Zn(NH_3)_3^{2+}]}{[Zn^{2+}]} - 3 \log [NH_3]$$

and rearranging gives

$$pNH_3 = \frac{1}{3} \log \beta_3 + \frac{1}{3} \log \frac{[Zn^{2+}]}{[Zn(NH_3)_3^{2+}]}$$

When the concentrations of Zn and $Zn(NH_3)_3^{2+}$ are equal, then

$$pNH_3 = \frac{1}{3} \log \beta_3 = 2.29$$

In general, for the metal–ligand complex ML_n, the step for a cumulative formation constant is

$$pL = \frac{1}{n} \log \beta_n$$

Figure 6.6.7 shows the complete ladder diagram for the Zn^{2+}–NH_3 system.

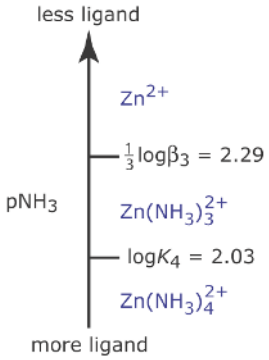


Figure 6.6.7 . Ladder diagram for Zn^{2+}–NH_3 metal–ligand complexation reactions showing both a step based on a cumulative formation constant and a step based on a stepwise formation constant.

Ladder Diagrams for Oxidation/Reduction Equilibria

We also can construct ladder diagrams to help us evaluate redox equilibria. Figure 6.6.8 shows a typical ladder diagram for two half-reactions in which the scale is the potential, E.

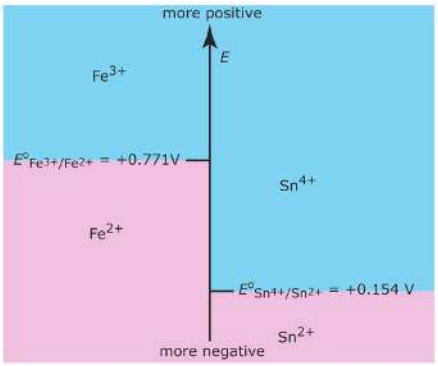


Figure 6.6.8 . Redox ladder diagram for Fe^{3+}/Fe^{2+} and for Sn^{4+}/Sn^{2+}. The areas shaded in blue show the potential range where the oxidized forms are the predominate species; the reduced forms are the predominate species in the areas shaded in pink. Note that a more positive potential favors the oxidized form.

The Nernst equation defines the areas of predominance. Using the Fe^{3+}/Fe^{2+} half-reaction as an example, we write

$$E = E° - \frac{RT}{nF}\ln\frac{[Fe^{2+}]}{[Fe^{3+}]} = 0.771 - 0.05916\log\frac{[Fe^{2+}]}{[Fe^{3+}]}$$

At a potential more positive than the standard state potential, the predominate species is Fe^{3+}, whereas Fe^{2+} predominates at potentials more negative than $E°$. When coupled with the step for the Sn^{4+}/Sn^{2+} half-reaction we see that Sn^{2+} is a useful reducing agent for Fe^{3+}. If Sn^{2+} is in excess, the potential of the resulting solution is near +0.154 V.

Because the steps on a redox ladder diagram are standard state potentials, a complication arises if solutes other than the oxidizing agent and reducing agent are present at non-standard state concentrations. For example, the potential for the half-reaction

$$UO_2^{2+}(aq) + 4H_3O^+(aq) + 2e^- \rightleftharpoons U^{4+}(aq) + 6H_2O(l)$$

depends on the solution's pH. To define areas of predominance in this case we begin with the Nernst equation

$$E = +0.327 - \frac{0.05916}{2}\log\frac{[U^{4+}]}{[UO_2^{2+}]\,[H_3O^+]^4}$$

and factor out the concentration of H_3O^+.

$$E = +0.327 + \frac{0.05916}{2}\log[H_3O^+]^4 - \frac{0.05916}{2}\log\frac{[U^{4+}]}{[UO_2^{2+}]}$$

From this equation we see that the area of predominance for UO_2^{2+} and U^{4+} is defined by a step at a potential where $[U^{4+}] = [UO_2^{2+}]$.

$$E = +0.327 + \frac{0.05916}{2}\log\left[H_3O^+\right]^4 = +0.327 - 0.1183pH$$

Figure 6.6.9 shows how pH affects the step for the UO_2^{2+} /U^{4+} half-reaction.

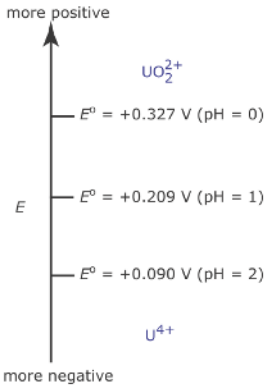


Figure 6.6.9 . Redox ladder diagram for the UO_2^{2+}/U^{4+} half-reaction showing the effect of pH on the step defined by the standard state's potential.

This page titled 9.1: Ladder Diagrams is shared under a CC BY-NC-SA 4.0 license and was authored, remixed, and/or curated by Kathryn Davis.

- **6.6: Ladder Diagrams** by David Harvey is licensed CC BY-NC-SA 4.0.

9.2: Solving Equilibrium Problems

Ladder diagrams are a useful tool for evaluating chemical reactivity and for providing a reasonable estimate of a chemical system's composition at equilibrium. If we need a more exact quantitative description of the equilibrium condition, then a ladder diagram is insufficient; instead, we need to find an algebraic solution. In this section we will learn how to set-up and solve equilibrium problems. We will start with a simple problem and work toward more complex problems.

A Simple Problem: The Solubility of $Pb(IO_3)_2$

If we place an insoluble compound such as $Pb(IO_3)_2$ in deionized water, the solid dissolves until the concentrations of Pb^{2+} and IO_3^- satisfy the solubility product for $Pb(IO_3)_2$. At equilibrium the solution is saturated with $Pb(IO_3)_2$, which means simply that no more solid can dissolve. How do we determine the equilibrium concentrations of Pb^{2+} and IO_3^-, and what is the molar solubility of $Pb(IO_3)_2$ in this saturated solution?

> When we first add solid $Pb(IO_3)_2$ to water, the concentrations of Pb^{2+} and IO_3^- are zero and the reaction quotient, Q_r, is
>
> $$Q_r = [Pb^{2+}]\,[IO_3^-]^2 = 0$$
>
> As the solid dissolves, the concentrations of these ions increase, but Q_r remains smaller than K_{sp}. We reach equilibrium and "satisfy the solubility product" when $Q_r = K_{sp}$.

We begin by writing the equilibrium reaction and the solubility product expression for $Pb(IO_3)_2$.

$$Pb(IO_3)_2(s) \rightleftharpoons Pb^{2+}(aq) + 2IO_3^-(aq)$$

e

$$K_{sp} = [Pb^{2+}]\,[IO_3^-]^2 = 2.5 \times 10^{-13} \tag{9.2.1}$$

As $Pb(IO_3)_2$ dissolves, two IO_3^- ions form for each ion of Pb^{2+}. If we assume that the change in the molar concentration of Pb^{2+} at equilibrium is x, then the change in the molar concentration of IO_3^- is $2x$. The following table helps us keep track of the initial concentrations, the change in con- centrations, and the equilibrium concentrations of Pb2+ and IO_3^-.

concentrations	$Pb(IO_3)_2$ (s)	$\rightleftharpoons$	Pb^{2+} (aq)	+	$2IO_3^-$ (aq)
initial	solid		0		0
change	solid		$+x$		$+\,2x$
equilibrium	solid		x		$2x$

> Because a solid, such as $Pb(IO_3)_2$, does not appear in the solubility product expression, we do not need to keep track of its concentration. Remember, however, that the K_{sp} value applies only if there is some solid $Pb(IO_3)_2$ present at equilibrium.

Substituting the equilibrium concentrations into Equation 9.2.1 and solving gives

$$(x)(2x)^2 = 4x^3 = 2.5 \times 10^{-13}$$

$$x = 3.97 \times 10^{-5}$$

Substituting this value of x back into the equilibrium concentration expressions for Pb^{2+} and IO_3^- gives their concentrations as

$$[Pb^{2+}] = x = 4.0 \times 10^{-5}\text{M and } [IO_3^-] = 2x = 7.9 \times 10^{-5}$$

Because one mole of $Pb(IO_3)_2$ contains one mole of Pb^{2+}, the molar solubility of $Pb(IO_3)_2$ is equal to the concentration of Pb^{2+}, or 4.0×10^{-5} M.

We can express a compound's solubility in two ways: as its molar solubility (mol/L) or as its mass solubility (g/L). Be sure to express your answer clearly.

Exercise 6.7.1

Calculate the molar solubility and the mass solubility for Hg_2Cl_2, given the following solubility reaction and K_{sp} value.

$$\mathbf{Hg_2Cl_2}(s) \rightleftharpoons \mathbf{Hg_2^{2+}}(aq) + 2\mathbf{Cl^-}(aq) \quad K_{sp} = 1.2 \times 10^{-8}$$

Answer

When Hg_2Cl_2 dissolves, two Cl^- are produced for each ion of $\mathbf{Hg_2^{2+}}$. If we assume x is the change in the molar concentration of $\mathbf{Hg_2^{2+}}$, then the change in the molar concentration of Cl^- is $2x$. The following table helps us keep track of our solution to this problem.

concentration	Hg_2Cl_2 (s)	$\rightleftharpoons$	$\mathbf{Hg_2^{2+}}$ (aq)	+	Cl^- (aq)
initial	solid		0		0
change	solid		$+x$		$+2x$
equilibrium	solid		x		$2x$

Substituting the equilibrium concentrations into the K_{sp} expression forHg_2Cl_2 gives

$$K_{sp} = [\mathbf{Hg_2^{2+}}]\,[\mathbf{Cl^-}]^2 = (x)(2x)^2 = 4x^3 = 1.2 \times 10^{-18}$$

$$x = 6.69 \times 10^{-7}$$

Substituting x back into the equilibrium expressions for $\mathbf{Hg_2^{2+}}$ and Cl^- gives their concentrations as

$$[\mathbf{Hg_2^{2+}}] = x = 6.7 \times 10^{-7}\ \mathbf{M} \quad [\mathbf{Cl^-}] = 2x = 1.3 \times 10^{-6}\ \mathbf{M}$$

The molar solubility is equal to $[\mathbf{Hg_2^{2+}}]$, or $\mathbf{6.7 \times 10^{-7}}$ mol/L.

A More Complex Problem: The Common Ion Effect

Calculating the solubility of $Pb(IO_3)_2$ in deionized water is a straightforward problem because the solid's dissolution is the only source of Pb^{2+} and $\mathbf{IO_3^-}$. But what if we add $Pb(IO_3)_2$ to a solution of 0.10 M $Pb(NO_3)_2$? Before we set-up and solve this problem algebraically, think about the system's chemistry and decide whether the solubility of $Pb(IO_3)_2$ will increase, decrease, or remain the same. Beginning a problem by thinking about the likely answer is a good habit to develop. Knowing what answers are reasonable will help you spot errors in your calculations and give you more confidence that your solution to a problem is correct. Because the solution already contains a source of Pb^{2+}, we can use Le Châtelier's principle to predict that the solubility of $Pb(IO_3)_2$ is smaller than that in our previous problem.

We begin by setting up a table to help us keep track of the concentrations of Pb^{2+} and $\mathbf{IO_3^-}$ as this system moves toward and reaches equilibrium.

concentrations	$Pb(IO_3)_2$ (s)	$\rightleftharpoons$	Pb^{2+} (aq)	+	$2\mathbf{IO_3^-}$ (aq)
initial	solid		0.10		0
change	solid		$+x$		$+ 2x$
equilibrium	solid		$0.10 + x$		$2x$

Substituting the equilibrium concentrations into Equation 9.2.1

$$(0.10 + x)(2x)^2 = 2.5 \times 10^{-13}$$

and multiplying out the terms on the equation's left side leaves us with

$$4x^3 + 0.40x^2 = 2.5 \times 10^{-13} \tag{9.2.2}$$

This is a more difficult equation to solve than that for the solubility of $Pb(IO_3)_2$ in deionized water, and its solution is not immediately obvious. We can find a rigorous solution to Equation 9.2.2 using computational software packages and spreadsheets, some of which are described in Chapter 6.10.

> There are several approaches to solving cubic equations, but none are computationally easy using just paper and pencil.

How might we solve Equation 9.2.2 if we do not have access to a computer? One approach is to use our understanding of chemistry to simplify the problem. From Le Châtelier's principle we know that a large initial concentration of Pb^{2+} will decrease significantly the solubility of $Pb(IO_3)_2$. One reasonable assumption is that the initial concentration of Pb^{2+} is very close to its equilibrium concentration. If this assumption is correct, then the following approximation is reasonable

$$[Pb^{2+}] = 0.10 + x \approx 0.10$$

Substituting this approximation into Equation 9.2.1 and solving for *x* gives

$$(0.10)(2x)^2 = 0.4x^2 = 2.5 \times 10^{-13}$$

$$x = 7.91 \times 10^{-7}$$

Before we accept this answer, we must verify that our approximation is reasonable. The difference between the actual concentration of Pb^{2+}, which is 0.10 + *x* M, and our assumption that the concentration of Pb^{2+} is 0.10 M is 7.9×10^{-7}, or 7.9×10^{-4} % of the assumed concentration. This is a negligible error. If we accept the result of our calculation, we find that the equilibrium concentrations of Pb^{2+} and IO_3^- are

$$[Pb^{2+}] = 0.10 + x \approx 0.10 \text{ M and } [IO_3^-] = 2x = 1.6 \times 10^{-6} \text{ M}$$

$$\begin{aligned} \%\text{ error } &= \frac{\text{actual } - \text{ assumed}}{\text{assumed}} \times 100 \\ &= \frac{(0.10 + x) - 0.10}{0.10} \times 100 \\ &= \frac{7.91 \times 10^{-7}}{0.10} \times 100 \\ &= 7.91 \times 10^{-4}\% \end{aligned}$$

The molar solubility of $Pb(IO_3)_2$ is equal to the additional concentration of Pb^{2+} in solution, or 7.9×10^{-4} mol/L. As expected, we find that $Pb(IO_3)_2$ is less soluble in the presence of a solution that already contains one of its ions. This is known as the ***common ion effect***.

As outlined in the following example, if an approximation leads to an error that is unacceptably large, then we can extend the process of making and evaluating approximations.

> One "rule of thumb" when making an approximation is that it should not introduce an error of more than ±5%. Although this is not an unreasonable choice, what matters is that the error makes sense within the context of the problem you are solving.

✔ Example 6.7.1

Calculate the solubility of $Pb(IO_3)_2$ in 1.0×10^{-4} M $Pb(NO_3)_2$.

Solution

If we let x equal the change in the concentration of Pb^{2+}, then the equilibrium concentrations of Pb^{2+} and IO_3^- are

$$[Pb^{2+}] = 1.0 \times 10^{-4} + x \text{ and } [IO_3^-] = 2x$$

Substituting these concentrations into Equation 9.2.1 leaves us with

$$(1.0 \times 10^{-4} + x)(2x)^2 = 2.5 \times 10^{-13}$$

To solve this equation for x, let's make the following assumption

$$[Pb^{2+}] = 1.0 \times 10^{-4} + x \approx 1.0 \times 10^{-4} \text{ M}$$

Solving for x gives its value as 2.50×10^{-5}; however, when we substitute this value for x back, we find that the calculated concentration of Pb^{2+} at equilibrium

$$[Pb^{2+}] = 1.0 \times 10^{-4} + x = 1.0 \times 10^{-4} + 2.50 \times 10^{-5} = 1.25 \times 10^{-4} \text{ M}$$

is 25% greater than our assumption of 1.0×10^{-4} M. This error is unreasonably large.

Rather than shouting in frustration, let's make a new assumption. Our first assumption—that the concentration of Pb^{2+} is 1.0×10^{-4} M—was too small. The calculated concentration of 1.25×10^{-4} M, therefore, probably is a too large, but closer to the correct concentration than was our first assumption. For our second approximation, let's assume that

$$[Pb^{2+}] = 1.0 \times 10^{-4} + x = 1.25 \times 10^{-4} \text{M}$$

Substituting into Equation 9.2.1 and solving for x gives its value as 2.24×10^{-5}. The resulting concentration of Pb^{2+} is

$$[Pb^{2+}] = 1.0 \times 10^{-4} + 2.24 \times 10^{-5} = 1.22 \times 10^{-4} \text{ M}$$

which differs from our assumption of 1.25×10^{-4} M by 2.4%. Because the original concentration of Pb^{2+} is given to two significant figure, this is a more reasonable error. Our final solution, to two significant figures, is

$$[Pb^{2+}] = 1.2 \times 10^{-4} \text{ M and } [IO_3] = 4.5 \times 10^{-5} \text{ M}$$

and the molar solubility of $Pb(IO_3)_2$ is 2.2×10^{-5} mol/L. This iterative approach to solving the problems is known as the ***method of successive approximations***.

? Exercise 6.7.2

Calculate the molar solubility for Hg_2Cl_2 in 0.10 M NaCl and compare your answer to its molar solubility in deionized water (see Exercise 6.7.1).

Answer

We begin by setting up a table to help us keep track of the concentrations Hg_2^{2+} and Cl^- as this system moves toward and reaches equilibrium.

concentration	Hg_2Cl_2 (s)	⇌	Hg_2^{2+} (aq)	+	Cl^- (aq)
initial	solid		0		0.10
change	solid		$+x$		$+2x$
equilibrium	solid		x		$0.1 + 2x$

Substituting the equilibrium concentrations into the K_{sp} expression for Hg_2Cl_2 leaves us with a difficult to solve cubic equation.

$$K_{sp} = [Hg_2^{2+}][Cl^-]^2 = (x)(0.10 + 2x)^2 = 4x^3 + 0.40x^2 + 0.010x$$

Let's make an assumption to simplify this problem. Because we expect the value of x to be small, let's assume that

$$[Cl^-] = 0.10 + 2x \approx 0.10$$

This simplifies our problem to

$$K_{sp} = [Hg_2^{2+}]\,[Cl^-]^2 = (x)(0.10)^2 = 0.010x = 1.2 \times 10^{-18}$$

which gives the value of x as 1.2×10^{-16} M. The difference between the actual concentration of Cl^-, which is (0.10 + 2x) M, and our assumption that it is 0.10 M introduces an error of 2.4×10^{-13} %. This is a negligible error. The molar solubility of Hg_2Cl_2 is the same as the concentration of Hg_2^{2+}, or 1.2×10^{-16} M. As expected, the molar solubility in 0.10 M NaCl is less than 6.7×10^{-7} mol/L, which is its solubility in water (see solution to Exercise 6.7.1).

A Systematic Approach to Solving Equilibrium Problems

Calculating the solubility of $Pb(IO_3)_2$ in a solution of $Pb(NO_3)_2$ is more complicated than calculating its solubility in deionized water. The calculation, however, is still relatively easy to organize and the simplifying assumptions are fairly obvious. This problem is reasonably straightforward because it involves only one equilibrium reaction and one equilibrium constant.

Determining the equilibrium composition of a system with multiple equilibrium reactions is more complicated. In this section we introduce a systematic approach to setting-up and solving equilibrium problems. As shown in Table 6.7.1 , this approach involves four steps.

Table 6.7.1 . Systematic Approach to Solving Equilibrium Problems

Step 1 Write all relevant equilibrium reactions and equilibrium constant expressions.
Step 2 Count the unique species that appear in the equilibrium constant expressions; these are your unknowns. You have enough information to solve the problem if the number of unknowns equals the number of equilibrium constant expressions. If not, add a mass balance equation and/or a charge balance equation. Continue adding equations until the number of equations equals the number of unknowns.
Step 3 Combine your equations and solve for one unknown. Whenever possible, simplify the algebra by making appropriate assumptions. If you make an assumption, set a limit for its error. This decision influences your evaluation of the assumption.
Step 4 Check your assumptions. If any assumption proves invalid, return to the previous step and continue solving. The problem is complete when you have an answer that does not violate any of your assumptions.

In addition to equilibrium constant expressions, two other equations are important to this systematic approach to solving an equilibrium problem. The first of these equations is a ***mass balance equation***, which simply is a statement that matter is conserved during a chemical reaction. In a solution of acetic acid, for example, the combined concentrations of the conjugate weak acid, CH_3COOH, and the conjugate weak base, CH_3COO^-, must equal acetic acid's initial concentration, C_{CH_3COOH}.

$$C_{CH_3COOH} = [CH_3COOH] + [CH_3COO^-]$$

You may recall from Chapter 2 that this is the difference between a formal concentration and a molar concentration. The variable C represents a formal concentration.

The second equation is a ***charge balance equation***, which requires that the total positive charge from the cations equal the total negative charge from the anions. Mathematically, the charge balance equation is

$$\sum_{i=1}^{n} (z^+)_i\,[C^{z+}]_i = -\sum_{j=1}^{m} (z^-)_j\,[A^{z-}]_j$$

where $[C^{z+}]_i$ and $[A^{z-}]_j$ are, respectively, the concentrations of the i^{th} cation and the j^{th} anion, and $(z^+)_i$ and $(z^-)_j$ are the charges for the i^{th} cation and the j^{th} anion. Every ion in solution, even if it does not appear in an equilibrium reaction, must appear in the charge

balance equation. For example, the charge balance equation for an aqueous solution of $Ca(NO_3)_2$ is

$$2 \times [Ca^{2+}] + [H_3O^+] = [OH^+] + [NO_3^-]$$

Note that we multiply the concentration of Ca^{2+} by two and that we include the concentrations of H_3O^+ and OH^-.

A charge balance is a conservation of a charge. The minus sign in front of the summation term on the right side of the charge balance equation ensures that both summations are positive. There are situations where it is impossible to write a charge balance equation because we do not have enough information about the solution's composition. For example, suppose we fix a solution's pH using a buffer. If the buffer's composition is not specified, then we cannot write a charge balance equation.

Example 6.7.2

Write mass balance equations and a charge balance equation for a 0.10 M solution of $NaHCO_3$.

Solution

It is easier to keep track of the species in solution if we write down the reactions that define the solution's composition. These reactions are the dissolution of a soluble salt

$$NaHCO_3(s) \rightarrow Na^+(aq) + HCO_3^-(aq)$$

and the acid–base dissociation reactions of HCO_3^- and H_2O

$$HCO_3^-(aq) + H_2O(l) \rightleftharpoons H_3O^+(aq) + CO_3^{2-}(aq)$$

$$HCO_3^-(aq) + H_2O(l) \rightleftharpoons OH^-(aq) + H_2CO_3(aq)$$

$$2H_2O(l) \rightleftharpoons H_3O^+(aq) + OH^-(aq)$$

The mass balance equations are

$$0.10M = [H_2CO_3] + [HCO_3^-] + [CO_3^{2-}]$$

$$0.10\ M = [Na^+]$$

and the charge balance equation is

$$[Na^+] + [H_3O^+] = [OH^-] + [HCO_3^-] + 2 \times [CO_3^{2-}]$$

Exercise 6.7.3

Write appropriate mass balance and charge balance equations for a solution containing 0.10 M KH_2PO_4 and 0.050 M Na_2HPO_4.

Answer

To help us determine what ions are in solution, let's write down all the reaction needed to prepare the solutions and the equilibrium reactions that take place within these solutions. These reactions are the dissolution of two soluble salts

$$KH_2PO_4(s) \longrightarrow K^+(aq) + H_2PO_4^-(aq)$$

$$NaHPO_4(s) \longrightarrow Na^+(aq) + HPO_4^{2-}(aq)$$

and the acid–base dissociation reactions for $H_2PO_4^-$, HPO_4^{2-}. and H_2O.

$$H_2PO_4^-(aq) + H_2O(l) \rightleftharpoons H_3O^+(aq) + HPO_4^{2-}(aq)$$

$$H_2PO_4^-(aq) + H_2O(l) \rightleftharpoons OH^-(aq) + H_3PO_4(aq)$$

$$HPO_4^{2-}(aq) + H_2O(l) \rightleftharpoons H_3O^+(aq) + PO_4^{3-}(aq)$$

$$2H_2O(l) \rightleftharpoons H_3O^+(aq) + OH^-(aq)$$

Note that we did not include the base dissociation reaction for HPO_4^{2-} because we already accounted for its product, $H_2PO_4^-$, in another reaction. The mass balance equations for K^+ and Na^+ are straightforward

$$[K^+] = 0.10\ M \text{ and } [Na^+] = 0.10\ M$$

but the mass balance equation for phosphate takes a bit more thought. Both $H_2PO_4^-$ and HPO_4^{2-} produce the same ions in solution. We can, therefore, imagine that the solution initially contains 0.15 M KH_2PO_4, which gives the following mass balance equation.

$$[H_3PO_4] + [H_2PO_4^-] + [HPO_4^{2-}] + [PO_4^{3-}] = 0.15\ M$$

The charge balance equation is

$$[H_3O^+] + [K^+] + [Na^+] = [H_2PO_4^-] + 2 \times [HPO_4^{2-}] + 3 \times [PO_4^{3-}] + [OH^-]$$

pH of a Monoprotic Weak Acid

To illustrate the systematic approach to solving equilibrium problems, let's calculate the pH of 1.0 M HF. Two equilibrium reactions affect the pH. The first, and most obvious, is the acid dissociation reaction for HF

$$HF(aq) + H_2O(l) \rightleftharpoons H_3O^+(aq) + F^-(aq)$$

for which the equilibrium constant expression is

$$K_a = \frac{[H_3O^+]\,[F^-]}{[HF]} = 6.8 \times 10^{-4} \tag{9.2.3}$$

The second equilibrium reaction is the dissociation of water, which is an obvious yet easily neglected reaction

$$2H_2O(l) \rightleftharpoons H_3O^+(aq) + OH^-(aq)$$

$$K_w = [H_3O^+]\,[OH^-] = 1.00 \times 10^{-14} \tag{9.2.4}$$

Counting unknowns, we find four: [HF], [F^-], [H_3O^+], and [OH^-]. To solve this problem we need two additional equations. These equations are a mass balance equation on hydrofluoric acid

$$C_{HF} = [HF] + [F^-] = 1.0M \tag{9.2.5}$$

and a charge balance equation

$$[H_3O^+] = [OH^-] + [F^-] \tag{9.2.6}$$

With four equations and four unknowns, we are ready to solve the problem. Before doing so, let's simplify the algebra by making two assumptions.

Assumption One. Because HF is a weak acid, we know that the solution is acidic. For an acidic solution it is reasonable to assume that

$$[H_3O^+] >> [OH^-]$$

which simplifies the charge balance equation to

$$[H_3O^+] = [F^-] \tag{9.2.7}$$

Assumption Two. Because HF is a weak acid, very little of it dissociates to form F^-. Most of the HF remains in its conjugate weak acid form and it is reasonable to assume that

$$[HF] >> [F^-]$$

which simplifies the mass balance equation to

$$C_{HF} = [HF] = 1.0\ M \tag{9.2.8}$$

For this exercise let's accept an assumption if it introduces an error of less than ±5%.

Substituting Equation 9.2.7 and Equation 9.2.8 into Equation 9.2.3, and solving for the concentration of H_3O^+ gives us

$$K_a = \frac{[H_3O^+][F^-]}{[HF]} = \frac{[H_3O^+][H_3O^+]}{C_{HF}} = \frac{[H_3O^+]^2}{C_{HF}} = 6.8 \times 10^{-4}$$

$$[H_3O^+] = \sqrt{K_a C_{HF}} = \sqrt{(6.8 \times 10^{-4})(1.0)} = 2.6 \times 10^{-2}$$

Before accepting this answer, we must verify our assumptions. The first assumption is that $[OH^-]$ is significantly smaller than $[H_3O^+]$. Using Equation 9.2.4, we find that

$$[OH^-] = \frac{K_w}{[H_3O^+]} = \frac{1.00 \times 10^{-14}}{2.6 \times 10^{-2}} = 3.8 \times 10^{-13}$$

Clearly this assumption is acceptable. The second assumption is that $[F^-]$ is significantly smaller than [HF]. From Equation 9.2.7 we have

$$[F^-] = 2.6 \times 10^{-2}\ M$$

Because $[F^-]$ is 2.60% of C_{HF}, this assumption also is acceptable. Given that $[H_3O^+]$ is 2.6×10^{-2} M, the pH of 1.0 M HF is 1.59.

How does the calculation change if we require that the error introduced in our assumptions be less than ±1%? In this case we no longer can assume that [HF] >> $[F^-]$ and we cannot simplify the mass balance equation. Solving the mass balance equation for [HF]

$$[HF] = C_{HF} - [F^-] = C_{HF} - [H_3O^+]$$

and substituting into the K_a expression along with Equation 9.2.7 gives

$$K_a = \frac{[H_3O^+]^2}{C_{HF} - [H_3O^+]}$$

Rearranging this equation leaves us with a quadratic equation

$$[H_3O^+]^2 + K_a[H_3O^+] - K_a C_{HF} = 0$$

which we solve using the quadratic formula

$$x = \frac{-b \pm \sqrt{b^2 - 4ac}}{2a}$$

where a, b, and c are the coefficients in the quadratic equation

$$ax^2 + bx + c = 0$$

Solving a quadratic equation gives two roots, only one of which has chemical significance. For our problem, the equation's roots are

$$x = \frac{-6.8 \times 10^{-4} \pm \sqrt{(6.8 \times 10^{-4})^2 - (4)(1)(-6.8 \times 10^{-4})}}{(2)(1)}$$

$$x = \frac{-6.8 \times 10^{-4} \pm 5.22 \times 10^{-2}}{2}$$

$$x = 2.57 \times 10^{-2} \text{ or } -2.64 \times 10^{-2}$$

Only the positive root is chemically significant because the negative root gives a negative concentration for H_3O^+. Thus, $[H_3O^+]$ is 2.57×10^{-2} M and the pH is 1.59.

You can extend this approach to calculating the pH of a monoprotic weak base by replacing K_a with K_b, replacing C_{HF} with the weak base's concentration, and solving for $[OH^-]$ in place of $[H_3O^+]$.

Exercise 6.7.4

Calculate the pH of 0.050 M NH_3. State any assumptions you make in solving the problem, limiting the error for any assumption to ±5%. The K_b value for NH_3 is 1.75×10^{-5}.

Answer

To determine the pH of 0.050 M NH_3, we need to consider two equilibrium reactions: the base dissociation reaction for NH_3

$$NH_3(aq) + H_2O(l) \rightleftharpoons OH^-(aq) + NH_4^+(aq)$$

and water's dissociation reaction.

$$2H_2O(l) \rightleftharpoons H_3O^+(aq) + OH^-(aq)$$

These two reactions contain four species whose concentrations we need to consider: NH_3, NH_4^+, H_3O^+, and OH^-. We need four equations to solve the problem—these equations are the K_b equation for NH_3

$$K_b = \frac{[NH_4^+]\,[OH^-]}{[NH_3]} = 1.75 \times 10^{-5}$$

the K_w equation for H_2O

$$K_w = [H_3O^+]\,[OH^-]$$

a mass balance equation on ammonia

$$C_{NH_3} = 0.050\ M = [NH_3] + [NH_4^+]$$

and a charge balance equation

$$[H_3O^+] + [NH_4^+] = [OH^-]$$

To solve this problem, we will make two assumptions. Because NH_3 is a base, our first assumption is

$$[OH^-] >> [H_3O^+]$$

which simplifies the charge balance equation to

$$[NH_4^+] = [OH^-]$$

Because NH_3 is a weak base, our second assumption is

$$[NH_3] >> [NH_4^+]$$

which simplifies the mass balance equation to

$$C_{NH_3} = 0.050\ M = [NH_3]$$

Substituting the simplified charge balance equation and mass balance equation into the K_b equation leave us with

$$K_b = \frac{[NH_4^+]\,[OH^-]}{[NH_3]} = \frac{[OH^-]\,[OH^-]}{C_{NH_3}} = \frac{[OH^-]^2}{C_{NH_3}} = 1.75 \times 10^{-5}$$

$$[OH^-] = \sqrt{K_b C_{NH_3}} = \sqrt{(1.75 \times 10^{-5})\,(0.050)} = 9.35 \times 10^{-4}$$

Before we accept this answer, we must verify our two assumptions. The first assumption is that the concentration of OH^- is significantly greater than the concentration of H_3O^+. Using K_w, we find that

$$[H_3O^+] = \frac{K_w}{[OH^-]} = \frac{1.00 \times 10^{-14}}{9.35 \times 10^{-4}} = 1.07 \times 10^{-11}$$

Clearly this assumption is acceptable. Our second assumption is that the concentration of NH_3 is significantly greater than the concentration of NH_4^+. Using our simplified charge balance equation, we find that

$$[NH_4^+] = [OH^-] = 9.35 \times 10^{-4}$$

Because the concentration of NH_4^+ is 1.9% of C_{NH_3}, our second assumption also is reasonable. Given that $[H_3O^+]$ is 1.07×10^{-11}, the pH is 10.97.

pH of a Polyprotic Acid or Base

A more challenging problem is to find the pH of a solution that contains a polyprotic weak acid or one of its conjugate species. As an example, consider the amino acid alanine, whose structure is shown in Figure 6.7.1 . The ladder diagram in Figure 6.7.2 shows alanine's three acid–base forms and their respective areas of predominance. For simplicity, we identify these species as H_2L^+, HL, and L^-.

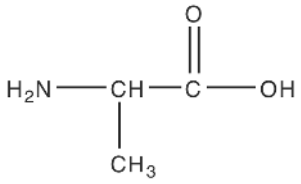


Figure 6.7.1 . Structure of the amino acid alanine, which has pK_a values of 2.348 (–COOH) and 9.867 ($–NH_2$).

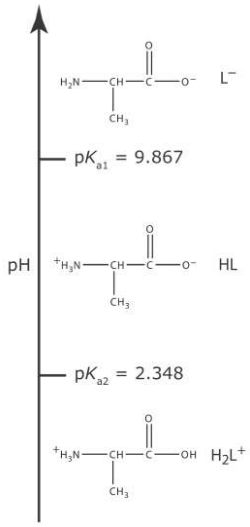


Figure 6.7.2 . Ladder diagram for alanine.

pH of 0.10 M Alanine Hydrochloride (H_2L^+)

Alanine hydrochloride is the salt of the diprotic weak acid H_2L^+ and Cl^-. Because H_2L^+ has two acid dissociation reactions, a complete systematic solution to this problem is more complicated than that for a monoprotic weak acid. The ladder diagram in Figure 6.7.2 helps us simplify the problem. Because the areas of predominance for H_2L^+ and L^- are so far apart, we can assume that a solution of H_2L^+ will not contain a significant amount of L^-. As a result, we can treat H_2L^+ as though it is a monoprotic weak acid. Calculating the pH of 0.10 M alanine hydrochloride, which is 1.72, is left to the reader as an exercise.

pH of 0.10 M Sodium Alaninate (L^-)

The alaninate ion is a diprotic weak base. Because L^- has two base dissociation reactions, a complete systematic solution to this problem is more complicated than that for a monoprotic weak base. Once again, the ladder diagram in Figure 6.7.2 helps us simplify the problem. Because the areas of predominance for H_2L^+ and L^- are so far apart, we can assume that a solution of L^- will not contain a significant amount of H_2L^+. As a result, we can treat L^- as though it is a monoprotic weak base. Calculating the pH of 0.10 M sodium alaninate, which is 11.42, is left to the reader as an exercise.

pH of 0.10 M Alanine (HL)

Finding the pH of a solution of alanine is more complicated than our previous two examples because we cannot ignore the presence of either H_2L^+ or L^-. To calculate the solution's pH we must consider alanine's acid dissociation reaction

$$HL(aq) + H_2O(l) \rightleftharpoons H_3O^+(aq) + L^-(aq)$$

and its base dissociation reaction

$$HL(aq) + H_2O(l) \rightleftharpoons OH^-(aq) + H_2L^+(aq)$$

and, as always, we must also consider the dissociation of water

$$2H_2O(l) \rightleftharpoons H_3O^+(aq) + OH^-(aq)$$

This leaves us with five unknowns—$[H_2L^+]$, [HL], $[L^-]$, $[H_3O^+]$, and $[OH^-]$—for which we need five equations. These equations are K_{a2} and K_{b2} for alanine

$$K_{a2} = \frac{[H_3O^+]\,[L^-]}{[HL]}$$

$$K_{b2} = \frac{K_w}{K_{a1}} = \frac{[OH^-]\,[H_2L^+]}{[HL]}$$

the K_w equation

$$K_w = [H_3O^+]\,[OH^-]$$

a mass balance equation for alanine

$$C_{HL} = [H_2L^+] + [HL] + [L^-]$$

and a charge balance equation

$$[H_2L^+] + [H_3O^+] = [OH^-] + [L^-]$$

Because HL is a weak acid and a weak base, it seems reasonable to assume that little of it will dissociate and that

$$[HL] >> [H_2L^+] + [L^-]$$

which allows us to simplify the mass balance equation to

$$C_{HL} = [HL]$$

Next we solve K_{b2} for $[H_2L^+]$

$$[H_2L^+] = \frac{K_w[HL]}{K_{a1}\,[OH^-]} = \frac{[H_3O^+]\,[HL]}{K_{a1}} = \frac{C_{HL}\,[H_3O^+]}{K_{a1}}$$

and solve K_{a2} for $[L^-]$

$$[L^-] = \frac{K_{a2}[HL]}{[H_3O^+]} = \frac{K_{a2}C_{HL}}{[H_3O^+]}$$

Substituting these equations for $[H_2L^+]$ and $[L^-]$, and the equation for K_w, into the charge balance equation give us

$$\frac{C_{HL}\,[H_3O^+]}{K_{a1}} + [H_3O^+] = \frac{K_w}{[H_3O^+]} + \frac{K_{a2}C_{HL}}{[H_3O^+]}$$

which we simplify to

$$[H_3O^+]\left(\frac{C_{HL}}{K_{a1}} + 1\right) = \frac{1}{[H_3O^+]}\left(K_w + K_{a2}C_{HL}\right)$$

$$[H_3O^+]^2 = \frac{(K_{a2}C_{HL} + K_w)}{\frac{C_{HL}}{K_{a1}} + 1} = \frac{K_{a1}\,(K_{a2}C_{HL} + K_w)}{C_{HL} + K_{a1}}$$

$$[H_3O^+] = \sqrt{\frac{(K_{a1}K_{a2}C_{HL} + K_{a1}K_w)}{C_{HL} + K_{a1}}}$$

We can further simplify this equation if $K_{a1}K_w << K_{a1}K_{a2}C_{HL}$, and if $K_{a1} << C_{HL}$, leaving us with

$$[H_3O^+] = \sqrt{K_{a1}K_{a2}}$$

For a solution of 0.10 M alanine the $[H_3O^+]$ is

$$[H_3O^+] = \sqrt{(4.487 \times 10^{-3})(1.358 \times 10^{-10})} = 7.806 \times 10^{-7}\ M$$

or a pH of 6.11.

? Exercise 6.7.5

Verify that each assumption in our solution for the pH of 0.10 M alanine is reasonable, using ±5% as the limit for the acceptable error.

Answer

In solving for the pH of 0.10 M alanine, we made the following three assumptions: (a) [HL] >> $[H_2L^+]$ + $[L^-]$; (b) $K_{a1}K_w << K_{a1}K_{a2}C_{HL}$; and (c) $K_{a1} << C_{HL}$. Assumptions (b) and (c) are easy to check. The value of K_{a1} (4.487×10^{-3}) is 4.5% of C_{HL} (0.10), and $K_{a1}Kw$ (4.487×10^{-17}) is 0.074% of $K_{a1}K_{a2}C_{HL}$ (6.093×10^{-14}). Each of these assumptions introduces an error of less than ±5%.

To test assumption (a) we need to calculate the concentrations of H_2L^+ and L^-, which we accomplish using the equations for K_{a1} and K_{a2}.

$$[H_2L^+] = \frac{[H_3O^+][HL]}{K_{a1}} = \frac{(7.807 \times 10^{-7})(0.10)}{4.487 \times 10^{-3}} = 1.74 \times 10^{-5}$$

$$[L^-] = \frac{K_{a2}[HL]}{[H_3O^+]} = \frac{(1.358 \times 10^{-10})(0.10)}{7.807 \times 10^{-7}} = 1.74 \times 10^{-5}$$

Because these concentrations are less than ±5% of *C*HL, the first assumption also is acceptable.

Effect of Complexation on Solubility

One method for increasing a precipitate's solubility is to add a ligand that forms soluble complexes with one of the precipitate's ions. For example, the solubility of AgI increases in the presence of NH_3 due to the formation of the soluble $Ag(NH_3)_2^+$ complex. As a final illustration of the systematic approach to solving equilibrium problems, let's calculate the molar solubility of AgI in 0.10 M NH_3.

We begin by writing the relevant equilibrium reactions, which includes the solubility of AgI, the acid–base chemistry of NH_3 and H_2O, and the metal-ligand complexation chemistry between Ag^+ and NH_3.

$$AgI(s) \rightleftharpoons Ag^+(aq) + I^-(aq)$$
$$NH_3(aq) + H_2O(l) \rightleftharpoons OH^-(aq) + NH_4^+(aq)$$
$$2H_2O(l) \rightleftharpoons H_3O^+(aq) + OH^-(aq)$$
$$Ag^+(aq) + 2NH_3(aq) \rightleftharpoons Ag(NH_3)_2^+(aq)$$

This leaves us with seven unknowns—$[Ag^+]$, $[I^-]$, $[NH_3]$, $[NH_4^+]$, $[OH^-]$, $[H_3O^+]$, and $[Ag(NH_3)_2^+]$—and a need for seven equations. Four of the equations we need to solve this problem are the equilibrium constant expressions

$$K_{sp} = [Ag^+][I^-] = 8.3 \times 10^{-17} \quad (9.2.9)$$

$$K_b = \frac{[NH_4^+][OH^-]}{[NH_3]} = 1.75 \times 10^{-5} \quad (9.2.10)$$

$$K_w = [H_3O^+]\,[OH^-] = 1.00 \times 10^{-14} \tag{9.2.11}$$

$$\beta_2 = \frac{[Ag(NH_3)_2^+]}{[Ag^+]\,[NH_3]^2} = 1.7 \times 10^7 \tag{9.2.12}$$

We still need three additional equations. The first of these equations is a mass balance for NH_3.

$$C_{NH_3} = [NH_3] + [NH_4^+] + 2 \times [Ag(NH_3)_2^+] \tag{9.2.13}$$

In writing this mass balance equation we multiply the concentration of $Ag(NH_3)_2^+$ by two since there are two moles of NH_3 per mole of $Ag(NH_3)_2^+$. The second additional equation is a mass balance between iodide and silver. Because AgI is the only source of I^- and Ag^+, each iodide in solution must have an associated silver ion, which may be Ag^+ or $Ag(NH_3)_2^+$; thus

$$[I^-] = [Ag^+] + [Ag(NH_3)_2^+] \tag{9.2.14}$$

Finally, we include a charge balance equation.

$$[Ag^+] + [Ag(NH_3)_2^+] + [NH_4^+] + [H_3O^+] = [OH^-] + [I^-] \tag{9.2.15}$$

Although the problem looks challenging, three assumptions greatly simplify the algebra.

Assumption One. Because the formation of the $Ag(NH_3)_2^+$ complex is so favorable (β_2 is 1.7×10^7), there is very little free Ag^+ in solution and it is reasonable to assume that

$$[Ag^+] << [Ag(NH_3)_2^+]$$

Assumption Two. Because NH_3 is a weak base we may reasonably assume that most uncomplexed ammonia remains as NH_3; thus

$$[NH_4^+] << [NH_3]$$

Assumption Three. Because K_{sp} for AgI is significantly smaller than β_2 for $Ag(NH_3)_2^+$, the solubility of AgI probably is small enough that very little ammonia is needed to form the metal–ligand complex; thus

$$[Ag(NH_3)_2^+] << [NH_3]$$

As we use these assumptions to simplify the algebra, let's set ±5% as the limit for error.

Assumption two and assumption three suggest that the concentration of NH_3 is much larger than the concentrations of either NH_4^+ or $Ag(NH_3)_2^+$, which allows us to simplify the mass balance equation for NH_3 to

$$C_{NH_3} = [NH_3] \tag{9.2.16}$$

Finally, using assumption one, which suggests that the concentration of $Ag(NH_3)_2^+$ is much larger than the concentration of Ag^+, we simplify the mass balance equation for I^- to

$$[I^-] = [Ag(NH_3)_2^+] \tag{9.2.17}$$

Now we are ready to combine equations and to solve the problem. We begin by solving Equation 9.2.9 for $[Ag^+]$ and substitute it into β_2 (Equation 9.2.12), which leaves us with

$$\beta_2 = \frac{[Ag(NH_3)_2^+]\,[I^-]}{K_{sp}\,[NH_3]^2} \tag{9.2.18}$$

Next we substitute Equation 9.2.16 and Equation 9.2.17 into Equation 9.2.18, obtaining

$$\beta_2 = \frac{[I^-]^2}{K_{sp}\,(C_{NH_3})^2} \tag{9.2.19}$$

Solving Equation 9.2.19 for $[I^-]$ gives

$$[I^-] = C_{NH_3}\sqrt{\beta_2 K_{sp}} =$$
$$(0.10)\sqrt{(1.7 \times 10^7)\,(8.3 \times 10^{-17})} = 3.76 \times 10^{-6}\ \text{M}$$

Because one mole of AgI produces one mole of I^-, the molar solubility of AgI is the same as the $[I^-]$, or 3.8×10^{-6} mol/L.

Before we accept this answer we need to check our assumptions. Substituting $[I^-]$ into Equation 9.2.9, we find that the concentration of Ag^+ is

$$[Ag^+] = \frac{K_p}{[I^-]} = \frac{8.3 \times 10^{-17}}{3.76 \times 10^{-6}} = 2.2 \times 10^{-11}\ M$$

Substituting the concentrations of I^- and Ag+ into the mass balance equation for iodide (Equation 9.2.14), gives the concentration of $Ag(NH_3)_2^+$ as

$$[Ag(NH_3)_2^+] = [I^-] - [Ag^+] = 3.76 \times 10^{-6} - 2.2 \times 10^{-11} = 3.76 \times 10^{-6}\ M$$

Our first assumption that $[Ag^+]$ is significantly smaller than the $[Ag(NH_3)_2^+]$ is reasonable.

Substituting the concentrations of Ag^+ and $Ag(NH_3)_2^+$ into Equation 9.2.12 and solving for $[NH_3]$, gives

$$[NH_3] = \sqrt{\frac{[Ag(NH_3)_2^+]}{[Ag^+]\,\beta_2}} = \sqrt{\frac{3.76 \times 10^{-6}}{(2.2 \times 10^{-11})\,(1.7 \times 10^{7})}} = 0.10\ M$$

From the mass balance equation for NH3 (Equation 9.2.12) we see that $[NH_4^+]$ is negligible, verifying our second assumption that $[NH_4^+]$ is significantly smaller than $[NH_3]$. Our third assumption that $[Ag(NH_3)_2^+]$ is significantly smaller than $[NH_3]$ also is reasonable.

> Did you notice that our solution to this problem did not make use of Equation 9.2.15, the charge balance equation? The reason for this is that we did not try to solve for the concentration of all seven species. If we need to know the reaction mixture's complete composition at equilibrium, then we will need to incorporate the charge balance equation into our solution.

This page titled 9.2: Solving Equilibrium Problems is shared under a CC BY-NC-SA 4.0 license and was authored, remixed, and/or curated by Kathryn Davis.

- **6.7: Solving Equilibrium Problems** by David Harvey is licensed CC BY-NC-SA 4.0.

9.3: Activity Effects

Careful measurements on the metal–ligand complex $Fe(SCN)^{2+}$ suggest its stability decreases in the presence of inert ions [Lister, M. W.; Rivington, D. E. *Can. J. Chem.* **1995**, *33*, 1572–1590]. We can demonstrate this by adding an inert salt to an equilibrium mixture of Fe^{3+} and SCN^-. Figure 6.9.1 a shows the result of mixing together equal volumes of 1.0 mM $FeCl_3$ and 1.5 mM KSCN, both of which are colorless. The solution's reddish–orange color is due to the formation of $Fe(SCN)^{2+}$.

$$Fe^{3+}(aq) + SCN^-(aq) \rightleftharpoons Fe(SCN)^{2+}(aq) \tag{9.3.1}$$

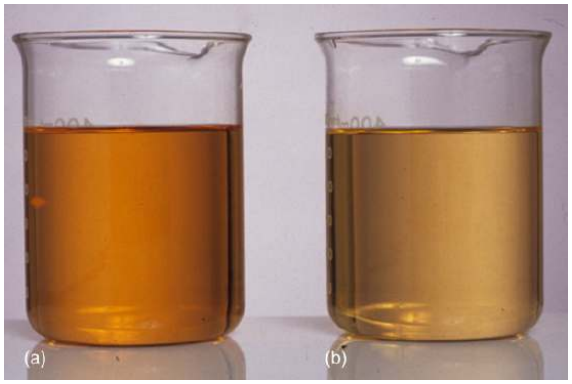


Figure 6.9.1 . The effect of a inert salt on a reaction's equilibrium position is shown by the solutions in these two beakers. The beaker on the left contains equal volumes of 1.0 mM $FeCl_3$ and 1.5 mM KSCN. The solution's color is due to the formation of the metal–ligand complex $Fe(SCN)^{2+}$. Adding 10 g of KNO_3 to the beaker on the left produces the result shown on the right. The lighter color suggests that there is less $Fe(SCN)^{2+}$ as a result of the equilibrium in reaction 9.3.1 shifting to the left.

Adding 10 g of KNO_3 to the solution and stirring to dissolve the solid, produces the result shown in Figure 6.9.1 b. The solution's lighter color suggests that adding KNO_3 shifts reaction 9.3.1 to the left, decreasing the concentration of $Fe(SCN)^{2+}$ and increasing the concentrations of Fe^{3+} and SCN^-. The result is a decrease in the complex's formation constant, K_1.

$$K_1 = \frac{[Fe(SCN)^{2+}]}{[Fe^{3+}]\,[SCN^-]} \tag{9.3.2}$$

Why should adding an inert electrolyte affect a reaction's equilibrium position? We can explain the effect of KNO_3 on the formation of $Fe(SCN)^{2+}$ if we consider the reaction on a microscopic scale. The solution in Figure 6.9.1 b contains a variety of cations and anions: Fe^{3+}, SCN^-, K^+, NO_3^-, H_3O^+, and OH^-. Although the solution is homogeneous, on average, there are slightly more anions in regions near the Fe^{3+} ions, and slightly more cations in regions near the SCN^- ions. As shown in Figure 6.9.2 , each Fe^{3+} ion and each SCN^- ion is surrounded by an ionic atmosphere of opposite charge (δ^- and δ^+) that partially screen the ions from each other. Because each ion's apparent charge at the edge of its ionic atmosphere is less than its actual charge, the force of attraction between the two ions is smaller. As a result, the formation of $Fe(SCN)^{2+}$ is slightly less favorable and the formation constant in Equation 9.3.2 is slightly smaller. Higher concentrations of KNO_3 increase δ^- and δ^+, resulting in even smaller values for the formation constant.

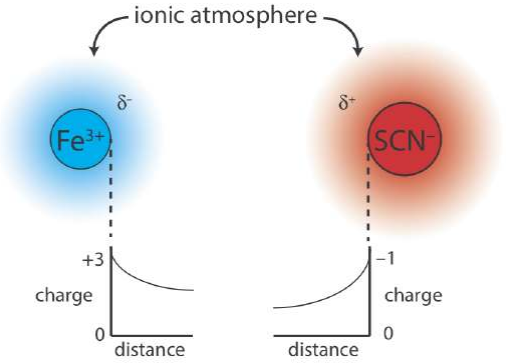


Figure 6.9.2 . Ions of Fe^{3+} and SCN^- are surrounded by ionic atmospheres with net charges of δ^- and δ^+. Because of these ionic atmospheres, each ion's apparent charge at the edge of its ionic atmosphere is less than the ion's actual charge.

Ionic Strength

To factor the concentration of ions into the formation constant for $Fe(SCN)^{2+}$, we need a way to express that concentration in a meaningful way. Because both an ion's concentration and its charge are important, we define the solution's ***ionic strength***, μ as

$$\mu = \frac{1}{2}\sum_{i=1}^{n} c_i z_i^2$$

where c_i and z_i are the concentration and charge of the i^{th} ion.

Example 6.9.1

Calculate the ionic strength of a solution of 0.10 M NaCl. Repeat the calculation for a solution of 0.10 M Na_2SO_4.

Solution

The ionic strength for 0.10 M NaCl is

$$\mu = \tfrac{1}{2}\left\{[Na^+] \times (+1)^2 + [Cl^-] \times (-1)^2\right\}$$
$$\mu = \tfrac{1}{2}\left\{(0.10) \times (+1)^2 + (0.10) \times (-1)^2\right\} = 0.10\ M$$

For 0.10 M Na_2SO_4 the ionic strength is

$$\mu = \tfrac{1}{2}\left\{[Na^+] \times (+1)^2 + [SO_4^{2-}] \times (-2)^2\right\}$$
$$\mu = \tfrac{1}{2}\left\{(0.20) \times (+1)^2 + (0.10) \times (-2)^2\right\} = 0.30\ M$$

In calculating the ionic strengths of these solutions we are ignoring the presence of H_3O^+ and OH^-, and, in the case of Na_2SO_4, the presence of HSO_4^- from the base dissociation reaction of SO_4^{2-}. In the case of 0.10 M NaCl, the concentrations of H_3O^+ and OH^- are 1.0×10^{-7}, which is significantly smaller than the concentrations of Na^+ and Cl^-. Because SO_4^{2-} is a very weak base ($K_b = 1.0 \times 10^{-12}$), the solution is only slightly basic (pH = 7.5), and the concentrations of H_3O^+, OH^-, and HSO_4^- are negligible. Although we can ignore the presence of H_3O^+, OH^-, and HSO_4^- when we calculate the ionic strength of these two solutions, be aware that an equilibrium reaction can generate ions that might affect the solution's ionic strength.

Note that the unit for ionic strength is molarity, but that a salt's ionic strength need not match its molar concentration. For a 1:1 salt, such as NaCl, ionic strength and molar concentration are identical. The ionic strength of a 2:1 electrolyte, such as Na_2SO_4, is three times larger than the electrolyte's molar concentration.

Activity and Activity Coefficients

Figure 6.9.1 shows that adding KNO_3 to a mixture of Fe^{3+} and SCN^- decreases the formation constant for $Fe(SCN)^{2+}$. This creates a contradiction. Earlier in this chapter we showed that there is a relationship between a reaction's standard-state free energy, ΔG^o, and its equilibrium constant, K.

$$\Delta G^\circ = -RT\ln K$$

Because a reaction has only one standard-state, its equilibrium constant must be independent of solution conditions. Although ionic strength affects the *apparent* formation constant for $Fe(SCN)^{2+}$, reaction 9.3.1 must have an underlying *thermodynamic* formation constant that is independent of ionic strength.

The apparent formation constant for $Fe(SCN)^{2+}$, as shown in Equation 9.3.2, is a function of concentrations. In place of concentrations, we define the true thermodynamic equilibrium constant using activities. The activity of species A, a_A, is the product of its concentration, $[A]$, and a solution-dependent activity coefficient, γ_A

$$a_A = [A]\gamma_A$$

The true thermodynamic formation constant for $Fe(SCN)^{2+}$, therefore, is

$$K_1 = \frac{a_{Fe(SCN)^{2+}}}{a_{Fe^{3+}} \times a_{SCN^-}} = \frac{[Fe(SCN)^{2+}]\,\gamma_{Fe(SCN)^{2+}}}{[Fe^{3+}]\,\gamma_{Fe^{3+}}\,[SCN^-]\,\gamma_{SCN^-}}$$

> Unless otherwise specified, the equilibrium constants in the appendices are thermodynamic equilibrium constants.

A species' ***activity coefficient*** corrects for any deviation between its physical concentration and its ideal value. For a gas, a pure solid, a pure liquid, or a non-ionic solute, the activity coefficient is approximately one under most reasonable experimental conditions.

> For a gas the proper terms are fugacity and fugacity coefficient, instead of activity and activity coefficient.

For a reaction that involves only these species, the difference between activity and concentration is negligible. The activity coefficient for an ion, however, depends on the solution's ionic strength, the ion's charge, and the ion's size. It is possible to estimate activity coefficients using the extended ***Debye-Hückel equation***

$$\log \gamma_A = \frac{-0.51 \times z_A^2 \times \sqrt{\mu}}{1 + 3.3 \times \alpha_A \times \sqrt{\mu}} \tag{9.3.3}$$

where z_A is the ion's charge, α_A is the hydrated ion's effective diameter in nanometers (Table 6.2), μ is the solution's ionic strength, and 0.51 and 3.3 are constants appropriate for an aqueous solution at 25°C. A hydrated ion's effective radius is the radius of the ion plus those water molecules closely bound to the ion. The effective radius is greater for smaller, more highly charged ions than it is for larger, less highly charged ions.

Table 6.9.1 . Effective Diameters (α) for Selected Ions

ion	effective diameter (nm)
H_3O^+	0.9
Li^+	0.6
Na^+, IO_3^-, HSO_3^-, HCO_3^-, $H_2PO_4^-$	0.45
OH^-, F^-, SCN^-, HS^-, ClO_3^-, ClO_4^-, MnO_4^-	0.35
K^+, Cl^-, Br^-, I^-, CN^-, NO_2^-, NO_3^-	0.3
Cs^+, Tl^+, Ag^+, NH_4^+	0.25
Mg^{2+}, Be^{2+}	0.8
Ca^{2+}, Cu^{2+}, Zn^{2+}, Sn^{2+}, Mn^{2+}, Fe^{2+}, Ni^{2+}, Co^{2+}	0.6
Sr^{2+}, Ba^{2+}, Cd^{2+}, Hg^{2+}, S^{2-}	0.5
Pb^{2+}, SO_4^{2-}, SO_3^{2-}	0.45
Hg_2^{2+}, SO_4^{2-}, $S_2O_3^{2-}$, CrO_4^{2-}, HPO_4^{2-}	0.40
Al^{3+}, Fe^{3+}, Cr^{3+}	0.9
PO_4^{3-}, $Fe(CN)_6^{3-}$	0.4
Zr^{4+}, Ce^{4+}, Sn^{4+}	1.1
$Fe(CN)_6^{4-}$	0.5
Source: Kielland, J. *J. Am. Chem. Soc.* **1937**, *59*, 1675–1678.	

Several features of Equation 9.3.3 deserve our attention. First, as the ionic strength approaches zero an ion's activity coefficient approaches a value of one. In a solution where $\mu = 0$, an ion's activity and its concentration are identical. We can take advantage of this fact to determine a reaction's thermodynamic equilibrium constant by measuring the apparent equilibrium constant for several

increasingly smaller ionic strengths and extrapolating back to an ionic strength of zero. Second, an activity coefficient is smaller, and the effect of activity is more important, for an ion with a higher charge and a smaller effective radius. Finally, the extended Debye-Hückel equation provides a reasonable estimate of an ion's activity coefficient when the ionic strength is less than 0.1. Modifications to Equation 9.3.3 extend the calculation of activity coefficients to higher ionic strengths [Davies, C. W. *Ion Association*, Butterworth: London, 1962].

Including Activity Coefficients When Solving Equilibrium Problems

Earlier in this chapter we calculated the solubility of $Pb(IO_3)_2$ in deionized water, obtaining a result of 4.0×10^{-5} mol/L. Because the only significant source of ions is from the solubility reaction, the ionic strength is very low and we can assume that $\gamma \approx 1$ for both Pb^{2+} and IO_3^-. In calculating the solubility of $Pb(IO_3)_2$ in deionized water, we do not need to account for ionic strength. But what if we need to know the solubility of $Pb(IO_3)_2$ in a solution that contains other, inert ions? In this case we need to include activity coefficients in our calculation.

Example 6.9.2

Calculate the solubility of $Pb(IO_3)_2$ in a matrix of 0.020 M $Mg(NO_3)_2$.

Solution

We begin by calculating the solution's ionic strength. Since $Pb(IO_3)_2$ is only sparingly soluble, we will assume we can ignore its contribution to the ionic strength; thus

$$\mu = \frac{1}{2}\left\{(0.020)(+2)^2 + (0.040)(-1)^2\right\} = 0.060 \text{ M}$$

Next, we use Equation 9.3.3 to calculate the activity coefficients for Pb^{2+} and IO_3^-.

$$\log \gamma_{Pb^{2+}} = \frac{-0.51 \times (+2)^2 \times \sqrt{0.060}}{1 + 3.3 \times 0.45 \times \sqrt{0.060}} = -0.366$$

$$\gamma_{Pb^{2+}} = 0.431$$

$$\log \gamma_{IO_3^-} = \frac{-0.51 \times (-1)^2 \times \sqrt{0.060}}{1 + 3.3 \times 0.45 \times \sqrt{0.060}} = -0.0916$$

$$\gamma_{IO_3^-} = 0.810$$

Defining the equilibrium concentrations of Pb^{2+} and IO_3^- in terms of the variable x

Concentrations	$Pb(IO_3)_2$ (s)	$\rightleftharpoons$	Pb^{2+} (aq)	+	$2IO_3^-$ (aq)
initial	solid		0		0
change	solid		$+x$		$+2x$
equilibrium	solid		x		$2x$

and substituting into the thermodynamic solubility product for $Pb(IO_3)_2$ leaves us with

$$K_{sp} = a_{Pb^{2+}} \times a_{IO_3^-}^2 = \gamma_{Pb^{2+}}\left[Pb^{2+}\right] \times \gamma_{IO_3^-}^2\left[IO_3^-\right]^2 = 2.5 \times 10^{-13}$$

$$K_{sp} = (0.431)(x)(0.810)^2(2x)^2 = 2.5 \times 10^{-13}$$

$$K_{sp} = 1.131x^3 = 2.5 \times 10^{-13}$$

Solving for x gives 6.0×10^{-5} and a molar solubility of 6.0×10^{-5} mol/L for $Pb(IO_3)_2$. If we ignore activity, as we did in our earlier calculation, we report the molar solubility as 4.0×10^{-5} mol/L. Failing to account for activity in this case underestimates the molar solubility of $Pb(IO_3)_2$ by 33%.

The solution's equilibrium composition is

$$[Pb^{2+}] = 6.0 \times 10^{-5}\ M$$
$$[IO_3^-] = 1.2 \times 10^{-4}\ M$$
$$[Mg^{2+}] = 0.020\ M$$
$$[NO_3^-] = 0.040\ M$$

Because the concentrations of both Pb^{2+} and IO_3^- are much smaller than the concentrations of Mg^{2+} and NO_3^- our decision to ignore the contribution of Pb^{2+} and IO_3^- to the ionic strength is reasonable.

How do we handle the calculation if we can not ignore the concentrations of Pb^{2+} and IO_3^- when calculating the ionic strength. One approach is to use the method of successive approximations. First, we recalculate the ionic strength using the concentrations of all ions, including Pb^{2+} and IO_3^-. Next, we recalculate the activity coefficients for Pb^{2+} and IO_3^- using this new ionic strength and then recalculate the molar solubility. We continue this cycle until two successive calculations yield the same molar solubility within an acceptable margin of error.

Exercise 6.9.1

Calculate the molar solubility of Hg_2Cl_2 in 0.10 M NaCl, taking into account the effect of ionic strength. Compare your answer to that from Exercise 6.7.2 in which you ignored the effect of ionic strength.

Answer

We begin by calculating the solution's ionic strength. Because NaCl is a 1:1 ionic salt, the ionic strength is the same as the concentration of NaCl; thus μ = 0.10 M. This assumes, of course, that we can ignore the contributions of Hg_2^{2+} and Cl^- from the solubility of Hg_2Cl_2.

Next we use Equation 9.3.3 to calculate the activity coefficients for Hg_2^{2+} and Cl^-.

$$\log \gamma_{Hg_2^{2+}} = \frac{-0.51 \times (+2)^2 \times \sqrt{0.10}}{1 + 3.3 \times 0.40 \times \sqrt{0.10}} = -0.455$$

$$\gamma_{Hg_2^{2+}} = 0.351$$

$$\log \gamma_{Cl^-} = \frac{-0.51 \times (-1)^2 \times \sqrt{0.10}}{1 + 3.3 \times 0.3 \times \sqrt{0.10}} = -0.12$$

$$\gamma_{Cl^-} = 0.75$$

Defining the equilibrium concentrations of Hg_2^{2+} and Cl^- in terms of the variable *x*

concentrations	Hg2Cl2 (*s*)	⇌	Hg_2^{2+} (*aq*)	+	$2Cl^-$ (*aq*)
initial	solid		0		0.10
change	solid		+*x*		+2*x*
equilibrium	solid		*x*		0.10 + 2*x*

and substituting into the thermodynamic solubility product for Hg_2Cl_2, leave us with

$$K_{sp} = a_{Hg_2^{2+}} (a_{Cl^-})^2 = \gamma_{Hg_2^{2+}} [Hg_2^{2+}] (\gamma_{Cl^-})^2 [Cl^-]^2 = 1.2 \times 10^{-18}$$

Because the value of *x* likely is small, let's simplify this equation to

$$(0.351)(x)(0.75)^2(0.1)^2 = 1.2 \times 10^{-18}$$

Solving for *x* gives its value as 6.1×10^{-16}. Because *x* is the concentration of Hg_2^{2+} and 2*x* is the concentration of Cl^-, our decision to ignore their contributions to the ionic strength is reasonable. The molar solubility of Hg_2Cl_2 in 0.10 M NaCl is

6.1×10^{-16} mol/L. In Exercise 6.7.2, where we ignored ionic strength, we determined that the molar solubility of Hg_2Cl_2 is 1.2×10^{-16} mol/L, a result that is $5\times$ smaller than the its actual value.

As Example 6.9.2 and Exercise 6.9.1 show, failing to correct for the effect of ionic strength can lead to a significant error in an equilibrium calculation. Nevertheless, it is not unusual to ignore activities and to assume that the equilibrium constant is expressed in terms of concentrations. There is a practical reason for this—in an analysis we rarely know the exact composition, much less the ionic strength of aqueous samples or of solid samples brought into solution. Equilibrium calculations are a useful guide when we develop an analytical method; however, it only is when we complete an analysis and evaluate the results that can we judge whether our theory matches reality. In the end, work in the laboratory is the most critical step in developing a reliable analytical method.

This is a good place to revisit the meaning of pH. In Chapter 2 we defined pH as

$$\mathrm{pH} = -\log [H_3O^+]$$

Now we see that the correct definition is

$$\mathrm{pH} = -\log a_{H_3O^+}$$
$$\mathrm{pH} = -\log \gamma_{H_3O^+} [H_3O^+]$$

Failing to account for the effect of ionic strength can lead to a significant error in the reported concentration of H_3O^+. For example, if the pH of a solution is 7.00 and the activity coefficient for H_3O^+ is 0.90, then the concentration of H_3O^+ is 1.11×10^{-7} M, not 1.00×10^{-7} M, an error of +11%. Fortunately, when we develop and carry out an analytical method, we are more interested in controlling pH than in calculating $[H_3O^+]$. As a result, the difference between the two definitions of pH rarely is of significant concern.

This page titled 9.3: Activity Effects is shared under a CC BY-NC-SA 4.0 license and was authored, remixed, and/or curated by Kathryn Davis.

- **6.9: Activity Effects** by David Harvey is licensed CC BY-NC-SA 4.0.

9.4: Precipitation Gravimetry

In precipitation gravimetry an insoluble compound forms when we add a precipitating reagent, or ***precipitant***, to a solution that contains our analyte. In most cases the precipitate is the product of a simple metathesis reaction between the analyte and the precipitant; however, any reaction that generates a precipitate potentially can serve as a gravimetric method.

> Most precipitation gravimetric methods were developed in the nineteenth century, or earlier, often for the analysis of ores. Figure 1.1.1 in Chapter 1, for example, illustrates a precipitation gravimetric method for the analysis of nickel in ores.

Theory and Practice

All precipitation gravimetric analyses share two important attributes. First, the precipitate must be of low solubility, of high purity, and of known composition if its mass is to reflect accurately the analyte's mass. Second, it must be easy to separate the precipitate from the reaction mixture.

Solubility Considerations

To provide an accurate result, a precipitate's solubility must be minimal. The accuracy of a total analysis technique typically is better than ±0.1%, which means the precipitate must account for at least 99.9% of the analyte. Extending this requirement to 99.99% ensures the precipitate's solubility will not limit the accuracy of a gravimetric analysis.

> A total analysis technique is one in which the analytical signal—mass in this case—is proportional to the absolute amount of analyte in the sample. See Chapter 3 for a discussion of the difference between total analysis techniques and concentration techniques.

We can minimize solubility losses by controlling the conditions under which the precipitate forms. This, in turn, requires that we account for every equilibrium reaction that might affect the precipitate's solubility. For example, we can determine Ag^+ gravimetrically by adding NaCl as a precipitant, forming a precipitate of AgCl.

$$Ag^+(aq) + Cl^-(aq) \rightleftharpoons AgCl(s) \tag{9.4.1}$$

If this is the only reaction we consider, then we predict that the precipitate's solubility, S_{AgCl}, is given by the following equation.

$$S_{AgCl} = [Ag^+] = \frac{K_{sp}}{[Cl^-]} \tag{9.4.2}$$

Equation 9.4.2 suggests that we can minimize solubility losses by adding a large excess of Cl^-. In fact, as shown in Figure 8.2.1 , adding a large excess of Cl^- increases the precipitate's solubility.

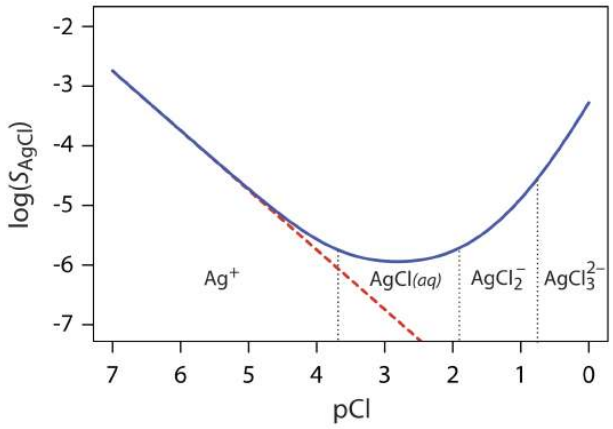


Figure 8.2.1 . Solubility of AgCl as a function of pCl. The dashed red line shows our prediction for S_{AgCl} if we assume incorrectly that only reaction 9.4.1 and Equation 9.4.2 affect silver chloride's solubility. The solid blue curve is calculated using Equation 9.4.7, which accounts for reaction 9.4.1 and reactions 9.4.3–9.4.5. Because the solubility of AgCl spans several orders of magnitude, S_{AgCl} is displayed on the *y*-axis in logarithmic form. The vertical dotted lines are a ladder diagram for the silver-chloro complexes.

To understand why the solubility of AgCl is more complicated than the relationship suggested by Equation 9.4.2, we must recall that Ag^+ also forms a series of soluble silver-chloro metal–ligand complexes.

$$Ag^+(aq) + Cl^-(aq) \rightleftharpoons AgCl(aq) \quad \log K_1 = 3.70 \tag{9.4.3}$$

$$AgCl(aq) + Cl^-(aq) \rightleftharpoons AgCl_2(aq) \quad \log K_2 = 1.92 \tag{9.4.4}$$

$$AgCl_2^-(aq) + Cl^-(aq) \rightleftharpoons AgCl_3^{2-}(aq) \quad \log K_3 = 0.78 \tag{9.4.5}$$

Note the difference between reaction 9.4.3, in which we form AgCl(*aq*) as a product, and reaction 9.4.1, in which we form AgCl(*s*) as a product. The formation of AgCl(*aq*) from AgCl(*s*)

$$AgCl(s) \rightleftharpoons AgCl(aq)$$

is called AgCl's intrinsic solubility.

The actual solubility of AgCl is the sum of the equilibrium concentrations for all soluble forms of Ag^+.

$$S_{AgCl} = [Ag^+] + [AgCl(aq)] + [AgCl_2^-] + [AgCl_3^{2-}] \tag{9.4.6}$$

By substituting into Equation 9.4.6 the equilibrium constant expressions for reaction 9.4.1 and reactions 9.4.3–9.4.5, we can define the solubility of AgCl as

$$S_{AgCl} = \frac{K_{sp}}{[Cl^-]} + K_1K_{sp} + K_1K_2K_{sp}[Cl^-] + K_1K_2K_3K_{sp}[Cl^-]^2 \tag{9.4.7}$$

Equation 9.4.7 explains the solubility curve for AgCl shown in Figure 8.2.1 . As we add NaCl to a solution of Ag^+, the solubility of AgCl initially decreases because of reaction 9.4.1. Under these conditions, the final three terms in Equation 9.4.7 are small and Equation 9.4.2 is sufficient to describe AgCl's solubility. For higher concentrations of Cl^-, reaction 9.4.4 and reaction 9.4.5 increase the solubility of AgCl. Clearly the equilibrium concentration of chloride is important if we wish to determine the concentration of silver by precipitating AgCl. In particular, we must avoid a large excess of chloride.

The predominate silver-chloro complexes for different values of pCl are shown by the ladder diagram along the *x*-axis in Figure 8.2.1 . Note that the increase in solubility begins when the higher-order soluble complexes of $AgCl_2^-$ and $AgCl_3^{2-}$ are the predominate species.

Another important parameter that may affect a precipitate's solubility is pH. For example, a hydroxide precipitate, such as $Fe(OH)_3$, is more soluble at lower pH levels where the concentration of OH^- is small. Because fluoride is a weak base, the

solubility of calcium fluoride, S_{CaF_2}, also is pH-dependent. We can derive an equation for S_{CaF_2} by considering the following equilibrium reactions

$$CaF_2(s) \rightleftharpoons Ca^{2+}(aq) + 2F^-(aq) \quad K_{sp} = 3.9 \times 10^{-11} \tag{9.4.8}$$

$$HF(aq) + H_2O(l) \rightleftharpoons H_3O^+(aq) + F^-(aq) \quad K_a = 6.8 \times 10^{-4} \tag{9.4.9}$$

and the following equation for the solubility of CaF_2.

$$S_{CaF_2} = [Ca^{2+}] = \frac{1}{2}\{[F^-] + [HF]\} \tag{9.4.10}$$

Be sure that Equation 9.4.10 makes sense to you. Reaction 9.4.8 tells us that the dissolution of CaF_2 produces one mole of Ca^{2+} for every two moles of F^-, which explains the term of 1/2 in Equation 9.4.10. Because F^- is a weak base, we must account for both chemical forms in solution, which explains why we include HF.

Substituting the equilibrium constant expressions for reaction 9.4.8 and reaction 9.4.9 into Equation 9.4.10 allows us to define the solubility of CaF_2 in terms of the equilibrium concentration of H_3O^+.

$$S_{CaF_2} = [Ca^{2+}] = \left\{\frac{K_p}{4}\left(1 + \frac{[H_3O^+]}{K_a}\right)^2\right\}^{1/3} \tag{9.4.11}$$

Figure 8.2.2 shows how pH affects the solubility of CaF_2. Depending on the solution's pH, the predominate form of fluoride is either HF or F^-. When the pH is greater than 4.17, the predominate species is F^- and the solubility of CaF_2 is independent of pH because only reaction 9.4.8 occurs to an appreciable extent. At more acidic pH levels, the solubility of CaF_2 increases because of the contribution of reaction 9.4.9.

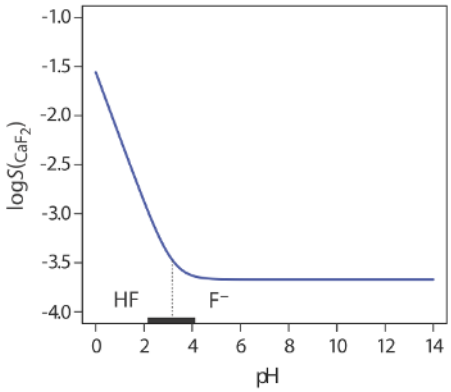


Figure 8.2.2 . Solubility of CaF_2 as a function of pH. The solid blue curve is a plot of Equation 9.4.11. The predominate form of fluoride in solution is shown by the ladder diagram along the *x*-axis, with the black rectangle indicating the region where both HF and F^- are important species. Note that the solubility of CaF_2 is independent of pH for pH levels greater than 4.17, and that its solubility increases dramatically at lower pH levels where HF is the predominate species. Because the solubility of CaF_2 spans several orders of magnitude, its solubility is shown in logarithmic form.

? Exercise 8.2.1

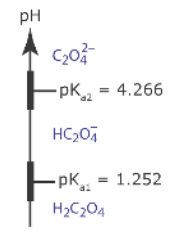
You can use a ladder diagram to predict the conditions that will minimize a precipitate's solubility. Draw a ladder diagram for oxalic acid, H_2C2O_4, and use it to predict the range of pH values that will minimize the solubility of CaC_2O_4. Relevant equilibrium constants are in the appendices.

Answer

The solubility reaction for CaC_2O_4 is

$$CaC_2O_4(s) \rightleftharpoons Ca^{2+}(aq) + C_2O_4^{2-}(aq)$$

To minimize solubility, the pH must be sufficiently basic that oxalate, $C_2O_4^{2-}$, does not react to form $HC_2O_4^-$ or $H_2C_2O_4$. The ladder diagram for oxalic acid, including approximate buffer ranges, is shown below. Maintaining a pH greater than 5.3 ensures that $C_2O_4^{2-}$ is the only important form of oxalic acid in solution, minimizing the solubility of CaC_2O_4.



When solubility is a concern, it may be possible to decrease solubility by using a non-aqueous solvent. A precipitate's solubility generally is greater in an aqueous solution because of water's ability to stabilize ions through solvation. The poorer solvating ability of a non-aqueous solvent, even those that are polar, leads to a smaller solubility product. For example, the K_{sp} of $PbSO_4$ is 2×10^{-8} in H_2O and 2.6×10^{-12} in a 50:50 mixture of H_2O and ethanol.

Avoiding Impurities

In addition to having a low solubility, a precipitate must be free from impurities. Because precipitation usually occurs in a solution that is rich in dissolved solids, the initial precipitate often is impure. To avoid a determinate error, we must remove these impurities before we determine the precipitate's mass.

The greatest source of impurities are chemical and physical interactions that take place at the precipitate's surface. A precipitate generally is crystalline—even if only on a microscopic scale—with a well-defined lattice of cations and anions. Those cations and anions at the precipitate's surface carry, respectively, a positive or a negative charge because they have incomplete coordination spheres. In a precipitate of AgCl, for example, each silver ion in the precipitate's interior is bound to six chloride ions. A silver ion at the surface, however, is bound to no more than five chloride ions and carries a partial positive charge (Figure 8.2.3). The presence of these partial charges makes the precipitate's surface an active site for the chemical and physical interactions that produce impurities.

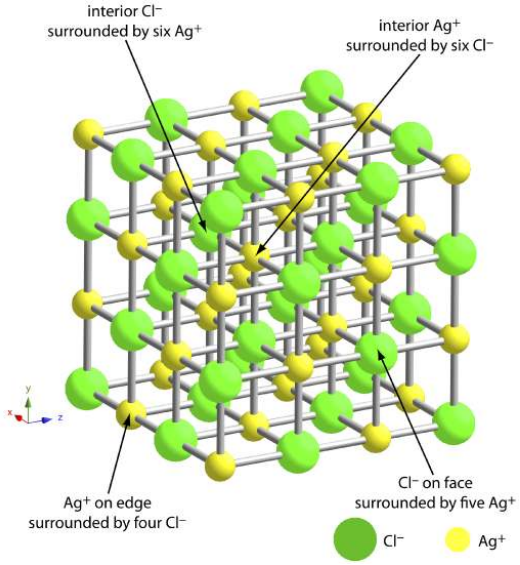


Figure 8.2.3 . Ball-and-stick model showing the lattice structure of AgCl. Each silver ion in the lattice's interior binds with six chloride ions and each chloride ion in the interior binds with six silver ions. Those ions on the lattice's surface or edges bind to fewer than six ions and carry a partial charge. A silver ion on the surface, for example, carries a partial positive charge. These charges make a precipitate's surface an active site for chemical and physical interactions.

One common impurity is an ***inclusion***, in which a potential interferent, whose size and charge is similar to a lattice ion, can substitute into the lattice structure if the interferent precipitates with the same crystal structure (Figure 8.2.4 a). The probability of

forming an inclusion is greatest when the interfering ion's concentration is substantially greater than the lattice ion's concentration. An inclusion does not decrease the amount of analyte that precipitates, provided that the precipitant is present in sufficient excess. Thus, the precipitate's mass always is larger than expected.

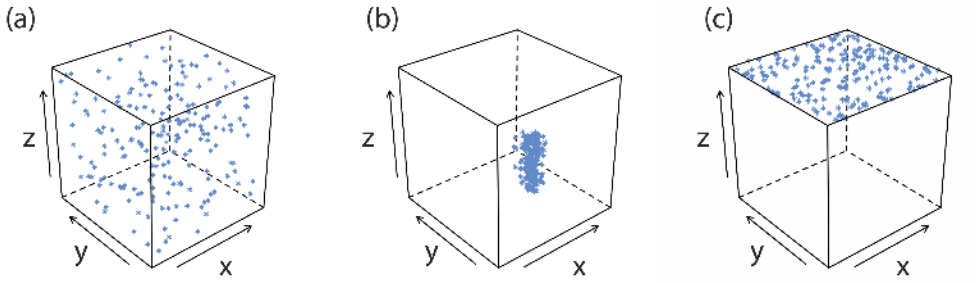


Figure 8.2.4 . Three examples of impurities that may form during precipitation. The cubic frame represents the precipitate and the blue marks are impurities present as (a) inclusions, (b) occlusions, and (c) surface adsorbates. Inclusions are randomly distributed throughout the precipitate. Occlusions are localized within the interior of the precipitate and surface adsorbates are localized on the precipitate's exterior. For ease of viewing, in (c) adsorption is shown on only one surface.

An inclusion is difficult to remove since it is chemically part of the precipitate's lattice. The only way to remove an inclusion is through ***reprecipitation*** in which we isolate the precipitate from its supernatant solution, dissolve the precipitate by heating in a small portion of a suitable solvent, and then reform the precipitate by allowing the solution to cool. Because the interferent's concentration after dissolving the precipitate is less than that in the original solution, the amount of included material decreases upon reprecipitation. We can repeat the process of reprecipitation until the inclusion's mass is insignificant. The loss of analyte during reprecipitation, however, is a potential source of determinate error.

> Suppose that 10% of an interferent forms an inclusion during each precipitation. When we initially form the precipitate, 10% of the original interferent is present as an inclusion. After the first reprecipitation, 10% of the included interferent remains, which is 1% of the original interferent. A second reprecipitation decreases the interferent to 0.1% of the original amount.

An ***occlusion*** forms when an interfering ions is trapped within the growing precipitate. Unlike an inclusion, which is randomly dispersed within the precipitate, an occlusion is localized, either along flaws within the precipitate's lattice structure or within aggregates of individual precipitate particles (Figure 8.2.4 b). An occlusion usually increases a precipitate's mass; however, the precipitate's mass is smaller if the occlusion includes the analyte in a lower molecular weight form than that of the precipitate.

We can minimize an occlusion by maintaining the precipitate in equilibrium with its supernatant solution for an extended time, a process called digestion. During a ***digestion***, the dynamic nature of the solubility–precipitation equilibria, in which the precipitate dissolves and reforms, ensures that the occlusion eventually is reexposed to the supernatant solution. Because the rates of dissolution and reprecipitation are slow, there is less opportunity for forming new occlusions.

After precipitation is complete the surface continues to attract ions from solution (Figure 8.2.4 c). These ***surface adsorbates*** comprise a third type of impurity. We can minimize surface adsorption by decreasing the precipitate's available surface area. One benefit of digestion is that it increases a precipitate's average particle size. Because the probability that a particle will dissolve completely is inversely proportional to its size, during digestion larger particles increase in size at the expense of smaller particles. One consequence of forming a smaller number of larger particles is an overall decrease in the precipitate's surface area. We also can remove surface adsorbates by washing the precipitate, although we cannot ignore the potential loss of analyte.

Inclusions, occlusions, and surface adsorbates are examples of ***coprecipitates***—otherwise soluble species that form along with the precipitate that contains the analyte. Another type of impurity is an interferent that forms an independent precipitate under the conditions of the analysis. For example, the precipitation of nickel dimethylglyoxime requires a slightly basic pH. Under these conditions any Fe^{3+} in the sample will precipitate as $Fe(OH)_3$. In addition, because most precipitants rarely are selective toward a single analyte, there is a risk that the precipitant will react with both the analyte and an interferent.

> In addition to forming a precipitate with Ni^{2+}, dimethylglyoxime also forms precipitates with Pd^{2+} and Pt^{2+}. These cations are potential interferents in an analysis for nickel.

We can minimize the formation of additional precipitates by controlling solution conditions. If an interferent forms a precipitate that is less soluble than the analyte's precipitate, we can precipitate the interferent and remove it by filtration, leaving the analyte behind in solution. Alternatively, we can mask the analyte or the interferent to prevent its precipitation. Both of the approaches outline above are illustrated in Fresenius' analytical method for the determination of Ni in ores that contain Pb^{2+}, Cu^{2+}, and Fe^{3+} (see Figure 1.1.1 in Chapter 1). Dissolving the ore in the presence of H_2SO_4 selectively precipitates Pb^{2+} as $PbSO_4$. Treating the resulting supernatant with H_2S precipitates Cu^{2+} as CuS. After removing the CuS by filtration, ammonia is added to precipitate Fe^{3+} as $Fe(OH)_3$. Nickel, which forms a soluble amine complex, remains in solution.

> Masking was introduced in Chapter 7.

Controlling Particle Size

Size matters when it comes to forming a precipitate. Larger particles are easier to filter and, as noted earlier, a smaller surface area means there is less opportunity for surface adsorbates to form. By controlling the reaction conditions we can significantly increase a precipitate's average particle size.

The formation of a precipitate consists of two distinct events: nucleation, the initial formation of smaller, stable particles of the precipitate, and particle growth. Larger particles form when the rate of particle growth exceeds the rate of nucleation. Understanding the conditions that favor particle growth is important when we design a gravimetric method of analysis.

We define a solute's ***relative supersaturation***, *RSS*, as

$$RSS = \frac{Q - S}{S} \tag{9.4.12}$$

where Q is the solute's actual concentration and S is the solute's concentration at equilibrium [Von Weimarn, P. P. *Chem. Revs*. **1925**, *2*, 217–242]. The numerator of Equation 9.4.12, $Q - S$, is a measure of the solute's supersaturation. A solution with a large, positive value of *RSS* has a high rate of nucleation and produces a precipitate with many small particles. When the *RSS* is small, precipitation is more likely to occur by particle growth than by nucleation.

> A supersaturated solution is one that contains more dissolved solute than that predicted by equilibrium chemistry. A supersaturated solution is inherently unstable and precipitates solute to reach its equilibrium position. How quickly precipitation occurs depends, in part, on the value of *RSS*.

Equation 9.4.12 suggests that we can minimize *RSS* if we decrease the solute's concentration, Q, or if we increase the precipitate's solubility, S. A precipitate's solubility usually increases at higher temperatures and adjusting pH may affect a precipitate's solubility if it contains an acidic or a basic ion. Temperature and pH, therefore, are useful ways to increase the value of S. Forming the precipitate in a dilute solution of analyte or adding the precipitant slowly and with vigorous stirring are ways to decrease the value of Q.

There are practical limits to minimizing *RSS*. Some precipitates, such as $Fe(OH)_3$ and PbS, are so insoluble that S is very small and a large *RSS* is unavoidable. Such solutes inevitably form small particles. In addition, conditions that favor a small *RSS* may lead to a relatively stable supersaturated solution that requires a long time to precipitate fully. For example, almost a month is required to form a visible precipitate of $BaSO_4$ under conditions in which the initial *RSS* is 5 [Bassett, J.; Denney, R. C.; Jeffery, G. H. Mendham. J. *Vogel's Textbook of Quantitative Inorganic Analysis*, Longman: London, 4th Ed., 1981, p. 408].

A visible precipitate takes longer to form when *RSS* is small both because there is a slow rate of nucleation and because there is a steady decrease in *RSS* as the precipitate forms. One solution to the latter problem is to generate the precipitant *in situ* as the product of a slow chemical reaction, which effectively maintains a constant *RSS*. Because the precipitate forms under conditions of low *RSS*, initial nucleation produces a small number of particles. As additional precipitant forms, particle growth supersedes nucleation, which results in larger particles of precipitate. This process is called a ***homogeneous precipitation*** [Gordon, L.; Salutsky, M. L.; Willard, H. H. *Precipitation from Homogeneous Solution*, Wiley: NY, 1959].

Two general methods are used for homogeneous precipitation. If the precipitate's solubility is pH-dependent, then we can mix the analyte and the precipitant under conditions where precipitation does not occur, and then increase or decrease the pH by chemically generating OH^- or H_3O^+. For example, the hydrolysis of urea, $CO(NH_2)_2$, is a source of OH^- because of the following two reactions.

$$CO\,(NH_2)_2\,(aq) + H_2O(l) \rightleftharpoons 2NH_3(aq) + CO_2(g)$$

$$NH_3(aq) + H_2O(l) \rightleftharpoons OH^-(aq) + NH_4^+(aq)$$

Because the hydrolysis of urea is temperature-dependent—the rate is negligible at room temperature—we can use temperature to control the rate of hydrolysis and the rate of precipitate formation. Precipitates of CaC_2O_4, for example, have been produced by this method. After dissolving a sample that contains Ca^{2+}, the solution is made acidic with HCl before adding a solution of 5% w/v $(NH_4)_2C_2O_4$. Because the solution is acidic, a precipitate of CaC_2O_4 does not form. The solution is heated to approximately 50°C and urea is added. After several minutes, a precipitate of CaC_2O_4 begins to form, with precipitation reaching completion in about 30 min.

In the second method of homogeneous precipitation, the precipitant is generated by a chemical reaction. For example, Pb^{2+} is precipitated homogeneously as $PbCrO_4$ by using bromate, BrO_3^-, to oxidize Cr^{3+} to CrO_4^{2-}.

$$6BrO_3^-(aq) + 10Cr^{3+}(aq) + 22H_2O(l) \rightleftharpoons 3Br_2(aq) + 10CrO_4^{2-}(aq) + 44H^+(aq)$$

Figure 8.2.5 shows the result of preparing $PbCrO_4$ by direct addition of K_2CrO_4 (Beaker A) and by homogenous precipitation (Beaker B). Both beakers contain the same amount of $PbCrO_4$. Because the direct addition of K_2CrO_4 leads to rapid precipitation and the formation of smaller particles, the precipitate remains less settled than the precipitate prepared homogeneously. Note, as well, the difference in the color of the two precipitates.

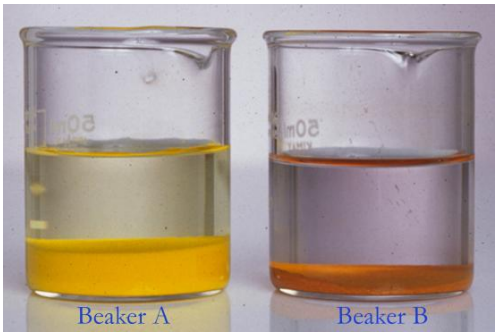


Figure 8.2.5 . Two precipitates of $PbCrO_4$. In Beaker A, mixing together 0.1 M $Pb(NO_3)_2$ and 0.1 M K_2CrO_4 forms the precipitate under conditions of high *RSS*. The precipitate forms rapidly and consists of very small particles. In Beaker B, heating a solution of 0.1 M $Pb(NO_3)_2$, 0.1 M $Cr(NO_3)_3$, and 0.1 M $KBrO_3$ slowly oxidizes Cr^{3+} to CrO_4^{2-}, precipitating $PbCrO_4$ under conditions of low *RSS*. The precipitate forms slowly and consists of much larger particles.

> The effect of particle size on color is well-known to geologists, who use a streak test to help identify minerals. The color of a bulk mineral and its color when powdered often are different. Rubbing a mineral across an unglazed porcelain plate leaves behind a small streak of the powdered mineral. Bulk samples of hematite, Fe_2O_3, are black in color, but its streak is a familiar rust-red. Crocite, the mineral $PbCrO_4$, is red-orange in color; its streak is orange-yellow.

A homogeneous precipitation produces large particles of precipitate that are relatively free from impurities. These advantages, however, are offset by the increased time needed to produce the precipitate and by a tendency for the precipitate to deposit as a thin film on the container's walls. The latter problem is particularly severe for hydroxide precipitates generated using urea.

An additional method for increasing particle size deserves mention. When a precipitate's particles are electrically neutral they tend to coagulate into larger particles that are easier to filter. Surface adsorption of excess lattice ions, however, provides the precipitate's particles with a net positive or a net negative surface charge. Electrostatic repulsion between particles of similar charge prevents them from coagulating into larger particles.

Let's use the precipitation of AgCl from a solution of $AgNO_3$ using NaCl as a precipitant to illustrate this effect. Early in the precipitation, when NaCl is the limiting reagent, excess Ag^+ ions chemically adsorb to the AgCl particles, forming a positively charged primary adsorption layer (Figure 8.2.6 a). The solution in contact with this layer contains more inert anions, NO_3^- in this case, than inert cations, Na^+, giving a secondary adsorption layer with a negative charge that balances the primary adsorption layer's positive charge. The solution outside the secondary adsorption layer remains electrically neutral. ***Coagulation*** cannot occur if the secondary adsorption layer is too thick because the individual particles of AgCl are unable to approach each other closely enough.

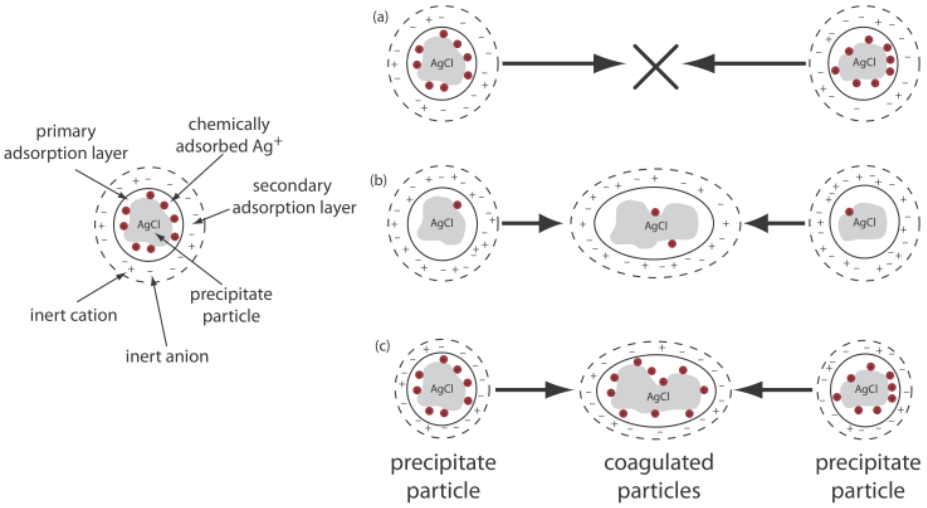


Figure 8.2.6 . Two methods for coagulating a precipitate of AgCl. (a) Coagulation does not occur due to the electrostatic repulsion between the positively charged particles. (b) Decreasing the charge within the primary adsorption layer, by adding additional NaCl, decreases the electrostatic repulsion and allows the particles to coagulate. (c) Adding additional inert ions decreases the thickness of the secondary adsorption layer. Because the particles can approach each other more closely, they are able to coagulate.

We can induce coagulation in three ways: by decreasing the number of chemically adsorbed Ag^+ ions, by increasing the concentration of inert ions, or by heating the solution. As we add additional NaCl, precipitating more of the excess Ag^+, the number of chemically adsorbed silver ions decreases and coagulation occurs (Figure 8.2.6 b). Adding too much NaCl, however, creates a primary adsorption layer of excess Cl^- with a loss of coagulation.

> The coagulation and decoagulation of AgCl as we add NaCl to a solution of $AgNO_3$ can serve as an endpoint for a titration. See Chapter 9 for additional details.

A second way to induce coagulation is to add an inert electrolyte, which increases the concentration of ions in the secondary adsorption layer (Figure 8.2.6 c). With more ions available, the thickness of the secondary absorption layer decreases. Particles of precipitate may now approach each other more closely, which allows the precipitate to coagulate. The amount of electrolyte needed to cause spontaneous coagulation is called the critical coagulation concentration.

Heating the solution and the precipitate provides a third way to induce coagulation. As the temperature increases, the number of ions in the primary adsorption layer decreases, which lowers the precipitate's surface charge. In addition, heating increases the particles' kinetic energy, allowing them to overcome the electrostatic repulsion that prevents coagulation at lower temperatures.

Filtering the Precipitate

After precipitating and digesting a precipitate, we separate it from solution by filtering. The most common filtration method uses filter paper, which is classified according to its speed, its size, and its ash content on ignition. Speed, or how quickly the supernatant passes through the filter paper, is a function of the paper's pore size. A larger pore size allows the supernatant to pass more quickly through the filter paper, but does not retain small particles of precipitate. Filter paper is rated as fast (retains particles larger than 20–25 μm), medium–fast (retains particles larger than 16 μm), medium (retains particles larger than 8 μm), and slow (retains particles larger than 2–3 μm). The proper choice of filtering speed is important. If the filtering speed is too fast, we may fail

to retain some of the precipitate, which causes a negative determinate error. On the other hand, the precipitate may clog the pores if we use a filter paper that is too slow.

> A filter paper's size is just its diameter. Filter paper comes in many sizes, including 4.25 cm, 7.0 cm, 11.0 cm, 12.5 cm, 15.0 cm, and 27.0 cm. Choose a size that fits comfortably into your funnel. For a typical 65-mm long-stem funnel, 11.0 cm and 12.5 cm filter paper are good choices.

Because filter paper is hygroscopic, it is not easy to dry it to a constant weight. When accuracy is important, the filter paper is removed before we determine the precipitate's mass. After transferring the precipitate and filter paper to a covered crucible, we heat the crucible to a temperature that coverts the paper to $CO_2(g)$ and $H_2O(g)$, a process called ***ignition***.

> Igniting a poor quality filter paper leaves behind a residue of inorganic ash. For quantitative work, use a low-ash filter paper. This grade of filter paper is pretreated with a mixture of HCl and HF to remove inorganic materials. Quantitative filter paper typically has an ash content of less than 0.010% w/w.

Gravity filtration is accomplished by folding the filter paper into a cone and placing it in a long-stem funnel (Figure 8.2.7). To form a tight seal between the filter cone and the funnel, we dampen the paper with water or supernatant and press the paper to the wall of the funnel. When prepared properly, the funnel's stem fills with the supernatant, increasing the rate of filtration.

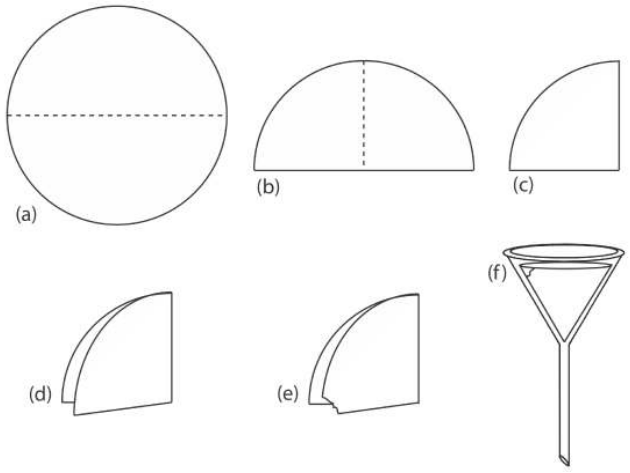


Figure 8.2.7 . To prepare a filter paper cone the filter paper circle is (a) folded in half (b), folded in half a second time (c), parted (d) and a small
corner is torn off (e) before the paper is opened up into a cone and placed in the funnel (f).

The precipitate is transferred to the filter in several steps. The first step is to decant the majority of the ***supernatant*** through the filter paper without transferring the precipitate (Figure 8.2.8). This prevents the filter paper from clogging at the beginning of the filtration process. The precipitate is rinsed while it remains in its beaker, with the rinsings decanted through the filter paper. Finally, the precipitate is transferred onto the filter paper using a stream of rinse solution. Any precipitate that clings to the walls of the beaker is transferred using a rubber policeman (a flexible rubber spatula attached to the end of a glass stirring rod).

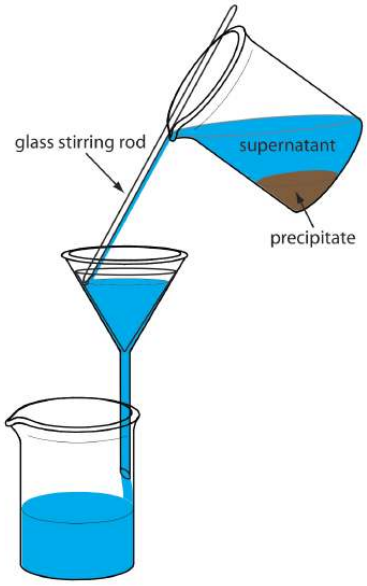


Figure 8.2.8 . Proper procedure for transferring the supernatant to the filter paper cone. The glass stirring rod allows the supernatant to trickle into the funnel without splashing.

An alternative method for filtering a precipitate is to use a filtering crucible. The most common option is a fritted-glass crucible that contains a porous glass disk filter. Fritted-glass crucibles are classified by their porosity: coarse (retaining particles larger than 40–60 μm), medium (retaining particles greater than 10–15 μm), and fine (retaining particles greater than 4–5.5 μm). Another type of filtering crucible is the Gooch crucible, which is a porcelain crucible with a perforated bottom. A glass fiber mat is placed in the crucible to retain the precipitate. For both types of crucibles, the pre- cipitate is transferred in the same manner described earlier for filter paper. Instead of using gravity, the supernatant is drawn through the crucible with the assistance of suction from a vacuum aspirator or pump (Figure 8.2.9).

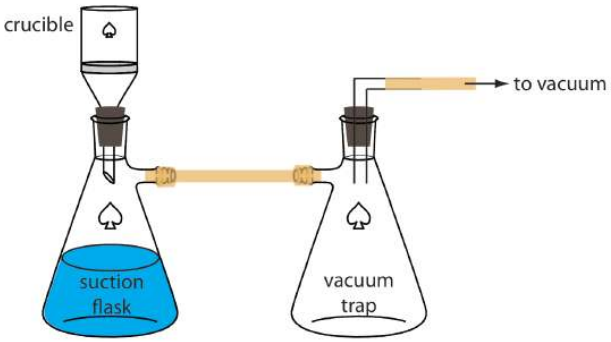


Figure 8.2.9 . Procedure for filtering a precipitate through a filtering crucible. The trap prevents water from the aspirator from back-washing into the suction flask.

Rinsing the Precipitate

Because the supernatant is rich with dissolved inert ions, we must remove residual traces of supernatant without incurring loss of analyte due to solubility. In many cases this simply involves the use of cold solvents or rinse solutions that contain organic solvents such as ethanol. The pH of the rinse solution is critical if the precipitate contains an acidic or a basic ion. When coagulation plays an important role in determining particle size, adding a volatile inert electrolyte to the rinse solution prevents the precipitate from reverting into smaller particles that might pass through the filter. This process of reverting to smaller particles is called ***peptization***. The volatile electrolyte is removed when drying the precipitate.

In general, we can minimize the loss of analyte if we use several small portions of rinse solution instead of a single large volume. Testing the used rinse solution for the presence of an impurity is another way to guard against over-rinsing the precipitate. For example, if Cl^- is a residual ion in the supernatant, we can test for its presence using $AgNO_3$. After we collect a small portion of the rinse solution, we add a few drops of $AgNO_3$ and look for the presence or absence of a precipitate of AgCl. If a precipitate forms,

then we know Cl^- is present and continue to rinse the precipitate. Additional rinsing is not needed if the $AgNO_3$ does not produce a precipitate.

Drying the Precipitate

After separating the precipitate from its supernatant solution, we dry the precipitate to remove residual traces of rinse solution and to remove any volatile impurities. The temperature and method of drying depend on the method of filtration and the precipitate's desired chemical form. Placing the precipitate in a laboratory oven and heating to a temperature of 110°C is sufficient to remove water and other easily volatilized impurities. Higher temperatures require a muffle furnace, a Bunsen burner, or a Meker burner, and are necessary if we need to decompose the precipitate before its weight is determined.

Because filter paper absorbs moisture, we must remove it before we weigh the precipitate. This is accomplished by folding the filter paper over the precipitate and transferring both the filter paper and the precipitate to a porcelain or platinum crucible. Gentle heating first dries and then chars the filter paper. Once the paper begins to char, we slowly increase the temperature until there is no trace of the filter paper and any remaining carbon is oxidized to CO_2.

Fritted-glass crucibles can not withstand high temperatures and are dried in an oven at a temperature below 200°C. The glass fiber mats used in Gooch crucibles can be heated to a maximum temperature of approximately 500°C.

Composition of the Final Precipitate

For a quantitative application, the final precipitate must have a well-defined composition. A precipitate that contains volatile ions or substantial amounts of hydrated water, usually is dried at a temperature that completely removes these volatile species. For example, one standard gravimetric method for the determination of magnesium involves its precipitation as $MgNH_4PO_4 \cdot 6H_2O$. Unfortunately, this precipitate is difficult to dry at lower temperatures without losing an inconsistent amount of hydrated water and ammonia. Instead, the precipitate is dried at a temperature greater than 1000°C where it decomposes to magnesium pyrophosphate, $Mg_2P_2O_7$.

An additional problem is encountered if the isolated solid is nonstoichiometric. For example, precipitating Mn^{2+} as $Mn(OH)_2$ and heating frequently produces a nonstoichiometric manganese oxide, MnO_x, where *x* varies between one and two. In this case the nonstoichiometric product is the result of forming a mixture of oxides with different oxidation state of manganese. Other nonstoichiometric compounds form as a result of lattice defects in the crystal structure [Ward, R., ed., *Non-Stoichiometric Compounds (Ad. Chem. Ser. 39)*, American Chemical Society: Washington, D. C., 1963].

Representative Method 8.2.1: Determination of Mg in Water and Wastewater

The best way to appreciate the theoretical and practical details discussed in this section is to carefully examine a typical precipitation gravimetric method. Although each method is unique, the determination of Mg^{2+} in water and wastewater by precipitating $MgNH_4PO_4 \cdot 6H_2O$ and isolating $Mg_2P_2O_7$ provides an instructive example of a typical procedure. The description here is based on Method 3500-Mg D in *Standard Methods for the Examination of Water and Wastewater*, 19th Ed., American Public Health Asso- ciation: Washington, D. C., 1995. With the publication of the 20th Edition in 1998, this method is no longer listed as an approved method.

Description of Method

Magnesium is precipitated as $MgNH_4PO_4 \cdot 6H_2O$ using $(NH_4)_2HPO_4$ as the precipitant. The precipitate's solubility in a neutral solution is relatively high (0.0065 g/100 mL in pure water at 10°C), but it is much less soluble in the presence of dilute ammonia (0.0003 g/100 mL in 0.6 M NH_3). Because the precipitant is not selective, a preliminary separation of Mg^{2+} from potential interferents is necessary. Calcium, which is the most significant interferent, is removed by precipitating it as CaC_2O_4. The presence of excess ammonium salts from the precipitant, or from the addition of too much ammonia, leads to the formation of $Mg(NH_4)_4(PO_4)_2$, which forms $Mg(PO_3)_2$ after drying. The precipitate is isolated by gravity filtration, using a rinse solution of dilute ammonia. After filtering, the precipitate is converted to $Mg_2P_2O_7$ and weighed.

Procedure

Transfer a sample that contains no more than 60 mg of Mg^{2+} into a 600-mL beaker. Add 2–3 drops of methyl red indicator, and, if necessary, adjust the volume to 150 mL. Acidify the solution with 6 M HCl and add 10 mL of 30% w/v $(NH_4)_2HPO_4$. After cooling and with constant stirring, add concentrated NH_3 dropwise until the methyl red indicator turns yellow (pH > 6.3). After stirring for

5 min, add 5 mL of concentrated NH_3 and continue to stir for an additional 10 min. Allow the resulting solution and precipitate to stand overnight. Isolate the precipitate by filtering through filter paper, rinsing with 5% v/v NH_3. Dissolve the precipitate in 50 mL of 10% v/v HCl and precipitate a second time following the same procedure. After filtering, carefully remove the filter paper by charring. Heat the precipitate at 500°C until the residue is white, and then bring the precipitate to constant weight at 1100°C.

Questions

1. Why does the procedure call for a sample that contains no more than 60 mg of Mg^{2+}?

A 60-mg portion of Mg^{2+} generates approximately 600 mg of $MgNH_4PO_4 \cdot 6H_2O$, which is a substantial amount of precipitate. A larger quantity of precipitate is difficult to filter and difficult to rinse free of impurities.

2. Why is the solution acidified with HCl before we add the precipitant?

The HCl ensures that $MgNH_4PO_4 \cdot 6H_2O$ does not precipitate immediately upon adding the precipitant. Because PO_4^{3-} is a weak base, the precipitate is soluble in a strongly acidic solution. If we add the precipitant under neutral or basic conditions (that is, a high *RSS*), then the resulting precipitate will consist of smaller, less pure particles. Increasing the pH by adding base allows the precipitate to form under more favorable (that is, a low *RSS*) conditions.

3. Why is the acid–base indicator methyl red added to the solution?

The indicator changes color at a pH of approximately 6.3, which indicates that there is sufficient NH_3 to neutralize the HCl added at the beginning of the procedure. The amount of NH_3 is crucial to this procedure. If we add insufficient NH_3, then the solution is too acidic, which increases the precipitate's solubility and leads to a negative determinate error. If we add too much NH_3, the precipitate may contain traces of $Mg(NH_4)_4(PO_4)_2$, which, on drying, forms $Mg(PO_3)_2$ instead of $Mg_2P_2O_7$. This increases the mass of the ignited precipitate, and gives a positive determinate error. After adding enough NH_3 to neutralize the HCl, we add an additional 5 mL of NH_3 to complete the quantitative precipitation of $MgNH_4PO_4 \cdot 6H_2O$.

4. Explain why forming $Mg(PO_3)_2$ instead of $Mg_2P_2O_7$ increases the precipitate's mass.

Each mole of $Mg_2P_2O_7$ contains two moles of magnesium and each mole of $Mg(PO_3)_2$ contains only one mole of magnesium. A conservation of mass, therefore, requires that two moles of $Mg(PO_3)_2$ form in place of each mole of $Mg_2P_2O_7$. One mole of $Mg_2P_2O_7$ weighs 222.6 g. Two moles of $Mg(PO_3)_2$ weigh 364.5 g. Any replacement of $Mg_2P_2O_7$ with $Mg(PO_3)_2$ must increase the precipitate's mass.

5. What additional steps, beyond those discussed in questions 2 and 3, help improve the precipitate's purity?

Two additional steps in the procedure help to form a precipitate that is free of impurities: digestion and reprecipitation.

6. Why is the precipitate rinsed with a solution of 5% v/v NH_3?

This is done for the same reason that the precipitation is carried out in an ammonical solution; using dilute ammonia minimizes solubility losses when we rinse the precipitate.

Quantitative Applications

Although no longer a common analytical technique, precipitation gravimetry still provides a reliable approach for assessing the accuracy of other methods of analysis, or for verifying the composition of standard reference materials. In this section we review the general application of precipitation gravimetry to the analysis of inorganic and organic compounds.

Inorganic Analysis

Table 8.2.1 provides a summary of precipitation gravimetric methods for inorganic cations and anions. Several methods for the homogeneous generation of precipitants are shown in Table 8.2.2 . The majority of inorganic precipitants show poor selectivity for the analyte. Many organic precipitants, however, are selective for one or two inorganic ions. Table 8.2.3 lists examples of several common organic precipitants.

Table 8.2.1 . Selected Precipitation Gravimetric Methods for Inorganic Cations and Anions (Arranged by Precipitant)

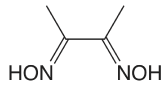
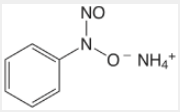
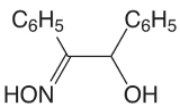
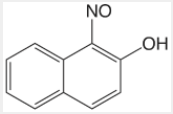
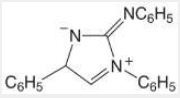
analyte	precipitant	precipitate formed	precipitate weighed
Ba^{2+}	$(NH_4)_2CrO_4$	$BaCrO_4$	$BaCrO_4$
Pb^{2+}	K_2CrO_4	$PbCrO_4$	$PbCrO_4$
Ag^{+}	HCl	AgCl	AgCl
Hg_2^{2+}	HCl	Hg_2Cl_2	Hg_2Cl_2
Al^{3+}	NH_3	$Al(OH)_3$	Al_2O_3
Be^{2+}	NH_3	$Be(OH)_2$	BeO
Fe^{3+}	NH_3	$Fe(OH)_3$	Fe_2O_3
Ca^{2+}	$(NH_4)_2CrO_4$	CaC_2O_4	$CaCO_3$ or CaO
Sb^{3+}	H_2S	Sb_2S_3	Sb_2S_3
As^{3+}	H_2S	As_2S_3	As_2S_3
Hg^{2+}	H_2S	HgS	HgS
Ba^{2+}	H_2SO_4	$BaSO_4$	$BaSO_4$
Pb^{2+}	H_2SO_4	$PbSO_4$	PbSO4
Sr^{2+}	H_2SO_4	$SrSO_4$	$SrSO_4$
Be^{2+}	$(NH_4)_2HPO_4$	NH_4BePO_4	$Be_2P_2O_7$
Mg^{2+}	$(NH_4)_2HPO_4$	NH_4MgPO_4	$Mg_2P_2O_7$
Zn^{2+}	$(NH_4)_2HPO_4$	NH_4ZnPO_4	$Zn_2P_2O_7$
Sr^{2+}	KH_2PO_4	$SrHPO_4$	$Sr_2P_2O_7$
CN^{-}	$AgNO_3$	AgCN	AgCN
I–	$AgNO_3$	AgI	AgI
Br^{-}	$AgNO_3$	AgBr	AgBr
Cl^{-}	$AgNO_3$	AgCl	AgCl
ClO_3^{-}	$FeSO_4/AgNO_3$	AgCl	AgCl
SCN^{-}	$SO_2/CuSO_4$	CuSCN	CuSCN
SO_4^{2}–	$BaCl_2$	$BaSO_4$	$BaSO_4$

Table 8.2.2 . Reactions for the Homogeneous Preparation of Selected Inorganic Precipitants

https://chem.libretexts.org/@go/page/556161

precipitant	reaction
OH–	$(NH_2)_2CO(aq) + 3H_2O(l) \rightleftharpoons 2NH_4^+(aq) + CO_2(g) + 2OH^-(aq)$
SO_4^{2-}	$NH_2HSO_3(aq) + 2H_2O(l) \rightleftharpoons NH_4^+(aq) + H_3O^+(aq) + SO_4^{2-}(aq)$
S^{2-}	$CH_3CSNH_2(aq) + H_2O(l) \rightleftharpoons CH_3CONH_2(aq) + H_2S(aq)$
IO_3^-	$HOCH_2CH_2OH(aq) + IO_4^-(aq) \rightleftharpoons 2HCHO(aq) + H_2O(l) + IO_3^-(aq)$
PO_4^{3-}	$(CH_3O)_3PO(aq) + 3H_2O(l) \rightleftharpoons 3CH_3OH(aq) + H_3PO_4(aq)$
$C_2O_4^{2-}$	$(C_2H_5)_2C_2O_4(aq) + 2H_2O(l) \rightleftharpoons 2C_2H_5OH(aq) + H_2C_2O_4(aq)$
CO_3^{2-}	$Cl_3CCOOH(aq) + 2OH^-(aq) \rightleftharpoons CHCl_3(aq) + CO_3^{2-}(aq) + H_2O(l)$

Table 8.2.3 . Selected Precipitation Gravimetric Methods for Inorganic Ions Using an Organic Precipitant

analyte	precipitant	structure	precipirate formed	precipitate weighed
Ni^{2+}	dimethylglyoxime		$Ni(C_4H_7O_2N_2)_2$	$Ni(C_4H_7O_2N_2)_2$
Fe^{3+}	cupferron		$Fe(C_6H_5N_2O_2)_3$	Fe_2O_3
Cu^{2+}	cupron		$CuC_{14}H_{11}O_2N$	$CuC_{14}H_{11}O_2N$
Co^{2+}	1-nitrso-2-napthol		$Co(C_{10}H_6O_2N)_3$	Co or $CoSO_4$
K^+	sodium tetraphenylborate	$Na[B(C_6H_5)_4]$	$K[B(C_6H_5)_4]$	$K[B(C_6H_5)_4]$
NO_3^-	nitron		$C_{20}H_{16}N_4HNO_3$	$C_{20}H_{16}N_4HNO_3$

Precipitation gravimetry continues to be listed as a standard method for the determination of SO_4^{2-} in water and wastewater analysis [Method 4500-SO42– C and Method 4500-SO42– D as published in *Standard Methods for the Examination of Waters and Wastewaters*, 20th Ed., American Public Health Association: Wash- ington, D. C., 1998]. Precipitation is carried out using $BaCl_2$ in an acidic solution (adjusted with HCl to a pH of 4.5–5.0) to prevent the precipitation of $BaCO_3$ or $Ba_3(PO_4)_2$, and at a temperature near the solution's boiling point. The precipitate is digested at 80–90°C for at least two hours. Ashless filter paper pulp is added to the precipitate to aid in its filtration. After filtering, the precipitate is ignited to constant weight at 800°C. Alternatively, the precipitate is filtered through a fine porosity fritted glass crucible (without adding filter paper pulp), and dried to constant weight at 105°C. This procedure is subject to a variety of errors, including occlusions of $Ba(NO_3)_2$, $BaCl_2$, and alkali sulfates.

> Other standard methods for the determination of sulfate in water and wastewater include ion chromatography (see Chapter 12), capillary ion electrophoresis (see Chapter 12), turbidimetry (see Chapter 10), and flow injection analysis (see Chapter 13).

Organic Analysis

Several organic functional groups or heteroatoms can be determined using precipitation gravimetric methods. Table 8.2.4 provides a summary of several representative examples. Note that the determination of alkoxy functional groups is an indirect analysis in which the functional group reacts with and excess of HI and the unreacted I^- determined by precipitating as AgCl.

Table 8.2.4 . Selected Precipitation Gravimetric Methods for the Analysis of Organic Functional Groups and Heteroatoms

analyte	treatment	precipitant	precipitate
organic halides (R-*X*) where *X* is Cl, Br, or I	oxidation with HNO_3 in the presence of Ag^+	$AgNO_3$	Ag*X*
organic halides (R-X) where *X* is Cl, Br, or I	combustion in O_2 (with a Pt catalyst) in the presence of Ag+	$AgNO_3$	AgX
organic sulfur	oxidation with HNO_3 in the presence of Ba^{2+}	$BaCl_2$	$BaSO_4$
organic sulfur	combustion in O_2 (with Pt catalyst) with SO_2 and SO_3 collected in dilute H_2O_2	$BaCl_2$	$BaSO_4$
alkoxy groups (–O-R or –COO-*R*) where R is $–CH_3$ or $–C_2H_5$	reaction with HI to produce RI	$AgNO_3$	AgI

Quantitative Calculations

The stoichiometry of a precipitation reaction provides a mathematical relationship between the analyte and the precipitate. Because a precipitation gravimetric method may involve additional chemical reactions to bring the analyte into a different chemical form, knowing the stoichiometry of the precipitation reaction is not always sufficient. Even if you do not have a complete set of balanced chemical reactions, you can use a conservation of mass to deduce the mathematical relationship between the analyte and the precipitate. The following example demonstrates this approach for the direct analysis of a single analyte.

✔ Example 8.2.1

To determine the amount of magnetite, Fe_3O_4, in an impure ore, a 1.5419-g sample is dissolved in concentrated HCl, resulting in a mixture of $Fe^{2+}$and Fe^{3+}. After adding HNO_3 to oxidize Fe^{2+} to Fe^{3+} and diluting with water, Fe^{3+} is precipitated as $Fe(OH)_3$ using NH_3. Filtering, rinsing, and igniting the precipitate provides 0.8525 g of pure Fe_2O_3. Calculate the %w/w Fe_3O_4 in the sample.

Solution

A conservation of mass requires that the precipitate of Fe_2O_3 contain all iron originally in the sample of ore. We know there are 2 moles of Fe per mole of Fe_2O_3 (FW = 159.69 g/mol) and 3 moles of Fe per mole of Fe_3O_4 (FW = 231.54 g/mol); thus

$$0.8525 \text{ g } Fe_2O_3 \times \frac{2 \text{ mol Fe}}{159.69 \text{ g } Fe_2O_3} \times \frac{231.54 \text{ g } Fe_3O_4}{3 \text{ mol Fe}} = 0.82405 \text{ g } Fe_3O_4$$

The % w/w Fe_3O_4 in the sample, therefore, is

$$\frac{0.82405 \text{ g } Fe_3O_4}{1.5419 \text{ g sample}} \times 100 = 53.44\%$$

? Exercise 8.2.2

A 0.7336-g sample of an alloy that contains copper and zinc is dissolved in 8 M HCl and diluted to 100 mL in a volumetric flask. In one analysis, the zinc in a 25.00-mL portion of the solution is precipitated as $ZnNH_4PO_4$, and isolated as $Zn_2P_2O_7$, yielding 0.1163 g. The copper in a separate 25.00-mL portion of the solution is treated to precipitate CuSCN, yielding 0.2383 g. Calculate the %w/w Zn and the %w/w Cu in the sample.

Answer

A conservation of mass requires that all zinc in the alloy is found in the final product, $Zn_2P_2O_7$. We know there are 2 moles of Zn per mole of $Zn_2P_2O_7$; thus

$$0.1163 \text{ g } Zn_2P_2O_7 \times \frac{2 \text{ mol Zn}}{304.70 \text{ g } Zn_2P_2O_7} \times \frac{65.38 \text{ g Zn}}{\text{mol Zn}} = 0.04991 \text{ g Zn}$$

This is the mass of Zn in 25% of the sample (a 25.00 mL portion of the 100.0 mL total volume). The %w/w Zn, therefore, is

$$\frac{0.04991 \text{ g Zn} \times 4}{0.7336 \text{ g sample}} \times 100 = 27.21\% \text{ w/wZn}$$

For copper, we find that

$$0.2383 \text{ g CuSCN} \times \frac{1 \text{ mol Zn}}{121.63 \text{ g CuSCN}} \times \frac{63.55 \text{ g Cu}}{\text{mol Cu}} = 0.1245 \text{ g Cu}$$

$$\frac{0.1245 \text{ g Cu} \times 4}{0.7336 \text{ g sample}} \times 100 = 67.88\% \text{ w/wCu}$$

In Practice Exercise 8.2.2 the sample contains two analytes. Because we can precipitate each analyte selectively, finding their respective concentrations is a straightforward stoichiometric calculation. But what if we cannot separately precipitate the two analytes? To find the concentrations of both analytes, we still need to generate two precipitates, at least one of which must contain both analytes. Although this complicates the calculations, we can still use a conservation of mass to solve the problem.

Example 8.2.2

A 0.611-g sample of an alloy that contains Al and Mg is dissolved and treated to prevent interferences by the alloy's other constituents. Aluminum and magnesium are precipitated using 8-hydroxyquinoline, which yields a mixed precipitate of $Al(C_9H_6NO)_3$ and $Mg(C_9H_6NO)_2$ that weighs 7.815 g. Igniting the precipitate converts it to a mixture of Al_2O_3 and MgO that weighs 1.002 g. Calculate the %w/w Al and %w/w Mg in the alloy.

Solution

The masses of the solids provide us with the following two equations.

$$\text{g Al}(C_9H_6NO)_3 + \text{ g Mg}(C_9H_6NO)_2 = 7.815 \text{ g}$$

$$\text{g } Al_2O_3 + \text{g MgO} = 1.002 \text{ g}$$

With two equations and four unknowns, we need two additional equations to solve the problem. A conservation of mass requires that all the aluminum in $Al(C_9H_6NO)_3$ also is in Al_2O_3; thus

$$\text{g } Al_2O_3 = \text{g Al}(C_9H_6NO)_3 \times \frac{1 \text{ mol Al}}{459.43 \text{ g Al}(C_9H_6NO)_3} \times \frac{101.96 \text{ g } Al_2O_3}{2 \text{ mol } Al_2O_3}$$

$$\text{g } Al_2O_3 = 0.11096 \times \text{g Al}(C_9H_6NO)_3$$

Using the same approach, a conservation of mass for magnesium gives

$$\text{g MgO} = \text{g Mg}(C_9H_6NO)_2 \times \frac{1 \text{ mol Mg}}{312.61 \text{ g Mg}(C_9H_6NO)_2} \times \frac{40.304 \text{ g MgO}}{\text{mol MgO}}$$

$$\text{g MgO} = 0.12893 \times \text{g Mg}(C_9H_6NO)_2$$

Substituting the equations for g MgO and g Al_2O_3 into the equation for the combined weights of MgO and Al_2O_3 leaves us with two equations and two unknowns.

$$\text{g Al}(C_9H_6NO)_3 + \text{g Mg}(C_9H_6NO)_2 = 7.815 \text{ g}$$

$$0.11096 \times \text{g Al}(C_9H_6NO)_3 + 0.12893 \times \text{g Mg}(C_9H_6NO)_2 = 1.002 \text{ g}$$

Multiplying the first equation by 0.11096 and subtracting the second equation gives

$$-0.01797 \times \text{g Mg}(C_9H_6NO)_2 = -0.1348 \text{ g}$$

$$\text{g Mg}(C_9H_6NO)_2 = 7.504 \text{ g}$$

$$\text{g Al}(C_9H_6NO)_3 = 7.815 \text{ g} - 7.504 \text{ g Mg}(C,H_6NO)_2 = 0.311 \text{ g}$$

Now we can finish the problem using the approach from Example 8.2.1 . A conservation of mass requires that all the aluminum and magnesium in the original sample of Dow metal is in the precipitates of $Al(C_9H_6NO)_3$ and the $Mg(C_9H_6NO)_2$. For aluminum, we find that

$$0.311 \text{ g Al}(C_9H_6NO)_3 \times \frac{1 \text{ mol Al}}{459.45 \text{ g Al}(C_9H_6NO)_3} \times \frac{26.982 \text{ g Al}}{\text{mol Al}} = 0.01826 \text{ g Al}$$

$$\frac{0.01826 \text{ g Al}}{0.611 \text{ g sample}} \times 100 = 2.99\%\text{w/wAl}$$

and for magnesium we have

$$7.504 \text{ g Mg}(C_9H_6NO)_2 \times \frac{1 \text{ mol Mg}}{312.61 \text{ g Mg}(C_9H_6NO)_2} \times \frac{24.305 \text{ g Mg}}{\text{mol MgO}} = 0.5834 \text{ g Mg}$$

$$\frac{0.5834 \text{ g Mg}}{0.611 \text{ g sample}} \times 100 = 95.5\%\text{w/wMg}$$

? Exercise 8.2.3

A sample of a silicate rock that weighs 0.8143 g is brought into solution and treated to yield a 0.2692-g mixture of NaCl and KCl. The mixture of chloride salts is dissolved in a mixture of ethanol and water, and treated with $HClO_4$, precipitating 0.3314 g of $KClO_4$. What is the %w/w Na_2O in the silicate rock?

Answer

The masses of the solids provide us with the following equations

$$\text{g NaCl} + \text{g KCl} = 0.2692 \text{ g}$$

$$\text{g KClO}_4 = 0.3314 \text{ g}$$

With two equations are three unknowns—g NaCl, g KCl, and g $KClO_4$—we need one additional equation to solve the problem. A conservation of mass requires that all the potassium originally in the KCl ends up in the $KClO_4$; thus

$$\text{g KClO}_4 = \text{g KCl} \times \frac{1 \text{ mol Cl}}{74.55 \text{ g KCl}} \times \frac{138.55 \text{ g KClO}_4}{\text{mol Cl}} = 1.8585 \times \text{ g KCl}$$

Given the mass of $KClO_4$, we use the third equation to solve for the mass of KCl in the mixture of chloride salts

$$\text{g KCl} = \frac{\text{g KClO}_4}{1.8585} = \frac{0.3314 \text{ g}}{1.8585} = 0.1783 \text{ g KCl}$$

The mass of NaCl in the mixture of chloride salts, therefore, is

$$\text{g NaCl} = 0.2692 \text{ g} - \text{g KCl} = 0.2692 \text{ g} - 0.1783 \text{ g KCl} = 0.0909 \text{ g NaCl}$$

Finally, to report the %w/w Na_2O in the sample, we use a conservation of mass on sodium to determine the mass of Na_2O

$$0.0909 \text{ g NaCl} \times \frac{1 \text{ mol Na}}{58.44 \text{ g NaCl}} \times \frac{61.98 \text{ g Na}_2\text{O}}{2 \text{ mol Na}} = 0.0482 \text{ g Na}_2\text{O}$$

giving the %w/w Na_2O as

$$\frac{0.0482 \text{ g Na}_2\text{O}}{0.8143 \text{ g sample}} \times 100 = 5.92\% \text{ w/w Na}_2\text{O}$$

The previous problems are examples of direct methods of analysis because the precipitate contains the analyte. In an indirect analysis the precipitate forms as a result of a reaction with the analyte, but the analyte is not part of the precipitate. As shown by the following example, despite the additional complexity, we still can use conservation principles to organize our calculations.

Example 8.2.3

An impure sample of Na_3PO_3 that weighs 0.1392 g is dissolved in 25 mL of water. A second solution that contains 50 mL of 3% w/v $HgCl_2$, 20 mL of 10% w/v sodium acetate, and 5 mL of glacial acetic acid is prepared. Adding the solution that contains the sample to the second solution oxidizes PO_3^{3-} to PO_4^{3-} and precipitates Hg_2Cl_2. After digesting, filtering, and rinsing the precipitate, 0.4320 g of Hg_2Cl_2 is obtained. Report the purity of the original sample as % w/w Na_3PO_3.

Solution

This is an example of an indirect analysis because the precipitate, Hg_2Cl_2, does not contain the analyte, Na_3PO_3. Although the stoichiometry of the reaction between Na_3PO_3 and $HgCl_2$ is given earlier in the chapter, let's see how we can solve the problem using conservation principles. (*Although you can write the balanced reactions for any analysis, applying conservation principles can save you a significant amount of time!*)

The reaction between Na_3PO_3 and $HgCl_2$ is an oxidation-reduction reaction in which phosphorous increases its oxidation state from +3 in Na_3PO_3 to +5 in Na_3PO_4, and in which mercury decreases its oxidation state from +2 in $HgCl_2$ to +1 in Hg_2Cl_2. A redox reaction must obey a conservation of electrons because all the electrons released by the reducing agent, Na_3PO_3, must be accepted by the oxidizing agent, $HgCl_2$. Knowing this, we write the following stoichiometric conversion factors:

$$\frac{2 \text{ mol } e^-}{\text{mol } Na_3PO_3} \text{ and } \frac{1 \text{mol } e^-}{\text{mol } HgCl_2}$$

Now we are ready to solve the problem. First, we use a conservation of mass for mercury to convert the precipitate's mass to the moles of $HgCl_2$.

$$0.4320 \text{ g } Hg_2Cl_2 \times \frac{2 \text{ mol Hg}}{472.09 \text{ g } Hg_2Cl_2} \times \frac{1 \text{ mol } HgCl_2}{\text{mol Hg}} = 1.8302 \times 10^{-3} \text{ mol } HgCl_2$$

Next, we use the conservation of electrons to find the mass of Na_3PO_3.

$$1.8302 \times 10^{-3} \text{ mol } HgCl_2 \times \frac{1 \text{ mol } e^-}{\text{mol } HgCl_2} \times \frac{1 \text{ mol } Na_3PO_4}{2 \text{ mol } e^-} \times \frac{147.94 \text{ g } Na_3PO_3}{\text{mol } Na_3PO_3} = 0.13538 \text{ g } Na_3PO_3$$

Finally, we calculate the %w/w Na_3PO_3 in the sample.

$$\frac{0.13538 \text{ g } Na_3PO_3}{0.1392 \text{ g sample}} \times 100 = 97.26\% \text{w/w} Na_3PO_3$$

As you become comfortable using conservation principles, you will see ways to further simplify problems. For example, a conservation of electrons requires that the electrons released by Na_3PO_3 end up in the product, Hg_2Cl_2, yielding the following stoichiometric conversion factor:

$$\frac{2 \text{ mol } Na_3PO_3}{\text{mol } Hg_2Cl_2}$$

This conversion factor provides a direct link between the mass of Hg_2Cl_2 and the mass of Na_3PO_3.

Exercise 8.2.4

One approach for determining phosphate, PO_4^{3-}, is to precipitate it as ammonium phosphomolybdate, $(NH_4)_3PO_4 \cdot 12MoO_3$. After we isolate the precipitate by filtration, we dissolve it in acid and precipitate and weigh the molybdate as $PbMoO_3$. Suppose we know that our sample is at least 12.5% Na_3PO_4 and that we need to recover a minimum of 0.600 g of $PbMoO_3$? What is the minimum amount of sample that we need for each analysis?

Answer

To find the mass of $(NH_4)_3PO_4$•$12MoO_3$ that will produce 0.600 g of $PbMoO_3$, we first use a conservation of mass for molybdenum; thus

$$0.600 \text{ g } PbMoO_3 \times \frac{1 \text{ mol Mo}}{351.2 \text{ g } PbMoO_3} \times \frac{1876.59 \text{ g } (NH_4)_3PO_4 \cdot 12MoO_3}{12 \text{ mol Mo}} = 0.2672 \text{ g } (NH_4)_3PO_4 \cdot 12MoO_3$$

Next, to convert this mass of $(NH_4)_3PO_4$•$12MoO_3$ to a mass of Na_3PO_4, we use a conservation of mass on PO_4^{3-}.

$$0.2672 \text{ g } (NH_4)_3PO_4 \cdot 12MoO_3 \times \frac{1 \text{ mol } PO_4^{3-}}{1876.59 \text{ g } (NH_4)_3PO_4 \cdot 12MoO_3} \times \frac{163.94 \text{ g } Na_3PO_4}{\text{mol } PO_4^{3-}} = 0.02334 \text{ g } Na_3PO_4$$

Finally, we convert this mass of Na_3PO_4 to the corresponding mass of sample.

$$0.02334 \text{ g } Na_3PO_4 \times \frac{100 \text{ g sample}}{12.5 \text{ g } Na_3PO_4} = 0.187 \text{ g sample}$$

A sample of 0.187 g is sufficient to guarantee that we recover a minimum of 0.600 g $PbMoO_3$. If a sample contains more than 12.5% Na_3PO_4, then a 0.187-g sample will produce more than 0.600 g of $PbMoO_3$.

Qualitative Applications

A precipitation reaction is a useful method for identifying inorganic and organic analytes. Because a qualitative analysis does not require quantitative measurements, the analytical signal is simply the observation that a precipitate forms. Although qualitative applications of precipitation gravimetry have been replaced by spectroscopic methods of analysis, they continue to find application in spot testing for the presence of specific analytes [Jungreis, E. *Spot Test Analysis*; 2nd Ed., Wiley: New York, 1997].

> Any of the precipitants listed in Table 8.2.1 , Table 8.2.3 , and Table 8.2.4 can be used for a qualitative analysis.

Evaluating Precipitation Gravimetry

Scale of Operation

The scale of operation for precipitation gravimetry is limited by the sensitivity of the balance and the availability of sample. To achieve an accuracy of ±0.1% using an analytical balance with a sensitivity of ±0.1 mg, we must isolate at least 100 mg of precipitate. As a consequence, precipitation gravimetry usually is limited to major or minor analytes, in macro or meso samples. The analysis of a trace level analyte or a micro sample requires a microanalytical balance.

Accuracy

For a macro sample that contains a major analyte, a relative error of 0.1– 0.2% is achieved routinely. The principal limitations are solubility losses, impurities in the precipitate, and the loss of precipitate during handling. When it is difficult to obtain a precipitate that is free from impurities, it often is possible to determine an empirical relationship between the precipitate's mass and the mass of the analyte by an appropriate calibration.

Precision

The relative precision of precipitation gravimetry depends on the sample's size and the precipitate's mass. For a smaller amount of sample or precipitate, a relative precision of 1–2 ppt is obtained routinely. When working with larger amounts of sample or precipitate, the relative precision extends to several ppm. Few quantitative techniques can achieve this level of precision.

Sensitivity

For any precipitation gravimetric method we can write the following general equation to relate the signal (grams of precipitate) to the absolute amount of analyte in the sample

$$\text{g precipitate} = k \times \text{g analyte} \tag{9.4.13}$$

where k, the method's sensitivity, is determined by the stoichiometry between the precipitate and the analyte.

Equation 9.4.13 assumes we used a suitable blank to correct the signal for any contributions of the reagent to the precipitate's mass.

Consider, for example, the determination of Fe as Fe_2O_3. Using a conservation of mass for iron, the precipitate's mass is

$$\text{g } Fe_2O_3 = \text{g Fe} \times \frac{\text{1 mol Fe}}{\text{AW Fe}} \times \frac{\text{FW } Fe_2O_3}{\text{2 mol Fe}}$$

and the value of *k* is

$$k = \frac{1}{2} \times \frac{\text{FW } Fe_2O_3}{\text{AW Fe}} \tag{9.4.14}$$

As we can see from Equation 9.4.14, there are two ways to improve a method's sensitivity. The most obvious way to improve sensitivity is to increase the ratio of the precipitate's molar mass to that of the analyte. In other words, it helps to form a precipitate with the largest possible formula weight. A less obvious way to improve a method's sensitivity is indicated by the term of 1/2 in Equation 9.4.14, which accounts for the stoichiometry between the analyte and precipitate. We can also improve sensitivity by forming a precipitate that contains fewer units of the analyte.

? Exercise 8.2.5

Suppose you wish to determine the amount of iron in a sample. Which of the following compounds—FeO, Fe_2O_3, or Fe_3O_4—provides the greatest sensitivity?

Answer

To determine which form has the greatest sensitivity, we use a conservation of mass for iron to find the relationship between the precipitate's mass and the mass of iron.

$$\text{g FeO} = \text{g Fe} \times \frac{\text{1 mol Fe}}{\text{55.85 g Fe}} \times \frac{\text{71.84 g FeO}}{\text{mol Fe}} = 1.286 \times \text{g Fe}$$

$$\text{g } Fe_2O_3 = \text{g Fe} \times \frac{\text{1 mol Fe}}{\text{55.85 g Fe}} \times \frac{\text{159.69 g } Fe_2O_3}{\text{2 mol Fe}} = 1.430 \times \text{g Fe}$$

$$\text{g } Fe_3O_4 = \text{g Fe} \times \frac{\text{1 mol Fe}}{\text{55.85 g Fe}} \times \frac{\text{231.53 g } Fe_3O_4}{\text{3 mol Fe}} = 1.382 \times \text{g Fe}$$

Of the three choices, the greatest sensitivity is obtained with Fe_2O_3 because it provides the largest value for *k*.

Selectivity

Due to the chemical nature of the precipitation process, precipitants usually are not selective for a single analyte. For example, silver is not a selective precipitant for chloride because it also forms precipitates with bromide and with iodide. Interferents often are a serious problem and must be considered if accurate results are to be obtained.

Time, Cost, and Equipment

Precipitation gravimetry is time intensive and rarely practical if you have a large number of samples to analyze; however, because much of the time invested in precipitation gravimetry does not require an analyst's immediate supervision, it is a practical alternative when working with only a few samples. Equipment needs are few—beakers, filtering devices, ovens or burners, and balances—inexpensive, routinely available in most laboratories, and easy to maintain.

This page titled 9.4: Precipitation Gravimetry is shared under a CC BY-NC-SA 4.0 license and was authored, remixed, and/or curated by Kathryn Davis.

- **8.2: Precipitation Gravimetry** by David Harvey is licensed CC BY-NC-SA 4.0.

Index

A

absorbance
- 6.2: Spectroscopy Based on Absorption
- 8.1: UV/Vis Analysis of Two-Component Mixtures

absorption
- 6.1: Overview of Spectroscopy
- 6.2: Spectroscopy Based on Absorption

Absorption Spectrometry
- 6.3: UV/Vis and IR Spectroscopy

absorption spectroscopy
- 6: Beyond Beer's Law- Quantitative Spectroscopic Analysis

accessible education
- InfoPage

accuracy
- 1.4: Characterizing Experimental Errors
- 9.4: Precipitation Gravimetry

acetate
- 9.1: Ladder Diagrams

acetic acid
- 3.1: Acid–Base Titrations
- 3.4: Buffer Solutions
- 9.1: Ladder Diagrams

acid
- 3.4: Buffer Solutions

acid base reactions
- 4.2: EDTA Ladder Diagrams

acid base titrimetry
- 4.3: Redox Titrations

acid dissociation constant
- 3.4: Buffer Solutions

activities
- 5.2: Potentiometric Methods

activity coefficients
- 9.3: Activity Effects

activity effects
- 9: Solubility Equilibria

adaptive learning
- InfoPage

AgCl solubility
- 4.4: Ladder Diagrams for Redox Titrations

alternative hypothesis
- 1.7: Statistical Analysis of Data
- 1.8: Statistical Methods for Normal Distributions

analysis of mixtures
- 7.6: Applications of Molecular Mass Spectrometry

analyte
- 1.1: Classifying Analytical Techniques
- 6.2: Spectroscopy Based on Absorption
- 8.2: Classifying Separation Techniques
- 8.4: Overview of Analytical Separations
- 9.4: Precipitation Gravimetry

analyte concentration
- 5: Electrochemical Instrumental Analysis
- 5.3: Coulometric Methods

analytical
- 4: There Are Other Titration Methods!

analytical calculations
- 2.2: Stoichiometric Calculations

analytical chemistry
- TitlePage
- 1.2: Measurements in Analytical Chemistry
- 1.5: Propagation of Uncertainty
- 2.1: Concentration
- 3.1: Acid–Base Titrations
- 3.2: Ladder Diagrams for Acid-Base Equilibria
- 4.1: Complexation Titrations
- 4.2: EDTA Ladder Diagrams
- 4.4: Ladder Diagrams for Redox Titrations
- 5.1: Overview of Electrochemistry
- 5.2: Potentiometric Methods
- 5.4: Voltammetric and Amperometric Methods
- 6.5: Photoluminescent Spectroscopy
- 7: Mass Spectrometry
- 7.2: Inductively Coupled Plasma Mass Spectrometer
- 7.4: Mass Spectrometers
- 8: Analysis and Separation of Mixtures
- 8.1: UV/Vis Analysis of Two-Component Mixtures
- 8.2: Classifying Separation Techniques
- 8.5: General Theory of Column Chromatography
- 8.6: Optimizing Chromatographic Separations
- 8.8: High-Performance Liquid Chromatography
- 8.9: Other Forms of Chromatography
- 8.10: Electrophoresis

analytical electrochemistry
- 5: Electrochemical Instrumental Analysis

analytical lab
- 2.3: Preparing Solutions

analytical method
- 6.2: Spectroscopy Based on Absorption

Analytical Methods
- 1.4: Characterizing Experimental Errors
- 3: Acid-Base Equilibria Affect Solution Conditions
- 4.4: Ladder Diagrams for Redox Titrations
- 6.3: UV/Vis and IR Spectroscopy

analytical technique
- 7.6: Applications of Molecular Mass Spectrometry

analytical techniques
- 1.1: Classifying Analytical Techniques
- 6.1: Overview of Spectroscopy
- 6.4: Atomic Absorption Spectroscopy

analytical titration
- 4.3: Redox Titrations

analyticalchemistry
- 6.6: Atomic Emission Spectroscopy

aqueous solvent
- 8.3: Liquid-Liquid Extractions

atomic absorption
- 6.4: Atomic Absorption Spectroscopy

atomic absorption spectroscopy
- 6: Beyond Beer's Law- Quantitative Spectroscopic Analysis
- 6.4: Atomic Absorption Spectroscopy

atomic emission
- 6.4: Atomic Absorption Spectroscopy
- 7.2: Inductively Coupled Plasma Mass Spectrometer

atomic emission spectroscopy
- 6: Beyond Beer's Law- Quantitative Spectroscopic Analysis

atomicemission
- 6.6: Atomic Emission Spectroscopy

atomization
- 6.6: Atomic Emission Spectroscopy

auxiliary electrode
- 5.4: Voltammetric and Amperometric Methods

B

balanced reaction
- 2: The Return of Stoichiometry
- 2.2: Stoichiometric Calculations

band broadening
- 8.6: Optimizing Chromatographic Separations

base
- 3.4: Buffer Solutions

base peak
- 7.3: Molecular Mass Spectra

Beer’s Law
- 6.3: UV/Vis and IR Spectroscopy

Beer's law
- 8.1: UV/Vis Analysis of Two-Component Mixtures

binomial distribution
- 1.6: The Distribution of Measurements and Results

buffer
- 3.1: Acid–Base Titrations
- 3.4: Buffer Solutions

buffer capacity
- 3.4: Buffer Solutions

buffer solutions
- 3: Acid-Base Equilibria Affect Solution Conditions

C

calibration
- 1.4: Characterizing Experimental Errors
- 1.5: Propagation of Uncertainty
- 6.6: Atomic Emission Spectroscopy

capillary columns
- 8.7: Gas Chromatography

capillary electrophoresis
- 8.10: Electrophoresis

central tendency
- 1.3: Characterizing Measurements and Results
- 1.4: Characterizing Experimental Errors

Centrifugation
- 8: Analysis and Separation of Mixtures

Chapter 20
- 7.1: Mass Spectrometers

charge balance equation
- 3.3: Solving Acid-Base Equilibrium Problems

CHEM 235
- TitlePage

chemical analysis
- 4.1: Complexation Titrations
- 4.3: Redox Titrations
- 8.8: High-Performance Liquid Chromatography

chemical calculations
- 1.5: Propagation of Uncertainty

chemical equilibrium
- 9.1: Ladder Diagrams
- 9.2: Solving Equilibrium Problems
- 9.3: Activity Effects

chemical interactions
- 3: Acid-Base Equilibria Affect Solution Conditions
- 8.4: Overview of Analytical Separations

chemical interferences
- 4.4: Ladder Diagrams for Redox Titrations

chemical ionization
- 7.5: Ion Sources

Chemical Properties
8: Analysis and Separation of Mixtures
8.2: Classifying Separation Techniques
chemical reactions
1.1: Classifying Analytical Techniques
1.2: Measurements in Analytical Chemistry
2.2: Stoichiometric Calculations
3.2: Ladder Diagrams for Acid-Base Equilibria
4.2: EDTA Ladder Diagrams
chemical reactivity
3.3: Solving Acid-Base Equilibrium Problems
9: Solubility Equilibria
9.2: Solving Equilibrium Problems
chemical solutions
2.1: Concentration
chemical structure
7.3: Molecular Mass Spectra
chemical systems
9: Solubility Equilibria
chemistry
TitlePage
4: There Are Other Titration Methods!
Chemistry Education
3.2: Ladder Diagrams for Acid-Base Equilibria
chromatogram
8.5: General Theory of Column Chromatography
chromatographic resolution
8.5: General Theory of Column Chromatography
chromatography
8: Analysis and Separation of Mixtures
8.2: Classifying Separation Techniques
8.4: Overview of Analytical Separations
8.5: General Theory of Column Chromatography
8.6: Optimizing Chromatographic Separations
chromatography methods
8.8: High-Performance Liquid Chromatography
chromatography techniques
8.4: Overview of Analytical Separations
8.9: Other Forms of Chromatography
collaboration
InfoPage
column chromatography
8.5: General Theory of Column Chromatography
common ion effect
9.2: Solving Equilibrium Problems
complexation
4: There Are Other Titration Methods!
4.1: Complexation Titrations
complexation equilibria
4.2: EDTA Ladder Diagrams
concentration
1.1: Classifying Analytical Techniques
1.2: Measurements in Analytical Chemistry
1.5: Propagation of Uncertainty
2: The Return of Stoichiometry
2.1: Concentration
2.3: Preparing Solutions
3.3: Solving Acid-Base Equilibrium Problems
concentrations
5.2: Potentiometric Methods
8.1: UV/Vis Analysis of Two-Component Mixtures
9.3: Activity Effects
confidence interval
1.7: Statistical Analysis of Data
1.8: Statistical Methods for Normal Distributions
confidence intervals
1.6: The Distribution of Measurements and Results
conservation of mass
2.2: Stoichiometric Calculations
coordination compounds
4.2: EDTA Ladder Diagrams
coulometry
5.3: Coulometric Methods
counter electrode
5.1: Overview of Electrochemistry
current efficiency
5.3: Coulometric Methods
current measurement
5.1: Overview of Electrochemistry
curriculum development
InfoPage

D

data analysis
1.3: Characterizing Measurements and Results
detection limit
8.7: Gas Chromatography
dilution
1.5: Propagation of Uncertainty
2.3: Preparing Solutions
dissociation reaction
3.2: Ladder Diagrams for Acid-Base Equilibria
dissociation reactions
3.3: Solving Acid-Base Equilibrium Problems
Distillation
8: Analysis and Separation of Mixtures
distribution ratio
8.3: Liquid-Liquid Extractions
DNA fragments
8.10: Electrophoresis

E

EDTA
4: There Are Other Titration Methods!
4.1: Complexation Titrations
9.1: Ladder Diagrams
education
TitlePage
InfoPage
electrochemical cell
5.3: Coulometric Methods
5.4: Voltammetric and Amperometric Methods
electrochemical cells
5: Electrochemical Instrumental Analysis
5.2: Potentiometric Methods
electrochemical techniques
5.1: Overview of Electrochemistry
5.3: Coulometric Methods
electrochemistry
1.1: Classifying Analytical Techniques
5: Electrochemical Instrumental Analysis
5.1: Overview of Electrochemistry
electrodes
5.2: Potentiometric Methods
electrolysis
5.3: Coulometric Methods
electromagnetic radiation
6: Beyond Beer's Law- Quantitative Spectroscopic Analysis
6.1: Overview of Spectroscopy
6.2: Spectroscopy Based on Absorption
Electromagnetic Spectrum
6.3: UV/Vis and IR Spectroscopy
electron configuration
6.5: Photoluminescent Spectroscopy
electron ionization
7.5: Ion Sources
electroosmotic flow
8.10: Electrophoresis
electrophoresis
8.10: Electrophoresis
electrophoretic mobility
8.10: Electrophoresis
electrospray ionization
7.5: Ion Sources
electrostatic analyzer
7.1: Mass Spectrometers
emission
6.1: Overview of Spectroscopy
energy levels
6.2: Spectroscopy Based on Absorption
energy transfer
6.1: Overview of Spectroscopy
environmental analytical method
8.3: Liquid-Liquid Extractions
Environmental Chemistry
6.3: UV/Vis and IR Spectroscopy
equilibrium
3: Acid-Base Equilibria Affect Solution Conditions
3.3: Solving Acid-Base Equilibrium Problems
4: There Are Other Titration Methods!
9.1: Ladder Diagrams
9.2: Solving Equilibrium Problems
equilibrium chemistry
4.2: EDTA Ladder Diagrams
4.4: Ladder Diagrams for Redox Titrations
9: Solubility Equilibria
equilibrium constant
1.2: Measurements in Analytical Chemistry
3.2: Ladder Diagrams for Acid-Base Equilibria
9: Solubility Equilibria
equilibrium constant expressions
3.3: Solving Acid-Base Equilibrium Problems
equilibrium problems
9: Solubility Equilibria
equivalence point
3.1: Acid–Base Titrations
errors
1.4: Characterizing Experimental Errors
3: Acid-Base Equilibria Affect Solution Conditions
excitation state
6.5: Photoluminescent Spectroscopy
extraction
8.2: Classifying Separation Techniques
extraction efficiency
8.3: Liquid-Liquid Extractions
extraction method
8.4: Overview of Analytical Separations

F

faradaic current
5.4: Voltammetric and Amperometric Methods
Fe3+
2.2: Stoichiometric Calculations
Fe3+/Fe2+ reaction
4.4: Ladder Diagrams for Redox Titrations
filtration
9.4: Precipitation Gravimetry

fluorescence
6.1: Overview of Spectroscopy
6.5: Photoluminescent Spectroscopy
formation constant
9.3: Activity Effects
formation constants
4.2: EDTA Ladder Diagrams
fragment ions
7.3: Molecular Mass Spectra
fragmentation
7.5: Ion Sources
fragmentation patterns
7.3: Molecular Mass Spectra
7.6: Applications of Molecular Mass Spectrometry

G
gas chromatography
7.4: Mass Spectrometers
7.6: Applications of Molecular Mass Spectrometry
8.3: Liquid-Liquid Extractions
8.6: Optimizing Chromatographic Separations
8.7: Gas Chromatography
gel electrophoresis
8.10: Electrophoresis
glassware
2.3: Preparing Solutions
gravimetric method
9: Solubility Equilibria
gravimetry
1.1: Classifying Analytical Techniques
9.4: Precipitation Gravimetry

H
HPLC
8.8: High-Performance Liquid Chromatography
8.9: Other Forms of Chromatography
hypothesis testing
1.7: Statistical Analysis of Data

I
icp
7.2: Inductively Coupled Plasma Mass Spectrometer
indicators
4.3: Redox Titrations
inductively coupled plasma
7: Mass Spectrometry
7.2: Inductively Coupled Plasma Mass Spectrometer
infrared
6: Beyond Beer's Law- Quantitative Spectroscopic Analysis
instrumentation
6.3: UV/Vis and IR Spectroscopy
6.4: Atomic Absorption Spectroscopy
interferent
8.2: Classifying Separation Techniques
ion separation
7.4: Mass Spectrometers
ionic strength
9.3: Activity Effects
ionization
7.2: Inductively Coupled Plasma Mass Spectrometer
ions
7.1: Mass Spectrometers
isotopic ratios
7.6: Applications of Molecular Mass Spectrometry

K
Kathy Davis
TitlePage
kinetic energy
7.1: Mass Spectrometers
Ksp
9.2: Solving Equilibrium Problems

L
laboratory techniques
8.8: High-Performance Liquid Chromatography
ladder diagrams
4.2: EDTA Ladder Diagrams
9: Solubility Equilibria
9.2: Solving Equilibrium Problems
Le Châtelier's principle
9.2: Solving Equilibrium Problems
LibreTexts
InfoPage
ligand
4: There Are Other Titration Methods!
4.1: Complexation Titrations
liquid chromatography
7.4: Mass Spectrometers
8.6: Optimizing Chromatographic Separations
8.8: High-Performance Liquid Chromatography
8.9: Other Forms of Chromatography

M
magnetic sector analyzer
7.1: Mass Spectrometers
magnetic sector mass analyzers
7.4: Mass Spectrometers
mass
1.1: Classifying Analytical Techniques
1.3: Characterizing Measurements and Results
1.6: The Distribution of Measurements and Results
9.4: Precipitation Gravimetry
mass analyzers
7.1: Mass Spectrometers
7.4: Mass Spectrometers
mass balance equation
3.3: Solving Acid-Base Equilibrium Problems
mass spectrometer
7: Mass Spectrometry
7.4: Mass Spectrometers
8.7: Gas Chromatography
mass spectrometry
7: Mass Spectrometry
7.2: Inductively Coupled Plasma Mass Spectrometer
7.3: Molecular Mass Spectra
7.5: Ion Sources
7.6: Applications of Molecular Mass Spectrometry
mass spectrum
7.3: Molecular Mass Spectra
7.4: Mass Spectrometers
7.5: Ion Sources
matrix interference
6.4: Atomic Absorption Spectroscopy
mean
1.3: Characterizing Measurements and Results
1.6: The Distribution of Measurements and Results
measurement error
1.2: Measurements in Analytical Chemistry
1.4: Characterizing Experimental Errors
measurement units
2: The Return of Stoichiometry
measurements
1.5: Propagation of Uncertainty
measures of spread
1.3: Characterizing Measurements and Results
median
1.3: Characterizing Measurements and Results
metal
4: There Are Other Titration Methods!
4.1: Complexation Titrations
metal complexes
8.1: UV/Vis Analysis of Two-Component Mixtures
metal ion
4.1: Complexation Titrations
metal ligand complex
9.3: Activity Effects
metal ligand complexes
4.2: EDTA Ladder Diagrams
method selection
6.4: Atomic Absorption Spectroscopy
methods
4: There Are Other Titration Methods!
9.4: Precipitation Gravimetry
mixtures
8.1: UV/Vis Analysis of Two-Component Mixtures
mobile phase
8.4: Overview of Analytical Separations
8.5: General Theory of Column Chromatography
8.6: Optimizing Chromatographic Separations
8.8: High-Performance Liquid Chromatography
8.9: Other Forms of Chromatography
molality
2.1: Concentration
molar absorptivity
8.1: UV/Vis Analysis of Two-Component Mixtures
molar solubility
9.3: Activity Effects
molarity
2.1: Concentration
2.3: Preparing Solutions
Molecular Absorption
6: Beyond Beer's Law- Quantitative Spectroscopic Analysis
6.3: UV/Vis and IR Spectroscopy
8: Analysis and Separation of Mixtures
molecular ion
7.3: Molecular Mass Spectra
molecular ions
7.5: Ion Sources
molecular mass spectra
7: Mass Spectrometry
molecular transitions
6.1: Overview of Spectroscopy
molecular weight
7.6: Applications of Molecular Mass Spectrometry
moles
2: The Return of Stoichiometry
2.2: Stoichiometric Calculations
multielemental
6.6: Atomic Emission Spectroscopy

N
NaOH
3.1: Acid–Base Titrations

Nernst equation
4.3: Redox Titrations
4.4: Ladder Diagrams for Redox Titrations
5: Electrochemical Instrumental Analysis
5.1: Overview of Electrochemistry
5.2: Potentiometric Methods
nitrophenolate
9.1: Ladder Diagrams
normal distribution
1.6: The Distribution of Measurements and Results
1.8: Statistical Methods for Normal Distributions
normality
2.1: Concentration
null hypothesis
1.7: Statistical Analysis of Data
1.8: Statistical Methods for Normal Distributions

O

OER
InfoPage
open licensing
InfoPage
organic solvent
8.3: Liquid-Liquid Extractions
oxidation
5: Electrochemical Instrumental Analysis
oxidation reduction
4.3: Redox Titrations
5.1: Overview of Electrochemistry
oxidizing agent
4.3: Redox Titrations

P

particle properties
6.1: Overview of Spectroscopy
partition coefficient
8.3: Liquid-Liquid Extractions
peak analysis
8.5: General Theory of Column Chromatography
penny
1.3: Characterizing Measurements and Results
pH
3: Acid-Base Equilibria Affect Solution Conditions
3.1: Acid–Base Titrations
3.2: Ladder Diagrams for Acid-Base Equilibria
3.4: Buffer Solutions
4.1: Complexation Titrations
9.1: Ladder Diagrams
9.2: Solving Equilibrium Problems
pH control
4.4: Ladder Diagrams for Redox Titrations
pH measurement
5.2: Potentiometric Methods
phosphorescence
6.5: Photoluminescent Spectroscopy
photoluminescence
6: Beyond Beer's Law- Quantitative Spectroscopic Analysis
6.5: Photoluminescent Spectroscopy
physical properties
8.2: Classifying Separation Techniques
population
1.6: The Distribution of Measurements and Results
population mean
1.7: Statistical Analysis of Data
potential measurement
5.1: Overview of Electrochemistry
potentiometric analysis
5.3: Coulometric Methods
potentiometry
5: Electrochemical Instrumental Analysis
5.2: Potentiometric Methods
potentiostat
5.4: Voltammetric and Amperometric Methods
precipitate
9.4: Precipitation Gravimetry
precipitation
9.4: Precipitation Gravimetry
precision
1.4: Characterizing Experimental Errors
preparing solutions
2: The Return of Stoichiometry
2.3: Preparing Solutions
probability distribution
1.6: The Distribution of Measurements and Results
products
2: The Return of Stoichiometry
propagation
1.5: Propagation of Uncertainty
proteins
8.10: Electrophoresis
pure compounds
7.6: Applications of Molecular Mass Spectrometry
purification
8.2: Classifying Separation Techniques

Q

quadrupole mass analyzers
7.4: Mass Spectrometers
qualitative
6.6: Atomic Emission Spectroscopy
qualitative analysis
7: Mass Spectrometry
7.2: Inductively Coupled Plasma Mass Spectrometer
7.6: Applications of Molecular Mass Spectrometry
8.7: Gas Chromatography
quantitative
6.6: Atomic Emission Spectroscopy
quantitative analysis
1.2: Measurements in Analytical Chemistry
2.1: Concentration
2.2: Stoichiometric Calculations
5.3: Coulometric Methods
6.3: UV/Vis and IR Spectroscopy
7: Mass Spectrometry
7.2: Inductively Coupled Plasma Mass Spectrometer
7.6: Applications of Molecular Mass Spectrometry
8.1: UV/Vis Analysis of Two-Component Mixtures
8.7: Gas Chromatography
8.10: Electrophoresis
quantum yield
6.5: Photoluminescent Spectroscopy

R

reactants
2: The Return of Stoichiometry
reaction conditions
9.3: Activity Effects
reaction rate
1.2: Measurements in Analytical Chemistry
redox
4: There Are Other Titration Methods!
redox equilibria
4.4: Ladder Diagrams for Redox Titrations
redox reactions
5.2: Potentiometric Methods
5.4: Voltammetric and Amperometric Methods
redox titration
4.3: Redox Titrations
5.3: Coulometric Methods
reducing agent
4.3: Redox Titrations
reference electrode
5.1: Overview of Electrochemistry
5.4: Voltammetric and Amperometric Methods
reference electrodes
5: Electrochemical Instrumental Analysis
relative abundance
7.3: Molecular Mass Spectra
relaxation mechanisms
6.5: Photoluminescent Spectroscopy
resolution
7.1: Mass Spectrometers
7.4: Mass Spectrometers
8.6: Optimizing Chromatographic Separations
retention time
8.5: General Theory of Column Chromatography
8.6: Optimizing Chromatographic Separations
8.9: Other Forms of Chromatography

S

sample
1.6: The Distribution of Measurements and Results
sample analysis
6.4: Atomic Absorption Spectroscopy
7: Mass Spectrometry
sample introduction
8.7: Gas Chromatography
sample mean
1.7: Statistical Analysis of Data
sample preparation
6.4: Atomic Absorption Spectroscopy
sample size
1.3: Characterizing Measurements and Results
1.8: Statistical Methods for Normal Distributions
scientific notation
1.2: Measurements in Analytical Chemistry
separation
8.2: Classifying Separation Techniques
8.4: Overview of Analytical Separations
8.8: High-Performance Liquid Chromatography
separation efficiency
8.7: Gas Chromatography
separation technique
8.3: Liquid-Liquid Extractions
separation techniques
8: Analysis and Separation of Mixtures
8.6: Optimizing Chromatographic Separations
8.10: Electrophoresis
significance testing
1.7: Statistical Analysis of Data
1.8: Statistical Methods for Normal Distributions
significant figures
1.2: Measurements in Analytical Chemistry
1.5: Propagation of Uncertainty
2.2: Stoichiometric Calculations

singlet state
6.5: Photoluminescent Spectroscopy
sodium acetate
3.4: Buffer Solutions
solubility
3: Acid-Base Equilibria Affect Solution Conditions
3.2: Ladder Diagrams for Acid-Base Equilibria
9.2: Solving Equilibrium Problems
9.4: Precipitation Gravimetry
solute
2: The Return of Stoichiometry
2.1: Concentration
solute partitioning
8.3: Liquid-Liquid Extractions
solute retention
8.8: High-Performance Liquid Chromatography
solute separation
8.4: Overview of Analytical Separations
8.5: General Theory of Column Chromatography
solution
2: The Return of Stoichiometry
2.1: Concentration
solution preparation
2.3: Preparing Solutions
Spectrophotometers
8: Analysis and Separation of Mixtures
Spectrophotometry
6.3: UV/Vis and IR Spectroscopy
Spectroscopy
1.1: Classifying Analytical Techniques
6: Beyond Beer's Law- Quantitative Spectroscopic Analysis
6.1: Overview of Spectroscopy
6.2: Spectroscopy Based on Absorption
6.4: Atomic Absorption Spectroscopy
6.6: Atomic Emission Spectroscopy
7.2: Inductively Coupled Plasma Mass Spectrometer
8: Analysis and Separation of Mixtures
8.1: UV/Vis Analysis of Two-Component Mixtures
stability
4.1: Complexation Titrations
9: Solubility Equilibria
9.3: Activity Effects
stability constants
4.2: EDTA Ladder Diagrams
standard deviation
1.3: Characterizing Measurements and Results
1.5: Propagation of Uncertainty
standard solution
2.3: Preparing Solutions
standards
1.4: Characterizing Experimental Errors
stationary phase
8.4: Overview of Analytical Separations
8.5: General Theory of Column Chromatography
8.7: Gas Chromatography
8.8: High-Performance Liquid Chromatography
8.9: Other Forms of Chromatography
statistical analysis
1.6: The Distribution of Measurements and Results
1.7: Statistical Analysis of Data
1.8: Statistical Methods for Normal Distributions
statistical parameter
1.4: Characterizing Experimental Errors
statistical tests
1.7: Statistical Analysis of Data
stock solutions
2.3: Preparing Solutions
stoichiometric calculations
2: The Return of Stoichiometry
stoichiometry
2.2: Stoichiometric Calculations
strong base
3.1: Acid–Base Titrations
supercritical fluid chromatography
8.9: Other Forms of Chromatography

T

tandem mass spectrometry
7.5: Ion Sources
techniques
8.2: Classifying Separation Techniques
textbook
TitlePage
textbooks
InfoPage
theoretical plates
8.6: Optimizing Chromatographic Separations
thermal conductivity detector
8.7: Gas Chromatography
thermodynamic equilibrium
9.3: Activity Effects
titration
2.2: Stoichiometric Calculations
3.1: Acid–Base Titrations
4.1: Complexation Titrations
titration curve
3.1: Acid–Base Titrations
4.3: Redox Titrations
titrations
3: Acid-Base Equilibria Affect Solution Conditions
4: There Are Other Titration Methods!
titrimetry
1.1: Classifying Analytical Techniques
traceanalysis
6.6: Atomic Emission Spectroscopy
transitions
6.2: Spectroscopy Based on Absorption
triplet state
6.5: Photoluminescent Spectroscopy

U

ultraviolet radiation
6.2: Spectroscopy Based on Absorption
uncertainty
1.5: Propagation of Uncertainty
units of measurement
1.2: Measurements in Analytical Chemistry
UV
6: Beyond Beer's Law- Quantitative Spectroscopic Analysis
8.1: UV/Vis Analysis of Two-Component Mixtures
UV/Vis Spectroscopy
6.3: UV/Vis and IR Spectroscopy
UVVis Analysis
8: Analysis and Separation of Mixtures

V

variability
1.3: Characterizing Measurements and Results
1.4: Characterizing Experimental Errors
variance
1.6: The Distribution of Measurements and Results
visible
6: Beyond Beer's Law- Quantitative Spectroscopic Analysis
visible radiation
6.2: Spectroscopy Based on Absorption
voltammetry
5: Electrochemical Instrumental Analysis
5.4: Voltammetric and Amperometric Methods
voltammogram
5.4: Voltammetric and Amperometric Methods
volume
1.1: Classifying Analytical Techniques
volumetric flask
2.3: Preparing Solutions

W

water analysis
9.4: Precipitation Gravimetry
wave properties
6.1: Overview of Spectroscopy
weak acid
3.1: Acid–Base Titrations
3.2: Ladder Diagrams for Acid-Base Equilibria
3.3: Solving Acid-Base Equilibrium Problems
3.4: Buffer Solutions
9.2: Solving Equilibrium Problems
weak base
3.2: Ladder Diagrams for Acid-Base Equilibria
3.3: Solving Acid-Base Equilibrium Problems
weight percent
2.1: Concentration
working electrode
5.1: Overview of Electrochemistry
5.4: Voltammetric and Amperometric Methods

Glossary

Sample Word 1 | Sample Definition 1

Detailed Licensing

Overview

Title: CHEM 235: Analytical Chemistry (Davis)

Webpages: 68

Applicable Restrictions: Noncommercial

All licenses found:

- CC BY-NC-SA 4.0: 73.5% (50 pages)
- Undeclared: 26.5% (18 pages)

By Page

- CHEM 235: Analytical Chemistry (Davis) - *CC BY-NC-SA 4.0*
  - Front Matter - *Undeclared*
    - TitlePage - *Undeclared*
    - InfoPage - *Undeclared*
    - Table of Contents - *Undeclared*
    - Licensing - *Undeclared*
  - 1: All Measurements Are Uncertain - *Undeclared*
    - 1.1: Classifying Analytical Techniques - *CC BY-NC-SA 4.0*
    - 1.2: Measurements in Analytical Chemistry - *CC BY-NC-SA 4.0*
    - 1.3: Characterizing Measurements and Results - *CC BY-NC-SA 4.0*
    - 1.4: Characterizing Experimental Errors - *CC BY-NC-SA 4.0*
    - 1.5: Propagation of Uncertainty - *CC BY-NC-SA 4.0*
    - 1.6: The Distribution of Measurements and Results - *CC BY-NC-SA 4.0*
    - 1.7: Statistical Analysis of Data - *CC BY-NC-SA 4.0*
    - 1.8: Statistical Methods for Normal Distributions - *CC BY-NC-SA 4.0*
  - 2: The Return of Stoichiometry - *Undeclared*
    - 2.1: Concentration - *CC BY-NC-SA 4.0*
    - 2.2: Stoichiometric Calculations - *CC BY-NC-SA 4.0*
    - 2.3: Preparing Solutions - *CC BY-NC-SA 4.0*
  - 3: Acid-Base Equilibria Affect Solution Conditions - *Undeclared*
    - 3.1: Acid–Base Titrations - *CC BY-NC-SA 4.0*
    - 3.2: Ladder Diagrams for Acid-Base Equilibria - *CC BY-NC-SA 4.0*
    - 3.3: Solving Acid-Base Equilibrium Problems - *CC BY-NC-SA 4.0*
    - 3.4: Buffer Solutions - *CC BY-NC-SA 4.0*
  - 4: There Are Other Titration Methods! - *Undeclared*
    - 4.1: Complexation Titrations - *CC BY-NC-SA 4.0*
    - 4.2: EDTA Ladder Diagrams - *CC BY-NC-SA 4.0*
    - 4.3: Redox Titrations - *CC BY-NC-SA 4.0*
    - 4.4: Ladder Diagrams for Redox Titrations - *CC BY-NC-SA 4.0*
  - 5: Electrochemical Instrumental Analysis - *Undeclared*
    - 5.1: Overview of Electrochemistry - *CC BY-NC-SA 4.0*
    - 5.2: Potentiometric Methods - *CC BY-NC-SA 4.0*
    - 5.3: Coulometric Methods - *CC BY-NC-SA 4.0*
    - 5.4: Voltammetric and Amperometric Methods - *CC BY-NC-SA 4.0*
  - 6: Beyond Beer's Law- Quantitative Spectroscopic Analysis - *Undeclared*
    - 6.1: Overview of Spectroscopy - *CC BY-NC-SA 4.0*
    - 6.2: Spectroscopy Based on Absorption - *CC BY-NC-SA 4.0*
    - 6.3: UV/Vis and IR Spectroscopy - *CC BY-NC-SA 4.0*
    - 6.4: Atomic Absorption Spectroscopy - *CC BY-NC-SA 4.0*
    - 6.5: Photoluminescent Spectroscopy - *CC BY-NC-SA 4.0*
    - 6.6: Atomic Emission Spectroscopy - *CC BY-NC-SA 4.0*
  - 7: Mass Spectrometry - *Undeclared*
    - 7.1: Mass Spectrometers - *CC BY-NC-SA 4.0*
    - 7.2: Inductively Coupled Plasma Mass Spectrometer - *CC BY-NC-SA 4.0*
    - 7.3: Molecular Mass Spectra - *CC BY-NC-SA 4.0*
    - 7.4: Mass Spectrometers - *CC BY-NC-SA 4.0*
    - 7.5: Ion Sources - *CC BY-NC-SA 4.0*
    - 7.6: Applications of Molecular Mass Spectrometry - *CC BY-NC-SA 4.0*
  - 8: Analysis and Separation of Mixtures - *Undeclared*

- 8.1: UV/Vis Analysis of Two-Component Mixtures - *CC BY-NC-SA 4.0*
- 8.2: Classifying Separation Techniques - *CC BY-NC-SA 4.0*
- 8.3: Liquid-Liquid Extractions - *CC BY-NC-SA 4.0*
- 8.4: Overview of Analytical Separations - *CC BY-NC-SA 4.0*
- 8.5: General Theory of Column Chromatography - *CC BY-NC-SA 4.0*
- 8.6: Optimizing Chromatographic Separations - *CC BY-NC-SA 4.0*
- 8.7: Gas Chromatography - *CC BY-NC-SA 4.0*
- 8.8: High-Performance Liquid Chromatography - *CC BY-NC-SA 4.0*
- 8.9: Other Forms of Chromatography - *CC BY-NC-SA 4.0*
- 8.10: Electrophoresis - *CC BY-NC-SA 4.0*

- 9: Solubility Equilibria - *Undeclared*
  - 9.1: Ladder Diagrams - *CC BY-NC-SA 4.0*
  - 9.2: Solving Equilibrium Problems - *CC BY-NC-SA 4.0*
  - 9.3: Activity Effects - *CC BY-NC-SA 4.0*
  - 9.4: Precipitation Gravimetry - *CC BY-NC-SA 4.0*
- Back Matter - *Undeclared*
  - Index - *Undeclared*
  - Glossary - *Undeclared*
  - Detailed Licensing - *Undeclared*